Ollscoil na hÉireann, Corcaigh

National University of Ireland, Cork

Exploring Early-Life Microbiome Transfer and Therapeutic Applications in Bovines and Humans

Thesis presented by

Kevin Anthony Linehan, BSc. (Hons)

for the degree of

Doctor of Philosophy

UCC Student No: 114467738

University College Cork

School of Microbiology, University College Cork, Cork, Ireland

Teagasc Food Research Centre, Moorepark, Fermoy, Co. Cork, Ireland

APC Microbiome Ireland, University College Cork, Cork, Ireland

Supervisor(s): Prof. Catherine Stanton, Prof. R. Paul Ross

Head of School/Department: Dr David Clarke

July 2023

Table of contents

Declaration

This is to certify that the work I am submitting is my own and has not been submitted for another degree, either at University College Cork or elsewhere. All external references and sources are clearly acknowledged and identified within the contents. I have read and understood the regulations of University College Cork concerning plagiarism and intellectual property.

Contributions

Chapter 3: The Contributions of the Placenta, Mode of Delivery, Maternal Oral Cavity, Prophylactic Antibiotics and Initial Feeding on the Meconium Microbiome: Performed DNA extractions. Prepared 16S rRNA compositional sequencing libraries. Performed bioinformatics analysis and statistical analysis. Drafted the manuscript. Dr. Eimear Hurley and Carol Anne O'Shea recruited the subjects, assisted with sample collections from Cork University Maternity Hospital and provided clinical metadata on the samples. Dr Kiera Murphy performed part of the bioinformatics analysis of 16S rRNA sequencing data. Prof. Eugene M. Dempsey, Prof. Anthony Ryan, Prof. R. Paul Ross and Prof. Catherine Stanton designed the study and acquired ethical approval.

Chapter 4: Characterising the Virome of Bovine Colostrum: Diversity, Community Structure and Implications for Veterinary and Human Applications: Collected bovine colostrum samples.Performed culture-based work, viral nucleic acid extractions and prepared samples for whole genome sequencing. Performed bioinformatics analysis and statistical analysis.Drafted the manuscript. Lisa Smith provided assistance with part of the bioinformatics analysis of virome data.

Chapter 5: Isolation, characterisation and efficacy of two novel temperate bacteriophages against bovine and human pathogenic Staphylococcus aureus isolates: Collected bovine colostrum samples**.** Performed culture-based work, phage isolation, phenotypic and genotypic experiments**.** Performed DNA extractions and prepared samples for whole genome sequencing**.** Performed bioinformatics analysis and statistical analysis. Drafted the manuscript. Dr. Katriona Lyons collected human milk samples as part of the INFAMILK study and provided assistance in the isolation of phage vB_SauS_HM1. Dr. Colin Buttimer assisted with CsCl gradient preparations and provided assistance with bioinformatic analysis. Prof. Aidan Coffey provided MRSA strains from St. James' Hospital for host range screening. Dr Horst Neve and his transmission electron microscopy team at the Max Rubner-Institut, Germany carried out TEM imaging.

Chapter 6: Emulsion-Based Postbiotic Formulation Is Comparable to Viable Cells in Eliciting a Localised Immune Response in Dairy Cows With Chronic Mastitis: Drafted the manuscript. Conducted ELISAs to quantify IL-8 titres.

Performed part of the bioinformatics analysis and statistical analysis Dr. Harsh Mathur prepared the various emulsion-based formulations for infusions, associated microbiological work, and ELISAs to quantify IL-8 titres. Jim Flynn conducted the SCC determinations and plating of pathogens. Noel Byrne performed treatment infusions.

Signature: _____ 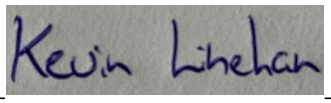 _____

Date: _____27/07/2023_____

Student number: 114467738

Acknowledgements

First and foremost, I would like to thank my research supervisors Catherine Stanton and Paul Ross for giving me the opportunity to carry out this PhD. Your expertise and mentorship have been truly invaluable throughout this journey. I am sincerely grateful for your unwavering help, support and input over the years.

My sincere gratitude goes out to my funding bodies at the APC microbiome institute and Science Foundation Ireland for their generosity and financial support which enabled this research.

A PhD represents the collective effort and support of many individuals and I could not have completed this undertaking without the love and support of my friends and family. To my friends and colleagues in Teagasc, past and present- thank you! There are a few individuals that I want to give a special mention to. Leonie, I can't thank you enough for your friendship and support which made this journey so much more enjoyable and kept me sane throughout the whole process. Ashok, thanks for always being a sensei and helping me find the peaks. A special thanks also to Aoife, Arghya, Clodagh, Conall, Dhrati, Fatma, Grace, Harsh, Kiera, Katriona, Kiz, Niamh, Ronan, Ruth and Sinead for your friendship, help, and advice over the years.

To all my friends outside of Moorepark, thanks for being the perfect remedy to academia. Too many to mention everyone here, but particularly (and in alphabetical order so nobody roasts me), Adam, Andrew, Darragh, David, Donagh, Mark, Paudie, Rory, Shane, and Steve.

Most importantly, thank you to my family. Mom, Dad and Denise, words will never be enough, but here's some anyway. Mom and Dad, all the characteritics that were needed to complete this thesis were instilled in me by you. Throughout my life, through your own example, you have imbued in me a passion for hard work, respect, and decency for others. You have always put my happiness first and this thesis is for you. Denise, you are not only the best sister but also an amazing friend. Your unwavering support, encouragement, and presence have meant the world to me. I truly appreciate everything you've done, and I know I can always count on you. Thank you for being there for me.

Abstract

The microbiome consists of intricate microbial communities, including bacteria, archaea, eukarya, viruses, bacteriophages, and their associated products. These dynamic entities establish symbiotic relationships with their bovine and human hosts, exerting direct or indirect influences on physiology throughout life, impacting both health and disease outcomes. The early-life microbiome exerts a profound impact on developmental trajectories and long-term health. The extent to which different maternal microbial sources and perinatal factors contribute and shape the initial colonisation, development, and functionality of the neonatal microbiome is a topic of ongoing research. Understanding these factors is crucial for comprehending the early establishment of the microbiome. Given the current antibiotic resistance crisis, there is significant importance in leveraging host-microbiome interactions to develop microbiome-based therapeutics. This thesis explores a number of research foci with a view to gain a better understanding of (1) the influence of different maternal microbial sources and perinatal factors on the initial establishment of the human infant gut microbiome, (2) harnessing the bioactive composition of bovine colostrum for bovine and human health applications, (3) characterising the virome of bovine colostrum and the influence of perinatal factors on its composition, and (4) the potential of microbiome-based therapeutics for disease treatment in bovines and humans. Chapter 1 discusses the impact of perinatal factors, including maternal nutrition, antibiotic use, gestational age, and mode of delivery, on the initial colonisation, development, and function of the human neonatal gut microbiome. The elucidation of the precise extent to which these factors influence gut microbiome establishment and identification of those with the most decisive effects on colonisation are essential for improving infant health. In Chapter 2, the diverse array of bioactive components in bovine colostrum suitable for the development of functional foods, nutraceuticals, and pharmaceuticals with veterinary and human health applications are discussed. The processing techniques used to produce high-value colostrum-based products, and recent studies utilizing bovine colostrum for veterinary and human health are also outlined. In Chapter 3, using a cohort of 18 healthy mother-infant dyads, the microbial composition of three potential maternal sources of microbial transmission (oral, vaginal and placental) to the microbiota of their new-born infant (oral and meconium microbiota) were characterised. This allowed investigation of the contribution of

numerous transmission routes and the impact of various perinatal factors on the initial establishment of the infant gut and oral microbiome. The results of this study consolidate and corroborate recent findings surrounding the existence of a meconium microbiome and the absence of a placental microbiome. Furthermore, the study shows that significant vertical transfer, primarily from the maternal oral cavity to the infant oral cavity occurs in early life. In Chapter 4, a reproducible, low cost and high-throughput virome extraction method was developed for bovine colostrum. Shotgun sequencing and viral specific metagenomics bioinformatics were performed on samples from 72 dairy cows, given dry cow therapy (n=48) or naturally dried off (n=24). The impact of farm level variables (location and parity) were also assessed. Phages carrying multidrug resistance genes (smeS, lfrA, kdpE and baeS) were identified. Antibiotic treatments significantly impacted virome composition and the presence of resistance genes specific to the administered antibiotic. This study provides novel insights into disease development and transmission in animals and humans, and the contribution of viruses to the spread of global antimicrobial resistance. In Chapter 5, two novel *Staphylococcus aureus* bacteriophage species from the genus *Phietavirus* were isolated. Phages were lytic against several human and bovine mastitis causing strains of Staphylococcus aureus (including MRSA). Phages displayed excellent characteristics for *in vivo* experiments, with no resistance genes present, stability to variations in pH (4 to 9), temperature (up to 60 °C), chloroform resistant and capable of replicating in mastitic milk. Finally, in Chapter 6, a field trial was undertaken to investigate the efficacy of emulsion based postbiotic and live-biotherapeutic formulations of *Lactococcus lactis* DPC3147, producer of the bacteriocin lacticin 3147, as alternative therapeutics for bovine mastitis. Twenty eight cows with chronic mastitis were treated with emulsion-based formulations containing either viable *L. lactis* DPC3147 cells (n=15) or heat-killed *L. lactis* DPC3147 cells (n=13). The efficacies of the two formulations in stimulating a localised immune response (measuring interleukin-8 concentrations in milk) and cure rates (somatic cell counts reductions and pathogen absence) were evaluated. This study demonstrated that the presence of heat-inactivated bacteria (a postbiotic) was as effective as the live bio-therapeutic in eliciting a localised immune response in cows with chronic mastitis. The results outlined in this thesis provide valuable insights into the intricate dynamics of early-life microbiome transfer and outline novel microbiome-based therapeutics for applications in bovines and humans.

Publications

Chapter 1: **Linehan, K.,** Dempsey, E. M., Ryan, C. A., Ross, R. P. & Stanton, C. 2022. First encounters of the microbial kind: perinatal factors direct infant gut microbiome establishment. *Microbiome Research Reports*, 1, 10. http://dx.doi.org/10.20517/mrr.2021.09

Chapter 2: **Linehan, K.,** Ross, R. P. & Stanton, C. 2022. Bovine Colostrum for Veterinary and Human Health Applications: A Critical Review. *Annual review of food science and technology*, 14**,** 387-410. https://doi.org/10.1146/annurev-food-060721-014650

Chapter 6: Mathur, H., **Linehan, K.,** Flynn, J., Byrne, N., Dillon, P., Conneely, M., Grimuad, G., Hill, C., Stanton, C. & Ross, R. P. 2022. Emulsion-Based Postbiotic Formulation Is Comparable to Viable Cells in Eliciting a Localised Immune Response in Dairy Cows With Chronic Mastitis. Frontiers in Microbiology, 13, 41. https://doi.org/10.3389/fmicb.2022.759649

Co-authored publications

Kuhl, G.C., Mazzon, R.R., Simas Porto, B.L., Zamboni Madaloz, T., Razzera, G., Patricio, D.D.O., **Linehan, K**., Ahern, G., Mathur, H., Ross, P., Stanton, C. and De Dea Linder, J. 2021. Oleate hydratase in *Lactobacillus delbrueckii* subsp. *bulgaricus* LBP UFSC 2230 catalyzes the reversible conversion between linoleic acid and ricinoleic acid. *Microbiology Spectrum*, 9, e01179-21. https://doi.org/10.1128/Spectrum.01179-21

Bauman, D.E., Lock, A.L., Conboy Stephenson, R., **Linehan, K.,** Ross, R.P., Stanton, C. (2020). Conjugated Linoleic Acid: Biosynthesis and Nutritional Significance. Advanced Dairy Chemistry, Volume 2: Lipids, 67-106. https://doi.org/10.1007/978-3-030-48686-0_3

Patangia, D.V.; Grimaud, G.; **Linehan, K**.; Ross, R.P.; Stanton, C. Microbiota and Resistome Analysis of Colostrum and Milk from Dairy Cows Treated with and without Dry Cow Therapies. *Antibiotics* **2023**, *12*, 1315. https://doi.org/10.3390/antibiotics12081315

Linehan, K.; Patangia, D.V.; Ross, R.P.; Stanton, C. Production, Composition and Nutritional Properties of Organic Milk: A Critical Review. Under review in *Foods*.

Co-authored an article discussing Chapter 6 of this thesis for the Teagasc TResearch Autumn 2022 magazine, targeted at non-research audiences: https://www.teagasc.ie/about/research--innovation/research-publications/tresearch-autumn-2022/finding-alternative-ways-to-treat-bovine-mastitis/

Conferences

1. Student Award Speaker for the International Milk Genomics Consortium 2022, University of California, Davis, USA. "*Microbiome Based Mastitis Therapeutics*".

2. Student Award Speaker for the International Milk Genomics Consortium 2023, University College Cork. "*Characterisation of the Bovine Colostrum Virome and Two Novel Staphylococcus Aureus Bacteriophages*".

Abbreviations

3′SL: 3′ sialyllactose

6′SL: 6′ sialyllactose

6′SLN: 6′ siayllactosamine

ACE2: angiotensin-converting enzyme 2

AMR: Antimicrobial resistance

ANCOM: analysis of the composition of microbiomes

ANI: Average nucleotide identity

ANOVA: Analysis of Variance

APGAR: Appearance, Pulse, Grimace, Activity and Respiration

APP: Acute-phase proteins

ASV: Amplicon Sequencing Variant

BH: Benjamini-Hochberg

BIMs: Bacteriophage-insensitive mutants

BLAST: Basic Local Alignment Search Tool

BMI: Body Mass Index

BCS: bovine colostrum silage

BPA: Baird Parker agar

bMEC: Bovine mammary epithelial cells

β: Beta

bp: Base Pair

BRED: Bacteriophage recombineering of electroporated DNA

CARD: Comprehensive Antibiotic Resistance Database

CHAP: N-terminal cysteine, histidine-dependent amidohydrolases/peptidases

CLA: Conjugated Linoleic Acid

CFU/ml: Colony forming units per milliliter

CRESS: Conserved RNA Element Search Software

CS: C-section

CDS: Coding sequence

CsCl: Cesium Chloride

DCT: Dry Cow Therapy

DNA: Deoxyribonucleic acid

DSL: Disialyllactose

ds: Double stranded

EGFs: Epidermal growth factors

ELISA: Enzyme-Linked Immunosorbent Assay

EOP: Efficiency of Plaquing

ESKAPE: Enterococcus faecium, Staphylococcus aureus, Klebsiella pneumoniae, Acinetobacter baumannii, Pseudomonas aeruginosa, and Enterobacter spp.

FAO: Food and Agriculture Organisation of the United Nations

FDR: False discovery rate

FMT: Fecal microbiota transplantation

Fc: fragment crystallisable

FOS: Fructo-Oligosaccharides

g: Gravitational force or gram

GABA: γ-aminobutyric acid

GDM: Gestational Diabetes Mellitus

GI: Gastrointestinal

GBS: Group B Streptococcus

GBDP: Genome-BLAST Distance Phylogeny

GRAS: Generally regarded as safe

HBC: Hyperimmune bovine colostrum

HGT: Horizontal gene transfer

HMOs: Human milk oligosaccharides

HPRA: Health Products Regulatory Authority

HPP: High-pressure processing

HGT: Horizontal gene transfer

HIV: Human immunodeficiency virus

HTST: High-temperature short-time

IAP: Intrapartum antimicrobial prophylaxis

ICSTs: Infant community state types

IBD: Inflammatory Bowel Disease

IGF: Insulin-like growth factor

Ig: Immunoglobulin

IgA: Immunoglobulin A

IgD: Immunoglobulin D

IgE: Immunoglobulin E

IgG: Immunoglobulin G

IgM: Immunoglobulin M

IL: Interleukin

ITCs: isothiocyanates

Kbp: Kilobase pair

KEGG: Kyoto Encyclopedia of Genes and Genomes

KO: KEGG Orthology

LAB: Lactic acid bacteria

LASL: Long-Read Linker-Amplified Shotgun Library

LCA: Lithocholic acid

LEfSe: Linear discriminant analysis Effect Size

LGT: Lateral gene transfer

LPS: Lipopolysaccharides

LDA: Linear discriminant analysis

LTLT: low-temperature long-time

LAB: Lactic acid bacteria

MDR: Multidrug resistant

MIC: Minimum inhibitory concentration

miRNAs: MicroRNAs

MOI: Multiplicity of Infection

MUFAs: monounsaturated fatty acids

NACs: N-acetylcysteine

NGS: Next-generation sequencing

NICU: Neonatal Intensive Care Unit

NCBI: National Centre for Biotechnology Information

NGS: Next-generation sequencing

NB: Natural Birth

NSAIDs: Nonsteroidal anti-inflammatory drugs

ORF: Open reading frame

PAS: Phage-antibiotic synergy

PCR: Polymerase chain reaction

PBS: Phosphate buffered saline

PCoA: Principal Coordinate Analysis

PEG: Polyethylene glycol

PERMANOVA: Permutational multivariate ANOVA

PICRUSt2: Phylogenetic Investigation of Communities by Reconstruction of Unobserved States

PMNs: polymorphonuclear leukocytes

PROM: premature rupture of membranes

ProkSee

pVOGs: prokaryotic viral orthologous groups

PUFA: polyunsaturated fatty acid

RID: radial immunodiffusion

RGI: Resistance Gene Identifier

RID: radial immunodiffusion

SCFA: Short-chain fatty acids

SCCs: somatic cell counts

SCVs: Small colony variants

SFA: saturated fatty acid

SL: sialyllactose

SLn: siayllactosamine

ss: single stranded

TGF: transforming growth factor

TFF: tangential-flow filtration

TNFs: tumor necrosis factors

TBC: total bacterial count

UV: Ultraviolet

VF: Virulence factor

VFDB: Virulence Factor Database

VEGF: Vascular endothelial growth factor

VLPs: virus-like particles

VRSA: vancomycin-resistant S. aureus

WHO: World Health Organisation

v: Version

vs.: Versus

Units

˚C: Degree Celsius

µg: Microgram

µg/ml: Microgram per millilitre

µl: Microliter

bp: Base Pair

cm: Centimetre

Da: Dalton

g: Gram

h: Hour

kDa: Kilodalton

KU: kiloUnit

L: Litre

M: Molar

mg/L: Milligram per litre

mg ml-1: Milligram per millilitre

min(s): Minute(s)

mm: Millimetre

mM: Millimolar

ng: Nanogram

nm: Nanometre

nt: Nucleotide

v/v: Volume per volume

V: Volt

w/v: Weight per volume

xg: Relative centrifugal force

Chapter 1

Mini Review

First encounters of the microbial kind: perinatal factors direct infant gut microbiome establishment

Kevin Linehan is first author of this invited review which is published in:

Linehan, K., Dempsey, E. M., Ryan, C. A., Ross, R. P. & Stanton, C. 2022. First encounters of the microbial kind: perinatal factors direct infant gut microbiome establishment. *Microbiome Research Reports,* 1, 10.

1.1 Abstract

The human gut microbiome harbours a diverse range of microbes that play a fundamental role in the health and well-being of their host. The early-life microbiome has a major influence on human development and long-term health. Perinatal factors such as maternal nutrition, antibiotic use, gestational age and mode of delivery influence the initial colonisation, development, and function of the neonatal gut microbiome. The perturbed early-life gut microbiome predisposes infants to diseases in early and later life. Understanding how perinatal factors guide and shape the composition of the early-life microbiome is essential to improving infant health. The following review provides a synopsis of perinatal factors with the most decisive influences on initial microbial colonisation of the infant gut.

1.2 Introduction

The microbiome depicts the microbiota and their "theatre of activity", encompassing the combined nucleic acids (including viruses and bacteriophages), structural components and microbial metabolites related to the microbiota (Berg et al., 2020). The gut microbiota describes the trillions of microbial cells (bacteria, archaea, protists, and fungi) occupying the intestine, with Bacteroidetes and Firmicutes accounting for 90% of the total bacterial inhabitants and Actinobacteria, Cyanobacteria, Fusobacteria, Proteobacteria and Verrucomicrobia constituting the remaining 10% (Lloyd-Price et al., 2016). These gut microbiota engage in a plethora of host biological responses, including the regulation of immunity (Gensollen et al., 2016), energy homeostasis, protection against pathogens and bioactive metabolite production (Nguyen et al., 2021b). Furthermore, the disparities in the intestinal microbiota have been linked to disease states such as metabolic disorder (Wiley et al., 2021a), cancer (Gopalakrishnan et al., 2018), and cardiovascular disease (Murphy et al., 2021a). The initial formation of the gut microbiota is essential in maintaining intestinal homeostasis and symbiosis in neonates, shaping and guiding the development of the immune and nervous systems during a critical developmental window (Clarke et al., 2014). Although the mechanism at present is not fully elucidated, the current consensus is that a disrupted microbiota in early life can leave a lasting footprint on health in early life and beyond (Fouhy et al., 2019). The first encounters of the neonatal gut with microbes are directed by intrinsic and extrinsic factors, collectively named "perinatal factors". These consist of maternal nutrition, antibiotic use, gestational age, genetics and mode of delivery (Wang et al., 2020a). Early-life gut microbiome imbalances predispose infants to colonisation by opportunistic pathogens, such as *Enterococcus*, *Enterobacter*, *Clostridium*, and *Klebsiella* species. Furthermore, infant gut dysbiosis can lead to impaired growth and an increased risk of sepsis and necrotizing enterocolitis (NEC), especially in preterm new-borns (Fundora et al., 2020). Longer-term consequences of perturbed microbial colonisation include allergies, asthma, metabolic syndrome, diabetes and inflammatory bowel disease (Milani et al., 2017). Therefore, it is essential to elucidate the extent to which perinatal factors may influence the microbial bond between mother and infant. Further understanding of how this intricate relationship may be influenced by perinatal factors

is imperative to optimise mother and infant health in the perinatal period and inform the adequate type and timing of therapeutic interventions. In this short review, we discuss the core microbes which initially colonise the infant gut and decipher the influence of perinatal factors on directing these first encounters.

1.3 Core Infant Gut Microbiome

The first encounters of microbes with the infant intestine represent the *de novo* assembly of a complex microbial community (Costello et al., 2012). In contrast to adults, the gut microbiome in early life is unstable, highly dynamic and low in diversity (Arrieta et al., 2014). At birth, the infant gut is an aerobic environment, inhabited by *Escherichia* and *Enterococcus*. These facultative bacteria thrive on residual oxygen present, resulting in a lowered redox potential and thus shifting the infant gut to an anaerobic environment. Obligate anaerobes, including Firmicutes such as *Clostridia*, Bacteroidetes and the bedrock of the infant gut microbiome, bifidobacteria, begin to flourish at this point (Collado et al., 2012). Bifidobacteria constitute up to 37% of the infant gut microbiota in early life (Duranti et al., 2017). Along with *Veillonella*, *Streptococcus*, *Citrobacter*, *Escherichia*, as well as *Bacteroides* and *Clostridium*, they dominate the core infant gut microbiome (Turroni et al., 2020). In Table 1.1, we summarize the characteristics and functions of these pioneering microbes in the infant gut. Despite large variance at the intra-individual level, a recent multi-population cohort meta-analysis revealed the existence of specific taxonomic patterns or infant community state types (ICSTs) (Mancabelli et al., 2020). This study subdivided ICSTs into four macro groups, < 1 month of age, between 1 and 6 months of age, between 6 and 12 months of age and between 1 and 3 years of age. Higher microbial complexity in samples from infants aged between 12 and 36 months compared to those from children less than one-month-old was observed. This increase in biodiversity appeared to have caused a reduction in the relative abundance of the *Bifidobacterium* genus in favour of *Bacteroides*, *Feacalibacterium*, *Blautia* and *Ruminococcus* genera. ICSTs are further modulated by birth mode and feeding type, which will be discussed later in this review.

Table 1.1 | Characteristics, Functions and Metabolites produced by the Core Infant Gut Microbiome Members

Microbes	**Key Functions & Characteristics in the Infant Gut**	**Microbial Metabolites Produced**	**Refs**
Bifidobacteria	Saccharolytic degradation of diet-derived glycans and host-provided carbohydrates (known as host glycans including mucins and HMOs).	γ-aminobutyric acid (GABA), Conjugated Linoleic Acid (CLA), Short Chain Fatty Acids (SCFA), Group B Vitamins (B1, B3, B6, B9, B12)	(Alessandri et al., 2021, Wiley et al., 2021b, Yoshii et al., 2019)
Genus *Bacteroides*	Metabolise HMOs, mucins and complex plant polysaccharides (starch, cellulose, xylans, and pectins). Proteolytic activity via extracellular proteases. Deconjugation of bile acids.	GABA, Vitamin K, SCFA, Group B Vitamins (B1, B2, B5, B6, B7, B9, B12)	(Marcobal et al., 2011, Otaru et al., 2021, Rios-Covian et al., 2017, Wiley et al., 2021b, Yoshii et al., 2019)
Genus *Veillonella*	Produce propionate from end products of carbohydrate fermentation (e.g., lactate). Propionate displays anti-inflammatory	SCFA	(Vipperla and O'Keefe, 2012)

	features, influences glucose and energy homeostasis and increases insulin sensitivity.		
Genus *Streptococcus*	Specific members of the genus *Streptococcus* form part of the core infant gut microbiota and are among the first established bacteria in the infant gut within the first 24 h following birth.	Serotonin, GABA, Histamine,	(Wiley et al., 2021b)
Genus *Collinsella*	Present in large amounts when infant gut microbiota is dominated by bifidobacteria. Currently comprises six species isolated from human faeces and vaginal tract.	Group B Vitamins (B6)	(Han et al., 2021, Magnúsdóttir et al., 2015, Yoshii et al., 2019)
Genus *Lactobacillus*	Vertical transmission of *Lactobacillus* species presents the origin of infant	Serotonin, GABA, Acetylcholine, Histamine, CLA, SCFA, Group B Vitamins (B1, B2, B7, B9, B12)	(Zhang et al., 2020, Wiley et al., 2021b, Yoshii et al., 2019)

	Lactobacillus microbiota component. May be related to the HMO metabolism of infant.		
Genus *Akkermansia*	*A. muciniphila* is the sole intestinal representative in the human gut from early life. May ferment HMOs. Target for therapeutics aimed at increasing barrier function.	Serotonin, SCFA	(Yaghoubfar et al., 2020)

1.4 Perinatal Factors and the First Microbial Encounters

In this section, we discuss the effect of perinatal factors on the initial colonisation of the infant gut with microbes (see Figure 1.1). The majority of studies on this topic relate the relative abundance of microbes in fecal samples to the composition of the gut microbiota, thus any changes or differences in microbial content discussed herein are based upon changes/differences in the relative abundance of microbes unless otherwise stated. While this review will focus on the establishment of bacteria in the infant gut, we acknowledge that these factors may also influence the infant gut virome (Taboada et al., 2021), mycobiome and sporobiota (Egan et al., 2021).

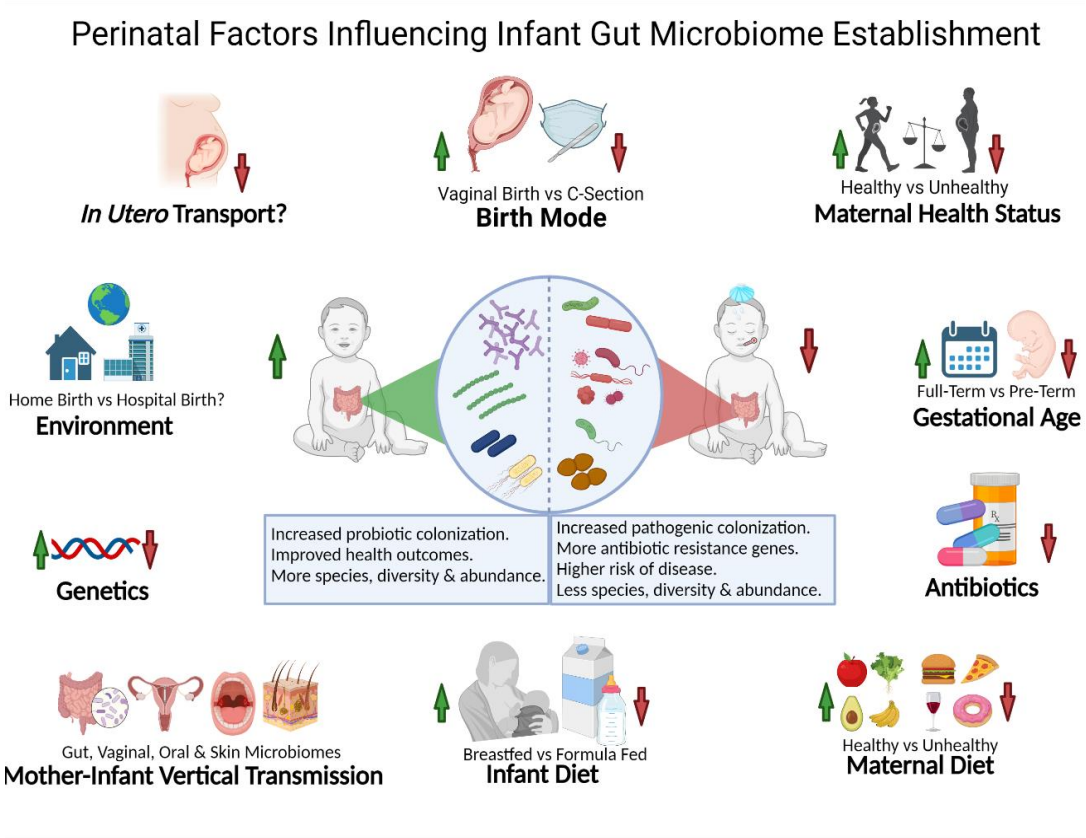

Figure 1.1 | Perinatal Factors Influencing Infant Gut Microbiome Establishment. Graphic outlining the factors that contribute to early the initial infant gut microbiome. Created with BioRender.com.

1.4.1 Maternal health status during pregnancy

Maternal health during pregnancy is a key input in fetal health and infant development. Numerous studies have described aberrant gut colonisation in infants born to mothers who suffered from elevated stress and cortisol levels throughout gestation (Naudé et al., 2020). Specifically, increased abundances of pathogenic bacteria Proteobacteria (*Escherichia*, *Enterobacter*, *Serratia*, *Citrobacter*, *Campylobacter*) and Firmicutes (*Veillonella* and *Finegoldia*) in addition to decreased abundances of beneficial bacteria such as lactic acid bacteria (*Lactobacillus*, *Lactococcus*, *Aerococcus*), Actinobacteria (bifidobacteria, *Collinsella*, *Eggerthella*) and *Akkermansia* have been noted (Naudé et al., 2020). While weight gain during pregnancy is a natural physiological response, excessive gestational weight gain (defined as 16 kg or above for women with BMI 19.8-25 or above 11.5 kg for women with BMI > 25 (Naudé et al., 2020) has been reported to lead to the increased relative abundance of *Escherichia* and *Dorea* in vaginally born infants (Singh et al., 2020). Metagenomic

analysis has also shown that gestational weight gain impacts the function of the initial infant gut microbiome (Baumann-Dudenhoeffer et al., 2018). Excessive maternal weight gain during pregnancy has been associated with enrichment of phenylalanine, cysteine/serine, folate, thiamine, biotin, and pyridoxine synthesis pathways and bacterial glucose pathways in infants (Baumann-Dudenhoeffer et al., 2018). These effects are seen up to eight months post-partum, highlighting a longer-term impact on microbiota function. Affecting one in every seven live births worldwide (Cho et al., 2018), gestational diabetes mellitus (GDM) presents the most frequent metabolic disorder that women encounter throughout gestation. The establishment of key pioneering taxa, important for establishing neonatal development, such as *Lactobacillus*, *Flavonifractor*, *Erysipelotrichaceae* and *Bacteroides* have shown to be decreased in infants born to mothers with GDM (Soderborg et al., 2020). Interestingly, the level of dysbiosis is postulated to occur differentially depending on the severity of the GDM condition (Sililas et al., 2021). Both extremes of the reproductive age (typically < 17 years and > 35 years) are considered as the highest risks for infant mortality and detrimental health outcomes for mother and infant. Fetal and maternal complications of GDM include fetal growth restriction, preterm birth, chromosomal and congenital abnormalities, pre-eclampsia and C-section (CS) birth (Kim et al., 2021, Frick, 2021, Attali and Yogev, 2021).

1.1.1 Maternal diet

Mounting evidence demonstrates the influence of a healthy maternal diet throughout the gestational period to optimize the acquisition of rich and diverse gut microbiota in neonates and improve long-term health outcomes (Maher et al., 2020). While the quintessential prenatal diet is not known, it is recommended that pregnant women consume “a balanced diet with the appropriate distribution of the basic food pyramid groups” (American College of Obstetricians and Gynecologists, 2019). Regarding studies of the influence of maternal diet on infant gut microbiome establishment, it must be noted that notable heterogeneity pervades multiple areas of the studies presented to date. For instance, most studies utilize cohorts of overweight or obese women, which are not representative of a normal population. At present, there is no clear consensus on the periods of assessment and time points during pregnancy at which assessments are carried out. A systematic review by Maher *et al.* (Maher et al., 2020) recently reported that inspection of detailed dietary data in pregnancy and its

impact on the microbiome must be carried out in detail in a cohort that is indicative of a normal obstetric population. Bereft of this information, current findings from subgroups are challenging to decipher and highly variable. Finally, the authors noted that the methods of reporting dietary intake are subject to bias, suggesting that combining both Food Frequency Questionnaires and food diaries may be a method to circumvent this problem. With these limitations in mind, high-fat maternal diet has been repeatedly associated with detrimental effects on the infant gut microbiome (Maher et al., 2020). High-fat maternal diet has been reported to be associated with the enrichment of *Enterococcus* and depletion in *Bacteroides* (Chu et al., 2016). A recent study reported that diet in a healthy cohort of pregnant women was correlated to both maternal and neonatal microbiota at the time of birth, in a delivery mode-dependent manner (Selma-Royo et al., 2021). Furthermore, the study indicated that fat intake in the form of saturated fatty acids and mono- and poly-unsaturated fatty acids (MUFA and PUFA) showed significant enrichment in Firmicutes phylum genera and depletion in Proteobacteria phylum genera in the offspring's microbiota. A high-fat diet has been related to a higher abundance of Firmicutes and a concurrent increase in BMI (Koliada et al., 2017, Serino et al., 2012). Maternal intestinal permeability is higher throughout pregnancy (Reyes et al., 2006) and excess dietary intake is known to enhance intestinal permeability (Rohr et al., 2020), which may have implications on the vertical transmission of specific genera influencing early neonatal colonisation. Prenatal diet has also been shown to modify the breast milk microbiome. High dietary intake of plant protein, fiber, and carbohydrates was associated with elevated *Staphylococcus*, *Bifidobacterium*, and *Lactobacillus* abundance (Cortes-Macías et al., 2021). The intake of food with high animal protein content and fats (n-3 PUFAs and MUFAs), exhibited a negative association with the abundance of *Enterococcus* and *Bifidobacterium* and a positive correlation with *Gemella* (Cortes-Macías et al., 2021) in the breast milk microbiome. Maternal diet may also modulate the human milk oligosaccharide (HMO) composition of breast milk (Seferovic et al., 2020). Modulation of the HMO profile of breast milk by dietary manipulation may represent a method to manipulate the establishment of microbial species in the infant gut (Seferovic et al., 2020). Further studies are required to elucidate this relationship fully.

1.1.2 In utero microbiome transfer

Microbiome studies of the *in utero* environment highlight numerous limitations of current next-generation sequencing (NGS) methodologies. Contamination (de Goffau et al., 2018) or the "kitome" (Olomu et al., 2020) represents a major issue when NGS and PCR-based approaches are applied to low-biomass samples, such as those encountered in the *in utero* environment (Bushman, 2019). Without stringent controls and method standardisation, these methodologies will amplify any DNA present in the sampled environment, regardless of bacterial viability (Amos et al., 2020), thus, inaccurately reflecting the microbiota present in the sample (Fricke and Ravel, 2021). Studies to date which have applied NGS methods informed by the potential for false-positive results have failed to detect a placental microbiome (Olomu et al., 2020). However, a well-controlled study by Edmond *et al.* (Edmond et al., 2012) indicated that the placenta represents a potential site of perinatal acquisition of *Streptococcus agalactiae* [group B *Streptococcus* (GBS)], a major cause of neonatal sepsis. Robust studies of amniotic fluid have failed to find a resident microbiome (Lim et al., 2018, Rehbinder et al., 2018, De Goffau et al., 2019). Indeed, *Enterobacter* and *Escherichia*, commonly identified contaminants in laboratory and extraction kit reagents (Salter et al., 2014, Tanner et al., 1998) have been reported as the most abundant genera detected in amniotic fluid (Liu et al., 2019, Collado et al., 2016). Similarly, controlled studies have reported that the microbial content of meconium does not differ from negative controls (Kennedy et al., 2021, Dos Santos et al., 2021). A recent study claimed to have detected bacterial DNA and viable bacteria in the fetal intestine using 16S rRNA gene sequencing, qPCR, electron microscopy, and bacterial culture of *Micrococcus luteus*-related bacteria, which appeared to show adaptations to the fetal environment, re-igniting the controversy surrounding the existence of *in utero* microbiomes (Rackaityte et al., 2021, de Goffau et al., 2021) . The studies presented thus far support the consensus that microbial colonisation of the infant occurs at birth and the establishment of replicating microbial cells does not commonly occur in healthy pregnancies, devoid of clinical infections (Blaser et al., 2021). This is in agreement with Walter and Horneff (Walter and Hornef, 2021), who highlighted that there is no overlap between the bacterial taxa detected *in utero* in the sequencing studies of the *in utero* environment, with evident conformity between the bacterial taxa identified *in utero* and the controls.

1.1.3 Birth mode

Throughout vaginal birth, the infant is primarily exposed to the maternal intestinal and vaginal microbiota (Li et al., 2021a). Microbes of the birth canal such as *Lactobacillus, Prevotella* and *Sneathia* are typically detected in the infant gut of vaginally born infants. *Bacteroides, Escherichia, Bifidobacterium,* and *Parabacteroides* are also usually found (Wampach et al., 2018). These genera dominate the infant microbiota and comprise up to 68% of all microbes present four days after birth (Shao et al., 2019). CS removes the infant's exposure to maternal intestinal and vaginal microbes, thus blocking vertical transmission and is the perinatal factor with the most uniform effects on the infant gut microbiota across individuals and studies (Korpela, 2021).A ubiquitous feature of the CS-born infant's gut microbiota is the low relative abundance of bifidobacteria and almost total lack of *Bacteroides* (Korpela and de Vos, 2018). The relative abundance of *Enterococcus, Staphylococcus, Streptococcus, Klebsiella, Enterobacter, Propioni bacterium,* and *Clostridium* is also higher in the CS born infant gut (Shaterian et al., 2021). Many of these taxa are common representatives of endemic opportunistic pathogens responsible for nosocomial infections (O'Neill et al., 2020) and are common to the maternal skin and hospital environment (Lax et al., 2017).The type of CS undertaken may further modulate its effects on the infant gut microbiome. For instance, the skin and vagina are thought to be the source of the gut microbiota in emergency CS, whereas the skin is considered to be the predominant microbial origin of the gut microbiota in infants born by elective CS (Chu et al., 2017). Recent studies have attempted to utilise orally delivered fecal microbiota transplantation (FMT) and oral administration of maternal vaginal microbiota to restore disturbed intestinal microbial colonisation in CS born infants (Korpela et al., 2020, Wilson et al., 2021). Despite its recent inception, FMT has yielded encouraging results (Korpela et al., 2020), while vaginal transplantation has delivered less comprehensive findings (Wilson et al., 2021).

1.1.4 Mother-infant vertical transmission

Following birth, infants appear to share 50% of microbial species in their gut with those found in the maternal gut, oral, vaginal, or skin microbiota indicating vertical transmission of microbes from mother to infant (Ferretti et al., 2018). A study by Ferretti *et al*. (Ferretti et al., 2018) reported that a significant proportion (50.7%) of the microbes present in the infant gut immediately post-partum, were transferred from

the mother's gut, vagina, oral cavity, or skin. The presence of these microbes was largely stable up to four months of age (Ferretti et al., 2018). The mother's gut accounted for the most significant proportion of microbes (22.1%), followed by the vagina (16.3%), the oral cavity (7.2%), and the skin (5%) (Ferretti et al., 2018). The maternal gut microbiota represents the greatest maternal source of infant-acquired strains immediately post-partum, with most strains from Actinobacteria and Bacteroidetes (Duranti et al., 2017). Furthermore, a recent large scale meta-analysis of whole metagenomic shotgun sequencing data of maternal and infant fecal samples identified a set of 26 mother-infant shared species (species of *B. uniformis*, *B. vulgatus*, *B. longum*, *P. distasonis*, *P. merdae* confirmed at strain level) with high prevalence and relative abundance across cohorts studied (Wang et al., 2021). The vaginal microbiome during gestation is dominated by *Lactobacillus* species, displaying decreased diversity and increased stability compared to non-pregnant women (Mortensen et al., 2021). The vaginally delivered infant gut microbiome is dominated by *Lactobacillus*, *Prevotella*, *Atopobium* or *Sneathia* species, which are typical of the mother's vaginal microbiome (Chen et al., 2021). The vaginal microbiomes impact on the infant before birth remains largely unknown, however gestational changes that happen during pregnancy could be part of an adaptive response to promote the correct development and health of the fetus (Mueller et al., 2015). While the vaginal microbiome does contribute bacteria to the infant gut microbiome it may be that this contribution is minimal, in terms of overall abundance due to the low diversity of the vaginal microbiome during pregnancy (O'Neill et al., 2020). The mother's oral cavity and skin represent the other possible maternal sources of microbes. The contributions of microbes from these areas to the initial infant gut microbiome are significantly less than the mothers gut, vaginal and breast milk microbiomes. Furthermore, bacteria transferred from these sites colonise the infant gut in a transient manner (Dominguez-Bello et al., 2010, Hurley et al., 2019). However, significant microbial transfer from the mother's skin and oral cavity to infants in later life is feasible, although additional studies are needed.

1.1.5 Gestational age

Gestational age is one of the most significant influencers of gut microbiota formation (Henderickx et al., 2019), defined as full-term (37-42 weeks), preterm (< 37 weeks) or post-term (> 42 weeks). The intestinal microbiota of the preterm infant is

distinguished by delayed colonisation, diminished species diversity and abundance. There is also a predilection to being colonised by pathogenic facultative anaerobes (e.g., *Enterobacter*, *Escherichia*, and *Klebsiella*) and decreased levels of commensal strictly anaerobic organisms (e.g., *Bifidobacterium*, *Bacteroides*, and *Clostridium*) (Pammi et al., 2017). Numerous studies have indicated a shared patterned progression of colonisation by bacilli, Gammaproteobacteria and Clostridia in preterm infants (La Rosa et al., 2014). In particular, *Enterococcus faecalis*, *Enterobacter cloacae*, *Staphylococcus epidermidis*, *E. coli*, *Klebsiella pneumoniae*, and *Klebsiella oxytoca* species are frequently found in the gut microbiota of preterm infants (Nguyen et al., 2021a). Preterm infants also encounter numerous distinctive environmental and host conditions, which can have deleterious effects on the establishment and subsequent formation of their gut microbiome. For instance, even before birth, between 25%-30% of preterm infants are exposed to microbes in the context of preterm premature rupture of membranes and intra-amniotic infection (Goldenberg et al., 2008). CS birth is also common in preterm birth cases; thus, colonisation by the skin and environmental conditions rather than vaginal and rectal microbiota commonly occur (Korpela, 2021). Furthermore, exposure to the Neonatal Intensive Care Unit (NICU) has been related with a NICU-associated core microbiota composed of bacterial families *Enterobacteriaceae* (genera *Klebsiella* and *Escherichia* in particular) and Enterococcaceae (Zwittink et al., 2017). A common NICU practice, respiratory support, has recently been shown to drive differences in microbiota development between extremely and very preterm infants (Zwittink et al., 2017). Specifically, preterm infants exhibited higher colonisation by facultative anaerobes and delayed colonisation by obligate anaerobes (Zwittink et al., 2017). As a result, with the shift in the ratio of facultative to obligate anaerobic bacteria, defense against pathogenic bacteria can often be impaired (Henderickx et al., 2019). Finally, antibiotic administration in NICUs is commonplace for treating and preventing infections and sepsis (Henderickx et al., 2019) and will be discussed in detail below.

1.1.1 Antibiotics

In light of the ever-evolving antimicrobial resistance (AMR) crisis (Ventola, 2015), deciphering the implications of perinatal antibiotic usage on the establishment of the infant gut microbiome is paramount. Oral antibiotic use in pregnancy or intravenous antibiotic prophylaxis during delivery is common practice - especially for maternal

GBS positivity, preterm premature rupture of the membranes, and/or as prophylaxis against wound infection in CS (Grech et al., 2021). Vertical transmission of antibiotics and antibiotic-resistant microorganisms from mother to infant has been proposed to negatively impact the development and succession of the infant gut microbiota (Patangia et al., 2022). Antibiotic usage presents two potential problems in the perinatal period, through the transfer of antibiotics and/or AMR strains from mother to infant via *in utero* transfer or breastfeeding. The majority of broad-spectrum antibiotics (e.g., amoxicillin, gentamicin, vancomycin) used in the perinatal period can be readily transmitted to the fetus *in utero* via the placenta and umbilical vein due to simple diffusion and blood flow (Nahum et al., 2006). Because of the restricted activity of fetal hepatic drug-metabolizing enzymes compared with adults, the non-metabolised drug thus accumulates in the fetal tissues (Morgan, 1997). There is strong evidence that maternal antibiotic treatment throughout gestation reaches the infant in adequate amounts to potentially impact their resistome profiles (Imoto et al., 2018). Numerous studies have explored the effect of antibiotic use in pregnancy on infants' intestinal microbiome composition and/or diversity. Reduced relative abundances of Actinobacteria, specifically *Bifidobacterium* (Imoto et al., 2018) and *Bacteroides* (Stearns et al., 2017a) are commonly observed in infants whose mothers were treated with antibiotics prenatally or during delivery compared to those without. Increased relative abundances of Firmicutes and Proteobacteria are also consistently reported (Mazzola et al., 2016). To date, most studies concentrate on the detrimental effects of antibiotics on the mother or fetus but lack exploration of the AMR aspects. There is also a pressing need for characterisation of the species and strains harbouring these resistance genes (Li et al., 2021b).

1.1.7 Infant diet

Human breast milk is the "gold standard" nutrition for infant health and development and is considered the second integral source of microbes to the infant after the birth canal (Pannaraj et al., 2017). Harbouring > 700 bacterial species, breast milk ensures the consumption of up to ~800,000 bacteria daily (Le Doare et al., 2018). HMOs modulate the immune system, prevent adhesion of pathogenic bacteria and act as metabolic substrates for gut bifidobacteria. In turn, bifidobacteria utilize their arsenal of membrane transporters and saccharolytic enzymes to cleave HMOs into their constituent monomers and internalize these or intact HMOs into the central catabolic

pathways, leading to the main end products, lactate, acetate, formate, and 1, 2-propandiol (Sakanaka et al., 2019). This process aids in suppressing the growth of opportunistic pathogenic species within *Clostridiaceae*, *Enterobacteriaceae*, and *Staphylococcaceae* (Matsuki et al., 2016). Multiple studies have isolated and identified bacterial strains, mostly *Bifidobacterium*, *Lactobacillus*, and *Staphylococcus*, which are common to both breast milk and infant faeces (Murphy et al., 2017). However, breastfeeding is not chosen/not possible in many circumstances. Exclusively formula-fed infants harbor a more diverse microbiota with lower abundances of HMO-utilizing *Bifidobacterium* species, often with increased abundances of *Clostridium* species (*C. difficile* and *C. perfringens*) and *Enterobacteriaceae* species (e.g., *E. coli*) (Bäckhed et al., 2015). While the gap between the composition of commercial formulas and breast milk is narrowing (Ahern et al., 2019), the gut microbiota of formula and breast-fed infants remain distinct (Baumann-Dudenhoeffer et al., 2018).

1.1.8 Probiotics

Probiotics are defined by the FAO/WHO as "live microorganisms which when administered in adequate amounts confer a health benefit on the host" (Gibson et al., 2017). Probiotic supplementation in infants to ameliorate aberrant colonisation, typically with *Bifidobacterium* and *Lactobacillus* strains, has yielded mixed results (Wang et al., 2020b). Probiotic usage for the prevention of NEC in preterm infants has yielded encouraging findings (Murphy et al., 2021b). A recent meta-analysis concluded that *L. acidophilus* LB was the best supplementation option for reducing NEC risk in preterm infants (Beghetti et al., 2021). A synbiotic is defined as "a mixture comprising live microorganisms and substrate(s) selectively utilised by host microorganisms that confers a health benefit on the host" (Swanson et al., 2020). A synbiotic consisting of short-chain galacto-oligosaccharides and long-chain fructo-oligosaccharides and the bifidobacterial strain *B. breve* M-16V, with a similar dosage to bacterial numbers of human milk, was reported to substantially increase levels of bifidobacteria in exclusively formula-fed infants (Phavichitr et al., 2021). Further studies of probiotic, prebiotic and synbiotic supplementation in the infant diet to ensure optimal microbial colonisation of the infant gut are warranted.

1.1.9 Genetics

Individuals with different genetic backgrounds harbour distinct microbes, as have been indicated by host and microbiome genome-wide association studies. These studies show similarities in the gut microbiome composition among phylogenetically-related individuals (Ley et al., 2008). For instance, twin studies indicate that the microbiome of monozygotic twins is significantly closer than that of dizygotic twins (Xie et al., 2016). Kurilshikov *et al.* (Kurilshikov et al., 2021) reported an age-dependent association between the lactase (*LCT*) gene locus and the *Bifidobacterium* genus in the MiBioGen consortium. Indeed, the functional SNP in the *LCT* locus, rs4988235, has been shown to determine the abundance of the *Bifidobacterium* genus (Bonder et al., 2016). The DR4-DQ8 allele, the highest risk associated allele for type 1 diabetes, has also been hypothesised to serve as a gatekeeper for the presence or absence of gut bacteria in early life (Patricia et al., 2021). A study of dichorionic triplets suggested that host genetics initially play a major role in determining microbial community composition; however, by year one, environmental factors are the major determinant in healthy infants (Murphy et al., 2015), suggesting that nurture has the potential to overcome the genetic nature of an individual. Collectively, the findings of these studies demonstrated the influence of host genetics in the formation and development of the human microbiota. Further studies are needed to fully elucidate how genetic differences may shape the mother-to-infant microbiota transmission and the formation of the gut microbiome in the initial stages of life.

1.1.10 Environment

Environmental factors such as place of birth and geographical location have also been reported to influence initial patterns of infant gut microbiota colonisation. For instance, while the hospital setting contributes an antiseptic environment for labor and delivery, it also presents a possible exposure route of antibiotic-resistant bacteria, especially in the case of CS birth (Lax et al., 2017). Lower beta diversity of *Bacteroides*, *Bifidobacterium*, *Streptococcus* and *Lactobacillus* and higher *Clostridium* and *Enterobacteriaceae* in hospital-born infants than babies delivered at home has been demonstrated (Combellick et al., 2018). Similarly, a study indicated that the microbiota of hospital-delivered infants was enriched with gram-positive anaerobic cocci, including the *Peptoniphilus* and *Finegoldia* genera, while those of home-delivered infants exhibited higher relative abundances of species from

the *Enterococcus* and *Bifidobacterium* genera (Selma-Royo et al., 2020). Geographical location and ethnicity are also proposed to impact the establishment of the infant gut microbiome; however, these microbiota differences seem to be associated with dietary and lifestyle patterns in a specific area or region (Rodríguez et al., 2015). For instance, children living in a rural village in Africa harbour a distinct microbiota to children residing in an urban region in Italy (De Filippo et al., 2010). African infants show an increased relative abundance of bacilli, while North American infants have more Bacteroidetes and less Actinobacteria than infants in other continents (Korpela and de Vos, 2018). Numerous additional studies have explored the geographical effect, as linked to ethnicity and/or diet, on microbial diversity and composition (Stearns et al., 2017b).

1.5 Conclusion

Evidence to date indicates that perinatal factors have a significant effect on the formation of the gut microbiota in the initial stages of life. Our understanding of exactly how such factors affect microbial colonisation and, in turn, influence infant health is mostly limited to correlation rather than causation studies due to a previously underpowered toolkit. Furthermore, direct comparisons of studies of infant gut microbiota and perinatal factors have been limited due to the cultivation techniques used and the use of 16S rRNA amplicon sequencing, which have informed most of our understanding of the human microbiome to date. Yet, these approaches are hampered by the limited number of cultivable species (Makino et al., 2011), primer design (Claesson et al., 2010), sample processing (Hill et al., 2016), small sample sizes (Bäckhed et al., 2015) and the low taxonomic resolution provided by 16S rRNA gene profiling (Bokulich et al., 2016). Most importantly, as 16S rRNA amplicon sequencing is only reliable to genus level, it does not provide information about the functional capacity of the microbiome. Fortunately, the advent of metagenomics sequencing (i.e., whole-genome shotgun sequencing) has illuminated much of the "dark matter" of our microbiome (de Vos, 2017) and will hopefully circumvent many of the limitations of previous studies. These methods allow characterisation of microbial activity, helping us to elucidate not only which microbes are present, but also what metabolic functionalities these microbes possess. Such knowledge could uncover associations between the presence of particular microbes and particular neonatal diseases.

A deeper understanding of how perinatal factors may stimulate or hinder the inheritance and/or choice of microbes by infants in early life constitutes a viable strategy in the investigation of next-generation probiotics for therapeutic interventions that maintain/improve the health of infants. Large scale longitudinal human studies, with greater, equally balanced cohorts given the same strains and prescription of either prebiotics, probiotics or synbiotics at comparable times and by related delivery routes are needed to target the vertical transmission of maternal microbes to infants with regards to specific bacteria at higher taxonomic resolution (e.g., strains) and the gross changes of the infant's microbiota. Studies investigating how multiple perinatal factors may interact with each other in the formation of the infant gut microbiome are also warranted. For instance, breastfeeding has been shown to beneficially alter the patterns of aberrant colonisation in CS born infants (Coker et al., 2021). Finally, detailed transcriptomics, metabolomics, lipidomics and proteomic investigations in combination with DNA and RNA sequencing will enable us to fully uncover the effects of perinatal factors on initial microbiome establishment and long-term functioning.

1.6 Acknowledgements

This research is supported by APC Microbiome Ireland, a research centre funded by Science Foundation Ireland (SFI), through the Irish Government's National Development Plan (Grant Number.12/RC/2273_P2).

1.7 References

AHERN, G. J., HENNESSY, A. A., RYAN, C. A., ROSS, R. P. & STANTON, C. 2019. Advances in Infant Formula Science. Annu Rev Food Sci Technol, 10, 75-102.

ALESSANDRI, G., VAN SINDEREN, D. & VENTURA, M. 2021. The genus bifidobacterium: From genomics to functionality of an important component of the mammalian gut microbiota running title: Bifidobacterial adaptation to and interaction with the host. Computational and Structural Biotechnology Journal.

AMOS, G. C. A., LOGAN, A., ANWAR, S., FRITZSCHE, M., MATE, R., BLEAZARD, T. & RIJPKEMA, S. 2020. Developing standards for the microbiome field. Microbiome, 8, 98.

ARRIETA, M. C., STIEMSMA, L. T., AMENYOGBE, N., BROWN, E. M. & FINLAY, B. 2014. The intestinal microbiome in early life: health and disease. Front Immunol, 5, 427.

ATTALI, E. & YOGEV, Y. 2021. The impact of advanced maternal age on pregnancy outcome. Best Pract Res Clin Obstet Gynaecol, 70, 2-9.

BÄCKHED, F., ROSWALL, J., PENG, Y., FENG, Q., JIA, H., KOVATCHEVA-DATCHARY, P., LI, Y., XIA, Y., XIE, H. & ZHONG, H. 2015. Dynamics and stabilization of the human gut microbiome during the first year of life. Cell host & microbe, 17, 690-703.

BAUMANN-DUDENHOEFFER, A. M., D'SOUZA, A. W., TARR, P. I., WARNER, B. B. & DANTAS, G. 2018. Infant diet and maternal gestational weight gain predict early metabolic maturation of gut microbiomes. Nat Med, 24, 1822-1829.

BEGHETTI, I., PANIZZA, D., LENZI, J., GORI, D., MARTINI, S., CORVAGLIA, L. & ACETI, A. 2021. Probiotics for Preventing Necrotizing Enterocolitis in Preterm Infants: A Network Meta-Analysis. Nutrients, 13.

BERG, G., RYBAKOVA, D., FISCHER, D., CERNAVA, T., VERGÈS, M. C., CHARLES, T., CHEN, X., COCOLIN, L., EVERSOLE, K., CORRAL, G. H., KAZOU, M., KINKEL, L., LANGE, L., LIMA, N., LOY, A., MACKLIN, J. A., MAGUIN, E., MAUCHLINE, T., MCCLURE, R., MITTER, B., RYAN, M., SARAND, I., SMIDT, H., SCHELKLE, B., ROUME, H., KIRAN, G. S., SELVIN, J., SOUZA, R. S. C., VAN OVERBEEK, L., SINGH, B. K., WAGNER, M., WALSH, A., SESSITSCH, A. & SCHLOTER, M. 2020. Microbiome definition re-visited: old concepts and new challenges. Microbiome, 8, 103.

BLASER, M. J., DEVKOTA, S., MCCOY, K. D., RELMAN, D. A., YASSOUR, M. & YOUNG, V. B. 2021. Lessons learned from the prenatal microbiome controversy. Microbiome, 9, 8.

BOKULICH, N. A., CHUNG, J., BATTAGLIA, T., HENDERSON, N., JAY, M., LI, H., D. LIEBER, A., WU, F., PEREZ-PEREZ, G. I. & CHEN, Y. 2016. Antibiotics, birth mode, and diet shape microbiome maturation during early life. Science translational medicine, 8, 343ra82-343ra82.

BONDER, M. J., KURILSHIKOV, A., TIGCHELAAR, E. F., MUJAGIC, Z., IMHANN, F., VILA, A. V., DEELEN, P., VATANEN, T., SCHIRMER, M., SMEEKENS, S. P., ZHERNAKOVA, D. V., JANKIPERSADSING, S. A., JAEGER, M., OOSTING, M., CENIT, M. C., MASCLEE, A. A., SWERTZ, M. A., LI, Y., KUMAR, V., JOOSTEN, L., HARMSEN, H., WEERSMA, R. K., FRANKE, L., HOFKER, M. H., XAVIER, R. J., JONKERS, D.,

NETEA, M. G., WIJMENGA, C., FU, J. & ZHERNAKOVA, A. 2016. The effect of host genetics on the gut microbiome. Nat Genet, 48, 1407-1412.

BUSHMAN, F. D. 2019. De-Discovery of the Placenta Microbiome. Am J Obstet Gynecol, 220, 213-214.

CHEN, X., LU, Y., CHEN, T. & LI, R. 2021. The Female Vaginal Microbiome in Health and Bacterial Vaginosis. Front Cell Infect Microbiol, 11, 631972.

CHO, N. H., SHAW, J. E., KARURANGA, S., HUANG, Y., DA ROCHA FERNANDES, J. D., OHLROGGE, A. W. & MALANDA, B. 2018. IDF Diabetes Atlas: Global estimates of diabetes prevalence for 2017 and projections for 2045. Diabetes Res Clin Pract, 138, 271-281.

CHU, D. M., ANTONY, K. M., MA, J., PRINCE, A. L., SHOWALTER, L., MOLLER, M. & AAGAARD, K. M. 2016. The early infant gut microbiome varies in association with a maternal high-fat diet. Genome Med, 8, 77.

CHU, D. M., MA, J., PRINCE, A. L., ANTONY, K. M., SEFEROVIC, M. D. & AAGAARD, K. M. 2017. Maturation of the infant microbiome community structure and function across multiple body sites and in relation to mode of delivery. Nature medicine, 23, 314-326.

CLAESSON, M. J., WANG, Q., O'SULLIVAN, O., GREENE-DINIZ, R., COLE, J. R., ROSS, R. P. & O'TOOLE, P. W. 2010. Comparison of two next-generation sequencing technologies for resolving highly complex microbiota composition using tandem variable 16S rRNA gene regions. Nucleic Acids Res, 38, e200.

CLARKE, G., O'MAHONY, S. M., DINAN, T. G. & CRYAN, J. F. 2014. Priming for health: gut microbiota acquired in early life regulates physiology, brain and behaviour. Acta Paediatr, 103, 812-9.

COKER, M. O., LAUE, H. E., HOEN, A. G., HILLIARD, M., DADE, E., LI, Z., PALYS, T., MORRISON, H. G., BAKER, E. & KARAGAS, M. R. 2021. Infant feeding alters the longitudinal impact of birth mode on the development of the gut microbiota in the first year of life. Frontiers in microbiology, 524.

COLLADO, M. C., CERNADA, M., BAÜERL, C., VENTO, M. & PÉREZ-MARTÍNEZ, G. 2012. Microbial ecology and host-microbiota interactions during early life stages. Gut Microbes, 3, 352-65.

COLLADO, M. C., RAUTAVA, S., AAKKO, J., ISOLAURI, E. & SALMINEN, S. 2016. Human gut colonisation may be initiated in utero by distinct microbial communities in the placenta and amniotic fluid. Sci Rep, 6, 23129.

COMBELLICK, J. L., SHIN, H., SHIN, D., CAI, Y., HAGAN, H., LACHER, C., LIN, D. L., MCCAULEY, K., LYNCH, S. V. & DOMINGUEZ-BELLO, M. G. 2018. Differences in the fecal microbiota of neonates born at home or in the hospital. Sci Rep, 8, 15660.

CORTES-MACÍAS, E., SELMA-ROYO, M., GARCÍA-MANTRANA, I., CALATAYUD, M., GONZÁLEZ, S., MARTÍNEZ-COSTA, C. & COLLADO, M. C. 2021. Maternal Diet Shapes the Breast Milk Microbiota Composition and Diversity: Impact of Mode of Delivery and Antibiotic Exposure. J Nutr, 151, 330-340.

COSTELLO, E. K., STAGAMAN, K., DETHLEFSEN, L., BOHANNAN, B. J. & RELMAN, D. A. 2012. The application of ecological theory toward an understanding of the human microbiome. Science, 336, 1255-62.

DE FILIPPO, C., CAVALIERI, D., DI PAOLA, M., RAMAZZOTTI, M., POULLET, J. B., MASSART, S., COLLINI, S., PIERACCINI, G. & LIONETTI, P. 2010. Impact of diet in shaping gut microbiota revealed by a comparative study in children from Europe and rural Africa. Proc Natl Acad Sci U S A, 107, 14691-6.

DE GOFFAU, M. C., CHARNOCK-JONES, D. S., SMITH, G. C. S. & PARKHILL, J. 2021. Batch effects account for the main findings of an in utero human intestinal bacterial colonisation study. Microbiome, 9, 6.

DE GOFFAU, M. C., LAGER, S., SALTER, S. J., WAGNER, J., KRONBICHLER, A., CHARNOCK-JONES, D. S., PEACOCK, S. J., SMITH, G. C. S. & PARKHILL, J. 2018. Recognizing the reagent microbiome. Nat Microbiol, 3, 851-853.

DE GOFFAU, M. C., LAGER, S., SOVIO, U., GACCIOLI, F., COOK, E., PEACOCK, S. J., PARKHILL, J., CHARNOCK-JONES, D. S. & SMITH, G. C. S. 2019. Human placenta has no microbiome but can contain potential pathogens. Nature, 572, 329-334.

DE VOS, W. M. 2017. Microbe Profile: Akkermansia muciniphila: a conserved intestinal symbiont that acts as the gatekeeper of our mucosa. Microbiology (Reading), 163, 646-648.

DOMINGUEZ-BELLO, M. G., COSTELLO, E. K., CONTRERAS, M., MAGRIS, M., HIDALGO, G., FIERER, N. & KNIGHT, R. 2010. Delivery mode shapes the acquisition and structure of the initial microbiota across multiple body habitats in newborns. Proceedings of the National Academy of Sciences, 107, 11971-11975.

DOS SANTOS, S. J., PAKZAD, Z., ELWOOD, C. N., ALBERT, A. Y. K., GANTT, S., MANGES, A. R., DUMONCEAUX, T. J., MAAN, E. J., HILL, J. E. & MONEY, D. M. 2021. Early Neonatal Meconium Does Not Have a Demonstrable Microbiota Determined through Use of Robust Negative Controls with cpn60-Based Microbiome Profiling. Microbiol Spectr, 9, e0006721.

DURANTI, S., LUGLI, G. A., MANCABELLI, L., ARMANINI, F., TURRONI, F., JAMES, K., FERRETTI, P., GORFER, V., FERRARIO, C. & MILANI, C. 2017. Maternal inheritance of bifidobacterial communities and bifidophages in infants through vertical transmission. Microbiome, 5, 1-13.

EDMOND, K. M., KORTSALIOUDAKI, C., SCOTT, S., SCHRAG, S. J., ZAIDI, A. K., COUSENS, S. & HEATH, P. T. 2012. Group B streptococcal disease in infants aged younger than 3 months: systematic review and meta-analysis. Lancet, 379, 547-56.

EGAN, M., DEMPSEY, E., RYAN, C. A., ROSS, R. P. & STANTON, C. 2021. The Sporobiota of the Human Gut. Gut Microbes, 13, 1-17.

FERRETTI, P., PASOLLI, E., TETT, A., ASNICAR, F., GORFER, V., FEDI, S., ARMANINI, F., TRUONG, D. T., MANARA, S. & ZOLFO, M. 2018. Mother-to-infant microbial transmission from different body sites shapes the developing infant gut microbiome. Cell host & microbe, 24, 133-145.

FOUHY, F., WATKINS, C., HILL, C. J., O'SHEA, C.-A., NAGLE, B., DEMPSEY, E. M., O'TOOLE, P. W., ROSS, R. P., RYAN, C. A. & STANTON, C. 2019. Perinatal factors affect the gut microbiota up to four years after birth. Nature communications, 10, 1-10.

FRICK, A. P. 2021. Advanced maternal age and adverse pregnancy outcomes. Best Pract Res Clin Obstet Gynaecol, 70, 92-100.

FRICKE, W. F. & RAVEL, J. 2021. Microbiome or no microbiome: are we looking at the prenatal environment through the right lens? Microbiome, 9, 9.

FUNDORA, J. B., GUHA, P., SHORES, D. R., PAMMI, M. & MAHESHWARI, A. 2020. Intestinal dysbiosis and necrotizing enterocolitis: assessment for causality using Bradford Hill criteria. Pediatric research, 87, 235-248.

GENSOLLEN, T., IYER, S. S., KASPER, D. L. & BLUMBERG, R. S. 2016. How colonisation by microbiota in early life shapes the immune system. Science, 352, 539-44.

GIBSON, G. R., HUTKINS, R., SANDERS, M. E., PRESCOTT, S. L., REIMER, R. A., SALMINEN, S. J., SCOTT, K., STANTON, C., SWANSON, K. S., CANI, P. D., VERBEKE, K. & REID, G. 2017. Expert consensus document: The International Scientific Association for Probiotics and Prebiotics (ISAPP) consensus statement on the definition and scope of prebiotics. Nat Rev Gastroenterol Hepatol, 14, 491-502.

GOLDENBERG, R. L., CULHANE, J. F., IAMS, J. D. & ROMERO, R. 2008. Epidemiology and causes of preterm birth. Lancet, 371, 75-84.

GOPALAKRISHNAN, V., HELMINK, B. A., SPENCER, C. N., REUBEN, A. & WARGO, J. A. 2018. The Influence of the Gut Microbiome on Cancer, Immunity, and Cancer Immunotherapy. Cancer Cell, 33, 570-580.

GRECH, A., COLLINS, C. E., HOLMES, A., LAL, R., DUNCANSON, K., TAYLOR, R. & GORDON, A. 2021. Maternal exposures and the infant gut microbiome: a systematic review with meta-analysis. Gut Microbes, 13, 1-30.

HAN, K.-I., KIM, J.-S., EOM, M. K., LEE, K. C., SUH, M. K., KIM, H. S., PARK, S.-H., LEE, J. H., KANG, S. W. & PARK, J.-E. 2021. Collinsella acetigenes sp. nov., an Anaerobic Actinobacterium Isolated from Human Feces, and Emended Description of the Genus Collinsella and Collinsella aerofaciens. Current Microbiology, 78, 3667-3673.

HENDERICKX, J. G. E., ZWITTINK, R. D., VAN LINGEN, R. A., KNOL, J. & BELZER, C. 2019. The preterm gut microbiota: An inconspicuous challenge in nutritional neonatal care. Frontiers in cellular and infection microbiology, 9, 85.

HILL, C. J., BROWN, J. R., LYNCH, D. B., JEFFERY, I. B., RYAN, C. A., ROSS, R. P., STANTON, C. & O'TOOLE, P. W. 2016. Effect of room temperature transport vials on DNA quality and phylogenetic composition of faecal microbiota of elderly adults and infants. Microbiome, 4, 19.

HURLEY, E., MULLINS, D., BARRETT, M. P., O'SHEA, C. A., KINIRONS, M., RYAN, C. A., STANTON, C., WHELTON, H., HARRIS, H. M. B. & O'TOOLE, P. W. 2019. The microbiota of the mother at birth and its influence on the emerging infant oral microbiota from birth to 1 year of age: a cohort study. Journal of Oral Microbiology, 11, 1599652.

IMOTO, N., MORITA, H., AMANUMA, F., MARUYAMA, H., WATANABE, S. & HASHIGUCHI, N. 2018. Maternal antimicrobial use at delivery has a stronger impact than mode of delivery on bifidobacterial colonisation in infants: a pilot study. J Perinatol, 38, 1174-1181.

KENNEDY, K. M., GERLACH, M. J., ADAM, T., HEIMESAAT, M. M., ROSSI, L., SURETTE, M. G., SLOBODA, D. M. & BRAUN, T. 2021. Fetal meconium does not have a detectable microbiota before birth. Nature Microbiology, 6, 865-873.

KIM, Y. N., CHOI, D. W., KIM, D. S., PARK, E. C. & KWON, J. Y. 2021. Maternal age and risk of early neonatal mortality: a national cohort study. Sci Rep, 11, 814.

KOLIADA, A., SYZENKO, G., MOSEIKO, V., BUDOVSKA, L., PUCHKOV, K., PEREDERIY, V., GAVALKO, Y., DOROFEYEV, A., ROMANENKO, M., TKACH, S., SINEOK, L., LUSHCHAK, O. & VAISERMAN, A. 2017. Association between body mass index and Firmicutes/Bacteroidetes ratio in an adult Ukrainian population. BMC Microbiol, 17, 120.

KORPELA, K. 2021. Impact of Delivery Mode on Infant Gut Microbiota. Ann Nutr Metab, 1-9.

KORPELA, K. & DE VOS, W. M. 2018. Early life colonisation of the human gut: microbes matter everywhere. Curr Opin Microbiol, 44, 70-78.

KORPELA, K., HELVE, O., KOLHO, K. L., SAISTO, T., SKOGBERG, K., DIKAREVA, E., STEFANOVIC, V., SALONEN, A., ANDERSSON, S. & DE VOS, W. M. 2020. Maternal Fecal Microbiota Transplantation in Cesarean-Born Infants Rapidly Restores Normal Gut Microbial Development: A Proof-of-Concept Study. Cell, 183, 324-334.e5.

KURILSHIKOV, A., MEDINA-GOMEZ, C., BACIGALUPE, R., RADJABZADEH, D., WANG, J., DEMIRKAN, A., LE ROY, C. I., RAYGOZA GARAY, J. A., FINNICUM, C. T., LIU, X., ZHERNAKOVA, D. V., BONDER, M. J., HANSEN, T. H., FROST, F., RÜHLEMANN, M. C., TURPIN, W., MOON, J. Y., KIM, H. N., LÜLL, K., BARKAN, E., SHAH, S. A., FORNAGE, M., SZOPINSKA-TOKOV, J., WALLEN, Z. D., BORISEVICH, D., AGREUS, L., ANDREASSON, A., BANG, C., BEDRANI, L., BELL, J. T., BISGAARD, H., BOEHNKE, M., BOOMSMA, D. I., BURK, R. D., CLARINGBOULD, A., CROITORU, K., DAVIES, G. E., VAN DUIJN, C. M., DUIJTS, L., FALONY, G., FU, J., VAN DER GRAAF, A., HANSEN, T., HOMUTH, G., HUGHES, D. A., IJZERMAN, R. G., JACKSON, M. A., JADDOE, V. W. V., JOOSSENS, M., JØRGENSEN, T., KESZTHELYI, D., KNIGHT, R., LAAKSO, M., LAUDES, M., LAUNER, L. J., LIEB, W., LUSIS, A. J., MASCLEE, A. A. M., MOLL, H. A., MUJAGIC, Z., QIBIN, Q., ROTHSCHILD, D., SHIN, H., SØRENSEN, S. J., STEVES, C. J., THORSEN, J., TIMPSON, N. J., TITO, R. Y., VIEIRA-SILVA, S., VÖLKER, U., VÖLZKE, H., VÕSA, U., WADE, K. H., WALTER, S., WATANABE, K., WEISS, S., WEISS, F. U., WEISSBROD, O., WESTRA, H. J., WILLEMSEN, G., PAYAMI, H., JONKERS, D., ARIAS VASQUEZ, A., DE GEUS, E. J. C., MEYER, K. A., STOKHOLM, J., SEGAL, E., ORG, E., WIJMENGA, C., KIM, H. L., KAPLAN, R. C., SPECTOR, T. D., UITTERLINDEN, A. G., RIVADENEIRA, F., FRANKE, A., LERCH, M. M., FRANKE, L., SANNA, S., D'AMATO, M., PEDERSEN, O., et al. 2021. Large-scale association analyses identify host factors influencing human gut microbiome composition. Nat Genet, 53, 156-165.

LA ROSA, P. S., WARNER, B. B., ZHOU, Y., WEINSTOCK, G. M., SODERGREN, E., HALL-MOORE, C. M., STEVENS, H. J., BENNETT, W. E., JR., SHAIKH, N., LINNEMAN, L. A., HOFFMANN, J. A., HAMVAS, A., DEYCH, E., SHANDS, B. A., SHANNON, W. D. & TARR, P. I. 2014. Patterned progression of bacterial populations in the premature infant gut. Proc Natl Acad Sci U S A, 111, 12522-7.

LAX, S., SANGWAN, N., SMITH, D., LARSEN, P., HANDLEY, K. M., RICHARDSON, M., GUYTON, K., KREZALEK, M., SHOGAN, B. D., DEFAZIO, J., FLEMMING, I., SHAKHSHEER, B., WEBER, S., LANDON, E., GARCIA-HOUCHINS, S., SIEGEL, J., ALVERDY, J., KNIGHT, R., STEPHENS, B. & GILBERT, J. A. 2017. Bacterial colonisation and succession in a newly opened hospital. Sci Transl Med, 9.

LE DOARE, K., HOLDER, B., BASSETT, A. & PANNARAJ, P. S. 2018. Mother's milk: a purposeful contribution to the development of the infant microbiota and immunity. Frontiers in immunology, 9, 361.

LEY, R. E., HAMADY, M., LOZUPONE, C., TURNBAUGH, P. J., RAMEY, R. R., BIRCHER, J. S., SCHLEGEL, M. L., TUCKER, T. A., SCHRENZEL, M. D., KNIGHT, R. & GORDON, J. I. 2008. Evolution of mammals and their gut microbes. Science, 320, 1647-51.

LI, N., LIANG, S., CHEN, Q., ZHAO, L., LI, B. & HUO, G. 2021a. Distinct gut microbiota and metabolite profiles induced by delivery mode in healthy Chinese infants. J Proteomics, 232, 104071.

LI, X., STOKHOLM, J., BREJNROD, A., VESTERGAARD, G. A., RUSSEL, J., TRIVEDI, U., THORSEN, J., GUPTA, S., HJELMSØ, M. H., SHAH, S. A., RASMUSSEN, M. A., BISGAARD, H. & SØRENSEN, S. J. 2021b. The infant gut resistome associates with E. coli, environmental exposures, gut microbiome maturity, and asthma-associated bacterial composition. Cell Host Microbe, 29, 975-987.e4.

LIM, E. S., RODRIGUEZ, C. & HOLTZ, L. R. 2018. Amniotic fluid from healthy term pregnancies does not harbor a detectable microbial community. Microbiome, 6, 87.

LIU, C. J., LIANG, X., NIU, Z. Y., JIN, Q., ZENG, X. Q., WANG, W. X., LI, M. Y., CHEN, X. R., MENG, H. Y., SHEN, R., SUN, S. Y., LUO, Y. Y., YANG, E., GENG, J. W. & LI, X. R. 2019. Is the delivery mode a critical factor for the microbial communities in the meconium? EBioMedicine, 49, 354-363.

LLOYD-PRICE, J., ABU-ALI, G. & HUTTENHOWER, C. 2016. The healthy human microbiome. Genome Medicine, 8.

MAGNÚSDÓTTIR, S., RAVCHEEV, D., DE CRÉCY-LAGARD, V. & THIELE, I. 2015. Systematic genome assessment of B-vitamin biosynthesis suggests co-operation among gut microbes. Frontiers in Genetics, 6, 148.

MAHER, S. E., O'BRIEN, E. C., MOORE, R. L., BYRNE, D. F., GERAGHTY, A. A., SALDOVA, R., MURPHY, E. F., VAN SINDEREN, D., COTTER, P. D. & MCAULIFFE, F. M. 2020. The association between the maternal diet and the maternal and infant gut microbiome: a systematic review. Br J Nutr, 1-29.

MAKINO, H., KUSHIRO, A., ISHIKAWA, E., MUYLAERT, D., KUBOTA, H., SAKAI, T., OISHI, K., MARTIN, R., BEN AMOR, K., OOZEER, R., KNOL, J. & TANAKA, R.

2011. Transmission of intestinal Bifidobacterium longum subsp. longum strains from mother to infant, determined by multilocus sequencing typing and amplified fragment length polymorphism. Appl Environ Microbiol, 77, 6788-93.

MANCABELLI, L., TARRACCHINI, C., MILANI, C., LUGLI, G. A., FONTANA, F., TURRONI, F., VAN SINDEREN, D. & VENTURA, M. 2020. Multi-population cohort meta-analysis of human intestinal microbiota in early life reveals the existence of infant community state types (ICSTs). Computational and Structural Biotechnology Journal, 18, 2480-2493.

MARCOBAL, A., BARBOZA, M., SONNENBURG, E. D., PUDLO, N., MARTENS, E. C., DESAI, P., LEBRILLA, C. B., WEIMER, B. C., MILLS, D. A. & GERMAN, J. B. 2011. Bacteroides in the infant gut consume milk oligosaccharides via mucus-utilization pathways. Cell host & microbe, 10, 507-514.

MATSUKI, T., YAHAGI, K., MORI, H., MATSUMOTO, H., HARA, T., TAJIMA, S., OGAWA, E., KODAMA, H., YAMAMOTO, K., YAMADA, T., MATSUMOTO, S. & KUROKAWA, K. 2016. A key genetic factor for fucosyllactose utilization affects infant gut microbiota development. Nat Commun, 7, 11939.

MAZZOLA, G., MURPHY, K., ROSS, R. P., DI GIOIA, D., BIAVATI, B., CORVAGLIA, L. T., FALDELLA, G. & STANTON, C. 2016. Early Gut Microbiota Perturbations Following Intrapartum Antibiotic Prophylaxis to Prevent Group B Streptococcal Disease. PLoS One, 11, e0157527.

MILANI, C., DURANTI, S., BOTTACINI, F., CASEY, E., TURRONI, F., MAHONY, J., BELZER, C., DELGADO PALACIO, S., ARBOLEYA MONTES, S. & MANCABELLI, L. 2017. The first microbial colonizers of the human gut: composition, activities, and health implications of the infant gut microbiota. Microbiology and molecular biology reviews, 81, e00036-17.

MORGAN, D. J. 1997. Drug disposition in mother and foetus. Clin Exp Pharmacol Physiol, 24, 869-73.

MORTENSEN, M. S., RASMUSSEN, M. A., STOKHOLM, J., BREJNROD, A. D., BALLE, C., THORSEN, J., KROGFELT, K. A., BISGAARD, H. & SØRENSEN, S. J. 2021. Modeling transfer of vaginal microbiota from mother to infant in early life. Elife, 10.

MUELLER, N. T., BAKACS, E., COMBELLICK, J., GRIGORYAN, Z. & DOMINGUEZ-BELLO, M. G. 2015. The infant microbiome development: mom matters. Trends Mol Med, 21, 109-17.

MURPHY, K., CA, O. S., RYAN, C. A., DEMPSEY, E. M., PW, O. T., STANTON, C. & ROSS, R. P. 2015. The gut microbiota composition in dichorionic triplet sets suggests a role for host genetic factors. PLoS One, 10, e0122561.

MURPHY, K., CURLEY, D., O'CALLAGHAN, T. F., O'SHEA, C. A., DEMPSEY, E. M., O'TOOLE, P. W., ROSS, R. P., RYAN, C. A. & STANTON, C. 2017. The Composition of Human Milk and Infant Faecal Microbiota Over the First Three Months of Life: A Pilot Study. Sci Rep, 7, 40597.

MURPHY, K., O'DONOVAN, A. N., CAPLICE, N. M., ROSS, R. P. & STANTON, C. 2021a. Exploring the Gut Microbiota and Cardiovascular Disease. Metabolites, 11.

MURPHY, K., ROSS, R. P., RYAN, C. A., DEMPSEY, E. M. & STANTON, C. 2021b. Probiotics, Prebiotics, and Synbiotics for the Prevention of Necrotizing Enterocolitis. Front Nutr, 8, 667188.

NAHUM, G. G., UHL, K. & KENNEDY, D. L. 2006. Antibiotic use in pregnancy and lactation: what is and is not known about teratogenic and toxic risks. Obstet Gynecol, 107, 1120-38.

NAUDÉ, P. J. W., CLAASSEN-WEITZ, S., GARDNER-LUBBE, S., BOTHA, G., KABA, M., ZAR, H. J., NICOL, M. P. & STEIN, D. J. 2020. Association of maternal prenatal psychological stressors and distress with maternal and early infant faecal bacterial profile. Acta Neuropsychiatr, 32, 32-42.

NGUYEN, M., HOLDBROOKS, H., MISHRA, P., ABRANTES, M. A., ESKEW, S., GARMA, M., OCA, C. G., MCGUCKIN, C., HEIN, C. B., MITCHELL, R. D., KAZI, S., CHEW, S., CASABURI, G., BROWN, H. K., FRESE, S. A. & HENRICK, B. M. 2021a. Impact of Probiotic B. infantis EVC001 Feeding in Premature Infants on the Gut Microbiome, Nosocomially Acquired Antibiotic Resistance, and Enteric Inflammation. Front Pediatr, 9, 618009.

NGUYEN, Q. P., KARAGAS, M. R., MADAN, J. C., DADE, E., PALYS, T. J., MORRISON, H. G., PATHMASIRI, W. W., MCRITCHE, S., SUMNER, S. J., FROST, H. R. & HOEN, A. G. 2021b. Associations between the gut microbiome and metabolome in early life. BMC Microbiol, 21, 238.

O'NEILL, I. J., SANCHEZ GALLARDO, R., SALDOVA, R., MURPHY, E. F., COTTER, P. D., MCAULIFFE, F. M. & VAN SINDEREN, D. 2020. Maternal and infant factors that shape neonatal gut colonisation by bacteria. Expert Rev Gastroenterol Hepatol, 14, 651-664.

OLOMU, I. N., PENA-CORTES, L. C., LONG, R. A., VYAS, A., KRICHEVSKIY, O., LUELLWITZ, R., SINGH, P. & MULKS, M. H. 2020. Elimination of "kitome" and "splashome" contamination results in lack of detection of a unique placental microbiome. BMC Microbiol, 20, 157.

OTARU, N., YE, K., MUJEZINOVIC, D., BERCHTOLD, L., CONSTANCIAS, F., CORNEJO, F. A., KRZYSTEK, A., DE WOUTERS, T., BRAEGGER, C., LACROIX, C. & PUGIN, B. 2021. GABA Production by Human Intestinal Bacteroides spp.: Prevalence, Regulation, and Role in Acid Stress Tolerance. Frontiers in Microbiology, 12, 860.

PAMMI, M., COPE, J., TARR, P. I., WARNER, B. B., MORROW, A. L., MAI, V., GREGORY, K. E., KROLL, J. S., MCMURTRY, V., FERRIS, M. J., ENGSTRAND, L., LILJA, H. E., HOLLISTER, E. B., VERSALOVIC, J. & NEU, J. 2017. Intestinal dysbiosis in preterm infants preceding necrotizing enterocolitis: a systematic review and meta-analysis. Microbiome, 5, 31.

PANNARAJ, P. S., LI, F., CERINI, C., BENDER, J. M., YANG, S., ROLLIE, A., ADISETIYO, H., ZABIH, S., LINCEZ, P. J., BITTINGER, K., BAILEY, A., BUSHMAN, F. D., SLEASMAN, J. W. & ALDROVANDI, G. M. 2017. Association Between Breast Milk Bacterial Communities and Establishment and Development of the Infant Gut Microbiome. JAMA Pediatr, 171, 647-654.

PATANGIA, D. V., RYAN, C. A., DEMPSEY, E., STANTON, C. & ROSS, R. P. 2022. Vertical transfer of antibiotics and antibiotic resistant strains across the mother/baby axis. Trends Microbiol, 30, 47-56.

PATRICIA, L. T., ANGELICA, P. A., JORDAN, T. R., ERIK, K., MEGHAN, A. B., JORMA, I., MARK, A. A., DESMOND, A. S., ERIC, W. T. & JOHNNY, L. 2021. Adolescent autism and autoimmune diagnoses linked to infant gut bacteria whose prevalence is associated with at-risk genetics and/or diet. medRxiv, 2021.06.07.21258510.

PHAVICHITR, N., WANG, S., CHOMTO, S., TANTIBHAEDHYANGKUL, R., KAKOUROU, A., INTARAKHAO, S., JONGPIPUTVANICH, S., ROESELERS, G. & KNOL, J. 2021. Impact of synbiotics on gut microbiota during early life: a randomised, double-blind study. Sci Rep, 11, 3534.

RACKAITYTE, E., HALKIAS, J., FUKUI, E. M., MENDOZA, V. F., HAYZELDEN, C., CRAWFORD, E. D., FUJIMURA, K. E., BURT, T. D. & LYNCH, S. V. 2021. Corroborating evidence refutes batch effect as explanation for fetal bacteria. Microbiome, 9, 10.

REHBINDER, E. M., LØDRUP CARLSEN, K. C., STAFF, A. C., ANGELL, I. L., LANDRØ, L., HILDE, K., GAUSTAD, P. & RUDI, K. 2018. Is amniotic fluid of women with uncomplicated term pregnancies free of bacteria? Am J Obstet Gynecol, 219, 289.e1-289.e12.

REYES, H., ZAPATA, R., HERNÁNDEZ, I., GOTTELAND, M., SANDOVAL, L., JIRÓN, M. I., PALMA, J., ALMUNA, R. & SILVA, J. J. 2006. Is a leaky gut involved in the pathogenesis of intrahepatic cholestasis of pregnancy? Hepatology, 43, 715-22.

RIOS-COVIAN, D., SALAZAR, N., GUEIMONDE, M. & DE LOS REYES-GAVILAN, C. G. 2017. Shaping the metabolism of intestinal Bacteroides population through diet to improve human health. Frontiers in microbiology, 8, 376.

RODRÍGUEZ, J. M., MURPHY, K., STANTON, C., ROSS, R. P., KOBER, O. I., JUGE, N., AVERSHINA, E., RUDI, K., NARBAD, A., JENMALM, M. C., MARCHESI, J. R. & COLLADO, M. C. 2015. The composition of the gut microbiota throughout life, with an emphasis on early life. Microb Ecol Health Dis, 26, 26050.

ROHR, M. W., NARASIMHULU, C. A., RUDESKI-ROHR, T. A. & PARTHASARATHY, S. 2020. Negative Effects of a High-Fat Diet on Intestinal Permeability: A Review. Adv Nutr, 11, 77-91.

SAKANAKA, M., GOTOH, A., YOSHIDA, K., ODAMAKI, T., KOGUCHI, H., XIAO, J. Z., KITAOKA, M. & KATAYAMA, T. 2019. Varied Pathways of Infant Gut-Associated Bifidobacterium to Assimilate Human Milk Oligosaccharides: Prevalence of the Gene Set and Its Correlation with Bifidobacteria-Rich Microbiota Formation. Nutrients, 12.

SALTER, S. J., COX, M. J., TUREK, E. M., CALUS, S. T., COOKSON, W. O., MOFFATT, M. F., TURNER, P., PARKHILL, J., LOMAN, N. J. & WALKER, A. W. 2014. Reagent and laboratory contamination can critically impact sequence-based microbiome analyses. BMC Biology, 12, 87.

SEFEROVIC, M. D., MOHAMMAD, M., PACE, R. M., ENGEVIK, M., VERSALOVIC, J., BODE, L., HAYMOND, M. & AAGAARD, K. M. 2020. Maternal diet alters human milk oligosaccharide composition with implications for the milk metagenome. Sci Rep, 10, 22092.

SELMA-ROYO, M., CALATAYUD ARROYO, M., GARCÍA-MANTRANA, I., PARRA-LLORCA, A., ESCURIET, R., MARTÍNEZ-COSTA, C. & COLLADO, M. C. 2020. Perinatal environment shapes microbiota colonisation and infant growth: impact on host response and intestinal function. Microbiome, 8, 167.

SELMA-ROYO, M., GARCÍA-MANTRANA, I., CALATAYUD, M., PARRA-LLORCA, A., MARTÍNEZ-COSTA, C. & COLLADO, M. C. 2021. Maternal diet during pregnancy and intestinal markers are associated with early gut microbiota. Eur J Nutr, 60, 1429-1442.

SERINO, M., LUCHE, E., GRES, S., BAYLAC, A., BERGÉ, M., CENAC, C., WAGET, A., KLOPP, P., IACOVONI, J., KLOPP, C., MARIETTE, J., BOUCHEZ, O., LLUCH, J., OUARNÉ, F., MONSAN, P., VALET, P., ROQUES, C., AMAR, J., BOULOUMIÉ, A., THÉODOROU, V. & BURCELIN, R. 2012. Metabolic adaptation to a high-fat diet is associated with a change in the gut microbiota. Gut, 61, 543-53.

SHAO, Y., FORSTER, S. C., TSALIKI, E., VERVIER, K., STRANG, A., SIMPSON, N., KUMAR, N., STARES, M. D., RODGER, A. & BROCKLEHURST, P. 2019. Stunted microbiota and opportunistic pathogen colonisation in caesarean-section birth. Nature, 574, 117-121.

SHATERIAN, N., ABDI, F., GHAVIDEL, N. & ALIDOST, F. 2021. Role of cesarean section in the development of neonatal gut microbiota: A systematic review. Open Med (Wars), 16, 624-639.

SILILAS, P., HUANG, L., THONUSIN, C., LUEWAN, S., CHATTIPAKORN, N., CHATTIPAKORN, S. & TONGSONG, T. 2021. Association between Gut Microbiota and Development of Gestational Diabetes Mellitus. Microorganisms, 9.

SINGH, S. B., MADAN, J., COKER, M., HOEN, A., BAKER, E. R., KARAGAS, M. R. & MUELLER, N. T. 2020. Does birth mode modify associations of maternal pre-pregnancy BMI and gestational weight gain with the infant gut microbiome? Int J Obes (Lond), 44, 23-32.

SODERBORG, T. K., CARPENTER, C. M., JANSSEN, R. C., WEIR, T. L., ROBERTSON, C. E., IR, D., YOUNG, B. E., KREBS, N. F., HERNANDEZ, T. L., BARBOUR, L. A., FRANK, D. N., KROEHL, M. & FRIEDMAN, J. E. 2020. Gestational Diabetes Is Uniquely Associated With Altered Early Seeding of the Infant Gut Microbiota. Front Endocrinol (Lausanne), 11, 603021.

SOCIETY FOR REPRODUCTIVE MEDICINE, AMERICAN COLLEGE OF OBSTETRICIANS AND GYNECOLOGISTS' COMMITTEE ON GYNECOLOGIC PRACTICE. Prepregnancy counseling: Committee Opinion No. 762. *Fertil Steril* 2019;111:32-42.

STEARNS, J. C., SIMIONI, J., GUNN, E., MCDONALD, H., HOLLOWAY, A. C., THABANE, L., MOUSSEAU, A., SCHERTZER, J. D., RATCLIFFE, E. M., ROSSI, L., SURETTE, M. G., MORRISON, K. M. & HUTTON, E. K. 2017a. Intrapartum antibiotics for GBS prophylaxis alter colonisation patterns in the early infant gut microbiome of low risk infants. Sci Rep, 7, 16527.

STEARNS, J. C., ZULYNIAK, M. A., DE SOUZA, R. J., CAMPBELL, N. C., FONTES, M., SHAIKH, M., SEARS, M. R., BECKER, A. B., MANDHANE, P. J., SUBBARAO, P.,

TURVEY, S. E., GUPTA, M., BEYENE, J., SURETTE, M. G. & ANAND, S. S. 2017b. Ethnic and diet-related differences in the healthy infant microbiome. Genome Med, 9, 32.

SWANSON, K. S., GIBSON, G. R., HUTKINS, R., REIMER, R. A., REID, G., VERBEKE, K., SCOTT, K. P., HOLSCHER, H. D., AZAD, M. B., DELZENNE, N. M. & SANDERS, M. E. 2020. The International Scientific Association for Probiotics and Prebiotics (ISAPP) consensus statement on the definition and scope of synbiotics. Nat Rev Gastroenterol Hepatol, 17, 687-701.

TABOADA, B., MORÁN, P., SERRANO-VÁZQUEZ, A., IŠA, P., ROJAS-VELÁZQUEZ, L., PÉREZ-JUÁREZ, H., LÓPEZ, S., TORRES, J., XIMENEZ, C. & ARIAS, C. F. 2021. The gut virome of healthy children during the first year of life is diverse and dynamic. PLoS One, 16, e0240958.

TANNER, M. A., GOEBEL, B. M., DOJKA, M. A. & PACE, N. R. 1998. Specific ribosomal DNA sequences from diverse environmental settings correlate with experimental contaminants. Appl Environ Microbiol, 64, 3110-3.

TURRONI, F., MILANI, C., DURANTI, S., LUGLI, G. A., BERNASCONI, S., MARGOLLES, A., DI PIERRO, F., VAN SINDEREN, D. & VENTURA, M. 2020. The infant gut microbiome as a microbial organ influencing host well-being. Ital J Pediatr, 46, 16.

VENTOLA, C. L. 2015. The antibiotic resistance crisis: part 1: causes and threats. P t, 40, 277-83.

VIPPERLA, K. & O'KEEFE, S. J. 2012. The microbiota and its metabolites in colonic mucosal health and cancer risk. Nutrition in Clinical Practice, 27, 624-635.

WALTER, J. & HORNEF, M. W. 2021. A philosophical perspective on the prenatal in utero microbiome debate. Microbiome, 9, 5.

WAMPACH, L., HEINTZ-BUSCHART, A., FRITZ, J. V., RAMIRO-GARCIA, J., HABIER, J., HEROLD, M., NARAYANASAMY, S., KAYSEN, A., HOGAN, A. H. & BINDL, L. 2018. Birth mode is associated with earliest strain-conferred gut microbiome functions and immunostimulatory potential. Nature communications, 9, 1-14.

WANG, S., EGAN, M., RYAN, C. A., BOYAVAL, P., DEMPSEY, E. M., ROSS, R. P. & STANTON, C. 2020a. A good start in life is important-perinatal factors dictate early microbiota development and longer term maturation. FEMS Microbiol Rev, 44, 763-781.

WANG, S., EGAN, M., RYAN, C. A., BOYAVAL, P., DEMPSEY, E. M., ROSS, R. P. & STANTON, C. 2020b. A good start in life is important—perinatal factors dictate early microbiota development and longer term maturation. FEMS Microbiology Reviews, 44, 763-781.

WANG, S., ZENG, S., EGAN, M., CHERRY, P., STRAIN, C., MORAIS, E., BOYAVAL, P., RYAN, C. A., DEMPSEY, E. & ROSS, R. P. 2021. Metagenomic analysis of mother-infant gut microbiome reveals global distinct and shared microbial signatures. Gut microbes, 13, 1911571.

WILEY, N. C., CRYAN, J. F., DINAN, T. G., ROSS, R. P. & STANTON, C. 2021a. Production of Psychoactive Metabolites by Gut Bacteria. Mod Trends Psychiatry, 32, 74-99.

WILEY, N. C., CRYAN, J. F., DINAN, T. G., ROSS, R. P. & STANTON, C. 2021b. Production of Psychoactive Metabolites by Gut Bacteria. Microbes and the Mind, 32, 74-99.

WILSON, B. C., BUTLER É, M., GRIGG, C. P., DERRAIK, J. G. B., CHIAVAROLI, V., WALKER, N., THAMPI, S., CREAGH, C., REYNOLDS, A. J., VATANEN, T., O'SULLIVAN, J. M. & CUTFIELD, W. S. 2021. Oral administration of maternal vaginal microbes at birth to restore gut microbiome development in infants born by caesarean section: A pilot randomised placebo-controlled trial. EBioMedicine, 69, 103443.

XIE, H., GUO, R., ZHONG, H., FENG, Q., LAN, Z., QIN, B., WARD, K. J., JACKSON, M. A., XIA, Y., CHEN, X., CHEN, B., XIA, H., XU, C., LI, F., XU, X., AL-AAMA, J. Y., YANG, H., WANG, J., KRISTIANSEN, K., WANG, J., STEVES, C. J., BELL, J. T., LI, J., SPECTOR, T. D. & JIA, H. 2016. Shotgun Metagenomics of 250 Adult Twins Reveals Genetic and Environmental Impacts on the Gut Microbiome. Cell Syst, 3, 572-584.e3.

YAGHOUBFAR, R., BEHROUZI, A., ASHRAFIAN, F., SHAHRYARI, A., MORADI, H. R., CHOOPANI, S., HADIFAR, S., VAZIRI, F., NOJOUMI, S. A. & FATEH, A. 2020. Modulation of serotonin signaling/metabolism by Akkermansia muciniphila and its extracellular vesicles through the gut-brain axis in mice. Scientific reports, 10, 1-12.

YOSHII, K., HOSOMI, K., SAWANE, K. & KUNISAWA, J. 2019. Metabolism of Dietary and Microbial Vitamin B Family in the Regulation of Host Immunity. Frontiers in Nutrition, 6, 48.

ZHANG, X., MUSHAJIANG, S., LUO, B., TIAN, F., NI, Y. & YAN, W. 2020. The composition and concordance of Lactobacillus populations of infant gut and the corresponding breast-milk and maternal gut. Frontiers in Microbiology, 11.

ZWITTINK, R. D., VAN ZOEREN-GROBBEN, D., MARTIN, R., VAN LINGEN, R. A., GROOT JEBBINK, L. J., BOEREN, S., RENES, I. B., VAN ELBURG, R. M., BELZER, C. & KNOL, J. 2017. Metaproteomics reveals functional differences in intestinal microbiota development of preterm infants. Mol Cell Proteomics, 16, 1610-1620.

Chapter 2

Literature Review

2 Bovine Colostrum for Veterinary and Human Health Applications: A Critical Review

Kevin Linehan is first author of this review which is published in:

Linehan, K., Ross, R. P. & Stanton, C. 2022. Bovine Colostrum for Veterinary and Human Health Applications: A Critical Review. *Annual review of food science and technology*, 14**,** 387-410.

2.1 Abstract

Bovine colostrum harbours a diverse array of bioactive components suitable for the development of functional foods, nutraceuticals, and pharmaceuticals with veterinary and human health applications. Bovine colostrum has a strong safety profile with applications across all age groups for health promotion and the amelioration of a variety of disease states. Increased worldwide milk production and novel processing technologies have resulted in substantial growth of the market for colostrum-based products. This review provides a synopsis of the bioactive components in bovine colostrum, the processing techniques used to produce high-value colostrum-based products, and recent studies utilizing bovine colostrum for veterinary and human health.

2.2 Introduction

Colostrum is the initial mammary secretion post-parturition, bestowing a complete nutritional profile and bioactive compounds vital for optimum nutrition and promoting the growth, development, and immunological defense of newborns. The composition, structure, and physicochemical properties of colostrum fluctuate significantly across different species (Roy et al., 2020). For this review, colostrum, unless otherwise defined, will refer to milk from dairy cows up to 3 days postpartum (McGrath et al., 2016b). Calves are agammaglobulinemic at birth, as the syndesmochorial placenta of cows prevents passive immunity transfer from the mother to the neonate during gestation. As a result, bovine colostrum contains high concentrations of bioactive compounds, particularly immunoglobulin G (IgG), to provide passive immunity. In addition, colostrum is rich in growth factors, lactoperoxidase, lysozyme, lactoferrin, cytokines, vitamins, peptides, leukocytes, hormones, minerals, and oligosaccharides. These components engage in a plethora of biological responses, including maturation of the gastrointestinal (GI) tract, immune functioning, energy homeostasis, and protection against pathogens (Lopez and Heinrichs, 2022b). To acquire passive immunity, newborn calves require at least 4 L of first-milking colostrum within 1–2 hours of birth, with an IgG concentration of more than 50 g/L (Godden et al., 2019). The enterocytes of the calf small intestine freely absorb IgG and other large molecules by pinocytosis for the first 6–12 hours postpartum, before intestinal permeability ceases at 24 hours (Lopez and Heinrichs, 2022a). Colostrum accounts for ~1% of a healthy cow's annual milk production, far in excess of the calves' needs (Scammell and Billakanti, 2022). Colostrum's bioactive components possess cross-species bioactivity, making it an attractive choice in the research and development of functional foods and pharmaceuticals with veterinary and human applications (Playford and Weiser, 2021). The market for colostrum products is developing rapidly and is projected to increase from $2.6 billion in 2019 to $4.3 billion in 2027, largely due to improved processing techniques and novel methods for the isolation and identification of previously concealed colostrum constituents (Sydney et al., 2022). A plethora of preclinical and clinical studies in humans have demonstrated the therapeutic benefits of colostrum supplementation for health promotion and the treatment of numerous diseases (Kaplan et al., 2021). Colostrum products have also been explored for use in animal husbandry and for the health and well-being of large

animals and domestic pets (Pagnoncelli et al., 2022). This review describes the bioactive composition of colostrum, current methods used to produce colostrum-based products, and, finally, recent studies of colostrum supplementation for veterinary and human health applications. An overview of the applications of bovine colostrum in veterinary and human health is presented in Figure 2.1.

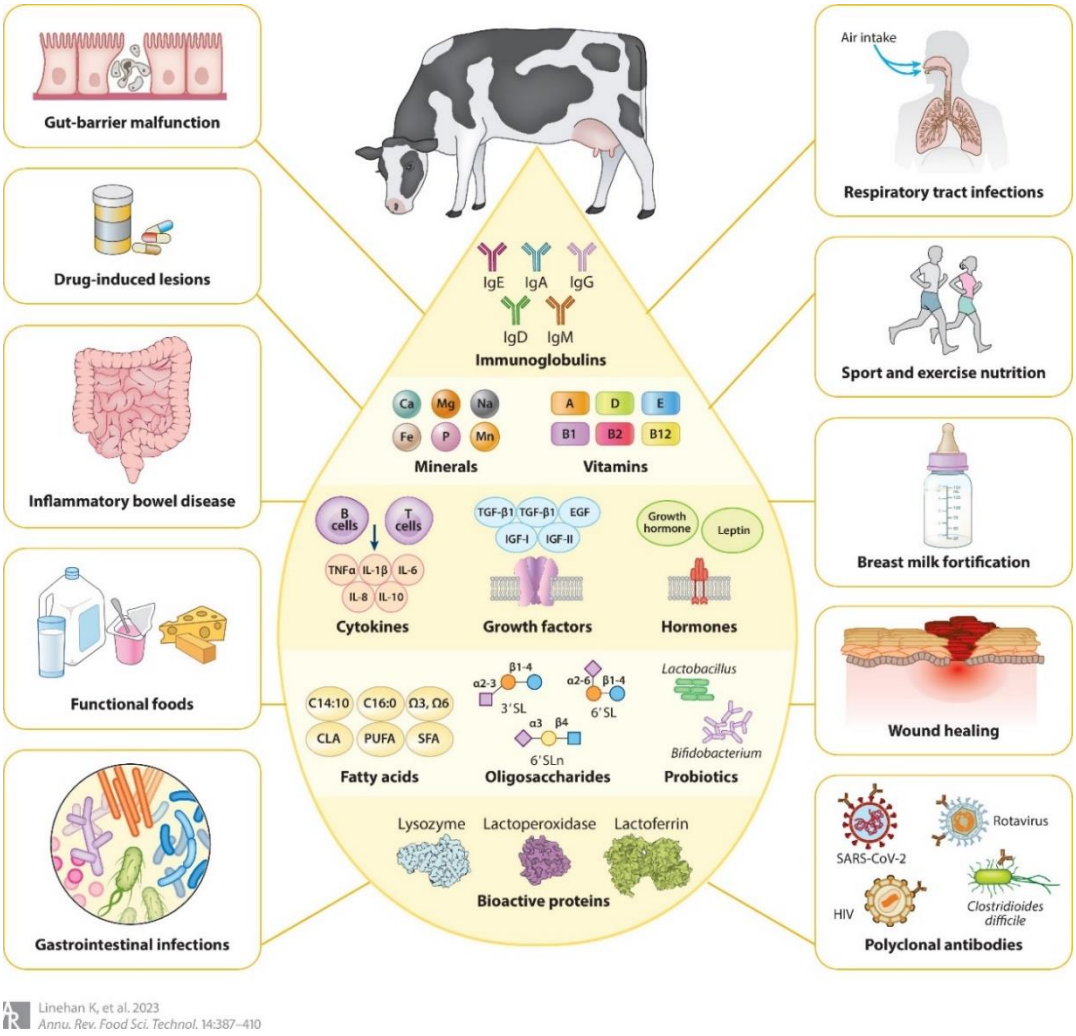

Figure 2.1 | An overview of the bioactive composition and applications of bovine colostrum in veterinary and human health. Figure adapted from images created with BioRender.com. Abbreviations: CLA, conjugated linoleic acid; EGF, epidermal growth factor; IgA, immunoglobulin A; IgD, immunoglobulin D; IgE, immunoglobulin E; IGF, insulin-like growth factor; IgG, immunoglobulin G; IgM, immunoglobulin M; PUFA, polyunsaturated fatty acid; SFA, saturated fatty acid; SL, sialyllactose; SLn, siayllactosamine; TGF, transforming growth factor.

2.3 The Bioactive Composition of Bovine Colostrum

The composition and physical properties of colostrum are highly variable due to factors such as individuality, age, breed, nutrition, antibiotics and disease exposure (Scammell and Billakanti, 2022). Generally, colostrum contains more fat, protein, vitamins, minerals, hormones, growth factors, cytokines and nucleotides and less lactose than mature milk (McGrath et al., 2016a). With the exception of lactose, all of these compounds decrease rapidly during the first 3 days of lactation before transitioning to mature milk (Playford and Weiser, 2021). The gross chemical and physical composition of colostrum is shown in Table 2.1.

Table 2.1 | Concentrations of select macronutrients, micronutrients, immunoglobulins, and general antimicrobial peptides present in bovine colostrum and mature milk

Component	**Colostrum**	**Milk**
Total solids (%)	24–28	12.9
Fat (%)	6–7	3.6–4.0
Protein (%)	14–16	3.1–3.2
Casein (%)	4.8	2.5–2.6
Lactose (%)	2–3	4.7–5.0
Immunoglobulins	**Colostrum**	**Milk**
IgG1 (g/L)	34.0–87.0	0.31–0.40
IgG2 (g/L)	1.6–6.0	0.03–0.08
IgA (g/L)	3.2–6.2	3.2–6.2
IgM (g/L)	3.7–6.1	0.03–0.06
Proteins	**Colostrum**	**Milk**
Lactoferrin (g/L)	1.5–5	0.02–0.75
Lactoperoxidase (mg/L)	11–45	13–30

Lysozyme (mg/L)	0.14–0.7	0.07–0.6
Growth Factors	**Colostrum**	**Milk**
Epidermal growth factor (ng/ml)	4-325	1-150
Insulin-like growth factor-I (ng/ml)	100-2000	5-100
Insulin-like growth factor-II (ng/ml)	150-600	5-100
Transforming growth factor- β1 (ng/ml)	1--50	<5
Transforming growth factor- β2 (ng/ml)	150-1150	10--70
Minerals	**Colostrum**	**Milk**
Calcium (g/kg)	2.6–4.7	1.2–1.3
Phosphorus (g/kg)	4.5	0.9–1.2
Potassium (g/kg)	1.4–2.8	1.5–1.7
Sodium (g/kg)	0.7–1.1	0.4
Magnesium (g/kg)	0.4–0.7	0.1
Zinc (mg/kg)	11.6–38.1	3.0–6.0
Fat	**Colostrum**	**Milk**
SFA (g/100 g)	66.12-74.05	64.88-64.47
MUFA (g/100 g)	24.54-30.09	31.51-31.79
PUFA (g/100 g)	3.79-3.88	3.61-3.74
Vitamins	**Colostrum**	**Milk**
Thiamin (B1) (µg/ml)	0.58–0.90	0.4–0.5
Riboflavin (B2) (µg/ml)	4.55–4.83	1.5–1.7
Niacin (B3) (µg/ml)	0.34–0.96	0.8–0.9

Cobalamin (B12) (µg/ml)	0.05–0.60	0.004–0.006
Vitamin A (µg/100 ml)	25	34
Vitamin D (IU/g fat)	0.89–1.81	0.41
Tocopherol (E) (µg/g)	2.92–5.63	0.06
Carbohydrates	**Colostrum**	**Milk**
3′-sialyllactose (g/L)	0.42-1.24	0.13
6′-sialyllactose (g/L)	0.05-0.13	0.04
6′-sialyl-N-acetyllactosamine (g/L)	0.07-0.42	0.01

Ranges are shown where available. Values obtained from (Arslan, et al. 2021, Bunyatratchata, et al. 2021, Playford and Weiser 2021). Abbreviations: MUFAs, monounsaturated fatty acids; PUFAs, polyunsaturated fatty acids; SFAs, saturated fatty acids.

2.3.1 Protein

The protein concentration of colostrum is 15% (weight/weight), falling to 3% in mature milk (Sats et al., 2020). Immunoglobulins (IgG, IgA, IgE, IgD, and IgM) constitute 70–80% of the protein in colostrum, with IgG accounting for 80–85% of the total immunoglobulin content (Playford and Weiser, 2021). The total immunoglobulin content of colostrum ranges from 42 to 90 g/L and falls to 0.4–0.9 g/L in mature milk. Immunoglobulins (antibodies) are glycoproteins produced by B cells of the immune system that specifically recognize and bind antigens present on bacteria and viruses (Ulfman et al., 2018). These Y-shaped molecules consist of four polypeptide chains, with two identical heavy chains and two identical light chains connected via disulfide bonds. Antigen binding to the two antigen binding fragments (Fab) of the N-terminal region causes immune complex formation and activation (Ghosh and Iacucci, 2021). The C-terminal region consists of two nonantigen binding fragments, termed the fragment crystallisable (Fc) region. The Fc region interacts with Fc receptors present on immune effector cells such as phagocytes, natural killer cells, dendritic cells, and $CD4^+$ T lymphocytes (Ghosh and Iacucci, 2021). This process presents pathogens to macrophages for destruction, activates T cells and B cells, modifies the intestinal microbiota, and induces local IgA production (Ulfman et al., 2018).. Specific

vaccination of cows against human or bovine pathogens (hyperimmunisation) results in the production of polyclonal, pathogen-specific antibodies in colostrum secretions, commonly referred to as hyperimmune bovine colostrum (HBC) (Ulfman et al., 2018).. HBC products have been shown to effectively neutralize a range of pathogens, including rotavirus, *Escherichia coli*, *Cryptosporidium*, *Shigella*, *Vibrio cholerae*, *Clostridioides difficile*, *Helicobacter pylori*, human immunodeficiency virus (HIV), *Candida albicans*, and *Streptococcus mutans* (Borad and Singh, 2022). Lactoperoxidase is an antimicrobial glycoprotein and a member of the heme peroxidase family of enzymes, which are known to inhibit bacterial metabolism. Lactoperoxidase catalyzes the oxidation of thiocyanate ions, at the expense of hydrogen peroxide, to generate reactive products that are toxic to numerous gram-positive and gram-negative bacteria, including *Pseudomonas aeruginosa*, *Salmonella typhimurium*, *Listeria monocytogenes*, and *Staphylococcus aureus* (Wolfson and Sumner, 1993). Concentrations of lactoperoxidase in colostrum (11–45 mg/L) are comparable to milk (13–30 mg/L), but the activity of lactoperoxidase is substantially higher in colostrum (McGrath et al., 2016a). Lysozyme is an antimicrobial enzyme that lyses the peptidoglycan layer of gram-positive and gram-negative bacterial cells by hydrolysis to cause cell lysis. Lysozyme concentrations in colostrum (0.14–0.7 mg/L) are higher than in mature milk (0.07–0.6 mg/L) (McGrath et al., 2016a). Lactoferrin is also found in colostrum and is an iron-binding glycoprotein and member of the transferrin family. Lactoferrin induces multiple valuable biological effects, including iron absorption, immune modulation, enhancement of the antimicrobial activity of lysozyme, and increase in the growth of epithelial cells and fibroblasts (Zhao et al., 2019). Colostrum is routinely used for the isolation of lactoferrin to add to infant formula, cosmetics, and nutritional supplements (Sydney et al., 2022).

2.3.2 Carbohydrates

Lactose is the predominant carbohydrate in colostrum (2.5%) and is present at lower concentrations than in mature milk (5%) (McGrath et al., 2016a). Oligosaccharides are the third most abundant solid component found in milk after lactose and lipids (Fong et al., 2011). These structurally and biologically diverse molecules, although resistant to digestion, are associated with various beneficial functions. Oligosaccharide concentrations are significantly higher in colostrum (0.7–1.2 g/L) than in mature milk (0.1 g/L) (ten Bruggencate et al., 2014). 3′ Sialyllactose (3′SL), 6′

sialyllactose (6′SL), 6′ siayllactosamine (6′SLN), and disialyllactose (DSL) are the major bovine colostrum oligosaccharides (BCOs), with 3′SL accounting for 70% of the oligosaccharide content in colostrum (Bunyatratchata et al., 2021). BCOs exert prebiotic effects by acting as metabolic substrates for beneficial bacteria such as bifidobacteria, which are important early colonisers of the calf gut (Bondue et al., 2016). Furthermore, BCOs act as competitive inhibitors to pathogenic bacteria (e.g., *E. coli*, *Cronobacter sakazakii*, and *H. pylori*) for binding sites on gut epithelial cells by mimicking epithelial cell surface carbohydrates (Morrin et al., 2019, Morrin et al., 2020). Advancements in enzymatic glycosylation have provided opportunities to alter the structure of bovine milk oligosaccharides to better resemble human milk oligosaccharides (Weinborn et al., 2020). Colostrum is also rich in glycosylated proteins, especially bovine glycomacropeptide, which has different glycosylated forms and is created via κ-casein proteolysis during digestion (McGrath et al., 2016a). Bovine glycomacropeptide has bifidogenic activity, as shown by its concentration-dependent growth promotion of *Bifidobacterium longum* subspecies *infantis* (O'Riordan et al., 2018). Colostrum also contains β-lactoglobulin, a whey protein with numerous human health benefits that is absent in human colostrum (Le Maux et al., 2014).

2.3.3 Fats

The fat component of colostrum is usually removed to facilitate commercial processing; however, it is not biologically inert and contains multiple beneficial components. Colostrum contains ∼7% fat, predominantly comprising milk-fat globules (Sats et al., 2022). There are lower concentrations of *trans*-fatty acids and short-chain fatty acids (C4–C10) in colostrum than in mature milk (Contarini et al., 2014). Colostrum contains approximately 65–75% saturated fatty acids (SFAs), 24–28% monounsaturated fatty acids (MUFAs), and 4–5% polyunsaturated fatty acids (PUFAs) (Wilms et al., 2022, O'Callaghan et al., 2020). Ω3 and Ω6 PUFAs are up to 25% higher in colostrum than mature milk (Wilms et al., 2022). Oleic acid (C18:1n-9), myristic acid (C14:0), and palmitic acid (C16:0) are the predominant fatty acids in colostrum (Wilms et al., 2022, O'Callaghan et al., 2020). Palmitate is important in early life nutrition (Miles and Calder, 2017) and oleic acid has been shown to exert beneficial effects in immunomodulation and cardiovascular health (Sales-Campos et al., 2013). Colostrum from primiparous cows has a significantly higher level of

conjugated linoleic acid (CLA; *cis*-9, *trans*-11) than that from multiparous cows; however, there are no overall differences between colostrum and mature milk (Wilms et al., 2022, O'Callaghan et al., 2020). CLA has attracted attention for its apparent benefits, including reduction of carcinogenesis, atherosclerosis, inflammation, obesity, and diabetes demonstrated in human and animal models (Yang et al., 2015).Further studies on the fat composition of colostrum are needed to allow the segregation of colostrum from mature milk. This information would minimize the undesirable mixing of raw milk with colostrum before processing, enable more efficient and targeted production of colostrum-based foods and food supplements, and avoid processing-related issues that have previously been reported with colostrum (Tsioulpas et al., 2007).

2.3.4 Vitamins, Minerals, and Hormones

The concentrations of fat-soluble vitamins (A, D, E) and carotenoids, as well as those of the water-soluble vitamins thiamine, riboflavin, vitamins B_1, B_2, B_6, and B_{12}, folate, and vitamin C, are higher in colostrum than in mature milk (Scammell and Billakanti, 2022). Colostrum is also richer in several essential minerals, including calcium, sodium, copper, selenium, iron, zinc, magnesium, manganese, and phosphorus (McGrath et al., 2016a). The vitamins and minerals found in colostrum help in the metabolism of fats and proteins, have antioxidant properties, and aid in proper functioning of the nervous system (Buttar et al., 2017). Colostrum also contains multiple hormones, including growth hormone, prolactin, somatostatin, oxytocin, luteinizing hormone–releasing hormone, leptin, thyroid-stimulating hormone, thyroxine, calcitonin, estrogen, and progesterone. Increased gut permeability in the neonatal period allows these factors to enter the circulatory system to influence the developing calf (Lopez and Heinrichs, 2022a).

2.3.5 Cytokines and Immune Regulators

Cytokines are a diverse group of proteins, peptides, and glycoproteins secreted by T-helper cells and activated macrophages. Although present at minute concentrations in colostrum (10–1,000 pg/ml), cytokines show pro- or anti-inflammatory activity that supports immune activation and recruitment against pathogenic bacteria, viruses, and fungi (Playford and Weiser, 2021). Cytokines in colostrum include interleukins (ILs), tumor necrosis factors (TNFs), and interferons. Several types and subtypes of

cytokines and IL are present in colostrum, including IL-1, IL-3, IL-4, IL-5, IL-6, IL-8, IL-10, IL-12, IL-13, IL-16, IL-18, IFN-γ, TNF-α, and TNF-γ receptors (McGrath et al., 2016a). Concentrations of IL-1β, IL-6, TNF-α, IFN-γ, and IL-1ra are higher in colostrum than in mature milk (McGrath et al., 2016a). Colostrum also comprises maternal leukocytes, such as B and T lymphocytes, macrophages, and neutrophils (Playford and Weiser, 2021). Leukocytes protect against enteric pathogens by directly acting on the microbe, in addition to stimulating a local immune response, such as the production of cytokines, IgG, and antimicrobial factors (Stelwagen et al., 2009). Unfortunately, commercial preparation techniques typically remove leukocytes from the final product. Colostrinin (or proline-rich polypeptide) is a polypeptide that helps regulate the production of cytokines and inhibits the production of damaging reactive oxygen species (Zabłocka et al., 2020). The amino acid compositions of colostrinin from ovine, bovine, and human colostrum are similar (Kruzel et al., 2001). Although not entirely chemically defined, colostrinin constitutes a mixture of at least 32 peptides with molecular weights ranging from 0.5 to 3 kDa (Rattray, 2005). Colostrinin has been shown to prevent allergic inflammation due to common indoor and outdoor allergens in a murine allergic airway inflammation model, and immunocompromised rats infected with enterotoxigenic *E. coli* (ETEC) had reduced endotoxin levels and infected lymph nodes when treated with colostrinin (Boldogh et al., 2008). MicroRNAs (miRNAs) with immune-regulating potential are also present in colostrum (Sun et al., 2013). miRNAs are short, noncoding RNA molecules that can regulate gene expression at the post-transcriptional level, representing a possible method of postnatal signaling from the mother to the neonate (Van Hese et al., 2020). miRNAs are packaged in microvesicles, allowing stability during passage through the GI tract, and may influence lymphoid cell function within the intestine (Van Hese et al., 2020). Research in other species suggests that once absorbed by the neonate, miRNAs from colostrum may be important in the differentiation and functional development of the intestinal epithelium and the maturation of the neonate's immune system (Hatmal et al., 2022).

2.3.6 Growth Factors

Growth factors are polypeptides that stimulate cellular processes, including cell proliferation, migration, and differentiation (Gauthier et al., 2006). Insulin-like growth factor (IGF) is the most abundant growth factor in colostrum (Scammell and

Billakanti, 2022). IGF-I and IGF-II concentrations in colostrum range from 50 to 2,000 μg/L and 200 to 600 μg/L, respectively, whereas their concentration in mature milk is less than 10 μg/L (McGrath et al., 2016a). IGF-I is an anabolic factor that enhances protein accumulation and mediates the growth-promoting action of growth hormone. Epidermal growth factors (EGFs) stimulate the proliferation of epithelial and epidermal cells, act as differentiation factors, and modulate hormone synthesis. The concentration of EGFs in colostrum varies from 4 to 320 μg/L and ranges from 2 to 155 μg/L in milk (Scammell and Billakanti, 2022). Transforming growth factors (TGFs) maintain the equilibrium between cell proliferation and differentiation. TGF-α helps in reducing gastric acid production, increasing gastric mucus production, and stimulating gut growth and repair (Coffey et al., 1995). TGF-β acts as a chemoattractant for neutrophils and increases epithelial cell migration at the edges of wounds (Pakyari et al., 2013). Concentrations of TGF-β in colostrum are much higher (20–40 mg/L) than in milk (1–2 mg/L) (Playford and Weiser, 2021). Vascular endothelial growth factor (VEGF) is a heparin-binding glycoprotein that stimulates proliferation and new vessel formation and vascular permeability-enhancing activity (Keck et al., 1989). Because of its angiogenic activity, the VEGF content of colostrum may have value in enhancing local vascular supply in conditions such as peptic ulceration (Playford and Weiser, 2021). Milk-fat globule-epidermal growth factor 8 (MFG-E8) is a secreted protein, forming an integral component of milk-fat globules. MFG-E8 is present in colostrum in high concentrations and may influence the immune and repair response of the suckling neonate (Chatterton et al., 2013). MFG-E8 enhances the removal of damaged and apoptotic cells by phagocytosis, induction of VEGF-mediated new vessel formation, and enhancement of mucosal healing (Yi, 2016).

2.3.7 Microbiome

The microbiome comprises the microbiota and its “theatre of activity,” encompassing the combined nucleic acids (including viruses and bacteriophages), structural components, and microbial metabolites related to the microbiota (Berg et al., 2020). Firmicutes, Bacteroidetes, Proteobacteria, and Actinobacteria are the most abundant bacterial phyla in colostrum (Vasquez et al., 2022, Yeoman et al., 2018). The colostrum microbiota was found to share approximately 10.6% and 9.6% of operational taxonomic units with luminal and mucosal microbiota of the calves,

respectively, suggesting colostrum contributes to the makeup of the calf GI tract microbiota in early life (Yeoman et al., 2018). Probiotics have been defined by the Food and Agriculture Organisation and World Health Organisation as "live microorganisms which when administered in adequate amounts confer a health benefit on the host" (FAO/WHO 2001, Hill et al. 2014). Colostrum contains various bacteria, including *Lacticaseibacillus casei*, *Lactiplantibacillus plantarum*, *Bifidobacterium pseudolongum*, and *Bacillus subtilis* (Vasquez et al., 2022, Yeoman et al., 2018). Colostrum is also a source of potentially pathogenic bacteria, including *Streptococcus uberis*, *Streptococcus agalactiae*, *Streptococcus dysgalactiae*, *Staphylococcus aureus*, and *Corynebacterium* spp. (Derakhshani et al., 2018, Fasse et al., 2021). Pathogens originate from mammary gland infections and improper colostrum harvest, handling, and storage (Godden et al., 2019). Colostrum quality is typically evaluated by the IgG content; however, total bacterial count (TBC) should also be considered due to negative effects on passive transfer of immunity in calves and industrial processing (Cummins et al., 2017, Fasse et al., 2021). TBCs of less than 100,000 colony forming units (CFU)/ml and coliform counts of less than 10,000 CFU/ml are considered acceptable (Godden et al., 2019). Calves fed colostrum with low TBC have decreased pathogenic bacterial colonisation and a higher prevalence of beneficial bacteria, including *Bifidobacterium* spp. and *Lactobacillus* spp. (Malmuthuge et al., 2015, Fischer et al., 2018). Recent human studies indicate that bacteriophages are transmitted from mother to infant via breastfeeding (Pannaraj et al., 2018); however, we are not aware of any studies that have investigated the presence of bacteriophages in bovine colostrum.

2.4 Production of Bovine Colostrum Products

Bulk milk tank collections exclude colostrum for the first 4–5 days postpartum because the low clotting temperature and high protein content hamper industrial processes (Hesami et al., 2020). Farmers that supply colostrum manufacturers normally ship frozen colostrum to central processing facilities, where it is used to produce whole colostrum powders via conventional dairy processing methods. Manufacturers also use colostrum to isolate individual components, typically IgG and lactoferrin, through a combination of chromatography and tangential flow filtration steps, for addition to dietary products such as infant milk formula and calf dietary supplements (Scammell and Billakanti, 2022). The United States, Canada, and India

are the main producers of colostrum products due to their practice of year-round calving, which ensures a consistent supply of colostrum for processing (Scammell and Billakanti, 2022). PanTheryx (Colorado, USA) is the leading supplier of colostrum products worldwide and recently received the generally recognised as safe classification from the US Food and Drug Administration (Sydney et al., 2022). Commercial products for both veterinary and human applications are typically in the form of capsules, lozenges, chewing gums, powder, or whole colostrum drinks. Whole colostrum has also been used as an additive in dairy products such as yogurt, kefir, fermented milk, ice cream, cheese, and butter to enhance their bioactive composition (Mehra et al., 2021). Traditional colostrum foods are also produced throughout the world, including khess (India), kalvdans (Scandinavia), abrystir (Iceland), råmelk (Norway), leipäjuusto (Finland), molozyvo (Ukraine), and groosniuys (Isle of Man) (Mehra et al., 2021). Elimination of bacterial contamination and preservation of bioactive components are the primary challenges of generating colostrum products (Kaplan et al., 2021). Preservation and processing methods used to produce colostrum products for supplementation in animal and human studies are discussed in the following section.

2.4.1 Refrigeration and Freezing

Up to 90% of Irish and US dairy producers freeze colostrum for on-farm and industrial usage (Cummins et al., 2016a, Usuga et al., 2022). Frozen colostrum is typically used to create a colostrum bank for newborn calves that cannot be fed their mothers' colostrum immediately after birth (Lopez and Heinrichs, 2022a). Freezing is the optimal preservation method for colostrum and storage for up to 1 year leads to no significant alterations in the bioactive composition (Godden et al., 2019). Thawing by the au bain-marie method with temperatures <40°C has been shown to have no effect on composition (Robbers et al., 2021). However, TBC and pH are significantly altered when colostrum is stored at >4°C (Cummins et al., 2016b). Gross increases in TBC and pH occur in the first 6 hours postpartum; therefore, rapid storage at ≤4°C is essential (Cummins et al., 2016b). Storage at ≤4°C for 2 days also sufficiently minimizes bacterial growth to levels suitable for processing and ensures passive transfer to calves occurs (Cummins et al., 2017).

2.4.2 Thermal Treatment

Pasteurisation is a heat treatment process used to reduce the total number of microorganisms and minimize the number of pathogens in colostrum (Robbers et al., 2021). High-temperature short-time (HTST) pasteurisation at 72°C for 15 seconds and low-temperature long-time (LTLT) pasteurisation at 60°C for 30 minutes are the two most common pasteurisation methods employed in producing colostrum products (Jay, 1998). The bioactive components in colostrum are heat labile; for instance, immunoglobulins unfold above 65°C and denature at 89°C and other significant bioactives denature between 62°C and 78°C (Indyk et al., 2008). HTST is efficient at pathogen elimination in colostrum but results in a significant loss of bioactives and increases viscosity, thus affecting downstream processing (Elsohaby et al., 2018). LTLT at 60°C for 30 or 60 minutes is the optimal pasteurisation method for colostrum for the reduction of microbial contamination and maintenance of bioactive components (Mann et al., 2020).

2.4.3 Drying

Drying colostrum to a powder form reduces the water activity (aw) to an aw below 0.2 and slows microbiological, chemical, and enzymatic activity, allowing for long storage periods without activity loss of bioactive components (Guiné, 2018). Spray drying refers to the conversion of a liquid feed to powder by spraying into a hot dryer to rapidly remove moisture (Kandasamy and Naveen, 2022). Freeze drying or lyophilisation refers to the elimination of moisture from frozen food molecules through sublimation (Kandasamy and Naveen, 2022). The thermo-labile nature of colostrum requires the omission of conventional pasteurisation of colostrum prior to spray drying; hence, spray-dried powder may contain pathogens and spoilage microorganisms (Borad et al., 2019). For instance, potentially harmful *Bacillus* species were detected in spray-dried colostrum powder sold in the US market (Hayes et al., 2012). Freeze drying is significantly more effective at preserving bioactive constituents than spray drying (Chatterton et al., 2020). However, high production costs, longer processing time, and problems in scaling up freeze drying have limited its industrial application for the manufacture of colostrum products. Therefore, spray drying is the most common drying method for colostrum (Chelack et al., 1993). Electrostatic spray drying is the newest drying technology

aimed at heat-sensitive materials and has the potential to reduce denaturation of heat-labile components in colostrum (Ackerman et al., 2019).

2.4.4 Emerging Processing Methods

Because of the thermal instability of bioactive constituents in colostrum, numerous nonthermal technologies have been explored for the production of colostrum products. Anaerobic fermentation, termed bovine colostrum silage (BCS), is produced by storage at mild temperatures (17–22.5°C) for a minimum period of 35 days (Kraus et al., 2021). BCS can be stored for 2 years, is low cost, does not require refrigeration, freezing, or use of additives, and can be used for feeding calves (Halavach et al., 2022). *Streptococcus lactis*, *Streptococcus thermophilus*, *Lactobacillus bulgaricus*, *Lactobacillus acidophilus*, and *L. plantarum* have been used to produce BCS (Halavach et al., 2022). High-pressure processing (HPP) exposes foodstuffs to elevated pressures (100–1,000 MPa) to achieve microbial destruction without affecting low-molecular-weight compounds (Li et al., 2006). HPP at 300–400 MPa for 30 minutes has been shown to effectively reduce TBC while maintaining IgG concentrations in colostrum (Foster et al., 2016). Irradiation utilizes ultraviolet light to inactivate microorganisms in food materials (Cutler and Zimmerman, 2011). A negative linear relationship between duration of continuous ultraviolet light treatment and the concentration of IgG and bacterial contaminants has been reported by (Pereira et al., 2014). Membrane processing, pulsed electric field, nanoencapsulation, and liposomal technologies are emerging food processing techniques warranting further investigation for the production of colostrum products (Borad and Singh, 2022, Kaplan et al., 2021).

2.5 Human Health Applications of Bovine Colostrum

Prior to the advent of antibiotics, bovine colostrum was consumed by humans for thousands of years for its antibacterial properties. For example, as part of Ayurveda, the ancient system of medical practice in India, colostrum was used in the treatment of eye infections (Buttar et al., 2017). At present, there are more than 120 clinical trials taking place worldwide investigating the use of colostrum in human health promotion and the amelioration of numerous disease states in adults and neonates (see **https://trialbulletin.com/lib/trials/term=Colostrum**). This section discusses recent preclinical and clinical studies of colostrum supplementation for human health

applications. Table 2.2 outlines a more detailed description of a selection of clinical trials of colostrum supplementation in humans.

Table 2.2 | A selection of human clinical trials studying the effects of supplementation of whole bovine colostrum or isolated compounds in human health promotion.

Application	**Studied Sample**	**Colostrum Form & Intervention**	**Benefits**	**References**
Necrotizing enterocolitis (NEC)	80 preterm neonates	Immuguard® (Dulex-Lab Pharmaceutical Co.) 20 ml/kg/day for first 2 weeks of life	Decrease of feeding intolerance, NEC, late-onset sepsis and mortality	(Ismail, et al. 2021)
Exercise-induced immune dysfunction	31 male athletes	Powdered whole colostrum. 20 g per day for 58 days	Prevented prolonged exercise-induced immunodepression	(Jones, et al. 2019)
Rotavirus and E. coli infection-related acute diarrhoea	160 children, aged 6 months- 2 years old	3 g BC powder diluted in 50 ml water, daily, orally, 1 week	Reduction of frequency and duration of vomit and diarrhoea episodes	(Barakat, et al. 2020)
Drug-induced lesions	62 children age 1–18 years old	Spray-dried BC powder (Biofiber-Damino™), 7.5–30 g/ day 1–3 daily doses, oral or nasogastric tube	No difference for neutropenic fever, intravenous antibiotics, incidence of bacteremia, or intestinal mucositis Reduction of the peak severity of oral mucositis	(Rathe, et al. 2020)

Enterotoxigenic E. coli (ETEC) infection	90 healthy volunteers	One or two tablets with 200 mg of HBC powder, three times a day for 7 days	Protection against the development of diarrhoea Reduction of abdominal pain complaints No effect on the viability of the challenge strains	(Otto, et al. 2011)
Dietary supplement for preterm infants	40 preterm infants	Powered colostrum product, ColoDan, Biofiber Damino, Gesten, Denmark) as a supplement to own mother's milk	Colostrum feeding showed no adverse clinical effects, increased enteral protein intake (when feeding with human milk), and/or a shortened time to reach full enteral feeding (when feeding with infant formula)	(Juhl, et al. 2018)

Abbreviations: BC, bovine colostrum; HBC, hyperimmune bovine colostrum; NEC, necrotizing enterocolitis.

2.5.1 Infant Health

In vitro studies have shown that fortification of human milk with bovine colostrum increases its antibacterial activity (Gao et al., 2021). Furthermore, in vitro studies have reported that colostrum-derived IgG fractions have prebiotic effects, as they are capable of increasing the adhesion of *Bifidobacterium* spp. and *Lactobacillus* spp., important early colonisers of the infant gut, to human intestinal cells (Morrin et al., 2020, Morrin et al., 2019). Stepwise pilot-phase safety trials of colostrum supplementation in preterm infants (<37 weeks gestation in humans) have shown a shortened time to reach full enteral feeding (when feeding with infant formula), no adverse clinical effects, and/or increased enteral protein intake (when feeding with human milk) (Juhl et al., 2018, Li et al., 2017). A larger clinical trial is currently taking place to investigate the use of bovine colostrum as a fortifier to human milk in preterm infants (n = 350) (see **https://clinicaltrials.gov/ct2/show/NCT03085277**). Necrotizing enterocolitis (NEC) is the leading cause of death from GI disease in infants, affecting 3–10% of hospitalised preterm infants worldwide (Burrin et al., 2020). Although encouraging results have been seen in animal models, human studies have so far not shown a significant benefit of colostrum products in reducing the incidence of or mortality from NEC in preterm infants; however, gut priming effects have been reported (Ismail et al., 2021, Sharma et al., 2020, Tao et al., 2020).

2.5.2 Sport and Exercise Nutrition

Colostrum has attracted significant interest within sports nutrition to influence body composition, physical performance, recovery, immune function, illness risk, and gut damage and permeability in athletes (Davison, 2021). The World Anti-Doping Agency previously advised athletes against taking colostrum for fear of causing a rise in circulatory levels of IGF-I, resulting in doping penalties, but this has since been proved false (Davison et al., 2019). Colostrum supplementation has been shown to ameliorate several performance decrements caused by periods of high-intensity, intermittent, and endurance performance (Kotsis et al., 2018). Daily colostrum supplementation for 2–12 weeks has been reported to have beneficial effects on clinically relevant immune functions and the risk of suffering upper respiratory tract infections or symptoms in athletes (Jones et al., 2016, Jones et al., 2019). Numerous studies have reported benefits of colostrum supplementation on gut permeability, especially during periods of intensified training (March et al., 2017, March et al., 2019). However, null effects

on GI permeability or damage markers in athletes have also been reported (Morrison et al., 2014, McKenna et al., 2017). The balance of available evidence for gut permeability and illness risk is positive, but further research is required to fully determine all mechanisms responsible for these effects in athletic populations (Davison, 2021).

2.5.3 Skincare

Colostrum and its components have been investigated for their usage in skincare products (Sydney et al., 2022). In vitro studies have demonstrated that colostrum induces proliferation and differentiation of skin cells and stimulates repair and reduces artificially induced inflammation in animal models (Kovacs et al., 2020, Hong and Park, 2014). More recently, combining colostrum with honey reduced scars and exudates, provided pain relief, protected against infection, and stimulated the growth of granulation tissue in rat models of cutaneous wound injuries (Tanideh et al., 2017). In human volunteers, topical administration of colostrum-derived lactoferrin reduced inflammation after exposure to skin allergens (Griffiths et al., 2001).

2.5.4 Respiratory Tract Infections

Human respiratory syncytial virus (RSV) is a common, contagious virus that causes respiratory infections, namely bronchiolitis, the common cold, and serious illness for infants and elderly persons (Nederend et al., 2020). Intranasal administration of colostrum-derived IgG prevented and neutralised RSV infections in mice (Nederend et al., 2020). Immunisation of pregnant cows with the S1 receptor-binding domain protein and trimeric S protein of severe acute respiratory syndrome coronavirus 2 (SARS-CoV-2) was recently used to develop SARS-CoV-2-specific neutralizing antibodies, which demonstrated blocking of the interaction between the trimeric S protein and angiotensin-converting enzyme 2 (ACE2) (Kangro et al., 2021). This study led to the formulation of a nasal spray, BioBlock, which is currently being investigated in a clinical trial (Uusküla et al., 2022).

2.5.5 Diarrhea

Colostrum has proved to be an effective adjuvant therapy for both viral and bacterial diarrhea in children and adults. A meta-analysis of five randomised control trials in children (n = 324) reported that colostrum supplementation significantly reduced stool

frequency and occurrence of diarrhea caused by rotavirus or *E. coli* (Li et al., 2019). Colostrum supplementation in a randomised control trial in adult patients (n = 42) with HIV-related diarrhea resulted in reduced stool frequency and fatigue and permitted weight gain compared to routine care alone (Kaducu et al., 2011). In adults, a randomised control trial (n = 90) showed colostrum supplementation was significantly effective at protecting against travelers' diarrhea caused by ETEC (Otto et al., 2011).The product used in the aforementioned study, TRAVELAN® (600 mg/day anti-*E. coli*/antidiarrheal HBC) is currently sold in several countries (Otto et al., 2011).

2.5.6 Drug-Induced Gut Injuries

Nonsteroidal anti-inflammatory drugs (NSAIDs) are the most commonly used drugs worldwide for the treatment of pain; however, they can cause gastric and intestinal damage such as peptic ulceration and injury to both the small and large intestine (Arslan et al., 2021). Colostrum protected against indomethacin-induced mucosal damage and increased villus height in vivo (mice and rats) and in vitro (HT-29 cells) (Playford et al., 2020, Yamamoto et al., 2013). Colostrum feeding decreased intestinal permeability and intestinal villi harm in rats with diclofenac-induced mucosal damage (Kim et al., 2005). Intestinal damage caused by chemotherapy treatment in pigs showed that colostrum supplementation reduced inflammatory markers and increased intestinal enzyme activity, resulting in reduced intestinal drug toxicity (Pontoppidan et al., 2015). Randomised crossover trials of indomethacin-induced intestinal permeability in humans indicate that colostrum supplementation protects against NSAID injury (Playford et al., 2001). Mechanistically, the beneficial effects of colostrum on NSAID injuries have been attributed to the affinity of the C-terminal half of lactoferrin (C-lobe) for NSAIDs (Mir et al., 2009).

2.5.7 Short Bowel Syndrome

Short bowel syndrome (SBS) is an intestinal insufficiency resulting from intestine resection due to infarction of the mesenteric vessels, trauma, abnormalities, or complications of Crohn's disease. Promising results from animal models of SBS suggest that the supplementation of diets with colostrum led to weight gain and significant improvements in intestinal (Aunsholt et al., 2018). Clinical trials in children and adults have not shown that colostrum provides significant improvements to SBS clinical markers (Aunsholt et al., 2014). Despite encouraging results from

animal studies, the requirement for invasive sampling for endpoint measurements of SBS has limited studies on the effects of colostrum supplementation on SBS in humans.

2.5.8 Inflammatory Bowel Disease (IBD)

Colostrum and its constituents have shown promising results in the treatment of inflammatory bowel disease (IBD), a group of diseases that affect the intestine, classified by two main phenotypes: ulcerative colitis and Crohn's disease (Sienkiewicz et al., 2021). In mouse models of chemically induced colitis, colostrum feeding was shown to prevent and reduce colitis (Filipescu et al., 2018, Spalinger et al., 2019). A recent study reported that colostrum supplementation in mice with colitis led to a reduction in inflammatory markers of colitis and stimulation in the growth of *Bifidobacterium* spp. and *Lactobacillus* spp. (Menchetti et al., 2020). In humans, colostrum was shown to improve the symptoms and histological scores of patients with distal colitis who received colostrum enemas in addition to mesalazine, a medication routinely used to treat IBD, compared to controls who only received mesalazine (Khan et al., 2002).

2.6 Veterinary Applications of Bovine Colostrum

Bovine colostrum is commonly used as a nutritional supplement and alternative source of passive immunity in domestic animals and pets. Furthermore, colostrum has been investigated in production animals to improve growth performance parameters such as body weight gain, feed intake, and feed conversion ratio. This section discusses studies of colostrum supplementation for veterinary applications.

2.6.1 Bovines

Failed passive transfer of immunity is a common issue for bovines (Lopez and Heinrichs, 2022a). Colostrum replacers (>100 g IgG per dose) in the form of dried powders are a viable alternative when maternal colostrum is unavailable or of poor quality for feeding (Godden et al., 2019). The ease of storage and preparation of colostrum replacers is particularly advantageous over thawing maternal colostrum from a colostrum bank (Lago et al., 2018). However, replacement products should not replace high-quality colostrum, as they typically lack antigen-specific antibodies against farm-specific pathogens (Cabral et al., 2013). Colostrum supplements (<100 g

IgG per dose) are commonly used in conjunction with maternal colostrum to ensure passive immune transfer occurs (Godden et al., 2019).

2.6.2 Pigs

Pigs represent the most widespread use of colostrum in non-bovines. Modern pig breeds often produce more offspring than the number of functional teats on sows; thus, bovine colostrum has been explored as an alternate source of passive immunisation for newborn piglets (Kirkden et al., 2013). Studies in preterm piglets, a model for preterm human infants, have shown that bovine colostrum is equally as effective as porcine colostrum at improving digestive and absorptive functions, inducing body and gut growth, dampening inflammation, protecting against NEC and late-onset sepsis, and improving systemic immunity relative to formula feeding (Yan et al., 2021). Furthermore, colostrum-fed preterm piglets display an exceptional capacity to rapidly adapt their gut and immune development to that in term pigs (within 1 to 2 weeks) (Rasmussen et al., 2016). As a basis for human trials, colostrum has been explored as a fortifier to donor human milk in preterm pigs in the first weeks of life. Fortification of donor human milk with colostrum was superior to formula-based fortifiers to support growth, gut function, nutrient absorption, mucosal defense, and reduction in the density of mucosa-associated bacteria and putative pathogens (Sun et al., 2019). It has been suggested that the growth-stimulating effect of adding colostrum to human milk or formula may relate to indirect effects via the developing gut microbiota, potentially via immunoglobulins, which, in turn, increase or decrease plasma amino acid levels so that the environment is more favourable to microbial growth (Jiang et al., 2022).Future studies are needed to investigate the ability of colostrum to regenerate a gut first exposed to a period of formula feeding (Brunse et al., 2019).

2.6.3 Poultry

Colostrum has been used as a feed additive in poultry production to maximize protein quality and growth performance and decrease feed costs (Playford and Weiser, 2021, Mehra et al., 2022). Studies have reported that supplementing the diet of broiler chickens with 2–5% colostrum/kg improved feed conversion efficiency, increased body weight, and reduced mortality rates compared to control diet groups (Afzal et al., 2017). In young broiler chickens (1–10 days old) under heat stress, colostrum feeding increased thigh and breast size (Afzal et al., 2017).

2.6.4 Fish

Colostrum and its constituents have shown encouraging results as a feed supplement in fish. Colostrum feeding to *Piaractus mesopotamicus* thickened muscle layers of the intestinal epithelium and increased nutrient absorption concentration of goblet cells and superoxide dismutase activity in the gut, indicating a protective effect on enteric cell protection (Moretti et al., 2019). Colostrum feeding also increased goblet cell concentrations in the enteric mucosa of *Salminus brasiliensis* (Nordi et al., 2016, da Cruz et al., 2016) Supplementation of bovine lactoferrin was shown to suppress the stress responses in Siberian sturgeon (Falahatkar et al., 2014)Bovine lactoferrin supplementation also enhanced immune function and disease resistance in Pacu and Dorado species (Machado-Neto et al., 2016).

2.6.5 Goats

Numerous authors have reported that colostrum products are an effective alternative to goat colostrum in newborn goat kids. Feeding bovine colostrum to newborn goat kids resulted in no difference in the enteric histology and histomorphometric features of the GI tract compared to feeding goat colostrum (Nordi et al., 2013). Interestingly, one study reported that the number of sialomucins, which have cytoprotective and antiadhesive effects, was higher in the jejunum epithelium of goat kids fed with lyophilised colostrum than in goat kids fed with goat colostrum (Machado-Neto et al., 2013).

2.6.6 Dogs

Several canine nutritional supplements and colostrum-based powdered dog foods are available (Beynen, 2020). Recently, weaned puppies fed diets supplemented with bovine colostrum demonstrated improved fecal scores when placed in a new environment that favored stress-related diarrhea (Giffard et al., 2004). Colostrum supplementation to 2–7-year-old huskies for 40 weeks increased fecal IgA levels compared to controls, suggesting enhanced gut-associated lymph tissue function (Satyaraj et al., 2013). Furthermore, these subjects responded to canine distemper virus (CDV) vaccination with higher plasma levels of anti-CDV IgG and had increased fecal microbiota diversity, suggesting positive effects on immune function and gut microbiome (Satyaraj et al., 2013). More recently, a pilot crossover trial in which male beagles were supplemented with 1 g of bovine colostrum per day for three weeks, in

addition to a set of four probiotic strains at 2.9×10^9 CFU, was associated with improvements in protein digestibility (Dequenne et al. 2014).

2.6.7 Cats

Kittens fed a diet containing 0.1% spray-dried bovine colostrum during the weaning period were shown to have increased fecal IgA expression and a faster and stronger antibody response to a rabies vaccine booster, indicative of better localised and systemic immune function, respectively (Gore et al., 2021). Supplementation also helped to maintain intestinal microbiota stability in kittens (Gore et al., 2021). These results show that colostrum supplementation can help strengthen the immune system and enhance the gut microbiota stability of growing kittens.

2.6.8 Horses

Colostrum has been explored to improve the immunological health and athletic performance of horses. Colostrum has been shown to be a suitable alternative for the transfer of passive immunity in (Holmes and Lunn, 1991). A bovine colostrum-based supplement was shown to significantly reduce the duration of respiratory disease in thoroughbred yearlings (Fenger et al., 2016). In addition, in a randomised crossover trial of racing thoroughbreds, colostrum supplementation led to better race performances and quicker returns to racing compared with controls (Fenger et al., 2014b). Colostrum supplementation in racehorses does not increase serum IGF-I concentrations; therefore, there are no regulatory concerns over its utilisation for athletic performance (Fenger et al., 2014a).

2.7 Future Challenges

Milk is already among the most versatile products in the food industry. World milk production was recorded at 823 million tons in 2017 and is expected to increase by 22% by 2027 (Marcel et al., 2018). This growing supply chain means that there will be more access to bovine colostrum for product manufacture. However, there are several issues to address in the manufacture of colostrum products to maximize its benefits for use in veterinary and human health.

2.7.1 Quality Control of Products

To interpret results from clinical trials accurately, especially when comparing results from different investigators, the colostrum products being used need appropriate

quality control. The quality of commercial colostrum products is usually accepted as involving the total protein and immunoglobulin concentrations with no specification to either individual growth factor concentrations or, of more value, total growth factor bioactivity. A recent study highlighted the severity of this issue, reporting up to sixfold differences in the bioactivity of 20 different commercial colostrum products (Playford, et al. 2020). These wide variations in bioactivity are of particular concern if colostrum is being used as a therapeutic agent for a medical condition, where consistency of the product is vital. Encouragingly, products that displayed high levels of bioactivity in this study had previously been shown to exert beneficial effects for numerous health applications (Playford, et al. 2020). If the bioactivity level of products was noted by researchers in their publications, it would be possible to determine dose-response profiles and establish the minimum efficacious dose of colostrum products.

2.7.2 Scaling Up of Polyclonal Antibody Production

Colostrum-derived polyclonal antibodies targeting pathogens, immune modulators, or cancerous cells continue to show promise, but to date this approach has been overtaken by the rapid development and cost reductions of monoclonal antibodies that have reshaped parts of the pharmaceutical industry. Bovine polyclonal antibodies have advantages, particularly considering direct targeting of disease in the lumen of the gut, but the developmental pathway, good manufacturing practices for repeatable potency, preclinical and clinical trials, and final regulatory approval remain challenging.

2.7.3 Measurement of Bioactive Constituents

At present, radial immunodiffusion (RID) is considered the gold standard for IgG detection but is slow and costly and cannot be performed in the field (Godden, et al. 2019). On-farm detection methods, such as refractometry, indirectly measure IgG and often overestimate actual concentrations (Godden, et al. 2019). As the composition of bovine colostrum is widely variable between individual cows, the development of rapid and accurate on-farm methods for the determination of colostrum quality will aid in the production and standardisation of high-quality colostrum products. One such example includes the recently developed split trehalase IgG quantification assay, which is comparable to RID testing and is compatible with on-farm application (Drikic, et al. 2018).

2.8 Conclusions and Future Perspectives

Bovine colostrum harbours a diverse array of bioactive components suitable for the development of functional foods, nutraceuticals, and pharmaceuticals with veterinary and human health applications. Increases in worldwide milk production and improving processing techniques indicate there is significant potential for expansion and growth in the colostrum-based products market. Studies in humans and animals have indicated benefits of colostrum-based products in the amelioration of disease states pertaining to all stages of life. At present, bovine colostrum is marketed as a health-food supplement and has better evidence across a wider range of applications than many of its competitors. However, colostrum products need to overcome several obstacles before consideration as pharmaceutical products. Stricter quality control, using methods such as bioassays, is imperative to accurately compare and interpret results from human clinical trials. Such assays would elucidate the dose-response effects in clinical settings, which is the norm for pharmaceutical products. Further studies are required to determine the effective dosages of colostrum products to elicit beneficial effects. Better-conducted clinical randomised control trials of colostrum supplementation are required, as systematic reviews of colostrum to date have been severely hampered by heterogeneous and poor-quality studies. Finally, more studies elucidating the mechanisms behind the beneficial effects of colostrum supplementation are needed.

2.9 Disclosure statement

The authors are not aware of any affiliations, memberships, funding, or financial holdings that might be perceived as affecting the objectivity of this review.

2.10 Acknowledgments

This research is supported by APC Microbiome Ireland, a research center funded by Science Foundation Ireland (SFI), through the Irish Government's National Development Plan (grant number 12/RC/2273_P2) and VISTAMILK [grant number 16/RC/3835].

2.11 References

ACKERMAN, T. E., BARNES, C. W., BRIGHT, A. C., HUFFMAN, D. C., KOCSIS, S. J., ROSKOS, K. E., PETER, G. R. S., SMITH, B. K., SZCZAP, J. P. & THÉNIN, M. R. 2019. Apparatus and method for spray drying. Google Patents.

AFZAL, I., KHAN, A. A., KHALIQ, T., HAMADANI, H., SHAFI, M. & RAJA, T. A. 2017. Effect of bovine colostrum supplemented diets on performance of broiler chicken.

ARSLAN, A., KAPLAN, M., DUMAN, H., BAYRAKTAR, A., ERTÜRK, M., HENRICK, B. M., FRESE, S. A. & KARAV, S. 2021. Bovine Colostrum and Its Potential for Human Health and Nutrition. Frontiers in Nutrition, 8.

AUNSHOLT, L., JEPPESEN, P. B., LUND, P., SANGILD, P. T., IFAOUI, I. B. R., QVIST, N. & HUSBY, S. 2014. Bovine colostrum to children with short bowel syndrome: a randomised, double-blind, crossover pilot study. Journal of Parenteral and Enteral Nutrition, 38, 99-106.

AUNSHOLT, L., QVIST, N., SANGILD, P. T., VEGGE, A., STOLL, B., BURRIN, D. G., JEPPESEN, P. B., ERIKSEN, T., HUSBY, S. & THYMANN, T. 2018. Minimal enteral nutrition to improve adaptation after intestinal resection in piglets and infants. Journal of Parenteral and Enteral Nutrition, 42, 446-454.

BERG, G., RYBAKOVA, D., FISCHER, D., CERNAVA, T., VERGÈS, M. C., CHARLES, T., CHEN, X., COCOLIN, L., EVERSOLE, K., CORRAL, G. H., KAZOU, M., KINKEL, L., LANGE, L., LIMA, N., LOY, A., MACKLIN, J. A., MAGUIN, E., MAUCHLINE, T., MCCLURE, R., MITTER, B., RYAN, M., SARAND, I., SMIDT, H., SCHELKLE, B., ROUME, H., KIRAN, G. S., SELVIN, J., SOUZA, R. S. C., VAN OVERBEEK, L., SINGH, B. K., WAGNER, M., WALSH, A., SESSITSCH, A. & SCHLOTER, M. 2020. Microbiome definition re-visited: old concepts and new challenges. Microbiome, 8, 103.

BEYNEN, A. 2020. Beynen AC, 2020. Bovine colostrum for dogs. 95-102.

BOLDOGH, I., AGUILERA-AGUIRRE, L., BACSI, A., CHOUDHURY, B. K., SAAVEDRA-MOLINA, A. & KRUZEL, M. 2008. Colostrinin decreases hypersensitivity and allergic responses to common allergens. International archives of allergy and immunology, 146, 298-306.

BONDUE, P., CRÈVECOEUR, S., BROSE, F., DAUBE, G., SEGHAYE, M.-C., GRIFFITHS, M. W., LAPOINTE, G. & DELCENSERIE, V. 2016. Cell-free spent media obtained from Bifidobacterium bifidum and Bifidobacterium crudilactis grown in media supplemented with 3′-sialyllactose modulate virulence gene expression in Escherichia coli O157: H7 and Salmonella typhimurium. Frontiers in Microbiology, 7, 1460.

BORAD, S. G. & SINGH, A. K. 2022. Immunoglobulins. In: MCSWEENEY, P. L. H. & MCNAMARA, J. P. (eds.) Encyclopedia of Dairy Sciences (Third Edition). Oxford: Academic Press.

BORAD, S. G., SINGH, A. K., KAPILA, S., BEHARE, P., ARORA, S. & SABIKHI, L. 2019. Influence of unit operations on immunoglobulins and thermal stability of colostrum fractions. International Dairy Journal, 93, 85-91.

BRUNSE, A., WORSØE, P., PORS, S. E., SKOVGAARD, K. & SANGILD, P. T. 2019. Oral Supplementation With Bovine Colostrum Prevents Septic Shock and Brain Barrier Disruption During Bloodstream Infection in Preterm Newborn Pigs. Shock, 51.

BUNYATRATCHATA, A., WEINBORN, V. & BARILE, D. 2021. Bioactive oligosaccharides in colostrum and other liquid feeds for calf's early life nutrition: A qualitative and quantitative investigation. International Dairy Journal, 121, 105100.

BURRIN, D., SANGILD, P. T., STOLL, B., THYMANN, T., BUDDINGTON, R., MARINI, J., OLUTOYE, O. & SHULMAN, R. J. 2020. Translational Advances in Pediatric Nutrition and Gastroenterology: New Insights from Pig Models. Annu Rev Anim Biosci, 8, 321-354.

BUTTAR, H. S., BAGWE, S. M., BHULLAR, S. K. & KAUR, G. 2017. Chapter 1 - Health Benefits of Bovine Colostrum in Children and Adults. In: WATSON, R. R., COLLIER, R. J. & PREEDY, V. R. (eds.) Dairy in Human Health and Disease Across the Lifespan. Academic Press.

CABRAL, R. G., CHAPMAN, C. E. & ERICKSON, P. S. 2013. REVIEW: Colostrum supplements and replacers for dairy calves11Partial funding was provided by the New Hampshire Agricultural Experiment Station. This is scientific contribution number 2503 of the New Hampshire Agricultural Experiment Station. This review is supported by the NC-1042 regional project. The Professional Animal Scientist, 29, 449-456.

CHATTERTON, D. E. W., AAGAARD, S., HESSELBALLE HANSEN, T., NGUYEN, D. N., DE GOBBA, C., LAMETSCH, R. & SANGILD, P. T. 2020. Bioactive proteins in bovine colostrum and effects of heating, drying and irradiation. Food Funct, 11, 2309-2327.

CHATTERTON, D. E. W., NGUYEN, D. N., BERING, S. B. & SANGILD, P. T. 2013. Anti-inflammatory mechanisms of bioactive milk proteins in the intestine of newborns. The international journal of biochemistry & cell biology, 45, 1730-1747.

CHELACK, B. J., MORLEY, P. S. & HAINES, D. M. 1993. Evaluation of methods for dehydration of bovine colostrum for total replacement of normal colostrum in calves. Can Vet J, 34, 407-12.

COFFEY, R. J., ROMANO, M. & GOLDENRING, J. 1995. Roles for transforming growth factor-alpha in the stomach. J Clin Gastroenterol, 21 Suppl 1, S36-9.

CONTARINI, G., POVOLO, M., PELIZZOLA, V., MONTI, L., BRUNI, A., PASSOLUNGO, L., ABENI, F. & DEGANO, L. 2014. Bovine colostrum: changes in lipid constituents in the first 5 days after parturition. J Dairy Sci, 97, 5065-72.

CUMMINS, C., BERRY, D. P., MURPHY, J. P., LORENZ, I. & KENNEDY, E. 2017. The effect of colostrum storage conditions on dairy heifer calf serum immunoglobulin G concentration and preweaning health and growth rate. Journal of dairy science, 100, 525-535.

CUMMINS, C., BERRY, D. P., SAYERS, R., LORENZ, I. & KENNEDY, E. 2016a. Questionnaire identifying management practices surrounding calving on spring-calving dairy farms and their associations with herd size and herd expansion. animal, 10, 868-877.

CUMMINS, C., LORENZ, I. & KENNEDY, E. 2016b. The effect of storage conditions over time on bovine colostral immunoglobulin G concentration, bacteria, and pH. Journal of dairy science, 99, 4857-4863.

CUTLER, T. D. & ZIMMERMAN, J. J. 2011. Ultraviolet irradiation and the mechanisms underlying its inactivation of infectious agents. Animal Health Research Reviews, 12, 15-23.

DA CRUZ, T. M. P., MORETTI, D. B., NORDI, W. M., CYRINO, J. E. P. & MACHADO-NETO, R. 2016. Intestinal epithelium of juvenile dourado Salminus brasiliensis (Cuvier, 1816) fed diet with lyophilised bovine colostrum. Aquaculture Research, 47, 561-569.

DAVISON, G. 2021. The Use of Bovine Colostrum in Sport and Exercise. Nutrients, 13.

DAVISON, G., JONES, A. W., MARCHBANK, T. & PLAYFORD, R. J. 2019. Oral bovine colostrum supplementation does not increase circulating insulin-like growth factor-1 concentration in healthy adults: results from short-and long-term administration studies. European Journal of Nutrition, 1-7.

DEQUENNE, M., ROBAYE, V., DOTREPPE, O., NEIZER, C., DELHALLE, L., THONART, P., BERTRAND, C., ROBERT, B., MOINET, B. & DIEZ, M. A supplement of bovine colostrum and probiotics increased protein digestibility in dogs but dit not influence microbiome. 2014.

DERAKHSHANI, H., PLAIZIER, J. C., DE BUCK, J., BARKEMA, H. W. & KHAFIPOUR, E. 2018. Composition of the teat canal and intramammary microbiota of dairy cows subjected to antimicrobial dry cow therapy and internal teat sealant. Journal of dairy science, 101, 10191-10205.

ELSOHABY, I., MCCLURE, J. T., DOW, N. & KEEFE, G. P. 2018. Effect of Heat-treatment on Accuracy of Infrared Spectroscopy and Digital and Optical Brix Refractometers for Measuring Immunoglobulin G Concentration in Bovine Colostrum. Journal of veterinary internal medicine, 32, 491-496.

FALAHATKAR, B., ESLAMLOO, K. & YOKOYAMA, S. 2014. Suppression of stress responses in Siberian sturgeon, Acipenser baeri, juveniles by the dietary administration of bovine lactoferrin. Journal of the World Aquaculture Society, 45, 699-708.

FASSE, S., ALARINTA, J., FRAHM, B. & WIRTANEN, G. 2021. Bovine Colostrum for Human Consumption—Improving Microbial Quality and Maintaining Bioactive Characteristics through Processing. Dairy, 2, 556-575.

FENGER, C., TOBIN, T., CASEY, P., LANGEMEIER, J. & HAINES, D. 2014a. Bovine colostrum supplementation does not influence serum insulin-like growth factor-1 in horses in race training. Journal of Equine Veterinary Science, 34, 1025-1027.

FENGER, C. K., TOBIN, T., CASEY, P. J., ROUALDES, E. A., LANGEMEIER, J. L., COWLES, R. & HAINES, D. M. 2016. Enhanced bovine colostrum supplementation shortens the duration of respiratory disease in thoroughbred yearlings. Journal of Equine Veterinary Science, 42, 77-81.

FENGER, C. K., TOBIN, T., CASEY, P. J., ROUALDES, E. A., LANGEMEIER, J. L. & HAINES, D. M. 2014b. Bovine colostrum supplementation optimises earnings, performance and recovery in racing Thoroughbreds. Comparative Exercise Physiology, 10, 233-238.

FILIPESCU, I. E., LEONARDI, L., MENCHETTI, L., GUELFI, G., TRAINA, G., CASAGRANDE-PROIETTI, P., PIRO, F., QUATTRONE, A., BARBATO, O. &

BRECCHIA, G. 2018. Preventive effects of bovine colostrum supplementation in TNBS-induced colitis in mice. PloS one, 13, e0202929.

FISCHER, A. J., SONG, Y., HE, Z., HAINES, D. M., GUAN, L. L. & STEELE, M. A. 2018. Effect of delaying colostrum feeding on passive transfer and intestinal bacterial colonization in neonatal male Holstein calves. Journal of dairy science, 101, 3099-3109.

FONG, B., MA, K. & MCJARROW, P. 2011. Quantification of bovine milk oligosaccharides using liquid chromatography–selected reaction monitoring–mass spectrometry. Journal of agricultural and food chemistry, 59, 9788-9795.

FOSTER, D. M., POULSEN, K. P., SYLVESTER, H. J., JACOB, M. E., CASULLI, K. E. & FARKAS, B. E. 2016. Effect of high-pressure processing of bovine colostrum on immunoglobulin G concentration, pathogens, viscosity, and transfer of passive immunity to calves. Journal of dairy science, 99, 8575-8588.

GAO, X., LI, Y., OLIN, A. B. & NGUYEN, D. N. 2021. Fortification With Bovine Colostrum Enhances Antibacterial Activity of Human Milk. JPEN J Parenter Enteral Nutr, 45, 1417-1424.

GAUTHIER, S. F., POULIOT, Y. & MAUBOIS, J.-L. 2006. Growth factors from bovine milk and colostrum: composition, extraction and biological activities. Le Lait, 86, 99-125.

GHOSH, S. & IACUCCI, M. 2021. Diverse immune effects of bovine colostrum and benefits in human health and disease. Nutrients, 13, 3798.

GIFFARD, C. J., SEINO, M. M., MARKWELL, P. J. & BEKTASH, R. M. 2004. Benefits of bovine colostrum on fecal quality in recently weaned puppies. The Journal of nutrition, 134, 2126S.

GODDEN, S. M., LOMBARD, J. E. & WOOLUMS, A. R. 2019. Colostrum Management for Dairy Calves. Vet Clin North Am Food Anim Pract, 35, 535-556.

GORE, A. M., SATYARAJ, E., LABUDA, J., ENGLER, R., SUN, P., KERR, W. & CONBOY-SCHMIDT, L. 2021. Supplementation of Diets With Bovine Colostrum Influences Immune and Gut Function in Kittens. Front Vet Sci, 8, 675712.

GRIFFITHS, C. E. M., CUMBERBATCH, M., TUCKER, S. C., DEARMAN, R. J., ANDREW, S., HEADON, D. R. & KIMBER, I. 2001. Exogenous topical lactoferrin inhibits allergen-induced Langerhans cell migration and cutaneous inflammation in humans. British Journal of Dermatology, 144, 715-725.

GUINÉ, R. 2018. The drying of foods and its effect on the physical-chemical, sensorial and nutritional properties. International Journal of Food Engineering, 2, 93-100.

HALAVACH, T., TARUN, E., DUDCHIK, N. V., ZHYGANKOV, V., ROMANOVICH, R. & ASAFOV, V. 2022. Functional value of fermented bovine colostrum.

HATMAL, M. M. M., AL-HATAMLEH, M. A. I., OLAIMAT, A. N., ALSHAER, W., HASAN, H., ALBAKRI, K. A., ALKHAFAJI, E., ISSA, N. N., AL-HOLY, M. A. & ABDERRAHMAN, S. M. 2022. Immunomodulatory Properties of Human Breast Milk: MicroRNA Contents and Potential Epigenetic Effects. Biomedicines, 10, 1219.

HAYES, M. M., HUGHES, T. A. & GREENE, A. K. 2012. Bacterial diversity in dried colostrum and whey sold as nutraceutical products. Journal of food science, 77, M359-M363.

HESAMI, S., SHAHRAKI, A.-D. F., ZAKIAN, A. & GHALAMKARI, G. 2020. The effect of various heat-treatment methods on colostrum quality, health and performance of dairy calves. Acta Scientiarum. Animal Sciences, 43.

HILL, C., GUARNER, F., REID, G., GIBSON, G. R., MERENSTEIN, D. J., POT, B., MORELLI, L., CANANI, R. B., FLINT, H. J. & SALMINEN, S. 2014. Expert consensus document: The International Scientific Association for Probiotics and Prebiotics consensus statement on the scope and appropriate use of the term probiotic. Nature reviews Gastroenterology & hepatology, 11, 506.

HOLMES, M. A. & LUNN, D. P. 1991. A study of bovine and equine immunoglobulin levels in pony foals fed bovine colostrum. Equine Veterinary Journal, 23, 116-118.

HONG, J. P. & PARK, S. W. 2014. The combined effect of recombinant human epidermal growth factor and erythropoietin on full-thickness wound healing in diabetic rat model. International wound journal, 11, 373-378.

INDYK, H. E., WILLIAMS, J. W. & PATEL, H. A. 2008. Analysis of denaturation of bovine IgG by heat and high pressure using an optical biosensor. International Dairy Journal, 18, 359-366.

ISMAIL, R. I. H., AWAD, H. A., IMAM, S. S., GAD, G. I., ABOUSHADY, N. M., ABDOU, R. M., EISSA, D. S., AZZAM, N. T., BARAKAT, M. M., YASSIN, M. M. & BARAKAT, N. M. 2021. Gut priming with bovine colostrum and T regulatory cells in preterm neonates: a randomised controlled trial. Pediatric Research, 90, 650-656.

JAY, J. M. 1998. High-temperature food preservation and characteristics of thermophilic microorganisms. Modern food microbiology. Springer.

JIANG, P. P., MUK, T., KRYCH, L., NIELSEN, D. S., KHAKIMOV, B., LI, Y., JUHL, S. M., GREISEN, G. & SANGILD, P. T. 2022. Gut colonization in preterm infants supplemented with bovine colostrum in the first week of life: An explorative pilot study. JPEN J Parenter Enteral Nutr, 46, 592-599.

JONES, A. W., MARCH, D. S., CURTIS, F. & BRIDLE, C. 2016. Bovine colostrum supplementation and upper respiratory symptoms during exercise training: a systematic review and meta-analysis of randomised controlled trials. BMC Sports Sci Med Rehabil, 8, 21.

JONES, A. W., MARCH, D. S., THATCHER, R., DIMENT, B., WALSH, N. P. & DAVISON, G. 2019. The effects of bovine colostrum supplementation on in vivo immunity following prolonged exercise: a randomised controlled trial. Eur J Nutr, 58, 335-344.

JUHL, S. M., YE, X., ZHOU, P., LI, Y., IYORE, E. O., ZHANG, L., JIANG, P., VAN GOUDOEVER, J. B., GREISEN, G. & SANGILD, P. T. 2018. Bovine colostrum for preterm infants in the first days of life: a randomised controlled pilot trial. Journal of pediatric gastroenterology and nutrition, 66, 471-478.

KADUCU, F. O., OKIA, S. A., UPENYTHO, G., ELFSTRAND, L. & FLORÉN, C. H. 2011. Effect of bovine colostrum-based food supplement in the treatment of HIV-associated diarrhea

in Northern Uganda: a randomised controlled trial. Indian Journal of Gastroenterology, 30, 270-276.

KANDASAMY, S. & NAVEEN, R. 2022. A review on the encapsulation of bioactive components using spray-drying and freeze-drying techniques. Journal of Food Process Engineering, e14059.

KANGRO, K., KURASHIN, M., GILDEMANN, K., SANKOVSKI, E., ZUSINAITE, E., LELLO, L. S., PERT, R., KAVAK, A., POIKALAINEN, V. & LEPASALU, L. 2021. Bovine colostrum derived antibodies against SARS-CoV-2 show great potential to serve as a prophylactic agent. medRxiv.

KAPLAN, M., ARSLAN, A., DUMAN, H., KARYELIOĞLU, M., BAYDEMIR, B., GÜNAR, B. B., ALKAN, M., BAYRAKTAR, A., TOSUN, H., ERTÜRK, M., ESKICI, G., DUAR, R. M., HENRICK, B. M., FRESE, S. A. & KARAV, S. 2021. Production of Bovine Colostrum for Human Consumption to Improve Health. Front Pharmacol, 12, 796824.

KECK, P. J., HAUSER, S. D., KRIVI, G., SANZO, K., WARREN, T., FEDER, J. & CONNOLLY, D. T. 1989. Vascular permeability factor, an endothelial cell mitogen related to PDGF. Science, 246, 1309-1312.

KHAN, Z., MACDONALD, C., WICKS, A. C., HOLT, M. P., FLOYD, D., GHOSH, S., WRIGHT, N. A. & PLAYFORD, R. J. 2002. Use of the 'nutriceutical', bovine colostrum, for the treatment of distal colitis: results from an initial study. Alimentary pharmacology & therapeutics, 16, 1917-1922.

KIM, J. W., JEON, W. K. & KIM, E. J. 2005. Combined effects of bovine colostrum and glutamine in diclofenac-induced bacterial translocation in rat. Clinical Nutrition, 24, 785-793.

KIRKDEN, R. D., BROOM, D. M. & ANDERSEN, I. L. 2013. Invited review: piglet mortality: management solutions. J Anim Sci, 91, 3361-89.

KOTSIS, Y., MIKELLIDI, A., ARESTI, C., PERSIA, E., SOTIROPOULOS, A., PANAGIOTAKOS, D. B., ANTONOPOULOU, S. & NOMIKOS, T. 2018. A low-dose, 6-week bovine colostrum supplementation maintains performance and attenuates inflammatory indices following a Loughborough Intermittent Shuttle Test in soccer players. Eur J Nutr, 57, 1181-1195.

KOVACS, D., MARESCA, V., FLORI, E., MASTROFRANCESCO, A., PICARDO, M. & CARDINALI, G. 2020. Bovine colostrum induces the differentiation of human primary keratinocytes. The FASEB Journal, 34, 6302-6321.

KRAUS, R. B., DOS SANTOS, P. R., KRUMMENAUER, A., PALHARES, K. E., LIMA, H. G. D., LADEIRA, S. R. L., PEREIRA, G. M., DORS, G. C., NASCENTE, P. D. S. & LUND, R. G. 2021. Bovine Colostrum Silage: Physicochemical and Microbiological Characteristics at Different Fermentation Times. Frontiers in Microbiology, 12.

KRUZEL, M. L., JANUSZ, M., LISOWSKI, J., FISCHLEIGH, R. V. & GEORGIADES, J. A. 2001. Towards an understanding of biological role of colostrinin peptides. Journal of Molecular Neuroscience, 17, 379-389.

LAGO, A., SOCHA, M., GEIGER, A., COOK, D., SILVA-DEL-RÍO, N., BLANC, C., QUESNELL, R. & LEONARDI, C. 2018. Efficacy of colostrum replacer versus maternal

colostrum on immunological status, health, and growth of preweaned dairy calves. Journal of dairy science, 101, 1344-1354.

LE MAUX, S., BOUHALLAB, S., GIBLIN, L., BRODKORB, A. & CROGUENNEC, T. 2014. Bovine β-lactoglobulin/fatty acid complexes: binding, structural, and biological properties. Dairy science & technology, 94, 409-426.

LI, J., XU, Y. W., JIANG, J. J. & SONG, Q. K. 2019. Bovine colostrum and product intervention associated with relief of childhood infectious diarrhea. Sci Rep, 9, 3093.

LI, S.-Q., ZHANG, H. Q., BALASUBRAMANIAM, V. M., LEE, Y.-Z., BOMSER, J. A., SCHWARTZ, S. J. & DUNNE, C. P. 2006. Comparison of effects of high-pressure processing and heat treatment on immunoactivity of bovine milk immunoglobulin G in enriched soymilk under equivalent microbial inactivation levels. Journal of agricultural and food chemistry, 54, 739-746.

LI, Y., JUHL, S. M., YE, X., SHEN, R. L., IYORE, E. O., DAI, Y., SANGILD, P. T. & GREISEN, G. O. 2017. A stepwise, pilot study of bovine colostrum to supplement the first enteral feeding in preterm infants (precolos): study protocol and initial results. Frontiers in pediatrics, 5, 42.

LOPEZ, A. J. & HEINRICHS, A. J. 2022a. Invited review: The importance of colostrum in the newborn dairy calf. Journal of Dairy Science, 105, 2733-2749.

LOPEZ, A. J. & HEINRICHS, A. J. 2022b. Invited review: The importance of colostrum in the newborn dairy calf. Journal of dairy science.

MACHADO-NETO, R., PONTIN, M. C. F., NORDI, W. M., LIMA, A. L. & MORETTI, D. B. 2013. Goblet cell mucin distribution in the small intestine of newborn goat kids fed lyophilised bovine colostrum. Livestock Science, 157, 125-131.

MACHADO-NETO, R., MORETTI, D. B., NORDI, W. M., DA CRUZ, T. M. P. & CYRINO, J. E. P. 2016. Growth performance of juvenile pacu (P iaractus mesopotamicus) and dourado (S alminus brasiliensis) fed with lyophilised bovine colostrum. Aquaculture Research, 47, 3551-3557.

MALMUTHUGE, N., CHEN, Y., LIANG, G. & GOONEWARDENE, L. A. 2015. Heat-treated colostrum feeding promotes beneficial bacteria colonization in the small intestine of neonatal calves. Journal of dairy science, 98, 8044-8053.

MANN, S., CURONE, G., CHANDLER, T. L., SIPKA, A., CHA, J., BHAWAL, R. & ZHANG, S. 2020. Heat treatment of bovine colostrum: II. Effects on calf serum immunoglobulin, insulin, and IGF-I concentrations, and the serum proteome. Journal of Dairy Science, 103, 9384-9406.

MARCEL, A., ENCISO, S. R. A., BOUBAKER, B.-B., JONATHAN, B., EMILY, C., CICERONE, G., KATIA, C., DE CAGNO, F., KOEN, D. & ANNELIES, D. 2018. OECD-FAO Agricultural Outlook 2018-2027. OECD-FAO Agricultural Outlook 2018-2027.

MARCH, D. S., JONES, A. W., THATCHER, R. & DAVISON, G. 2019. The effect of bovine colostrum supplementation on intestinal injury and circulating intestinal bacterial DNA following exercise in the heat. Eur J Nutr, 58, 1441-1451.

MARCH, D. S., MARCHBANK, T., PLAYFORD, R. J., JONES, A. W., THATCHER, R. & DAVISON, G. 2017. Intestinal fatty acid-binding protein and gut permeability responses to exercise. Eur J Appl Physiol, 117, 931-941.

MCGRATH, B. A., FOX, P. F., MCSWEENEY, P. L. H. & KELLY, A. L. 2016a. Composition and properties of bovine colostrum: a review. Dairy Science & Technology, 96, 133-158.

MCGRATH, B. A., FOX, P. F., MCSWEENEY, P. L. H. & KELLY, A. L. 2016b. Composition and properties of bovine colostrum: a review. Dairy Science & Technology, 96, 133-158.

MCKENNA, Z., BERKEMEIER, Q., NAYLOR, A., KLEINT, A., GORINI, F., NG, J., KIM, J. K., SULLIVAN, S. & GILLUM, T. 2017. Bovine colostrum supplementation does not affect plasma I-FABP concentrations following exercise in a hot and humid environment. Eur J Appl Physiol, 117, 2561-2567.

MEHRA, R., GARHWAL, R., SANGWAN, K., GUINÉ, R. P. F., LEMOS, E. T., BUTTAR, H. S., VISEN, P. K., KUMAR, N., BHARDWAJ, A. & KUMAR, H. 2022. Insights into the Research Trends on Bovine Colostrum: Beneficial Health Perspectives with Special Reference to Manufacturing of Functional Foods and Feed Supplements. Nutrients, 14.

MEHRA, R., SINGH, R., NAYAN, V., BUTTAR, H. S., KUMAR, N., KUMAR, S., BHARDWAJ, A., KAUSHIK, R. & KUMAR, H. 2021. Nutritional attributes of bovine colostrum components in human health and disease: A comprehensive review. Food Bioscience, 40, 100907.

MENCHETTI, L., CURONE, G., FILIPESCU, I. E., BARBATO, O., LEONARDI, L., GUELFI, G., TRAINA, G., CASAGRANDE-PROIETTI, P., RIVA, F. & CASANO, A. B. 2020. The Prophylactic Use of Bovine Colostrum in a Murine Model of TNBS-Induced Colitis. Animals, 10, 492.

MILES, E. A. & CALDER, P. C. 2017. The influence of the position of palmitate in infant formula triacylglycerols on health outcomes. Nutrition Research, 44, 1-8.

MIR, R., SINGH, N., VIKRAM, G., KUMAR, R. P., SINHA, M., BHUSHAN, A., KAUR, P., SRINIVASAN, A., SHARMA, S. & SINGH, T. P. 2009. The Structural Basis for the Prevention of Nonsteroidal Antiinflammatory Drug-Induced Gastrointestinal Tract Damage by the C-Lobe of Bovine Colostrum Lactoferrin. Biophysical Journal, 97, 3178-3186.

MORETTI, D. B., NORDI, W. M. & MACHADO-NETO, R. 2019. Redox balance and tissue development of juvenile Piaractus mesopotamicus subjected to high stocking density and fed dry diets containing nutraceutical food. Latin american journal of aquatic research, 47, 423-432.

MORRIN, S. T., LANE, J. A., MAROTTA, M., BODE, L., CARRINGTON, S. D., IRWIN, J. A. & HICKEY, R. M. 2019. Bovine colostrum-driven modulation of intestinal epithelial cells for increased commensal colonisation. Applied microbiology and biotechnology, 103, 2745-2758.

MORRIN, S. T., MCCARTHY, G., KENNEDY, D., MAROTTA, M., IRWIN, J. A. & HICKEY, R. M. 2020. Immunoglobulin G from bovine milk primes intestinal epithelial cells for increased colonization of bifidobacteria. AMB Express, 10, 1-10.

MORRISON, S. A., CHEUNG, S. S. & COTTER, J. D. 2014. Bovine colostrum, training status, and gastrointestinal permeability during exercise in the heat: a placebo-controlled double-blind study. Appl Physiol Nutr Metab, 39, 1070-82.

NEDEREND, M., VAN STIGT, A. H., JANSEN, J. H. M., JACOBINO, S. R., BRUGMAN, S., DE HAAN, C. A. M., BONT, L. J., VAN NEERVEN, R. J. J. & LEUSEN, J. H. W. 2020. Bovine IgG Prevents Experimental Infection With RSV and Facilitates Human T Cell Responses to RSV. Front Immunol, 11, 1701.

NORDI, W. M., MORETTI, D. B., DA CRUZ, T. M. P., CYRINO, J. E. P. & MACHADO-NETO, R. 2016. Enteric, hepatic and muscle tissue development of juvenile dourado Salminus brasiliensis fed with lyophilised bovine colostrum. Fisheries science, 82, 321-326.

NORDI, W. M., MORETTI, D. B., LIMA, A. L., PAULETTI, P., SUSIN, I. & MACHADO-NETO, R. 2013. Intestinal histology of newborn goat kids fed lyophilised bovine colostrum. Czech Journal of Animal Science, 58, 232-241.

O'CALLAGHAN, T. F., O'DONOVAN, M., MURPHY, J. P., SUGRUE, K., MANNION, D., MCCARTHY, W. P., TIMLIN, M., KILCAWLEY, K. N., HICKEY, R. M. & TOBIN, J. T. 2020. Evolution of the bovine milk fatty acid profile–From colostrum to milk five days post parturition. International Dairy Journal, 104, 104655.

Organ. Econ. Co-op. Dev. 2018. OECD-FAO Agricultural Outlook 2018–2027. Paris: OECD Publ. https://stats.oecd.org/Index.aspx?DataSetCode=HIGH_AGLINK_2018

O'RIORDAN, N., O'CALLAGHAN, J., BUTTÒ, L. F., KILCOYNE, M., JOSHI, L. & HICKEY, R. M. 2018. Bovine glycomacropeptide promotes the growth of Bifidobacterium longum ssp. infantis and modulates its gene expression. Journal of dairy science, 101, 6730-6741.

OTTO, W., NAJNIGIER, B., STELMASIAK, T. & ROBINS-BROWNE, R. M. 2011. Randomised control trials using a tablet formulation of hyperimmune bovine colostrum to prevent diarrhea caused by enterotoxigenic Escherichia coli in volunteers. Scandinavian journal of gastroenterology, 46, 862-868.

PAGNONCELLI, M. G. B., DO PRADO, F. G., MACHADO, J. M. C., ANSCHAU, A. & SOCCOL, C. R. 2022. Potential bovine colostrum for human and animal therapy. Current Developments in Biotechnology and Bioengineering, 377-395.

PAKYARI, M., FARROKHI, A., MAHARLOOEI, M. K. & GHAHARY, A. 2013. Critical Role of Transforming Growth Factor Beta in Different Phases of Wound Healing. Adv Wound Care (New Rochelle), 2, 215-224.

PANNARAJ, P. S., LY, M., CERINI, C., SAAVEDRA, M., ALDROVANDI, G. M., SABOORY, A. A., JOHNSON, K. M. & PRIDE, D. T. 2018. Shared and distinct features of human milk and infant stool viromes. Frontiers in microbiology, 9, 1162.

PEREIRA, R. V., BICALHO, M. L., MACHADO, V. S., LIMA, S., TEIXEIRA, A. G., WARNICK, L. D. & BICALHO, R. C. 2014. Evaluation of the effects of ultraviolet light on bacterial contaminants inoculated into whole milk and colostrum, and on colostrum immunoglobulin G. Journal of Dairy Science, 97, 2866-2875.

PLAYFORD, R. J., CATTELL, M. & MARCHBANK, T. 2020. Marked variability in bioactivity between commercially available bovine colostrum for human use; implications for clinical trials. PLoS One, 15, e0234719.

PLAYFORD, R. J., MACDONALD, C. E., CALNAN, D. P., FLOYD, D. N., PODAS, T., JOHNSON, W., WICKS, A. C., BASHIR, O. & MARCHBANK, T. 2001. Co-administration of the health food supplement, bovine colostrum, reduces the acute non-steroidal anti-inflammatory drug-induced increase in intestinal permeability. Clin Sci (Lond), 100, 627-33.

PLAYFORD, R. J. & WEISER, M. J. 2021. Bovine colostrum: its constituents and uses. Nutrients, 13, 265.

PONTOPPIDAN, P. E. L., SHEN, R. L., CILIEBORG, M. S., JIANG, P., KISSOW, H., PETERSEN, B. L., THYMANN, T., HEILMANN, C., MÜLLER, K. & SANGILD, P. T. 2015. Bovine Colostrum Modulates Myeloablative Chemotherapy–Induced Gut Toxicity in Piglets. The Journal of Nutrition, 145, 1472-1480.

RASMUSSEN, S. O., MARTIN, L., ØSTERGAARD, M. V., RUDLOFF, S., LI, Y., ROGGENBUCK, M., BERING, S. B. & SANGILD, P. T. 2016. Bovine colostrum improves neonatal growth, digestive function, and gut immunity relative to donor human milk and infant formula in preterm pigs. Am J Physiol Gastrointest Liver Physiol, 311, G480-91.

RATTRAY, M. 2005. Technology evaluation: colostrinin, ReGen. Current opinion in molecular therapeutics, 7, 78-84.

ROBBERS, L., JORRITSMA, R., NIELEN, M. & KOETS, A. 2021. A Scoping Review of On-Farm Colostrum Management Practices for Optimal Transfer of Immunity in Dairy Calves. Frontiers in Veterinary Science, 8.

ROY, D., YE, A., MOUGHAN, P. J. & SINGH, H. 2020. Composition, structure, and digestive dynamics of milk from different species—A review. Frontiers in Nutrition, 7, 577759.

SALES-CAMPOS, H., SOUZA, P. R., PEGHINI, B. C., DA SILVA, J. S. & CARDOSO, C. R. 2013. An overview of the modulatory effects of oleic acid in health and disease. Mini Rev Med Chem, 13, 201-10.

SATS, A., KAART, T., POIKALAINEN, V., AARE, A., LEPASALU, L., ANDRESON, H. & JÕUDU, I. 2020. Bovine colostrum whey: Postpartum changes of particle size distribution and immunoglobulin G concentration at different filtration pore sizes. Journal of Dairy Science, 103, 6810-6819.

SATS, A., YURCHENKO, S., KAART, T., TATAR, V., LUTTER, L. & JÕUDU, I. 2022. Bovine colostrum: Postpartum changes in fat globule size distribution and fatty acid profile. Journal of Dairy Science, 105, 3846-3860.

SATYARAJ, E., REYNOLDS, A., PELKER, R., LABUDA, J., ZHANG, P. & SUN, P. 2013. Supplementation of diets with bovine colostrum influences immune function in dogs. British Journal of Nutrition, 110, 2216-2221.

SCAMMELL, A. W. & BILLAKANTI, J. 2022. Colostrum. In: MCSWEENEY, P. L. H. & MCNAMARA, J. P. (eds.) Encyclopedia of Dairy Sciences (Third Edition). Oxford: Academic Press.

SHARMA, D., KAUR, A., FARAHBAKHSH, N. & AGARWAL, S. 2020. Role of Oropharyngeal Administration of Colostrum in Very Low Birth Weight Infants for Reducing Necrotizing Enterocolitis: A Randomised Controlled Trial. Am J Perinatol, 37, 716-721.

SIENKIEWICZ, M., SZYMAŃSKA, P. & FICHNA, J. 2021. Supplementation of Bovine Colostrum in Inflammatory Bowel Disease: Benefits and Contraindications. Advances in Nutrition, 12, 533-545.

SPALINGER, M. R., ATROTT, K., BAEBLER, K., SCHWARZFISCHER, M., MELHEM, H., PERES, D. R., LALAZAR, G., ROGLER, G., SCHARL, M. & FREY-WAGNER, I. 2019. Administration of the hyper-immune bovine colostrum extract IMM-124E ameliorates experimental murine colitis. Journal of Crohn's and Colitis, 13, 785-797.

STELWAGEN, K., CARPENTER, E., HAIGH, B., HODGKINSON, A. & WHEELER, T. T. 2009. Immune components of bovine colostrum and milk. Journal of animal science, 87, 3-9.

SUN, J., LI, Y., PAN, X., NGUYEN, D. N., BRUNSE, A., BOJESEN, A. M., RUDLOFF, S., MORTENSEN, M. S., BURRIN, D. G. & SANGILD, P. T. 2019. Human Milk Fortification with Bovine Colostrum Is Superior to Formula-Based Fortifiers to Prevent Gut Dysfunction, Necrotizing Enterocolitis, and Systemic Infection in Preterm Pigs. JPEN J Parenter Enteral Nutr, 43, 252-262.

SUN, Q., CHEN, X., YU, J., ZEN, K., ZHANG, C. Y. & LI, L. 2013. Immune modulatory function of abundant immune-related microRNAs in microvesicles from bovine colostrum. Protein Cell, 4, 197-210.

SYDNEY, A. C. N., IKEDA, I. K., DE OLIVEIRA RIBEIRO, M. C., SYDNEY, E. B., DE CARVALHO NETO, D. P., KARP, S. G., RODRIGUES, C. & SOCCOL, C. R. 2022. Colostrum new insights: products and processes. Current Developments in Biotechnology and Bioengineering. Elsevier.

TANIDEH, N., ABDORDIDEH, E., YOUSEFABAD, S. L. A., DANESHI, S., HOSSEINABADI, O. K. & SAMANI, S. M. 2017. Evaluation of the healing effect of honey and colostrum in treatment of cutaneous wound in rat. Comparative Clinical Pathology, 26, 71-77.

TAO, J., MAO, J., YANG, J. & SU, Y. 2020. Effects of oropharyngeal administration of colostrum on the incidence of necrotizing enterocolitis, late-onset sepsis, and death in preterm infants: a meta-analysis of RCTs. European Journal of Clinical Nutrition, 74, 1122-1131.

TEN BRUGGENCATE, S. J. M., BOVEE-OUDENHOVEN, I. M. J., FEITSMA, A. L., VAN HOFFEN, E. & SCHOTERMAN, M. H. C. 2014. Functional role and mechanisms of sialyllactose and other sialylated milk oligosaccharides. Nutrition Reviews, 72, 377-389.

TSIOULPAS, A., GRANDISON, A. S. & LEWIS, M. J. 2007. Changes in physical properties of bovine milk from the colostrum period to early lactation. Journal of dairy science, 90, 5012-5017.

ULFMAN, L. H., LEUSEN, J. H. W., SAVELKOUL, H. F. J., WARNER, J. O. & VAN NEERVEN, R. J. 2018. Effects of bovine immunoglobulins on immune function, allergy, and infection. Frontiers in nutrition, 5, 52.

USUGA, A., ZABALA, D. A., MEDINA, L. C., HERNANDEZ, D. V., RAMIREZ, W. V. & ROJANO, B. A. 2022. Effect of three storage methods on physical and chemical properties of colostrum from Bos indicus cows. Ciência Rural, 52.

UUSKÜLA, A., KEIS, A., TOOMPERE, K., PLANKEN, A. & REBROV, K. 2022. Cluster randomised, controlled, triple-blind trial assessing the efficacy of intranasally administered virus-neutralising bovine colostrum supplement in preventing SARS-CoV-2 infection in household contacts of SARS-CoV-2-positive individuals: a study protocol. Trials, 23, 92.

VAN HESE, I., GOOSSENS, K., VANDAELE, L. & OPSOMER, G. 2020. Invited review: MicroRNAs in bovine colostrum—Focus on their origin and potential health benefits for the calf. Journal of dairy science, 103, 1-15.

VASQUEZ, A., NYDAM, D., FODITSCH, C., WARNICK, L., WOLFE, C., DOSTER, E. & MORLEY, P. S. 2022. Characterization and comparison of the microbiomes and resistomes of colostrum from selectively treated dry cows. Journal of Dairy Science, 105, 637-653.

WEINBORN, V., LI, Y., SHAH, I. M., YU, H., DALLAS, D. C., GERMAN, J. B., MILLS, D. A., CHEN, X. & BARILE, D. 2020. Production of functional mimics of human milk oligosaccharides by enzymatic glycosylation of bovine milk oligosaccharides. International dairy journal, 102, 104583.

WILMS, J. N., HARE, K. S., FISCHER-TLUSTOS, A. J., VAHMANI, P., DUGAN, M. E. R., LEAL, L. N. & STEELE, M. A. 2022. Fatty acid profile characterization in colostrum, transition milk, and mature milk of primi-and multiparous cows during the first week of lactation. Journal of Dairy Science.

WOLFSON, L. M. & SUMNER, S. S. 1993. Antibacterial activity of the lactoperoxidase system: a review. Journal of Food Protection, 56, 887-892.

YAMAMOTO, M., MURANISHI, H., INAGAKI, M., UCHIDA, K., YAMASHITA, K., SAITO, S., YABE, T. & KANAMARU, Y. 2013. Skimmed, sterilised, and concentrated bovine late colostrum promotes both prevention and recovery from intestinal tissue damage in mice. Journal of dairy science, 96, 1347-1355.

YAN, X., SANGILD, P. T., PENG, Y., LI, Y., BERING, S. B. & PAN, X. 2021. Supplementary Bovine Colostrum Feedings to Formula-Fed Preterm Pigs Improve Gut Function and Reduce Necrotizing Enterocolitis. Journal of Pediatric Gastroenterology and Nutrition, 73, e39-e46.

YANG, B., CHEN, H., STANTON, C., ROSS, R. P., ZHANG, H., CHEN, Y. Q. & CHEN, W. 2015. Review of the roles of conjugated linoleic acid in health and disease. Journal of Functional Foods, 15, 314-325.

YEOMAN, C. J., ISHAQ, S. L., BICHI, E., OLIVO, S. K., LOWE, J. & ALDRIDGE, B. M. 2018. Biogeographical differences in the influence of maternal microbial sources on the early successional development of the bovine neonatal gastrointestinal tract. Scientific reports, 8, 1-14.

YI, Y.-S. 2016. Functional role of milk fat globule-epidermal growth factor VIII in macrophage-mediated inflammatory responses and inflammatory/autoimmune diseases. Mediators of inflammation, 2016.

ZABŁOCKA, A., SOKOŁOWSKA, A., MACAŁA, J., BARTOSZEWSKA, M., MITKIEWICZ, M., JANUSZ, M., WILUSZ, T. & POLANOWSKI, A. 2020. Colostral proline-rich polypeptide complexes. Comparative study of the antioxidant properties, cytokine-inducing activity, and nitric oxide release of preparations produced by a laboratory and a large-scale method. International Journal of Peptide Research and Therapeutics, 26, 685-694.

ZHAO, X., XU, X.-X., LIU, Y., XI, E.-Z., AN, J.-J., TABYS, D. & LIU, N. 2019. The in vitro protective role of bovine lactoferrin on intestinal epithelial barrier. Molecules, 24, 148.

Chapter 3

3 The Oral Placenta Infant Microbiota Study (OPIuM Study)

3.1 Abstract

The initial formation of the infant microbiota is crucial for preserving intestinal homeostasis and symbiosis in neonates, nurturing the development of the immune and nervous systems during a critical developmental stage. While the specific mechanisms are not yet fully understood, the current consensus is that a disturbed microbiota during infancy can have a lasting impact on health in early life and beyond. Extensive research exists on the human microbiome. However, a number of outstanding questions remain regarding the infant microbiome in the initial stages of life. In this study, using a cohort of 18 healthy mother-infant dyads, we characterised the microbiota composition of three potential maternal sources of microbial transmission (oral, vaginal and placental) to the microbiota of their new-born infant (oral and meconium microbiota). This allowed us to investigate the contribution of numerous transmission routes and the impact of various perinatal factors on the initial establishment of the infant gut and oral microbiome. Our results consolidate and corroborate recent findings surrounding the existence of a meconium microbiome and the absence of a placental microbiome. We show that significant vertical transfer, primarily from the maternal oral cavity the infant oral cavity occurs in early life. Moreover, we were able to provide further evidence on how perinatal factors influence the microbial bond between mother and infant and the establishment of the infant microbiome.

3.2 Introduction

The human microbiome is composed of microbial communities encompassing multiple divisions of the tree of life, including protozoa, fungi, viruses and prokaryota, inhabiting any accessible area of the human body. The defined niches with stable communities in humans and other mammals are currently generalised to the respiratory system (Lloyd and Marsland, 2017), nasal (Liu et al., 2015) and oral cavities (Dewhirst et al., 2010), skin (Byrd et al., 2018), vagina (Lamont et al., 2011), urinary tract (Neugent et al., 2020), and the gastrointestinal system (Ruan *et* al., 2020). The significance of these microscopic communities in the health and disease status of their macroscopic hosts has been well established (Wirbel et al., 2019). An individual's microbiome is a chimeric organ and a constant companion from birth to death (Clarke et al., 2014b, Evans et al., 2013, Possemiers et al., 2011, Eckburg et al., 2005). The initial formation of the infant microbiota is crucial for preserving intestinal homeostasis and symbiosis in neonates, nurturing the development of the immune and nervous systems during a critical developmental stage (Clarke et al., 2014a, Vemuri and Herath, 2023). While the specific mechanisms are not yet fully understood, the current consensus is that a disturbed microbiota during infancy can have a lasting impact on health status in early life and beyond (Fouhy et al., 2019). For instance, aberrant establishment of the infant gut microbiome increases the risk of colonisation by opportunistic pathogens, such as *Enterococcus*, *Enterobacter*, *Clostridium*, and *Klebsiella* species (Lax et al., 2017, O'Neill et al., 2020). Furthermore, infant gut dysbiosis can lead to impaired growth and an increased risk of sepsis and necrotizing enterocolitis (NEC), particularly in preterm new-borns (Fundora et al., 2020). Imbalances in the early life microbiome also appear to influence the development of emotional behaviour, stress and pain modulation systems and brain neurotransmitter systems (Morais et al., 2020). Long-term effects of disrupted initial microbial colonisation include allergies, asthma, metabolic syndrome, diabetes and inflammatory bowel disease (Milani et al., 2017).

The infant microbiome undergoes significant and rapid shifts in microbial diversity and functionality in the initial stages of life (Mackie et al., 1999, Matamoros et al., 2013). At present, it is exceptionally challenging to define a universally accepted 'gold standard' for the assembly and development of infant microbiome. However, with increases in cohort sample sizes, advancements in sequencing technologies and

evolving bioinformatic analysis tools, non-random and predictable patterns are emerging (Charbonneau et al., 2016, Rao et al., 2021, Derrien et al., 2019, Stewart et al., 2018, Yatsunenko et al., 2012, Bäckhed et al., 2015, Lim et al., 2015, Palmer et al., 2007, Vatanen et al., 2019). For instance, despite large variance at the intra-individual level, a recent multi-population cohort meta-analysis, revealed the existence of specific taxonomic patterns or infant community state types (ICSTs) (Mancabelli et al., 2020). This study subdivided ICSTs into four macro groups, < 1 month of age, between 1 and 6 months of age, between 6 and 12 months of age and between 1 and 3 years of age. Higher microbial complexity in samples from infants aged between 12 and 36 months compared to those from children less than one-month-old was observed. Overall, *Lactobacillus*, *Enterobacter*, *Escherichia*, *Bacteroides*, *Parabacteroides* and *Prevote lla* are believed to be the pioneering bacterial species which colonise the infants gut, mouth and skin (Shen et al., 2023, Li et al., 2023, Zeng et al., 2022). These microbes engage in a plethora of host biological responses, essential for the health and wellbeing of the neonate including the regulation of immunity (Gensollen et al., 2016), energy homeostasis, protection against pathogens and bioactive metabolite production (Nguyen et al., 2021). Specific functions include saccharolytic degradation of diet-derived glycans and host-provided carbohydrates, known as host glycans, including mucins and human milk oligosaccharides (HMOs) (Alessandri et al., 2021). Bioactive metabolites produced by these microbes include short-chain fatty acids (SCFAs), γ-aminobutyric acid (GABA), serotonin, conjugated linoleic acid (CLA) and Group B vitamins (B1, B2, B3, B5, B6, B7, B9, B12) (Alessandri et al., 2021, Wiley et al., 2021, Yoshii et al., 2019).

A crucial topic of study pertaining to the infant microbiome is the exact timing of microbial colonisation. At present the initial microbial colonisation of humans remains controversial (Kennedy et al., 2022). Numerous studies in recent years have explored the presence of live microorganisms within the prenatal intrauterine environment (placenta, amniotic fluid, fetus, and meconium), reaching irreconcilable conclusions (Bolte et al., 2022, Kennedy et al., 2022). Microbiome studies of the *in utero* environment highlight numerous limitations of current next-generation sequencing (NGS) methodologies. Contamination (de Goffau et al., 2018) or the "kitome" (Olomu et al., 2020) represent major issues when NGS and PCR-based

approaches are applied to low-biomass samples, such as those encountered in the *in utero* environment (Bushman, 2019). Without stringent controls and method standardisation, these methodologies will amplify any DNA present in the sampled environment, regardless of bacterial viability (Amos et al., 2020), thus, inaccurately reflecting the microbiota present in the sample (Fricke and Ravel, 2021). Interestingly, neonates born at term are not immunologically naive and are specifically adapted to cope with abrupt exposure to microbial, dietary and environmental stimuli (Hornef and Torow, 2020, Torow et al., 2017). However, our mechanistic understanding of how and when immune priming by microorganisms occurs, and the factors that drive it, is incomplete (Kennedy et al., 2022). Studies to date investigating the *in utero* environment have typically focussed on interrogating one sample at a time, without consideration of the impact of perinatal factors. In light of this information, understanding when microbial colonisation occurs in the infant is essential for our understanding of human immune development, and will allow us to optimise clinical therapeutic interventions and to illustrate common pitfalls in the microbial analyses of many other low-biomass environments (Kennedy et al., 2022).

The first encounters of the neonate with microbes represents the *de novo* assembly of a complex microbial community (Linehan et al., 2022). Strain levels analyses have indicated that the majority of these microbes are acquired through vertical transfer from mother to infant via multiple different pathways (Yassour et al., 2018, Wampach et al., 2018, Ferretti et al., 2018). Studies to date indicate that the maternal gut is the primary source of infant microbial seeding, followed by skin, the tongue dorsum, vagina and breast milk (Browne et al., 2022, Wang et al., 2020b). The formation of the infant microbiome is further directed by intrinsic and extrinsic factors, collectively named "perinatal factors" (Wang et al., 2020a). These include mode of delivery (Hill et al., 2017), gestational age at birth (Fouhy et al., 2019), feeding type (Bezirtzoglou et al., 2011), maternal health status (Collado et al., 2010) and exposure to intrapartum and postnatal antibiotics (Tapiainen et al., 2019). For instance, vaginally delivered infants are primarily exposed to microbes of the mother's birth canal (*Lactobacillus*, *Prevotella* and *Sneathia*) and intestinal microbiota (*Bacteroides*, *Escherichia, Bifidobacterium,* and *Parabacteroides*) (Li et al., 2020, Wampach et al., 2018), whereas, C-section (CS) delivery removes the infant's exposure to maternal intestinal and vaginal microbes, thus blocking vertical

transmission, disrupting community establishment in all body sites and is the perinatal factor with the most uniform effects on the infant gut microbiota across individuals and studies (Korpela, 2021). CS born infants typically have lowered relative abundance of highly beneficial microbes such as *Bifidobacterium* and *Bacteroides* (Korpela, 2021). CS born infants also display higher relative abundances of endemic opportunistic pathogens common to maternal skin and hospital environment such as *Enterococcus*, *Staphylococcus*, *Streptococcus*, *Klebsiella*, *Enterobacter*, *Propionibacterium*, and *Clostridium* (Shaterian et al., 2021). The microbiome of vaginally born, exclusively breastfed infants at term, with no previous exposure to antibiotics either directly or indirectly from the mother, could be considered the 'gold standard' (Warda et al., 2022). By contrast, antibiotic exposure, C-section (CS) birth or formula feeding are known to be associated with altered gut microbiome compared with 'gold standard' babies, and this may be associated with poorer health status in early and later life (Kuperman and Koren, 2016).

While extensive research exists on the human microbiome, a number of outstanding questions remain regarding the infant microbiome in the initial stages of life (Wang et al., 2020b). In this study we aimed to investigate three research questions highlighted in the review article by (Wang et al., 2020b). Firstly, is the intrauterine environment sterile, and what is the exact timing of the first microorganisms colonizing the human, that is, during pregnancy or after birth? Secondly, what is the contribution of each main maternal microbial source (gut, breast milk, vagina, skin, and oral cavity) to their offspring? Thirdly, what are the potential drivers that control species inheritance and/or selection by infants in early life? To answer these questions, we focussed on three potential maternal sources of microbial transmission (oral, vaginal and placental) to the microbiota of their new-born infant (oral and meconium microbiota) and sought to investigate the contribution of numerous transmission routes and the impact of numerous perinatal factors on the initial establishment of the infant gut and oral microbiome.

3.3 Materials and Methods

3.3.1 Study Design, Ethics and Recruitment

Subjects were recruited and clinically investigated at Cork University Maternity Hospital (CUMH). The study design was to recruit healthy mothers and their full term infants naturally born (NB) or via CS, for sampling in the first few days post-partum. A total of 63 mother-infant dyads were recruited between November 2015 and February 2019 at CUMH as part of the Oral Placenta Infant Microbiota Study (OPIuM Study). Ethical approval was obtained from the Cork Teaching Hospitals Clinical Research Ethics Committee (ethical approval reference: ECM 4 (v) 12/08/14). Information about the infants was collected at delivery using medical records. Exclusion criteria included infants born <35 weeks gestation, infants admitted to the neonatal intensive care unit (NICU) and ill mothers. For the purposes of this analysis, we included a subset of 18 mother-infant dyads for whom all five types of samples were collected, i.e. vaginal, mother saliva, placenta, infant saliva and infant meconium that were available. The clinical characteristics of these 18 mother-infant dyads are shown in Table 3.1. None of the infants included in this subset were treated with antibiotics.

3.3.2 Sample Collection

A CatchAll™ collection swab (Cambio, UK) with a hard pack for storage after collection was used to collect all vaginal and oral cavity (saliva) samples (Hurley et al., 2019). For vaginal samples, the midwife or gynaecologist collected mid-vaginal samples from the mother within one hour before delivery, samples were immediately placed on dry ice and stored at −80°C. Placenta samples were collected within one hour of delivery by obstetricians. Four cross-sectional samples were randomly excised using sterile gloves and surgical instruments from each placenta to incorporate both the maternal and fetal sides. Placental samples were immediately placed on dry ice and stored at −80°C. Saliva samples from the mother were collected using a CatchAll™ collection swab, from pooled saliva within the floor of the oral cavity within 24 h of the infant being delivered, placed on dry ice and stored −80°C. Saliva samples from the infant were collected from the oral cavity using a CatchAll™ collection swab within 4 days of delivery. Meconium samples were collected from infants within 4 days of delivery. Meconium samples were analysed for colour and

texture and only samples that had typical meconium characteristics (dark colour, sticky and tar-like) were considered for this study. Meconium and infant saliva samples collected at the hospital were immediately placed on dry ice, and stored at −80°C. Meconium and infant saliva samples collected at home by the mother were placed at 4°C, before collection in a temperature-controlled transport collection case by the research nurse for transport to the laboratory for long term storage at −80°C.

3.3.3 DNA Extractions

Extraction of DNA from samples collected via swabbing (vagina and saliva/oral cavity) was carried out using the MO BIO PowerSoil DNA Isolation kit (Qiagen), using a CatchAll™ collection swab rather than a soil sample as previously described (Hurley et al., 2019, Dominguez-Bello et al., 2010a). The sample (vagina and saliva/oral cavity) was contained in a CatchAll™ collection swab on the end of a collection tube, which was thawed before processing. The tube was cut 1 cm above this swab, and this was inserted into the PowerBead Pro tubes containing 600 µl of solution C1. Samples were then homogenised for 3 mins at maximum speed using the Mini Beadbeater (BioSpec). Samples were incubated at 65°C for 10 mins to lyse the cells. The remainder of the protocol was followed as per manufacturer's instructions. DNA was eluted in 50 µl solution C6. DNA was extracted from meconium samples using the repeated bead-beating plus column protocol as described by (Yu and Morrison, 2004) in combination with the QIAamp Fast DNA Stool Mini kit (Qiagen, UK) described by Fouhy et al. (Fouhy et al., 2015). Briefly, 1 ml of lysis buffer (500mM NaCl, 50mM Tris-HCl pH 8.0, 50mM EDTA and 4% (w/v) sodium dodecyl sulphate) was added to the bead beating tubes containing 0.25g of meconium sample. Samples were homogenised for 3 mins at maximum speed using the Mini Beadbeater (BioSpec). Samples were incubated at 70°C for 15 mins to lyse the cells and then centrifuged at 4°C for five min at 16,000 x g. Following centrifugation the supernatant was removed and the bead beating steps were repeated. Following pooling of the supernatant, samples were treated with ammonium acetate (Sigma Aldrich, Ireland) and then the DNA was pelleted and washed with 70% ethanol. The DNA was then treated with RNAse and proteinase K. Finally the DNA was washed using buffers AW1 and AW2 (QIAmp Fast DNA Stool Mini kit; Qiagen, UK) and eluted in 50 µl of buffer AE. DNA extractions for placenta samples was performed using the DNeasy Blood and Tissue Kit (QIAGEN) (Parnell et al., 2017). Briefly, 0.25g of frozen tissue

samples were cut into small pieces using sterile scalpels and were suspended in 2 ml screw cap microcentrifuge tubes containing 180 µl tissue lysis butter (ALT) and 1 sterile, 5 mm stainless steel bead (QIAGEN, Cat No: 69989). Tissues were homogenised at a frequency (1/s) of 30 for 20 sec using the Tissuelyser II (QIAGEN). 20 µl of proteinase K (20 mg/ml) was added to each sample and incubated at 56°C in a shaking incubator. Samples were vortex mixed every 30 mins to ensure complete lysis of the tissue. The remainder of the protocol was followed as per manufacturer's instructions. DNA was eluted in 50 µl of buffer AE. An extraction control consisting of 250 µl sterile molecular biology grade water (CORNING) was used for each sample studied. The quantity of DNA from every sample was measured by the Qubit™ 4 Fluorometer (Thermo Fisher Scientific, Waltham, MA, USA) using dsDNA HS assay Kit (Thermo Fisher Scientific). The limit of detection was 10 pg/µl. All extracted DNA was stored at −30°C.

3.3.4 16S rRNA gene amplification and MiSeq sequencing

Using the 16S metagenomic sequencing library protocol (Illumina), the V3-V4 hypervariable region of the 16S rRNA gene was amplified from 90 DNA samples. A no-sample (buffer only) DNA extraction blank for every sample type studied and no-template, negative-control sample for every sequencing library was prepared. DNA was amplified with primers specific to the V3-V4 region; forward primer 5' TCGTCGGCAGCGTCAGATGTGTATAAGAGACAGCCTACGGGNGGCWGCAG; and reverse primer 5' GTCTCGTGGGCTCGGAGATGTGTATAAGAGACAGGACTACHVGGGTATCTAATCC. Each PCR reaction contained template DNA (5 ng/µl), 1 µl forward primer (5 µM), 1 µl reverse primer (5 µM), 12.5 µl 2X KAPA2G Robust HotStart ReadyMix (Anachem, Dublin, Ireland) and PCR grade water. PCR conditions for amplification consisted of heated lid 110°C, initial denaturation at 95 °C × 3 min, 30 cycles of 95°C × 30 s, 55°C × 30 s, 72°C × 30 s, followed by 72°C × 5 min and holding at 4°C. PCR amplicons were visualised using gel electrophoresis (1X TAE buffer, 1.5% agarose, 100 V) stained with SYBR safe (Thermofisher, MA, USA). Amplicons were cleaned using AMPure XP magnetic bead based purification (Labplan, Dublin, Ireland) and subject to a second PCR reaction. Illumina sequencing adapters and dual-index barcodes (Illumina Nextera XT indexing primers, Illumina, Sweden) were added to the purified DNA (5 µl) to index each of the samples, allowing the library to be

pooled for sequencing as outlined in the Illumina library preparation protocol. Samples were quantified using the Qubit™ 3.0 Fluorometer using dsDNA HS assay Kit and samples were then pooled in an equimolar fashion. The pooled sample was run on the Agilent Bioanalyser for quality analysis prior to sequencing. The sample pool was prepared following Illumina guidelines. Samples were sequenced on the MiSeq sequencing platform in the Teagasc Sequencing facility, using a 2 × 300 cycle V3 kit, following standard Illumina sequencing protocols.

3.3.5 Bioinformatics analysis

Raw sequence quality was assessed using Multiqc (v1.9) before filtering and trimming. Primers were trimmed from FASTQ files using Cutadapt (v2.10) (Martin, 2011). The DADA2 library (v1.14) in R (v4.1.2) was used to derive amplicon sequence variants (ASVs) (Callahan et al., 2016a). Quality filtering, dereplication, error modelling, denoising, pair merging, and chimera removal were performed using default parameters. ASVs were taxonomically classified using the SILVA high quality rRNA database (v.138) (Quast et al., 2012). The *assignTaxonomy* and *assignSpecies* functions were used to combine exact genus- and species-level matching. Phyloseq (v1.24) was used to integrate the sample metadata, ASV table, phylogenetic tree and taxonomic assignments for statistical analyses (McMurdie and Holmes, 2013). The ASVs were then decontaminated using the decontam R package (v1.16.0) (Davis et al., 2018). This algorithm statistically assesses if an ASV is likely to be technical contamination considering its presence in negative-control samples and the DNA concentration in the samples, assuming that contaminating sequences have a higher frequency in low-concentration samples. Only ASVs that had a less than 5% chance of being contaminants were kept for further analysis. Taxa identified as Cyanobacteria, Mitochondria, Eukaryota or Archaea were removed, similar to previous microbiome studies investigating samples in early life (Turunen et al., 2021). Furthermore, samples with <5k reads and genera that were only detected as non-zero in 10% or fewer total samples were removed prior to downstream analysis. These criteria led to ten placental samples containing zero reads which were then discarded from further analysis. A *de novo* phylogenetic tree based on ASV sequences was built by performing a multiple-alignment using DECIPHER R package (v.2.16.1), followed by the construction of a neighbour-joining tree using phangorn R package (v.2.5.5) (Schliep, 2011) before fitting a GTR+G+I (Generalised time-reversible with Gamma

rate variation) maximum likelihood tree using the neighbour-joining tree as a starting point as recommended by (Callahan et al., 2016b). From the raw DADA2 output, the Phylogenetic Investigation of Communities by Reconstruction of Unobserved States (PICRUSt2) (v2.5.1) (Douglas et al., 2020) pipeline was used to predict putative microbial functions by mapping 16S rRNA marker gene sequences to known reference genomes, containing full 16S rRNA genes from bacterial and archaeal genomes in the Integrated Microbial Genomes (IMG) database (Markowitz et al., 2012). From this, k the most abundant Kyoto Encyclopaedia of Genes and Genomes (KEGG) pathways (Kanehisa et al., 2012) were identified for each sample as a result of the inferred analysis. Pathways were interrogated at KEGG Level 3. The *add_descriptions.py* convenience script for PICRUSt2, which adds a quick description of each functional category was also used.

3.3.6 Statistical Analysis

Further data handling was done in R (v4.1.2) with the RStudio GUI (v1.4.1717). Plotting was handled using ggplot2 (v3.4.1). To identify ASVs present in each sample type, presence in at least 50% of the 18 samples analysed and a cut off of >0.001 was used. These abundance-occurrence values are typically used in microbiome studies with similar sample sizes to this study (Neu et al., 2021). Further annotation of ASVs identified as core microbiota members was performed by taking the top BLASTn hit against the NCBI 16S rRNA gene database (Zhang et al., 2000). Five perinatal factors, mother antibiotic usage, delivery mode, feed type, gender and premature rupture of membranes (PROM) were assessed for their impact on the microbiome of each sample type. PROM refers to a patient who is beyond 37 weeks' gestation and has presented with rupture of membranes prior to the onset of labour. The iNEXT library was used to compute alpha diversity for the first three hill numbers (Chao1, Shannon entropy and Simpson Index) (Hsieh et al., 2016). Differences in alpha diversity (within-sample diversity) were assessed using linear models. Principal component analysis was performed on centred log-ratio transformed (clr) values as a visual companion to the beta diversity analysis. Zeroes were imputed using the *"const"* method (Lubbe et al., 2021). Beta diversity was computed in terms of Aitchison distance (Euclidean distance of clr-transformed counts) (Aitchison et al., 2000). Differences in beta diversity (between-sample diversity) were assessed using the adonis() PERMANOVA function in the vegan library (v2.6.4) and the value of *p*

were adjusted using the Bonferroni-Holm correction method. A difference was considered statistically significant if the adjusted $p < 0.05$. The Analysis of Composition of Microbiomes with Brown-Correction (ANCOM-BC) method was used to identify differentially abundant bacterial taxa. ANCOM-BC is a statistical framework designed to test for differential abundance in compositional data (Lin and Peddada, 2020). ANCOM-BC firstly computes a weighted average presence/absence score for each taxon and then uses these scores to perform a statistical test for each taxon, adjusting for the effects of total abundance and sample size. This method accounts for the compositional nature of the data, avoiding the use of simple fold changes or ratios, which can be unreliable in this context. Statistical Analysis of Metagenomic Profiles (STAMP) v2.1.3 (Parks et al., 2014) software was used to detect differentially abundant KEGG pathways generated by PICRUSt2 between perinatal factors of interest. Statistical significance was set at $p < 0.05$ (two-sided) following adjusted measures.

3.4 Results

3.4.1 Cohort Characteristics

Table 3.1 represents the characteristics of the 18 mother infant dyads included in this study at the time of sample collection. Briefly, the infant study population comprised of males (55.6%) and females (44.6%), with eight infants born by CS (44.4%) and 10 (55.6%) born vaginally. The mean birth weight of infants was 3,667.2g (standard deviation (SD) ± 386.6), mean gestational age was 39 weeks (SD ± 0.97) and mean Appearance, pulse, grimace, activity and respiration (Apgar) score was 9 (SD ± 1.15). The Apgar score is a standard assessment tool used to evaluate the physical condition of a new-born infant immediately after delivery. The score is based on five criteria: appearance (skin colour), pulse rate, grimace response, activity level, and respiration. Each criterion is scored from 0-2, with a maximum total score of 10 indicating a healthy new-born. PROM birth occurred for seven (38.9%) of infants in the study. Ten (55.6%) infants were breast fed, six (33.3%) infants were formula fed and the feed type of two infants (11.1%) was not noted. No infants in the studied subset received antibiotics. Regarding clinical characteristics of mothers, ten (55.6%) received antibiotics and eight (44.4%) received no antibiotics. Of the ten mothers who received antibiotics, the type of antibiotics received by two mothers was noted, these were Amoxicillin (Augmentin) and Flucloxocillin. Finally, the mean gravida (number of

pregnancies) of mothers was three (SD ± 1.5) and mean parity (number of births) was two (SD ± 1.3).

Table 3.1 | Clinical characteristics of the 18 mother infant dyads in this study.

Variables	
Infant Characteristics	**Cohort (*n*=18)**
Gender	
Male	10/18 (55.6%)
Female	8/18 (44.6%)
Delivery Mode	
Caesarean	8/18 (44.4%)
Vaginal	10/18 (55.6%)
Birth weight (g), mean (SD)	3667.2 (386.6)
Gestational age (in weeks), mean (SD)	39 (0.97)
AGPAR, mean (SD)	9 (1.15)
PROM	
Yes	7/18 (38.9%)
No	11/18 (61.1%)
Feed Type	
Breast Fed	10/18 (55.6%)
Formula	6/18 (33.3%)
Not Noted	2/18 (11.1%)
Maternal Characteristics	**Cohort (*n*=18)**
Intrapartum Antibiotic	
Yes	10/18 (55.6%)
No	8/18 (44.4%)
Amoxicillin (Augmentin)	1/18 (5.6%)
Flucloxocillin	1/18 (5.6%)
Type of antibiotic not noted	16/18 (88.8%)
Gravida, mean (SD)	3 (1.5)
Parity, mean (SD)	2 (1.3)

Continuous variables are presented as mean (+SD). Categorical variables are presented as number of participants (percentages). Abbreviations: SD, Standard

deviation; APGAR, Appearance, Pulse, Grimace, Activity and Respiration; PROM, Premature rupture of membranes.

3.4.2 The Placental Microbiome Does Not Differ From Negative Controls

Sequencing of placental tissues yielded a total of 666,018 reads with mean read lengths of 251 bp. The average reads per sample was 79,820, (standard deviation of 111,793). Following quality filtering, dereplication, error modelling, denoising, pair merging, and chimera removal were performed using default parameters in DADA2, ten samples contained zero reads and were discarded from further analysis. The average reads per sample of the remaining eight samples at this point was 29,774 (range 8,630-38,251). Of the 964 ASVs obtained across the 10 samples after taxonomic classification, 835 were flagged as contaminants by the Decontam software, corresponding to 43.7% to 67% of the ASVs present in each placental sample (median, 57%). The 129 remaining ASVs could not be classified to the species level. The filtering step, used for all other sample types in this study to remove genera that were only detected as non-zero in 10% or fewer total samples led to no ASVs in placental samples for downstream analysis. This step was therefore removed to investigate the ASVs found in placenta samples. DNA extraction blanks and amplicon PCR blanks and were used for each sample investigated in this study and we used the ASVs detected in these samples as a comparison to the ASVs found in placental samples. *Actinobacteriota*, *Firmicutes* and *Proteobacteria* were the only three phyla detected in DNA extraction blanks, PCR blanks and placental samples (Figure 3.1A). Five families were detected across the three sample types, *Bacillaceae*, *Corynebacteriaceae*, *Micrococcaceae*, *Streptococcaceae* and *Xanthbacteraceae* (Figure 3.1B), while six genera were detected *Afpia*, *Bacillus*, *Corynebacterium*, *Enhydrobacter*, *Micrococcus* and *Streptococcus* (Figure 3.1C).

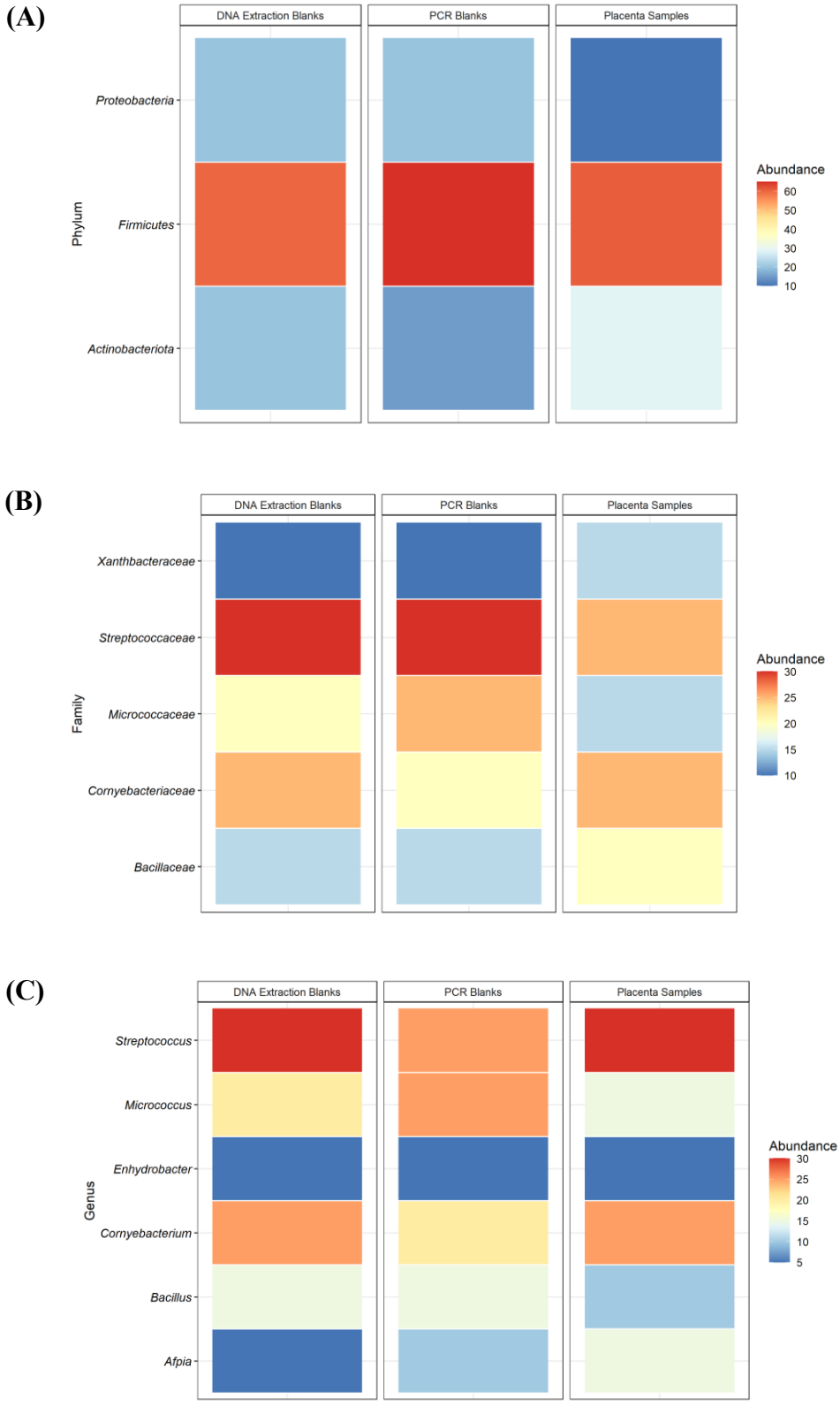

Figure 3.1 | Heat maps of average relative abundances at (A) phylum, (B) family and (C) genus level of DNA extraction blanks (n=5), amplicon PCR blanks (n=5) and placenta samples (n=8).

3.4.3 Phylogenetic Diversity, Core Microbiome and Metabolic Pathways in Infant Samples

Sequencing of infant meconium samples yielded a total of 2,234,980 reads with mean read lengths of 270 bp (251-301 bp). On average, each sample contained 79,820 reads (standard deviation of 57,324). After quality control, each sample contained an average of 67,689 reads (range 24,637-154,404). The phylogenetic diversities of the eight phyla detected in meconium and the relative abundances of the 301 ASVs identified across all samples are shown in Figure 3.2A. *Firmicutes* (57%), *Proteobacteria* (21%) *Actinobacteria* (18%) were the most dominant of the eight phyla detected. *Staphylococcaceae* (23%), *Enterobacteriaceae* (18%) and *Bifidobacteriaceae* (18%) were the most abundant families. *Staphylococcus* (25%), *Escherichia-Shigella* (18%) and *Bifidobacterium* (17%) were the most prevalent genera. Finally, the most abundant species were *Bifidobacterium bifidum* (*B. bifidum*) (37%), *Bifidobacterium longum* (*B. longum*) (16%), and *Rothia mucilaginosa* (*R. mucilaginosa*) (13%) (Figure 3.2B). Figure 3.2B displays the phylogenetic diversity of the ten most abundant species found in meconium. 12 ASVs (present in ≥50% of samples, cut-off >0.001) were identified as the core meconium microbiome (Figure 3.2C). ASV3, aligning significantly with *Staphylococcus epidermis* (*S. epidermis*) (BLASTn), was the only ASV present in all 18 samples. PICRUSt2 analysis identified 418 functional pathways across all meconium samples. Figure 3.2D shows the top 25 most abundant functional pathways across all samples. The most abundant pathways were the pentose phosphate pathway (non-oxidative branch), L-isoleucine biosynthesis, glycolysis, branched chain amino acid and aromatic amino acid biosynthesis pathways (Figure 3.2D).

(A)

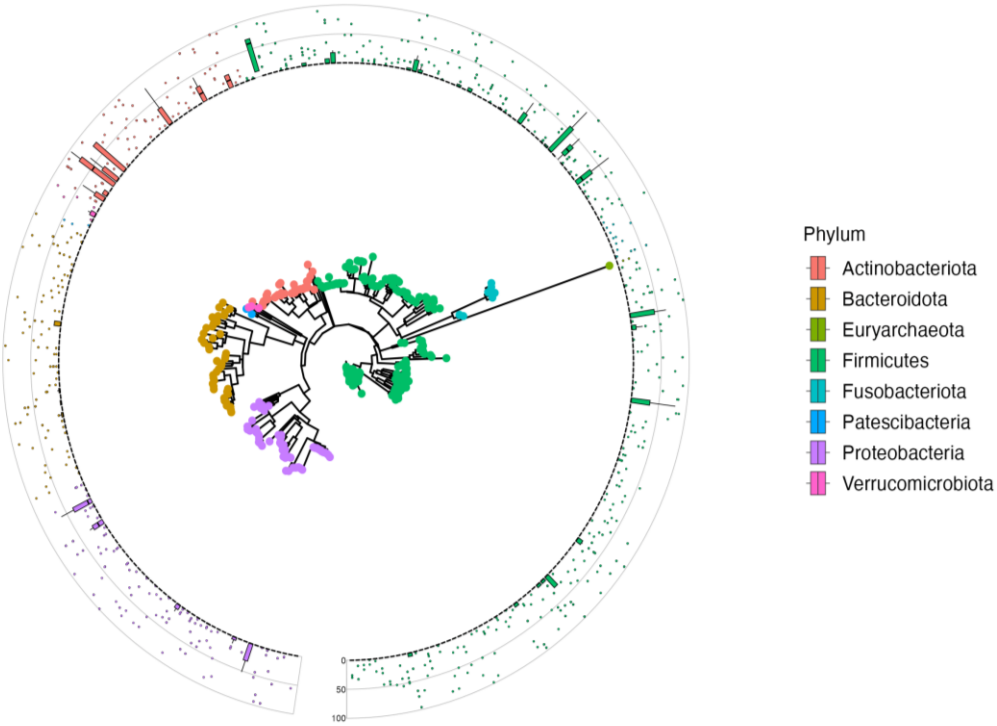
Phylum
Actinobacteriota
Bacteroidota
Euryarchaeota
Firmicutes
Fusobacteriota
Patescibacteria
Proteobacteria
Verrucomicrobiota
0
50
100

(B)

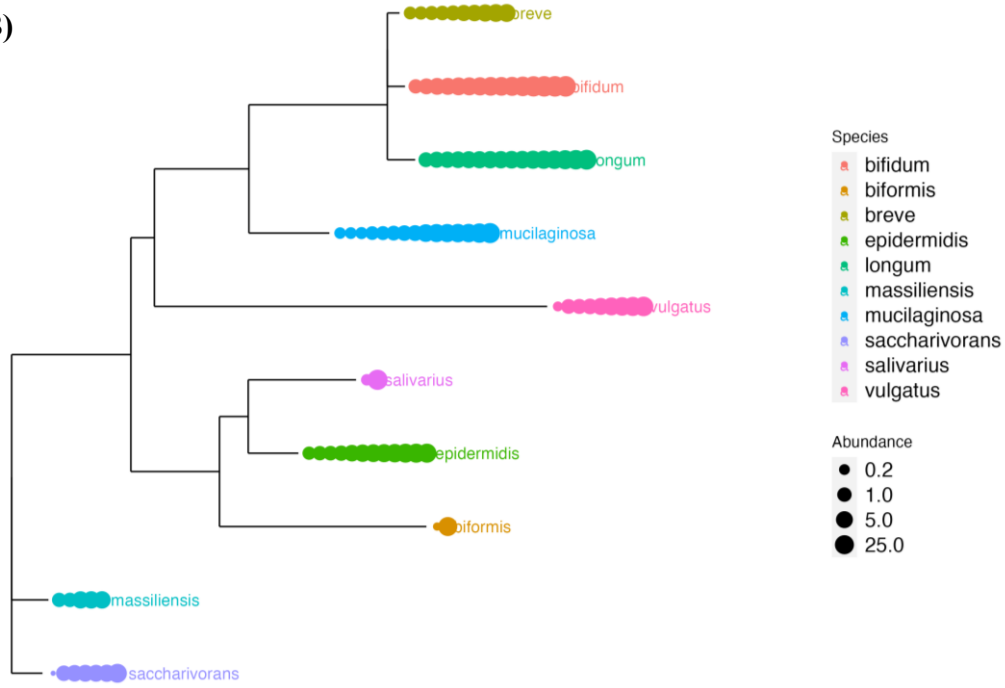
breve
bifidum
longum
mucilaginosa
vulgatus
salivarius
epidermidis
biformis
massiliensis
saccharivorans
Species
bifidum
biformis
breve
epidermidis
longum
massiliensis
mucilaginosa
saccharivorans
salivarius
vulgatus
Abundance
0.2
1.0
5.0
25.0

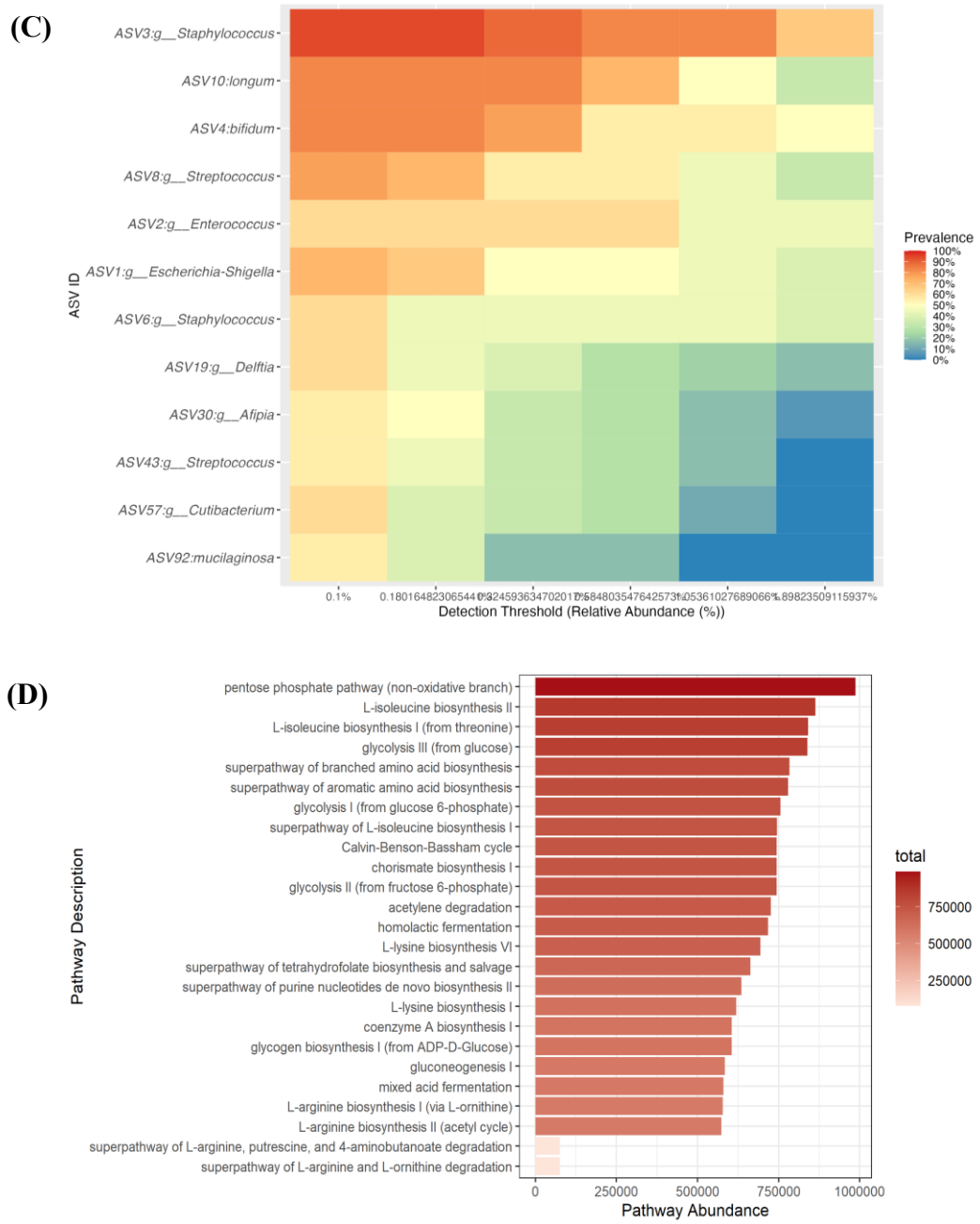

Figure 3.2 | (A) Phylogenetic tree with ASV relative abundance distribution shown as boxplots for Phylum-level abundances. Symbolic points coloured by phylum represent species abundances. (B) Phylogenetic tree with ASV relative abundance distribution for the top ten species in meconium samples. Node size represents relative abundance. (C) Heatmap of the core meconium microbiome, showing relative abundance and prevalence (> 0.001 cut-off and 50% cut-off, respectively) for the 18 samples analysed. ASVs are labelled with their ID and lowest taxonomic classification. (D) Predictive metabolic pathways associated with the meconium microbiome, displaying the top 25 abundant pathways based on abundance levels.

Sequencing of infant saliva samples yielded a total of 3,414,062 reads with mean read lengths of 301bp. On average, each sample contained 77,592 (standard deviation of 66,592). Following quality control, an average of 18,040 reads (range 11,438-58,257) per sample was obtained. Figure 3.3A depicts the phylogenetic diversities and relative abundances of the 341 ASVs identified across all samples. *Firmicutes* (63%), *Actinobacteriota* (20%) and *Proteobacteria* (10%) were the dominant of the nine phyla detected (Figure 3.3A). *Streptococcaceae* (41%), *Staphylococcaceae* (15%) and *Micrococcaceae* (14%) were the most abundant families (Figure 3.3A). *Streptococcus* (43%), *Staphylococcus* (18%) and *Rothia* (15%) were the most prevalent genera (Figure 3.3A). Finally, *R. mucilaginosa* (60%), *Staphylococcus lugdunensis* (*S. lugdunensis*) (8%), *Haemophilus parainfluenzae* (*H. parainfluenzae*) (7%), *Streptococcus oralis* (*S. oralis*) (6%) and *Streptococcus salivarius* (*S. salivarius*) (6%) were the most abundant species (Figure 3.3A). Figure 3.3B displays the phylogenetic diversity of the ten most abundant species found in infant oral samples. Of the 341 ASVs detected, seven ASVs (present in ≥50% of samples, cut-off >0.001) were identified as the core infant oral microbiome (Figure 3.3C). ASV1, aligning most significantly with *S. oralis* species (BLASTn analysis), was the only ASV present in all 18 samples. PICRUSt2 analysis identified 402 functional pathways across all infant saliva samples. Figure 3.3D shows the top 25 most abundant functional pathways across all samples. The predominant pathways included adenosine and guanosine deoxyribonucleotides *de novo* biosynthesis, cytidine diphosphate (CDP)-diacylglycerol biosynthesis, phospholipid biosynthesis and phosphatidylglycerol biosynthesis pathways (Figure 3.3D).

(A)

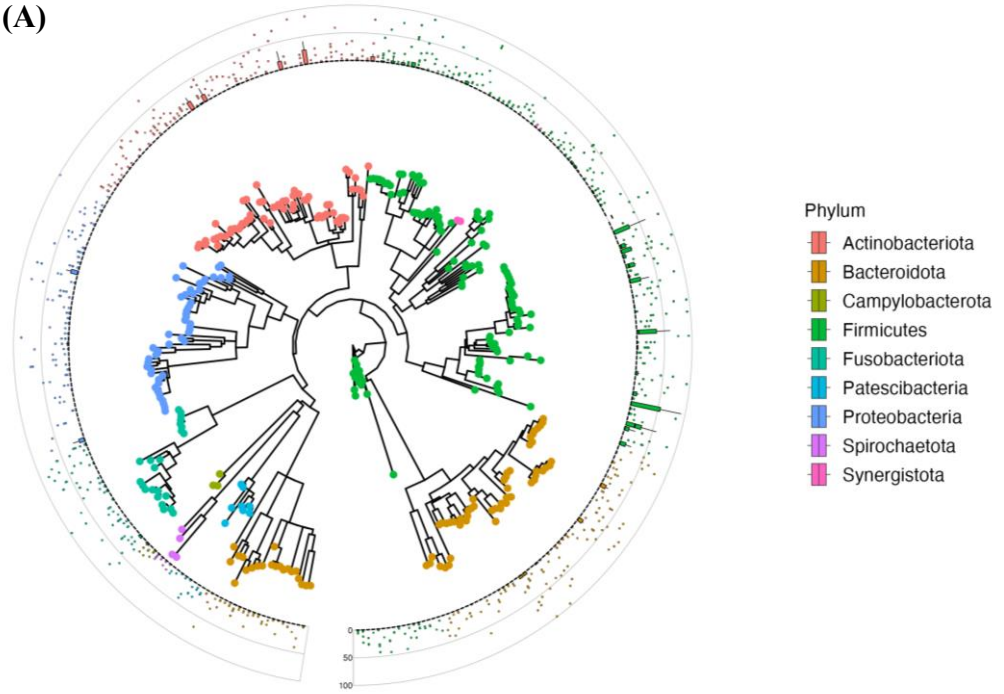
Phylum
Actinobacteriota
Bacteroidota
Campylobacterota
Firmicutes
Fusobacteriota
Patescibacteria
Proteobacteria
Spirochaetota
Synergistota
0
50
100

(B)

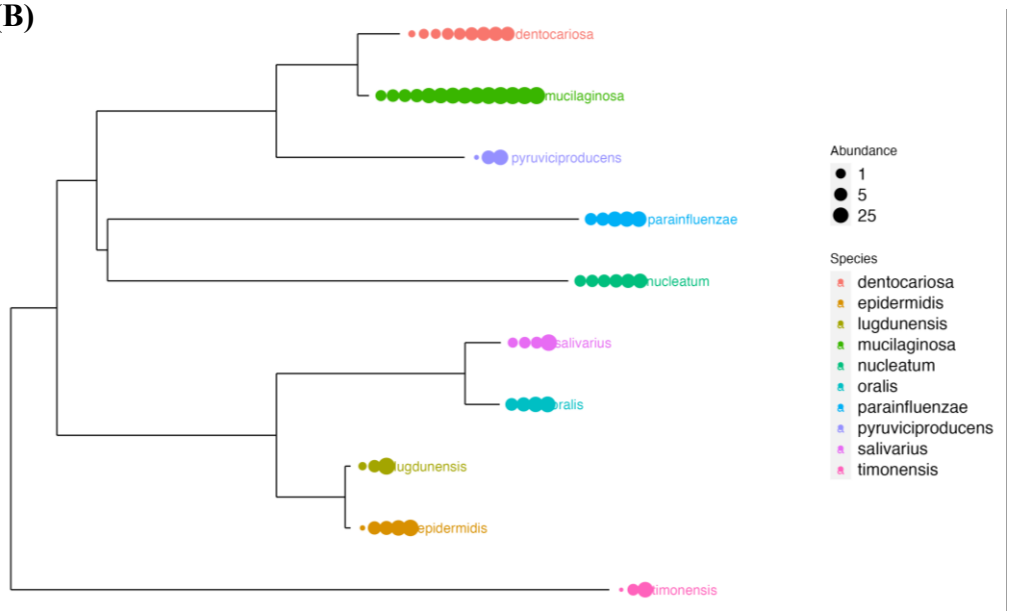
dentocariosa
mucilaginosa
pyruviciproducens
parainfluenzae
nucleatum
salivarius
oralis
lugdunensis
epidermidis
timonensis
Abundance
1
5
25
Species
dentocariosa
epidermidis
lugdunensis
mucilaginosa
nucleatum
oralis
parainfluenzae
pyruviciproducens
salivarius
timonensis

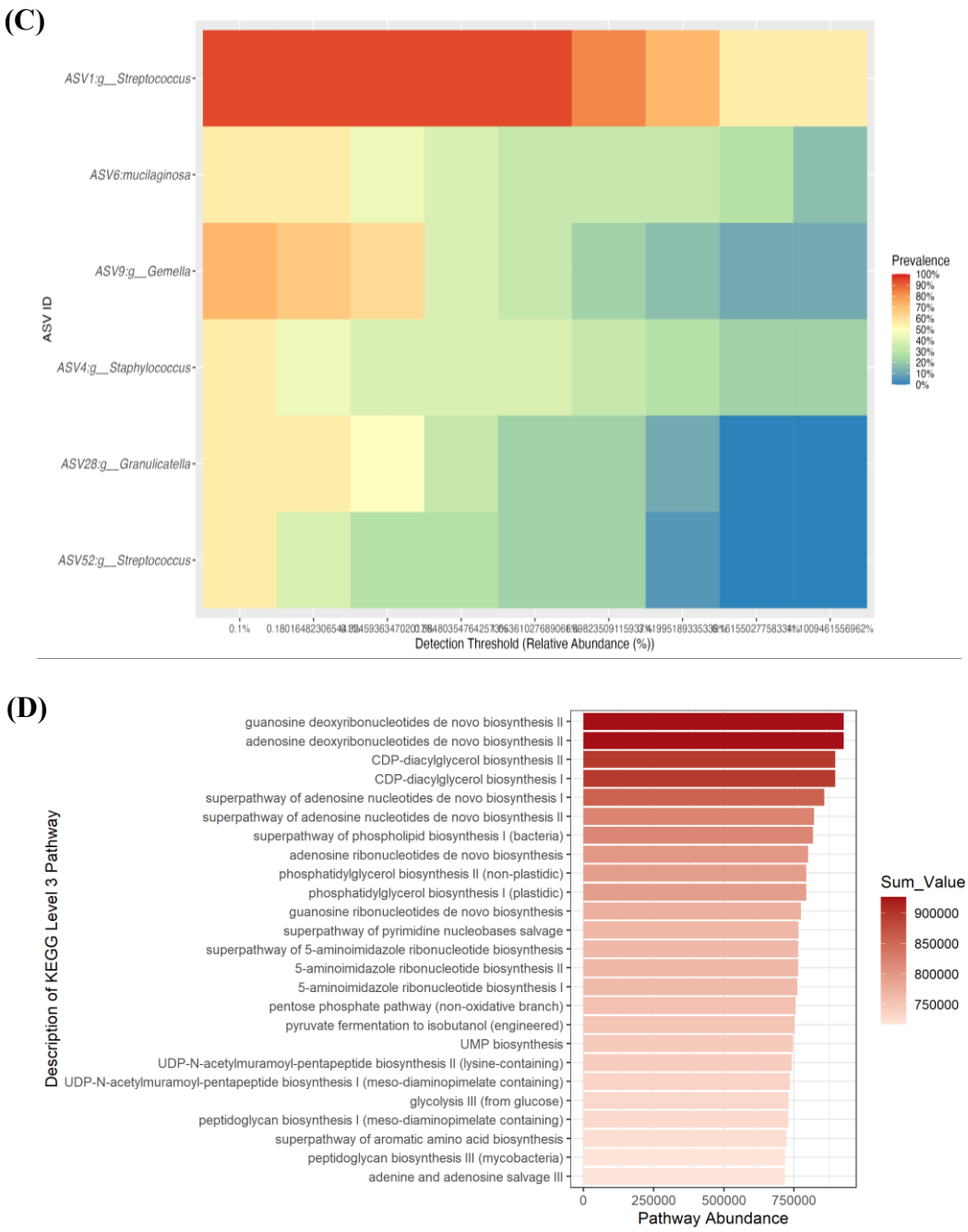

Figure 3.3 | (A) Phylogenetic tree with ASV relative abundance distribution shown as boxplots for Phylum-level abundances. Symbolic points coloured by phylum represent species abundances. (B) Phylogenetic tree with ASV relative abundance distribution for the top ten species in infant oral samples. Node size represents relative abundance. (C) Infant oral core microbiome heatmap, showing relative abundance and prevalence (> 0.001 cut-off and 50% cut-off, respectively) for the 18 samples analysed. ASVs are labelled with their ID and lowest taxonomic classification. (D) Predictive metabolic pathways associated with the infant oral microbiome, displaying the top 25 abundant pathways based on abundance level.

3.4.4 Phylogenetic Diversity, Core Microbiome and Metabolic Pathways in Maternal Samples

Sequencing of maternal saliva samples yielded a total of 5,781,180 reads with mean read lengths of 301bp. On average, each sample contained 123,003 reads (standard deviation of 165,745). Following quality control, an average of 40,254 (range 20,812-88,827) reads per sample was obtained. The phylogenetic diversities and relative abundances of the 456 ASVs identified across all samples are shown in Figure 3.4A. *Firmicutes* (48%), *Proteobacteria* (25%) *Actinobacteria* (12%) were the most dominant of the nine phyla detected in maternal saliva samples. *Streptococcaceae* (37%), *Neisseriaceae* (29%) and *Micrococcaceae* (11%) were most abundant families. *Streptococcus* (38%), *Neisseria* (20%) and *Rothia* (11%) were the most prevalent genera. Finally, *R. mucilaginosa* (*R. mucilaginosa*) (43%), *H. parainfluenzae* (15.6%) and *Prevotella melaninogenica* (*P. melaninogenica*) (11%) were the most abundant species found in maternal salvia samples. Figure 3.4B displays the phylogenetic diversity of the ten most abundant species found in maternal saliva samples. Of the 456 ASVs detected, 25 ASVs (present in ≥50% of samples, cut-off >0.001) were identified as core maternal oral microbiome (Figure 3.4C). ASV1, aligning significantly with *Streptococcus oralis* species (BLASTn), was the only ASV found to be present in all maternal saliva samples. PICRUSt2 analysis identified 418 functional pathways across all maternal saliva samples. Figure 3.4D shows the top 25 most abundant functional pathways across all samples. The most prevalent pathways included pyruvate fermentation to isobutanol, the pentose phosphate pathway, guanosine and adenosine deoxyribonucleotides *de novo* biosynthesis, L-isoleucine, CDP-diacylglycerol biosynthesis and L-valine biosynthesis pathways (Figure 3.4D).

(A)

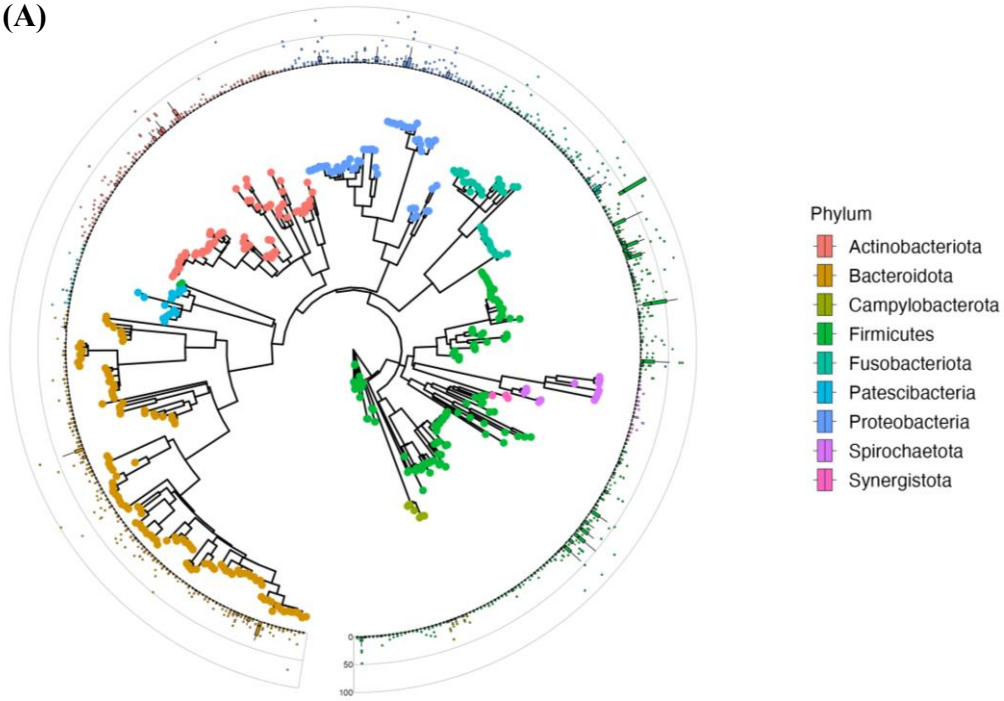
Phylum
Actinobacteriota
Bacteroidota
Campylobacterota
Firmicutes
Fusobacteriota
Patescibacteria
Proteobacteria
Spirochaetota
Synergistota
0
50
100

(B)

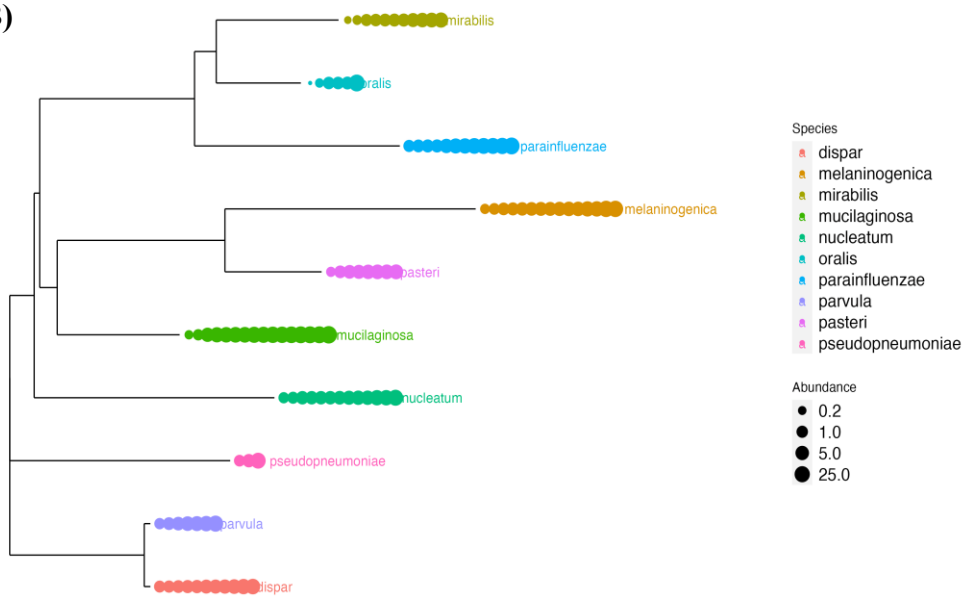
mirabilis
oralis
parainfluenzae
melaninogenica
pasteri
mucilaginosa
nucleatum
pseudopneumoniae
parvula
dispar
Species
dispar
melaninogenica
mirabilis
mucilaginosa
nucleatum
oralis
parainfluenzae
parvula
pasteri
pseudopneumoniae
Abundance
0.2
1.0
5.0
25.0

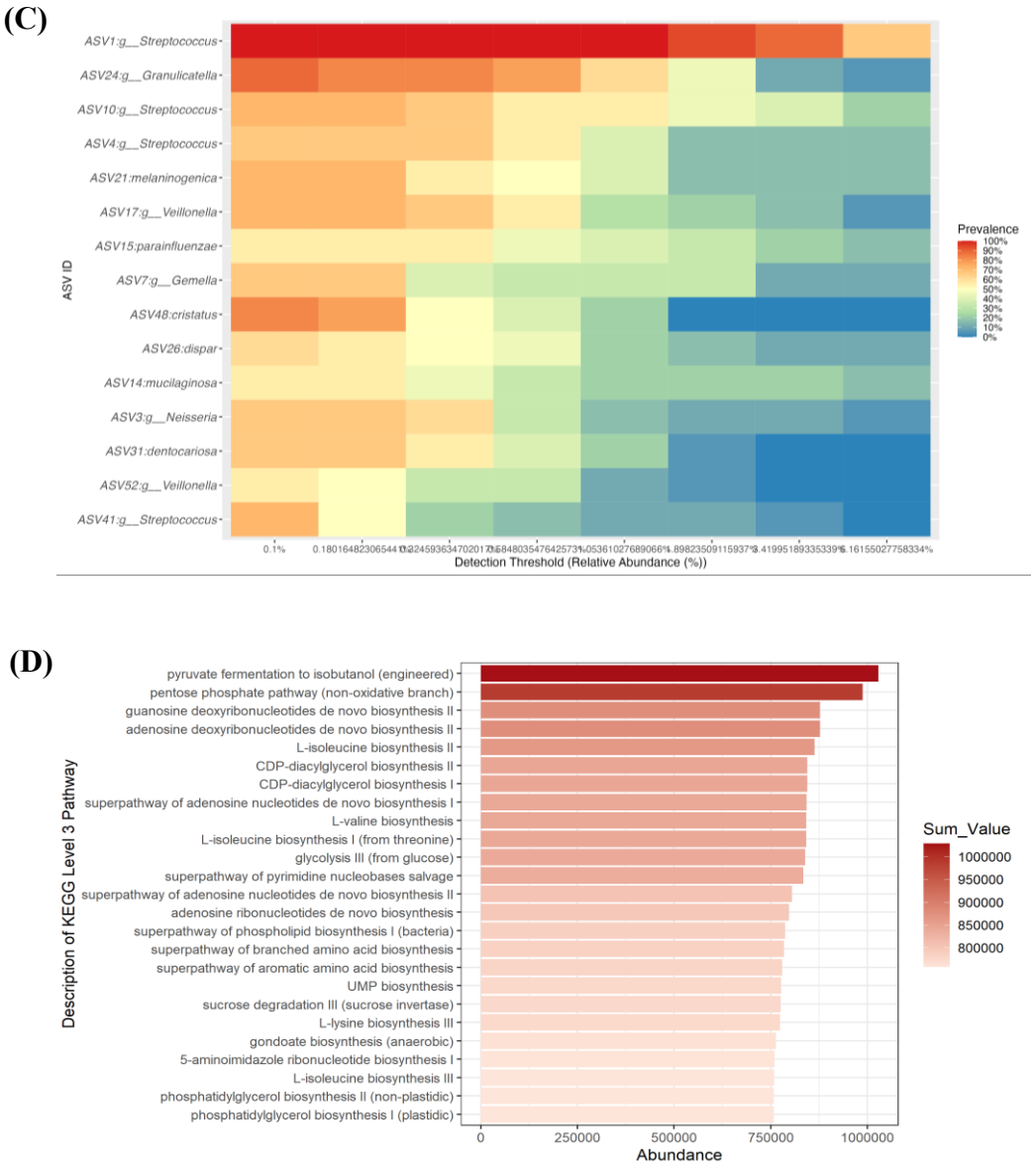

Figure 3.4 | (A) Phylogenetic tree with ASV relative abundance distribution shown as boxplots for phylum-level abundances. Symbolic points coloured by phylum represent species abundances. (B) Phylogenetic tree with ASV relative abundance distribution for the top ten species in maternal saliva samples. Node size represents relative abundance. (C) Maternal oral core microbiome heatmap, showing relative abundance and prevalence (> 0.001 cut-off and 50% cut-off, respectively) for the 18 samples analysed. ASVs are labelled with their ID and lowest taxonomic classification. (D) Predictive metabolic pathways associated with the maternal oral microbiome, displaying the top 25 abundant pathways based on abundance levels.

Sequencing of maternal vaginal swabs samples yielded a total of 2,063,808 reads with mean read lengths of 301bp. The average reads per sample was 103,190 (standard deviation of 109,261). Following quality control, an average of 18,440 (24,637-123,787) reads per sample were obtained. The phylogenetic diversities and relative abundances of the 89 ASVs identified across all samples are shown in Figure 3.5A. *Firmicutes* (73%) and *Actinobacteriota* (26%) were the most dominant of the seven phyla detected in vaginal swabs. *Family XI* (56%), *Corynebacteriaceae* (20%) and *Lactobacillaceae* (12%) were most abundant families. *Finegoldia* (22%), *Corynebacterium* (21%) and *Anaerococcus* (21%) were the most prevalent genera. Finally, *Corynebacterium pyruviciproducens* (*C. pyruviciproducens*) (30%), *Campylobacter ureolyticus* (*C. ureolyticus*) (16%) and *Peptostreptococcus anaerobius* (*P. anaerobius*) (14%) were the most abundant species. Figure 3.5B displays the phylogenetic diversity of the ten most abundant species found in the vaginal samples. Of the 89 ASVs detected, 8 ASVs (present in ≥50% of samples, cut-off >0.001) were identified as the core vaginal microbiome (Figure 3.5C). No ASV was found to be present in all vaginal samples. However, ASV5 which aligned significantly with *Finegoldia magna* (*F. magna*) and ASV16 which aligned significantly with *Peptoniphilus faecalis* (*P. faecalis*) were both found to be present in 17 out of 18 samples. PICRUSt2 analysis identified 363 functional pathways across all vaginal samples. Figure 3.5D shows the 25 most abundant functional pathways across all samples. The most abundant metabolic pathways were pyruvate fermentation to acetate and lactate, guanosine and adenosine and deoxyribonucleotides *de novo* biosynthesis, pentose phosphate pathway, phospholipid biosynthesis and CDP-diacylglycerol biosynthesis pathways (Figure 3.5D). The alpha diversity of the vaginal microbiome was significantly lower than meconium (Chao1, p= 0.0161) and the maternal oral microbiome (Chao1, p <0.0001), (Shannon p= 0.0208) (Figure 3.6).

(A)

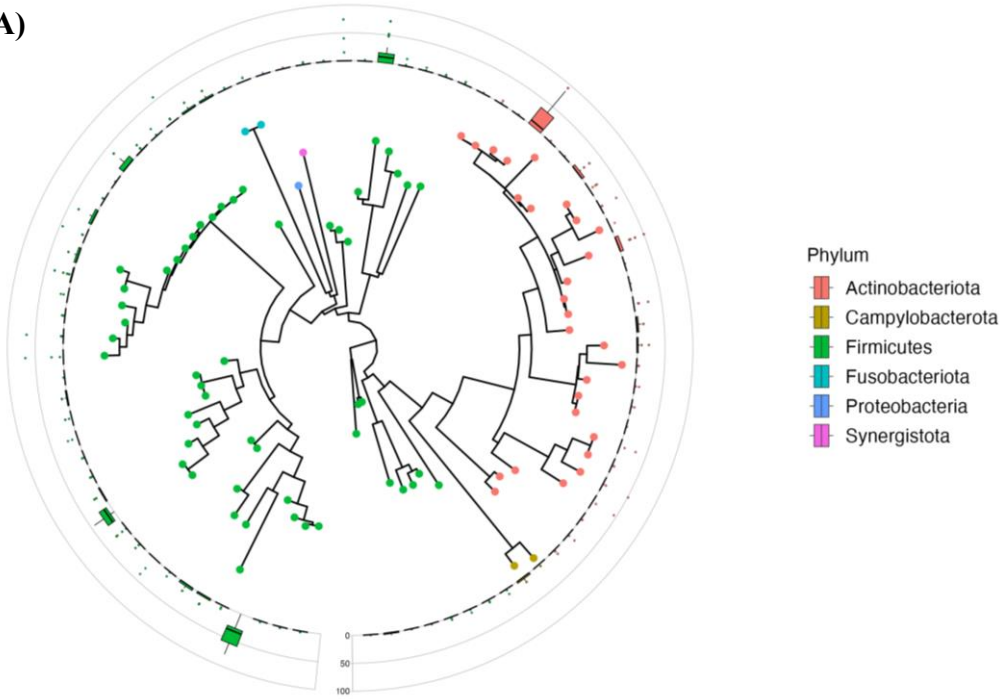
0
50
100
Phylum
Actinobacteriota
Campylobacterota
Firmicutes
Fusobacteriota
Proteobacteria
Synergistota

(B)

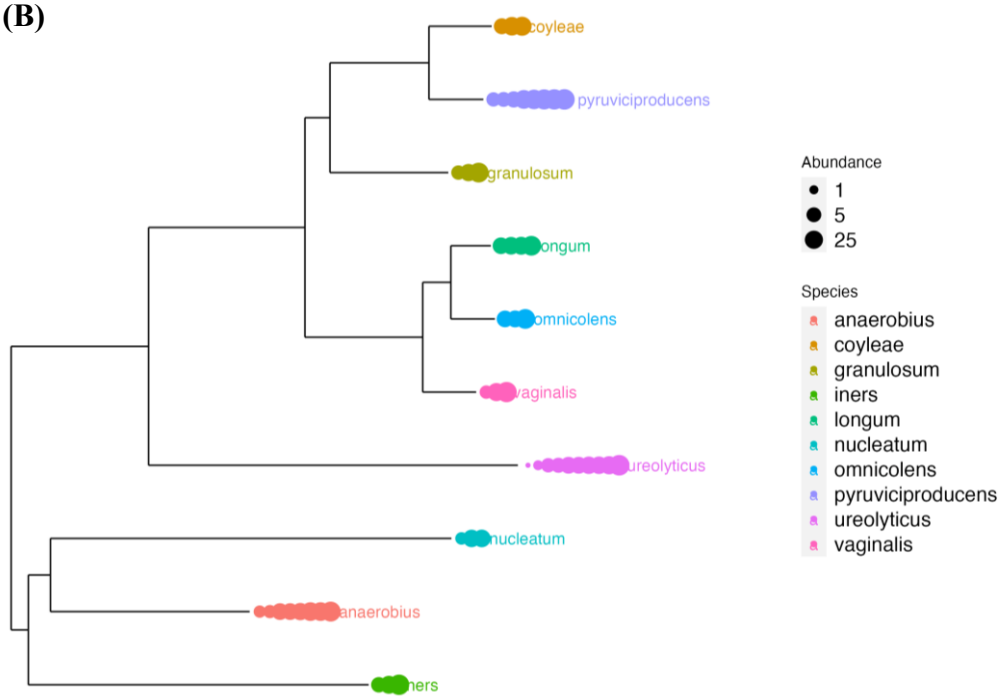
coyleae
pyruviciproducens
granulosum
ongum
omnicolens
vaginalis
ureolyticus
nucleatum
anaerobius
ners
Abundance
1
5
25
Species
anaerobius
coyleae
granulosum
iners
longum
nucleatum
omnicolens
pyruviciproducens
ureolyticus
vaginalis

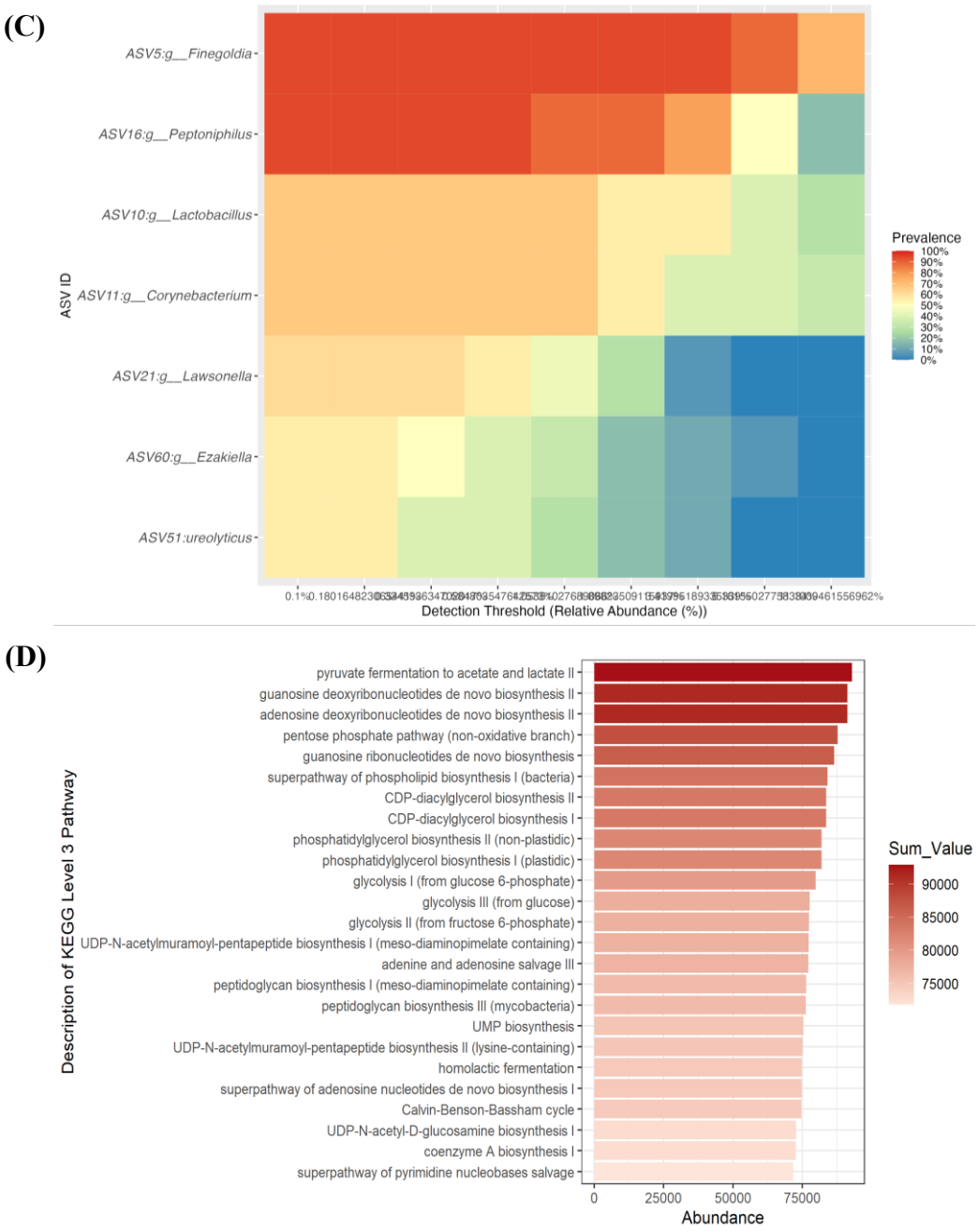

Figure 3.5 | (A) Phylogenetic tree with ASV relative abundance distribution shown as boxplots for phylum-level abundances. Symbolic points coloured by phylum represent species abundances. (B) Phylogenetic tree with ASV relative abundance distribution for the top ten species in vaginal samples. Node size represents relative abundance. (C) Vaginal core microbiome heatmap, showing relative abundance and prevalence (> 0.001 cut-off and 50% cut-off, respectively) for the 18 samples analysed. ASVs are labelled with their ID and lowest taxonomic classification. (D) Predictive metabolic pathways associated with the vaginal microbiome, displaying the top 25 abundant pathways based on abundance levels.

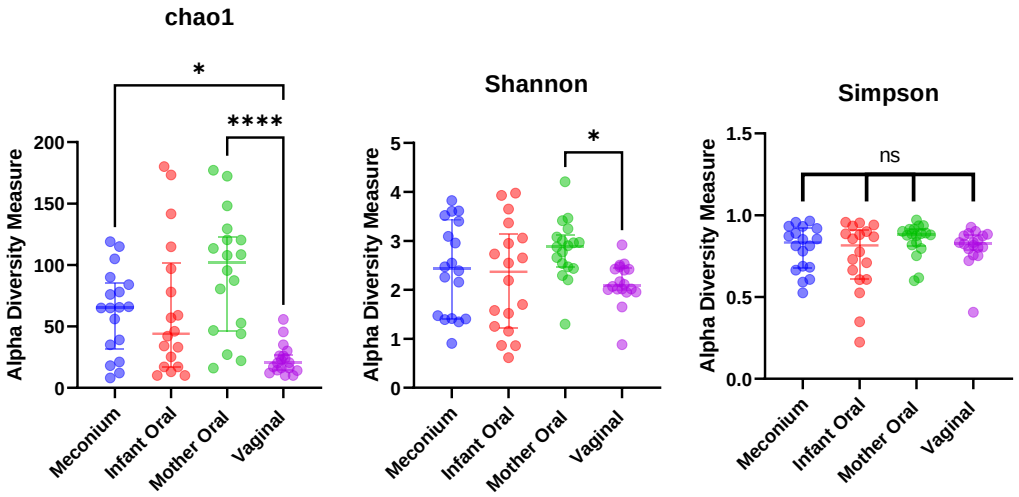

Figure 3.6 | Alpha diversity analysis of mother and infant samples. Statistical significance assessed by Mann-Whitney test ($p < 0.05$).

3.4.5 Site Specific Vertical transmission of Microbiota from Mother to Infant

To explore site specific vertical transmission of maternal microbiota to the infant microbiota, we identified bacterial taxa shared between the communities of mothers and their related infants. Figure 3.7 gives an overview of the overall microbial composition and their relative abundances of the four sample types investigated in this study.

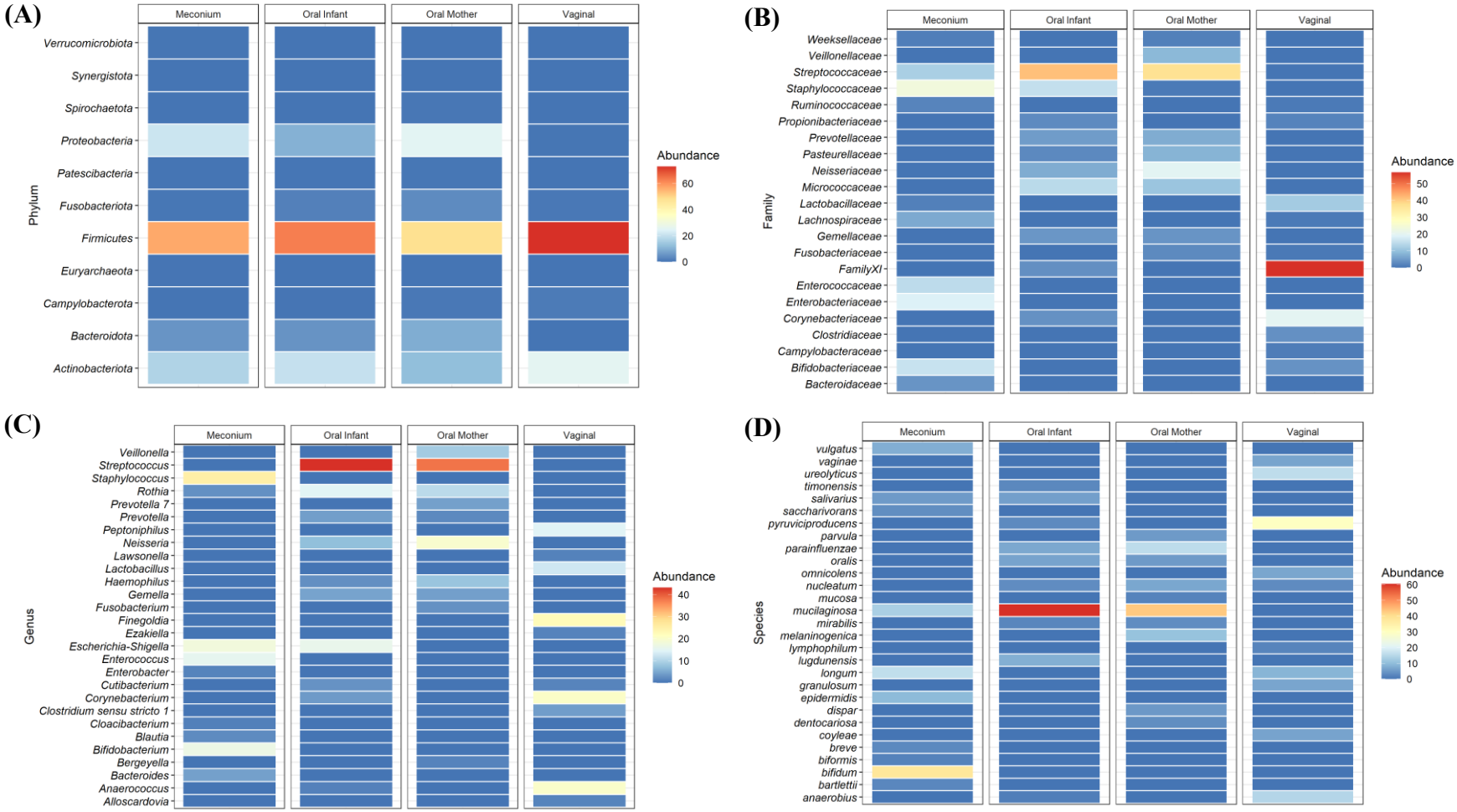

Figure 3.7 | Heat maps of average relative abundances at (A) phylum, (B) family and (C) genus level of meconium, oral saliva, maternal saliva and vaginal samples.

Regarding establishment of the infant's oral microbiome, on average, a related mother and infant's oral microbiota shared 45 taxa (Figure 3.8A), accounting for 65% of the total reads in the infant's sample (Figure 3.8B). Perinatal factors had no effect on the amount of the infants' oral microbiome that was shared with their mother. *R. mucilaginosa* was found present in all 18 mother-infant oral sample dyads. *S. oralis, H. parainfluenzae* and *Fusobacterium nucleatum* (*F. nucleatum*) were found in 15 dyads. On average, a related mother's vaginal microbiome and infant's oral microbiota shared 15 bacterial taxa (Figure 3.8C) which accounted for 15% of the total reads in the infant's sample (Figure 3.8D). When comparing NB infants versus by CS and we found that route of delivery had a significant effect on the amount of the infants' oral microbiome that was shared with their mother's vaginal microbiome (Mann Whitney Test, $p = 0.045$) (Figure S1). *C. pyruvicproducens* was present in all 18 mother-infant dyads when comparing vaginal and oral samples and was the only species common to oral and vaginal samples. *F. nucleatum* was present in 15 dyads. On average, a related mother's oral microbiota and infant's meconium microbiota shared eight bacterial taxa (Figure 3.8E) which accounted for 6% of the total reads in the infant's sample (Figure 3.8F). We next examined if the amount of the infants' meconium microbiome that was shared with their mother's oral microbiota differed according to the various perinatal factors investigated in previous sections, however there was no significant correlations. Regarding species sharing, *R. mucilaginosa* was the only shared species and was present in all 18 mother-infant dyads. On average, a related mother's vaginal microbiota and infant's meconium microbiota shared 38 bacterial taxa (Figure 3.8G) which accounted for 21% of the total reads in the infant's sample (Figure 3.8H). We next examined if the amount of the infants' meconium microbiome that was shared with their mother's oral microbiome differed according to the various perinatal factors investigated in previous sections, however there was no significant correlations. Regarding species sharing, *B. longum* was the only shared species.

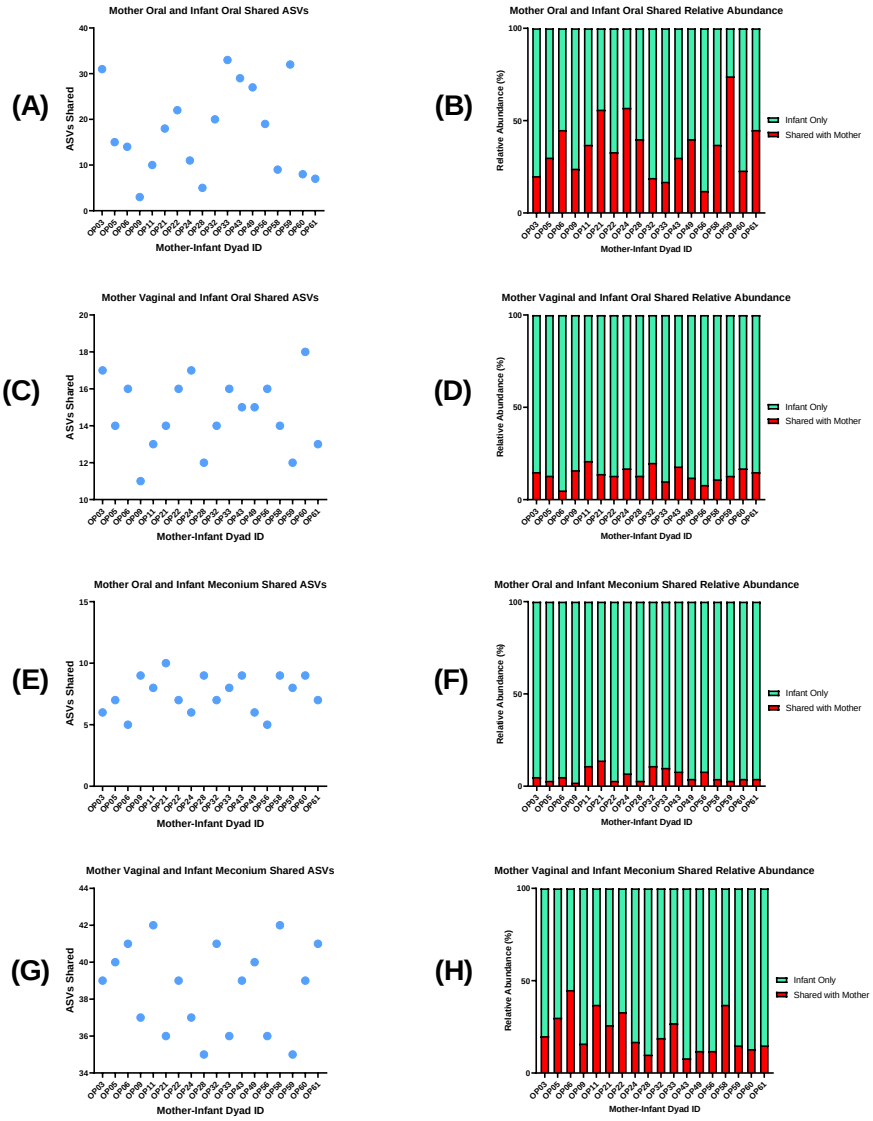

Figure 3.8 | (A) Number of ASVs shared between mother oral and infant oral dyad samples. (B) Relative abundance of infant oral microbiome shared with their mother's oral microbiome. (C) Number of ASVs shared between mother vaginal and infant oral dyad samples. (D) Relative abundance of infant oral microbiome shared with their mother's vaginal microbiome. (E) Number of ASVs shared between mother oral and infant meconium dyad samples. (F) Relative abundance of infant meconium microbiome shared with their mother's oral microbiome. (G) Number of ASVs shared between mother vaginal and infant meconium dyad samples. (H) Relative abundance of infant meconium microbiome shared with their mother's vaginal microbiome.

3.4.6 Impact of Perinatal Factors on the Meconium Microbiome

Maternal antibiotic usage had a significant effect on the beta diversity of meconium (R^2 = 0.0764, p = 0.069). 16 ASVs were differentially abundant in the "no" group at the genus level, most significantly *Eubacterium hallii* group, *Dialister* and *CAG-56*. At the species level, eight ASVs were differentially abundant, most significantly *Blautia obeum* (*B. obeum*), *Dorea formicigenerans* (*D. formicigenerans*) and *Bacteroides fragilis* (*B. fragilis*) (Figure 3.9A). 15 ASVs were differentially abundant in the "yes" group at the genus level, most significantly, *Pantoea, Enterobacter* and *Neisseria*. At the species level, eight ASVs were differentially abundant, most significantly was *Ruminococcus bromii* (*R. bromii*), *Fusobacterium periodonticum* (*F. periodonticum*) and *Gemella sanguinis* (*G. sanguinis*) (Figure 3.9A). 14 functional pathways primarily involving L-aspartate and L-asparagine biosynthesis and starch and glycogen degradation were associated with the "no" group (Figure 3.10A). 47 functional pathways, most significant included heme biosynthesis from glycine, and degradation pathways of phenylethylamine, salicylate, catechol and toluene were associated with the "yes" group (Figure 3.10A). Regarding delivery mode, CS delivery resulted in a significant increase in species richness in meconium (Chao1, p = 0.07). Ten ASVs were differentially abundant in NB infants at the genus level, most significantly, *Cloacibacterium*, *Bifidobacterium* and *Brevundimonas*. At the species level, eight ASVs were differentially abundant, most significantly, *B. longum*, *Bacillus niacin* (*B. niacin*) and *R. bromii* (Figure 3.9B). 21 ASVs were differentially abundant in CS-born infants at the genus level, most significantly *Fusicantentibacter*, *Eubacterium eligens* group and *Intestinibacter*. At the species level, seven ASVs were differentially abundant in CS-born infants, most significantly *Fusicatenibacter saccharivorans* (*F. saccharivorans*), *Veillonella tobersuensis* (*V. tobersuensis*) and *Intestinibacter bartlettii* (*I. bartlettii*) (Figure 3.9B). Seven functional pathways were significantly associated with NB infants (Figure 3.10B), including heterolactic fermentation and the *Bifidobacterium* shunt pathway (Figure 3.10B). Four functional pathways were significantly associated with CS infants, involving L-tryptophan, L-phenyalanine and tetrapyrrole biosynthesis (Figure 3.10B). Regarding feed type, 21 ASVs were differentially abundant in breast fed infants at the genus level, most significantly *Delftia*, *Afipia*, and *Escherichia-Shigella*. At the species level, 11 ASVs were differentially abundant, most significantly *Bacillus niacin*, *R. bromii*,

Bacteroides vulgatus (*B. vulgatus*) and *Bacteroides uniformis* (*B. uniformis*) (Figure 3.9C). 14 ASVs were differentially abundant in formula fed infants at the genus level, most significantly *Eubacterium eligens group, CAG-56* and *Eubacterium hallii group*. At the species level, seven ASVs were differentially abundant in formula fed infants, most significantly *Blautia obeum* (*B. obeum)*, *Dorea formicigenera*ns (*D. formicigenera*ns) and *Coproccus comes* (*C. comes*) (Figure 3.9C). 24 functional pathways were significantly associated with the meconium microbiome of breast fed infants, including fatty acid oxidation, the glycoxylate cycle, demethylmenaquinol biosynthesis and the pyridoxal 5'-phopshate biosynthesis pathway (Figure 3.10C). Formula feeding showed most significant associations with phosphatidyglycerol biosynthesis, L-threonine, L-isoleucine and coenzyme A biosynthesis (Figure 3.10C). Regarding gender, ten ASVs were differentially abundant in males at the genus level, most significantly *Gemella,* and *Neochlamydia* (Figure 3.9D). 11 ASVs were differentially abundant in males at the species level, most significantly *Anaerostipes hadrus* (*A. hadrus*), *Turicibacter sanguinis* (*T. sanguinis*) and *Acinetobacter radioresistens* (*A. radioresistens*) (Figure 3.9D). 15 ASVs were differentially abundant in females at the genus level, most significantly *Massilia, Eubacterium ventriosum* group and *UCG-002*. Seven species were differentially abundant in females, most significantly, *G. morbillorum, Rothia dentocariosa* (*R. dentocariosa*) and *Fusobacterium periodonticum* (*F. periodonticum*) (Figure 3.9D). Regarding PROM birth, 29 ASVs were differentially abundant in the "no" group at genus level, most significantly *Eubacterium eligens group*, *Eubacterium ventriosum group* and *CAG-56*. 12 ASVs were differentially abundant in the "no" group at species level, most significantly *B. obeum*, *D. formicigenerans* and *Veillonella rogosae* (*V. rogosae*) (Figure 3.9E). Eight ASVs were differentially abundant in the "yes" group at genus level, most significantly *Delftia, Afipia* and *Cutibacterium*. Eight species were differentially abundant in the "yes" group, most significantly *R. bromii, G. morbillorum* and *Cloacibacterium normanense* (*Cloacibacterium normanense*) (Figure 3.9E).

(A)

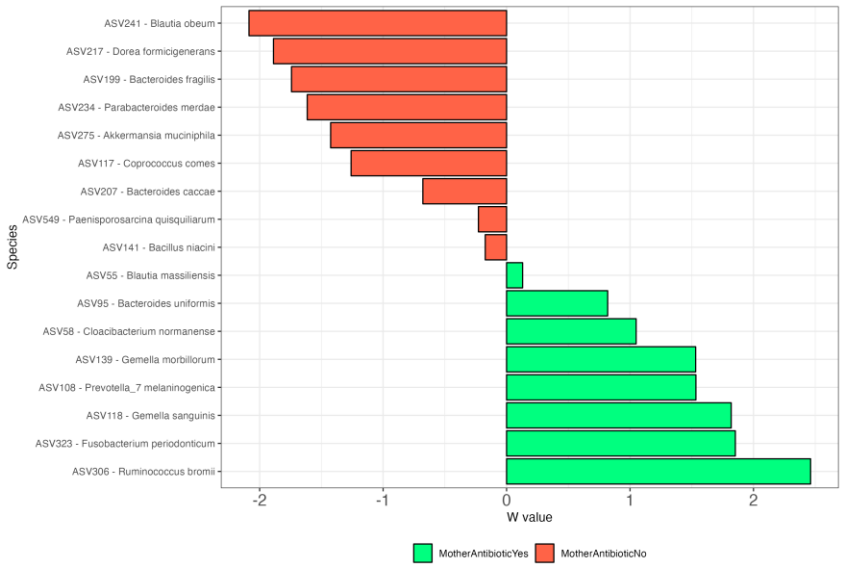
ASV241 - Blautia obeum
ASV217 - Dorea formicigenerans
ASV199 - Bacteroides fragilis
ASV234 - Parabacteroides merdae
ASV275 - Akkermansia muciniphila
ASV117 - Coprococcus comes
ASV207 - Bacteroides caccae
ASV549 - Paenisporosarcina quisquiliarum
ASV141 - Bacillus niacini
ASV55 - Blautia massiliensis
ASV95 - Bacteroides uniformis
ASV58 - Cloacibacterium normanense
ASV139 - Gemella morbillorum
ASV108 - Prevotella_7 melaninogenica
ASV118 - Gemella sanguinis
ASV323 - Fusobacterium periodonticum
ASV306 - Ruminococcus bromii
Species
-2
-1
0
1
2
W value
MotherAntibioticYes
MotherAntibioticNo

(B)

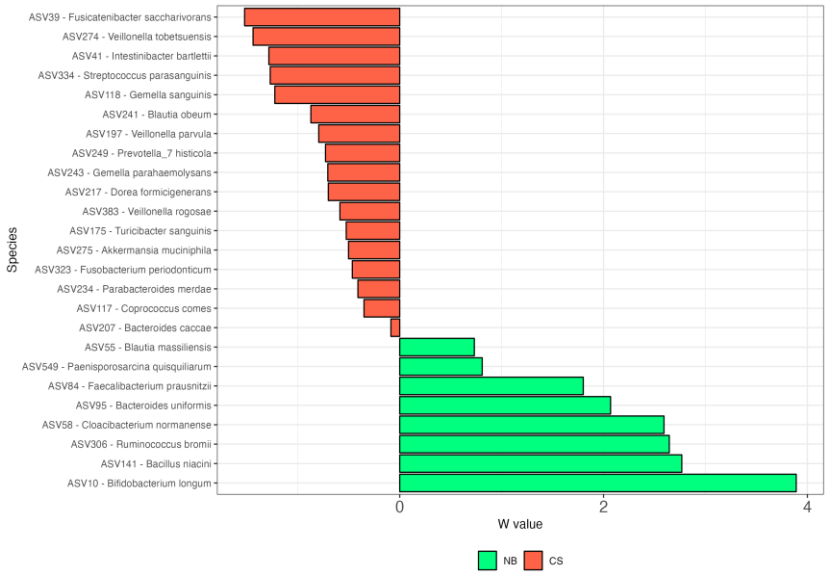
ASV39 - Fusicatenibacter saccharivorans
ASV274 - Veillonella tobetsuensis
ASV41 - Intestinibacter bartlettii
ASV334 - Streptococcus parasanguinis
ASV118 - Gemella sanguinis
ASV241 - Blautia obeum
ASV197 - Veillonella parvula
ASV249 - Prevotella_7 histicola
ASV243 - Gemella parahaemolysans
ASV217 - Dorea formicigenerans
ASV383 - Veillonella rogosae
ASV175 - Turicibacter sanguinis
ASV275 - Akkermansia muciniphila
ASV323 - Fusobacterium periodonticum
ASV234 - Parabacteroides merdae
ASV117 - Coprococcus comes
ASV207 - Bacteroides caccae
ASV55 - Blautia massiliensis
ASV549 - Paenisporosarcina quisquiliarum
ASV84 - Faecalibacterium prausnitzii
ASV95 - Bacteroides uniformis
ASV58 - Cloacibacterium normanense
ASV306 - Ruminococcus bromii
ASV141 - Bacillus niacini
ASV10 - Bifidobacterium longum
Species
0
2
4
W value
NB
CS

(C)

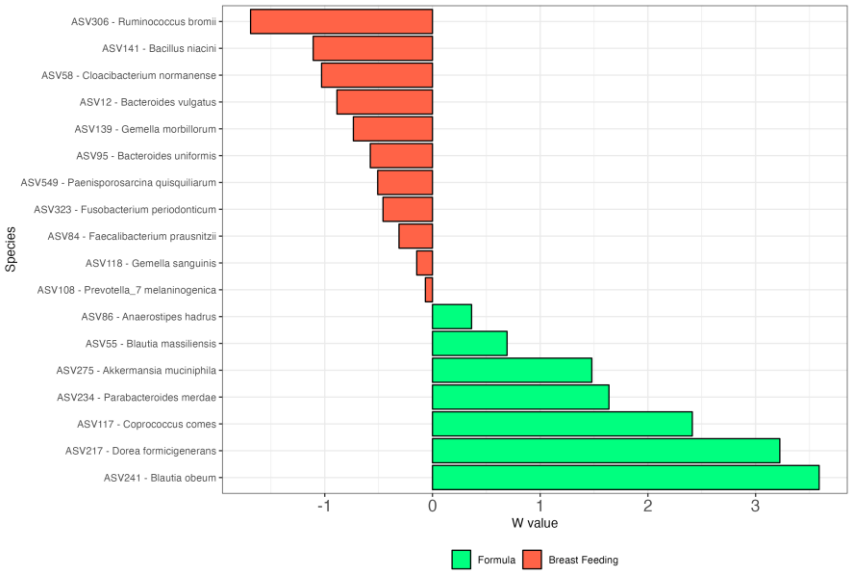
ASV306 - Ruminococcus bromii
ASV141 - Bacillus niacini
ASV58 - Cloacibacterium normanense
ASV12 - Bacteroides vulgatus
ASV139 - Gemella morbillorum
ASV95 - Bacteroides uniformis
ASV549 - Paenisporosarcina quisquiliarum
ASV323 - Fusobacterium periodonticum
ASV84 - Faecalibacterium prausnitzii
ASV118 - Gemella sanguinis
ASV108 - Prevotella_7 melaninogenica
ASV86 - Anaerostipes hadrus
ASV55 - Blautia massiliensis
ASV275 - Akkermansia muciniphila
ASV234 - Parabacteroides merdae
ASV117 - Coprococcus comes
ASV217 - Dorea formicigenerans
ASV241 - Blautia obeum
Species
-1
0
1
2
3
W value
Formula
Breast Feeding

(D)

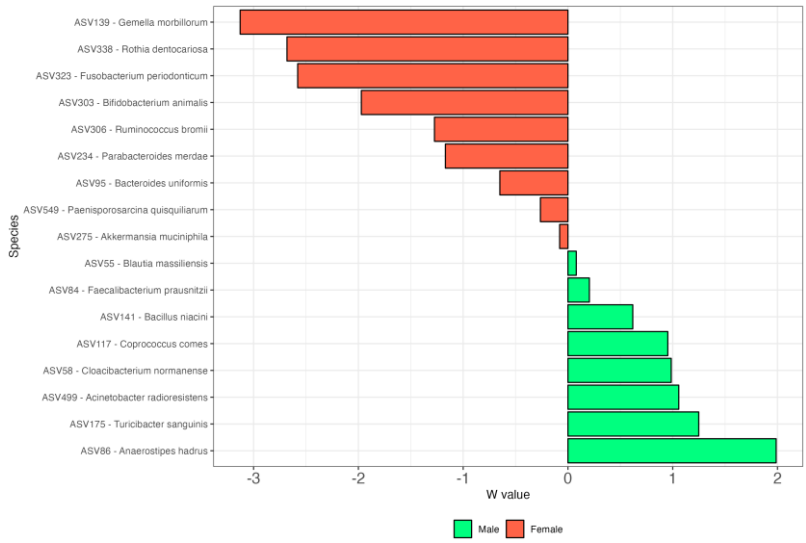

(E)

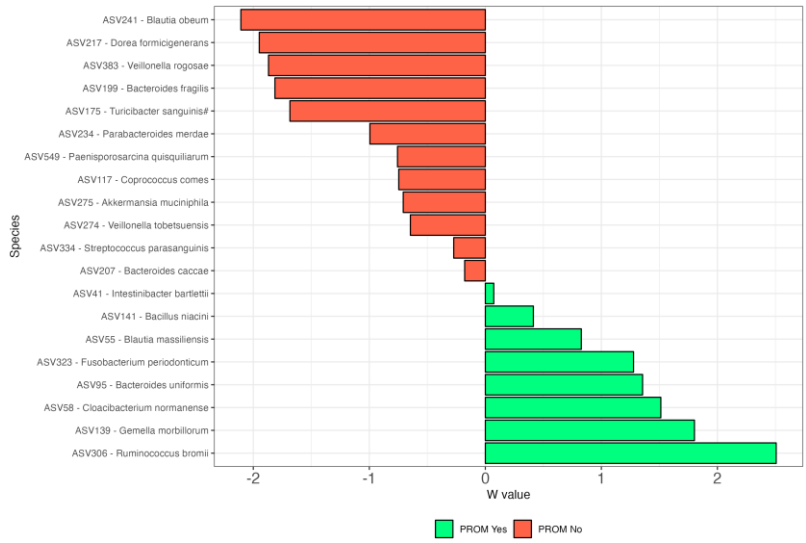

Figure 3.9| Bar-plots of differentially abundant ASVs within meconium samples at the species level. Perinatal factors are shown as green and red, respectively. (A) Mother antibiotic usage. (B) Delivery Mode. (C) Feed Type. (D) Gender. (E) PROM. Differential abundant ASVs were identified using analysis of the composition of microbiomes (ANCOM) method. Only statistically significant ASVs that fall within a distribution based on W values are shown.

(A)

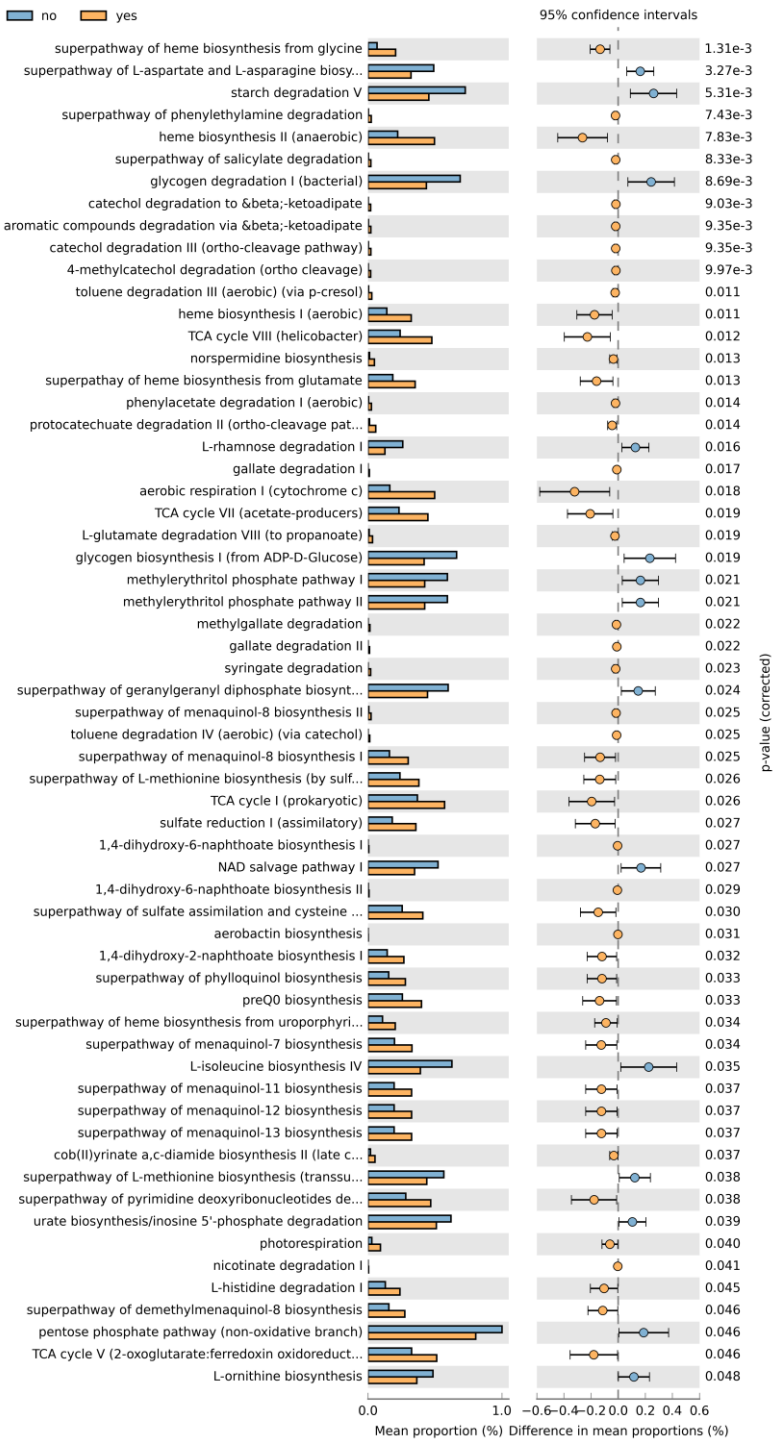
no
yes
95% confidence intervals
superpathway of heme biosynthesis from glycine
superpathway of L-aspartate and L-asparagine biosy...
starch degradation V
superpathway of phenylethylamine degradation
heme biosynthesis II (anaerobic)
superpathway of salicylate degradation
glycogen degradation I (bacterial)
catechol degradation to β-ketoadipate
aromatic compounds degradation via β-ketoadipate
catechol degradation III (ortho-cleavage pathway)
4-methylcatechol degradation (ortho cleavage)
toluene degradation III (aerobic) (via p-cresol)
heme biosynthesis I (aerobic)
TCA cycle VIII (helicobacter)
norspermidine biosynthesis
superpathay of heme biosynthesis from glutamate
phenylacetate degradation I (aerobic)
protocatechuate degradation II (ortho-cleavage pat...
L-rhamnose degradation I
gallate degradation I
aerobic respiration I (cytochrome c)
TCA cycle VII (acetate-producers)
L-glutamate degradation VIII (to propanoate)
glycogen biosynthesis I (from ADP-D-Glucose)
methylerythritol phosphate pathway I
methylerythritol phosphate pathway II
methylgallate degradation
gallate degradation II
syringate degradation
superpathway of geranylgeranyl diphosphate biosynt...
superpathway of menaquinol-8 biosynthesis II
toluene degradation IV (aerobic) (via catechol)
superpathway of menaquinol-8 biosynthesis I
superpathway of L-methionine biosynthesis (by sulf...
TCA cycle I (prokaryotic)
sulfate reduction I (assimilatory)
1,4-dihydroxy-6-naphthoate biosynthesis I
NAD salvage pathway I
1,4-dihydroxy-6-naphthoate biosynthesis II
superpathway of sulfate assimilation and cysteine ...
aerobactin biosynthesis
1,4-dihydroxy-2-naphthoate biosynthesis I
superpathway of phylloquinol biosynthesis
preQ0 biosynthesis
superpathway of heme biosynthesis from uroporphyri...
superpathway of menaquinol-7 biosynthesis
L-isoleucine biosynthesis IV
superpathway of menaquinol-11 biosynthesis
superpathway of menaquinol-12 biosynthesis
superpathway of menaquinol-13 biosynthesis
cob(II)yrinate a,c-diamide biosynthesis II (late c...
superpathway of L-methionine biosynthesis (transsu...
superpathway of pyrimidine deoxyribonucleotides de...
urate biosynthesis/inosine 5'-phosphate degradation
photorespiration
nicotinate degradation I
L-histidine degradation I
superpathway of demethylmenaquinol-8 biosynthesis
pentose phosphate pathway (non-oxidative branch)
TCA cycle V (2-oxoglutarate:ferredoxin oxidoreduct...
L-ornithine biosynthesis
1.31e-3
3.27e-3
5.31e-3
7.43e-3
7.83e-3
8.33e-3
8.69e-3
9.03e-3
9.35e-3
9.35e-3
9.97e-3
0.011
0.011
0.012
0.013
0.013
0.013
0.014
0.014
0.016
0.017
0.018
0.019
0.019
0.019
0.021
0.021
0.022
0.022
0.023
0.024
0.025
0.025
0.025
0.026
0.026
0.027
0.027
0.027
0.029
0.030
0.031
0.032
0.033
0.033
0.034
0.034
0.035
0.037
0.037
0.037
0.037
0.038
0.038
0.039
0.040
0.041
0.045
0.046
0.046
0.046
0.048
p-value (corrected)
0.0
1.0
Mean proportion (%)
−0.6 −0.4 −0.2 0.0 0.2 0.4 0.6
Difference in mean proportions (%)

(B)

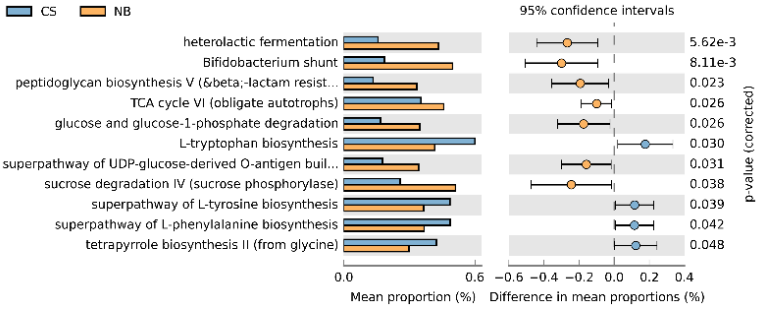
CS
NB
95% confidence intervals
heterolactic fermentation
Bifidobacterium shunt
peptidoglycan biosynthesis V (β-lactam resist...
TCA cycle VI (obligate autotrophs)
glucose and glucose-1-phosphate degradation
L-tryptophan biosynthesis
superpathway of UDP-glucose-derived O-antigen buil...
sucrose degradation IV (sucrose phosphorylase)
superpathway of L-tyrosine biosynthesis
superpathway of L-phenylalanine biosynthesis
tetrapyrrole biosynthesis II (from glycine)
5.62e-3
8.11e-3
0.023
0.026
0.026
0.030
0.031
0.038
0.039
0.042
0.048
p-value (corrected)
0.0
0.6
Mean proportion (%)
−0.6 −0.4 −0.2 0.0 0.2 0.4
Difference in mean proportions (%)

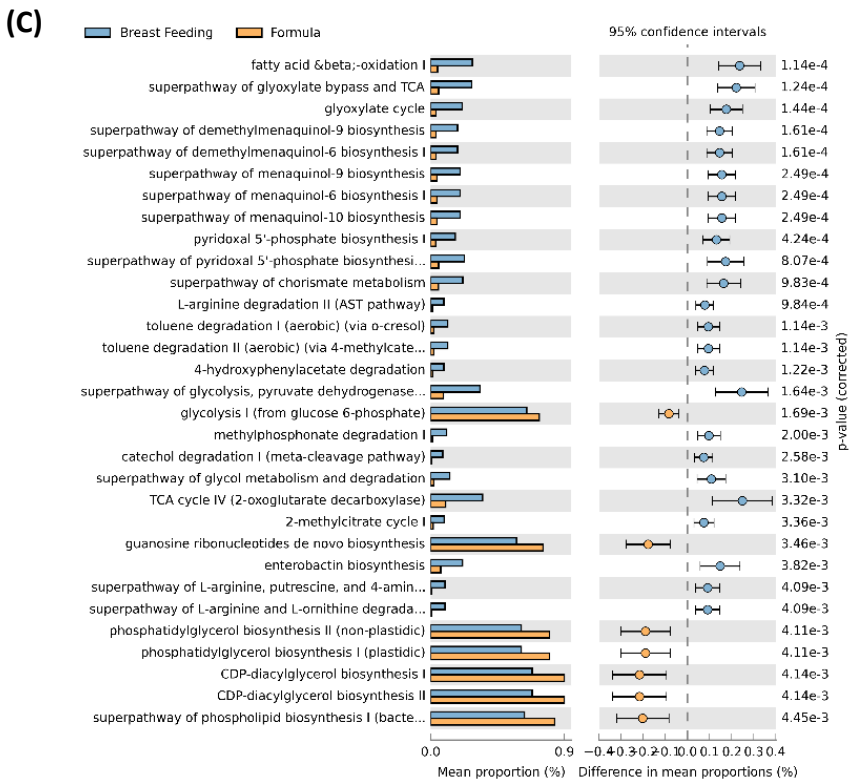

Figure 3.10 | Impact of perinatal factors on meconium microbiome functionality. Extended error bar plots comparing predicted KEGG functions using PICRUSt2. Bar plots show mean proportions of functional pathways, with error bars representing group differences. Error bars are color-coded based on the group with higher proportions. (A) Mother antibiotic usage. (B) Delivery Mode. (C) Feed Type. Welch's t-test was used with $p < 0.05$ (two-sided) as the significance threshold. Abbreviations: CS, C-section; NB, Natural Birth.

3.4.7 Impact of Perinatal Factors on the Infant Oral Microbiome

In this study, maternal antibiotic usage, PROM and gender had no significant effects on the infant oral microbiome. Regarding delivery mode, six ASVs were differentially abundant in NB infants at the genus level, most significantly *Parvimonas*, *Anaeroglobus* and *Oribacterium*. At the species level, 12 ASVs were differentially abundant in NB infants, most significantly *Bifidobacterium longum*, *Veillonella atypica* (*V. atypica*) and *Veillonella parvula* (*V. parvula*) (Figure 3.11A). 18 ASVs were differentially abundant at the genus level in CS-born infants, most significantly *Lautropia*, *Enhydrobacter*, *Kocuria*. 16 ASVs were differentially abundant at the species level in CS-born infants, most significantly *Lautropia mirabilis* (*L. mirabilis*), *Corynebacterium durum* (*C. durum*) and *Veillonella rogosae* (*V. rogosae*) (Figure 3.11A). 15 functional pathways, most significantly peptidoglycan biosynthesis, L-arginine biosynthesis and starch degradation pathways were associated with NB infants (Figure 3.12A). 25 functional pathways were significantly associated with CS-born infants, primarily involving L-arginine biosynthesis, fatty acid salvage and L-tryptophan biosynthesis (Figure 3.12A). Feed type had a significant effect on beta diversity ($R^2 = 0.1148$, $p = 0.049$) (Table 3.3). 27 ASVs were differentially abundant in breast fed infants at the genus level, most significantly *Eubacterium brachy group*, *Parvimonas* and *Anaeroglobus*. 27 ASVs were differentially abundant in breast fed infants at the species level, most significantly *Prevotella saccharolytica* (*P. saccharolytica*), *Treponema maltophilum* (*T. maltophilum*) and *Johnsonella ignava* (*J. ignava*) (Figure 3.11B). 14 ASVs were differentially abundant in formula fed infants at the genus level, most significantly *Lautropua*, *Acinetobacter* and *Escherichia-Shigella*. At the species level, 15 ASVs were differentially abundant in formula fed infants, most significantly *S. oralis*, *G. morbillorum* and *V. atypica* (Figure 3.11B). Hexitol degradation, taxadiene biosynthesis and the Cob(II)yrinate a,c-diamide biosynthesis I pathway were associated with the oral microbiome of breast fed infants (Figure 3.12B) Fatty acid salvage was the only pathway associated with formula fed infants (Figure 3.12B).

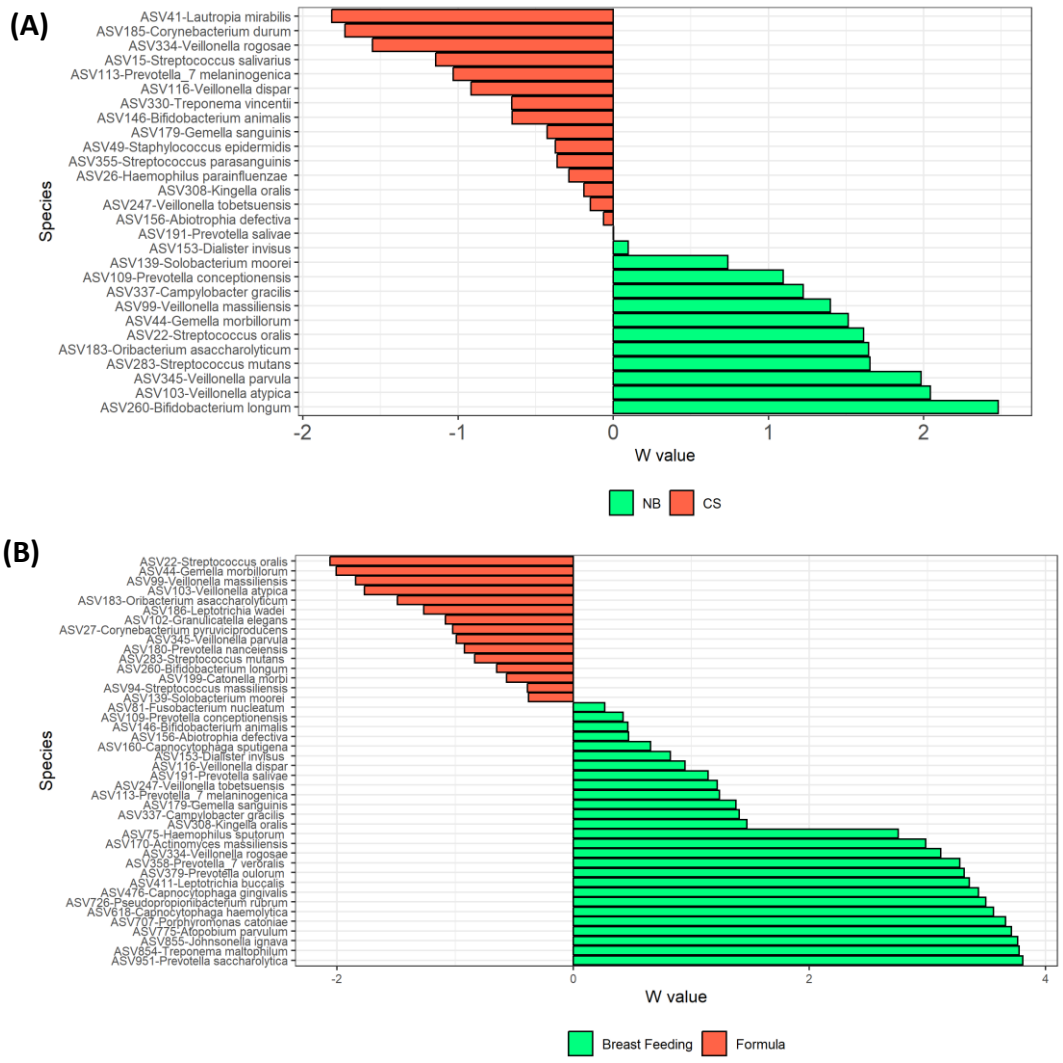

Figure 3.11 | Bar-plots of differentially abundant ASVs within infant oral samples at the species level. Perinatal factors are shown as green and red, respectively. (A) Delivery Mode. (B) Feed Type. Differential abundant ASVs were identified using analysis of the composition of microbiomes (ANCOM) method. Only statistically significant ASVs that fall within a distribution based on W values are shown (Supplementary Table for W values). Abbreviations; CS= C-section, NB= Natural Birth.

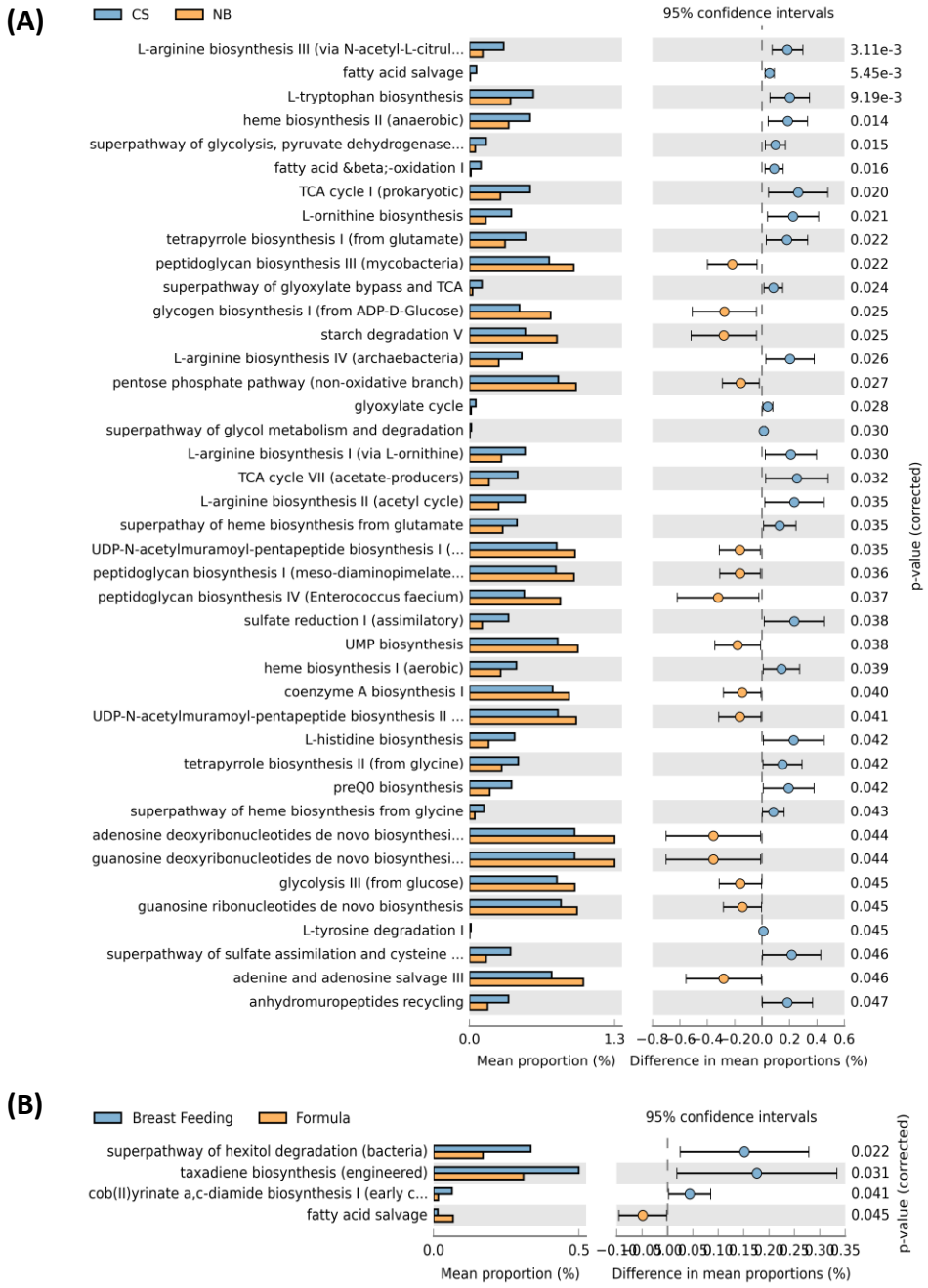

Figure 3.12 | Impact of perinatal factors on meconium microbiome functionality. Extended error bar plots for two-group analysis module comparison of PICRUSt2 predicted KEGG functions. Bar plots on the left represent the mean proportion of each functional pathway and error bars represents the difference between the two groups. Colouring of the error bar is according with the group with the higher proportion of the respective function. (A) Delivery Mode. (B) Feed Type. Welch's t-test for unequal variances. Statistical significance was set at $p < 0.05$ (two-sided) following adjusted measures. Abbreviations; CS= C-section, NB= Natural Birth.

3.4.8 Impact of Perinatal Factors on the Maternal Oral Microbiome

Maternal antibiotic usage had significant effects on the beta diversity of maternal oral microbiome (R^2 = 0.0877, p = 0.013). Seven ASVs were differentially abundant in the "no" group at the genus level, most significantly *Mycoplasma, Filifactor* and *Anaeroglobus.* 20 ASVs were differentially abundant in the "no" group at the species level, most significantly *Streptococcus mutans* (*S. mutans*), *Leptotrichia hongkongensis* (*L. hongkongensis*) *and Granulicatella elegans* (*G. elegans*) (Figure 3.13A). Four ASVs were differentially abundant in the "yes" group at genus level, most significantly, *Oribacterium*, *Mogibacterium* and *Anaerococcus.* At the species level, 16 ASVs were differentially abundant in the "yes" group, most significantly *Oribacterium sinus* (*O. sinus*), *Prevotella_7 veroralis* (*P. veroralis*) and *Prevotella_7 denticola* (*P. denticola*) (Figure 3.13A). Antibiotic usage was significantly associated with 18 pathways including mixed acid fermentation, guanosine pentaphosphate (ppGpp) biosynthesis and tRNA processing (Figure 3.14A). Five pathways, including pyruvate fermentation to acetate and lactate, myo-inositol degradation and D-galacturonate degradation were associated with mothers that did not receive antibiotics (Figure 3.14A). Regarding delivery mode, four ASVs were differentially abundant in the NB group at genus level, most significantly Anaerococcus, Enyhdrobacter and Candidatus Saccharimonas. At the species level, seven ASVs were differentially abundant in the NB group, most significantly *Haemophilus haemolyticus*, *Veillonella massiliensis* and *A. naeslundii* (Figure 3.13B). Nine ASVs were differentially abundant after CS birth at genus level, most significantly, *Filifactor*, *Mycoplasma* and *Eubacterium yurri* group. 18 ASVs were differentially abundant after CS birth at species level, most significantly, *Prevotella oris* (*P. oris*), *Filifactor alocis* (*F. alocis*) and *V. parvula* (Figure 3.13B). CS birth was associated with three functional pathways, most significantly anhydromuropeptides recycling (cell wall recycling), L-arginine biosynthesis III (via N-acetyl-L-citrulline) and norspermidine biosynthesis (Figure 3.14B). Infant gender had no significant effects on the maternal oral microbiome. PROM birth had a significant effect on beta diversity (R2 = 0.0874, p = 0.022). 15 ASVs were differentially abundant in the "no" group at the genus level, predominantly *Staphylococcus*, *Mycoplasma* and *Filifactor*. At the species level, 36 ASVs were differentially abundant in the "no" group, predominantly *L. hongkongensis*, *V. parvula* and *G. morbillorum* (Figure 3.13C). Six ASVs were

differentially abundant in the “yes” group at genus level, most significantly *Scardovia*, *Anaerococcus* and *Lactobacillus*. Ten ASVs were differentially abundant in the “yes” group, most significantly *O. sinus*, *A. naeslundii* and *Capnocytophaga leadbetteri* (*C. leadbetteri*) (Figure 3.13C). Eight functional pathways also associated with the “no” group, primarily thiazole biosynthesis II, thiamine diphosphate biosynthesis and D-galacturonate degradation (Figure 3.14C). Eight different functional pathways were associated with the “yes” group, including mixed acid fermentation, nitrate reduction and 2-methylcitrate cycle (Figure 3.14C).

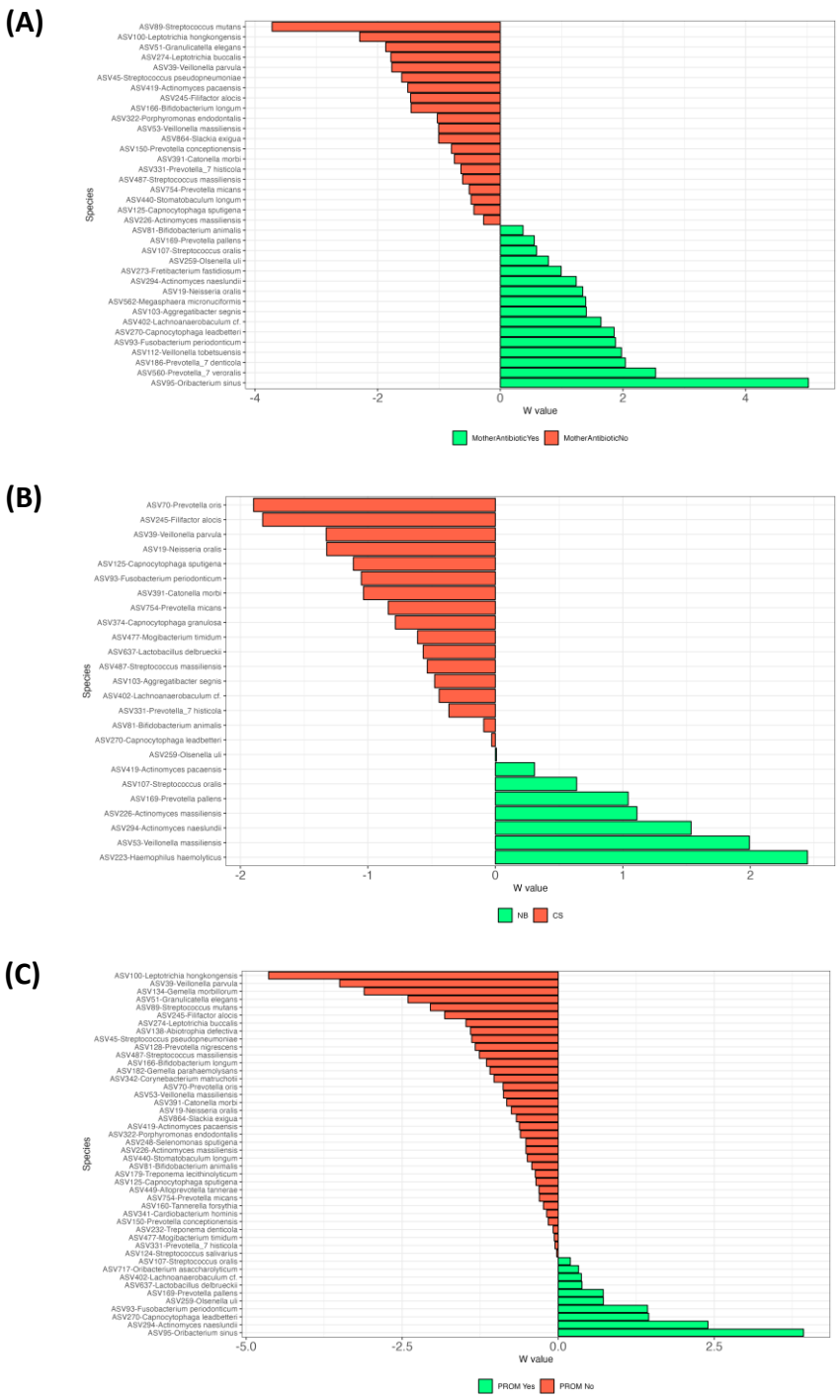

Figure 3.13 | Bar-plots of differentially abundant ASVs within maternal saliva samples at the species level. Perinatal factors are shown as green and red, respectively. (A) Mother antibiotic usage. (B) Delivery Mode. (C) PROM. Differential abundant ASVs were identified using analysis of the composition of microbiomes (ANCOM) method. Only statistically significant ASVs that fall within a distribution based on W values are shown.

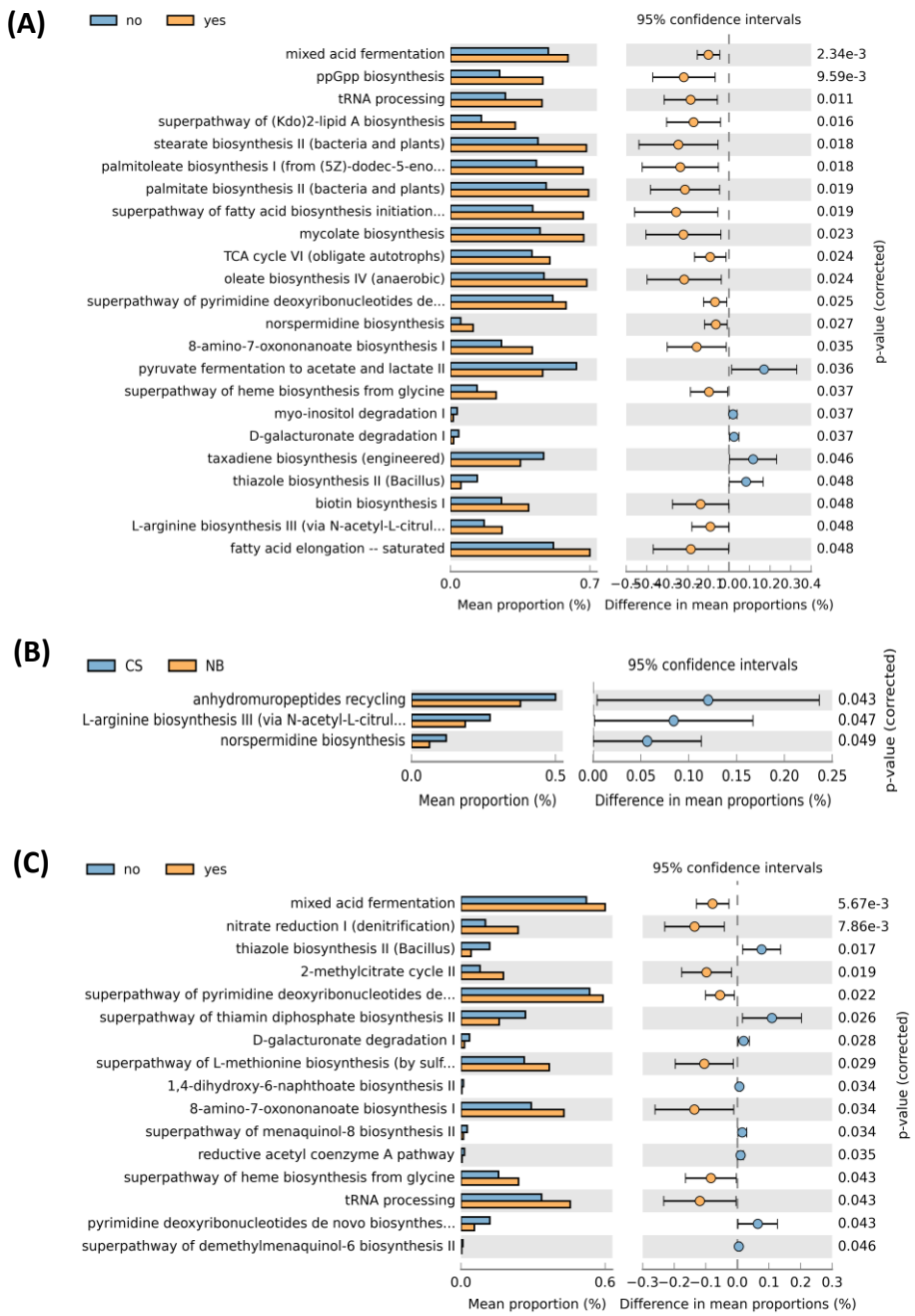

Figure 3.14| Impact of perinatal factors on maternal oral microbiome functionality. Extended error bar plots for two-group analysis module comparison of PICRUSt2 predicted KEGG functions. Bar plots on the left represent the mean proportion of each functional pathway and error bars represents the difference between the two groups. Colouring of the error bar is according with the group with the higher proportion of the respective function. (A) Mother antibiotic usage. (B) Delivery Mode. (C) PROM. Type. Welch's t-test for unequal variances. Statistical significance was set at $p < 0.05$ (two-sided) following adjusted measures. Abbreviations; CS= C-section, NB= Natural Birth.

3.4.9 Impact of Perinatal Factors on the Maternal Vaginal Microbiome

Regarding maternal antibiotic usage and the vaginal microbiome, two ASVs were differentially abundant in the "no" group at the genus level, most significantly *Clostridium sensu stricto 1* and *Staphylococcus*. Two ASVs were differentially abundant in the "no" group at the species level, most significantly *B. longum* and *Lactobacillus iners* (*L. iners*) (Figure 3.15A). Nine ASVs were differentially in the "yes" group at genus level, most significantly *Fenollaria*, *Fastidiosipila* and *Alloscardovia*. At species level, five ASVs were differentially in the "yes" group, most significantly *Alloscardovia omnicolens* (*A. omnicolens*), *Corynebacterium coyleae* (*C.coyleae*) and *F. nucleatum* (Figure 3.15A). 11 functional pathways, primarily involving hexitol fermentation were associated with the "no" group (Figure 3.16A). 42 functional pathways were associated with the "yes" group, most significantly the reductive TCA cycle, L-methionine and L-tryptophan biosynthesis and glucose and xylose degradation pathways (Figure 3.16A). Regarding delivery mode and the vaginal microbiome CS delivery resulted in a significant increase in species richness in vaginal samples (Chao1, $p = 0.091$). At species level five ASVs were differentially abundant after NB delivery, *Corynebacterium pyruviciproducens* (*C. pyruviciproducens*), *L. iners*, *Cutibacterium granulosum* (*C. granulosum*), *B. longum* and *Propionimicrobium lymphophilum* (*P. lymphophilum*) (Figure 3.15B). Nine functional pathways were significantly associated with NB delivery, primarily involving menaquinol biosynthesis and hexuronide and hexuronate degradation (Figure 3.16B). CS birth was associated with 13 functional pathways, most significantly Calvin-Benson-Bassham cycle, tRNA charging, pentose phosphate pathways, and 5-aminoimidazole ribonucleotide biosynthesis (Figure 3.16B). PROM birth significantly increased alpha diversity (Chao1, $p= 0.085$), (Shannon, $p= 0.015$). Two genera, *Clostridium sensu stricto 1and Staphylococcus* were found to be differentially abundant in the "no" group. Six genera were found to be differentially abundant in the "yes" group, most significantly *Alloscardovia*, *Fusobacterium* and Propionimicrobium (Figure 3.15C). Four species, *A.*, *F. nucleatum*, *P. lymphophilum* and *B. longum* were found to be differentially abundant in the "yes" group (Figure 3.15C). The "no" group was significantly associated with 5 pathways, these primarily involved adenosine and guanosine biosynthesis pathways and pyruvate fermentation to acetate and lactate (Figure 3.16C). The "yes" group was significantly associated

with 27 pathways primarily involving the TCA cycle, glucose and xylose degradation, L-methionine and L-tryptophan biosynthesis, and photorespiration (Figure 3.16C).

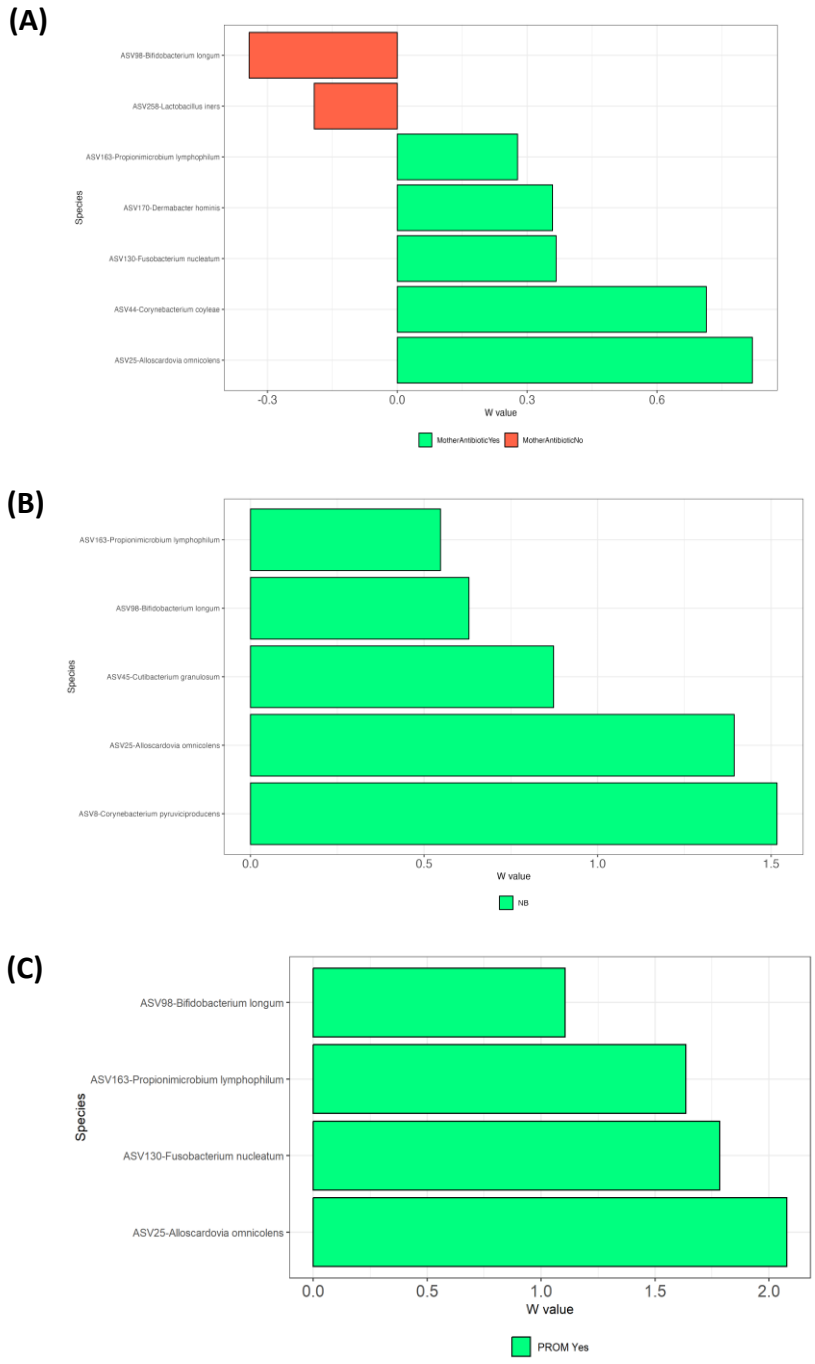

Figure 3.15 | Bar-plots of differentially abundant ASVs within maternal vaginal samples at the species level. Perinatal factors are shown as green and red, respectively. (A) Mother antibiotic usage. (B) Delivery Mode. (C) PROM. Differential abundant ASVs were identified using analysis of the composition of microbiomes (ANCOM) method. Only statistically significant ASVs that fall within a distribution based on W values are shown (Supplementary Table for W values).

(A)

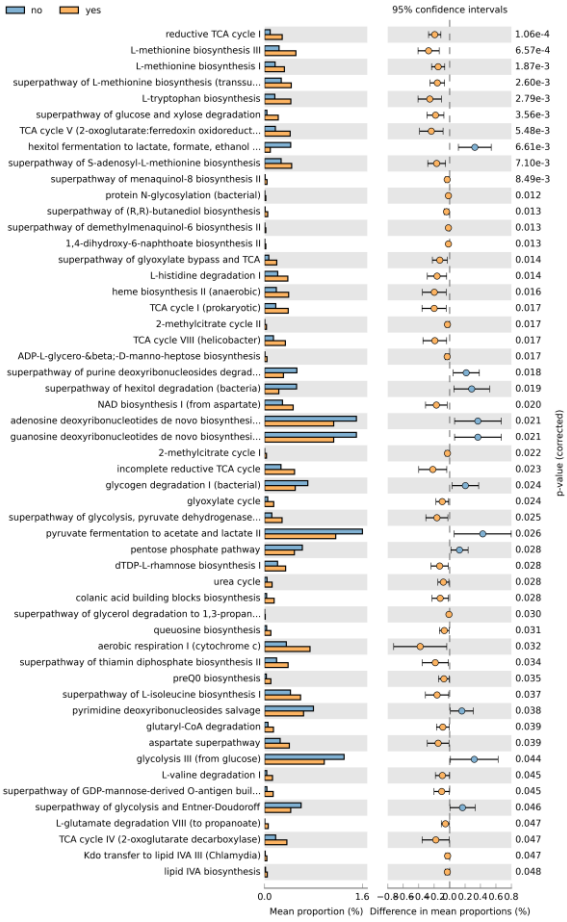
no
yes
95% confidence intervals
reductive TCA cycle I 1.06e-4
L-methionine biosynthesis III 6.57e-4
L-methionine biosynthesis I 1.87e-3
superpathway of L-methionine biosynthesis (transsu... 2.60e-3
L-tryptophan biosynthesis 2.79e-3
superpathway of glucose and xylose degradation 3.56e-3
TCA cycle V (2-oxoglutarate:ferredoxin oxidoreduct... 5.48e-3
hexitol fermentation to lactate, formate, ethanol ... 6.61e-3
superpathway of S-adenosyl-L-methionine biosynthesis 7.10e-3
superpathway of menaquinol-8 biosynthesis II 8.49e-3
protein N-glycosylation (bacterial) 0.012
superpathway of (R,R)-butanediol biosynthesis 0.013
superpathway of demethylmenaquinol-6 biosynthesis II 0.013
1,4-dihydroxy-6-naphthoate biosynthesis II 0.013
superpathway of glyoxylate bypass and TCA 0.014
L-histidine degradation I 0.014
heme biosynthesis II (anaerobic) 0.016
TCA cycle I (prokaryotic) 0.017
2-methylcitrate cycle II 0.017
TCA cycle VIII (helicobacter) 0.017
ADP-L-glycero-β-D-manno-heptose biosynthesis 0.017
superpathway of purine deoxyribonucleosides degrad... 0.018
superpathway of hexitol degradation (bacteria) 0.019
NAD biosynthesis I (from aspartate) 0.020
adenosine deoxyribonucleotides de novo biosynthesi... 0.021
guanosine deoxyribonucleotides de novo biosynthesi... 0.021
2-methylcitrate cycle I 0.022
incomplete reductive TCA cycle 0.023
glycogen degradation I (bacterial) 0.024
glyoxylate cycle 0.024
superpathway of glycolysis, pyruvate dehydrogenase... 0.025
pyruvate fermentation to acetate and lactate II 0.026
pentose phosphate pathway 0.028
dTDP-L-rhamnose biosynthesis I 0.028
urea cycle 0.028
colanic acid building blocks biosynthesis 0.028
superpathway of glycerol degradation to 1,3-propan... 0.030
queuosine biosynthesis 0.031
aerobic respiration I (cytochrome c) 0.032
superpathway of thiamin diphosphate biosynthesis II 0.034
preQ0 biosynthesis 0.035
superpathway of L-isoleucine biosynthesis I 0.037
pyrimidine deoxyribonucleosides salvage 0.038
glutaryl-CoA degradation 0.039
aspartate superpathway 0.039
glycolysis III (from glucose) 0.044
L-valine degradation I 0.045
superpathway of GDP-mannose-derived O-antigen buil... 0.045
superpathway of glycolysis and Entner-Doudoroff 0.046
L-glutamate degradation VIII (to propanoate) 0.047
TCA cycle IV (2-oxoglutarate decarboxylase) 0.047
Kdo transfer to lipid IVA III (Chlamydia) 0.047
lipid IVA biosynthesis 0.048
p-value (corrected)
0.0
1.6
Mean proportion (%)
−0.8 −0.6 −0.4 −0.2 0.0 0.2 0.4 0.6 0.8
Difference in mean proportions (%)

(B)

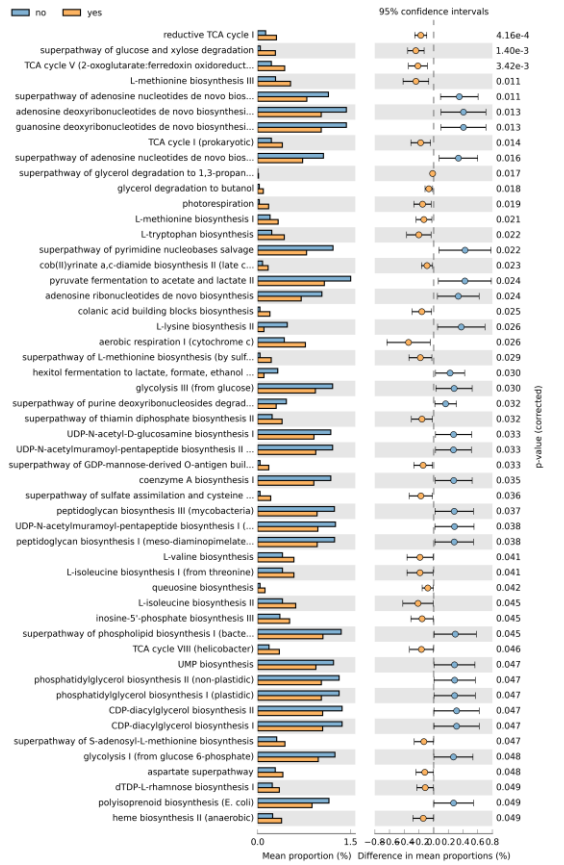
no
yes
95% confidence intervals
reductive TCA cycle I 4.16e-4
superpathway of glucose and xylose degradation 1.40e-3
TCA cycle V (2-oxoglutarate:ferredoxin oxidoreduct... 3.42e-3
L-methionine biosynthesis III 0.011
superpathway of adenosine nucleotides de novo bios... 0.011
adenosine deoxyribonucleotides de novo biosynthesi... 0.013
guanosine deoxyribonucleotides de novo biosynthesi... 0.013
TCA cycle I (prokaryotic) 0.014
superpathway of adenosine nucleotides de novo bios... 0.016
superpathway of glycerol degradation to 1,3-propan... 0.017
glycerol degradation to butanol 0.018
photorespiration 0.019
L-methionine biosynthesis I 0.021
L-tryptophan biosynthesis 0.022
superpathway of pyrimidine nucleobases salvage 0.022
cob(II)yrinate a,c-diamide biosynthesis II (late c... 0.023
pyruvate fermentation to acetate and lactate II 0.024
adenosine ribonucleotides de novo biosynthesis 0.024
colanic acid building blocks biosynthesis 0.025
L-lysine biosynthesis II 0.026
aerobic respiration I (cytochrome c) 0.026
superpathway of L-methionine biosynthesis (by sulf... 0.029
hexitol fermentation to lactate, formate, ethanol ... 0.030
glycolysis III (from glucose) 0.030
superpathway of purine deoxyribonucleosides degrad... 0.032
superpathway of thiamin diphosphate biosynthesis II 0.032
UDP-N-acetyl-D-glucosamine biosynthesis I 0.033
UDP-N-acetylmuramoyl-pentapeptide biosynthesis II ... 0.033
superpathway of GDP-mannose-derived O-antigen buil... 0.033
coenzyme A biosynthesis I 0.035
superpathway of sulfate assimilation and cysteine ... 0.036
peptidoglycan biosynthesis III (mycobacteria) 0.037
UDP-N-acetylmuramoyl-pentapeptide biosynthesis I (... 0.038
peptidoglycan biosynthesis I (meso-diaminopimelate... 0.038
L-valine biosynthesis 0.041
L-isoleucine biosynthesis I (from threonine) 0.041
queuosine biosynthesis 0.042
L-isoleucine biosynthesis II 0.045
inosine-5'-phosphate biosynthesis III 0.045
superpathway of phospholipid biosynthesis I (bacte... 0.045
TCA cycle VIII (helicobacter) 0.046
UMP biosynthesis 0.047
phosphatidylglycerol biosynthesis II (non-plastidic) 0.047
phosphatidylglycerol biosynthesis I (plastidic) 0.047
CDP-diacylglycerol biosynthesis II 0.047
CDP-diacylglycerol biosynthesis I 0.047
superpathway of S-adenosyl-L-methionine biosynthesis 0.047
glycolysis I (from glucose 6-phosphate) 0.048
aspartate superpathway 0.048
dTDP-L-rhamnose biosynthesis I 0.049
polyisoprenoid biosynthesis (E. coli) 0.049
heme biosynthesis II (anaerobic) 0.049
p-value (corrected)
0.0
1.5
Mean proportion (%)
−0.8 −0.6 −0.4 −0.2 0.0 0.2 0.4 0.6 0.8
Difference in mean proportions (%)

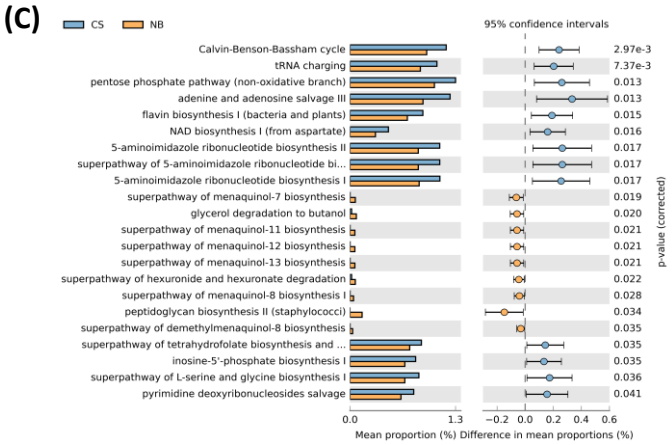

Figure 3.16 | Impact of perinatal factors on maternal vaginal microbiome functionality. Extended error bar plots for two-group analysis module comparison of PICRUSt predicted KEGG functions. Bar plots on the left represent the mean proportion of each functional pathway and error bars represents the difference between the two groups. Colouring of the error bar is according with the group with the higher proportion of the respective function. (A) Mother antibiotic usage. (B) Delivery Mode. (C) PROM. Type. Welch's t-test for unequal variances. Statistical significance was set at $p < 0.05$ (two-sided) following adjusted measures. Abbreviations; CS= C-section, NB= Natural Birth.

3.5 Discussion

In this study, using a cohort of 18 healthy mother-infant dyads, we characterised the microbiota composition of three potential maternal sources of microbial transmission (oral, vaginal and placental) to the microbiota of their new-born infant (oral and meconium microbiota). This allowed us to investigate the contribution of numerous transmission routes and the impact of various perinatal factors on the initial establishment of the infant gut and oral microbiome. Our results consolidate and corroborate recent findings surrounding the existence of a meconium microbiome and the absence of a placental microbiome. We show that significant vertical transfer, primarily from the maternal oral cavity to the infant oral cavity occurs in early life. Moreover, we were able to provide further evidence on how perinatal factors influence the microbial bond between mother and infant and the establishment of the infant microbiome.

One major outstanding question regarding infant microbiome development is the sterility of the intrauterine environment and what is the exact timing of the first microorganisms colonizing the human, that is, during pregnancy or after birth? Fetal meconium has been shown to not have a detectable microbiota before birth (Kennedy et al., 2021). While the presence of a microbiome in neonatal (first-pass) meconium, which is formed before birth, has been debated (Kennedy et al., 2023). Similarly, the existence of a placental microbiome has been disputed (Briana et al., 2021, Blaser et al., 2021). As the existence of microorganisms is not established in these samples, they have been categorised as 'potential no (zero) biomass samples' (Kennedy et al., 2023). In this study, to ensure accurate microbial detection and to identify and remove contaminants, we included 'blank' negative DNA extraction and amplicon sequencing controls and followed post-sequencing analyses steps recommend for low biomass samples by de Goffau et al. (de Goffau et al., 2018) and Heida et al. (Heida et al., 2021). *Staphylococcus*, *Bifidobacterium*, *Streptococcus*, *Enterococcus*, *Escherichia-shigella*, *Delftia*, *Afipia*, *Cutibacterium* and *Rothia* genera represented the core meconium microbiome in our samples. Furthermore, *S. epidermis*, the predominant bacteria in colostrum and milk from healthy women, was the only species present in all meconium sample. *S. epidermis* has repeatedly identified in breastfed neonates meconium (Altuntas, 2015, Moles et al., 2013, Jiménez et al., 2008). In agreement with our findings, several studies have shown that neonatal meconium contains

microbial profiles reflecting populations acquired during and after birth (Klopp et al., 2022, Kang et al., 2022, Rocha-Viggiano et al., 2022, Vemuri and Herath, 2023). Regarding the metabolic pathways present in meconium we used PICRUSt2. Contrary to most feature engineering methods, PICRUSt2 utilises new information from an outside source, such as the MetaCy (Caspi et al., 2014) database to transform each feature to many new informative ones. The pentose phosphate pathway was the most abundant metabolic pathway in meconium. This a metabolic pathway that generates NADPH (Nicotinamide adenine dinucleotide phosphate) and ribose-5-phosphate. NADPH is an essential molecule required for a range of biosynthetic reactions, including the production of fatty acids, steroids, and amino acids. Additionally, NADPH is necessary for the regeneration of the antioxidant, glutathione, which protects cells from oxidative stress. Ribose-5-phosphate, on the other hand, is required for the synthesis of nucleotides, which form the building blocks of DNA and RNA, as well as coenzymes such as ATP (adenosine triphosphate) and NADH (Nicotinamide adenine dinucleotide). Other highly prevalent pathways included the L-isoleucine biosynthesis pathway, branched chain and aromatic amino acid biosynthesis pathways, and glycolysis pathways. These pathways all contribute to the production of energy and/or biosynthesis of amino acids and other essential molecules. Regarding the existence of a placental microbiome, we did not detect any non-contaminant ASVs in placental samples, consistent with a plethora of other studies (Panzer et al., 2022, Sterpu et al., 2021, Leiby et al., 2018). As an exploratory analysis, we removed decontamination steps and prevalence filtering steps used for other samples in study to compare the ASVs found in placental samples with our DNA extraction and amplicon PCR blanks. The phyla (*Actinobacteriota*, *Firmicutes* and *Proteobacteria*), families (*Bacillaceae*, *Corynebacteriaceae*, *Micrococcaceae*, *Streptococcaceae* and *Xanthbacteraceae*) and genera (*Afpia*, *Bacillus*, *Corynebacterium*, *Enhydrobacter*, *Micrococcus* and *Streptococcus*) we detected in placental and control samples were nearly identical, both in terms of presence and relative abundances. All of these microbial taxa are commonly identified as contaminants in laboratory and extraction kit reagents (Salter et al., 2014, Tanner et al., 1998). Overall, our findings are in agreement with studies presented thus far which support the consensus that microbial colonisation of the infant occurs at birth and the establishment of replicating microbial cells does not commonly occur in healthy pregnancies, devoid of clinical infections (Blaser et al., 2021).

The second aim of this study was to elucidate the contribution of each main maternal microbial source (vagina, oral cavity and placenta) to their offspring (gut and oral cavity). To explore this question we investigated overall microbial composition of each sample type and deciphered vertical microbiota transfer in the 18 mother-infant dyads. As we have discussed the meconium microbiome in the previous section, we begin with the infant oral microbiome. The overall composition of the oral microbiome of infants in this study was consistent with other studies, predominantly consisting of *Streptoccous, Rothia, Prevotella, Neisseria, Escherichia-Shigella, Gemella, Haemophilus* genera (Belda-Ferre et al., 2012). *S. salivarius, S. oralis, R. mucilaginosa, S. epidermidis, F. nucleatum* were highly abundant and are some of the most frequently detected early colonisers in the oral cavity (Mason et al., 2018, Dzidic et al., 2018, Xiao et al., 2020). *Prevotella, Streptoccous, Veillonella, Rothia, Neisseria, Haemophilus* and *Fusobacterium* were the predominant genera present in our maternal oral samples, consistent with other studies (La et al., 2022, Jang et al., 2021, DiGiulio et al., 2015). At the species level, *R. mucilaginosa, H. parainfluenzae, P. melaninogenica F. nucleatum* represented some of the most abundant strains in maternal oral microbiome, which is commonly reported (Jo et al., 2021, Dashper et al., 2019, Lif Holgerson et al., 2020). We found that the vaginal microbiome demonstrated the most unique microbial composition in comparison to meconium, infant and maternal oral microbial communities. Indeed, the diversity of the vaginal microbiota was significantly lower than meconium and maternal oral microbiome, consistent with previous findings (Hurley et al., 2019). To date, in non- pregnant and pregnant women, no single core vaginal microbiota has been identified, but rather there are multiple core microbiota which can be classified into six 'community state types' (CSTs) based on differences in species composition and their relative abundances (Gajer et al., 2012, DiGiulio et al., 2015). Our samples were dominated by *Peptoniphilus, Lactobacillus, Finegoldia, Corynebacterium, Clostridium sensu stricto 1* and *Anaeroccus* genera. *Lactobacillus* dominance is a key feature of a healthy vaginal microbiome. These species are essential for restoring the vaginal ecosystem and maintaining a low pH, which functions as a barrier against invading and colonizing pathogens (Petrova et al., 2015). Overall our samples are indicative of CSTs 4-A and 4-B, which are characterised by decreased levels of lactic acid bacteria and increased proportions of strictly anaerobic bacteria (Ravel et al., 2011, Gajer et al., 2012). *F. magna* and *P. faecalis* were both found to be present in 17 out of 18

samples which have both been associated with bacterial vaginosis (Shipitsyna et al., 2013, Ceccarani et al., 2019). The most abundant metabolic pathways present in the vaginal microbiome of our samples have been shown to be conserved across vaginal samples previously (Liu et al., 2021).

Regarding vertical transmission, it has been well established that the gut, which harbours the most heavily populated microbiota in the human body, dominates the transmission of mother-to-infant microbiota (Bäckhed et al., 2015). Therefore, in this study we focussed on the contribution of the maternal oral cavity and vaginal microbiomes to the infant oral and gut microbiomes. The overall compositions of the infant and maternal oral microbiomes of our samples were highly similar both in terms of taxa and abundance, with the exception of the presence of *Escherichia-shigella*, *Cutibacterium* and *Corynebacterium* genera in infants. Investigation of mother-infant pairs revealed that on average, the infants' oral microbiota shared 45 ASVs which accounted for 65% of the total reads in the infant's sample. Although perinatal factors did not significantly influence the levels of sharing in this study, Kageyama et al. recently reported greater acquisition of maternal oral bacteria in formula-fed infants compared to breast-fed and mixed-fed infants (Kageyama et al., 2022). In our study, commensal bacteria such as *Streptococcus*, *Veillonella*, *Neisseria*, *Haemophilus*, *Fusobacterium* and *Rothia* were highly shared by infants and their parents, also reported by (Jo et al., 2021). *S. oralis*, *H. parainfluenzae*, *F. nucleatum* and *R. Mucilaginosa* exhibited high levels of sharing, similar to previous studies (Jo et al., 2021). *S. oralis* was the only species to be found in all infant oral samples and all maternal oral samples. *S. oralis* is one of a number commensal oral streptococci which are regarded as a primary colonisers and the major species colonizing infants and mucosal sites in adults (Marsh et al., 2009, Cephas et al., 2011). *H. parainfluenzae* and *R. Mucilaginosa* also form part of the flora of the mouth (Verma et al., 2018). By contrast, *F. nucleatum* is involved in periodontal disease (Moore and Moore, 1994, Yang et al., 2014) and also shared at a high rate. Overall the compositional and bacterial sharing similarities observed in this study are in agreement with previous studies which have indicated that about 70% of the initial neonatal oral microbiota are maternal in origin with 65% derived from maternal oral microbiota through vertical transmission (Yu et al., 2023, Gomez-Arango et al., 2017). Regarding vaginal microbiome transfer to the oral cavity of the infant, on average, a related mother's

vaginal microbiome and infant's oral microbiota shared 15 bacterial taxa which accounted for 15% of the total reads in the infant's sample (Figure 3.). When comparing NB infants versus by CS and we found that route of delivery had a significant effect on the amount of the infants' oral microbiome that was shared with their mother's vaginal microbiome (Mann Whitney Test, $p = 0.045$) (Figure 3.), also reported by (Dominguez-Bello et al., 2010b, Li et al., 2018). *C. pyruvicproducens* was present in all in all 18 mother-infant dyads and was the only species common to oral and vaginal samples. *C. pyruvicproducens* is a pyruvic acid producer which has recently been described as a putative human pathogen (Bartlett et al., 2022). The potential aforementioned pathogen, *F. nucleatum* was also highly prevalent and was present in 15 dyads. Regarding maternal oral microbiota transfer to the infant's meconium microbiome, on average, a related mother's oral microbiota and infant's meconium microbiota shared 8 bacterial taxa which accounted for 6% of the total reads in the infant's sample (Figure 3.). Perinatal factors had no effect on the levels of sharing. Regarding species sharing, *R. mucilaginosa* was the only shared species and was present in all 18 mother-infant dyads. *R. mucilaginosa* is a common commensal of the oral cavity and upper respiratory tract which has anti-inflammatory activity by NF-κB pathway inactivation (Rigauts et al., 2022). Regarding maternal vaginal microbiota transfer to the infant's meconium microbiome, on average, a related mother's vaginal microbiota and infant's meconium microbiota shared 38 bacterial taxa which accounted for 21% of the total reads in the infant's sample (Figure 3.). Perinatal factors had no effect on the levels of species sharing. Regarding species sharing, *B. longum* was the only shared species between vaginal and meconium samples and was present in all 18 dyads. *B. longum* is a commensal gastrointestinal tract (GIT) inhabitant that is recognised as a significant member of the human gut microbiota and is the most abundant species in the infant gut (Turroni et al., 2012), exerting numerous beneficial effects (Arboleya et al., 2016) ranging from production of bioactive substances to bifidobacterial surface-associated molecules that interact with the host (Zhang et al., 2019). Research to date indicates that *B. longum* has a range of applications to treat or prevent a range of diseases beginning in neonatal life and beyond (Mills et al., 2023).

The third and final aim of this study was to investigate the potential drivers that control strain inheritance and/or selection by infants in early life. Understanding how those

factors exert their influences on the microbiota communities in early life will facilitate our understanding of various medical conditions occurring in early life and beyond and thereby inform development of new preventive and therapeutic treatments.

Regarding maternal antibiotic usage, we observed a number of significant and interesting results. Firstly, in meconium samples we found significant differences in beta diversity. While the timing of antibiotic intervention was not noted in our study, a recent study noted that the beta diversity of meconium was significantly different between prenatal and intrapartum antibiotic administration, suggesting that timing of antibiotic prophylaxis is critical for the microbial community of infants during their first days of life (Bossung et al., 2022). In our study, *Gemella* and *Fusobacterium* spp., considered opportunistic pathogens which can contribute to biofilm formation (García López and Martín-Galiano, 2020, Okuda et al., 2012), were both differentially abundant in the meconium of infants born to mothers who received antibiotics. Antibiotic exposure significantly increased heme biosynthesis, an iron-containing cofactor that is required by bacterial pathogens for essential functions and virulence (Choby and Skaar, 2016, Palmer and Skaar, 2016). Similar findings regarding the effect of prenatal maternal antibiotic treatment on the establishment of thee gut microbiome and immune functioning in offspring have recently been reported in C57BL/6J mouse models (Madany et al., 2022). In maternal saliva samples, beta diversity was also significantly affected by maternal antibiotic usage. Antibiotic use was associated with increased *Prevotella* spp., *Fusobacterium* spp., linked to periodontitis (Costalonga and Herzberg, 2014). Non-antibiotic use was strongly associated with *Streptococcus*, *Actinomyces*, and *Granulicatella* spp. associated with periodontal health (Liu et al., 2012). In this study, mother antibiotic usage had the most profound effects on the vaginal microbiome. Significant increases in Chao1, Shannon and Simpson alpha diversity indexes and differences in beta diversity were also observed. Intrapartum antibiotic prophylaxis has previously been shown to modify the vaginal microbiota composition, decreasing abundances of *Lactobacillus* spp. causing higher microbial diversity (Shabayek et al., 2022). *L. iners*, a vaginal symbiont, recognised as the most prevalent *Lactobacillus* species in the vaginal econiche (Zheng et al., 2021, Campisciano et al., 2020) was differentially abundant in the no antibiotic group. A significant number of metabolic pathways were associated with maternal antibiotic usage. Most significantly the reductive TCA cycle and L-

methionine biosynthesis pathways, which can produce succinate. A high ratio of succinate to lactic acid was the original marker of bacterial vaginosis (Piot et al., 1982, Ison et al., 1983), and high succinate concentrations distinguish bacterial vaginosis from the similar but distinct condition of aerobic vaginitis (Donders et al., 2002). Increasing succinate at the expense of lactate results in a self-perpetuating condition whereby an elevated pH and a more reduced environment supports the growth of the anaerobic bacteria noted in bacterial vaginosis (Holmes et al., 1985). Encouragingly, this group also saw significant increases in tryptophan biosynthesis associated with vaginal health (Ceccarani et al., 2019). The non-antibiotic group was significantly associated with pathways involving the production of lactate, the primary marker of vaginal health (Ceccarani et al., 2019, Srinivasan et al., 2015).

Regarding delivery mode, we observed increased species richness in meconium samples of CS-born infants, which may be indicative of aberrant microbial colonisation. Maternal skin related *Streptococcus* spp. and potentially harmful *Intestinibacte*r and *Veillonella* spp., typically overrepresented in the gut microbiome of CS delivered infancolots (Liu et al., 2019), were differentially abundant in the meconium of CS infants. Delivery mode also significantly impacted the meconium microbiome of NB and CS delivered infants. NB was associated with heterolactic fermentation which produces lactic acid as a by-product, indicative of high levels of commensal bacteria such as lactobacilli and bifidobacteria, which utilise lactic acid as an energy source (Louis et al., 2022). Lactate production is also essential to maintain a low pH for digestive enzyme activation and serve as energy sources for colonocytes (Fukuda et al., 2011). The *Bifidobacterium* shunt pathway, also referred to as the fructose-6-phosphate (F6P) phosphoketolase (bifid shunt) pathway, was associated with NB infants. Bifidobacteria degrade the hexose sugars glucose and fructose through this unique ATP-generating pathway (Pokusaeva et al., 2011). The metabolites from this pathway primarily produce acetate and lactate (Yu et al., 2013), which antagonise pathogenic bacteria, form a barrier against infection (Sanchez et al., 2010) and serve as nutrients for cross-feeding between gut bacteria (Chia et al., 2021). Tetrapyrrole biosynthesis, important for the synthesis of heme, was associated with CS birth, which may indicate high levels of pathogenic bacteria (Choby and Skaar, 2016). Mode of delivery has been shown to affect oral microbiota establishment in infants (Lif Holgerson et al., 2011, Dzidic et al., 2018, Li et al., 2018). In our study,

important early colonisers of the infant oral microbiome *Bifidobacterium longum, V. atypica, V. parvula, S. oralis and S. mutans* were differentially abundant in NB infants. *Streptococcus* is perhaps the most ubiquitous bacteria detected in the infant oral microbiome in early life, primarily because of its ability to adhere to and colonise the mucosal surface lining (Sampaio-Maia and Monteiro-Silva, 2014). The metabolic products (such as lactic acid) derived from *Streptococcus* species from the dietary oligosaccharides in breast milk have been note to pave the way for the establishment of other microorganisms in the oral cavity, including bacterial genera like *Veillonella* (Gomez and Nelson, 2017, Wernersson et al., 2006). *L. mirabilis*, a known oral commensal which is a Gram-negative, motile, coccus bacteria which has been associated with periodontal health (Papapanou et al., 2020, Colombo et al., 2009), was differentially abundant in CS delivered infants. *C. durum* associated with Celiac diseases (Francavilla et al., 2014, Xiao et al., 2020) was also differentially abundant after CS delivery. By contrast, *V. rogosae*, reportedly enriched in caries-free individuals (Zhou et al., 2021) was also differentially abundant after CS delivery. In maternal oral samples, organisms associated with periodontitis, specifically *Fusobacterium* spp. and *Prevotella* spp. (Costalonga and Herzberg, 2014) and *F. alocis* (Griffen et al., 2012) were differentially abundant in the oral microbiome of mothers that underwent CS. By contrast the NB group was differentially abundant in *S. oralis, A. naeslundii, A. massiliensis and A. pacaensis*, which are typically associated with periodontal health (Liu et al., 2012). L-arginine biosynthesis was associated with the CS group. L-arginine has been reported to decrease the risk of dental caries by destabilizing and removing established oral biofilms (Zheng et al., 2017, Acevedo et al., 2005). Biosynthesis of the polyamine molecule norspermidine, was also associated with the CS group. Upregulation of norspermidine biosynthesis has been reported in the oral cavity of squamous cell carcinoma (Yang et al., 2021, Ganly et al., 2019) and has been reported to be involved in biofilm disassembly (He et al., 2020). Similar to maternal antibiotic use, CS delivery resulted in significantly increased species richness in the vaginal microbiome. Furthermore, akin to mothers that weren't given antibiotics, *L. iners*, was differentially abundant after NB. This finding was also reported by (Zhang et al., 2022). NB was associated with functional pathways beneficial to the infant, most significantly menaquinol (Vitamin K_2) biosynthesis, essential for blood clotting and bone health (Institute of et al., 2002).

Regarding feed type, breast feeding was associated with increased *Bacteroides* spp., which have been shown to shown to be able to metabolize HMOs (Pace et al., 2021, Marcobal et al., 2010). By contrast, formula feeding was associated with a more diverse bacterial community and differentially abundant taxa including *Blautia* spp. and *Dorea* spp. which are indicative of a more mature infant gut microbiome, among the most age-discriminatory species from six to 24 months of age in healthy infants (Robertson et al., 2019). Breast feeding was associated with a number of health promoting metabolic pathways, including, the demethylmenaquinol biosynthesis pathway important for the synthesis of Vitamin K_2. Furthermore, pyridoxal 5'-phopshate biosynthesis pathways which synthesise vitamin B6, important for amino acid metabolism, neurotransmitter synthesis and immune function (Mach and Clark, 2017), was also associated with breast feeding. Three important metabolic functional pathways were associated with the oral microbiome of breast fed infants. Hexitol degradation, which enables the metabolism of sugars like sorbitol and mannitol, which are present in breast milk. Taxadiene biosynthesis, which is a pathway involved in the biosynthesis of terpenoids, shown to have antimicrobial properties (Masyita et al., 2022). Finally, the Cob(II)yrinate a,c-diamide biosynthesis I pathway, involved in the biosynthesis of vitamin B12. Vitamin B12 is a water-soluble vitamin primarily obtained from meat, poultry, and dairy products and is essential for normal functioning of the central nervous system, red blood cell production, and DNA synthesis (Hunt et al., 2014). Fatty acid salvage was the only pathway associated with formula fed infants. This pathway allows bacteria to convert fatty acids, which are not directly usable, into a form that can be used as an energy source, which may be particularly important for the oral microbiome of formula-fed infants who are not receiving the same complex sugars and other nutrients present in breast milk.

Regarding gender, the only significant effects were observed in meconium samples. While there was no significant impact on the diversity metrics tested or functionality of the meconium microbiome, which has been reported (Cong et al., 2016), we did observe differentially abundant taxa which could correlate with different clinical outcomes. *B. animalis, B. uniformis* and *P.merdae* were differentially abundant in females. One other study has made a similar observation in female infants at three months old (Kozyrskyj et al., 2016). To date the mechanism of the gender specific differences on gut microbiome community remains poorly understood and requires

further study. It has been speculated that the variation of gut microbiome communities influenced by gender are related to hormone-immune-microbe interactions and genetic traits (Gomez et al., 2015).

Finally, regarding PROM birth, significant effects were observed in meconium, maternal oral and vaginal samples. In meconium samples there was no clear deleterious effects in terms of differential abundance with commensal *Eubacterium* spp. (Mukherjee et al., 2020) higher in the PROM birth infants. Beta diversity in maternal oral samples was significantly affected by PROM birth and the pathogenic species *C. leadbetteri* (Frandsen et al., 2008) was differentially abundant after PROM birth. Encouragingly, a number of metabolic pathways involved in pathogen clearance in the oral microbiome, primarily involving nitrate reduction (Hezel and Weitzberg, 2015) were associated with PROM birth. In vaginal samples we observed increased alpha diversity and decreased *Lactobacillus* spp. These finding have been reported by numerous studies, supporting the general consensus that lacking the protection of *Lactobacillus* is one of the major causes of PROM occurrence (Liu et al., 2022). While we did not observe other differentially abundant taxa, recent clinical trials have explored the use of vaginal probiotics (*L. rhamnosus* and *L. gasseri*) on the outcomes of PROM in pregnant women (Moraes et al., 2023).

There were a number of limitations in this study. Firstly, regarding the study design, utilizing a subset of samples led to a small sample size for analyses which may have restricted our ability to draw precise conclusions about the influence of perinatal factors on the development of the infant microbiome. A larger sample size would have provided more statistical power and allowed for a more robust analysis. Additionally, the lack of longitudinal design prevented the tracking of changes in the microbiome over time, which is important for understanding how it develops and responds to various environmental factors. Future studies should consider using larger sample sizes and longitudinal designs to build upon our findings and expand our understanding of this complex process. Limitations of the 16S rRNA gene sequencing limit the ability to draw definitive conclusions from this study. For instance, the low taxonomic resolution provided by 16S rRNA gene profiling (Bokulich et al., 2016), to identify bacteria reliably below the genus level does not allow the discrimination of pathogenic and non-pathogenic strains in the aforementioned genera, or indeed accurate evaluation of the functional capacity of the microbiome. It is also possible

that the apparent abundance of bacterial species was artificially inflated through PCR kinetics early in the amplicon methodology. To validate these findings in future studies, other methods, such as targeted qPCR or amplification-free metagenomics, would be required. Other possible methodologies to investigate low biomass samples include quantitative PCR (qPCR), fluorescent in situ hybridisation (FISH), scanning electron microscopy (SEM), microbial culturing and spiking with control DNA to allow calculation of absolute microbial abundance would have also improved this study. Furthermore, we used PICRUSt2 to estimate metabolic functional differences between the groups which has a number of limitations. Firstly, PICRUSt2 predictions exhibit bias toward established reference genomes, diminishing the likelihood of identifying rare, environment-specific functions. However, this constraint is gradually easing with the ongoing expansion of high-quality genomes. PICRUSt2 offers flexibility by enabling users to employ custom genomes for predictions, facilitating the study of specific environments. The second critique involves the inability of amplicon-based predictions to discern strain-specific functionality. This represents a notable constraint inherent in PICRUSt2 and any amplicon-based analysis, as differentiation is limited to variations in the amplified marker gene sequence. This limitation can be overcome by using a shotgun metagenomic approach which allows accuarate measurement of the relatavie abundance of functional genes and provides strain level accuracy. Finally, studies investigating how multiple perinatal factors may interact with each other in the formation of the infant gut microbiome are also warranted. For instance, breastfeeding has been shown to beneficially alter the patterns of aberrant colonisation in infants born by C-section (Coker et al., 2021). While complex, it is essential to understand the transmission routes and elucidate the extent to which perinatal factors may influence the microbial bond between mother and infant. A deeper understanding of how perinatal factors may stimulate or hinder the inheritance and/or choice of microbes by infants in early life constitutes a viable strategy in the investigation of next-generation probiotics for therapeutic interventions that maintain/improve the health of infants.

3.6 Acknowledgements

The authors wish to extend their most grateful thanks to all the families who agreed to participate in the OPIuM study. We thank the OPIuM research nurses and research teams for their assistance and support throughout. We thank Prof. Eugene M. Dempsey

and Prof. Anthony Ryan for their assistance in study design, ethical approval and manuscript prepatation. Additionally, we thank Dr. Kiera Murphy for assistance with the bioinformatics pipeline, and for helpful discussions. Finally, we thank Ms. Elaine Lawton, Dr. Fiona Crispie, Dr. Lisa Olohan and Prof. Paul Cotter from the Teagasc Sequencing Facility in relation to the 16S rRNA sequencing.

3.7 Financial Support

This research is supported by APC Microbiome Ireland, a research centre funded by Science Foundation Ireland (SFI), through the Irish Government's National Development Plan (Grant Number. 12/RC/2273_P2).

3.8 References

ACEVEDO, A. M., MACHADO, C., WOLFF, M. & KLEINBERG, P. I. 2005. The Inhibitory Effect of an Arginine Bicarbonate/Calcium Carbonate (CaviStat")-Containing Dentifrice on the Development of. J Clin dent, 16, 63-70.

AITCHISON, J., BARCELÓ-VIDAL, C., MARTÍN-FERNÁNDEZ, J. A. & PAWLOWSKY-GLAHN, V. 2000. Logratio analysis and compositional distance. Mathematical geology, 32, 271-275.

ALESSANDRI, G., VAN SINDEREN, D. & VENTURA, M. 2021. The genus bifidobacterium: From genomics to functionality of an important component of the mammalian gut microbiota running title: Bifidobacterial adaptation to and interaction with the host. Comput Struct Biotechnol J, 19, 1472-1487.

ALTUNTAS, E. G. 2015. Isolation, identification and characterization of Staphylococcus epidermidis in human milk. LWT-Food Science and Technology, 60, 36-41.

AMOS, G. C. A., LOGAN, A., ANWAR, S., FRITZSCHE, M., MATE, R., BLEAZARD, T. & RIJPKEMA, S. 2020. Developing standards for the microbiome field. Microbiome, 8, 98.

ARBOLEYA, S., WATKINS, C., STANTON, C. & ROSS, R. P. 2016. Gut bifidobacteria populations in human health and aging. Frontiers in microbiology, 7, 1204.

BÄCKHED, F., ROSWALL, J., PENG, Y., FENG, Q., JIA, H., KOVATCHEVA-DATCHARY, P., LI, Y., XIA, Y., XIE, H. & ZHONG, H. 2015. Dynamics and stabilization of the human gut microbiome during the first year of life. Cell host & microbe, 17, 690-703.

BARTLETT, A., PADFIELD, D., LEAR, L., BENDALL, R. & VOS, M. 2022. A comprehensive list of bacterial pathogens infecting humans. Microbiology, 168, 001269.

BELDA-FERRE, P., ALCARAZ, L. D., CABRERA-RUBIO, R., ROMERO, H., SIMON-SORO, A., PIGNATELLI, M. & MIRA, A. 2012. The oral metagenome in health and disease. The ISME journal, 6, 46-56.

BEZIRTZOGLOU, E., TSIOTSIAS, A. & WELLING, G. W. 2011. Microbiota profile in feces of breast-and formula-fed newborns by using fluorescence in situ hybridization (FISH). Anaerobe, 17, 478-482.

BLASER, M. J., DEVKOTA, S., MCCOY, K. D., RELMAN, D. A., YASSOUR, M. & YOUNG, V. B. 2021. Lessons learned from the prenatal microbiome controversy. Microbiome, 9, 8.

BOKULICH, N. A., CHUNG, J., BATTAGLIA, T., HENDERSON, N., JAY, M., LI, H., D. LIEBER, A., WU, F., PEREZ-PEREZ, G. I. & CHEN, Y. 2016. Antibiotics, birth mode, and diet shape microbiome maturation during early life. Science translational medicine, 8, 343ra82-343ra82.

BOLTE, E. E., MOORSHEAD, D. & AAGAARD, K. M. 2022. Maternal and early life exposures and their potential to influence development of the microbiome. Genome Medicine, 14, 1-29.

BOSSUNG, V., LUPATSII, M., DASHDORJ, L., TASSIELLO, O., JONASSEN, S., PAGEL, J., DEMMERT, M., WOLF, E. A., RODY, A., WASCHINA, S., GRASPEUNTNER, S., RUPP, J. & HÄRTEL, C. 2022. Timing of antimicrobial prophylaxis for cesarean section is critical for gut microbiome development in term born infants. Gut Microbes, 14, 2038855.

BRIANA, D. D., PAPAEVANGELOU, V. & MALAMITSI-PUCHNER, A. 2021. The jury is still out on the existence of a placental microbiome. Acta Paediatrica, 110, 2958-2963.

BROWNE, H. P., SHAO, Y. & LAWLEY, T. D. 2022. Mother–infant transmission of human microbiota. Current Opinion in Microbiology, 69, 102173.

BUSHMAN, F. D. 2019. De-Discovery of the Placenta Microbiome. Am J Obstet Gynecol, 220, 213-214.

BYRD, A. L., BELKAID, Y. & SEGRE, J. A. 2018. The human skin microbiome. Nature Reviews Microbiology, 16, 143-155.

CALLAHAN, B. J., MCMURDIE, P. J., ROSEN, M. J., HAN, A. W., JOHNSON, A. J. A. & HOLMES, S. P. 2016a. DADA2: High-resolution sample inference from Illumina amplicon data. Nature methods, 13, 581-583.

CALLAHAN, B. J., SANKARAN, K., FUKUYAMA, J. A., MCMURDIE, P. J. & HOLMES, S. P. 2016b. Bioconductor workflow for microbiome data analysis: from raw reads to community analyses. F1000Research, 5.

CAMPISCIANO, G., IEBBA, V., ZITO, G., LUPPI, S., MARTINELLI, M., FISCHER, L., DE SETA, F., BASILE, G., RICCI, G. & COMAR, M. 2020. Lactobacillus iners and gasseri, Prevotella bivia and HPV belong to the microbiological signature negatively affecting human reproduction. Microorganisms, 9, 39.

CASPI, R., ALTMAN, T., BILLINGTON, R., DREHER, K., FOERSTER, H., FULCHER, C. A., HOLLAND, T. A., KESELER, I. M., KOTHARI, A. & KUBO, A. 2014. The MetaCyc database of metabolic pathways and enzymes and the BioCyc collection of Pathway/Genome Databases. Nucleic acids research, 42, D459-D471.

CECCARANI, C., FOSCHI, C., PAROLIN, C., D'ANTUONO, A., GASPARI, V., CONSOLANDI, C., LAGHI, L., CAMBONI, T., VITALI, B., SEVERGNINI, M. & MARANGONI, A. 2019. Diversity of vaginal microbiome and metabolome during genital infections. Sci Rep, 9, 14095.

CEPHAS, K. D., KIM, J., MATHAI, R. A., BARRY, K. A., DOWD, S. E., MELINE, B. S. & SWANSON, K. S. 2011. Comparative analysis of salivary bacterial microbiome diversity in edentulous infants and their mothers or primary care givers using pyrosequencing. PloS one, 6, e23503.

CHARBONNEAU, M. R., BLANTON, L. V., DIGIULIO, D. B., RELMAN, D. A., LEBRILLA, C. B., MILLS, D. A. & GORDON, J. I. 2016. A microbial perspective of human developmental biology. Nature, 535, 48-55.

CHIA, L. W., MANK, M., BLIJENBERG, B., BONGERS, R. S., VAN LIMPT, K., WOPEREIS, H., TIMS, S., STAHL, B., BELZER, C. & KNOL, J. 2021. Cross-feeding between Bifidobacterium infantis and Anaerostipes caccae on lactose and human milk oligosaccharides. Beneficial microbes, 12, 69-83.

CHOBY, J. E. & SKAAR, E. P. 2016. Heme synthesis and acquisition in bacterial pathogens. Journal of molecular biology, 428, 3408-3428.

CLARKE, G., O'MAHONY, S. M., DINAN, T. G. & CRYAN, J. F. 2014a. Priming for health: gut microbiota acquired in early life regulates physiology, brain and behaviour. Acta Paediatr, 103, 812-9.

CLARKE, G., STILLING, R. M., KENNEDY, P. J., STANTON, C., CRYAN, J. F. & DINAN, T. G. 2014b. Minireview: gut microbiota: the neglected endocrine organ. Molecular endocrinology, 28, 1221-1238.

COKER, M. O., LAUE, H. E., HOEN, A. G., HILLIARD, M., DADE, E., LI, Z., PALYS, T., MORRISON, H. G., BAKER, E. & KARAGAS, M. R. 2021. Infant feeding alters the longitudinal impact of birth mode on the development of the gut microbiota in the first year of life. Frontiers in microbiology, 524.

COLLADO, M. C., ISOLAURI, E., LAITINEN, K. & SALMINEN, S. 2010. Effect of mother's weight on infant's microbiota acquisition, composition, and activity during early infancy: a prospective follow-up study initiated in early pregnancy. The American journal of clinical nutrition, 92, 1023-1030.

COLOMBO, A. P. V., BOCHES, S. K., COTTON, S. L., GOODSON, J. M., KENT, R., HAFFAJEE, A. D., SOCRANSKY, S. S., HASTURK, H., VAN DYKE, T. E. & DEWHIRST, F. 2009. Comparisons of subgingival microbial profiles of refractory periodontitis, severe periodontitis, and periodontal health using the human oral microbe identification microarray. Journal of periodontology, 80, 1421-1432.

CONG, X., XU, W., JANTON, S., HENDERSON, W. A., MATSON, A., MCGRATH, J. M., MAAS, K. & GRAF, J. 2016. Gut microbiome developmental patterns in early life of preterm infants: impacts of feeding and gender. PloS one, 11, e0152751.

COSTALONGA, M. & HERZBERG, M. C. 2014. The oral microbiome and the immunobiology of periodontal disease and caries. Immunol Lett, 162, 22-38.

DASHPER, S. G., MITCHELL, H. L., LÊ CAO, K. A., CARPENTER, L., GUSSY, M. G., CALACHE, H., GLADMAN, S. L., BULACH, D. M., HOFFMANN, B. & CATMULL, D. V. 2019. Temporal development of the oral microbiome and prediction of early childhood caries. Scientific reports, 9, 19732.

DAVIS, N. M., PROCTOR, D. M., HOLMES, S. P., RELMAN, D. A. & CALLAHAN, B. J. 2018. Simple statistical identification and removal of contaminant sequences in marker-gene and metagenomics data. Microbiome, 6, 226.

DE GOFFAU, M. C., LAGER, S., SALTER, S. J., WAGNER, J., KRONBICHLER, A., CHARNOCK-JONES, D. S., PEACOCK, S. J., SMITH, G. C. S. & PARKHILL, J. 2018. Recognizing the reagent microbiome. Nat Microbiol, 3, 851-853.

DERRIEN, M., ALVAREZ, A.-S. & DE VOS, W. M. 2019. The gut microbiota in the first decade of life. Trends in microbiology, 27, 997-1010.

DEWHIRST, F. E., CHEN, T., IZARD, J., PASTER, B. J., TANNER, A. C. R., YU, W.-H., LAKSHMANAN, A. & WADE, W. G. 2010. The human oral microbiome. Journal of bacteriology, 192, 5002-5017.

DIGIULIO, D. B., CALLAHAN, B. J., MCMURDIE, P. J., COSTELLO, E. K., LYELL, D. J., ROBACZEWSKA, A., SUN, C. L., GOLTSMAN, D. S. A., WONG, R. J., SHAW, G., STEVENSON, D. K., HOLMES, S. P. & RELMAN, D. A. 2015. Temporal and spatial variation of the human microbiota during pregnancy. Proceedings of the National Academy of Sciences, 112, 11060-11065.

DOMINGUEZ-BELLO, M. G., COSTELLO, E. K., CONTRERAS, M., MAGRIS, M., HIDALGO, G., FIERER, N. & KNIGHT, R. 2010a. Delivery mode shapes the acquisition and structure of the initial microbiota across multiple body habitats in newborns. Proc Natl Acad Sci U S A, 107, 11971-5.

DOMINGUEZ-BELLO, M. G., COSTELLO, E. K., CONTRERAS, M., MAGRIS, M., HIDALGO, G., FIERER, N. & KNIGHT, R. 2010b. Delivery mode shapes the acquisition and structure of the initial microbiota across multiple body habitats in newborns. Proceedings of the National Academy of Sciences, 107, 11971-11975.

DONDERS, G. G. G., VEREECKEN, A., BOSMANS, E., DEKEERSMAECKER, A., SALEMBIER, G. & SPITZ, B. 2002. Definition of a type of abnormal vaginal flora that is distinct from bacterial vaginosis: aerobic vaginitis. BJOG: an international journal of obstetrics and gynaecology, 109, 34-43.

DOUGLAS, G. M., MAFFEI, V. J., ZANEVELD, J. R., YURGEL, S. N., BROWN, J. R., TAYLOR, C. M., HUTTENHOWER, C. & LANGILLE, M. G. I. 2020. PICRUSt2 for prediction of metagenome functions. Nat Biotechnol, 38, 685-688.

DZIDIC, M., COLLADO, M. C., ABRAHAMSSON, T., ARTACHO, A., STENSSON, M., JENMALM, M. C. & MIRA, A. 2018. Oral microbiome development during childhood: an ecological succession influenced by postnatal factors and associated with tooth decay. The ISME journal, 12, 2292-2306.

ECKBURG, P. B., BIK, E. M., BERNSTEIN, C. N., PURDOM, E., DETHLEFSEN, L., SARGENT, M., GILL, S. R., NELSON, K. E. & RELMAN, D. A. 2005. Diversity of the human intestinal microbial flora. science, 308, 1635-1638.

EVANS, J. M., MORRIS, L. S. & MARCHESI, J. R. 2013. The gut microbiome: the role of a virtual organ in the endocrinology of the host. J Endocrinol, 218, R37-47.

FERRETTI, P., PASOLLI, E., TETT, A., ASNICAR, F., GORFER, V., FEDI, S., ARMANINI, F., TRUONG, D. T., MANARA, S. & ZOLFO, M. 2018. Mother-to-infant microbial transmission from different body sites shapes the developing infant gut microbiome. Cell host & microbe, 24, 133-145.

FOUHY, F., DEANE, J., REA, M. C., O'SULLIVAN, Ó., ROSS, R. P., O'CALLAGHAN, G., PLANT, B. J. & STANTON, C. 2015. The effects of freezing on faecal microbiota as determined using MiSeq sequencing and culture-based investigations. PloS one, 10, e0119355.

FOUHY, F., WATKINS, C., HILL, C. J., O'SHEA, C.-A., NAGLE, B., DEMPSEY, E. M., O'TOOLE, P. W., ROSS, R. P., RYAN, C. A. & STANTON, C. 2019. Perinatal factors affect the gut microbiota up to four years after birth. Nature communications, 10, 1-10.

FRANCAVILLA, R., ERCOLINI, D., PICCOLO, M., VANNINI, L., SIRAGUSA, S., DE FILIPPIS, F., DE PASQUALE, I., DI CAGNO, R., DI TOMA, M. & GOZZI, G. 2014. Salivary microbiota and metabolome associated with celiac disease. Applied and environmental microbiology, 80, 3416-3425.

FRANDSEN, E. V. G., POULSEN, K., KONONEN, E. & KILIAN, M. 2008. Diversity of Capnocytophaga species in children and description of Capnocytophaga leadbetteri sp. nov. and Capnocytophaga genospecies AHN8471. International journal of systematic and evolutionary microbiology, 58, 324-336.

FRICKE, W. F. & RAVEL, J. 2021. Microbiome or no microbiome: are we looking at the prenatal environment through the right lens? Microbiome, 9, 9.

FUKUDA, S., TOH, H., HASE, K., OSHIMA, K., NAKANISHI, Y., YOSHIMURA, K., TOBE, T., CLARKE, J. M., TOPPING, D. L. & SUZUKI, T. 2011. Bifidobacteria can protect from enteropathogenic infection through production of acetate. Nature, 469, 543-547.

FUNDORA, J. B., GUHA, P., SHORES, D. R., PAMMI, M. & MAHESHWARI, A. 2020. Intestinal dysbiosis and necrotizing enterocolitis: assessment for causality using Bradford Hill criteria. Pediatric research, 87, 235-248.

GAJER, P., BROTMAN, R. M., BAI, G., SAKAMOTO, J., SCHÜTTE, U. M., ZHONG, X., KOENIG, S. S., FU, L., MA, Z. S., ZHOU, X., ABDO, Z., FORNEY, L. J. & RAVEL, J. 2012. Temporal dynamics of the human vaginal microbiota. Sci Transl Med, 4, 132ra52.

GANLY, I., YANG, L., GIESE, R. A., HAO, Y., NOSSA, C. W., MORRIS, L. G. T., ROSENTHAL, M., MIGLIACCI, J., KELLY, D., TSENG, W., HU, J., LI, H., BROWN, S. & PEI, Z. 2019. Periodontal pathogens are a risk factor of oral cavity squamous cell carcinoma, independent of tobacco and alcohol and human papillomavirus. Int J Cancer, 145, 775-784.

GARCÍA LÓPEZ, E. & MARTÍN-GALIANO, A. J. 2020. The versatility of opportunistic infections caused by Gemella isolates is supported by the carriage of virulence factors from multiple origins. Frontiers in microbiology, 11, 524.

GENSOLLEN, T., IYER, S. S., KASPER, D. L. & BLUMBERG, R. S. 2016. How colonization by microbiota in early life shapes the immune system. Science, 352, 539-44.

GOMEZ-ARANGO, L. F., BARRETT, H. L., MCINTYRE, H. D., CALLAWAY, L. K., MORRISON, M. & DEKKER NITERT, M. 2017. Antibiotic treatment at delivery shapes the initial oral microbiome in neonates. Sci Rep, 7, 43481.

GOMEZ, A., LUCKEY, D. & TANEJA, V. 2015. The gut microbiome in autoimmunity: sex matters. Clinical immunology, 159, 154-162.

GOMEZ, A. & NELSON, K. E. 2017. The oral microbiome of children: development, disease, and implications beyond oral health. Microbial ecology, 73, 492-503.

GRIFFEN, A. L., BEALL, C. J., CAMPBELL, J. H., FIRESTONE, N. D., KUMAR, P. S., YANG, Z. K., PODAR, M. & LEYS, E. J. 2012. Distinct and complex bacterial profiles in human periodontitis and health revealed by 16S pyrosequencing. The ISME journal, 6, 1176-1185.

HE, Y., CAO, Y., XIANG, Y., HU, F., TANG, F., ZHANG, Y., ALBASHARI, A. A., XING, Z., LUO, L. & SUN, Y. 2020. An evaluation of norspermidine on anti-fungal effect on mature Candida albicans biofilms and angiogenesis potential of dental pulp stem cells. Frontiers in Bioengineering and Biotechnology, 8, 948.

HEIDA, F. H., KOOI, E. M. W., WAGNER, J., NGUYEN, T.-Y., HULSCHER, J. B. F., VAN ZOONEN, A. G. J. F., BOS, A. F., HARMSEN, H. J. M. & DE GOFFAU, M. C. 2021. Weight shapes the intestinal microbiome in preterm infants: results of a prospective observational study. BMC microbiology, 21, 1-12.

HEZEL, M. P. & WEITZBERG, E. 2015. The oral microbiome and nitric oxide homoeostasis. Oral diseases, 21, 7-16.

HILL, C. J., LYNCH, D. B., MURPHY, K., ULASZEWSKA, M., JEFFERY, I. B., O'SHEA, C. A., WATKINS, C., DEMPSEY, E., MATTIVI, F. & TUOHY, K. 2017. Evolution of gut microbiota composition from birth to 24 weeks in the INFANTMET Cohort. Microbiome. 2017; 5: 4.

HOLMES, K. K., CHEN, K. C. S., LIPINSKI, C. M. & ESCHENBACH, D. A. 1985. Vaginal redox potential in bacterial vaginosis (nonspecific vaginitis). Journal of Infectious Diseases, 152, 379-382.

HORNEF, M. W. & TOROW, N. 2020. 'Layered immunity'and the 'neonatal window of opportunity'–timed succession of non-redundant phases to establish mucosal host–microbial homeostasis after birth. Immunology, 159, 15-25.

HSIEH, T. C., MA, K. H. & CHAO, A. 2016. iNEXT: an R package for rarefaction and extrapolation of species diversity (H ill numbers). Methods in Ecology and Evolution, 7, 1451-1456.

HUNT, A., HARRINGTON, D. & ROBINSON, S. 2014. Vitamin B12 deficiency. Bmj, 349.

HURLEY, E., MULLINS, D., BARRETT, M. P., O'SHEA, C. A., KINIRONS, M., RYAN, C. A., STANTON, C., WHELTON, H., HARRIS, H. M. B. & O'TOOLE, P. W. 2019. The

microbiota of the mother at birth and its influence on the emerging infant oral microbiota from birth to 1 year of age: a cohort study. Journal of Oral Microbiology, 11, 1599652.

INSTITUTE OF, M., PANEL ON, M., NUTRITION, B., SUBCOMMITTEES ON UPPER REFERENCE LEVELS OF, N., OF, I., USE OF DIETARY REFERENCE, I., STANDING COMMITTEE ON THE SCIENTIFIC EVALUATION OF DIETARY REFERENCE, I., SUBCOMMITTEE OF, I., USES OF DIETARY REFERENCE, I. & SUBCOMMITTEE ON UPPER REFERENCE LEVELS OF, N. 2002. Dietary reference intakes for vitamin A, vitamin K, arsenic, boron, chromium, copper, iodine, iron, manganese, molybdenum, nickel, silicon, vanadium, and zinc, Dietary Reference Intakes.

ISON, C. A., EASMON, C. S., DAWSON, S. G., SOUTHERTON, G. & HARRIS, J. W. 1983. Non-volatile fatty acids in the diagnosis of non-specific vaginitis. Journal of clinical pathology, 36, 1367-1370.

JANG, H., PATOINE, A., WU, T. T., CASTILLO, D. A. & XIAO, J. 2021. Oral microflora and pregnancy: a systematic review and meta-analysis. Sci Rep, 11, 16870.

JIMÉNEZ, E., DELGADO, S., MALDONADO, A., ARROYO, R., ALBÚJAR, M., GARCÍA, N., JARIOD, M., FERNÁNDEZ, L., GÓMEZ, A. & RODRÍGUEZ, J. M. 2008. Staphylococcus epidermidis: a differential trait of the fecal microbiota of breast-fed infants. BMC microbiology, 8, 1-11.

JO, R., YAMA, K., AITA, Y., TSUTSUMI, K., ISHIHARA, C., MARUYAMA, M., TAKEDA, K., NISHINAGA, E., SHIBASAKI, K.-I. & MORISHIMA, S. 2021. Comparison of oral microbiome profiles in 18-month-old infants and their parents. Scientific Reports, 11, 861.

KAGEYAMA, S., FURUTA, M., TAKESHITA, T., MA, J., ASAKAWA, M. & YAMASHITA, Y. 2022. High-level acquisition of maternal oral bacteria in formula-fed infant oral microbiota. Mbio, 13, e03452-21.

KANEHISA, M., GOTO, S., SATO, Y., FURUMICHI, M. & TANABE, M. 2012. KEGG for integration and interpretation of large-scale molecular data sets. Nucleic acids research, 40, D109-D114.

KANG, H. M., KIM, S., HWANG-BO, S., YOO, I. H., SEO, Y. M., OH, M. Y., IM, S. A. & YOUN, Y. A. 2022. Compositional Differences of Meconium Microbiomes of Preterm and Term Infants, and Infants That Developed Necrotizing Enterocolitis or Feeding Intolerance. Pathogens, 12.

KENNEDY, K. M., DE GOFFAU, M. C., PEREZ-MUÑOZ, M. E., ARRIETA, M.-C., BÄCKHED, F., BORK, P., BRAUN, T., BUSHMAN, F. D., DORE, J., DE VOS, W. M., EARL, A. M., EISEN, J. A., ELOVITZ, M. A., GANAL-VONARBURG, S. C., GÄNZLE, M. G., GARRETT, W. S., HALL, L. J., HORNEF, M. W., HUTTENHOWER, C., KONNIKOVA, L., LEBEER, S., MACPHERSON, A. J., MASSEY, R. C., MCHARDY, A. C., KOREN, O., LAWLEY, T. D., LEY, R. E., O'MAHONY, L., O'TOOLE, P. W., PAMER, E. G., PARKHILL, J., RAES, J., RATTEI, T., SALONEN, A., SEGAL, E., SEGATA, N., SHANAHAN, F., SLOBODA, D. M., SMITH, G. C. S., SOKOL, H., SPECTOR, T. D., SURETTE, M. G., TANNOCK, G. W., WALKER, A. W., YASSOUR, M. & WALTER, J. 2023. Questioning the fetal microbiome illustrates pitfalls of low-biomass microbial studies. Nature, 613, 639-649.

KENNEDY, K. M., DE GOFFAU, M. C., PEREZ-MUÑOZ, M. E., ARRIETA, M.-C., BÄCKHED, F., BORK, P. & SMITH, G. 2022. The “fetal microbiome” and pitfalls of low-biomass microbial studies.

KENNEDY, K. M., GERLACH, M. J., ADAM, T., HEIMESAAT, M. M., ROSSI, L., SURETTE, M. G., SLOBODA, D. M. & BRAUN, T. 2021. Fetal meconium does not have a detectable microbiota before birth. Nature Microbiology, 6, 865-873.

KLOPP, J., FERRETTI, P., MEYER, C. U., HILBERT, K., HAIß, A., MARIßEN, J., HENNEKE, P., HUDALLA, H., PIRR, S. & VIEMANN, D. 2022. Meconium microbiome of very preterm infants across Germany. MSphere, 7, e00808-21.

KORPELA, K. 2021. Impact of Delivery Mode on Infant Gut Microbiota. Ann Nutr Metab, 1-9.

KOZYRSKYJ, A. L., KALU, R., KOLEVA, P. T. & BRIDGMAN, S. L. 2016. Fetal programming of overweight through the microbiome: boys are disproportionately affected. Journal of developmental origins of health and disease, 7, 25-34.

KUPERMAN, A. A. & KOREN, O. 2016. Antibiotic use during pregnancy: how bad is it? BMC medicine, 14, 1-7.

LA, X., JIANG, H., CHEN, A., ZHENG, H., SHEN, L., CHEN, W., YANG, F., ZHANG, L., CAI, X., MAO, H. & CHENG, L. 2022. Profile of the oral microbiota from preconception to the third trimester of pregnancy and its association with oral hygiene practices. J Oral Microbiol, 14, 2053389.

LAMONT, R. F., SOBEL, J. D., AKINS, R. A., HASSAN, S. S., CHAIWORAPONGSA, T., KUSANOVIC, J. P. & ROMERO, R. 2011. The vaginal microbiome: new information about genital tract flora using molecular based techniques. BJOG: An International Journal of Obstetrics & Gynaecology, 118, 533-549.

LAX, S., SANGWAN, N., SMITH, D., LARSEN, P., HANDLEY, K. M., RICHARDSON, M., GUYTON, K., KREZALEK, M., SHOGAN, B. D. & DEFAZIO, J. 2017. Bacterial colonization and succession in a newly opened hospital. Science translational medicine, 9.

LEIBY, J. S., MCCORMICK, K., SHERRILL-MIX, S., CLARKE, E. L., KESSLER, L. R., TAYLOR, L. J., HOFSTAEDTER, C. E., ROCHE, A. M., MATTEI, L. M. & BITTINGER, K. 2018. Lack of detection of a human placenta microbiome in samples from preterm and term deliveries. Microbiome, 6, 1-11.

LI, H., WANG, J., WU, L., LUO, J., LIANG, X., XIAO, B. & ZHU, Y. 2018. The impacts of delivery mode on infant’s oral microflora. Scientific reports, 8, 11938.

LI, N., YAN, F., WANG, N., SONG, Y., YUE, Y., GUAN, J., LI, B. & HUO, G. 2020. Distinct gut microbiota and metabolite profiles induced by different feeding methods in healthy Chinese infants. Frontiers in Microbiology, 11, 714.

LI, Y., SARAITHONG, P., ZHANG, L., DILLS, A., PASTER, B. J., XIAO, J., WU, T. T. & JONES, Z. 2023. Dynamics of oral microbiome acquisition in healthy infants: A pilot study. Frontiers in Oral Health, 4, 1152601.

LIF HOLGERSON, P., ESBERG, A., SJÖDIN, A., WEST, C. E. & JOHANSSON, I. 2020. A longitudinal study of the development of the saliva microbiome in infants 2 days to 5 years compared to the microbiome in adolescents. Scientific Reports, 10, 1-14.

LIF HOLGERSON, P., HARNEVIK, L., HERNELL, O., TANNER, A. C. & JOHANSSON, I. 2011. Mode of birth delivery affects oral microbiota in infants. J Dent Res, 90, 1183-8.

LIM, E. S., ZHOU, Y., ZHAO, G., BAUER, I. K., DROIT, L., NDAO, I. M., WARNER, B. B., TARR, P. I., WANG, D. & HOLTZ, L. R. 2015. Early life dynamics of the human gut virome and bacterial microbiome in infants. Nature medicine, 21, 1228-1234.

LIN, H. & PEDDADA, S. D. 2020. Analysis of compositions of microbiomes with bias correction. Nature Communications, 11, 3514.

LINEHAN, K., DEMPSEY, E. M., RYAN, C. A., ROSS, R. P. & STANTON, C. 2022. First encounters of the microbial kind: perinatal factors direct infant gut microbiome establishment. Microbiome Research Reports, 1, 10.

LIU, B., FALLER, L. L., KLITGORD, N., MAZUMDAR, V., GHODSI, M., SOMMER, D. D., GIBBONS, T. R., TREANGEN, T. J., CHANG, Y. C., LI, S., STINE, O. C., HASTURK, H., KASIF, S., SEGRÈ, D., POP, M. & AMAR, S. 2012. Deep sequencing of the oral microbiome reveals signatures of periodontal disease. PLoS One, 7, e37919.

LIU, C. M., PRICE, L. B., HUNGATE, B. A., ABRAHAM, A. G., LARSEN, L. A., CHRISTENSEN, K., STEGGER, M., SKOV, R. & ANDERSEN, P. S. 2015. Staphylococcus aureus and the ecology of the nasal microbiome. Science advances, 1, e1400216.

LIU, F., ZHOU, Y., ZHU, L., WANG, Z., MA, L., HE, Y. & FU, P. 2021. Comparative metagenomic analysis of the vaginal microbiome in healthy women. Synth Syst Biotechnol, 6, 77-84.

LIU, L., CHEN, J., CHEN, Y., JIANG, S., XU, H., ZHAN, H., REN, Y., XU, D., XU, Z. & CHEN, D. 2022. Characterization of Vaginal Microbiota in Third Trimester Premature Rupture of Membranes Patients through 16S rDNA Sequencing. Pathogens [Online], 11.

LIU, Y., QIN, S., SONG, Y., FENG, Y., LV, N., XUE, Y., LIU, F., WANG, S., ZHU, B. & MA, J. 2019. The perturbation of infant gut microbiota caused by cesarean delivery is partially restored by exclusive breastfeeding. Frontiers in Microbiology, 10, 598.

LLOYD, C. M. & MARSLAND, B. J. 2017. Lung homeostasis: influence of age, microbes, and the immune system. Immunity, 46, 549-561.

LOUIS, P., DUNCAN, S. H., SHERIDAN, P. O., WALKER, A. W. & FLINT, H. J. 2022. Microbial lactate utilisation and the stability of the gut microbiome. Gut Microbiome, 3, e3.

LUBBE, S., FILZMOSER, P. & TEMPL, M. 2021. Comparison of zero replacement strategies for compositional data with large numbers of zeros. Chemometrics and Intelligent Laboratory Systems, 210, 104248.

MACH, N. & CLARK, A. 2017. Micronutrient deficiencies and the human gut microbiota. Trends in microbiology, 25, 607-610.

MACKIE, R. I., SGHIR, A. & GASKINS, H. R. 1999. Developmental microbial ecology of the neonatal gastrointestinal tract. The American journal of clinical nutrition, 69, 1035s-1045s.

MADANY, A. M., HUGHES, H. K. & ASHWOOD, P. 2022. Prenatal Maternal Antibiotics Treatment Alters the Gut Microbiota and Immune Function of Post-Weaned Prepubescent Offspring. International Journal of Molecular Sciences, 23, 12879.

MANCABELLI, L., TARRACCHINI, C., MILANI, C., LUGLI, G. A., FONTANA, F., TURRONI, F., VAN SINDEREN, D. & VENTURA, M. 2020. Multi-population cohort meta-analysis of human intestinal microbiota in early life reveals the existence of infant community state types (ICSTs). Computational and Structural Biotechnology Journal, 18, 2480-2493.

MARCOBAL, A., BARBOZA, M., FROEHLICH, J. W., BLOCK, D. E., GERMAN, J. B., LEBRILLA, C. B. & MILLS, D. A. 2010. Consumption of human milk oligosaccharides by gut-related microbes. Journal of agricultural and food chemistry, 58, 5334-5340.

MARKOWITZ, V. M., CHEN, I. M. A., PALANIAPPAN, K., CHU, K., SZETO, E., GRECHKIN, Y., RATNER, A., JACOB, B., HUANG, J. & WILLIAMS, P. 2012. IMG: the integrated microbial genomes database and comparative analysis system. Nucleic acids research, 40, D115-D122.

MARSH, P. D., LEWIS, M. A. O., WILLIAMS, D. & MARTIN, M. V. 2009. Oral microbiology e-book, Elsevier health sciences.

MARTIN, M. 2011. Cutadapt removes adapter sequences from high-throughput sequencing reads. EMBnet. journal, 17, 10-12.

MASON, M. R., CHAMBERS, S., DABDOUB, S. M., THIKKURISSY, S. & KUMAR, P. S. 2018. Characterizing oral microbial communities across dentition states and colonization niches. Microbiome, 6, 1-10.

MASYITA, A., MUSTIKA SARI, R., DWI ASTUTI, A., YASIR, B., RAHMA RUMATA, N., EMRAN, T. B., NAINU, F. & SIMAL-GANDARA, J. 2022. Terpenes and terpenoids as main bioactive compounds of essential oils, their roles in human health and potential application as natural food preservatives. Food Chem X, 13, 100217.

MATAMOROS, S., GRAS-LEGUEN, C., LE VACON, F., POTEL, G. & DE LA COCHETIERE, M.-F. 2013. Development of intestinal microbiota in infants and its impact on health. Trends in microbiology, 21, 167-173.

MCMURDIE, P. J. & HOLMES, S. 2013. phyloseq: an R package for reproducible interactive analysis and graphics of microbiome census data. PloS one, 8, e61217.

MILANI, C., DURANTI, S., BOTTACINI, F., CASEY, E., TURRONI, F., MAHONY, J., BELZER, C., DELGADO PALACIO, S., ARBOLEYA MONTES, S. & MANCABELLI, L. 2017. The first microbial colonizers of the human gut: composition, activities, and health implications of the infant gut microbiota. Microbiology and molecular biology reviews, 81, e00036-17.

MILLS, S., YANG, B., SMITH, G. J., STANTON, C. & ROSS, R. P. 2023. Efficacy of Bifidobacterium longum alone or in multi-strain probiotic formulations during early life and beyond. Gut Microbes, 15, 2186098.

MOLES, L., GOMEZ, M., HEILIG, H., BUSTOS, G., FUENTES, S., DE VOS, W., FERNANDEZ, L., RODRÍGUEZ, J. M. & JIMENEZ, E. 2013. Bacterial diversity in

meconium of preterm neonates and evolution of their fecal microbiota during the first month of life. PloS one, 8, e66986.

MOORE, W. E. C. & MOORE, L. V. H. 1994. The bacteria of periodontal diseases. Periodontology 2000, 5, 66-77.

MORAES, D. V., QUEIROZ, D. B. & ELEUTÉRIO, J. J. 2023. Vaginal probiotics on the outcomes of premature rupture of membranes: a pilot randomised clinical trial. J Obstet Gynaecol, 2151349.

MORAIS, L. H., GOLUBEVA, A. V., MOLONEY, G. M., MOYA-PÉREZ, A., VENTURA-SILVA, A. P., ARBOLEYA, S., BASTIAANSSEN, T. F. S., O'SULLIVAN, O., REA, K. & BORRE, Y. 2020. Enduring behavioral effects induced by birth by caesarean section in the mouse. Current Biology, 30, 3761-3774.

MUKHERJEE, A., LORDAN, C., ROSS, R. P. & COTTER, P. D. 2020. Gut microbes from the phylogenetically diverse genus Eubacterium and their various contributions to gut health. Gut Microbes, 12, 1802866.

NEU, A. T., ALLEN, E. E. & ROY, K. 2021. Defining and quantifying the core microbiome: Challenges and prospects. Proceedings of the National Academy of Sciences, 118, e2104429118.

NEUGENT, M. L., HULYALKAR, N. V., NGUYEN, V. H., ZIMMERN, P. E. & DE NISCO, N. J. 2020. Advances in understanding the human urinary microbiome and its potential role in urinary tract infection. MBio, 11, e00218-20.

NGUYEN, Q. P., KARAGAS, M. R., MADAN, J. C., DADE, E., PALYS, T. J., MORRISON, H. G., PATHMASIRI, W. W., MCRITCHE, S., SUMNER, S. J., FROST, H. R. & HOEN, A. G. 2021. Associations between the gut microbiome and metabolome in early life. BMC Microbiol, 21, 238.

O'NEILL, I. J., SANCHEZ GALLARDO, R., SALDOVA, R., MURPHY, E. F., COTTER, P. D., MCAULIFFE, F. M. & VAN SINDEREN, D. 2020. Maternal and infant factors that shape neonatal gut colonization by bacteria. Expert Review of Gastroenterology & Hepatology, 14, 651-664.

OKUDA, T., KOKUBU, E., KAWANA, T., SAITO, A., OKUDA, K. & ISHIHARA, K. 2012. Synergy in biofilm formation between Fusobacterium nucleatum and Prevotella species. Anaerobe, 18, 110-116.

OLOMU, I. N., PENA-CORTES, L. C., LONG, R. A., VYAS, A., KRICHEVSKIY, O., LUELLWITZ, R., SINGH, P. & MULKS, M. H. 2020. Elimination of "kitome" and "splashome" contamination results in lack of detection of a unique placental microbiome. BMC Microbiol, 20, 157.

PACE, R. M., WILLIAMS, J. E., ROBERTSON, B., LACKEY, K. A., MEEHAN, C. L., PRICE, W. J., FOSTER, J. A., SELLEN, D. W., KAMAU-MBUTHIA, E. W. & KAMUNDIA, E. W. 2021. Variation in human milk composition is related to differences in milk and infant fecal microbial communities. Microorganisms, 9, 1153.

PALMER, C., BIK, E. M., DIGIULIO, D. B., RELMAN, D. A. & BROWN, P. O. 2007. Development of the human infant intestinal microbiota. PLoS biology, 5, e177.

PALMER, L. D. & SKAAR, E. P. 2016. Transition metals and virulence in bacteria. Annual review of genetics, 50, 67-91.

PANZER, J., ROMERO, R., GREENBERG, J. M., WINTERS, A. D., GALAZ, J., GOMEZ-LOPEZ, N. & THEIS, K. R. 2022. Is there a placental microbiota? A critical review and re-analysis of published placental microbiota datasets. bioRxiv, 2022-07.

PAPAPANOU, P. N., PARK, H., CHENG, B., KOKARAS, A., PASTER, B., BURKETT, S., WATSON, C. W. M., ANNAVAJHALA, M. K., UHLEMANN, A. C. & NOBLE, J. M. 2020. Subgingival microbiome and clinical periodontal status in an elderly cohort: The WHICAP ancillary study of oral health. Journal of periodontology, 91, S56-S67.

PARKS, D. H., TYSON, G. W., HUGENHOLTZ, P. & BEIKO, R. G. 2014. STAMP: statistical analysis of taxonomic and functional profiles. Bioinformatics, 30, 3123-3124.

PARNELL, L. A., BRIGGS, C. M., CAO, B., DELANNOY-BRUNO, O., SCHRIEFFER, A. E. & MYSOREKAR, I. U. 2017. Microbial communities in placentas from term normal pregnancy exhibit spatially variable profiles. Scientific Reports, 7, 11200.

PETROVA, M. I., LIEVENS, E., MALIK, S., IMHOLZ, N. & LEBEER, S. 2015. Lactobacillus species as biomarkers and agents that can promote various aspects of vaginal health. Frontiers in physiology, 6, 81.

PIOT, P., VAN DYCK, E., GODTS, P. & VANDERHEYDEN, J. 1982. The vaginal microbial flora in non-specific vaginitis. European Journal of Clinical Microbiology, 1, 301-306.

POKUSAEVA, K., FITZGERALD, G. F. & VAN SINDEREN, D. 2011. Carbohydrate metabolism in Bifidobacteria. Genes & nutrition, 6, 285-306.

POSSEMIERS, S., BOLCA, S., VERSTRAETE, W. & HEYERICK, A. 2011. The intestinal microbiome: a separate organ inside the body with the metabolic potential to influence the bioactivity of botanicals. Fitoterapia, 82, 53-66.

QUAST, C., PRUESSE, E., YILMAZ, P., GERKEN, J., SCHWEER, T., YARZA, P., PEPLIES, J. & GLÖCKNER, F. O. 2012. The SILVA ribosomal RNA gene database project: improved data processing and web-based tools. Nucleic acids research, 41, D590-D596.

RAO, C., COYTE, K. Z., BAINTER, W., GEHA, R. S., MARTIN, C. R. & RAKOFF-NAHOUM, S. 2021. Multi-kingdom ecological drivers of microbiota assembly in preterm infants. Nature, 591, 633-638.

RAVEL, J., GAJER, P., ABDO, Z., SCHNEIDER, G. M., KOENIG, S. S. K., MCCULLE, S. L., KARLEBACH, S., GORLE, R., RUSSELL, J. & TACKET, C. O. 2011. Vaginal microbiome of reproductive-age women. Proceedings of the National Academy of Sciences, 108, 4680-4687.

RIGAUTS, C., AIZAWA, J., TAYLOR, S. L., ROGERS, G. B., GOVAERTS, M., COS, P., OSTYN, L., SIMS, S., VANDEPLASSCHE, E., SZE, M., DONDELINGER, Y., VEREECKE, L., VAN ACKER, H., SIMPSON, J. L., BURR, L., WILLEMS, A., TUNNEY, M. M., CIGANA, C., BRAGONZI, A., COENYE, T. & CRABBÉ, A. 2022. R othia mucilaginosa is an anti-inflammatory bacterium in the respiratory tract of patients with chronic lung disease. Eur Respir J, 59.

ROBERTSON, R. C., MANGES, A. R., FINLAY, B. B. & PRENDERGAST, A. J. 2019. The human microbiome and child growth–first 1000 days and beyond. Trends in microbiology, 27, 131-147.

ROCHA-VIGGIANO, A. K., ARANDA-ROMO, S., SALGADO-BUSTAMANTE, M. & OVANDO-VÁZQUEZ, C. 2022. Meconium Microbiota Composition and Association with Birth Delivery Mode. Advanced Gut & Microbiome Research, 2022.

RUAN, W., ENGEVIK, M. A., SPINLER, J. K. & VERSALOVIC, J. 2020. Healthy human gastrointestinal microbiome: composition and function after a decade of exploration. Digestive diseases and sciences, 65, 695-705.

SALTER, S. J., COX, M. J., TUREK, E. M., CALUS, S. T., COOKSON, W. O., MOFFATT, M. F., TURNER, P., PARKHILL, J., LOMAN, N. J. & WALKER, A. W. 2014. Reagent and laboratory contamination can critically impact sequence-based microbiome analyses. BMC Biology, 12, 87.

SAMPAIO-MAIA, B. & MONTEIRO-SILVA, F. 2014. Acquisition and maturation of oral microbiome throughout childhood: An update. Dental research journal, 11, 291.

SANCHEZ, B., URDACI, M. C. & MARGOLLES, A. 2010. Extracellular proteins secreted by probiotic bacteria as mediators of effects that promote mucosa–bacteria interactions. Microbiology, 156, 3232-3242.

SCHLIEP, K. P. 2011. phangorn: phylogenetic analysis in R. Bioinformatics, 27, 592-593.

SHABAYEK, S., ABDELLAH, A. M., SALAH, M., RAMADAN, M. & FAHMY, N. 2022. Alterations of the vaginal microbiome in healthy pregnant women positive for group B Streptococcus colonization during the third trimester. BMC microbiology, 22, 313.

SHATERIAN, N., ABDI, F., GHAVIDEL, N. & ALIDOST, F. 2021. Role of cesarean section in the development of neonatal gut microbiota: A systematic review. Open Med (Wars), 16, 624-639.

SHEN, Z., ROBERT, L., STOLPMAN, M., CHE, Y., WALSH, A., SAFFERY, R., ALLEN, K. J., ECKERT, J., YOUNG, A. & DEMING, C. 2023. A genome catalog of the early-life human skin microbiome. bioRxiv, 2023-05.

SHIPITSYNA, E., ROOS, A., DATCU, R., HALLÉN, A., FREDLUND, H., JENSEN, J. S., ENGSTRAND, L. & UNEMO, M. 2013. Composition of the vaginal microbiota in women of reproductive age–sensitive and specific molecular diagnosis of bacterial vaginosis is possible? PloS one, 8, e60670.

SRINIVASAN, S., MORGAN, M. T., FIEDLER, T. L., DJUKOVIC, D., HOFFMAN, N. G., RAFTERY, D., MARRAZZO, J. M. & FREDRICKS, D. N. 2015. Metabolic signatures of bacterial vaginosis. MBio, 6, e00204-15.

STERPU, I., FRANSSON, E., HUGERTH, L. W., DU, J., PEREIRA, M., CHENG, L., RADU, S. A., CALDERÓN-PÉREZ, L., ZHA, Y., ANGELIDOU, P., PENNHAG, A., BOULUND, F., SCHEYNIUS, A., ENGSTRAND, L., WIBERG-ITZEL, E. & SCHUPPE-KOISTINEN, I. 2021. No evidence for a placental microbiome in human pregnancies at term. American Journal of Obstetrics and Gynecology, 224, 296.e1-296.e23.

STEWART, C. J., AJAMI, N. J., O'BRIEN, J. L., HUTCHINSON, D. S., SMITH, D. P., WONG, M. C., ROSS, M. C., LLOYD, R. E., DODDAPANENI, H. & METCALF, G. A. 2018. Temporal development of the gut microbiome in early childhood from the TEDDY study. Nature, 562, 583-588.

TANNER, M. A., GOEBEL, B. M., DOJKA, M. A. & PACE, N. R. 1998. Specific ribosomal DNA sequences from diverse environmental settings correlate with experimental contaminants. Appl Environ Microbiol, 64, 3110-3.

TAPIAINEN, T., KOIVUSAARI, P., BRINKAC, L., LORENZI, H. A., SALO, J., RENKO, M., PRUIKKONEN, H., POKKA, T., LI, W. & NELSON, K. 2019. Impact of intrapartum and postnatal antibiotics on the gut microbiome and emergence of antimicrobial resistance in infants. Scientific reports, 9, 1-11.

TOROW, N., MARSLAND, B. J., HORNEF, M. W. & GOLLWITZER, E. S. 2017. Neonatal mucosal immunology. Mucosal immunology, 10, 5-17.

TURRONI, F., PEANO, C., PASS, D. A., FORONI, E., SEVERGNINI, M., CLAESSON, M. J., KERR, C., HOURIHANE, J., MURRAY, D. & FULIGNI, F. 2012. Diversity of bifidobacteria within the infant gut microbiota. PloS one, 7, e36957.

TURUNEN, J., TEJESVI, M. V., PAALANNE, N., HEKKALA, J., LINDGREN, O., KAAKINEN, M., POKKA, T., KAISANLAHTI, A., REUNANEN, J. & TAPIAINEN, T. 2021. Presence of distinctive microbiome in the first-pass meconium of newborn infants. Sci Rep, 11, 19449.

VATANEN, T., PLICHTA, D. R., SOMANI, J., MÜNCH, P. C., ARTHUR, T. D., HALL, A. B., RUDOLF, S., OAKELEY, E. J., KE, X. & YOUNG, R. A. 2019. Genomic variation and strain-specific functional adaptation in the human gut microbiome during early life. Nature microbiology, 4, 470-479.

VEMURI, R. & HERATH, M. P. 2023. Beyond the Gut, Emerging Microbiome Areas of Research: A Focus on Early-Life Microbial Colonization. Microorganisms [Online], 11.

VERMA, D., GARG, P. K. & DUBEY, A. K. 2018. Insights into the human oral microbiome. Archives of microbiology, 200, 525-540.

WAMPACH, L., HEINTZ-BUSCHART, A., FRITZ, J. V., RAMIRO-GARCIA, J., HABIER, J., HEROLD, M., NARAYANASAMY, S., KAYSEN, A., HOGAN, A. H. & BINDL, L. 2018. Birth mode is associated with earliest strain-conferred gut microbiome functions and immunostimulatory potential. Nature communications, 9, 1-14.

WANG, S., EGAN, M., RYAN, C. A., BOYAVAL, P., DEMPSEY, E. M., ROSS, R. P. & STANTON, C. 2020a. A good start in life is important-perinatal factors dictate early microbiota development and longer term maturation. FEMS Microbiol Rev, 44, 763-781.

WANG, S., RYAN, C. A., BOYAVAL, P., DEMPSEY, E. M., ROSS, R. P. & STANTON, C. 2020b. Maternal vertical transmission affecting early-life microbiota development. Trends in microbiology, 28, 28-45.

WARDA, A. K., DEMPSEY, E. M., FORSSTEN, S. D., RYAN, C. A., CRYAN, J. F., PATTERSON, E., O'RIORDAN, M. N., O'SHEA, C.-A., KEOHANE, F. & MEEHAN, G. 2022. Cross-sectional observational study protocol: missing microbes in infants born by

caesarean section (MiMIC): antenatal antibiotics and mode of delivery. BMJ open, 12, e064398.

WERNERSSON, J., NIEMI, L. D., EINARSON, S., HERNELL, O. & JOHANSSON, I. 2006. Effects of human milk on adhesion of Streptococcus mutans to saliva-coated hydroxyapatite in vitro. Caries research, 40, 412-417.

WILEY, N. C., CRYAN, J. F., DINAN, T. G., ROSS, R. P. & STANTON, C. 2021. Production of Psychoactive Metabolites by Gut Bacteria. Mod Trends Psychiatry, 32, 74-99.

WIRBEL, J., PYL, P. T., KARTAL, E., ZYCH, K., KASHANI, A., MILANESE, A., FLECK, J. S., VOIGT, A. Y., PALLEJA, A. & PONNUDURAI, R. 2019. Meta-analysis of fecal metagenomes reveals global microbial signatures that are specific for colorectal cancer. Nature medicine, 25, 679-689.

XIAO, J., FISCELLA, K. A. & GILL, S. R. 2020. Oral microbiome: possible harbinger for children's health. International journal of oral science, 12, 12.

YANG, K., WANG, Y., ZHANG, S., ZHANG, D., HU, L., ZHAO, T. & ZHENG, H. 2021. Oral Microbiota Analysis of Tissue Pairs and Saliva Samples From Patients With Oral Squamous Cell Carcinoma - A Pilot Study. Front Microbiol, 12, 719601.

YANG, N. Y., ZHANG, Q., LI, J. L., YANG, S. H. & SHI, Q. 2014. Progression of periodontal inflammation in adolescents is associated with increased number of P orphyromonas gingivalis, P revotella intermedia, T annerella forsythensis, and F usobacterium nucleatum. International journal of paediatric dentistry, 24, 226-233.

YASSOUR, M., JASON, E., HOGSTROM, L. J., ARTHUR, T. D., TRIPATHI, S., SILJANDER, H., SELVENIUS, J., OIKARINEN, S., HYÖTY, H. & VIRTANEN, S. M. 2018. Strain-level analysis of mother-to-child bacterial transmission during the first few months of life. Cell host & microbe, 24, 146-154.

YATSUNENKO, T., REY, F. E., MANARY, M. J., TREHAN, I., DOMINGUEZ-BELLO, M. G., CONTRERAS, M., MAGRIS, M., HIDALGO, G., BALDASSANO, R. N. & ANOKHIN, A. P. 2012. Human gut microbiome viewed across age and geography. nature, 486, 222-227.

YOSHII, K., HOSOMI, K., SAWANE, K. & KUNISAWA, J. 2019. Metabolism of Dietary and Microbial Vitamin B Family in the Regulation of Host Immunity. Front Nutr, 6, 48.

YU, J. C., KHODADADI, H., SALLES, É. L., NAEINI, S. E., THRELKELD, E., BHANDARI, B., MEGHIL, M., WANG, P. L. & BABAN, B. 2023. Oral Microbiome and Innate Immunity in Health and Disease: Building a Predictive, Preventive and Personalised Therapeutic Approach. Microbiome in 3P Medicine Strategies: The First Exploitation Guide, 391-409.

YU, Z.-T., CHEN, C. & NEWBURG, D. S. 2013. Utilization of major fucosylated and sialylated human milk oligosaccharides by isolated human gut microbes. Glycobiology, 23, 1281-1292.

YU, Z. & MORRISON, M. 2004. Improved extraction of PCR-quality community DNA from digesta and fecal samples. Biotechniques, 36, 808-812.

ZENG, S., PATANGIA, D., ALMEIDA, A., ZHOU, Z., MU, D., PAUL ROSS, R., STANTON, C. & WANG, S. 2022. A compendium of 32,277 metagenome-assembled genomes and over 80 million genes from the early-life human gut microbiome. Nature Communications, 13, 5139.

ZHANG, C., YU, Z., ZHAO, J., ZHANG, H., ZHAI, Q. & CHEN, W. 2019. Colonization and probiotic function of Bifidobacterium longum. Journal of Functional Foods, 53, 157-165.

ZHANG, X., ZHAI, Q., WANG, J., MA, X., XING, B., FAN, H., GAO, Z., ZHAO, F. & LIU, W. 2022. Variation of the Vaginal Microbiome During and After Pregnancy in Chinese Women. Genomics Proteomics Bioinformatics, 20, 322-333.

ZHANG, Z., SCHWARTZ, S., WAGNER, L. & MILLER, W. 2000. A greedy algorithm for aligning DNA sequences. Journal of Computational biology, 7, 203-214.

ZHENG, N., GUO, R., WANG, J., ZHOU, W. & LING, Z. 2021. Contribution of Lactobacillus iners to Vaginal Health and Diseases: A Systematic Review. Front Cell Infect Microbiol, 11, 792787.

ZHENG, X., HE, J., WANG, L., ZHOU, S., PENG, X., HUANG, S., ZHENG, L., CHENG, L., HAO, Y., LI, J., XU, J., XU, X. & ZHOU, X. 2017. Ecological Effect of Arginine on Oral Microbiota. Scientific Reports, 7, 7206.

ZHOU, P., MANOIL, D., BELIBASAKIS, G. N. & KOTSAKIS, G. A. 2021. Veillonellae: beyond bridging species in oral biofilm ecology. Frontiers in oral health, 79.

Chapter 4

4 Characterising the Virome of Bovine Colostrum: Diversity, Community Structure and Implications for Veterinary and Human Applications

4.1 Abstract

The virome, representing the viral component of the microbiome, plays a crucial yet understudied role in microbial ecosystems. Bovine colostrum harbours diverse bioactive components essential to calf health and has attracted significant interest for health applications in humans. Investigating the virome of colostrum could have important implications for calf health, the spread of antimicrobial resistance in the environment and the transmission of diseases through colostrum-based products. In this study, using a cohort of 72 cows, given dry cow therapy (n=48) or naturally dried off (n=24), we characterised the virome composition of first milking bovine colostrum. A dedicated extraction protocol was developed to extract the virome from colostrum samples. Viral metagenomics was employed to explore the diversity, community structure, and ecological roles of viruses within bovine colostrum. The impact of farm-level variables, including location, parity, and dry cow antibiotic treatment, on the colostrum virome were assessed. Single stranded DNA (ssDNA) viruses, including *Circoviridae*, *Papillomaviridae* and *Microviridae* dominated the virome. Double stranded DNA (dsDNA) bacteriophages (phages) carrying multidrug resistance genes (*smeS*, lfrA, *kdpE* and *baeS*) were identified. Antibiotic treatments significantly impacted virome composition and the presence of resistance genes specific to the administered antibiotic. This study contributes to the growing field of virome research and emphasizes the significance of characterizing viral communities in livestock animals. These findings will enhance our understanding of the role of the virome in microbial ecosystems, animal health, and the broader implications for human health and the environment.

4.2 Introduction

The microbiome refers to complex microbial communities consisting of bacteria, archaea, eukarya, viruses, bacteriophages (phages), and their products. The intricate relationship between the bacterial microbiome (bacteriome) and their mammalian hosts in health and disease has been extensively studied (Zheng et al., 2020). However, the virome, which represents the viral component of the microbiome, remains one of the least documented and poorly understood aspects of global biodiversity (Carlson Colin et al., 2022). It is estimated that just 1% of mammalian viruses have been described to date (Carlson et al., 2019). The virome comprises various nucleic acids (ssDNA, dsDNA, ssRNA, and dsRNA), including eukaryotic viruses, viruses infecting archaea, prokaryotes (phages), and viral elements integrated into host chromosomes, all associated with the virus-like particles (VLPs) within a specific ecosystem (Carlson Colin et al., 2022). Viruses, primarily phages, are the most abundant biological entities on Earth, outnumbering their prokaryotic counterparts by a factor of 10, with an estimated 10^{31} VLPs in the biosphere (Mushegian, 2020). The field of virology has been revolutionised by the advent of high-throughput culture-independent next-generation sequencing (NGS) technologies, which have dramatically expanded our understanding of the 'virosphere' (Smith et al., 2022). Viral-focused shotgun metagenomic studies have significantly contributed to our understanding of virus diversity, taxonomy, and evolution across diverse ecological niches. Investigations in key environments such as the ocean (Elbehery and Deng, 2022), soil (Bi et al., 2022), and the human gut (Pargin et al., 2023) have deepened our knowledge of viral communities. These studies have significantly increased our understanding of zoonotic disease development and transmission (Kawasaki et al., 2023). Virome studies have also revealed the multifaceted environmental roles of phages. Phages can manipulate bacterial populations and communities through mechanisms such as lytic infection (Barr, 2019). Phage can also integrate into the host genome as prophages (lysogeny), altering host metabolism and fitness (Campbell et al., 2020). Furthermore, phages contribute to gene transfer (phage transduction), potentially conferring advantages to the host, such as antibiotic resistance (Schneider, 2021).

While viral metagenomic data continues to accumulate rapidly, the quantification of viral diversity and the characterisation of their functional attributes face numerous technical and methodological limitations. 'Viral dark matter' represents 60-95% of the

newly identified viral sequences in viromic datasets as they cannot be taxonomically classified (Santiago-Rodriguez and Hollister, 2022). This problem is compounded by the inability to culture the vast majority of the global virome due to host recalcitrance, rendering them inaccessible to standard laboratory approaches (Suh et al., 2022). Additionally, unlike bacteria with widely used phylogenetic markers like the 16S rRNA or the chaperonin-60 (cpn60) gene, virology lacks a single equivalent marker, further complicating the assignment of taxonomic ranks to this 'viral dark matter' (Shkoporov and Hill, 2019). The lack of reliable and robust, “capture-all” protocols for extracting genetic material from all the VLPs present in environmental samples has also hampered virome studies (Thurber et al., 2009). Sample specific protocols are often required, therefore, viral concentration and extraction methods contrast greatly amidst studies, limiting the reproducibility of research findings and making it difficult to compare results between studies of the same sample type (Mahony and van Sinderen, 2022). Encouragingly, advanced tools for detecting putative viral genomes are now available, enabling a more thorough exploration of previously untraceable "viral dark matter" in metagenomic data. For instance, these tools have led to the discovery of numerous novel viral clades, including crAss-like phages, thought to be the most abundant phages in the human gut (Fitzgerald et al., 2021).

In recent years, the importance of characterizing species-specific metagenomes as a surveillance baseline for early detection and monitoring of pathogen movements across diverse hosts has been highlighted by initiatives like the Global Virome Project (Albery et al., 2021). In this regard, virome research of livestock animals and their produce has grown significantly (Mahony and van Sinderen, 2022, Kwok et al., 2020). This interest has been further fuelled by the COVID-19 pandemic, which has emphasised the significance of understanding viruses with zoonotic potential (Harvey and Holmes, 2022). The global health crisis has underscored the urgent need to identify and study animal viromes to proactively prevent future cross-species transmission outbreaks (Harvey and Holmes, 2022).

Virome studies in livestock animals have primarily focussed on pigs, given the emergence and global spread of swine viruses, such as porcine epidemic diarrhoea virus and African swine fever virus (Goede and Morrison, 2016, Gallardo et al., 2015). Virome research of cows, sheep and goats are much more limited (Park and Kim, 2020, Kwok et al., 2020). Viral metagenomics studies in bovine samples have

predominantly detected viruses associated with enteric and respiratory diseases, including families such as *Astroviridae*, *Picornaviridae*, *Retroviridae*, as well as DNA viruses like *Papillomaviridae* and *Polyomaviridae* (Kaszab et al., 2020). Bovine body sites which have been investigated thus far include the rumen, nasal tract, slurry, plasma, and vaginal swabs (Kwok et al., 2020). Notably, a recent study reported a highly diverse virome dominated by lytic phages in dairy cattle slurry, with a significant proportion representing novel genera (Cook et al., 2021). Furthermore, this study also reported phages encoding a wide range of AMGs including virulence determinants and putative antibiotic-resistance genes (ARGs), suggesting that the agricultural slurry used for land application may contribute to bacterial virulence and antimicrobial resistance in the environment (Cook et al., 2021). Virome analysis of bovine produce, such as milk is especially challenging, due to their highly variable macromolecular content, texture and solubility (Muhammed et al., 2017, Mahony and van Sinderen, 2022). Moreover, investigating the bovine milk microbiome poses challenges due to its low biomass nature, susceptibility to contamination during collection, and the potential presence of extraction kit contaminants (Ruegg, 2022). Additionally, inter-individual variations in microbiota (Porcellato et al., 2020), diverse farming practices (Metzger et al., 2018), and the absence of standardised protocols further complicate the study of this microbiome. Consequently, viral nucleic acid extractions within the dairy matrix require optimised and sample-specific protocols to achieve sufficient yields for sequencing, while maintaining minimal bacterial DNA contamination (Muhammed et al., 2017, Mahony and van Sinderen, 2022). However, in recent years, optimised virome extraction protocols have been reported for dairy samples, primarily cheese (Dugat-Bony et al., 2020, Muhammed et al., 2017). Bovine colostrum, the initial mammary secretion after parturition, is renowned for its comprehensive nutritional profile and bioactive compounds which play a critical role in providing optimal nutrition, supporting immunological development and shaping the calf gut microbiota (Abdelsattar et al., 2022). The bioactive components present in colostrum have garnered significant interest as potential sources for developing health products in both veterinary and human medicine (Linehan et al., 2023). With a view to ensuring optimal calf health and safe colostrum product development, numerous studies have explored the microbial content of colostrum (Lima et al., 2017, Chen et al., 2021, Van Hese et al., 2022). In addition to potential probiotic species (*Bifidobacterium* spp. and *Lactobacillus* spp.), colostrum can also contain pathogenic

bacteria, including *Listeria monocytogenes*, *Streptococcus* spp., and *Staphylococcus* spp. (Linehan et al., 2023). Colostrum is suggested as a potential source of ARGs for calf gut microbiota in the absence of antibiotic use in calves (Liu et al., 2019, Thames et al., 2012). This has been partly attributed to antibiotic dry cow treatment (DCT) in the pre-partum period (Hazards et al., 2017). Therefore, colostrum based products have also been reported as a potential exposure route of antibiotic-resistant pathogens and ARGs to other animals which consume colostrum-based products (Miranda et al., 2023). To the best of our knowledge, no studies have investigated the virome of colostrum. Investigating the virome of bovine colostrum holds paramount importance for calf health, consumer health, understanding zoonotic diseases and potential spread of antimicrobial resistance in the environment. Based on the aforementioned information, this study aimed to accomplish three main objectives: (1) Establish a specialised virome extraction protocol specifically designed for the analysis of bovine colostrum. (2) Employ viral metagenomics to explore the diversity, community structure, and ecological functions of viral populations present in Irish bovine colostrum. (3) Evaluate the influence of farm-level variables, including location, parity, and dry cow antibiotic treatment, on the composition and characteristics of the colostrum virome.

4.3 Materials and Methods

4.3.1 Enrolment Criteria and Treatment for Cows

First milking colostrum samples were collected from Holstein-Friesian cows (n= 72) from five different commercial Irish dairy farms located in County Cork, Ireland between February and April 2020. Cows on all farms were treated with a teat sealant, Boviseal, a sterile, non-antibiotic intramammary paste used to protect from infections and seal the teat canal in cows during the dry period. The cows included in this study were categorised into three groups based on DCT treatment: NOAB (n=23), CEF (n=24), and UBRO (n=25). NOAB did not use any antibiotics during the drying-off period (natural drying off using teat sealant). UBRO group was treated with Ubro Red Dry Cow intramammary suspension at drying off; of which the active ingredients are Framycetin Sulfate (100 mg), Penethamate Hydriodide (100 mg) and Procaine Penicillin (300 mg). CEF group was treated with Cephaguard DC intramammary ointment at drying off, the active ingredient is Cefquinome (150 mg) (a fourth generation cephalosporin). Cows showing signs of mastitis or any other infections

were excluded from the study and milk samples were collected only from healthy cows. Cows were not subjected to additional antibiotic treatments during the dry period or during the time interval of sample collection.

4.3.2 Sample and Data Collection

All farms and personnel who collected samples included in this study are Bord Bia quality assurance certified members. Standard recommendations from the National Mastitis Council's Laboratory Handbook on bovine mastitis were followed for sample collection (Adkins and Middleton, 2017). Farmers were provided with instructions for sterile sample collection. All samples were collected within the first hour post-partum. Briefly, teats were disinfected with iodine tincture, dried and thoroughly disinfected with wipes soaked in 70% alcohol. Initial colostrum streams were discarded and then 25 ml of colostrum from the front right quarter of each cow's udder was collected into sterile 50 ml falcon tubes (Sarstedt). The tubes were labelled with the cow's identification number and the collection date, and immediately frozen in a chest freezer (-20°C) on the farm. Subsequently, the samples were transported (-20°C) to Teagasc, Moorepark, Co. Cork, and stored at -80°C. Metadata regarding the parity of cows, any previous infections, the treatment used for DCT and any other medications were collected from the farms (Table 4.1).

4.3.3 Virome Extraction Protocol Optimisation

The strategy for optimisation of protocols is described in Figure 4.2. The primary goal of this strategy was to minimize the loss (>50%) of spiked phage at each extraction step and effectively remove bulk protein, as evidenced by improved sample transparency (Muhammed et al., 2017, Dugat-Bony et al., 2020). For each method trialled, frozen colostrum samples were thawed overnight at 4°C and centrifuged at 300 x g for 5 min in order to pellet large aggregates. The samples were then spiked with ~10^6 plaque forming units (PFU)/ml of *Escherichia coli* phage T4 (DSM: 4505) (phage T4). Recovery of infective, spiked phages was enumerated after each protocol step by double agar overlay plaque assay (Kropinski et al., 2009). Protocol 1, adapted from a cheese whey virome extraction method (Muhammed et al., 2017), involved the following steps. First, samples were incubated with 1 M NaCl (wt/vol) (Sigma-Aldrich, USA) for 1 h at 4°C. Casein precipitation was achieved by adjusting the sample to pH ~4.6 using 1 M HCl and/or 1 M NaOH, followed by centrifugation at

28,000 x g for 15 min at 4°C. The resulting supernatant was incubated with 10% polyethylene glycol (PEG) 6000 (wt/vol) (Sigma-Aldrich) for 1 h at 4°C. Viruses were subsequently pelleted by centrifugation at 15,000 x *g* for 15 min at 4°C. The resulting pellet was re-suspended in 1 ml of SM buffer (100 mM NaCl, 8 mM $MgSO_4 \cdot 7H_2O$, 50 mM Tris-Cl, pH = 7.5) supplemented with 1.3 g ml^{-1} of Caesium Chloride (CsCl) (Sigma-Aldrich) and incubated for 1 h at 4°C.

Protocol 2 was based on a virome extraction method used for cheese rinds (Dugat-Bony et al., 2020). Samples were diluted (1:1) with ice cold trisodium citrate (2% w/v) and centrifuged at 5,000 x g for 45 min at 4°C. The resulting supernatant was diluted 1:5 with SM buffer, pre-filtered using glass vacuum filter holders (Millipore) before filtration with 0.45-µm pore PES membrane filters. The filtrate was incubated with 10% PEG 6000 overnight at 4°C. The next day, samples were centrifuged at 6,000 x g for 1 h at 4°C. Pellets were re-suspended in 2 ml of ice-cold (0°C) SM buffer.

Protocol 3 was based on a PEG virome extraction method used for human faecal samples (Shkoporov et al., 2018). Samples were diluted 1:1 with SM buffer and homogenised by vigorous vortexing for 5 min. Sample tubes were then chilled on ice for 5 min prior to centrifugation at 5,000 x g for 10 min at 4°C. Supernatants were transferred to new tubes, and centrifugation was repeated. Supernatants were subsequently filtered twice through 0.45-µm pore PES membrane filters. NaCl and PEG-8000 were added to filtrates at a final concentration of 0.5 M and 10% w/v respectively. Once completely dissolved, samples were incubated overnight at 4°C. Samples were then centrifuged at 5,000 x g for 20 min at 4°C to collect precipitate. Supernatant was removed, and tubes were left in an inverted position on paper towels for 5 min to remove last traces of supernatant. Pellets were then re-suspended in 400 µl of SM buffer.

Protocol 4 was based on a tangential-flow filtration (TFF) virome extraction method used for human faecal samples (Castro-Mejía et al., 2015). Samples were diluted 1:1 with SM buffer, homogenised by vigorous vortexing for 5 min and centrifuged at 5,000 x g for 45 min at 4°C. The supernatants were recovered and pre-filtrated (dead-end filtration) using glass fiber filters and passed through a 100-kDa MWCO membrane centriprep device (Millipore, PXC100C50) according to manufacturer's instructions, to concentrate phage particles and remove low molecular weight

residuals. Resulting supernatants were then placed in the outer tube of the centriprep device. Samples were then centrifuged at 5,000 x g for 30 min, 10 min and finally 3 min. The liquid filtered into the inner tube was poured off after each centrifugation step. 200 µl SM buffer was added to the inner tube at the end and centrifuged at 1,000 x g for 3 min. After the final centrifugation step, the concentrated virome solution (~500 µl) was collected from the outer tube.

4.3.4 Virome Nucleic Acid Extraction

The extraction of viral DNA and RNA was performed using the method described in Shkoporov et al. (2018), with some modifications. Briefly, 400 µl of reconstituted PEG pellets were aspirated into clean Eppendorf tubes and mixed with 40 µl of a solution of 10 mM $CaCl_2$ and 50 mM $MgCl_2$. After addition of 8 U of TURBO DNase (Ambion/ThermoFisher Scientific) and 20 U of RNase I (ThermoFisher Scientific) free DNA/ RNA digestion was carried out at 37°C for 1 h. Enzymes were then inactivated by incubation at 70°C for 10 min. Proteinase K (40 µg) and 20 µl of 10% SDS (both from Sigma-Aldrich) were then added to the tubes which were then incubated for 20 min at 56°C. Finally, viral particles were lysed by addition of 100 µl of phage lysis buffer (4.5 M guanidinium isothiocyanate, 44 mM sodium citrate pH 7.0, 0.88% sarkosyl, 0.72% 2- mercaptoethanol) and incubated at 65°C for 10 min. Lysates were then extracted twice by gentle vortexing with equal volumes of Phenol/Chloroform/Isoamyl Alcohol 25: 24:1 (Fisher Scientific) followed by centrifugation at 8,000 x g for 5 min at room temperature. The resulting aqueous phase was subjected to a final round of purification using DNeasy Blood & Tissue Kit (Qiagen) according to manufacturer's instruction with a final elution volume of 50 µl. Purified DNA was quantified using the Qubit dsDNA High Sensitivity kit (ThermoFisher Scientific).

4.3.5 Virome Library Processing

Reverse transcription (RT) of extracted VLPs, regardless of concentration, was performed using Superscript IV first strand system (Thermo Scientific), in a 2x reaction (40 µl final), according to the manufacturer's random hexamer primer protocol. RT reaction products were immediately frozen at -20^{o}C. For DNA fragmentation, 20 µl of RT product was taken for sonication after adjusting the volume to 52.5 µl with low-EDTA TE buffer in a microTUBE-50 (Covaris). Shearing of

unamplified DNA/cDNA mixture (variable amounts of DNA) was performed on M220 Focused-Ultrasonicator (Covaris) with the following settings: peak power of 50 W, duty factor of 20%, 200 cycles per burst, total duration of 35s. Samples were then concentrated using a DNA Clean & Concentrator kit (Zymo research) according to the manufacturer's instructions. Samples were immediately stored at -20^{o}C. Library preparation was carried out using Accel-NGS 1S plus kit (Swift Biosciences), in accordance with the manufacturer's protocol, using a 0.8 DNA/AMPure beads v/v ratio across all purification steps. Libraries were quantified on an Agilent 2100 Bioanalyzer (Agilent) using an Agilent High Sensitivity DNA Kit (Agilent) following the manufacturer's guidelines and electropherograms were visualised and fragment size determined using the Agilent Bioanalyzer 2100 expert software. Samples were once again quantified by Qubit, and converted to nM using the following formula:

$$(\text{ng/µl from Qubit}) \times (10^{6}) / (\text{Avg frag size}) \times (660)$$

Samples were subsequently pooled in an equimolar (10nM) fashion and sequenced using 2x150 nt paired-end sequencing run on an Illumina HiSeq 4000 platform at Genewiz, Germany.

4.3.6 Bioinformatic Analysis

The bioinformatics pipeline utilised in this study is summarised in Figure 4.1.

Figure 4.1 | Bioinformatics pipeline used for analysis of shotgun sequencing data. Abbreviations: nt - nucleotides; QC - quality control; bp - base pairs; DB - database.

Raw sequence (4,606,499 ± 242,973 per sample) quality was assessed using MultiQC (v1.9). Levels of bacterial contamination were estimated by classifying reads with SortMeRNA (v2.0) against the SILVA (v129) database. Filtering and trimming was performed with TrimGalore! (v0.6.1). Host sequences aligning to the *Bos taurus* (NCBI: ARS-UCD1.3) and *Homo sapiens* (NCBI: GRCh38.p14) reference genomes from NCBI were removed with Bowtie2 (v 2.4.4), resulting in 3,794,343 ± 232,625 sequences per sample. Reads were assembled on a per sample basis using metaSPAdes assembler (v3.10). Assembled contigs larger than 1kb were subsequently pooled and retained. Redundancy between samples was removed by aligning all contigs against each other with CD-HIT (v4.7) with the following parameters: "-g 1, -c 0.9, -s 0.9 -aS 0.9 –sc1". For each resulting family, the longest representative contig was taken to create a non-redundant contig catalogue consisting of 9,201 contigs. To identify a set of confident viral contigs, the viral sequence identification standard operating procedure (SOP) with from protocols.io (dx.doi.org/10.17504/protocols.io.bwm5pc86), which combines VirSorter2 (v2.2.3), CheckV (v1.0.1) , and DRAMv (v1.4.6), was employed. Contigs with no BLASTn alignments to the Genbank nucleotide database or the viral Refseq database (v.89), using an e-value of $\leq 10^{-10}$, covering > 90% of contig length at > 50% identity, were removed. Contigs aligning to the phage T4 spike were also removed at this point. This resulted in a set of 673 confident viral contigs. Quality filtered reads were subsequently aligned to the reference set of 673 confident viral contigs on a per sample basis, using Bowtie2 (v2.4.4) in the 'end-to-end' alignment mode. A count table was then generated using SAMTools (v1.10). Sequence coverage was calculated per nucleotide position, per contig and per sample using SAMTools 'mpileup' command. To remove spurious Bowtie2 alignments, read counts which featured a breadth of contig coverage of less than 1X for 75% of a contig length, were set to zero. Virus-like sequences that were classified as exogenous phage T4 were excluded at this point. Finally, the decontam R package (v1.16.0) was used to remove contaminating contigs using the prevalence mode based on the assumption that contaminating sequences are prevalent in the negative-control samples. These criteria yielded a final catalogue of 586 virus-like sequences for downstream analysis. Open reading frames (ORF) were predicted using Prodigal (v2.6.3) in metagenomic mode. A Hidden Markov Model (HMM) algorithm (hmmscan from HMMER v3.1b1 package) was used to search amino acid sequences of predicted protein products against an HMM database

prokaryotic viral orthologous groups (pVOGs) (Grazziotin et al., 2016). Significant hits were considered at e-value threshold of 10^{-5}. Contigs aligning to the phage T4 spike were assessed using the QUAST V 5.1.9 assembly quality test, against the T4 reference genome (NCBI:txid2681598). Estimated viral loads were calculated based on the initial spiked concentration of phage T4 using an in house script (Shkoporov et al., 2018). Family-level taxonomic annotations were assigned to viral contigs using the Demovir script (https://github.com/feargalr/Demovir) with default parameters and database. This script performs a search for amino acid sequence homologies between proteins encoded by a contigs query and a viral subset of the TrEMBL database, then uses a voting approach incorporated in the software to decide on taxonomic assignment. For contigs which could be taxonomically assigned at family level, genus-level taxonomic classification was assigned using VirusTaxo (Raju et al., 2022). To identify VLPs present in each sample type, presence in at least 50% of the 18 samples analysed and a cut off of >0.001 was used. The 69 VLPs which passed this threshold were visualised as proteomic trees using the ViPTree server (Nishimura et al., 2017). Circular genome maps of VLPs were drawn using ProkSee (Grant et al., 2023). Antibiotic resistance analysis of viral contigs was performed using RGI (v6.0.0) (Resistance Gene Identifier) main and the CARD (v3.2.5) (Comprehensive Antibiotic Resistance Database) (McArthur et al., 2013). The "--low_quality", was specified to allow prediction of partial open reading frames by Prodigal, recommended for low quality/coverage assemblies, metagenomic merged reads, small plasmids or assembly contigs (<20,000 bp). The "--include_nudge" and "Perfect, Strict and Loose Hits" options were chosen. Prediction of likely bacterial hosts for the curated set of contigs was done by searching for CRISPR spacer matches. Three genomic databases were used as sources for CRISPR spacer prediction: (1) Bacterial section of NCBI RefSeq (release 89, 50,971 draft and complete genome assemblies, 1,547,225 CRISPR spacers) (O'Leary et al., 2016). (2) 3,055 draft and complete bacterial genome assemblies in the Human Microbiome Project (HMP) database (35,544 spacers) (Human Microbiome Jumpstart Reference Strains et al., 2010). MinCED v0.4.2 (Bland et al., 2007) (using default settings) was used to identify CRISPR spacers in bacterial genomic sequences. BLASTn (Altschul et al., 1990) of spacer matches was performed against putative viral contigs using the following parameters: "blastn-short, e-value < 10^{-2}, bitscore ≥ 45". Assignment of bacterial host to phage

contigs was done at genus level. In cases of ambiguity, genus producing highest number of individual CRISPR hits was considered as primary host.

4.3.7 Statistical Analysis

Further data handling was performed in R (v4.1.2) with the RStudio GUI (v1.4.1717). Plotting was handled using ggplot2 (v3.4.1). The iNEXT library was used to compute alpha diversity for the first three hill numbers (Chao1, Shannon entropy and Simpson Index) (Hsieh et al., 2016). Differences in alpha diversity (within-sample diversity) were assessed using linear models. Principal component analysis was performed on centred log-ratio transformed (clr) values as a visual companion to the beta diversity analysis. Zeroes were imputed using the *"const"* method (Lubbe et al., 2021). Beta diversity was computed in terms of Aitchison distance (Euclidean distance of clr-transformed counts) (Aitchison et al., 2000). Network analysis was performed using a Bray-Curtis distance similarity matrix in the igraph (v 1.5.0) R package. Differences in beta diversity (between-sample diversity) were assessed using the adonis() PERMANOVA function in the vegan library (v2.6.4) and the value of p were adjusted using the Bonferroni-Holm correction method. A difference was considered statistically significant if the adjusted $p < 0.05$. Differential abundance analysis was carried out with R package *MaAsLin2* v1.13.0 (Mallick et al., 2021). The general linear model, no transformation and CLR-normalisation were selected as the parameters. CEF and UBRO were chosen as fixed effects and NOAB as the reference effect.

4.4 Results

4.4.1 Cohort characteristics

Table 4.1 presents the characteristics of the 72 cows included in this study. The study population was categorised into three groups based on antibiotic dry cow treatment: NOAB (n=23), CEF (n=24), and UBRO (n=25). The mean parity of the cohort was 2.85 (standard deviation [SD] ± 2.3) and the mean age was 4.85 (SD ± 2.3) years. Samples were collected from five different farms, including farm 1 (n=16), farm 2 (n=14), farm 3 (n=13), farm 4 (n=15), and farm 5 (n=14). Farm 1 did not practice antibiotic DCT.

Table 4.1 | Metadata for cows included in this study.

ID	Farm	Parity	Age (years)	Parous	Antibiotic
C10	Farm 1	2	4	Multiparous	None
C11	Farm 1	4	6	Multiparous	None
C13	Farm 1	1	3	Primiparous	None
C16	Farm 1	0	2	Nulliparous	None
C17	Farm 1	6	8	Multiparous	None
C18	Farm 1	4	6	Multiparous	None
C19	Farm 1	0	2	Nulliparous	None
C1	Farm 1	1	3	Primiparous	None
C20	Farm 1	4	6	Multiparous	None
C2	Farm 1	0	2	Nulliparous	None
C3	Farm 1	1	3	Primiparous	None
C5	Farm 1	0	2	Nulliparous	None
C6	Farm 1	3	5	Multiparous	None
C7	Farm 1	1	3	Primiparous	None
C8	Farm 1	4	6	Multiparous	None
C9	Farm 1	4	6	Multiparous	None
D10	Farm 2	8	10	Multiparous	Cefquinome
D11	Farm 2	2	4	Multiparous	Cefquinome
D12	Farm 2	4	6	Multiparous	Cefquinome
D13	Farm 2	1	3	Primiparous	Cefquinome
D14	Farm 2	1	3	Primiparous	Cefquinome
D15	Farm 2	3	5	Multiparous	Cefquinome
D17	Farm 2	2	4	Multiparous	Cefquinome
D18	Farm 2	7	9	Multiparous	Cefquinome
D19	Farm 2	4	6	Multiparous	Cefquinome
D1	Farm 2	8	10	Multiparous	Cefquinome
D20	Farm 2	0	2	Nulliparous	None
D5	Farm 2	7	9	Multiparous	Cefquinome
D7	Farm 2	3	5	Multiparous	Cefquinome
D9	Farm 2	1	3	Primiparous	Cefquinome

L10	Farm 3	3	5	Multiparous	Ubro Red
L12	Farm 3	5	7	Multiparous	Ubro Red
P14	Farm 4	1	3	Primiparous	Ubro Red
L14	Farm 3	6	8	Multiparous	Ubro Red
L15	Farm 3	0	2	Nulliparous	None
L18	Farm 3	7	9	Multiparous	Ubro Red
L19	Farm 3	2	4	Multiparous	Ubro Red
L2	Farm 3	3	5	Multiparous	Ubro Red
L3	Farm 3	1	3	Primiparous	Ubro Red
L5	Farm 3	1	3	Primiparous	Ubro Red
L7	Farm 3	2	4	Multiparous	Ubro Red
L8	Farm 3	5	7	Multiparous	Ubro Red
L9	Farm 3	7	9	Multiparous	Ubro Red
P10	Farm 4	1	3	Primiparous	Cefquinome
P11	Farm 4	6	8	Multiparous	Cefquinome
P12	Farm 4	2	4	Multiparous	Cefquinome
P13	Farm 4	5	7	Multiparous	Cefquinome
L13	Farm 3	0	2	Nulliparous	None
P15	Farm 4	7	9	Multiparous	Ubro Red
P16	Farm 4	0	2	Nulliparous	None
P18	Farm 4	0	2	Nulliparous	None
P19	Farm 4	1	3	Primiparous	Cefquinome
P1	Farm 4	4	6	Multiparous	Cefquinome
P5	Farm 4	5	7	Multiparous	Cefquinome
P6	Farm 4	5	7	Multiparous	Cefquinome
P7	Farm 4	4	6	Multiparous	Cefquinome
P8	Farm 4	2	4	Multiparous	Cefquinome
P9	Farm 4	1	3	Primiparous	Cefquinome
T10	Farm 5	3	5	Multiparous	Ubro Red
T11	Farm 5	0	2	Nulliparous	None
T12	Farm 5	2	4	Multiparous	Ubro Red
T16	Farm 5	3	5	Multiparous	Ubro Red

T17	Farm 5	1	3	Primiparous	Ubro Red
T18	Farm 5	2	4	Multiparous	Ubro Red
T19	Farm 5	2	4	Multiparous	Ubro Red
T1	Farm 5	5	7	Multiparous	Ubro Red
T20	Farm 5	2	4	Multiparous	Ubro Red
T4	Farm 5	1	3	Primiparous	Ubro Red
T5	Farm 5	2	4	Multiparous	Ubro Red
T6	Farm 5	0	2	Nulliparous	None
T7	Farm 5	7	9	Multiparous	Ubro Red
T8	Farm 5	3	5	Multiparous	Ubro Red

4.4.2 Virome Extraction Protocol Optimisation

The optimised protocol used for crude processing and extraction of viral nucleic acids from colostrum samples was ultimately based on protocol 3. This protocol was originally developed for virome extraction from human faeces (Shkoporov et al., 2018). Several key modifications were made to adapt the protocol for colostrum samples. The strategy for identifying suitable crude processing steps for viral particle separation is illustrated in Figure 4.2. The suitability of processing steps employed by various published protocols were assessed by two performance parameters: (i) removal of bulk protein, assessed visually, and (ii) recovery of spiked phages. Several approaches were investigated, including different NaCl concentrations, centrifugation/ultracentrifugation speeds, solution dilution buffers, filtration methods (dead-end and tangential-flow), and two phage particle concentration techniques (PEG and TFF). For PEG-based protocols, PEG 6000 was used as it dissolved more readily in colostrum samples compared to PEG 8000, with no significant differences in spike recovery. Isoelectric precipitation of casein by adjusting sample pH to 4.6, a common practice in the dairy industry, was found to be effective in sample clarification and recovery of spiked phages. Centrifugation at modest speeds (5,000 x g) yielded significantly higher recovery of spiked phage T4 compared to ultracentrifugation (28,000 x g). The inclusion of glass fiber filters had no significant impact on spike retrieval but greatly facilitated fat removal and filtration. The recovery rate of spiked-in phage T4 is shown in Figure 4.3.

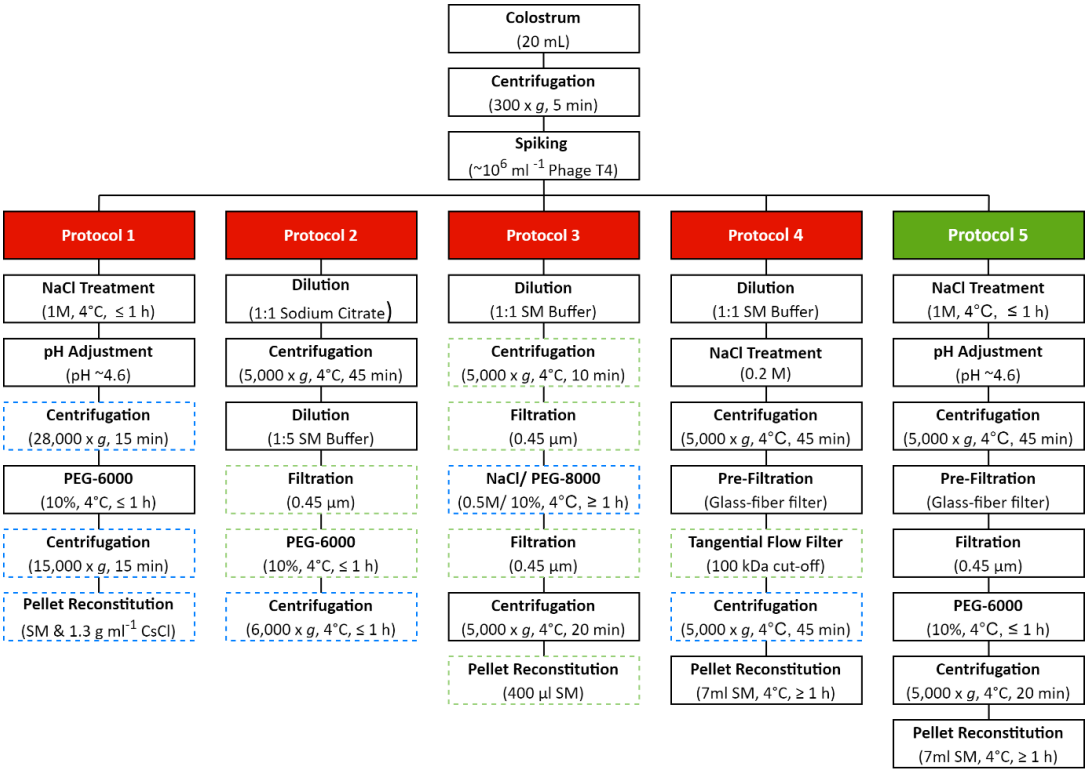

Figure 4.2 | Strategy for colostrum virome extraction protocol optimisation. Techniques assessed for protein separation and recovery of spiked *Escherichia coli* phage T4 from colostrum samples. Non-continuous line boxes: unsuitable for bacteriophage extraction (high loss of spiked phages). Green-line boxes: impure samples (low molecular weight impurities). Blue-line boxes: ≥50% loss of spiked bacteriophages. Continuous boldface line boxes: significant protein removal and/or high recovery of spiked phages. Final optimised protocol (protocol 5) developed based on steps with highest recovery. PEG: polyethylene glycol; SM: sodium-magnesium (buffer).

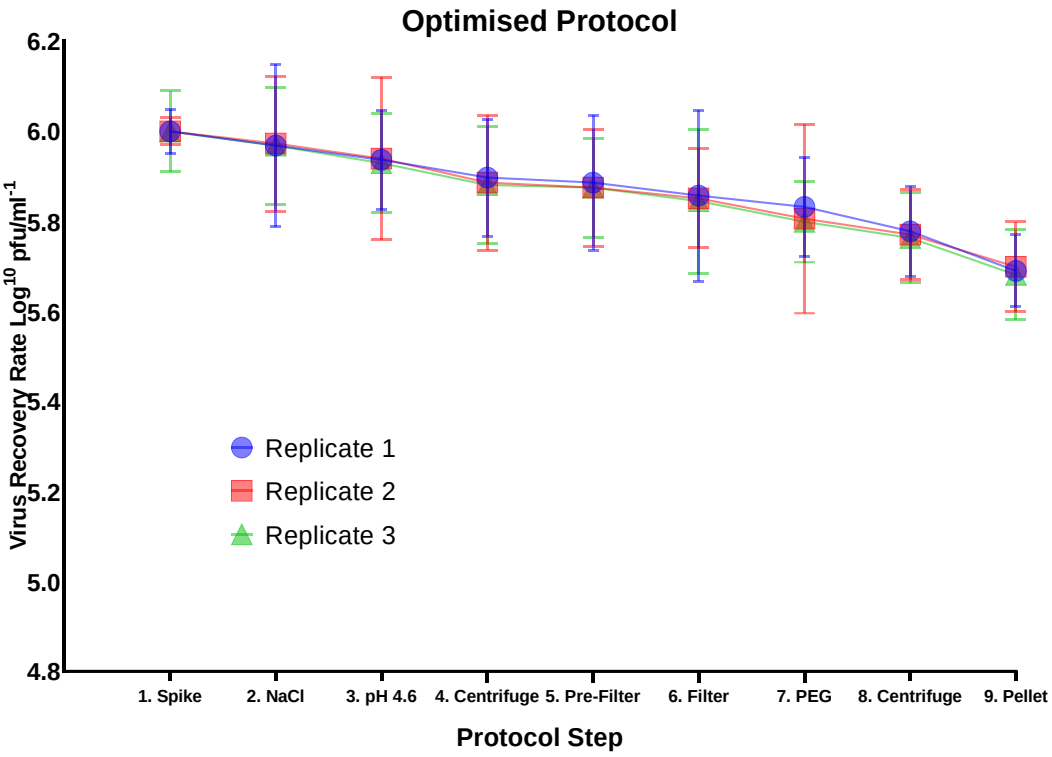

Figure 4.3 | Phage T4 spike-in recovery for optimised protocol. The percentages of phages recovered (y axis) were determined by plaque assay at each different sampling point (x axis). Error bars represent the standard deviation of biological repeats (n=3).

4.4.3 Sequencing Results and Recovery of Spike-In Phages

The amount of reads per sample retained at each step of DNA processing are shown in Table S4.1. Shotgun sequencing of colostrum samples yielded an average of 4,606,499 ± 242,973 reads per sample. Following read trimming, filtering, and host removal, an average of 3,794,343 ± 232,625 (median = 2,278,080, min = 19,626, max = 15,988,450), reads per sample remained. An average of 2.7% of reads in the pre-filtration dataset aligned to 16S rRNA, which is an accepted standard for virome studies (Jurasz et al., 2021). The final dataset for viral analysis consisted of 586 non-redundant complete and partial viral genomes. Contigs of various sizes were recovered, mainly representing genomic fragments (1×10^3 to 2×10^4 bp) with low-to-moderate levels of sequence coverage (1–100 ×) (Figure 4.4). The phage T4 spike genome was successfully assembled into a single contig (~168 kb) in all samples. This contig represented 99.5% of the NCBI reference T4 genome, exhibiting no miss-assemblies, 138 mismatches, and 57 indels, as confirmed by the QUAST assembly quality test. The phage T4 reference genome (168,903 bp) was aligned against the

contig recovered as the spike genome (168,052 bp), which showed that 851 base pairs were missing from the 5' and 3' ends of the genome.

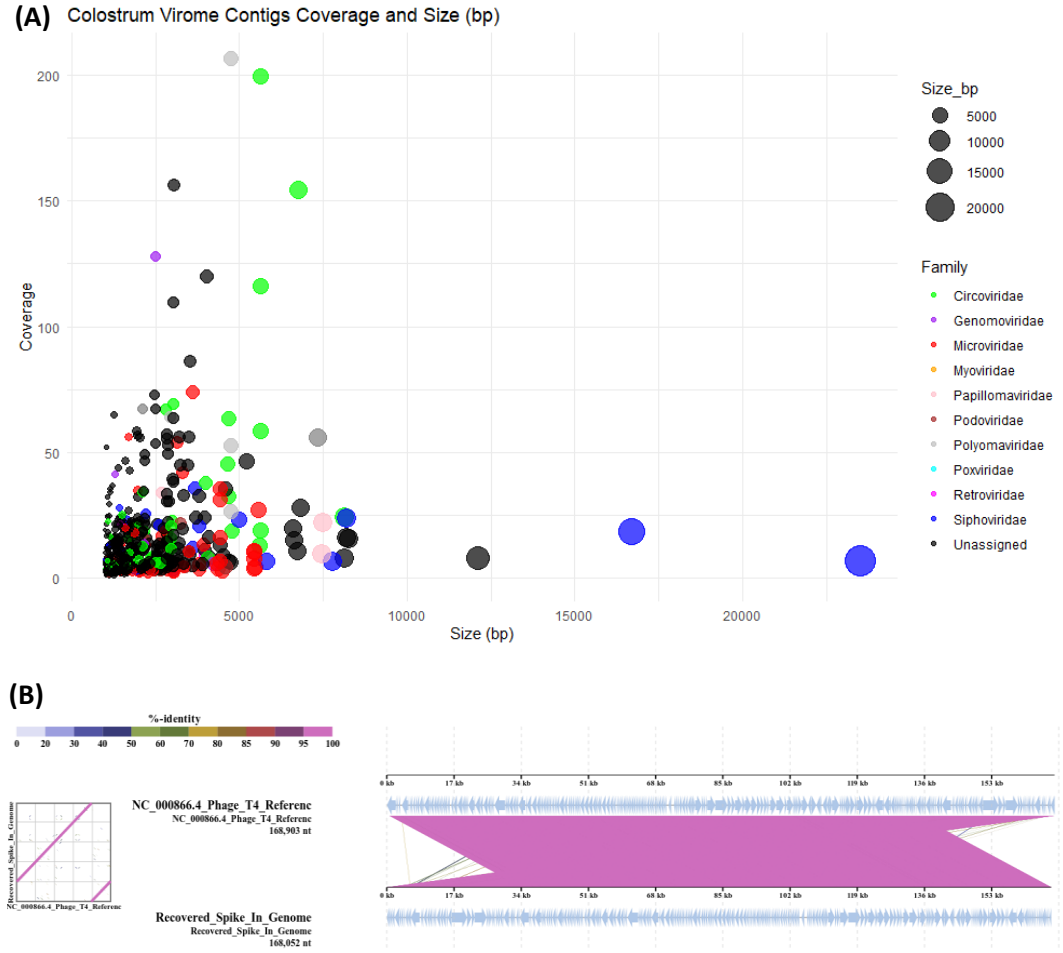

Figure 4.4 | (A) Colostrum virome contigs coverage and size (bp). (B) Pairwise comparison of phage T4 reference and spike-in genomes using ViPTree. Genomes shown linearly with CDS transcription direction indicated by arrows. tBLASTx alignments represented by coloured lines, with colour scale indicating percent identity.

4.4.4 Taxonomic Classification

Taxonomic classification of viral contigs revealed the following distribution: 47% were identified as ssDNA viruses, 48% were dsDNA viruses, 0.1% were ssRNA viruses and 28% were classified as dsDNA phages. A total of 20% of contigs contained genes for integrases or site-specific recombinases, indicating a possible temperate lifestyle. The estimated total viral load ranged from approximately 1.1 x 10^4 to 1.1 x 10^9 PFU/ml genome copies per gram of colostrum. On average, the viral load was approximately 1.1 x 10^6 PFU/ml. At the family level, a total of ten viral families were

identified, with the majority of contigs remaining unassigned. The identified viral genomes encompassed diverse types, including circular ssDNA viruses such as *Circoviridae* and *Genomoviridae*, linear double-stranded DNA viruses including *Myoviridae*, *Microviridae*, *Papillomaviridae*, *Podoviridae*, *Polyomaviridae*, *Poxviridae*, and *Siphoviridae*, as well as ssRNA viruses classified as *Retroviridae*. At the genus level, taxonomic classification using VirusTaxo identified a total of 48 distinct genera (Figure S4.1). The three most prominent genera which could be identified were *Circovirus*, *Lederbergvirus*, and *Liefievirus*.

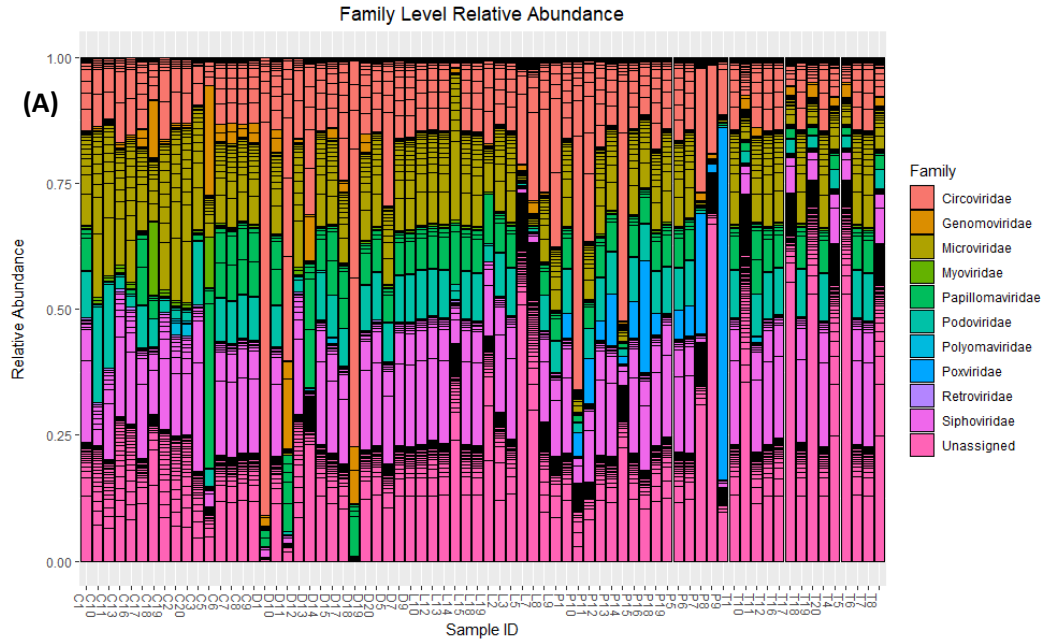
Family Level Relative Abundance
(A)
Relative Abundance
1.00
0.75
0.50
0.25
0.00
Sample ID
Family
Circoviridae
Genomoviridae
Microviridae
Myoviridae
Papillomaviridae
Podoviridae
Polyomaviridae
Poxviridae
Retroviridae
Siphoviridae
Unassigned

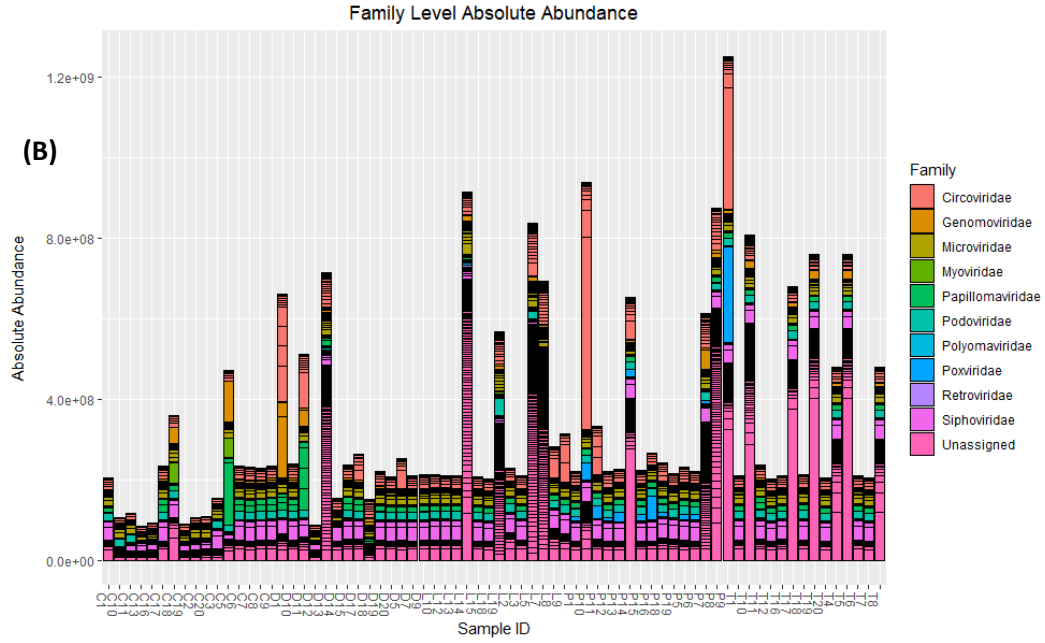
Family Level Absolute Abundance
(B)
Absolute Abundance
1.2e+09
8.0e+08
4.0e+08
0.0e+00
Sample ID
Family
Circoviridae
Genomoviridae
Microviridae
Myoviridae
Papillomaviridae
Podoviridae
Polyomaviridae
Poxviridae
Retroviridae
Siphoviridae
Unassigned

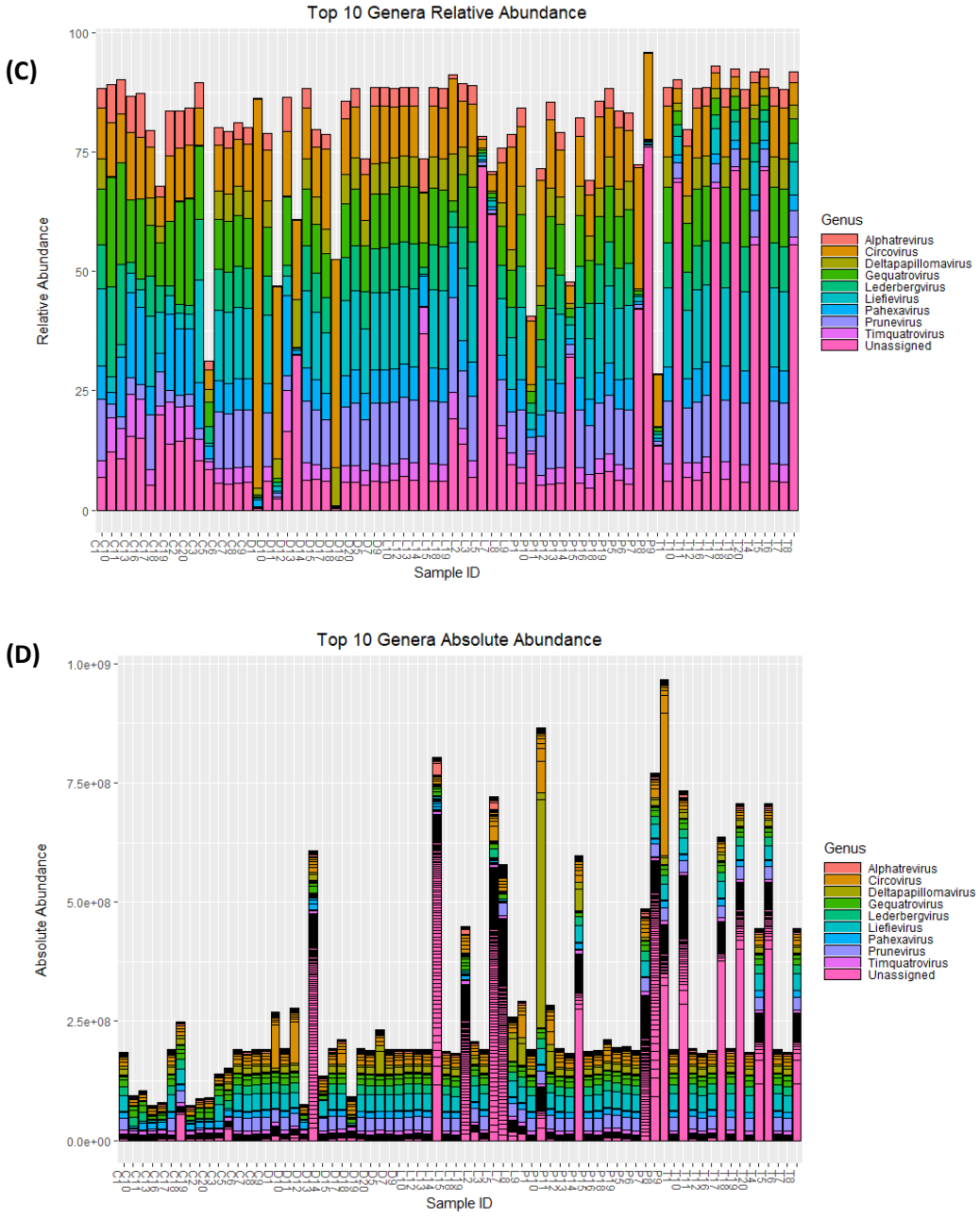

Figure 4.5 | (A) Family level relative abundance. (B) Family level absolute abundance. (C) Relative abundance of top ten genera. (D) Absolute abundance of top ten genera.

Core Virome Analysis

Out of the 586 VLPs detected, 69 VLPs (present in ≥50% of samples, cut-off >0.001) were identified as the core colostrum virome (Figure 4.6A). These VLPs were all ssDNA and dsDNA in nature. The core virome VLPs exhibited relative abundances ranging from 17% to 99.7% of the total viral abundance in each of the samples, with an average relative abundance of 89.2% (Figure 4.6B). The median relative abundance was 96%, and the standard deviation was 24.5%, indicating large variability in their abundance across the samples.

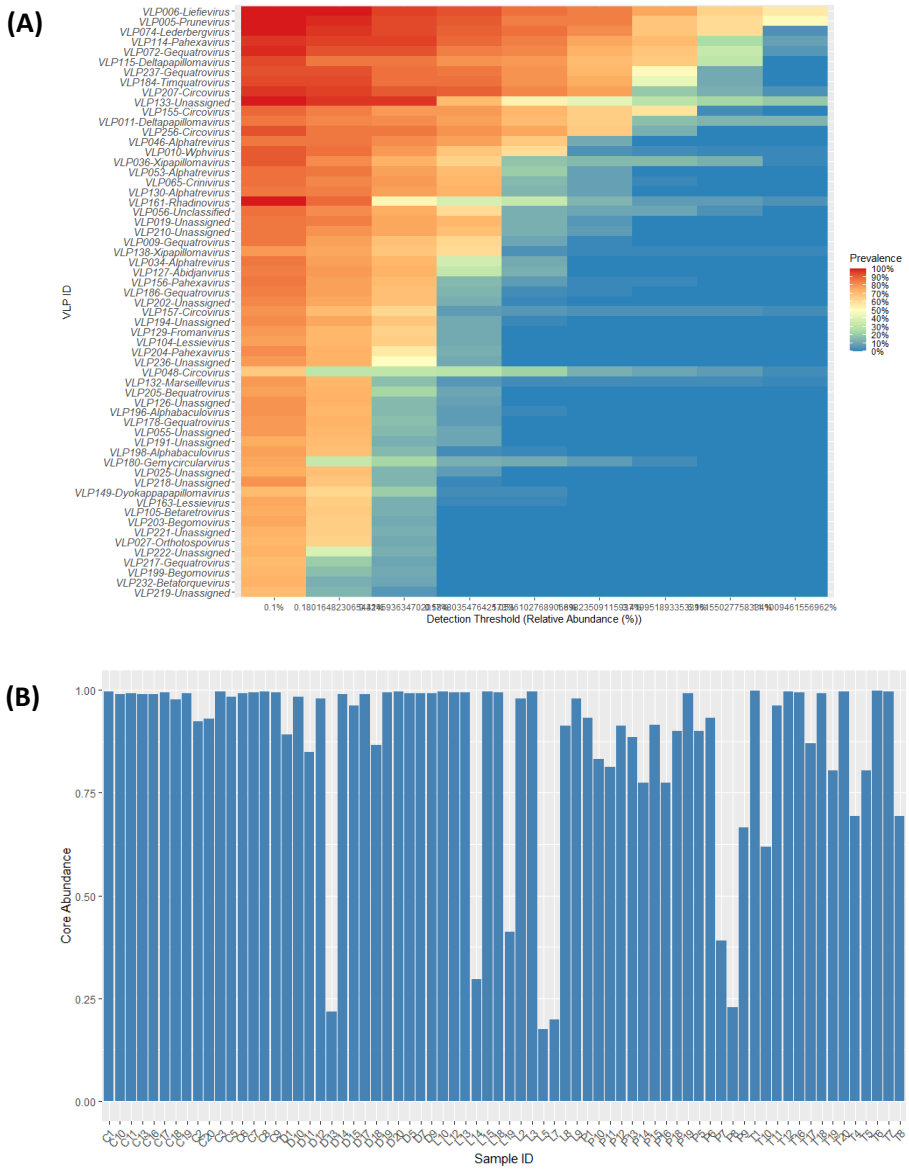

Figure 4.6 | (A) Colostrum core virome heatmap. Abundance of core VLPs in 72 samples (>0.001 cut-off) and prevalence (50% cut-off) with VLP ID and taxonomic

classification. (B) Percentage of which core contigs contributed to the total abundance in each sample.

In the absence of a robust phylogeny-based taxonomic classification and due to the fact that the vast majority of viral sequences cannot be assigned to any known taxon below the family level, we grouped viral contigs identified as the core virome using proteomic trees analysis. The 69 VLPs identified as the core virome were further clustered against all ssDNA virus genomes (1,796) (Figure 4.7A) and all dsDNA virus genomes (6,428) (Figure 4.7B) available from the VipTree server (Accessed 1st July 2023). Regarding VLPs which could not be classified, distinct clustering was observed towards

Parvoviridae, *Circoviridae* and *Geminiviridae*. Overall, this analysis further supported the taxonomic classifications made by Demovir and VirusTaxo. A total of 16 VLPs were shown to be shared among all samples (Table S4.2). Among these shared VLPs, two novel CRESS DNA viruses, namely VLP048 and VLP155, were identified, annotated and visualised using Proksee (Figure S4.2).

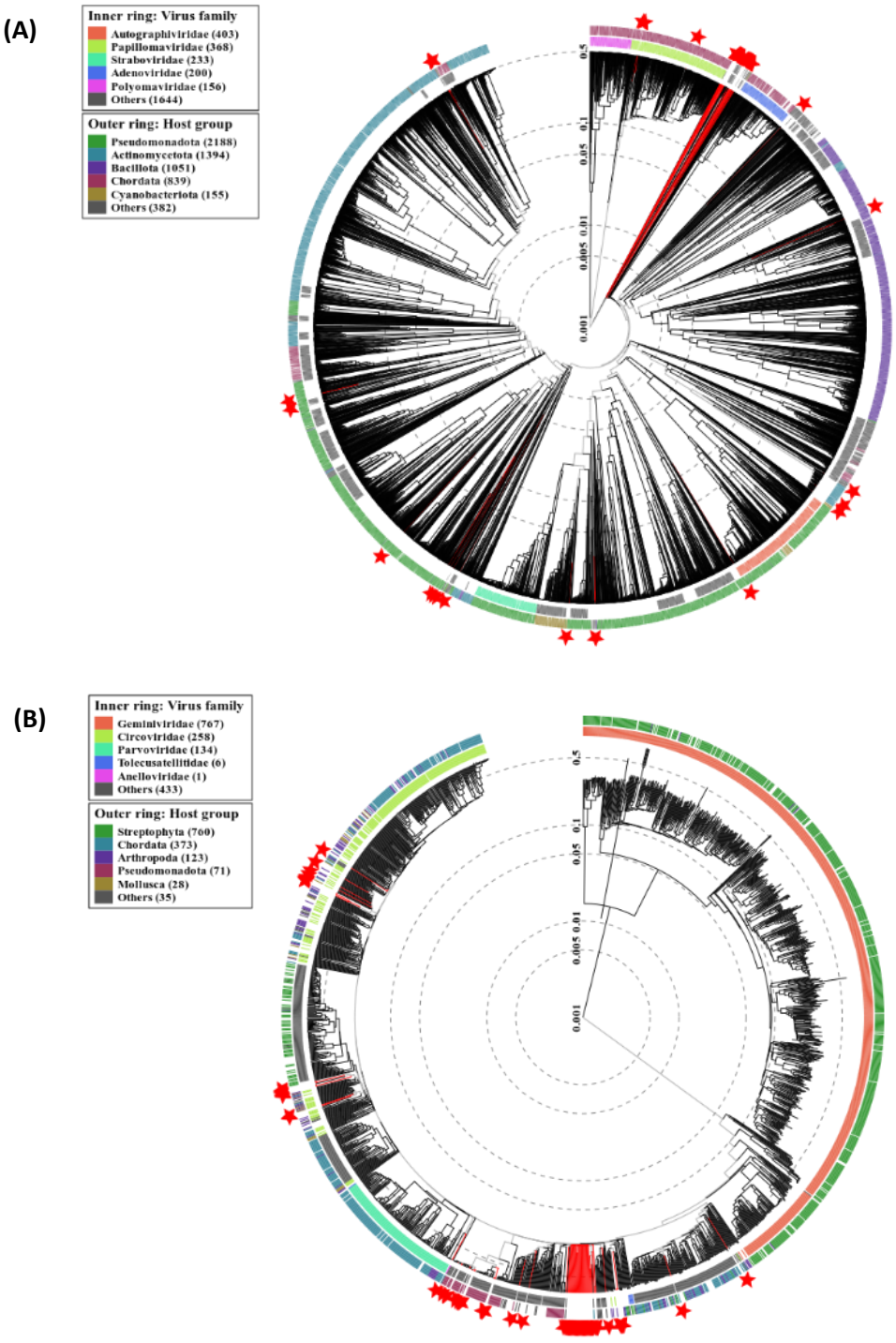

Figure 4.7 | (A) Circular proteomic tree based on genome-wide similarities of core virome VLPs (marked with a red star), top matches on BLASTn, and 1,796 ssDNA viral genomes. (B) Circular proteomic tree based on genome-wide similarities of core virome VLPs (marked with a red star), top matches on BLASTn, and 6,428 dsDNA viral genomes. Viptree server accessed 1st July 2023.

4.4.5 Detection of Putative Antimicrobial Resistance Genes and Bacterial Hosts

RGI main and the CARD database were used to predict ARGs present in the 586 viral contigs identified in this study. In total, 16 ARGs belonging to 10 AMR gene families conferring resistance to 15 different classes of antibiotics were found (Table 4.2). Of these, 17 ARGs conferred resistance to more than one class of antibiotic. Three ARGs were classified as multi-drug resistance (MDR) genes as they conferred resistance to three or more classes of antibiotics. ARGs were found to be present in 23 VLPs, which were all classified as DNA fragments of dsDNA phage genomes. Three ARGs (*kdpE*, *baeS*, *smeS*) were identified which are resistant to the antibiotic used in the UBRO group. The *smeS* gen also confers resistance to the antibiotic used in the CEF group. Overall, 28% (164) of VLPs identified in this study were identified as phage. Investigation of the bacterial hosts of these VLPs resulted in 23 VLPs identified to infect 39 different bacterial strains (Table 4.3). The most commonly identified host genera were *Actinoalloteichus*, *Mycobacterium*, *Staphylococcus* and *Bifidobacterium*.

Table 4.2 | The 16 antibiotic resistance genes identified in 23 VLPs identified in this study.

No.	Gene Name	Drug Class	Resistance Mechanism
1	*DfrA38*	diaminopyrimidine antibiotic	antibiotic target replacement
2	*baeS*	aminoglycoside antibiotic; aminocoumarin antibiotic	antibiotic efflux
3	*vmlR*	lincosamide antibiotic; streptogramin antibiotic; streptogramin B antibiotic	antibiotic target protection
4	*macB*	macrolide antibiotic	antibiotic efflux
5	*vanR_in_vanO_cl*	glycopeptide antibiotic	antibiotic target alteration
6	*basS*	peptide antibiotic	antibiotic target alteration; antibiotic efflux
7	*oleC*	macrolide antibiotic	antibiotic efflux
8	*lfrA*	fluoroquinolone antibiotic	antibiotic efflux
9	*kdpE*	aminoglycoside antibiotic	antibiotic efflux
10	*smeS*	aminoglycoside antibiotic; cephalosporin; cephamycin; penam	antibiotic efflux

11	*TxR*	tetracycline antibiotic	antibiotic efflux
12	*dfrA20*	diaminopyrimidine antibiotic	antibiotic target replacement
13	*bcrA*	peptide antibiotic	antibiotic efflux
14	*Erm(50)*	macrolide antibiotic; lincosamide antibiotic; streptogramin antibiotic	antibiotic target alteration
15	*lmrC*	lincosamide antibiotic	antibiotic target protection
16	*Mtub_thyA_PAS*	salicylic acid antibiotic	antibiotic target alteration

Gene name, drug class and resistance mechanism were identified by RGI (v6.0.0) (Resistance Gene Identifier) main and the CARD (v3.2.5) (Comprehensive Antibiotic Resistance Database).

Table 4.3 | Table outlining 23 VLPs phage and their corresponding host genera.

No.	**VLP Name**	**Host Genus**
1	VLP006-Liefievirus	*Mycobacterium*
2	VLP004-Unassigned	*Streptococcus*
3	VLP013-Unassigned	*Bifidobacterium*
4	VLP066-Unassigned	*Clostridioides*
5	VLP124-Unassigned	*Actinoalloteichus*
6	VLP170-Unassigned	*Staphylococcus*
7	VLP209-Unassigned	*Prevotella*
8	VLP226-Unassigned	*Pseudomonas*
9	VLP247-Unassigned	*Chryseobacterium*
10	VLP305-Unassigned	*Curvibacter*
11	VLP330-Unassigned	*Acinetobacter*
12	VLP350-Unassigned	*Anoxybacillus*
13	VLP366-Unassigned	*Ruminococcaceae*
14	VLP382-Unassigned	*Bacillus*
15	VLP403-Unassigned	*Paracoccus*
16	VLP428-Unassigned	*Xanthomonas*
17	VLP444-Unassigned	*Enterobacter*
18	VLP457-Unassigned	*Butyrivibrio*
19	VLP129-Fromanvirus	*Mycobacterium*
20	VLP482-Unassigned	*Actinoalloteichus*
21	VLP500-Unassigned	*Actinoalloteichus*
22	VLP519-Unassigned	*Actinoalloteichus*
23	VLP540-Unassigned	*Staphylococcus*

4.4.6 Impact of Farm Level Variables on the Colostrum Virome

Chao1, Shannon and Simpson diversity indices were used to calculate the alpha diversity of the virome within groups. The Chao1 index estimates the total number of viral species in a community based on the abundance of observed species. The Shannon index calculates the overall diversity of a community by considering both the abundance and evenness of species present. The Simpson index measures the dominance or concentration of species in a community. Alpha diversity was significantly different between the UBRO and the NOAB group (Chao1, $p = 2.7 \times 10^{-5}$) and (Simpson, $p = 0.0028$) (Figure 4.8A). Beta diversity of the virome was calculated using Bray-Curtis distance similarity matrix and observed using PCoA. Beta diversity between the NOAB and antibiotic groups (UBRO and CEF) demonstrated distinct clustering overall. Indeed, beta diversity was significantly different between the UBRO and the NOAB group ($p = 0.003$) and the CEF and the NOAB group ($p = 0.006$) (Figure 4.8B). Network analysis was also performed using Bray-Curtis distance similarity matrix and also showed distinct clustering of the NOAB group away from antibiotic groups (Figure 4.8C). 16 VLPs were differentially abundant in the NOAB group at the genus level, most significantly VLP459 (*Alphanudivirus*), VLP090 (*Gervaisevirus*) and VLP011 (*Deltapapillomavirus*) (Figure 4.8D). 16 VLPs were differentially abundant in the antibiotic groups (Figure 4.8D). Most significantly in the UBRO group were VLP132 (*Marseillevirus*), VLP180 (*Gemycircularvirus*) and VLP232 (*Betatorquevirus*). Most significantly in the CEF group were VLP132 (*Marseillevirus*), VLP046 (*Alphatrevirus*) and VLP072 (*Gequatrovirus*) (Figure 4.8D). Overall 16 VLPs were shared across treatment types, 18 were only found in the NOAB group, one was only found in the CEF group and no VLPs were specific to the UBRO group.

(A)

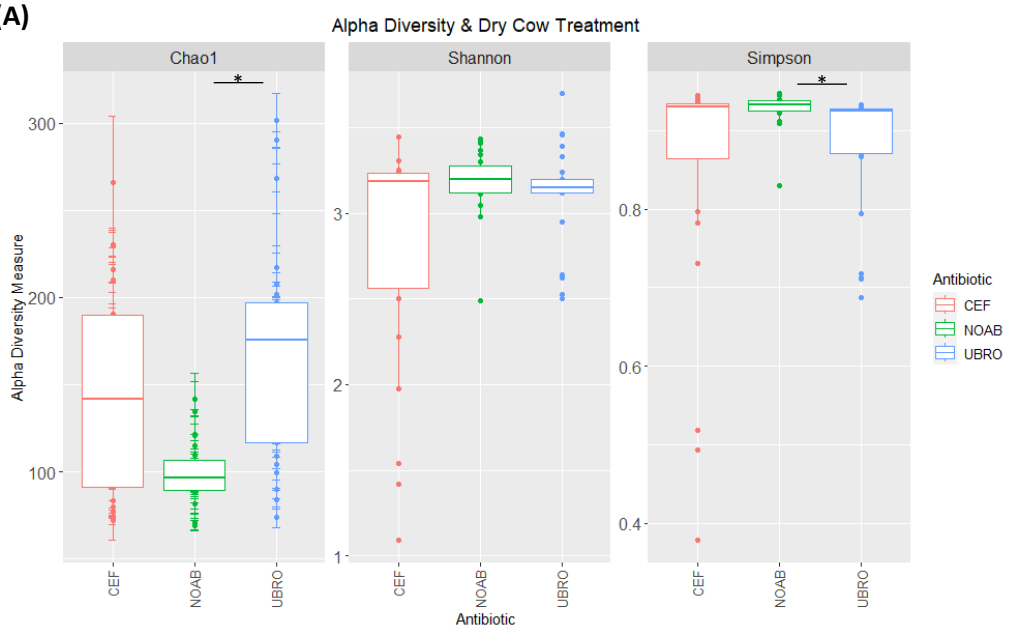
Alpha Diversity & Dry Cow Treatment
Chao1
Shannon
Simpson
Alpha Diversity Measure
300
200
100
3
2
1
0.8
0.6
0.4
*
*
CEF
NOAB
UBRO
Antibiotic
Antibiotic
CEF
NOAB
UBRO

(B)

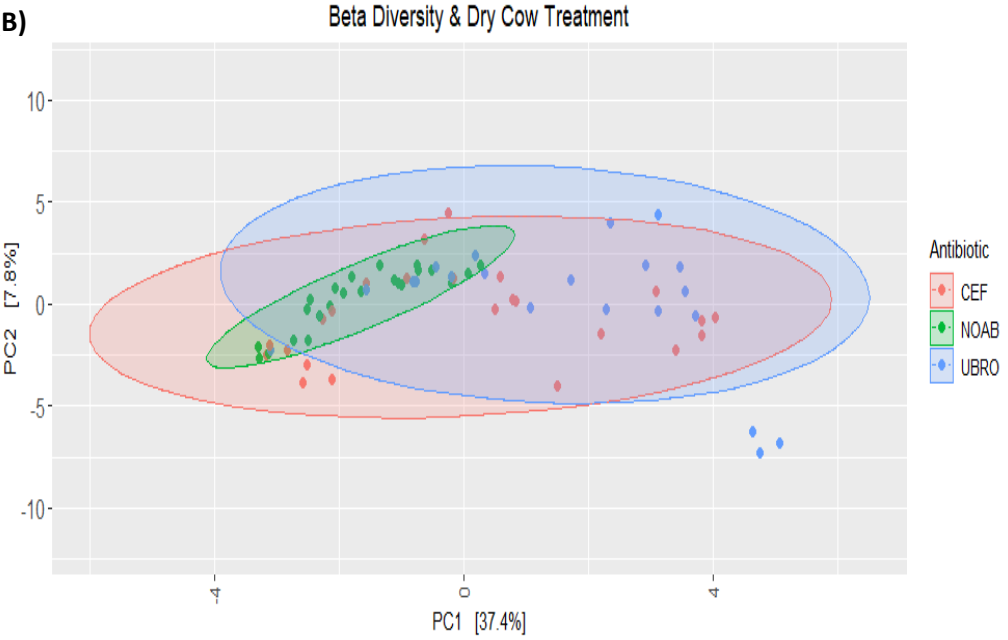
Beta Diversity & Dry Cow Treatment
10
5
0
-5
-10
PC2 [7.8%]
-4
0
4
PC1 [37.4%]
Antibiotic
CEF
NOAB
UBRO

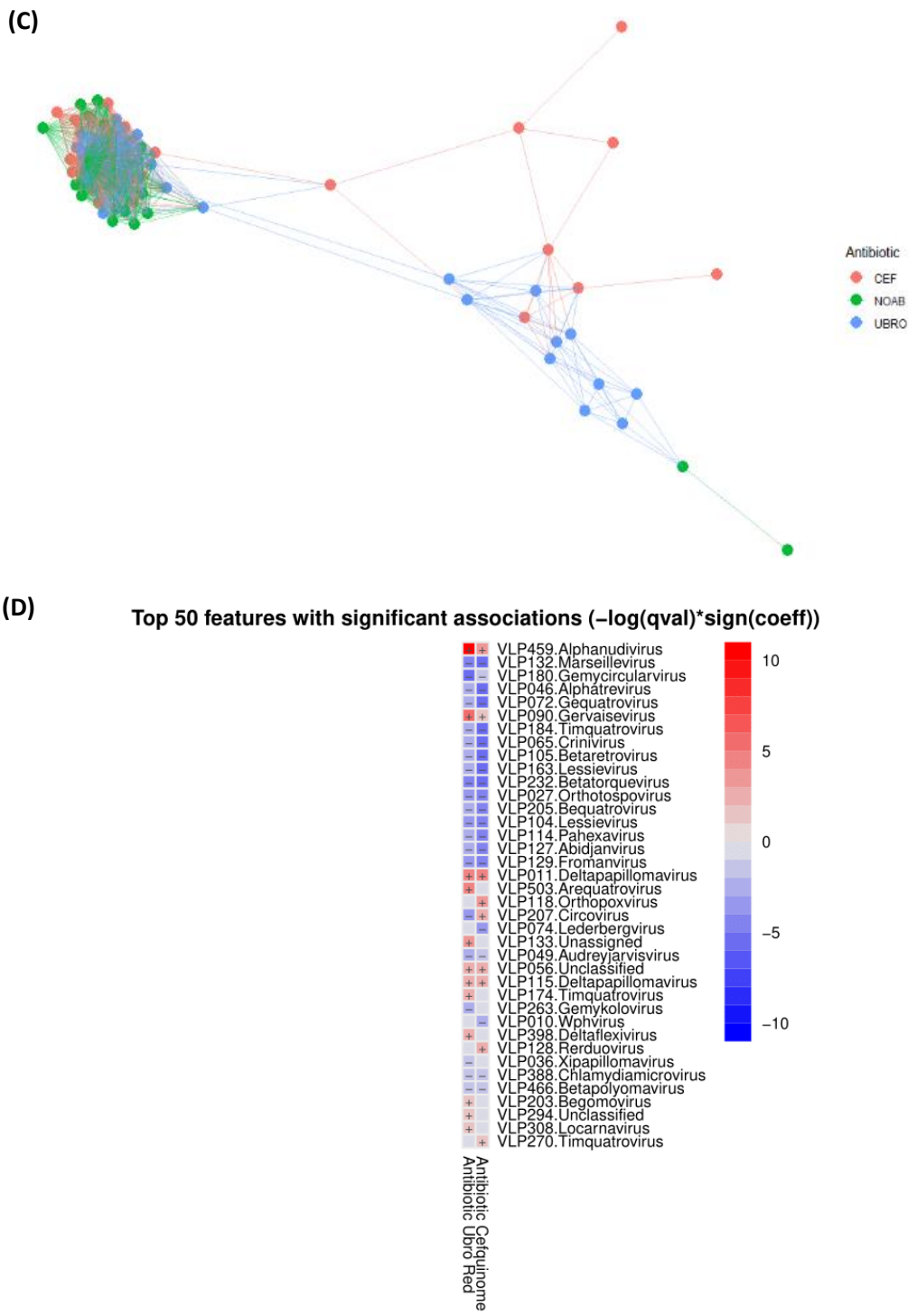

Figure 4.8 | Analysis of colostrum virome diversity and dry cow treatment. (A) Alpha diversity assessed using Chao1, Simpson and Shannon diversity metrics. (B) PCoA plot using Bray-Curtis distance matrix between the three groups. (C) Differentially abundant VLPs identified by MaAsLin2. Blue (reference) associated with no antibiotic. Red is associated with stated antibiotic. (D) Network analysis where node colours represent different dry cow treatment type.

Similar to distinct clustering of the NOAB group from antibiotic treated groups overall, we also observed clustering based on farms, where farm 1 (i.e., the farm using DCT without antibiotics) clusters separately from the other antibiotic treated farms (farm 2 and farm 4 are CEF, while farm 3 and farm 5 are UBRO) (Figure 4.9). Alpha diversity was significantly different between farm 1 and farm 3 (Chao1, p= 0.023), farm 4 (Chao1, p= 0.017) and farm 5 (Simpson, p= 0.028) (Figure 4.9A). Similarly, beta diversity was significantly different between farm 1 and farm 3 (p= 0.01), farm 4 (p= 0.01) and farm 5 (p= 0.01) (Figure 4.9B). These results were in agreement with the aforementioned results for the effect of DCT on virome composition as every cow on Farm 1 did not receive any antibiotic treatment. No distinct clustering based on farm was observed in network analysis (Figure 4.9C). 25 VLPs were differentially abundant in Farm 1 at the genus level, most significantly VLP180 (*Gemycircularvirus*), VLP132 (*Marseillevirus*) and VLP046 (*Alphatrevirus*) (Figure 4.9D). 20 VLPs were differentially abundant in farms which gave antibiotics compared to the non-antibiotic farm (Figure 4.9D). Most significantly were VLP011 (*Deltapapillomavirus*), VLP056 (Unclassified) and VLP115 (*Deltapapillomavirus*) (Figure 4.9D). Overall, 13 VLPs were shared across farms, six VLPs were specific to Farm 1, two VLPs were specific to Farm 4 and no VLPs were specific to Farm 2, Farm 3 and Farm 5.

(A)

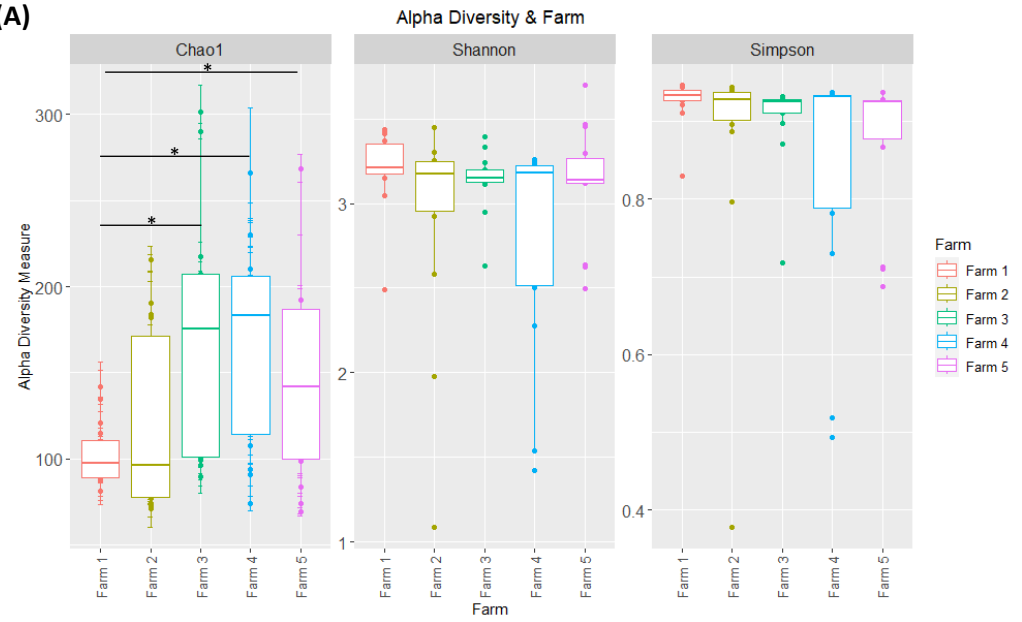
Alpha Diversity & Farm
Chao1
Shannon
Simpson
Alpha Diversity Measure
Farm
Farm 1
Farm 2
Farm 3
Farm 4
Farm 5

(B)

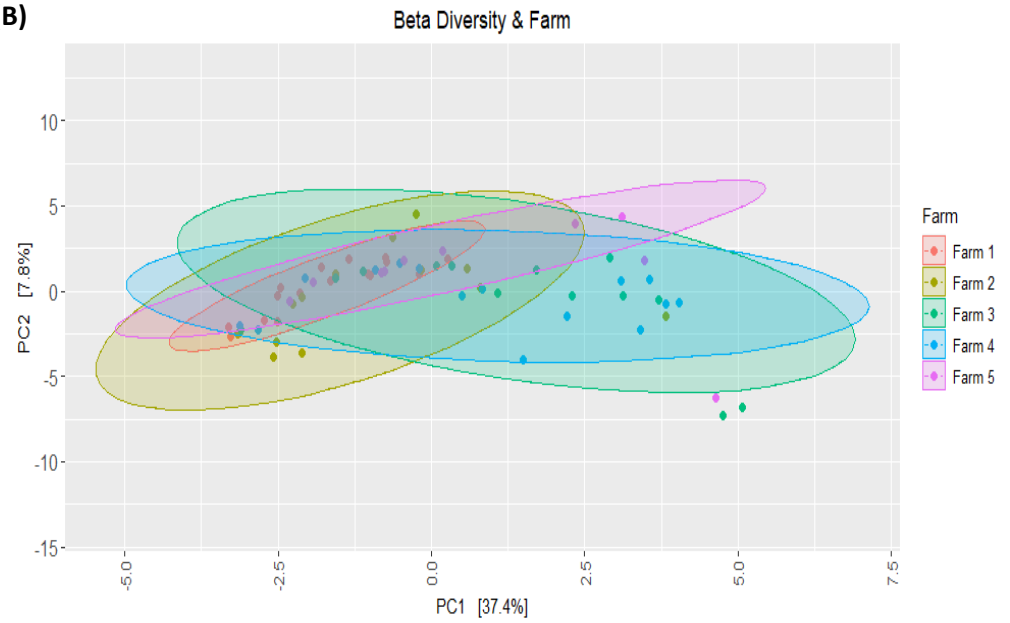
Beta Diversity & Farm
PC2 [7.8%]
PC1 [37.4%]
Farm
Farm 1
Farm 2
Farm 3
Farm 4
Farm 5

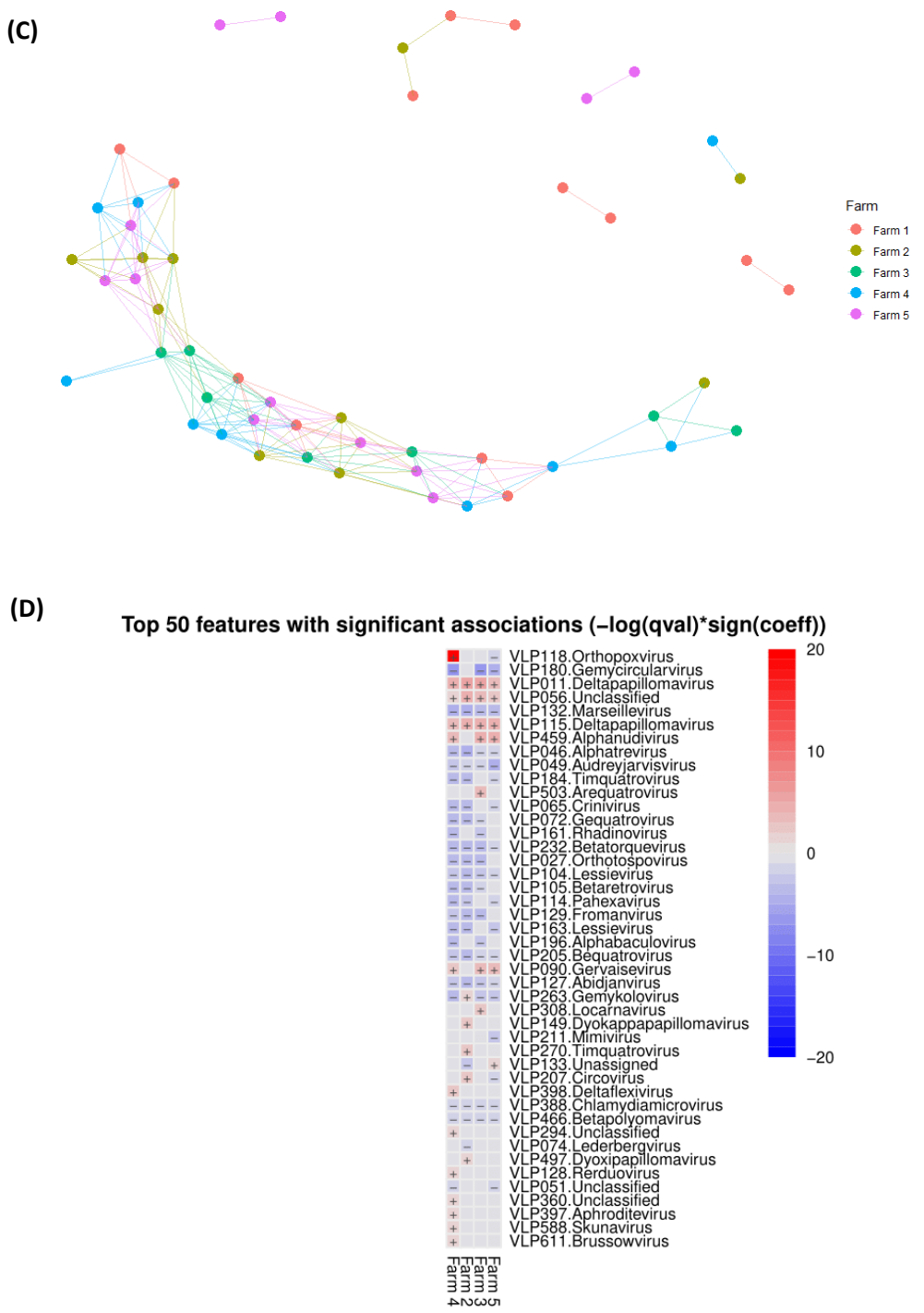

Figure 4.9 | Analysis of colostrum virome diversity based on farms from which samples were collected. (A) Alpha diversity assessed using Chao1, Simpson and Shannon diversity metrics. (B) PCoA plot using Bray-Curtis distance matrix between the five farms. (C) Differentially abundant VLPs identified by MaAsLin2. Blue (reference) associated with farm 1. Red is associated with stated farm. (D) Network analysis where node colours represent different farms.

Regarding the impact of parity on the virome, alpha diversity was significantly different between cows of parity zero and cows of parity two (Chao1, p= 0.041) (Figure 4.10A). There was no significant differences in the beta diversity between different parity values (Figure 4.10B). Network analysis showed distinct clustering of cows of parity zero (Figure 4.10C).). Eight VLPs were differentially abundant in cows of parity zero (Figure 4.10D). Most significantly, VLP104 (*Lessievirus*), VLP127 (*Abidjanvirus*) and VLP132 (*Marseillevirus*) (Figure 4.10D). VLP459 (*Alphanudivirus*) and VLP090 (*Gervaisevirus*) were differentially abundant in cows of parity one and two (Figure 4.10D). Overall, 13 VLPs were shared regardless of parity. There was only VLP specifically found in cows with a parity of four or more and no VLPs were specific to the other parities.

(A)

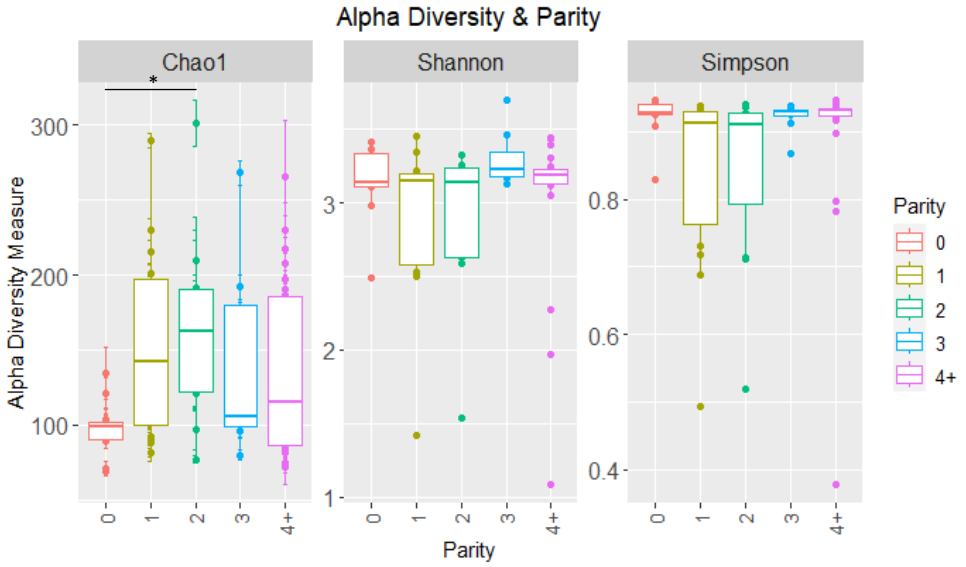
Alpha Diversity & Parity
Chao1
Shannon
Simpson
Alpha Diversity Measure
Parity
0
1
2
3
4+

(B)

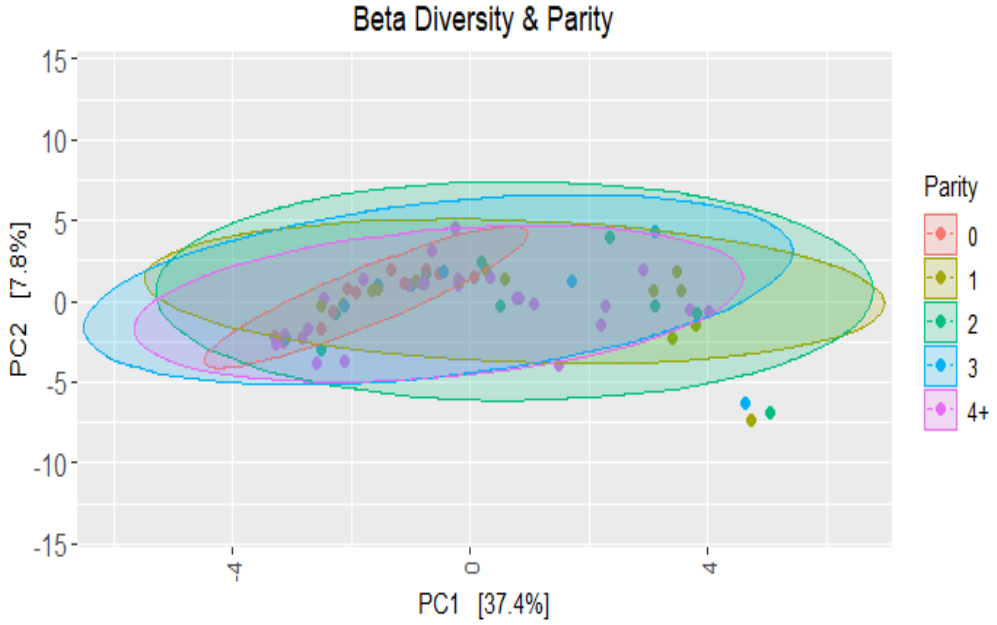
Beta Diversity & Parity
PC2 [7.8%]
PC1 [37.4%]
Parity
0
1
2
3
4+

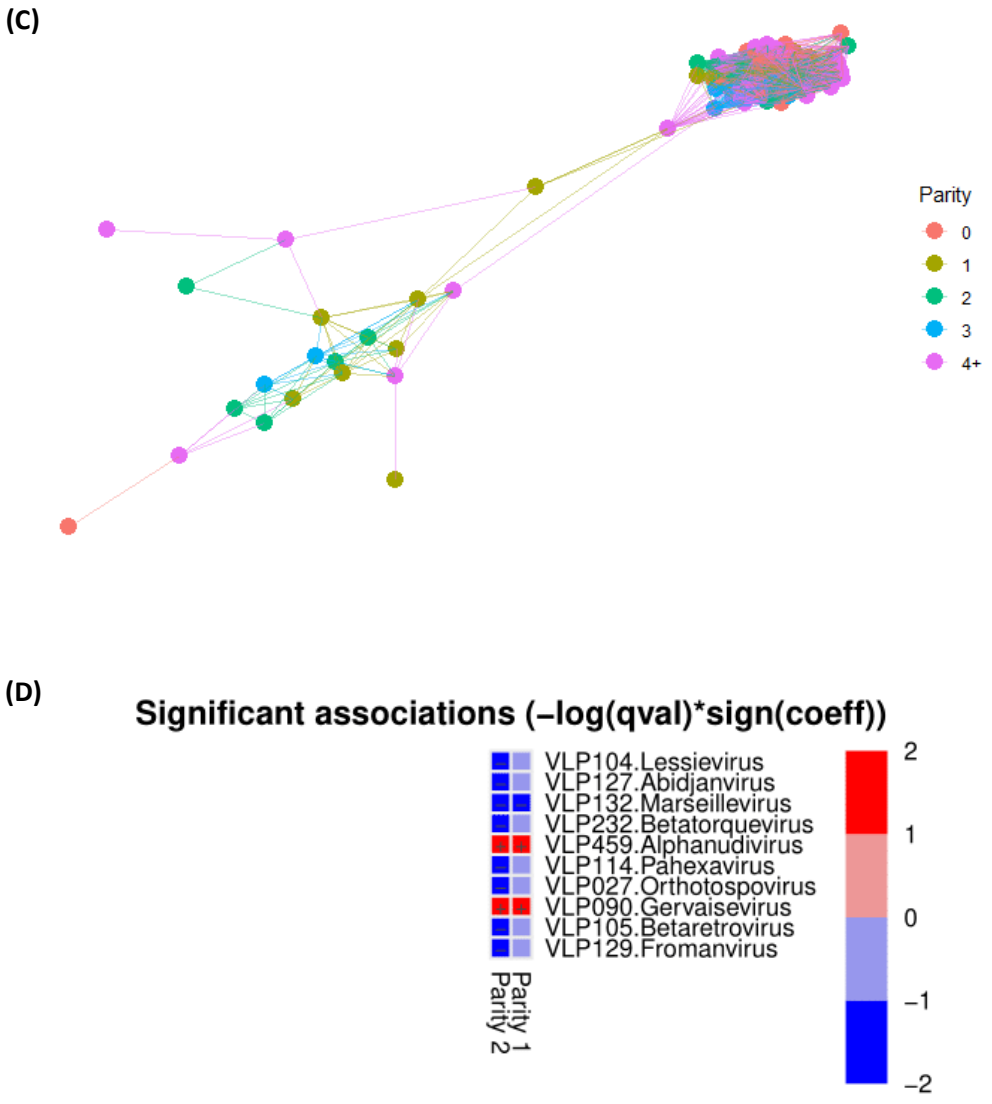

Figure 4.10 | Analysis of colostrum virome diversity based on parity. (A) Alpha diversity assessed using Chao1, Simpson and Shannon diversity metrics. (B) PCoA plot using Bray-Curtis distance matrix based on parity (C) Differentially abundant VLPs identified by MaAsLin2. Blue (reference) associated with parity 0. Red is associated with stated parity. (D) Network analysis where node colours represent different parity levels.

4.5 Discussion

In this study the virome of bovine colostrum was investigated. We developed a colostrum-specific virome extraction protocol and employed viral metagenomics to explore the diversity, community structure, and ecological roles of viruses in Irish bovine colostrum. Additionally, we evaluated the influence of farm-level variables, including location, parity, and dry cow antibiotic treatment, on the composition of the colostrum virome. Our findings reveal that the colostrum virome is predominantly comprised of ssDNA viruses and dsDNA phages which have the potential to carry antibiotic resistance genes. Notably, we identified a significant impact of farm-level variables, particularly antibiotic dry cow treatment, on the composition of the virome.

The first objective of this study was to establish a specialised virome extraction protocol specifically designed for the analysis of bovine colostrum. Virome extraction protocols encompass several crucial steps to facilitate the characterisation and quantification of nucleic acids from uncultured viruses, irrespective of their environmental origin. These steps involve (i) acquiring and storing the samples, (ii) separating viral particles, (iii) extracting pure nucleic acids while eliminating free nucleic acids and contaminating cells and (iv) successfully sequencing and bioinformatic analysis of the nucleic acids (Callanan et al., 2021). Recent studies have reported optimised methods for virome extraction from dairy-based foods and agricultural samples, with sample solubilisation, enzymatic treatment and filtration being the most frequently adjusted steps (Mahony and van Sinderen, 2022). Nevertheless, extracting the virome from bovine milk samples presents specific challenges, particularly in effectively separating various residues (e.g., proteins, bacterial cells, and cell debris) before concentrating the viruses (Muhammed et al., 2017). These challenges are further amplified in the case of colostrum due to its unique composition and higher concentration of proteins and fat (McGrath et al., 2016). In this study, we employed a pH adjustment of approximately 4.6 to facilitate sample clarification, a method previously utilised in the investigation of cheese whey viromes (Muhammed et al., 2017). This pH adjustment proved effective in removing a significant portion of residues through low-speed centrifugation. To enhance sample filtration and eliminate fat, we incorporated glass fiber filters, which yielded notable improvements. Instead of using 0.2 μm filters, which may lead to a reduction in virus detection and potentially overlook giant viruses (Conceição-Neto et al., 2015, Hoyles

et al., 2014), we opted for a 0.45 μm filtration step. Furthermore, we refrained from utilising CsCl gradients for viral particle purification, as this labour-intensive technique is not well-suited for high-throughput studies and shows poor reproducibility (d'Humières et al., 2019). However, it has been reported that including a CsCl step can improve the size of viral contigs recovered in virome studies (d'Humières et al., 2019). Instead, our approach involved a combination of microfiltration, PEG-precipitation of viral particles, and DNase/RNase treatment to remove free nucleic acids. Library preparation techniques in virome studies exhibit significant variation and can influence the results. Initially, viromes were sequenced after undergoing multiple displacement amplification (MDA) to achieve the amount of DNA required for library preparation. Nevertheless, it became evident that MDA introduced a bias favouring small circular single-stranded DNA (ssDNA) viral genomes, typically ranging from approximately 2,000 to 7,000 nucleotides in length (Kim and Bae, 2011). Newer technologies, such as the adaptase technology (Swift Biosciences) which attaches special adaptors to each DNA fragment thereby minimising potential amplification biases, are available to overcome this problem and was selected for our study. However, this kit includes a sonication step, which has been reported by some groups to shear ssDNA more efficiently than dsDNA, therefore introducing another bias in virome sequencing (Petit et al., 2022). To overcome this problem, approaches such as the short MDA method consisting of reducing the incubation time of the standard MDA treatment and the use of the T7 DNA polymerase have been proposed recently (Petit et al., 2022).

The second primary objective of this study was to explore the diversity, community structure, and ecological functions of viral populations in Irish bovine colostrum using viral metagenomics. The virome extraction protocol employed in this study yielded an average of 3,794,343 (± 232,625) quality filtered reads, indicating successful recovery of high-quality data with minimal bacterial contamination. Furthermore, the ability of the protocol used in this study to recover almost all of the phage T4 spike-in genome suggests it would be suitable for metagenomic characterisation of large viruses. However, the relatively small final catalogue of 586 viral contigs and their short lengths, raises some concerns and suggests the need for exploring alternative bioinformatics pipelines for analysis of the dataset. While the tools used in this study are commonly employed in virome studies (Chitcharoen et al., 2022), the constantly

evolving field of bioinformatics offers a range of emerging tools and pipelines aimed at improving the analysis of viral sequences (Smith et al., 2022). For example, SPAdes meta has recently been identified as a top performer for accurate virome assembly (Sutton et al., 2019). It is important to consider these advancements and explore tailor-made pipelines for the analysis of viral sequences (Zhou et al., 2023, Ma, 2023). However, it must be noted that in similar studies to ours, similar amounts of contigs and contigs sizes were recovered (Dugat-Bony et al., 2020, Muhammed et al., 2017, Colombo et al., 2018).

Regarding the taxonomic composition of the samples in this study, we observed the presence of ten viral families and identified 48 genera. These findings align with the 33 viral families identified in bovine virome studies to date (Kwok et al., 2020). While studies in farm animals have not yet reported the total viral load in their samples, research on the human gut, known for its high viral density, has estimated viral loads to be around 10^{10} per gram of faeces (Shkoporov and Hill, 2019). However, these estimates are typically based on the initial spiked concentration of phages, such as *Lactococcus lactis* phage Q33, assuming the VLPs in the study have an average genome length of 31,100 bp. In our study, we had to assume the overall genome sizes of the viruses were equal to that of phage T4 (~168,000 bp). Notably, *Circovius*, *Prunevirus* and *Liefievirus* were the most abundant genera in our samples, with average genome sizes of 2,000 bp, 8,700 bp, and 42,000 bp, respectively. Considering these genome sizes, a spike-in phage with a smaller genome might have been better suited for accurate quantification of the total viral load.

Regarding core virome analysis, 69 VLPs dominated the total viral abundance present across all samples. These VLPs were primarily members of the families *Circoviridae*, *Papillomaviridae* and *Microviridae*. *Circovirus* are a genus of small, non-enveloped viruses belonging to the family *Circoviridae* (Rosario et al., 2017). They possess a circular, single-stranded DNA genome and have been shown to infect all types of farm animals (e.g., goats, cattle, pigs, and chickens) and farm workers (Li et al., 2010). Epidemiological studies have shown that porcine *Circovirus* type 3, which porcine dermatitis, nephropathy syndrome, multi systemic inflammation and reproductive failure to be highly prevalent in bovines (Wang et al., 2019). *Papillomaviruses*, including *Deltapapillomavirus*, *Xipapillomavirus* and *Xipapillomavirus* were highly abundant in the samples in this study. *Papillomaviruses* are a heterogeneous group of

small, non-enveloped, double-stranded DNA viruses containing approximately 8,000 bp distributed worldwide, are known to infect mesenchymal tissues and are considered to be highly pathogenic to bovines (Daudt et al., 2018). Indeed *Papillomavirus* lesions on the teats and nipples of dairy cows cause mastitis, low milk yield and teat deformities ultimately leading to significant economic losses (Kale et al., 2023). Furthermore, *Papillomavirus* infections typically serve as a foundation for secondary infections, which significantly raises the prevalence of the illnesses and their cost of care (Kale et al., 2023).

Interestingly, our analysis revealed that approximately 28% (164) of the VLPs identified in this study were classified as dsDNA phages. Further analysis revealed that these phages carried ARGs. Notably three specific ARGs (*kdpE*, *baeS*, *smeS*) were identified, which are known to confer resistance to antibiotics used in the UBRO and CEF groups in this study. *KdpE* is a transcriptional activator involved in the regulation of potassium transport and known for its role in pathogenic bacteria's virulence and intracellular survival (Freeman et al., 2013). *BaeS* is a sensor kinase in the BaeSR regulatory system which confer resistance to aminoglycoside and aminocoumarin antibiotics (Nishino et al., 2005). *smeS* is the protein kinase sensor component of a two component signal transduction system that includes *smeR* which confer resistance to antibiotics such as aminoglycoside, cephalosporin, cephamycin and penams (Li et al., 2002). We were also able to identify a number of host bacterial genera of these dsDNA phage VLPs including *Streptococcus*, *Bifidobacterium*, *Staphylococcus*, *Acinetobacter* and *Pseudomonas* which have all been identified as core bacterial genera in colostrum previously (Chen et al., 2021).

The third and final objective of this study was to evaluate the influence of farm-level variables, including location, parity, and dry cow antibiotic treatment, on the composition and characteristics of the colostrum virome. In our study, antibiotic treatments significantly impacted virome composition. The antibiotics used in this study were cephaguard (cefquinome – 4th generation cephalosporin) and Ubro red (Framycetin sulfate, Penethamate hydroiodide, and Procaine Penicillin). Cephaguard targets mastitis-causing organisms such as *Streptococcus* spp. and *Staphylococcus aureus*, while UBRO red targets a broader range of bacteria including *Staphylococcus* spp., *Streptococcus* spp., *Corynebacterium* spp., *Escherichia* spp., *Klebsiella*, and *Pseudomonas* spp. Cefquinome is classified as a category B (restricted use) antibiotic

by the European Medicine Agency, while caution is advised for the use of Framycetin (source: https://www.gov.ie/en/collection/45f45-antimicrobial-resistance amr/?referrer=http://www.agriculture.gov.ie/amr/). Numerous studies have investigated the impact of DCT on the microbial composition of colostrum, with conflicting results (Derakhshani et al., 2018, Vasquez et al., 2022). Therefore, investigating the composition of the virome and microbiome of colostrum concurrently would be an interesting future study with our sample set.

While there were a number of limitations to this study, the findings reported herein inform a number of potential future studies. Firstly, we used short-read sequencing as it is commonly used in virome studies (Paez-Espino et al., 2016). However, this method is not without limitations. For instance, viruses which contain genomic islands and/or have high micro-diversity can cause genome fragmentation during assembly (Roux et al., 2017). Long-read sequencing technologies, such as Pacific Biosciences (PacBio) and Oxford Nanopore Technologies (ONT) offer solutions to such issues. The longer reads are potentially able to span the length of entire viral genomes, overcoming assembly issues resulting from repeat regions and low coverage (Olson et al., 2019). More recently, a Long-Read Linker-Amplified Shotgun Library (LASL) approach was developed that combines LASL library preparation with ONT MinION sequencing and has been found to recover more high-quality viral genomes than long or short-reads alone (Warwick-Dugdale et al., 2019, Cook et al., 2021). Such approaches could be applied to our extracted DNA to increase the number of VLPs for downstream analysis. The presence of viruses in our samples, particularly those capable of infecting both bovines and humans, has significant implications for calf health, farm hygiene, and the potential development of food products using colostrum. It is crucial to determine the environmental sources of these viruses by sampling the calving environment. For example, the frequent detection of *Liefievirus*, a plant pathogen, raises questions about its origin. Could it be originating from the bedding environment or even food sources like silage? Therefore, applying our approach to optimising virome extraction from other farm samples would be valuable in identifying the locations where viruses reside in the farm environment. This is particularly intriguing considering that we also identified phages carrying antibiotic resistance genes in the environment. Investigating the prevalence and distribution of these phages can provide further insights into the potential dissemination of antibiotic

resistance in the farm setting. Additionally, the lack of longitudinal design prevented the tracking of changes in the virome over time, which is important for understanding how it develops and responds to various environmental factors.

4.6 Acknowledgements

We would like to extend our thanks to the farmers who assisted with the sample collections. We thank Dr. Lorraine Draper for advice and support with regards nucleic acid extractions and library preparation. We thank Professor Colin Hill and Ms. Lisa Smith for support in bioinformatics analysis.

4.7 Financial Support

Science Foundation Ireland funding to APC Microbiome Ireland and Vistamilk. DAFM funding of Project 2022IRLNZ114, entitled RUmen microbiome MINING for bacterial cultures to reduce methane.

4.8 Ethics

None required/ Not applicable

4.9 Conflict of Interest

None declared

4.10 References

ABDELSATTAR, M. M., RASHWAN, A. K., YOUNES, H. A., ABDEL-HAMID, M., ROMEIH, E., MEHANNI, A.-H. E., VARGAS-BELLO-PÉREZ, E., CHEN, W. & ZHANG, N. 2022. An updated and comprehensive review on the composition and preservation strategies of bovine colostrum and its contributions to animal health. Animal Feed Science and Technology, 115379.

ADKINS, P. R. F. & MIDDLETON, J. R. 2017. Laboratory handbook on bovine mastitis, National Mastitis Council, Incorporated.

AITCHISON, J., BARCELÓ-VIDAL, C., MARTÍN-FERNÁNDEZ, J. A. & PAWLOWSKY-GLAHN, V. 2000. Logratio analysis and compositional distance. Mathematical geology, 32, 271-275.

ALBERY, G. F., BECKER, D. J., BRIERLEY, L., BROOK, C. E., CHRISTOFFERSON, R. C., COHEN, L. E., DALLAS, T. A., ESKEW, E. A., FAGRE, A., FARRELL, M. J., GLENNON, E., GUTH, S., JOSEPH, M. B., MOLLENTZE, N., NEELY, B. A., POISOT, T., RASMUSSEN, A. L., RYAN, S. J., SEIFERT, S., SJODIN, A. R., SORRELL, E. M. & CARLSON, C. J. 2021. The science of the host–virus network. Nature Microbiology, 6, 1483-1492.

ALTSCHUL, S. F., GISH, W., MILLER, W., MYERS, E. W. & LIPMAN, D. J. 1990. Basic local alignment search tool. Journal of molecular biology, 215, 403-410.

BARR, J. J. 2019. Precision Engineers: Bacteriophages Modulate the Gut Microbiome and Metabolome. Cell Host & Microbe, 25, 771-773.

BI, L., YU, D.-T., HAN, L.-L., DU, S., YUAN, C.-Y., HE, J.-Z. & HU, H.-W. 2022. Unravelling the ecological complexity of soil viromes: Challenges and opportunities. Science of The Total Environment, 812, 152217.

BLAND, C., RAMSEY, T. L., SABREE, F., LOWE, M., BROWN, K., KYRPIDES, N. C. & HUGENHOLTZ, P. 2007. CRISPR recognition tool (CRT): a tool for automatic detection of clustered regularly interspaced palindromic repeats. BMC bioinformatics, 8, 1-8.

BOKULICH, N. A., CHUNG, J., BATTAGLIA, T., HENDERSON, N., JAY, M., LI, H., D. LIEBER, A., WU, F., PEREZ-PEREZ, G. I. & CHEN, Y. 2016. Antibiotics, birth mode, and diet shape microbiome maturation during early life. Science translational medicine, 8, 343ra82-343ra82.

CALLANAN, J., STOCKDALE, S. R., SHKOPOROV, A., DRAPER, L. A., ROSS, R. P. & HILL, C. 2020. Expansion of known ssRNA phage genomes: from tens to over a thousand. Science advances, 6, eaay5981.

CALLANAN, J., STOCKDALE, S. R., SHKOPOROV, A., DRAPER, L. A., ROSS, R. P. & HILL, C. 2021. Biases in viral metagenomics-based detection, cataloguing and quantification of bacteriophage genomes in human faeces, a review. Microorganisms, 9, 524.

CAMPBELL, D. E., LY, L. K., RIDLON, J. M., HSIAO, A., WHITAKER, R. J. & DEGNAN, P. H. 2020. Infection with bacteroides phage BV01 alters the host transcriptome and bile acid metabolism in a common human gut microbe. Cell reports, 32.

CARLSON, C. J., ZIPFEL, C. M., GARNIER, R. & BANSAL, S. 2019. Global estimates of mammalian viral diversity accounting for host sharing. Nature Ecology & Evolution, 3, 1070-1075.

CARLSON COLIN, J., GIBB RORY, J., ALBERY GREGORY, F., BRIERLEY, L., CONNOR RYAN, P., DALLAS TAD, A., ESKEW EVAN, A., FAGRE ANNA, C., FARRELL MAXWELL, J., FRANK HANNAH, K., MUYLAERT RENATA, L., POISOT, T., RASMUSSEN ANGELA, L., RYAN SADIE, J. & SEIFERT STEPHANIE, N. 2022. The Global Virome in One Network (VIRION): an Atlas of Vertebrate-Virus Associations. mBio, 13, e02985-21.

CASTRO-MEJÍA, J. L., MUHAMMED, M. K., KOT, W., NEVE, H., FRANZ, C. M. A. P., HANSEN, L. H., VOGENSEN, F. K. & NIELSEN, D. S. 2015. Optimizing protocols for extraction of bacteriophages prior to metagenomic analyses of phage communities in the human gut. Microbiome, 3, 64.

CHEN, B., TANG, G., GUO, W., LEI, J., YAO, J. & XU, X. 2021. Detection of the Core bacteria in colostrum and their association with the rectal microbiota and with Milk composition in two dairy cow farms. Animals, 11, 3363.

CHITCHAROEN, S., SIVAPORNNUKUL, P. & PAYUNGPORN, S. 2022. Revolutionised virome research using systems microbiology approaches. Experimental Biology and Medicine, 247, 1135-1147.

COLOMBO, S., ARIOLI, S., GARGARI, G., NERI, E., DELLA SCALA, G. & MORA, D. 2018. Characterization of airborne viromes in cheese production plants. Journal of applied microbiology, 125, 1444-1454.

CONCEIÇÃO-NETO, N., ZELLER, M., LEFRÈRE, H., DE BRUYN, P., BELLER, L., DEBOUTTE, W., YINDA, C. K., LAVIGNE, R., MAES, P. & VAN RANST, M. 2015. Modular approach to customise sample preparation procedures for viral metagenomics: a reproducible protocol for virome analysis. Scientific reports, 5, 1-14.

COOK, R., HOOTON, S., TRIVEDI, U., KING, L., DODD, C. E. R., HOBMAN, J. L., STEKEL, D. J., JONES, M. A. & MILLARD, A. D. 2021. Hybrid assembly of an agricultural slurry virome reveals a diverse and stable community with the potential to alter the metabolism and virulence of veterinary pathogens. Microbiome, 9, 1-17.

D'HUMIÈRES, C., TOUCHON, M., DION, S., CURY, J., GHOZLANE, A., GARCIA-GARCERA, M., BOUCHIER, C., MA, L., DENAMUR, E. & PC ROCHA, E. 2019. A simple, reproducible and cost-effective procedure to analyse gut phageome: from phage isolation to bioinformatic approach. Scientific Reports, 9, 11331.

DAUDT, C., DA SILVA, F. R. C., LUNARDI, M., ALVES, C., WEBER, M. N., CIBULSKI, S. P., ALFIERI, A. F., ALFIERI, A. A. & CANAL, C. W. 2018. Papillomaviruses in ruminants: An update. Transbound Emerg Dis, 65, 1381-1395.

DERAKHSHANI, H., PLAIZIER, J. C., DE BUCK, J., BARKEMA, H. W. & KHAFIPOUR, E. 2018. Association of bovine major histocompatibility complex (BoLA) gene polymorphism with colostrum and milk microbiota of dairy cows during the first week of lactation. Microbiome, 6, 203.

DUGAT-BONY, E., LOSSOUARN, J., DE PAEPE, M., SARTHOU, A.-S., FEDALA, Y., PETIT, M.-A. & CHAILLOU, S. 2020. Viral metagenomic analysis of the cheese surface: A comparative study of rapid procedures for extracting viral particles. Food microbiology, 85, 103278.

ELBEHERY, A. H. A. & DENG, L. 2022. Insights into the global freshwater virome. Front Microbiol, 13, 953500.

FITZGERALD, C. B., SHKOPOROV, A. N., UPADRASTA, A., KHOKHLOVA, E. V., ROSS, R. P. & HILL, C. 2021. Probing the "Dark Matter" of the human gut phageome: culture assisted metagenomics enables rapid discovery and host-linking for novel bacteriophages. Frontiers in cellular and infection microbiology, 11, 616918.

FREEMAN, Z. N., DORUS, S. & WATERFIELD, N. R. 2013. The KdpD/KdpE two-component system: integrating K^+ homeostasis and virulence. PLoS Pathog, 9, e1003201.

GALLARDO, M. C., REOYO, A. D. L. T., FERNÁNDEZ-PINERO, J., IGLESIAS, I., MUÑOZ, M. J. & ARIAS, M. L. 2015. African swine fever: a global view of the current challenge. Porcine Health Management, 1, 1-14.

GOEDE, D. & MORRISON, R. B. 2016. Production impact & time to stability in sow herds infected with porcine epidemic diarrhea virus (PEDV). Preventive veterinary medicine, 123, 202-207.

GRANT, J. R., ENNS, E., MARINIER, E., MANDAL, A., HERMAN, E. K., CHEN, C.-Y., GRAHAM, M., VAN DOMSELAAR, G. & STOTHARD, P. 2023. Proksee: in-depth characterization and visualization of bacterial genomes. Nucleic Acids Research, gkad326.

GRAZZIOTIN, A. L., KOONIN, E. V. & KRISTENSEN, D. M. 2016. Prokaryotic Virus Orthologous Groups (pVOGs): a resource for comparative genomics and protein family annotation. Nucleic acids research, gkw975.

HARVEY, E. & HOLMES, E. C. 2022. Diversity and evolution of the animal virome. Nature Reviews Microbiology, 20, 321-334.

HAZARDS, E. P. O. B., RICCI, A., ALLENDE, A., BOLTON, D., CHEMALY, M., DAVIES, R., FERNÁNDEZ ESCÁMEZ, P. S., GIRONES, R., KOUTSOUMANIS, K. & LINDQVIST, R. 2017. Risk for the development of Antimicrobial Resistance (AMR) due to feeding of calves with milk containing residues of antibiotics. Efsa Journal, 15, e04665.

HOYLES, L., MCCARTNEY, A. L., NEVE, H., GIBSON, G. R., SANDERSON, J. D., HELLER, K. J. & VAN SINDEREN, D. 2014. Characterization of virus-like particles associated with the human faecal and caecal microbiota. Research in microbiology, 165, 803-812.

HSIEH, T. C., MA, K. H. & CHAO, A. 2016. iNEXT: an R package for rarefaction and extrapolation of species diversity (H ill numbers). Methods in Ecology and Evolution, 7, 1451-1456.

HUMAN MICROBIOME JUMPSTART REFERENCE STRAINS, C., NELSON, K. E., WEINSTOCK, G. M., HIGHLANDER, S. K., WORLEY, K. C., CREASY, H. H., WORTMAN, J. R., RUSCH, D. B., MITREVA, M. & SODERGREN, E. 2010. A catalog of reference genomes from the human microbiome. Science, 328, 994-999.

JURASZ, H., PAWŁOWSKI, T. & PERLEJEWSKI, K. 2021. Contamination issue in viral metagenomics: problems, solutions, and clinical perspectives. Frontiers in Microbiology, 12, 745076.

KALE, M., YıLDıRıM, Y., ÖZMEN, Ö., ÇAĞıRGAN, A. A., SÖKEL, S., USTA, A., KÜÇÜK, A. & ORTA, Y. S. 2023. Diagnosis and phylogenetic analysis of bovine papillomaviruses in cattle papillomatosis cases by different methods. Tropical Animal Health and Production, 55, 191.

KASZAB, E., DOSZPOLY, A., LANAVE, G., VERMA, A., BÁNYAI, K., MALIK, Y. S. & MARTON, S. 2020. Chapter 2 - Metagenomics revealing new virus species in farm and pet animals and aquaculture. In: MALIK, Y. S., BARH, D., AZEVEDO, V. & KHURANA, S. M. P. (eds.) Genomics and Biotechnological Advances in Veterinary, Poultry, and Fisheries. Academic Press.

KAWASAKI, J., TOMONAGA, K. & HORIE, M. 2023. Large-scale investigation of zoonotic viruses in the era of high-throughput sequencing. Microbiology and Immunology, 67, 1-13.

KIM, K.-H. & BAE, J.-W. 2011. Amplification methods bias metagenomic libraries of uncultured single-stranded and double-stranded DNA viruses. Applied and environmental microbiology, 77, 7663-7668.

KROPINSKI, A. M., MAZZOCCO, A., WADDELL, T. E., LINGOHR, E. & JOHNSON, R. P. 2009. Enumeration of bacteriophages by double agar overlay plaque assay. Bacteriophages: methods and protocols, volume 1: isolation, characterization, and interactions, 69-76.

KWOK, K. T. T., NIEUWENHUIJSE, D. F., PHAN, M. V. T. & KOOPMANS, M. P. G. 2020. Virus metagenomics in farm animals: a systematic review. Viruses, 12, 107.

LI, L., KAPOOR, A., SLIKAS, B., BAMIDELE, O. S., WANG, C., SHAUKAT, S., MASROOR, M. A., WILSON, M. L., NDJANGO, J.-B. N. & PEETERS, M. 2010. Multiple diverse circoviruses infect farm animals and are commonly found in human and chimpanzee feces. Journal of virology, 84, 1674-1682.

LI, X. Z., ZHANG, L. & POOLE, K. 2002. SmeC, an outer membrane multidrug efflux protein of Stenotrophomonas maltophilia. Antimicrob Agents Chemother, 46, 333-43.

LIMA, S. F., TEIXEIRA, A. G. V., LIMA, F. S., GANDA, E. K., HIGGINS, C. H., OIKONOMOU, G. & BICALHO, R. C. 2017. The bovine colostrum microbiome and its association with clinical mastitis. Journal of dairy science, 100, 3031-3042.

LINEHAN, K., ROSS, R. P. & STANTON, C. 2023. Bovine Colostrum for Veterinary and Human Health Applications: A Critical Review. Annual Review of Food Science and Technology, 14, 387-410.

LIU, J., TAFT, D. H., MALDONADO-GOMEZ, M. X., JOHNSON, D., TREIBER, M. L., LEMAY, D. G., DEPETERS, E. J. & MILLS, D. A. 2019. The fecal resistome of dairy cattle is associated with diet during nursing. Nature communications, 10, 4406.

LUBBE, S., FILZMOSER, P. & TEMPL, M. 2021. Comparison of zero replacement strategies for compositional data with large numbers of zeros. Chemometrics and Intelligent Laboratory Systems, 210, 104248.

MA, Z. 2023. Virome comparison (VC): A novel approach to comparing viromes based on virus species specificity and virome specificity diversity. Journal of Medical Virology, 95, e28682.

MAHONY, J. & VAN SINDEREN, D. 2022. Virome studies of food production systems: time for 'farm to fork' analyses. Current Opinion in Biotechnology, 73, 22-27.

MALLICK, H., RAHNAVARD, A., MCIVER, L. J., MA, S., ZHANG, Y., NGUYEN, L. H., TICKLE, T. L., WEINGART, G., REN, B. & SCHWAGER, E. H. 2021. Multivariable association discovery in population-scale meta-omics studies. PLoS computational biology, 17, e1009442.

MCARTHUR, A. G., WAGLECHNER, N., NIZAM, F., YAN, A., AZAD, M. A., BAYLAY, A. J., BHULLAR, K., CANOVA, M. J., DE PASCALE, G. & EJIM, L. 2013. The comprehensive antibiotic resistance database. Antimicrobial agents and chemotherapy, 57, 3348-3357.

MCGRATH, B. A., FOX, P. F., MCSWEENEY, P. L. H. & KELLY, A. L. 2016. Composition and properties of bovine colostrum: a review. Dairy Science & Technology, 96, 133-158.

MIRANDA, C., IGREJAS, G. & POETA, P. 2023. Bovine Colostrum: Human and Animal Health Benefits or Route Transmission of Antibiotic Resistance—One Health Perspective. Antibiotics [Online], 12.

MUHAMMED, M. K., KOT, W., NEVE, H., MAHONY, J., CASTRO-MEJÍA, J. L., KRYCH, L., HANSEN, L. H., NIELSEN, D. S., SØRENSEN, S. J. & HELLER, K. J. 2017. Metagenomic analysis of dairy bacteriophages: Extraction method and pilot study on whey samples derived from using undefined and defined mesophilic starter cultures. Appl. Environ. Microbiol., 83, e00888-17.

MUSHEGIAN, A. R. 2020. Are There 1031 Virus Particles on Earth, or More, or Fewer? Journal of Bacteriology, 202, 10.1128/jb.00052-20.

NISHIMURA, Y., YOSHIDA, T., KURONISHI, M., UEHARA, H., OGATA, H. & GOTO, S. 2017. ViPTree: the viral proteomic tree server. Bioinformatics, 33, 2379-2380.

NISHINO, K., HONDA, T. & YAMAGUCHI, A. 2005. Genome-wide analyses of Escherichia coli gene expression responsive to the BaeSR two-component regulatory system. J Bacteriol, 187, 1763-72.

O'LEARY, N. A., WRIGHT, M. W., BRISTER, J. R., CIUFO, S., HADDAD, D., MCVEIGH, R., RAJPUT, B., ROBBERTSE, B., SMITH-WHITE, B., AKO-ADJEI, D., ASTASHYN, A., BADRETDIN, A., BAO, Y., BLINKOVA, O., BROVER, V., CHETVERNIN, V., CHOI, J., COX, E., ERMOLAEVA, O., FARRELL, C. M., GOLDFARB, T., GUPTA, T., HAFT, D., HATCHER, E., HLAVINA, W., JOARDAR, V. S., KODALI, V. K., LI, W., MAGLOTT, D., MASTERSON, P., MCGARVEY, K. M., MURPHY, M. R., O'NEILL, K., PUJAR, S., RANGWALA, S. H., RAUSCH, D., RIDDICK, L. D., SCHOCH, C., SHKEDA, A., STORZ, S. S., SUN, H., THIBAUD-NISSEN, F., TOLSTOY, I., TULLY, R. E., VATSAN, A. R., WALLIN, C., WEBB, D., WU, W., LANDRUM, M. J., KIMCHI, A., TATUSOVA, T., DICUCCIO, M., KITTS, P., MURPHY, T. D. & PRUITT, K. D. 2016. Reference sequence (RefSeq) database at NCBI: current status, taxonomic expansion, and functional annotation. Nucleic Acids Res, 44, D733-45.

OLSON, N. D., TREANGEN, T. J., HILL, C. M., CEPEDA-ESPINOZA, V., GHURYE, J., KOREN, S. & POP, M. 2019. Metagenomic assembly through the lens of validation: recent advances in assessing and improving the quality of genomes assembled from metagenomes. Briefings in bioinformatics, 20, 1140-1150.

PAEZ-ESPINO, D., ELOE-FADROSH, E. A., PAVLOPOULOS, G. A., THOMAS, A. D., HUNTEMANN, M., MIKHAILOVA, N., RUBIN, E., IVANOVA, N. N. & KYRPIDES, N. C. 2016. Uncovering Earth's virome. Nature, 536, 425-430.

PARGIN, E., ROACH, M. J., SKYE, A., PAPUDESHI, B., INGLIS, L. K., MALLAWAARACHCHI, V., GRIGSON, S. R., HARKER, C., EDWARDS, R. A. & GILES, S. K. 2023. The human gut virome: composition, colonization, interactions, and impacts on human health. Frontiers in Microbiology, 14, 963173.

PARK, J. & KIM, E. B. 2020. Differences in microbiome and virome between cattle and horses in the same farm. Asian-Australasian Journal of Animal Sciences, 33, 1042-1055.

PETIT, M.-A., BILLAUD, M., THEODOROU, I., SHAH, S. A., DE SORDI, L. & DE PAEPE, M. 2022. An alternative method to multiple displacement amplification for preparing virome DNA in a way adapted for the sequencing of both double-strand and single-strand DNA viruses. bioRxiv, 2022-12.

RAJU, R. S., AL NAHID, A., CHONDROW DEV, P. & ISLAM, R. 2022. VirusTaxo: Taxonomic classification of viruses from the genome sequence using k-mer enrichment. Genomics, 114, 110414.

ROSARIO, K., BREITBART, M., HARRACH, B., SEGALÉS, J., DELWART, E., BIAGINI, P. & VARSANI, A. 2017. Revisiting the taxonomy of the family Circoviridae: establishment of the genus Cyclovirus and removal of the genus Gyrovirus. Archives of Virology, 162, 1447-1463.

ROUX, S., EMERSON, J. B., ELOE-FADROSH, E. A. & SULLIVAN, M. B. 2017. Benchmarking viromics: an in silico evaluation of metagenome-enabled estimates of viral community composition and diversity. PeerJ, 5, e3817.

RUEGG, P. L. 2022. The bovine milk microbiome–an evolving Science. Domestic Animal Endocrinology, 79, 106708.

SANTIAGO-RODRIGUEZ, T. M. & HOLLISTER, E. B. 2022. Unraveling the viral dark matter through viral metagenomics. Frontiers in Immunology, 13, 1005107.

SCHNEIDER, C. L. 2021. Bacteriophage-Mediated Horizontal Gene Transfer: Transduction. In: HARPER, D. R., ABEDON, S. T., BURROWES, B. H. & MCCONVILLE, M. L. (eds.) Bacteriophages: Biology, Technology, Therapy. Cham: Springer International Publishing.

SHKOPOROV, A. N. & HILL, C. 2019. Bacteriophages of the human gut: the "known unknown" of the microbiome. Cell host & microbe, 25, 195-209.

SHKOPOROV, A. N., RYAN, F. J., DRAPER, L. A., FORDE, A., STOCKDALE, S. R., DALY, K. M., MCDONNELL, S. A., NOLAN, J. A., SUTTON, T. D. S. & DALMASSO, M. 2018. Reproducible protocols for metagenomic analysis of human faecal phageomes. Microbiome, 6, 68.

SMITH, S. E., HUANG, W., TIAMANI, K., UNTERER, M., KHAN MIRZAEI, M. & DENG, L. 2022. Emerging technologies in the study of the virome. Current Opinion in Virology, 54, 101231.

SUH, G. A., LODISE, T. P., TAMMA, P. D., KNISELY, J. M., ALEXANDER, J., ASLAM, S., BARTON, K. D., BIZZELL, E., TOTTEN, K. M. C. & CAMPBELL, J. L. 2022. Considerations for the use of phage therapy in clinical practice. Antimicrobial agents and chemotherapy, 66, e02071-21.

THAMES, C. H., PRUDEN, A., JAMES, R. E., RAY, P. P. & KNOWLTON, K. F. 2012. Excretion of antibiotic resistance genes by dairy calves fed milk replacers with varying doses of antibiotics. Frontiers in microbiology, 3, 139.

THURBER, R. V., HAYNES, M., BREITBART, M., WEGLEY, L. & ROHWER, F. 2009. Laboratory procedures to generate viral metagenomes. Nature protocols, 4, 470-483.

VAN HESE, I., GOOSSENS, K., AMPE, B., HAEGEMAN, A. & OPSOMER, G. 2022. Exploring the microbial composition of Holstein Friesian and Belgian Blue colostrum in relation to the transfer of passive immunity. Journal of Dairy Science, 105, 7623-7641.

VASQUEZ, A., NYDAM, D., FODITSCH, C., WARNICK, L., WOLFE, C., DOSTER, E. & MORLEY, P. S. 2022. Characterization and comparison of the microbiomes and resistomes of colostrum from selectively treated dry cows. Journal of Dairy Science, 105, 637-653.

WANG, W., SUN, W., CAO, L., ZHENG, M., ZHU, Y., LI, W., LIU, C., ZHUANG, X., XING, J. & LU, H. 2019. An epidemiological investigation of porcine circovirus 3 infection in cattle in Shandong province, China. BMC veterinary research, 15, 1-8.

WARWICK-DUGDALE, J., SOLONENKO, N., MOORE, K., CHITTICK, L., GREGORY, A. C., ALLEN, M. J., SULLIVAN, M. B. & TEMPERTON, B. 2019. Long-read viral metagenomics captures abundant and microdiverse viral populations and their niche-defining genomic islands. PeerJ, 7, e6800.

ZHENG, D., LIWINSKI, T. & ELINAV, E. 2020. Interaction between microbiota and immunity in health and disease. Cell Research, 30, 492-506.

ZHOU, Z., MARTIN, C., KOSMOPOULOS, J. C. & ANANTHARAMAN, K. 2023. ViWrap: A modular pipeline to identify, bin, classify, and predict viral–host relationships for viruses from metagenomes. iMeta, e118.

4.11 Supplementary material

Supplementary Figures:

Figure S4.1 | (A) Relative abundance of the 48 genera identified using VirusTaxo (B) Absolute abundance of the 48 genera identified.

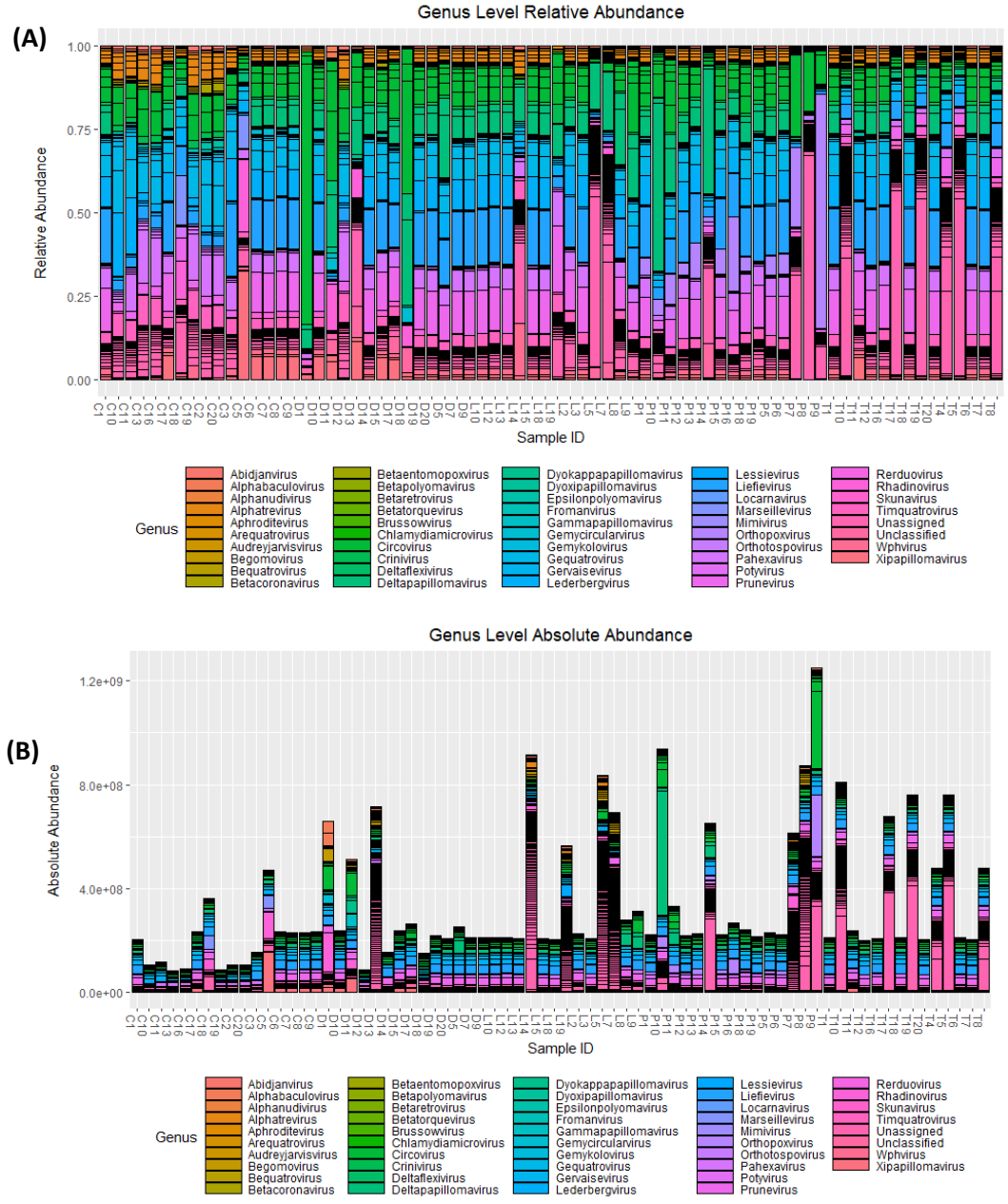

Figure S4.2 | (A) Genus level abundance of the 48 genera identified. (B) Absolute abundance of the 48 genera identified.

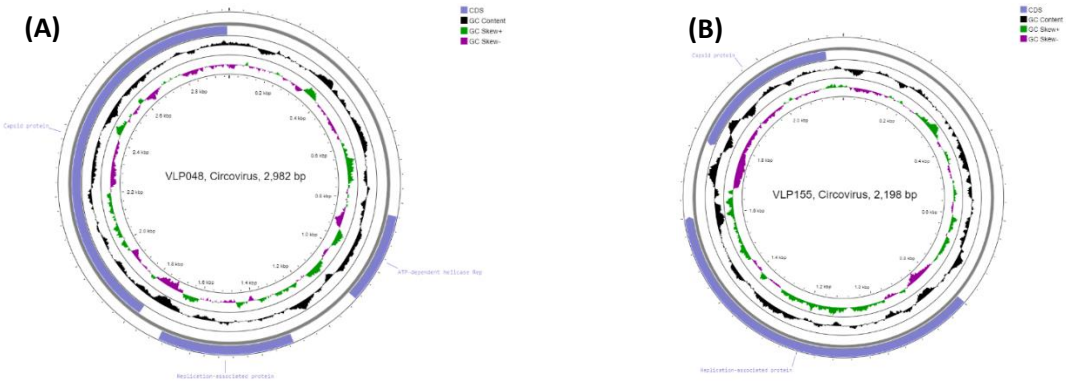

Figure S4.3 | (A) Circular genome map of VLP048 (B) Circular genome map of VLP155.

Supplementary Tables:

Table S4.1 | Table showing amount of reads in raw samples, post quality control (QC) and levels of bacterial contamination per sample.

	Total no. of reads		**Bacterial contamination**
Sample ID	Raw	Post QC	% of reads mapped to 16S rRNA
C10	4119866	2227625	0.28
C11	4489885	2149889	0.29
C13	12363	6260	0.1
C16	3523930	1946177	0.12
C17	5711014	2241080	0.19
C18	5839289	4709015	0.21
C19	4648707	1793375	0.34
C1	4003032	1614294	0.21
C20	2647144	938963	0.28
C2	2942847	989948	0.23
C3	6361550	2582551	0.4
C5	1501963	1291332	9.78
C6	4372807	3900751	6.66
C7	3059437	2780600	11.17
C8	3102275	2795797	2.77
C9	12576786	8811517	0.2
D10	5521233	5002932	2.21

D11	4339849	3952583	0.93
D12	67691	39414	0.88
D13	8225154	7685813	0.15
D14	3612068	2177971	7.06
D15	3737450	3406352	0.63
D17	3876787	3618611	0.74
D18	2261029	1624717	0.18
D19	32034	19626	1.05
D1	6066931	5612399	0.37
D20	223386	190813	5.19
D5	17169283	15988450	0.34
D7	8652296	8048881	1.19
D9	3280656	3074010	0.3
L10	6877166	6363628	0.53
L12	1539219	1396891	0.73
P14	5371381	4802340	1.19
L14	5821355	5401378	1.19
L15	4195209	3762070	0.41
L18	3597515	3349594	0.61
L19	6004657	5646837	0.8
L2	3206991	2338948	3.98
L3	4084783	3403068	4.6
L5	3956566	3571583	4.34
L7	2899934	2087919	5.3
L8	3921445	3021673	4.81
L9	4454975	3933829	4.47
P10	4197667	3689624	4.35
P11	3585062	3271000	2.66
P12	3208898	2785448	3.2
P13	13532718	12766778	0.36
L13	9329583	8727178	0.82
P15	3028804	2167390	8.61
P16	5934255	4547460	0.23
P18	5308581	4919510	0.53
P19	3842762	3154056	2.82
P1	3437375	2958163	2.11
P5	9444322	8396490	0.69
P6	8414148	7898433	0.47
P7	7247326	1686274	0.34
P8	3174489	2430889	6.98
P9	2153307	1650316	5.33
T10	2586027	2179305	7.66
T11	3901974	3596183	4.27
T12	8806708	8241602	0.56
T16	8238101	7681489	0.26

T17	3289502	2997059	0.97
T18	2569239	1952842	11.11
T19	3360921	2829222	2.02
T1	729017	597943	9.17
T20	4350889	3992299	0.38
T4	6724960	6288722	0.45
T5	2415240	2131280	3.08
T6	3455304	2832191	6.94
T7	4621486	4209880	2.16
T8	5571318	3689738	5.32

Table S4.2 | Table showing the 16 VLPs which were shared across all samples in this study and the characteristics of the hosts they infect.

VLP Name & Viral Genus	**Host Characteristics**
VLP005-*Prunevirus*	Plants
VLP006-*Liefievirus*	Mycobacteria
VLP011-*Deltapapillomavirus*	Ruminants
VLP036-*Xipapillomavirus*	Bovines
VLP048-*Circovirus*	Birds and mammals
VLP056-Unassigned	N/A
VLP074-*Lederbergvirus*	Bacteria
VLP115-*Deltapapillomavirus*	Ruminants
VLP133-Unassigned	N/A
VLP149-*Dyokappapapillomavirus*	Ruminants
VLP155-*Circovirus*	Birds and mammals
VLP161-*Rhadinovirus*	Humans, mammals
VLP180-*Gemycircularvirus*	Humans, mammals, birds
VLP196-*Alphabaculovirus*	Winged insects
VLP200-*Begomovirus*	Plants
VLP207-*Circovirus*	Birds and mammals

Chapter 5

5 Isolation, characterisation and efficacy of two novel temperate bacteriophages against bovine and human pathogenic *Staphylococcus aureus* isolates

5.1 Abstract

Staphylococcus aureus, known to coexist harmlessly as a commensal bacterium, can transform into a formidable pathogen capable of causing severe and life-threatening infections. The challenge of treating *S. aureus* infections has been exacerbated by the global antimicrobial resistance (AMR) crisis. Therefore, interest in exploring alternative therapeutic approaches has grown significantly. Among these approaches, bacteriophage (phage) therapy has emerged as one of the most promising avenues. The isolation of phages from bovine colostrum and human breast milk has not been explored previously. Therefore, the objective of this study was to isolate and evaluate the therapeutic applicability of *S. aureus* phages from bovine colostrum and human breast milk. In this study, vB_SauS_HM1 and vB_SauS_BC1 were isolated. *In vitro* analysis revealed that these phages have a number of favourable therapeutic characteristics, including broad host ranges, species specificity and lytic activity in milk enabling their potential use for future therapeutic applications against *S. aureus* infections. Furthermore, either individually or applied as a cocktail, they displayed the ability to reduce the bacterial growth of *S. aureus* in pasteurised, raw and mastitic milk samples. Bioinformatics analysis showed that these phages belong to subfamily *Azeredovirinae* and genus *Phietavirus.* As temperate phages are not recommended for phage therapy, future studies will explore genetic engineering techniques to make these phages applicable for clinical use.

5.2 Introduction

Staphylococcus aureus (*S. aureus*) is a gram-positive, commensal bacterium commonly inhabiting the skin and mucous membranes of animals and humans (Parlet et al., 2019). *S. aureus* can also cause illnesses ranging from minor skin infections to life-threatening diseases such as mastitis, sepsis, pneumonia and toxic shock syndrome (Cheung et al., 2021). This versatility in virulence is facilitated by the remarkable genomic plasticity of *S. aureus*, which allows for rearrangements driven by mobile genetic elements such as plasmids, pathogenicity islands, insertion sequences, transposons, and temperate phages (Atshan et al., 2023). The current global antimicrobial resistance (AMR) crisis has led to the emergence of multidrug resistant (MDR) *S. aureus* strains, exponentially increasing the difficulty of preventing and controlling *S. aureus* infections (Guo et al., 2020). The public health threat of MDR *S. aureus* strains has been underlined by the World Health Organisation (WHO), which placed methicillin-resistant *S. aureus* (MRSA) and vancomycin-resistant *S. aureus* (VRSA) on their global high-priority list of pathogens for which new antimicrobial development is urgently needed (Shrivastava et al., 2018). The escalating AMR crisis has spurred research into alternative therapeutics, with one of the most promising avenues being bacteriophage therapy (Hill et al., 2018, Hitchcock et al., 2023). Bacteriophages, or phages, are viruses which exclusively infect and replicate within bacterial cells. Phages offer several advantages over antibiotic prophylaxis, including lower discovery and production costs, a narrow spectrum of activity which preserves the host's normal microbiota and the ability to multiply at the site of infection (Ling et al., 2022). Furthermore, combining phages and antibiotics, referred to as phage-antibiotic synergy (PAS), has gained significant traction as an effective treatment against antibiotic resistant bacterial infections, including MRSA (Kebriaei et al., 2023, Simon et al., 2021).

Based on their lifecycle, phages are differentiated into lytic phages and temperate phages. Lytic phage reproduction invariably results in host cell death through cell lysis, facilitated by their endolysin enzyme. Temperate phage reproduction involves integration into the host genome and replication along with the host. This integration renders a bacterium and temperate phage as a lysogen and a prophage, respectively. Prophages can exit lysogeny, typically when the bacterium is in a condition of stress,

to begin their replication, lysis and release similar to lytic phages. Lytic phages were previously advised for phage therapy, primarily due to the potential of temperate phages to facilitate the horizontal transfer of antibiotic resistance and virulence genes (Borodovich et al., 2022, Strathdee et al., 2023). However, recent advancements in genetic engineering have rendered temperate phages as viable candidates for therapeutic applications (Hussain et al., 2023, Zhou et al., 2023, Oromí-Bosch et al., 2023). Techniques including CRISPR-Cas genome editing (Balcha and Neja, 2023), bacteriophage recombineering of electroporated DNA (BRED) (Payaslian et al., 2021), yeast-based platforms (Pires et al., 2021) and homologous recombination (Kilcher and Loessner, 2019) have been explored. Furthermore, temperate phages can be engineered to exhibit obligatorily lytic behaviour. This is especially encouraging for infections caused by bacterial species where lytic phages are scarce, such as *Clostridioides difficile* (Raeisi et al., 2023) and *Mycobacterium abscessus* (Dedrick et al., 2023). Utilising the CRISPR-Cas system, temperate phages can be manipulated to reduce the potential for horizontal transfer of antibiotic genes and re-sensitize bacteria to antibiotics (Khambhati et al., 2023, Gordillo Altamirano et al., 2021). In addition, temperate phages can be utilised as carriers for therapeutic RNAs, targeted drug delivery, gene therapy, and vaccines (Monteiro et al., 2019). Finally, endolysins derived from temperate phages can be produced recombinantly and utilised as effective antimicrobial and anti-biofilm agents (Lee et al., 2022).

S. aureus is one of the primary etiological agents of bovine mastitis. Bovine mastitis, defined as an infection and inflammation of the udder, represents the dairy production disease with the greatest economic impact on farmers worldwide (Hogeveen et al., 2019). Several potential candidates have been identified for phage therapy against mastitis-associated *S. aureus* (Titze et al., 2020, Iwano et al., 2018, Breyne et al., 2017, Li and Zhang, 2014, Kwak et al., 2023). However, the results of field trials to date are highly variable (Tomanić et al., 2023, Angelopoulou et al., 2019). To maximise the utility of phages against bovine mastitis, several factors affecting phage efficacy must be optimised. These include the dose and timing of administration, the presence of neutralizing antibodies, and the relative spectrum or specificity of the phage (Venturini et al., 2022). Furthermore, the ability of phages to replicate in the complex medium of milk, composed of lipids, milk proteins (caseins, whey proteins), enzymes, lactose, minerals, trace elements, vitamins and microbes must also be considered (Titze et al.,

2020). Indeed, the adsorption of Phage K to the cell surface in raw bovine milk, an exclusively lytic *S. aureus* phage belonging to the *Myoviridae* family, was inhibited by immunoglobulin activity and the clumping of *S. aureus* cells to fat globules and whey proteins in field trials (O'Flaherty et al., 2005a). Recent attempts to circumvent these issues have been explored with encouraging results. Phage cocktails, which combine multiple different phages have been shown to improve the efficacy of phage therapy against *S. aureus*-induced intramammary infection in murine models (Brouillette et al., 2023). Furthermore, phage endolysin preparations have shown significant efficacy against *S. aureus* associated with bovine mastitis (Park et al., 2023).

Numerous successful human clinical trials of phage therapy have been performed in recent years in the U.S. and Europe. Encouraging results have primarily been observed for the treatment of chronic non-healing wounds (Gupta et al., 2019), chronic rhinosinusitis (Ooi et al., 2019) and severe *S. aureus* infections (Petrovic Fabijan et al., 2020). Multiple clinical trials are ongoing for patients with acute diseases, such as prosthetic joint infections, bone and joint infections, urinary tract infections, implant infections, wound infections, diabetic foot infections, and acute tonsillitis (Hitchcock et al., 2023). However, there are a number of challenges to circumvent before phage therapy becomes commonplace in human clinical practice. Regarding safety, phage-mediated bacterial lysis may result in the release of bacteria-encoded endotoxins which can have deleterious effects on eukaryotic cells (Liang et al., 2023). Phages are susceptible to heat and chemical denaturation, with numerous phage preparations showing poor stability in gastric acid conditions and insufficient retention time in the intestine for therapeutic efficiency (Durr and Leipzig, 2023). The frequent and almost inevitable emergence of bacteriophage-insensitive mutants (BIMs) is another cause for concern (Mangalea and Duerkop, 2020). Despite these issues, a number of innovative approaches have been developed to improve the efficacy of phage therapy in the clinical setting. Various protocols, such as affinity chromatography have been developed to successfully remove endotoxins from phage preparations (Van Belleghem et al., 2017). Numerous methods have been explored to enhance the stability and delivery of phage products to the site of infection including liposome encapsulation, polymer encapsulation, electrospun fibre-encapsulation and microneedling (Ling et al., 2022). In addition, the aforementioned phage cocktails

have shown promising results in the reduction of BIMs (Abedon et al., 2021, Liu et al., 2022).

Regarding isolation sources, *S. aureus* phages for therapeutic usage in bovines have primarily been derived from milk and the farm environment (e.g. wastewater, sewage, silage effluent) (Angelopoulou et al., 2019, Tomanić et al., 2023). Bovine colostrum is the initial mammary secretion post-parturition, bestowing a complete nutritional profile and bioactive compounds vital for optimum nutrition and promoting the growth, development, and immunological defence of newborns (Roy et al., 2020). Calves are born immunoglobulin deficient at birth, as the syndesmochorial placenta of cows prevents passive immunity transfer from the mother to the neonate during gestation (Weaver et al., 2000). As a result, bovine colostrum contains high concentrations of bioactive compounds, particularly immunoglobulin G (IgG), to provide passive immunity (Linehan et al., 2023). In addition, colostrum is rich in growth factors, lactoperoxidase, lysozyme, lactoferrin, cytokines, vitamins, peptides, leukocytes, hormones, minerals, oligosaccharides, and probiotic bacteria (Linehan et al., 2023). However, no studies have been conducted to investigate the presence of phages in bovine colostrum. *S. aureus* phages for therapeutic use in humans have typically been isolated from clinical samples (blood, wound swabs), sewage and wastewater, faecal samples or induced from pathogenic strains (Atshan et al., 2023). Human breast milk is the gold standard feeding regime for newborn infants, contains the optimal amount of macro and micronutrients, and provides complete nutrition for the infant (Lyons et al., 2020). In addition to these nutrients, breast milk contains an array of bioactive and immune factors such as antibodies, lysozyme, growth factors, antimicrobial peptides, microRNAs, stem cells, human milk oligosaccharides (HMOs), and probiotic bacteria which all most likely influence the developing infant immune system and provide defence against pathogens (Yi and Kim, 2021). Recent human studies indicate that bacteriophages are transmitted from mother to infant via breastfeeding (Dinleyici et al., 2021, Pannaraj et al., 2018). However, we are not aware of any studies attempting to isolate phages from human milk samples for therapeutic applications. Therefore, in this study we aimed to isolate and characterise *S. aureus* phages from bovine colostrum and human breast milk. We report the isolation, characterisation and therapeutic application of two novel *S. aureus* phages vB_SauS_HM1 (phage HM1) and vB_SauS_BC1 (phage BC1). Using *in vitro*

approaches the therapeutic application of these phages was tested against pathogenic *S. aureus* strains of bovine and human origin. The application of these phages to mastitic milk was also explored. Finally, bioinformatic analysis was performed to describe the nature of the phages.

5.3 Materials and Methods

5.3.1 Sample collection

Bovine colostrum samples were collected from Holstein-Friesian dairy cows on a commercial dairy farm in north Cork, Ireland, during the spring calving season between February and April 2020. The cows included in the study had not received antibiotic treatment within 12 weeks prior to sampling. All samples were collected from the front right quarter immediately before first milking post-partum. Standard recommendations from the National Mastitis Council's Laboratory Handbook on bovine mastitis were followed for sample collection (Adkins and Middleton, 2017). Briefly, teats were disinfected with iodine tincture, dried and thoroughly disinfected with wipes soaked in 70% alcohol. Initial milk streams were discarded and then 25 ml of colostrum from the front right quarter of each cow's udder was collected into sterile 50 ml falcon tubes (Sarstedt). The tubes were labelled with the cow's identification number and the collection date, and immediately frozen at -20°C on the farm. Subsequently, the samples were transported to Teagasc, Moorepark, Co. Cork, and stored at -80°C. Human breast milk samples were collected as part of the INFAMILK study, which was approved by the Clinical Research Ethics Committee of the Cork Teaching Hospitals. For food application assays, pasteurised whole milk was purchased at a local supermarket (Cork, Ireland). Raw milk was obtained from the same farm colostrum samples were collected. Mastitic milk samples used in this study were collected as part of the study described in Chapter 6 of this thesis, before the administration of prophylactic treatments. The absence of *S. aureus* in pasteurised, raw and mastitic milk samples was confirmed by plating samples on Baird Parker agar (Oxoid) BPA supplemented with Egg Yolk Tellurite Emulsion (Oxoid) and on Blood agar (Oxoid Ltd., Basingstoke, Hampshire, United Kingdom) and incubated at 37°C for 48 h aerobically. The absence of antibiotic residues in pasteurised, raw and mastitic milk samples was confirmed by using the Delvotest® Strarter Kit (DSM; Co-Op Superstores).

5.3.2 Bacterial Strains and Cultivation Conditions

Strains with the prefix '**DPC**' were acquired from the Dairy Products Research Centre culture collection (n=12). MRSA strains (n=21) were acquired from the Irish National MRSA Reference Laboratory, St. James' Hospital, Dublin, Ireland (Shore et al., 2008). All strains were routinely cultured in Brain Heart Infusion broth (BHI; Merck, Darmstadt, Germany) or on BHI agar (Merck, Darmstadt, Germany) aerobically at 37°C. For long-term preservation, strains were stocked in BHI broth containing 40% glycerol and stored at −80°C. Table S5.1 and S5.2 provide additional information on the strains included in this study.

5.3.3 Phage Isolation

Phages were isolated using a standard enrichment method for bovine milk samples adapted from Kutter and Sulakvelidze (2004) and Kwiatek et al., (2012b). Briefly, 1 ml of bovine colostrum or human breast milk samples were suspended in 10 ml Tryptic soy broth (TSB; Difco™, Becton-Dickinson, Ltd., Ireland) supplemented with 10mM $MgS0_4$ and mixed with 1 ml of 18 h bacterial cultures (Table S5.3). The mixture was incubated for 24 h at 37°C, followed by shaking with 2 ml chloroform and centrifugation at 5,000 x g for 10 mins to pellet bacterial matter. The supernatant was then filter sterilised twice using 0.45 µm pore-size filters (Sarstedt, Nümbrecht, Germany) to obtain phage sample lysates, which were stored at 4°C prior to spot assays. Spot and plaque assays were conducted using the overlay method. Tryptic soy agar (TSA; Difco™, Becton-Dickinson, Ltd., Ireland) containing 1.5% (w/v) agar was used as the base agar in a 100 mm × 15 mm petri dish. For spot assays, 100 µl of 18 h bacterial cultures and 40 µl of 1M $MgSO_4$ (final concentration 10 mM) were added to 4 ml of soft TSA (0.75% agar w/v) kept at 55°C. This mixture was poured on top of the TSA base agar and allowed to solidify. Next, 10 µl of phage sample lysates were pipetted onto the agar and allowed to dry. Plates were then incubated for 24 h at 37°C. Cleared zones on the bacterial lawn indicated the presence of lytic phages. For plaque assays, 40 µl of 1 M $CaCl_2$ (final concentration 10 mM), 100 µl of phage lysate and 100 µl of 18 h bacterial cultures were added to 4 ml of soft TSA agar kept at 55°C. The mixture was poured on top of the TSA base agar and allowed to solidify. Plates were incubated for 24 h at 37°C. Isolated single plaques were picked into SM buffer (50 mM Tris.HCl pH 7.5, 100 mM NaCl, 8 mM $MgSO_4$). Isolated plaques from human breast milk and bovine colostrum were designated "HM" and "BC", respectively.

Single plaque purification was performed by propagating a single plaque and conducting a plaque assay three times.

5.3.4 Phage Characteristic Testing

5.3.4.1 Host range and Efficiency of Plaquing (EOP)

The host range of phages was determined by spotting a 1 µl volume of a serially diluted phage suspension (10^{-1} to 10^{-10}) onto TSA overlays seeded with the bacterial strain of interest. Bacterial sensitivity to the phage was determined by observing bacterial lysis at the spot where the phage was deposited. According to the degrees of clarity, the spots were differentiated into two categories: clear (+) and no reaction (-) (Jensen et al., 2015). This assay was performed in triplicate for three independent experiments. The Efficiency of Plaquing (EOP) was determined by dividing the ratio of the phage titre on each test strain by the phage titre of the reference host strain (*S. aureus* DPC5245). The experiment was performed in triplicate. Based on the mean ± SD score of EOP, each phage/bacterial strain combination was classified into one of four production levels, high (EOP ≥ 0.5), medium (0.1 ≤ EOP < 0.5), low (0.001 ≤ EOP < 0.1), or no production (EOP ≤ 0.001) (Shahin et al., 2019).

5.3.4.2 Optimal Multiplicity of Infection (MOI)

To determine the optimal Multiplicity of Infection (MOI), *S. aureus* DPC5245 cultures were grown to early logarithmic phase, corresponding to an OD_{600} of 0.18–0.2 (~ 1 x 10^8 colony forming unit (CFU)/ ml). Bacterial cultures (1 ml) were then inoculated with 10^8, 10^7, 10^6 and 10^5 plaque forming units (PFU)/ml at the MOIs 1, 0.1, 0.01 and 0.001 respectively. Bacterial growth was monitored at 37°C by measuring the OD_{600} at 30 min intervals up to 240 min. The mixture was centrifuged at 5,000 × g for 20 min at 4°C to pellet solid matter. The supernatant was then passed through 0.45 µm filters, diluted in SM buffer and the phage titre was immediately determined using plaque assays. This assay was performed in triplicate for three independent experiments.

5.3.4.3 One Step Growth Curve

To determine the latent period and phage burst size, one-step growth curve analysis was performed as described previously for *S. aureus* phages with some modifications (Chang et al., 2015, Kwiatek et al., 2012a, Wang et al., 2016). *S. aureus* DPC5245 was grown to early logarithmic phase, followed by centrifugation at 10,000 × g for 1

min to pellet bacteria. The pellet was re-suspended in 1 ml of TSB phage suspension to yield an approximate MOI of 0.001, and incubated at 37°C for 10 min with shaking (100 rpm). Subsequently, the mixture was centrifuged at 10,000 × g for 1 min, to pellet bacteria and the supernatant was removed to separate bound from unbound phages. The bacterial pellet containing bound phages was re-suspended in 10 ml of pre-warmed TSB 37°C and incubated in a water bath at 37°C with gentle shaking (100 rpm). At 5 min intervals, aliquots were taken, filtered through 0.45 µm filters, diluted and the phage titre was immediately determined using plaque assays. The latent-period, representing the interval between phage adsorption by the host and the beginning of lysis, was estimated from the one-step growth curve. The burst size, defined as the ratio of the final average number of phage particles liberated, was calculated by dividing number of phages present at the end of lysis by the initial number of bacterial cells at the time of infection (Xu et al., 2021).

5.3.4.4 Adsorption assay

An adsorption assay was performed as described previously for *S. aureus* phages with some modifications (Ajuebor et al., 2018, Zhang et al., 2015). 100 µL of early logarithmic phase cultures of host strains were mixed with 100 µl of phage, titered at approximately 1 x 10^5 PFU/ml, to achieve a MOI of 0.001. The mixtures were then incubated at 37°C with gentle shaking (100 rpm). At 5, 10, 15, 20, 30, and 40 min, 100 µL aliquots were collected. To separate bound phages from free phages, the samples were centrifuged at 10,000 × g for 5 min. The adsorption of phages to each strain was determined by calculating the difference between the total input PFU/ml and the number of unbound phages (per ml). The adsorption efficiency was expressed as a percentage relative to the propagating strain, *S. aureus* DPC5245.

5.3.4.5 Biophysical stability

Biophysical stability refers to the ability of phages, used in therapeutic studies, to maintain their physical integrity and functionality under various conditions, such as temperature, pH, and exposure to environmental stresses. To assess phage biophysical stability, the following tests were conducted. Phage thermostability was evaluated by incubating a phage suspension (10^{10} PFU/ml) in SM buffer at 24°C 37°C, 50°C, 60°C and 70 °C. Aliquots were taken at 5-minute intervals for up to 60 min. Phage pH stability was tested by incubating the phage suspension in pH buffers ranging from 3 to 12 (adjusted with NaOH or HCl) at 37°C for 1 h. Phage chloroform stability was

examined by mixing phage suspensions with different concentrations of chloroform (5%, 25%, 50%, and 75%), shaking vigorously, and incubating at 37°C for 30 min (Guo et al., 2021). After centrifugation at 1,000 × g for 15 min, the hydrophilic layer was collected and titered by plaque assay. Phage UV stability was assessed by exposing sterile Petri dishes containing phage suspensions to UV light (20W) at a distance of 40cm, with a dose of 50 J/m2. Aliquots were taken at 5-min intervals for up to 60 mins (Rodriguez et al., 2014). All assays were performed in triplicate for three independent experiments.

5.3.5 Therapeutic Suitability Assays

5.3.5.1 Bacteriophage-Insensitive Mutants (BIMs) Induction and Complementary Tests

BIMs were isolated as described previously (O'Flynn et al., 2004, Liu et al., 2022). Briefly, early logarithmic phase cultures of host strains were mixed with 100 µL of phage, tittered at approximately 1 x 10^5 PFU/ml, to achieve a MOI of 0.001. After incubation at 37 °C for 10 min, 4mlof 0.4% TSA was added. This mixture was poured on top of 1.5% TSA and incubated at 37 °C for 24 h up to 48 h until BIMs appeared. Single bacteriophage-insensitive mutant colonies were picked and the procedure was repeated at least 5 times. Spot assays were used to test phage sensitivity to BIM. Confluent lysis zones observed on plates were defined as phage-sensitive (S), semi-confluent lysis zones were defined as phage-intermediate-resistant (I), and no plaques were defined as phage-resistant (R).

5.3.5.2 Determining the Frequency and Emergence of BIMs

The frequency of BIMs was determined as previously described (O'Flynn et al., 2004, Liu et al., 2022). Briefly, early logarithmic phase cultures of host strains were mixed with 100 µL of individual phages, or in a cocktail (ratio 1:1), tittered at approximately 1 x 10^5 PFU/ml, to achieve a MOI of 0.001. After incubation at 37 °C for 10 min, mixtures were serially diluted and plated on a TSA-containing agar plate. Following overnight incubation at 37 °C, the number of remaining cells were counted, and the BIMs frequency was determined by dividing the number of remaining cells by the initial viable cell number. All assays were performed in triplicate for three independent experiments.

5.3.5.3 Bacterial challenge assay

The bacterial challenge assay was performed using 96-well plates as previously described, with slight modifications (Chang et al., 2019, Dalmasso et al., 2016). *S. aureus* DPC5245 (1%) was sub-inoculated into 50 ml of fresh TSB and the culture was aerobically incubated with shaking at 220 rpm at 37 °C until it reached the early exponential growth phase (OD_{600} = 0.18–0.2, ~10^8 CFU/ml). 100 µl of bacterial culture was mixed with 100 µl of diluted phage lysate to give an MOI of 0.001. This mixture was incubated at 37 °C for up to 32 h, with OD_{600} readings taken every 1 h using a plate reader (Synergy HT, BioTek). All assays were performed in triplicate for three independent experiments.

5.3.5.4 Potential Lysogens Test

The potential lysogen of isolated phages was tested as previously described with some modifications (Chang et al., 2019). Briefly, *S. aureus* DPC5245 was infected with phage suspensions (MOI of 0.001). Following 32 h of incubation, the surviving colonies were isolated, and induced with mitomycin C (0.5 µg/ml, final concentration) at 37 °C for 2 h. The culture was centrifuged at 10,000 × g for 5 min and filtered by a 0.22 µm syringe filter. Spot assays were performed with the filtered supernatant. The number of resistant colonies that were able to reproduce plaques by mitomycin C induction were regarded as lysogenised colonies and counted (Goffart-Roskam, 1965). The rate of lysogen formation was calculated by dividing the number of lysogenised colonies with the initial number of randomly selected colonies (fifty colonies) (Chang et al., 2019). These experiments were performed in triplicate, and the rate of lysogen formation is indicated as a % value with standard deviations.

5.3.5.5 Phage Bactericidal Activity in Pasteurised, Raw and Mastitic Milk

Food application assays were performed as described previously (Titze et al., 2020, Chang et al., 2019), with some modifications. Pasteurised, raw and mastitic bovine milk samples were inoculated with *S. aureus* DPC5245 at a concentration of ~ 1 × 10^5 CFU/ml. 1 ml of phage mixture was added to 5 ml inoculated milk, to give a final phage concentration of ~ 1× 10^9 PFU/ml. Samples were mixed by vortexing before incubating at 37 °C aerobically without shaking. Samples were taken at two-hour intervals up to eight hours. Bacterial counts were determined by spread plating on BPA. In parallel, control experiments were performed, which C included cultures

without phages (*S. aureus* inoculated milk) and negative control (non-inoculated milk). All assays were performed in triplicate for three independent experiments.

5.3.6 Assessment of Phage Morphological Characteristics

5.3.6.1 Caesium Chloride Gradient Purification

Isopycnic centrifugation through caesium chloride (CsCl) gradients was performed, as previously described (Sambrook and Russell, 2006), with some modifications. A high-titre phage lysate (>1 x 10^9 PFU/ml) was concentrated by centrifugation at 50,000 x g using the Sorvall wx ultra series with a FS5L-6 rotor for 2 hours at 5°C. The 180 ml phage lysate was concentrated to 6 ml. Where necessary, a chloroform phase separation step (1:1) was conducted to remove debris. The resulting phage preparation was placed on to a CsCl step gradient consisting of layers with densities of 1.3, 1.5, and 1.7 g/ml. Ultracentrifugation was carried out at 50,000 x g for 2 h at 5°C. The phage bands obtained were collected and subjected to dialysis for 18 h with two changes of SM buffer at 4°C.

5.3.6.2 Transmission Electron Microscopy (TEM)

CsCl purified phages were adsorbed onto freshly prepared ultra-thin carbon films. Phages were negatively stained with 1% (w/v) uranyl acetate for 20 min. A Tecnai 10 transmission electron microscope (FEI Thermo Fisher, Eindhoven, The Netherlands) at an acceleration voltage of 80 kV was used for analysis. Digital micrographs were acquired with a MegaView G2 CCD camera (EMSIS, Muenster, Germany) and examined at the Max Rubner-Institut, Department of Microbiology and Biotechnology, Hermann-Weigmann-Straße 1, 24103 Kiel, Germany.

5.3.7 Viral DNA Extraction, Amplification, Library Preparation, and Sequencing

Viral DNA Extraction was performed as described previously (Lewis et al., 2020), with some modifications. To 1 ml of high titre phage lysate (>1 x 10^9 PFU/ml), 100 µL of 10 × Nuclease Buffer (50 mM $CaCl_2$; 10 mM $MgCl_2$), was added. The mixture was treated with 20 U of DNase I and 10 U of RNase I (final concentrations; Ambion) for 1 h at 37°C. Nucleases were then inactivated at 70°C for 10 min. Phage capsids were degraded for 20 min at 56°C using 2 µl of freshly prepared Proteinase K (20 mg/µl). Phage DNA extractions were performed using Norgen BioTek Corp Phage DNA Isolation Kit, starting from the addition of Lysis Buffer B. DNA was eluted in

50 µl of Elution Buffer B. DNA quantification was conducted using the Invitrogen Qubit 4 fluorometer (Thermo Fisher Scientific, Renfrew, UK) following the manufacturer's protocol. The resulting DNA samples were sent to MicrobesNG (Birmingham, UK) for whole genome sequencing (WGS). Genomic DNA libraries were prepared using a Nextera XT Library Prep Kit (Illumina, San Diego, USA) and sequenced on an Illumina HiSeq, generating paired-end reads of 2 x 250 base pair (bp) reads.

5.3.8 Bioinformatic Analysis

5.3.8.1 Genome Overview

Raw Illumina paired-end reads were first quality-checked using FastQC v0.11.8 (Bioinformatics, 2019). The reads were then filtered and trimmed using trimgalore v0.6.1 (Krueger, 2015). Subsampling of reads was performed using Seqtk v1.4 (Shen et al., 2016). Genome assembly was conducted using metaSPAdes (Nurk et al., 2017) with standard parameters. The assembled contigs were visually inspected using Bandage v0.8.1 (Wick et al., 2015). Circularised contigs with the highest coverage and a length of >10,000 bp were selected as the phage genome. Assembly validation, coverage per contig extraction and error detection and correction were carried out using BBMap v38.22 (Bushnell, 2014), Pilon v1.24 (Walker et al., 2014) and SAMtools (Li et al., 2009). PHASTER (Arndt et al., 2016), PhageClouds (Rangel-Pineros et al., 2021) and BLAST were utilised to identify the closest phage sequences. Genome termini were identified using PhageTerm v1.0.12 (Garneau et al., 2017). To assess synteny and genome conservation, all complete sequences of the *Phietavirus* genus were downloaded from Genbank and aligned with the novel phage genomes. Multiple sequence alignment was performed using Clinker (Gilchrist and Chooi, 2021). The start and end positions of the new phage genomes were determined based on the most closely related species, *Staphylococcus* phage DW2, using manual genome reordering perl scripts provided by Shen and Millard (2021). Phage genomes were initially annotated with RASTtk (Aziz et al., 2008). Open reading frames (ORFs) were further investigated with BLASTp using the nr database, PFAM (HMMSCAN) (Finn et al., 2010) and HHpred (Söding et al., 2005). ARAGORN (Laslett and Canback, 2004) and tRNAscan-SE v. 2.0 (Chan et al., 2021) were employed for tRNA gene identification. The molecular weights of the predicted ORFs were estimated using the batch protein molecular weight determination of the sequence manipulation

suite (Stothard, 2000). Antibiotic resistance analysis of phage genomes was performed using RGI (Resistance Gene Identifier) main v6.0.0 and the Comprehensive Antibiotic Resistance Database (CARD) v3.2.5 (McArthur et al., 2013). Phage lifestyle prediction was carried out with PhageLeads (Yukgehnaish et al., 2022), PHACTS (McNair et al., 2012) and PhageAI (Tynecki et al., 2020). Potential Rho-independent terminators were identified using ARNold (Naville et al., 2011) with Mfold QuikFold (Zuker, 2003) using RNA energy rules 3.0 to verify predictions, with putative single-stranded hairpin promoters identification being assisted with Mfold QuikFold using DNA energy rules. Putative promotors of phages were determined by submitting 100bp of DNA sequence upstream of each gene to MEME (Multiple Em for Motif Elicitation) (Bailey et al., 2009). Circular genome maps of phages were drawn using ProkSee (Grant et al., 2023).

5.3.8.2 Comparative genomics

A total proteome comparison between phages was conducted using CoreGenes5 (Davis et al., 2022) with the BLASTP threshold set at 75% (Davis et al., 2022). Linear genomic comparison maps were generated using TBLASTX and visualised with Easyfig (Sullivan et al., 2011). Genome-based taxonomy was conducted according to the guidelines by Turner et al., (2021). For family-level classification, a proteome-based clustering strategy was applied using the ViPTree server (Nishimura et al., 2017), considering closely related phages and other dsDNA prokaryotic viruses. Phages with highest VipTree tBLASTx scores (S_G) were selected to construct a more detailed rectangular proteomic tree. To classify the phage at taxonomic levels below the family level (genus and species), a phylogenetic analysis of genome-genome distance was performed. This analysis involved comparing the isolated phage with BLASTn top hits, phages of highest (S_G) on ViPTree and an outgroup consisting of other morphotypes and families. The genome-genome distance was computed by Virus Classification and Tree Building Online Resource (VICTOR) (Meier-Kolthoff and Göker, 2017). Pairwise comparisons of amino acid sequences were conducted using the Genome-BLAST Distance Phylogeny (GBDP) method (Meier-Kolthoff et al., 2013) with recommended settings for prokaryotic viruses (Meier-Kolthoff and Göker, 2017). The resulting intergenomic distances were used to infer a balanced minimum evolution tree with branch support via FASTME including SPR post-processing (Lefort et al., 2015) for each of the formulas D0, D4 and D6, respectively.

Branch support was inferred from 100 pseudo-bootstrap replicates each. Trees were rooted at the midpoint (Farris, 1972) and visualised with ggtree (Yu, 2020). Taxon boundaries at the species, genus and family level were estimated with the OPTSIL program (Göker et al., 2009), the recommended clustering thresholds (Meier-Kolthoff and Göker, 2017) and an F value (fraction of links required for cluster fusion) of 0.5 (Meier-Kolthoff et al., 2014). In addition, VIRIDIC (Virus Intergenomic Distance Calculator) (Moraru et al., 2020) was used to identify intergenomic similarities of the isolated phage genomes to the closest phage homologs in BLASTn and other closely related phages from the genus *Phietavirus*. Phages from the NCBI database were selected according to the following criteria, they belonged to the *Caudoviricetes* order, possessed a complete RefSeq genome and had a genome length ranging from 40Kb - 60Kb and were associated with *Gammaproteobacteria* hosts. The FASTA sequence of the filtered phages were downloaded and used for VIRIDIC analysis. VIRIDIC utilizes the traditional algorithm recommended by the ICTV to calculate pairwise intergenomic distances/similarities. Additionally, the genomic relationships between the phage and reference phage sequences from NCBI-GenBank were analysed using PhageClouds (Rangel-Pineros et al., 2021), an alignment-free method which calculates intergenomic distances, with the threshold set to 0.1. To identify shared signature genes among the phage and its close relatives, pan-genomic analysis was conducted using CoreGenes5 (Davis et al., 2022). The amino acid sequence alignments of the highly conserved signature genes, encoding the terminase large subunit, the major capsid protein, and the portal protein, were used for further confirmation of genus- and family-level phylogeny using the phylogeny.fr web-based tool (Dereeper et al., 2008). The amino acid sequences of the selected conserved genes of the selected phages were aligned by MUSCLE and the evolutionary history was inferred by the maximum likelihood method with Le_Gascuel model (Le and Gascuel, 2008). The robustness of the trees was assessed with 1000 bootstrap replicates. The evolutionary rate differences among sites were modelled by a discrete gamma distribution. Tree branch lengths were measured in number of substitutions per site, while all gaps and missing data were entirely removed. The trees of the phylogenetic analyses were constructed in MEGA (v11) (Tamura et al., 2021).

5.4 Results

The standard enrichment method for phage isolation was used to isolate phages from bovine colostrum and breast milk. This resulted in the isolation of phage HM1 and phage BC1, which were both isolated with *S. aureus* DPC5245.

5.4.1 Characteristic Testing

5.4.1.1 Host range

Phage HM1 and phage BC1 demonstrated a broad host range, capable of lysing the majority of *S. aureus* strains included in this study (Table S5.2 and Table S5.3). Phage HM1 exhibited lytic activity against 25 out of 33 strains (75.8%), while phage BC1 showed lytic activity against 17 out of 33 strains (51.5%) (Table 5.1). The host range was extended to 25 out of 33 strains (75.8%) when phages were combined as a cocktail (Supplementary TableTable 5.1). The susceptible strains identified through spot testing were subjected to EOP analysis. A wide range of EOP values were obtained, with phage HM1 ranging from 0.05 ± 0.07 to 0.85 ± 0.06 and phage BC1 ranging from 0.04 ± 0.01 to 0.88 ± 0.11. For phage HM1, 20% of the tested strains exhibited high EOP (EOP ≥ 0.05), another 20% showed medium EOP (0.1 ≤ EOP < 0.5) and 20% displayed low EOP (0.001 ≤ EOP < 0.1). Similarly, for phage BC1, 18% of the tested strains exhibited high EOP, 18% showed medium EOP, and 20% displayed low EOP. Both phages were found to be specific to *S. aureus* strains, as no plaque formation or inhibition was observed for any other bacterial species tested (Tables S5.2 and S5.3).

Table 5.1 | Host ranges of phage HM1 and phage BC1 on *S. aureus* strains (n=33) determined by spot testing with serial dilutions of phage suspensions.

			Spot Test		**Efficacy of Plaquing (EOP) (mean ± SD)**	
No.	**Strain**	**Source[a]**	**HM1**	**BC1**	**HM1**	**BC1**
1	0.0066(IIv)ST239	I	+	-	0.5 ± 0.1	no plaques
2	0.1206(IV)ST250	I	+	+	0.34 ± 0.12	0.44 ± 0.11
3	0.1239(III)ST239	I	-	-	no plaques	no plaques
4	0.1345(II)ST5	I	-	-	no plaques	no plaques
5	0073(III)ST239	I	+	-	0.55 ± 0.32	no plaques

6	0104(III)ST239	I	+	-	0.37 ± 0.04	no plaques
7	0220(II)ST5	I	+	-	0.46 ± 0.02	no plaques
8	0242(IV)ST30	I	+	+	0.16 ± 0.06	0.24 ± 0.01
9	0308(IA)ST247	I	+	+	0.05 ± 0.07	0.11 ± 0.04
10	3045(IIv)ST8	I	+	+	0.25 ± 0.01	0.31 ± 0.02
11	3144(IIv)ST8	I	+	-	0.12 ± 0.1	0.12 ± 0.04
12	3488(vv)ST8	I	-	-	no plaques	no plaques
13	3581(IA)ST247	I	-	-	no plaques	no plaques
14	3594(II)ST36	I	+	-	0.62 ± 0.1	no plaques
15	3596(IIv)ST8	I	+	-	0.36 ± 0.09	no plaques
16	E1038(IIv)ST8	I	+	+	0.06 ± 0.03	0.04 ± 0.01
17	E1139(IV)ST45	I	-	-	no plaques	no plaques
18	E1174(IV)ST22	I	+	+	0.54 ± 0.01	0.46 ± 0.03
19	E1185(IV)ST12	I	+	+	0.14 ± 0.02	0.11 ± 0.04
20	E1202(II)ST496	I	+	+	0.44 ± 0.07	0.51 ± 0.02
21	M03/0073(III)ST239	I	+	-	0.38 ± 0.12	no plaques
22	DPC5646	II	+	+	0.76 ± 0.04	0.74 ± 0.14
23	DPC5645	II	+	+	0.85 ± 0.06	0.88 ± 0.12
24	DPC5647	II	-	-	no plaques	no plaques
25	DPC5245*	II	+	+	1.0 ± 0	1.0 ± 0
26	DPC5246	II	-	-	no plaques	no plaques
27	DPC5247	II	+	+	0.56 ± 0.02	0.49 ± 0.03
28	DPC5644	II	-	-	no plaques	no plaques
29	DPC5970	II	+	+	0.23 ± 0.05	0.26 ± 0.01
30	DPC5971	II	+	+	0.55 ± 0.1	0.61 ± 0.07
31	DPC6868	II	+	+	0.58 ± 0.02	0.67 ± 0.06
32	DPC6869	II	+	+	0.51 ± 0.04	0.56 ± 0.03
33	DPC7016	II	+	+	0.13 ± 0.01	0.09 ± 0.06

The efficiency of plaquing (EOP) values were determined for sensitive strains. Results recorded as +, sensitive; −, no infection; * host strain of phages. [a]I, 21 MRSAs of

differing sequence types obtained from the Irish National MRSA collection. [a]II, 12 *S. aureus* strains obtained from the DPC culture collection.

5.1.1.1 Growth Characteristics

The growth characteristics of the phages were examined in order to understand their behaviour and stability. All following tests were performed using *S. aureus* DPC5245. The optimal MOI was determined to be 0.001, resulting in titres of 6.7×10^{10} PFU/ml for phage HM1 and 8.9×10^{10} PFU/ml 23for phage BC1 (Figure 5.1A). The adsorption rate of the phages was evaluated, showing that approximately 98.1% of phage HM1 and 73% of phage BC1 were adsorbed to host cells at 5 min post-infection, which increased to 99% and 98.1%, respectively, after 40 minutes (Figure 5.1B). Phage stability under different environmental conditions was also investigated. Chloroform stability tests indicated that phage activity remained stable at chloroform concentrations up to 75% (v/v), with a 61% and 64% loss of activity for phage HM1 and phage BC1, respectively, when the concentration reached 100% (Figure 5.1C). Thermal stability experiments demonstrated that both phages were stable at temperatures up to 50°C, but became completely inactivated at 70°C (Figure 5.1D). pH sensitivity tests revealed that the phages survived within a pH range of 5 to 9, with optimal growth conditions observed at pH 6 to 8. However, they became inactivated below pH 5 or above pH 9, indicating sensitivity to strong acid or alkali conditions (Figure 5.1E). Additionally, under 20W ultraviolet light, both phages remained relatively stable for the first 35 min, but their titres decreased sharply after this timepoint, with complete loss of activity occurring after 50 minutes (Figure 5.1F). Finally, one-step growth curves were determined for both phages based on the optimal MOI of 0.001. Phage HM1 showed a latent period of 20 min with an approximate burst size of 93 ± 8 PFU/ml (Figure 5.2B). Phage BC1 exhibited a latent period of 20 min and an approximate burst size of 58 ± 3 PFU/ml (Figure 5.2A).

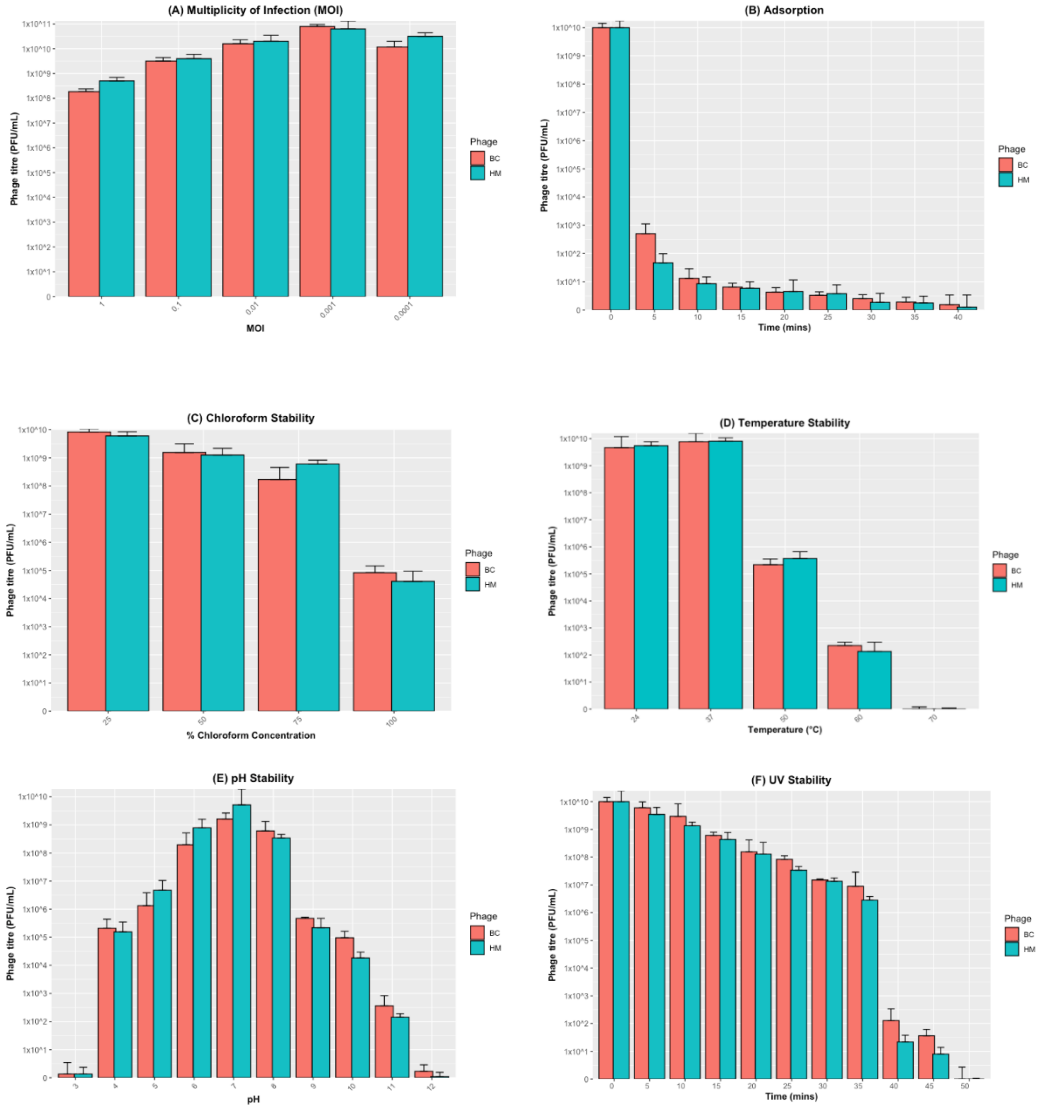

Figure 5.1 | Stability of phage HM1 and phage BC1 under various conditions performed with *S. aureus* DPC5245 (A) MOI, (B) Adsorption, (C) Chloroform, (D) Temperature, (E) pH, (F) UV. Error bars represent the standard deviation of biological repeats (n=3).

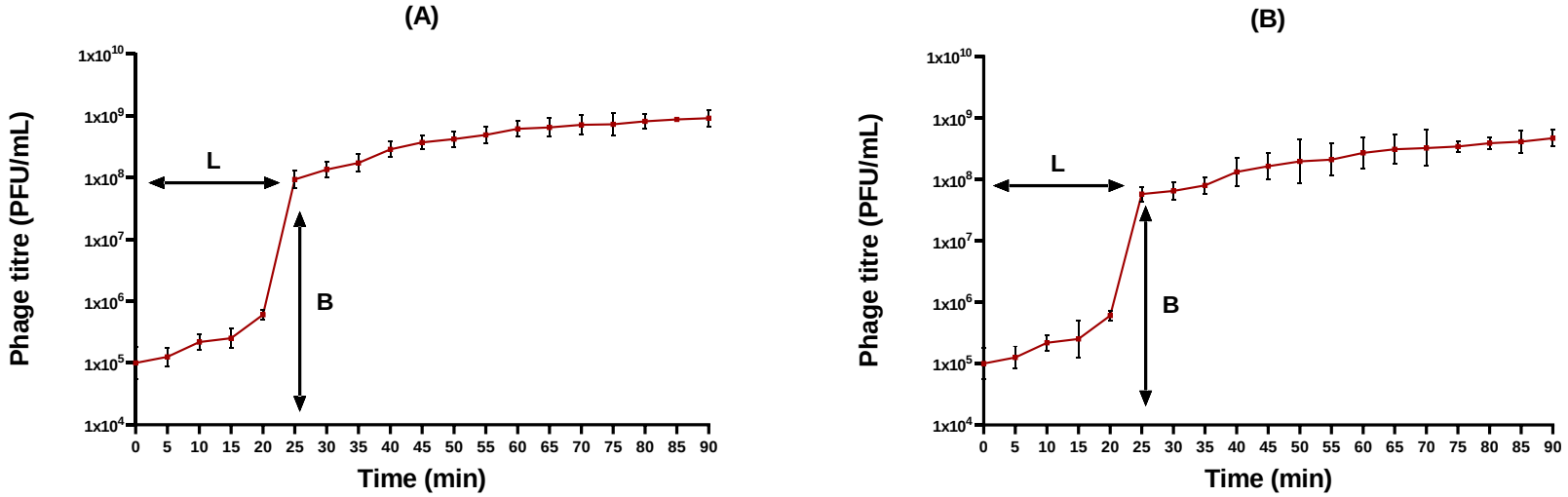

Figure 5.2 | One-step growth curve analysis of phage HM1 and phage BC1. (A) Phage HM1 infection of *S. aureus* strain DPC5245. (B) Phage BC1 infection of *S. aureus* strain DPC5245. The phage growth parameters, latent period (L) and burst size (B) are indicated. Data points represent the mean of three independent experiments while the error bars represent the standard deviation of biological repeats (n=3).

5.4.2 Therapeutic Suitability Assays

To determine the therapeutic suitability of phage HM1 and phage BC1, a number of assays were performed. Firstly, BIMs were generated with *S. aureus* DPC5245 and the activity of phages against them was determined. Table 5.2A shows that BIMs resistant to one phage demonstrated either sensitivity or intermediate sensitivity to the other phage. Furthermore, the frequency of BIM generation of the individual phages and of the phage cocktail formulation was determined. Phages showed good complementarity as a cocktail, with a reduced frequency of BIM generation compared to any of the single phages from the cocktail (Table 5.2B). The rate of lysogeny formation for phage HM1 and phage BC1 was $65.02 \pm 4.23\%$ and $69.45 \pm 3.13\%$, respectively. To investigate growth inhibition patterns, a challenge assay of phage HM1, phage BC1 and the cocktail formulation against *S. aureus* DPC5245 was conducted (Figure 5.3). Following infection with phage HM1 and phage BC1, *S. aureus* DPC5245 initially exhibited growth similar to the non-phage treated control for 5 h. Subsequently, host cell lysis was initiated and the inhibition of host growth persisted for 28 h until BIMs emerged. Following infection with the cocktail formulation, *S. aureus* DPC5245 exhibited growth similar to the non-phage treated control for 3 h. Subsequently, host cell lysis was initiated, leading to inhibition of host growth, which was sustained for 32 h. Investigation of phage bactericidal activity against *S. aureus* DPC5245 in pasteurised milk revealed that phage HM1, phage BC1 and the cocktail formulation reduced bacterial titres by 1.67, 1.4 and 2.46 log, respectively, 8 h after treatment (Figure 5.4A). The non-phage treated control grew by 1.94 log (Figure 5.4A). In raw milk, phage HM1, phage BC1 and the cocktail formulation reduced DPC5245 bacterial titres by 0.88, 0.7 and 1.55 log, respectively, 8 h after treatment (Figure 5.4B). The non-phage treated control grew by 2.78 log (Figure 5.4B). Finally, in bovine mastitic milk, phage HM1, phage BC1 and the cocktail formulation reduced *S. aureus* DPC5245 bacterial titres by 0.32, 0.32 and 0.9 log, respectively, 8 h after treatment (Figure 5.4C). The non-phage treated control grew by 3.12 log (Figure 5.4C). The negative controls (non-inoculated milk) showed no S. aureus growth as revealed by agar plating.

Table 5.2 | Sensitivity/Resistance of Bacteriophage-Insensitive Mutants (BIMs) to Phage HM1 and Phage BC1, and Frequency of BIM Emergence.

(A)		
Strain Name	**HM1**	**BC1**
DPC5245 Original	S	S
DPC5245/HM1 R1	R	I
DPC5245/HM1 R2	R	S
DPC5245/HM1 R3	I	S
DPC5245/HM1 R4	I	S
DPC5245/HM1 R5	R	S
DPC5245/BC1 R6	I	I
DPC5245/BC1 R7	S	R
DPC5245/BC1 R8	S	R
DPC5245/BC1 R9	S	I
DPC5245/BC1 R10	S	R

(B)	
Phage	**Bacteriophage-insensitive mutants Frequency ± (Mean SD)**
HM1	0.45×10^{-6}
BC1	0.19×10^{-6}
Cocktail	0.21×10^{-7}

(A) Sensitivity/resistance of bacteriophage-insensitive mutants (BIMs) to phage HM1 and phage BC1. (B) The frequency of the emergence of BIMs. DPC5245: Parent strain; R1–10: DPC5245 BIMs for phage HM1 and BC1. S: susceptible to the phage (clear plaque), I: intermediate sensitivity to the phage (turbid plaque), R: Resistant to the phage. The average of three independent experiments is shown.

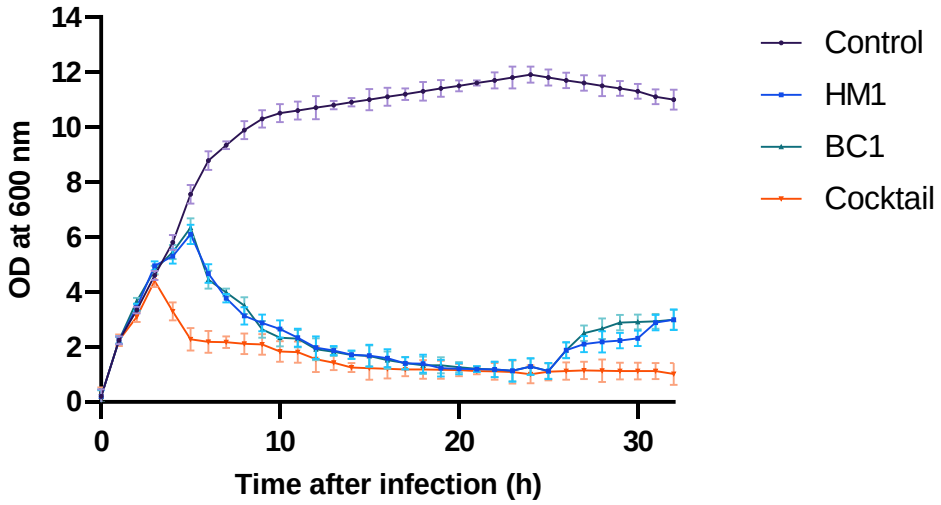

Figure 5.3 | Bacterial challenge test of *Staphylococcus* phages HM1, BC1 and cocktail formulation (10^8 PFU/ml each) with *S. aureus* DPC5245 (MOI of 0.001, 10^5 CFU/ml). Purple line depicts control containing non-phage treated *S. aureus* DPC5245. Blue line depicts phage HM1 treated *S. aureus* DPC5245. Green line depicts phage BC1 treated *S. aureus* DPC5245. Orange line depicts Cocktail treated *S. aureus* DPC5245. Error bars represent the standard deviation of biological repeats (n=3).

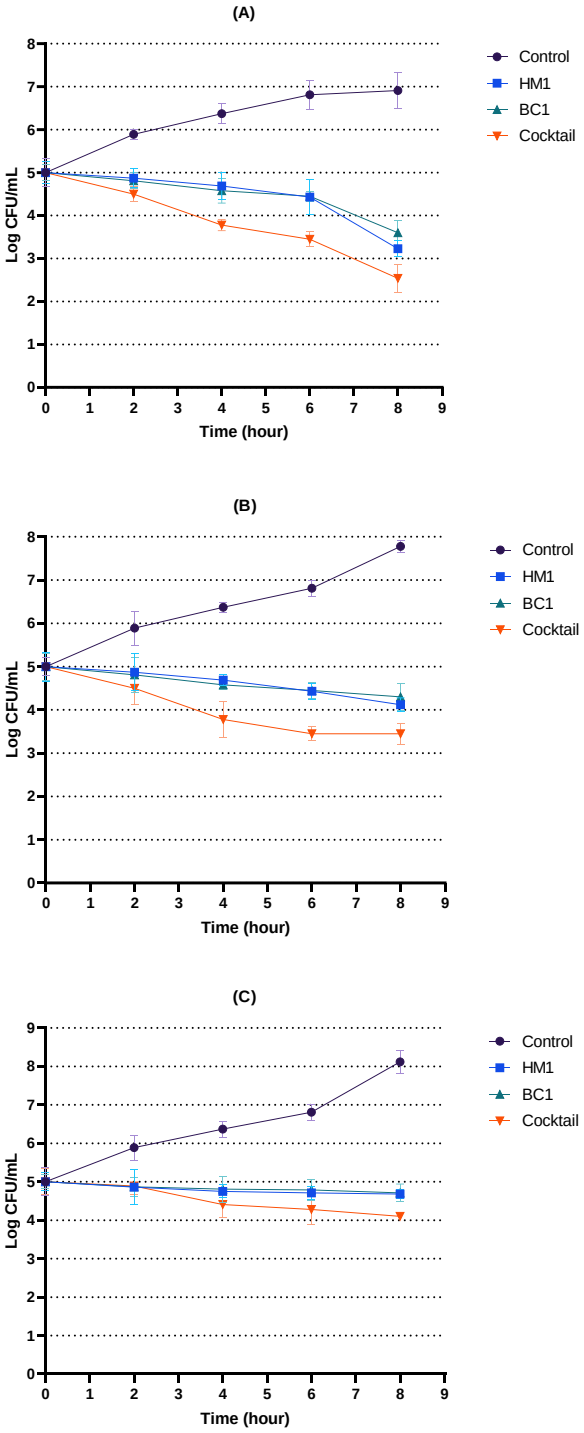

Figure 5.4 | Bactericidal activity test of *Staphylococcus* phages HM1 and BC1 and cocktail formulation (~10^9 PFU/ml each) against *S. aureus* DPC5245 (~ 1 × 10^5 CFU/ml) in (A) pasteurised, (B) raw and (C) mastitic milk. Purple line depicts control containing non-phage treated *S. aureus* DPC5245. Blue line depicts phage HM1 treated *S. aureus* DPC5245. Green line depicts phage BC1 treated *S. aureus* DPC5245. Orange line depicts cocktail treated *S. aureus* DPC5245. Error bars represent the standard deviation of biological repeats (n=3).

5.4.3 Morphological Characteristics

Morphological examination by TEM revealed that phage HM1 possesses an icosahedral head with a diameter of approximately 50nm and a non-contractile tail, which is around 165nm in length and 5nm in diameter (Figure 5.5A). Similarly, phage BC1 exhibits an icosahedral head with a diameter of approximately 50nm, along with a non-contractile tail measuring approximately 140nm in length and 5nm in diameter (Figure 5.5B). These morphological features align with the siphoviral morphotype, specifically the legacy family *Siphoviridae* of the order *Caudovirales*, as defined by the ninth report of the International Committee on Taxonomy of Viruses (ICTV) (King et al., 2011). Moreover, both phages possess a B1 morphotype (Ackermann, 2001). The phages were named in accordance with the bacterial virus nomenclature set out by Kropinski et al., (2009).

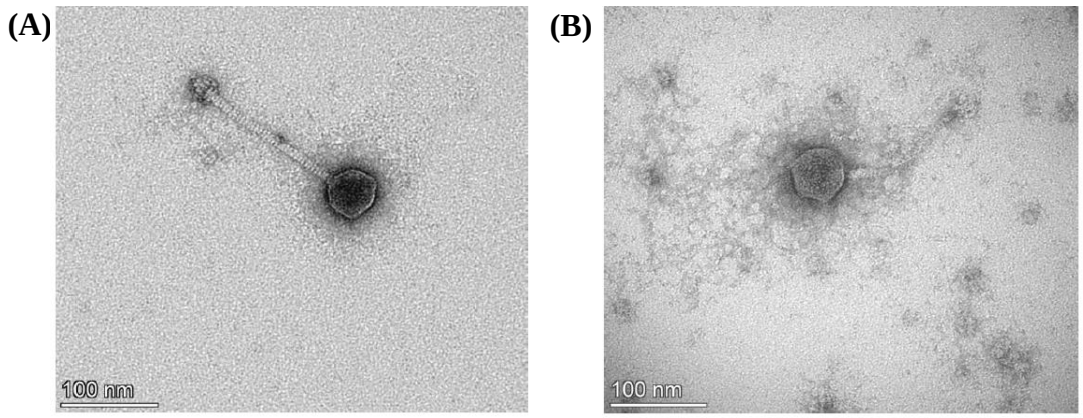

Figure 5.5 | Transmission electron micrographs of negatively stained *Staphylococcus* phages (A) HM1 and (B) BC1 using 2% (w/v) uranyl acetate. Scale bar represents 100 nm.

5.4.4 Bioinformatic Analysis

5.4.4.1 Genome Overview

Both phages were found to possess linear, double-stranded DNA (dsDNA) genomes. Phage HM1 had a genome size of 40,674 bp, with a coverage of 85.9, an average G+C content of 35.88% and 65 ORFs. Phage BC1 exhibited a genome size of 42,161 bp, with a coverage of 56.1, an average G+C content of 36% and 66 ORFs. Based on the classification scheme (Kwan et al., 2005), the genome sizes of both phages designate

them as class II staphylococcal phages (~40 kb). Of the total ORFs identified, 29 ORFs (44.62%) in phage HM1 and 33 ORFs (50%) in phage BC1 could be assigned a specific function, while the remaining ORFs were designated as hypothetical proteins. The first five ORFs and the final ORF of both phages were found to be in the reverse orientation, while all other ORFs were in the forward orientation. The average gene product sizes for phage HM1 and phage BC1 were 238 and 251 amino acids, respectively. Both phage genomes were found to exhibit a modular structure typical of temperate staphylococcal *Siphoviridae* phages. These modules consist of gene clusters representing each of the following functions: lysogeny, DNA replication, gene expression, DNA packaging, head morphogenesis, tail morphogenesis, and lysis (Ingmer et al., 2019). The presence of ORF1, encoding DNA integrase, confirmed the lysogenic nature of both phages. Additional typical lysogen-related proteins, such as repressor (ORF05), HTH cro/C1 type (ORF06) and antirepressor (ORF07), were also identified. The classification of both phages as temperate was further supported by lifestyle prediction software (PhageLeads, PHACTS, and PhageAI). Both genomes exhibited several annotated ORFs related to DNA replication and gene expression, including host-nuclease inhibitor protein Gam, essential recombination function protein, single-stranded DNA-binding protein, putative HNHc nuclease, replication initiation protein, putative acetyltransferase, dUTPase, transcriptional activators RinB and RinA, terminase small and large subunits, and portal protein. The head and tail morphogenesis modules in phage HM1 and phage BC1 start at ORF 39 and ORF 40, respectively, which encode the prohead protein. Other identified ORFs related to phage morphology include scaffold protein, major capsid protein, head-tail adapter, putative tail-component, major tail protein, tail assembly chaperone protein, tape measure protein, distal tail protein, tail protein, putative major teichoic acid biosynthesis protein C and baseplate upper protein. Lysis-related ORFs begin at ORF59 in HM1 and ORF60 in BC1, encoding a mannosyl-glycoprotein endo-beta-N-acetylglucosaminidase, followed by ORFs encoding a tail fiber protein, holin, and endolysin. The final annotated ORF in both genomes was acetyltransferase. Notably, no ORFs were found to encode tRNAs, virulence factors, or antibiotic-resistance genes. The complete annotated genome sequences of phage BC1 and phage HM1 are shown as circular genome maps in Figure 5.6 and Table S5.4 and Table S5.5.

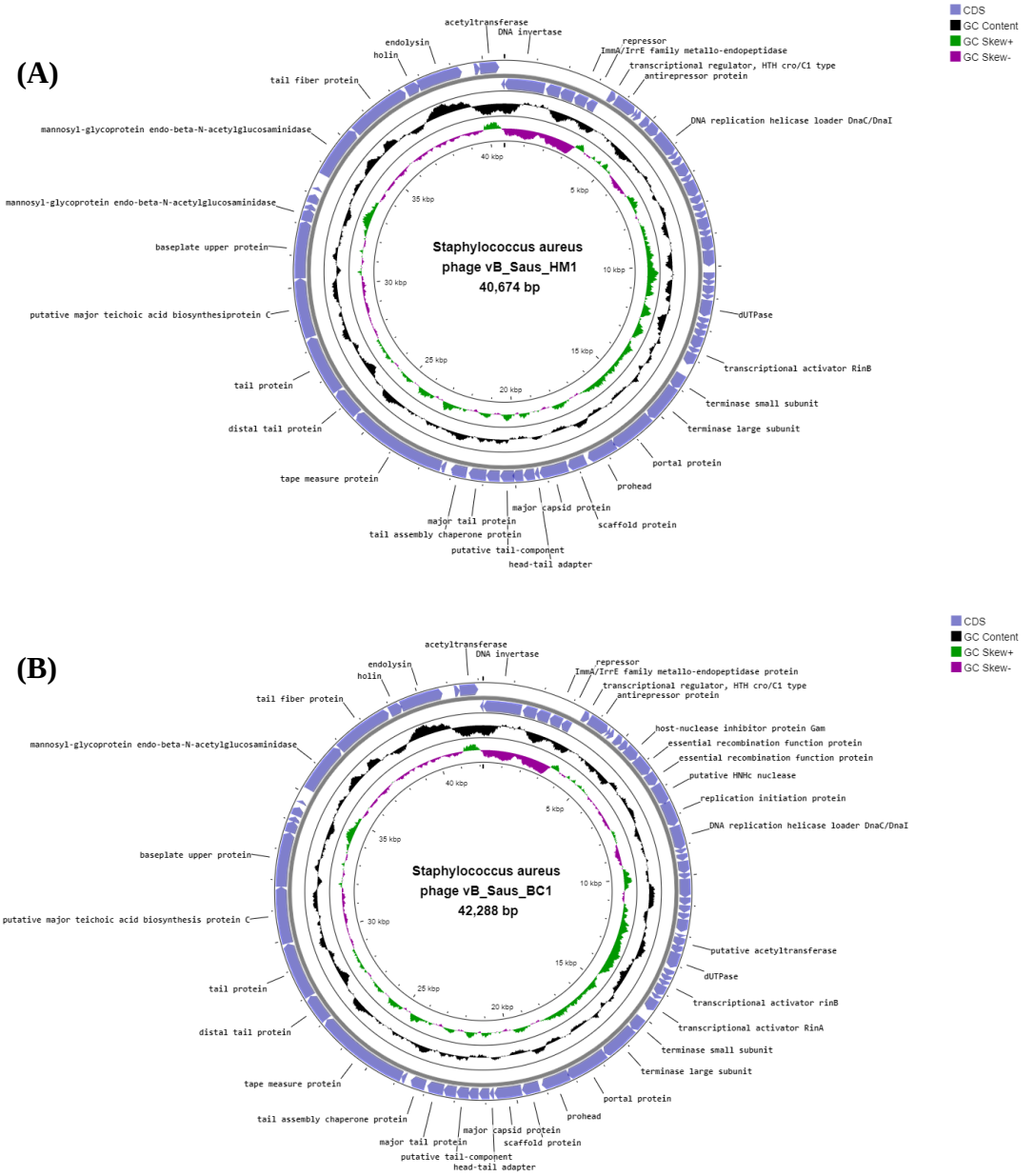

Figure 5.6 | Summary of the genomic organisation of the genomes of *Staphylococcus* phages HM1 and BC1. On the outer ring, putative open reading frames (ORFs) are represented by purple arrowheads labelled with predicted function where possible. On the middle ring is shown GC content relative to the mean GC content of the genome. On the inner ring, GC shew is illustrated where green represents a positive skew and purple a negative skew. Created using ProKsee.

5.4.4.2 Comparative genomics

Based on genome-wide nucleotide identity using the BLASTN algorithm (coverage multiplied by identity), phage HM1 and phage BC1 exhibited a nucleotide homology of 86.97%. According to the guidelines of the International Committee on Taxonomy of Viruses (ICTV) (Turner et al., 2021), a shared nucleotide similarity of <95%, but ≥70% sequence similarity indicates that both phages represent novel species. CoreGenes analysis indicated that phage HM1 and phage BC1 share 56 proteins (Table S5.6). Feature variations were primarily located in the DNA replication and packaging regions (Figure 5.7). Specifically, ORFs encoding hypothetical proteins, dUTPase, transcriptional activator rinA, single-stranded DNA-binding protein, essential recombination function protein and host-nuclease inhibitor protein Gam were identified as non-homologous (Table S5.6). To explore the phylogenetic neighbourhood of phage HM1, the whole genome was aligned against the NCBI nucleotide database using the megablast algorithm. The analysis revealed that *Staphylococcus* phage DW2 (NC_024391.1) had the highest level of similarity, exhibiting 95.29% identity over 85% of the phage HM1 genome. Other closely related nucleotide sequences included *Staphylococcus* phage Vb_SauS_I73, sharing 92.14% identity over 65% of the genome, and *Staphylococcus* phage B166 (NC_028859.1), with 94.52% identity over 63% of the phage HM1 genome. The top 25 phages identified with high similarity to phage HM1 (> 80% sequence identity over 49% - 85% coverage) are outlined in Table S5.7. Similarly, aligning the BC1 genome against the NCBI nucleotide database showed that phage DW2 had the highest level of similarity, exhibiting 95.29% identity over 94% of the BC1 genome. Other closely related nucleotide sequences included *Staphylococcus* phage vB_SauS_I73 (OM439672.1), sharing 92.14% identity over 66% of the genome, and *Staphylococcus* phage B122 (NC_054979.1), with 94.5% identity over 55% of the BC1 genome. Table S5.7 outlines the top 25 phages identified with high similarity to BC1 (>80% sequence identity over 51%-94% coverage). Pairwise comparisons of phage HM1 and phage BC1 with the aforementioned most closely related phages are shown in Figure 5.8. The major variations among these phages are primarily located in their lysogeny, DNA replication, and packaging regions. High levels of homology were observed in ORFs encoding genes for head morphogenesis, tail morphogenesis, and lysis. Additional analysis with CoreGenes indicated that phage HM1, phage BC1 and phage DW2 share 47 proteins.

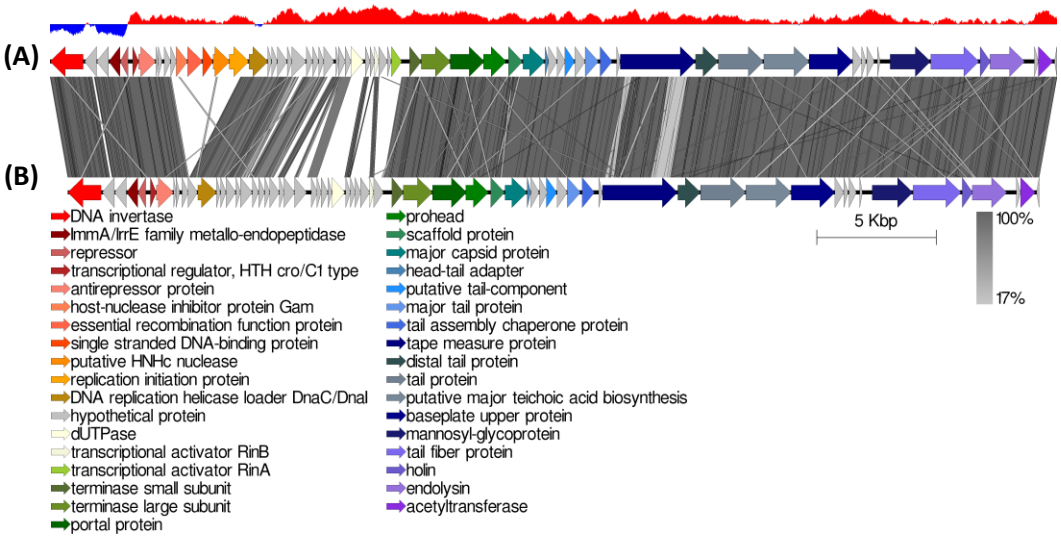

Figure 5.7 | Linear genome map and genome comparisons of *Staphylococcus* phages BC1 (A) and HM1 (B) employing BLASTn and visualisation with Easyfig. The genome maps display arrows indicating the locations and orientation of ORFs among different phage genomes. Arrows have been colour-coded describing their predicted roles (see key). Regions of grey between the two genomes depict sequence similarity, shaded according to % tBLASTx identity as shown in the key (bottom right). The genome annotations are color-coded according to function, as shown in the key. The graph above phage BC1 shows variation above (red) and below (blue) the average GC content (49.97%; black line).

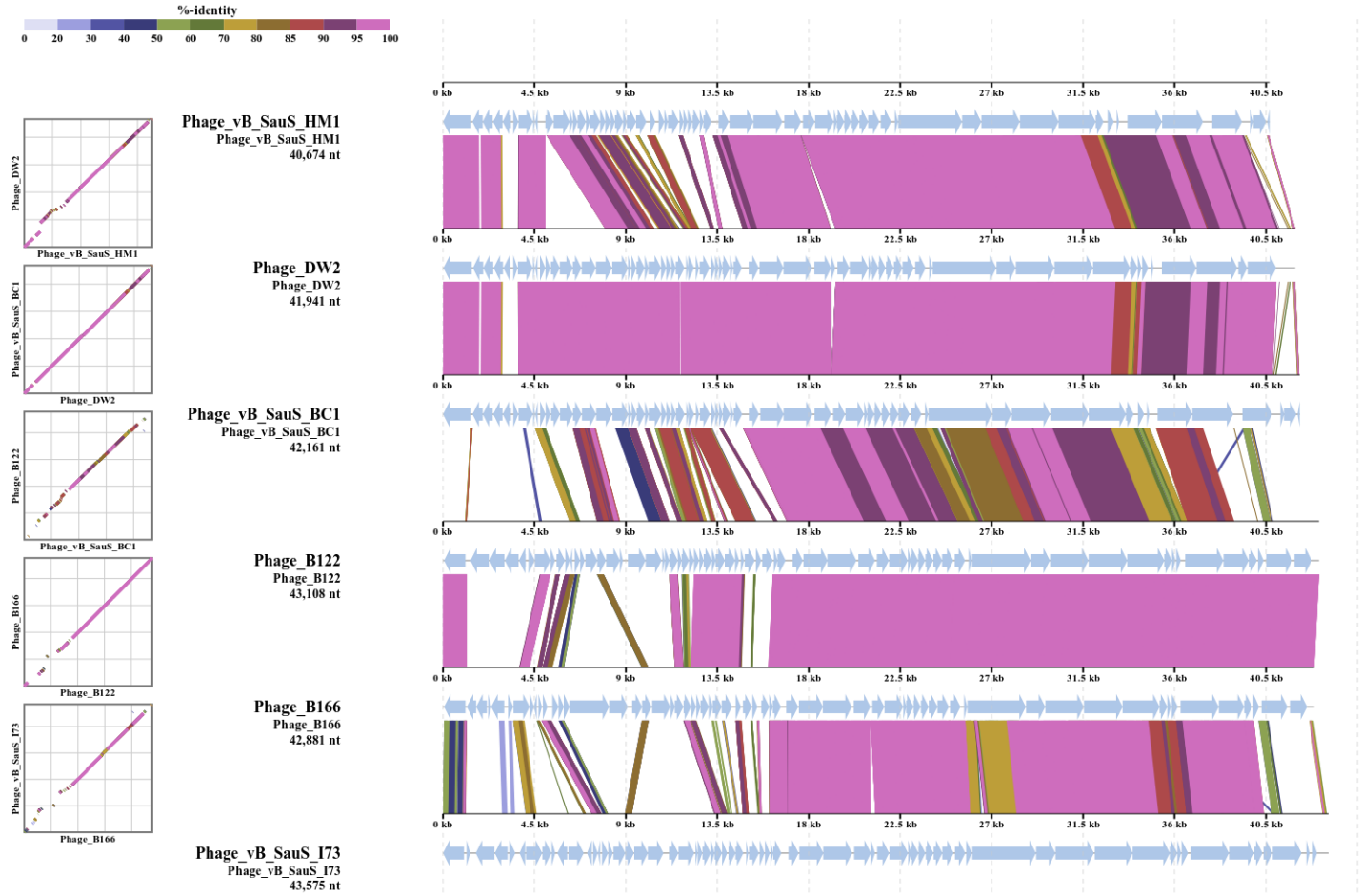

Figure 5.8 | Pairwise comparison of the genomes of Staphylococcus phages HM1 and BC1 with the genomes of Staphylococcus phages DW2, vB_SauS_I73, B122 and B166 using ViPTree. Genomes are represented linearly and the direction of the arrows is in line with transcription direction of each coding sequence (CDS). All tBLASTx alignments are represented by coloured lines between two genomes. Colour scale represents the tBLASTx percent identity.

Proteome-based phylogeny was employed to compare phage HM1 and phage BC1 with 803 and 862 closely related phages, respectively, using VipTree. Phage HM1, phage BC1 and phage DW2 were clustered together with other *Siphoviruses* whose bacterial hosts belong to the class *Bacillota* (Figure 5.9A). For the construction of a rectangular proteomic tree, phage BC1, HM1, and the top 50 phages with the highest VipTree SG were selected (Figure 5.9B). The rectangular proteomic tree grouped BC1 and HM1 with other *Siphoviruses* in a clade that is distinct from *Siphoviruses* of subfamily *Azerdovirinae* with $S_G \leq 0.05$.

Amino acid sequence-based whole-genome comparison was conducted using VICTOR, and the resulting phylogram (formula, D4, yielding an average support of 34%), supported the placement of both phages into subfamily *Azeredovirinae* and genus *Phietavirus* (Figure 5.10A). To complement the VICTOR results, VIRIDIC was employed to calculate intergenomic similarities among phage HM1, phage BC1 and closely related phages (Figure 5.10B). Unlike VICTOR, VIRIDIC can analyse more than 100 genomes; however, it cannot determine relationships between phages with similarity below 65%. Therefore, phages exhibiting intergenomic similarity above 60% with phage HM1 and phage BC1 were shortlisted, and their analysis results were visually represented as a heat map (Figure 5.10B). The calculated intergenomic similarity analysis using VIRIDIC for phage HM1, BC1 and 42 RefSeq genomes of the genus *Phietavirus* are provided in the supplementary material (Table S5.9). VIRIDIC clustered phage HM1, phage BC1 and the selected 13 phages into 15 species clusters, with each phage occupying a distinct species. At the genus level, VIRIDIC clustered the phages into nine different genera, and notably, phage HM1, phage BC1 and phage DW2 were placed in the same genus cluster (Figure 5.10A). The intergenomic similarity between phage HM1 and phage BC1 was determined to be 92.7%, while the similarity between phage HM1 and phage DW2 was 81.1% (Figure 5.10B). Likewise, the intergenomic similarity between phage BC1 and DW2 was 88.6% (Figure 5.10B). These results establish that these three phages belong to the same genus, but different species (default VIRIDIC similarity thresholds: 95% for species and 70% for genus). Another protein-protein network-based approach, PhageCloud was employed to investigate the genomic relationship of phage HM1 and phage BC1 with phage genomes on NCBI-GenBank. Of 5,240 analysed complete genomes, using the most stringent parameters (0.1 distance), 15 phages were top matched to HM1 and BC1 and with a distance range of 0.02 to 0.1 (Figure S5.1). Several of the top matched phages were also identified as closely related phages in the VICTOR and VIRIDIC analyses, further supporting their genomic similarity (Table S5.10 and Table S5.11). Accordingly,

phylogenetic analysis based on conserved signature proteins (i.e., major capsid protein, terminase large subunit and portal protein) was performed (Figure 5.11). In this analysis, phage HM1 and phage BC1 were monophyletic to each other (Figure 5.11).

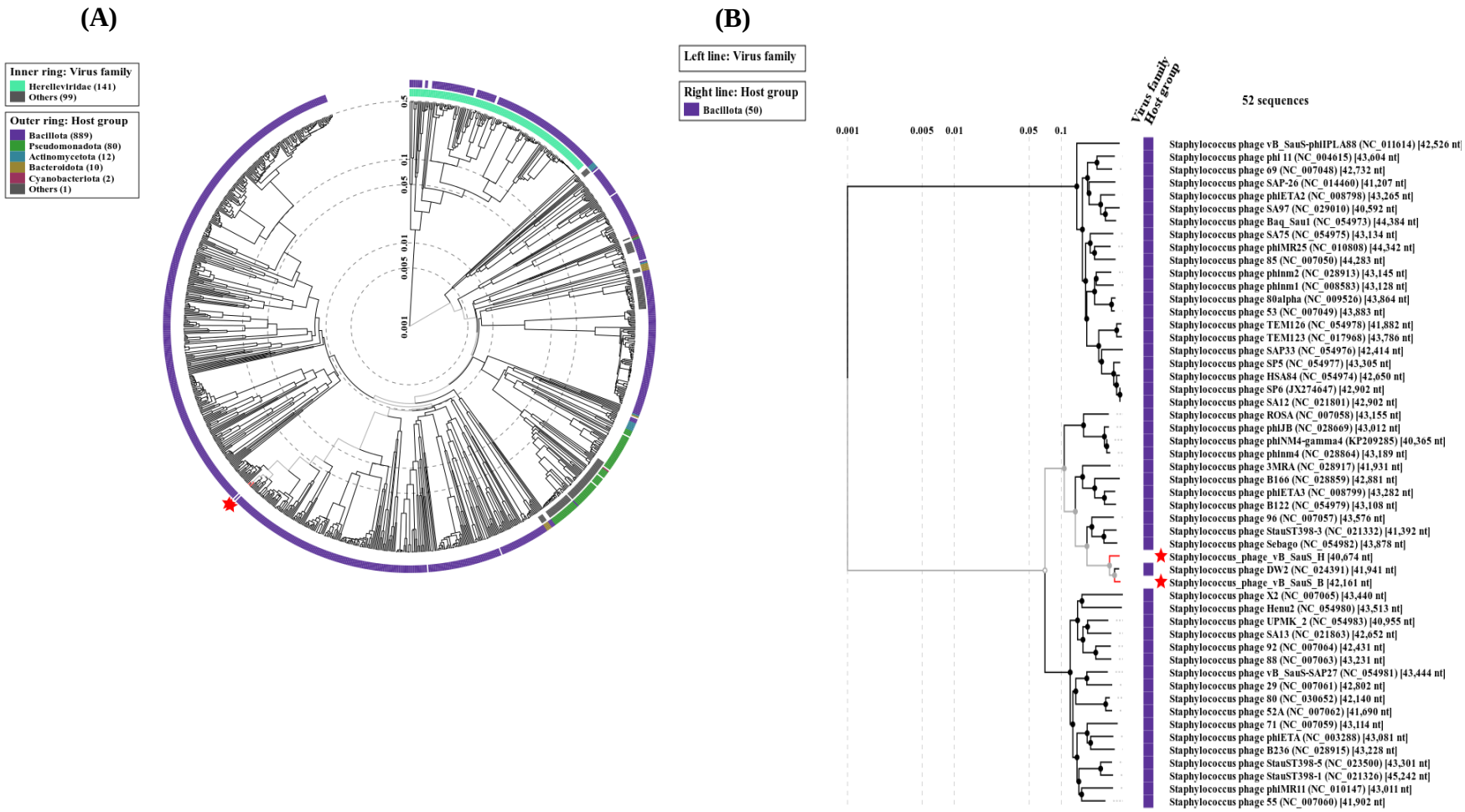

Figure 5.9 | Proteomic trees of *Staphylococcus* phages HM1 and BC1. (A) Circular proteomic tree based on genome-wide similarities of phage HM1 and phage BC1 (marked with a red star), top matches on BLASTn, and 1013 closely related reference phage genomes. (B) Rectangular proteomic trees of phage HM1 and phage BC1 50 phages with highest ViPTree SG scores.

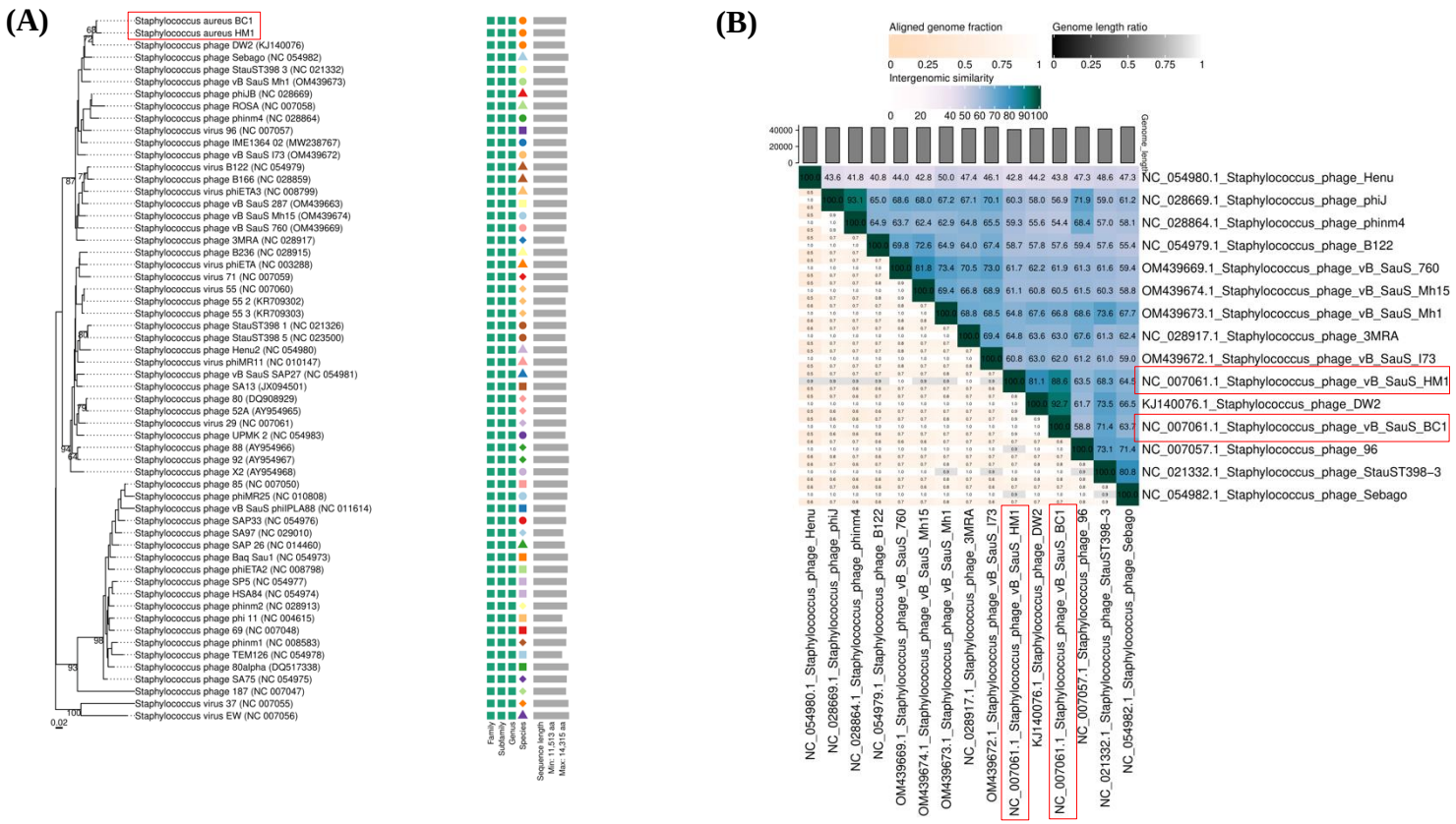

Figure 5.10 | (A) VICTOR generated phylogenomic GBDP trees of *Staphylococcus* phage HM1 and phage BC1 and 56 members of the *Azeredovirinae* subfamily inferred using formula D4 and yielding average support of 34 %. The numbers above branches are GBDP pseudobootstrap support values from 100 replications. Members of the *Phietavirus* and *Dubowvirus* genus are illustrated. (B) VIRIDIC heatmap for the intergenomic similarity between phage HM1, phage BC1 and closely related phages according to genome BLASTn top hits. Three factors of the alignment capacity were considered to calculate the relatedness between the phages: intergenomic similarities (hue of green to blue), the percentage of aligned genome sequence in a pair (shade of pink) and their length ratio (shade of black).

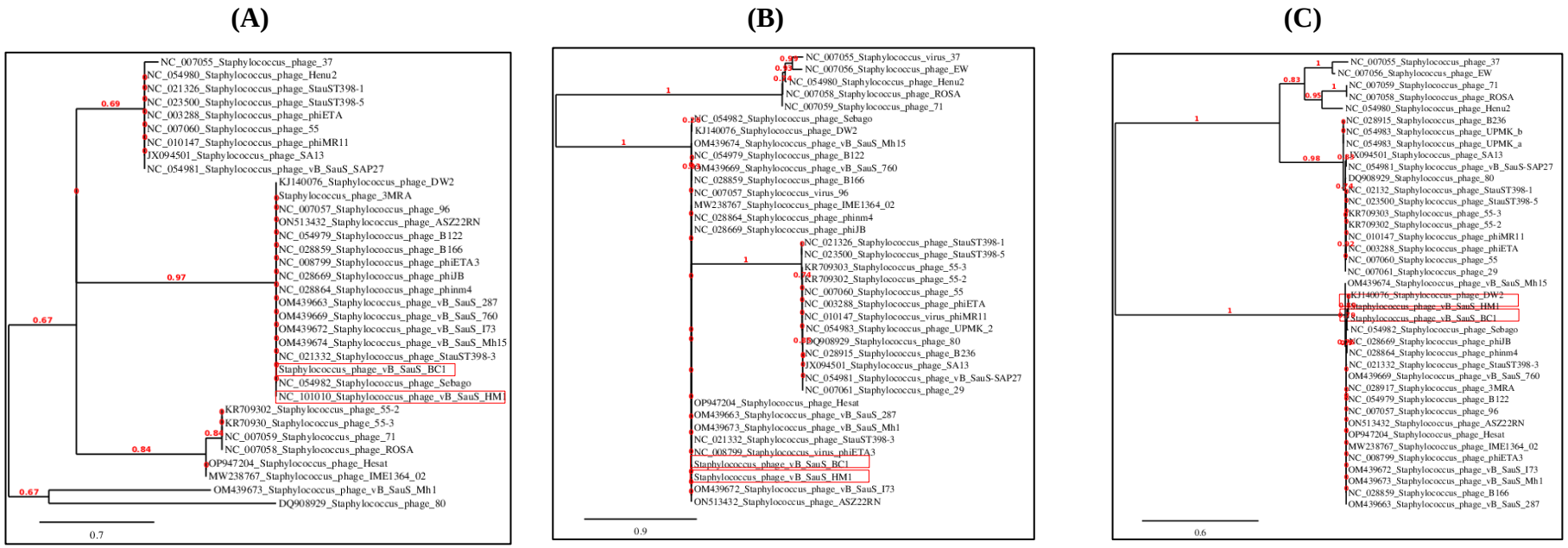

Figure 5.11 | Viral conserved signature protein-based phylogenetic tree. Phylogenetic trees for the evolutionary relatedness of the (A) major capsid protein, (B) large terminase and (C) portal proteins of phage HM1, phage BC1 and their orthologs in closely related phages. Phages included in the evolutionary analysis were chosen based on the closest relatives according to the proteomic tree, intergenomic similarity analysis and whether they had a gene annotated for the aforementioned genes in their Genbank file. The phylogenetic distance was inferred by the Maximum likelihood method and supported with a bootstrap of 1000 replicates, and the trees were constructed by MEGA11. Phage HM1 and phage BC1 clusters are outlined in red based on the protein homology in both trees of the highest log likelihood (-12536.16, -5522.81 and -1839.71, respectively).

5.5 Discussion

S. aureus, known to coexist harmlessly as a commensal bacterium, can transform into a formidable pathogen capable of causing severe and life-threatening infections. The current global AMR crisis has further complicated the treatment of *S. aureus* infections, necessitating the exploration of alternative therapeutic strategies. Phage therapy has emerged as one of the most promising avenues for combating *S. aureus* infections. *S. aureus* phages have been isolated from a vast range of ecological niches. While the bioactive compositions of bovine colostrum and human breast milk have been extensively studied, the investigation and isolation of phages from these sources remain largely unexplored. Therefore, in this study we isolated and assessed the therapeutic potential of lytic or temperate *S. aureus* phages derived from bovine colostrum and human breast milk.

The difficulty in direct isolation of phages from milk has been previously noted (Titze et al., 2020). In our study, attempts to isolate phages directly from colostrum and human milk samples proved unsuccessful, therefore an enrichment step was required. Subsequently, clear zones of lysis were observed against the *S. aureus* strain DPC5245, which was selected as the host strain for further analysis. *S. aureus* DPC5245 is a bovine mastitis clinical isolate, used in numerous previous studies for the study of anti-staphylococcal phages (Fitzgerald et al., 1997, O'Flaherty et al., 2005b, O'Flaherty et al., 2005c). Following similar studies on lytic and temperate phages effective against pathogenic *S. aureus* strains, laboratory tests were conducted to assess the therapeutic applicability of the phages isolated in this study (Ding et al., 2018, Zhang et al., 2022, Wang et al., 2016, Ajuebor et al., 2018, Liu et al., 2022). A thorough evaluation of phage characteristics is crucial to maximize their potential as effective alternatives for combating antimicrobial-resistant bacterial infections (Fernández et al., 2019, Philipson et al., 2018). One of the most significant obstacles to developing generalised phage therapy is the narrow host range of phages. Therefore, phages with broad host ranges are preferred for therapeutic applications (Ross et al., 2016). Enrichment using multiple host bacteria is an efficient approach to enable isolation of phages with broad host ranges (Ross et al., 2016). Furthermore, due to the homogenous structures of *S. aureus* bacteria, phages against *S. aureus* are typically reported to have a relatively broad host range (Göller et al., 2021). Phage HM1 and

phage BC1 exhibited a wide host range and high EOP values against the screened *S. aureus* strains. Phage HM1 was able to infect more strains than phage BC1. When combined as a cocktail, the host range was equal to that of phage HM1. Importantly, both phages demonstrated specificity to *S. aureus* strains, which is advantageous for therapeutic applications as it reduces the risk of disrupting the natural microbial balance in the host (Fernández et al., 2019). Both phages exhibited rapid adsorption rates and potent antibacterial activity across a range of MOI values (1 - 0.0001). Phages typically exhibit limited stability in solution and substantial decreases in concentration during processing and storage (Durr and Leipzig, 2023). This poses a challenge for their development as regulated pharmaceuticals, where maintaining stable dosage and precisely defined pharmacokinetics and pharmacodynamics are essential requirements (Malik et al., 2017). Phage HM1 and phage BC1 demonstrated good stability under different temperatures (24–50 °C), pH (5−9), chloroform and UV exposure conditions. One-step growth curve experiments demonstrated that both phages exhibit latent periods and burst sizes comparable to *S. aureus* phages with favourable characteristics for therapeutic applications (Zhang et al., 2022, Feng et al., 2021, Abdurahman et al., 2021). Finally, whole genome sequencing demonstrated that these two phages did not encode virulence factors, or antibiotic-resistance genes, which are essential prerequisite for therapeutic phages.

To evaluate the efficacy of host growth inhibition, a number of assays were performed as previously explored with *S. aureus* phages (Chang et al., 2019). A major limitation of phage therapy is the emergence of phage-resistant bacteria (Oromí-Bosch et al., 2023). Like antibiotics, phages impose strong selective pressures on their hosts to evolve resistance and prevent attack. These cellular mechanisms typically involve modifying or blocking phage host receptors, as well as the CRISPR-Cas system described as adaptive immunity for prokaryotes (Gummalla et al., 2023). BIMs were readily formed against phage HM1 and phage BC1 and high rates of lysogeny were observed. Phage cocktails have frequently been reported to offer a lower frequency of BIM emergence (Kebriaei et al., 2023). Encouragingly, in our study, the utilisation of phage HM1 and phage BC1 as a cocktail resulted in a one-log decrease in the rate of BIM development compared to their individual application. Regarding bacterial challenge assays, our study revealed that the application of phage HM1 or phage BC1 individually initiated host cell lysis after 5 h, which continued for 28 h. However,

beyond this time frame, the growth inhibition was no longer sustained, possibly suggesting the emergence of BIMs. Promisingly, the utilisation of HM1 and BC1 as a cocktail initiated host cell lysis after 3 hours, which was sustained for the 32 h duration of the experiment, further supporting the consensus that phage cocktails are effective at lowering the frequency of BIM emergence.

The difficulty of phage replication in the complex medium of milk has been reported previously (O'Flaherty et al., 2005a, Titze et al., 2020). This represents a major obstacle to the utilisation of phages for controlling *S. aureus* infections causing conditions such as mastitis. Temperate, lytic and virulent mutant phages have been explored to reduce *S. aureus* in milk (Kwak et al., 2023, Chang et al., 2019, García et al., 2009)**.** In this study, the utility of phage HM1 and phage BC1 individually or as a cocktail to reduce *S. aureus* in pasteurised, raw, and mastitic milk was assessed. Control samples containing *S. aureus* strain DPC5245 displayed a steady increase in the bacterial count in all milk sample types. Addition of phages, either alone or in combination as a cocktail to each of the milk sample types prevented the growth of *S. aureus* strain DPC5245. The phage cocktail displayed superior decreases in *S. aureus* strain DPC5245 bacterial counts in all milk sample types compared to the application of individual phages. The magnitude of bacterial growth reduction gradually decreased from pasteurised milk samples to raw and mastitic milk samples. Mastitic milk typically displays higher levels of somatic cells, bacterial load and alterations in the concentration of various components such as fat, protein, lactose, and minerals compared to pasteurised milk (Gonçalves et al., 2020). Such compositional changes may have affected the reduction in *S. aureus* bacterial counts observed in this study. Previous studies using similar experimental designs have achieved significantly higher reduction in *S. aureus*-contaminated milk samples using lytic phage cocktails (Titze et al., 2020, García et al., 2009).

Morphological and bioinformatics analysis confirmed that phage HM1 and phage BC1 are novel species belonging to the subfamily *Azeredovirinae* in the family *Siphoviridae*. Whole genome sequencing demonstrated that phage HM1 and phage BC1 contained genes typically reported in the functional modules of temperate staphylococcal *Siphoviridae* phages (Ingmer et al., 2019). Phylogenetic analysis indicated that phage HM1 and BC1 shared a number of characteristics with members

of the *Phietavirus* genus. In particular, they established a distinct clade with phage DW2, which was previously isolated from farmyard effluent, using *S. aureus* DPC5246 (O'Flaherty et al., 2005b). The high level of homology between *Staphylococcus* phages HM1, BC1 and DW2 raises questions regarding the origins of the novel phages described in this study. *S. aureus* isolates are typically known to carry multiple prophages in their genomes (Ingmer et al., 2019). Therefore, it is highly likely that phage HM1 and phage BC1 originated as prophages present in the screening strains belonging to the DPC culture collection used in the enrichment step, rather than from the bovine colostrum and human milk samples. CoreGenes analysis indicated that lysis-related genes were homologous between *Staphylococcus* phages HM1, BC1 and DW2. The endolysin of these phages consists of a C-terminal SH3b cell wall binding domain (398–466aa) and two peptidoglycan hydrolysing domains (Keary et al., 2014). The peptidoglycan hydrolysing domains consist of a centrally located N-acetylmuramoyl-l-alanine amidase domain (188–338aa), which cleaves the peptidoglycan bond between the N-acetylmuramoyl residues and L-amino acid residues and an N-terminal cysteine, histidine-dependent amidohydrolases/peptidases (CHAP) domain (13–148aa). CHAP domains are exclusive to phages that target Gram-positive bacteria and exhibit functional diversity, as CHAP domains from various phages are known to specifically cleave different bonds within the peptidoglycan structure (Broendum et al., 2018). This functional domain pattern is prevalent among the endolysins of staphylococcal phages, including those with diverse morphology and genome sizes (Ingmer et al., 2019). These phages also contain a phage tail hydrolase, consisting of a C-terminal lysozyme 2 (Lyz_2) subfamily domain (413–559aa) and a truncated N-terminal CHAP (2–86aa). In previous studies of phage DW2, recombinant proteins based on the endolysin and tail hydrolase were produced and shown to be lytic against the bovine mastitis-associated isolate, *S. aureus* DPC5246 (Keary et al., 2014). Despite the high level of homology between phages HM1, BC1 and DW2, a number of interesting differences were observed. For instance, phage HM1 and phage BC1 showed no lytic activity towards *S. aureus* DPC5246, the strain on which phage DW2 is routinely propagated(O'Flaherty et al., 2005b). Furthermore, ORF15 and ORF24 of phage DW2 were shown to encode two major virulence-related genes (Keary et al., 2014). However, ORF15 and ORF24 of phage DW2 showed no homology to ORFs present in phage HM1 and phage BC1.

While the phages described in this study show good antibacterial activity and therapeutic characteristics, their temperate nature is a limitation of using them in their current form. For instance, a recent study demonstrated that the temperate *Staphylococcus* phage PHB21, which did not contain antimicrobial resistance or virulence genes, enhanced the virulence of MRSA strains by increasing transcription of multiple virulence factor genes after integration into the host genome (Yang et al., 2022). Therefore, temperate phages, even those not carrying harmful genes, may also pose safety problems. A DNA random deletion method based on treatment with pyrophosphate has been used in numerous studies to mutate temperate phages to lytic phages (Gutiérrez et al., 2018). Two recent studies have used this method to mutate temperate *S. aureus* phages (Wang et al., 2023, Chang et al., 2019). The therapeutic characteristics of the phages were not negatively affected and the BIM frequency was decreased once mutated (Wang et al., 2023, Chang et al., 2019). This method represents a simple but potent way to increase the therapeutic potential of temperate phages. Therefore, future studies should involve subjecting phage HM1 and phage BC1 to phage-mutation assays.

Although our assays were conducted on a small scale, the results support the consensus that phage cocktails may be effective at overcoming bacterial resistance to phage infections (Oromí-Bosch et al., 2023). The three most common *S. aureus*-bacteriophage families are *Myoviridae*, *Podoviridae* and *Siphoviridae*. Therefore, an optimal phage cocktail to fight *S. aureus* would thus include bacteriophages of all three families, with the idea that point mutations which eliminate the receptor of one bacteriophage might not automatically lead to the exclusion of the other bacteriophages in the cocktail. Hence, future studies should explore combining phages HM1 and BC1 with *S. aureus* phages of the *Myoviridae* and *Podoviridae* families. With regards to studies which could utilise the phages without any genetic engineering, a potential experiment could explore combining antibiotic treatment with phage treatment. For instance, temperate phage-antibiotic synergy was shown to eradicate pathogenic *Escherichia coli in vitro* through the depletion of lysogens (Al-Anany et al., 2021). Another study of these phages could explore their utility against biofilm formation, which plays a key role in the pathogenesis of MRSA (Tong et al., 2015, Doulgeraki et al., 2017).

In summary, this study presents two novel temperate phages vB_SauS_HM1 and vB_SauS_BC1. *In vitro* analysis revealed that these phages have a number of favourable characteristics for potential therapeutic applications against *S. aureus* infections. Furthermore, either individually or applied as a cocktail, they displayed the ability to reduce the bacterial growth of *S. aureus* in pasteurised, raw and mastitic milk samples. Bioinformatics analysis showed that these phages belong to subfamily *Azeredovirinae* and genus *Phietavirus.* As temperate phages are not recommended for phage therapy, future studies should explore genetic engineering techniques to make these phages applicable for phage therapy.

5.6 Acknowledgements

We would like to extend our thanks to the farmers who assisted with the sample collections. We thank Professor Colin Hill and Dr. Colin Buttimer for support in CsCl gradient preparations and bioinformatic analysis. We thank Prof. Aidan Coffey for providing MRSA strains from St. James' Hospital for host range screening. We thank Dr Horst Neve and his transmission electron microscopy team at the Max Rubner-Institut, Germany for performing TEM imaging.

5.7 Financial Support

Science Foundation Ireland funding to APC Microbiome Ireland and Vistamilk. DAFM funding of Project 2022IRLNZ114, entitled RUmen microbiome MINING for bacterial cultures to reduce methane.

5.8 Ethics

None required/ Not applicable

5.9 Conflict of Interest

None declared

5.10 References

ABDURAHMAN, M., TOSUN, I., DURUKAN, I., KHORSHIDTALAB, M. & KıLıÇ, A. 2021. Four temperate bacteriophages from methicillin-resistant Staphylococcus aureus show broad bactericidal and biofilm removal activities. Kafkas Universitesi Veteriner Fakultesi Dergisi, 27.

ABEDON, S. T., DANIS-WLODARCZYK, K. M. & WOZNIAK, D. J. 2021. Phage Cocktail Development for Bacteriophage Therapy: Toward Improving Spectrum of Activity Breadth and Depth. Pharmaceuticals (Basel), 14.

ACKERMANN, H. W. 2001. Frequency of morphological phage descriptions in the year 2000. Archives of virology, 146, 843-857.

ADKINS, P. R. F. & MIDDLETON, J. R. 2017. Laboratory handbook on bovine mastitis, National Mastitis Council, Incorporated.

AJUEBOR, J., BUTTIMER, C., ARROYO-MORENO, S., CHANISHVILI, N., GABRIEL, E. M., O'MAHONY, J., MCAULIFFE, O., NEVE, H., FRANZ, C. & COFFEY, A. 2018. Comparison of Staphylococcus phage K with close phage relatives commonly employed in phage therapeutics. Antibiotics, 7, 37.

AL-ANANY, A. M., FATIMA, R. & HYNES, A. P. 2021. Temperate phage-antibiotic synergy eradicates bacteria through depletion of lysogens. Cell Reports, 35, 109172.

ANGELOPOULOU, A., WARDA, A. K., HILL, C. & ROSS, R. P. 2019. Non-antibiotic microbial solutions for bovine mastitis–live biotherapeutics, bacteriophage, and phage lysins. Critical reviews in microbiology, 45, 564-580.

ARNDT, D., GRANT, J. R., MARCU, A., SAJED, T., PON, A., LIANG, Y. & WISHART, D. S. 2016. PHASTER: a better, faster version of the PHAST phage search tool. Nucleic acids research, 44, W16-W21.

ARROYO-MORENO, S., BUTTIMER, C., BOTTACINI, F., CHANISHVILI, N., ROSS, P., HILL, C. & COFFEY, A. 2022. Insights into Gene Transcriptional Regulation of Kayvirus Bacteriophages Obtained from Therapeutic Mixtures. Viruses, 14, 626.

ATSHAN, S. S., HAMAT, R. A., ALJABERI, M. A., CHEN, J.-S., HUANG, S.-W., LIN, C.-Y., MULLINS, B. J. & KICIC, A. 2023. Phage Therapy as an Alternative Treatment Modality for Resistant Staphylococcus aureus Infections. Antibiotics, 12, 286.

AZIZ, R. K., BARTELS, D., BEST, A. A., DEJONGH, M., DISZ, T., EDWARDS, R. A., FORMSMA, K., GERDES, S., GLASS, E. M. & KUBAL, M. 2008. The RAST Server: rapid annotations using subsystems technology. BMC genomics, 9, 1-15.

BAILEY, T. L., BODEN, M., BUSKE, F. A., FRITH, M., GRANT, C. E., CLEMENTI, L., REN, J., LI, W. W. & NOBLE, W. S. 2009. MEME SUITE: tools for motif discovery and searching. Nucleic acids research, 37, W202-W208.

BALCHA, F. B. & NEJA, S. A. 2023. CRISPR-Cas9 mediated phage therapy as an alternative to antibiotics. Animal Diseases, 3, 1-11.

BIOINFORMATICS, B. 2019. FastQC: A quality control tool for high throughput sequence data. Version 0.11. 9.

BORODOVICH, T., SHKOPOROV, A. N., ROSS, R. P. & HILL, C. 2022. Phage-mediated horizontal gene transfer and its implications for the human gut microbiome. Gastroenterology Report, 10.

BREYNE, K., HONAKER, R. W., HOBBS, Z., RICHTER, M., ŻACZEK, M., SPANGLER, T., STEENBRUGGE, J., LU, R., KINKHABWALA, A. & MARCHON, B. 2017. Efficacy and safety of a bovine-associated Staphylococcus aureus phage cocktail in a murine model of mastitis. Frontiers in microbiology, 8, 2348.

BROENDUM, S. S., BUCKLE, A. M. & MCGOWAN, S. 2018. Catalytic diversity and cell wall binding repeats in the phage-encoded endolysins. Molecular microbiology, 110, 879-896.

BROUILLETTE, E., MILLETTE, G., CHAMBERLAND, S., ROY, J.-P., STER, C., KIROS, T., HICKEY, S., HITTLE, L., WOOLSTON, J. & MALOUIN, F. 2023. Effective Treatment of Staphylococcus aureus Intramammary Infection in a Murine Model Using the Bacteriophage Cocktail StaphLyse™. Viruses, 15, 887.

BUSHNELL, B. 2014. BBMap: a fast, accurate, splice-aware aligner. Lawrence Berkeley National Lab.(LBNL), Berkeley, CA (United States).

CHAN, PATRICIA P., LIN, BRIAN Y., MAK, ALLYSIA J. & LOWE, TODD M. 2021. tRNAscan-SE 2.0: improved detection and functional classification of transfer RNA genes. Nucleic Acids Research, 49, 9077-9096.

CHANG, Y., BAI, J., LEE, J.-H. & RYU, S. 2019. Mutation of a Staphylococcus aureus temperate bacteriophage to a virulent one and evaluation of its application. Food microbiology, 82, 523-532.

CHANG, Y., SHIN, H., LEE, J.-H., PARK, C. J., PAIK, S.-Y. & RYU, S. 2015. Isolation and genome characterization of the virulent Staphylococcus aureus bacteriophage SA97. Viruses, 7, 5225-5242.

CHEUNG, G. Y. C., BAE, J. S. & OTTO, M. 2021. Pathogenicity and virulence of Staphylococcus aureus. Virulence, 12, 547-569.

DALMASSO, M., STRAIN, R., NEVE, H., FRANZ, C. M. A. P., COUSIN, F. J., ROSS, R. P. & HILL, C. 2016. Three new Escherichia coli phages from the human gut show promising potential for phage therapy. PloS one, 11, e0156773.

DAVIS, P., SETO, D. & MAHADEVAN, P. 2022. CoreGenes5. 0: An Updated User-Friendly Webserver for the Determination of Core Genes from Sets of Viral and Bacterial Genomes. Viruses, 14, 2534.

DEDRICK, R. M., SMITH, B. E., CRISTINZIANO, M., FREEMAN, K. G., JACOBS-SERA, D., BELESSIS, Y., WHITNEY BROWN, A., COHEN, K. A., DAVIDSON, R. M. & VAN DUIN, D. 2023. Phage Therapy of Mycobacterium Infections: Compassionate Use of Phages in 20 Patients With Drug-Resistant Mycobacterial Disease. Clinical infectious diseases, 76, 103-112.

DEREEPER, A., GUIGNON, V., BLANC, G., AUDIC, S., BUFFET, S., CHEVENET, F., DUFAYARD, J. F., GUINDON, S., LEFORT, V. & LESCOT, M. 2008. Phylogeny. fr: robust phylogenetic analysis for the non-specialist. Nucleic acids research, 36, W465-W469.

DING, B., LI, Q., GUO, M., DONG, K., ZHANG, Y., GUO, X., LIU, Q., LI, L. & CUI, Z. 2018. Prevention of dermal abscess formation caused by Staphylococcus aureus using phage JD007 in nude mice. Frontiers in Microbiology, 9, 1553.

DINLEYICI, M., PÉREZ-BROCAL, V., ARSLANOGLU, S., AYDEMIR, O., SEVUK OZUMUT, S., TEKIN, N., VANDENPLAS, Y., MOYA, A. & DINLEYICI, E. C. 2021. Human Milk Virome Analysis: Changing Pattern Regarding Mode of Delivery, Birth Weight, and Lactational Stage. Nutrients, 13.

DOULGERAKI, A. I., DI CICCIO, P., IANIERI, A. & NYCHAS, G.-J. E. 2017. Methicillin-resistant food-related Staphylococcus aureus: a review of current knowledge and biofilm formation for future studies and applications. Research in microbiology, 168, 1-15.

DURR, H. A. & LEIPZIG, N. D. 2023. Advancements in bacteriophage therapies and delivery for bacterial infection. Materials Advances, 4, 1249-1257.

FARRIS, J. S. 1972. Estimating phylogenetic trees from distance matrices. The American Naturalist, 106, 645-668.

FENG, T., LEPTIHN, S., DONG, K., LOH, B., ZHANG, Y., STEFAN, M. I., LI, M., GUO, X. & CUI, Z. 2021. JD419, a Staphylococcus aureus phage with a unique morphology and broad host range. Frontiers in microbiology, 12, 602902.

FERNÁNDEZ, L., GUTIÉRREZ, D., GARCÍA, P. & RODRÍGUEZ, A. 2019. The Perfect Bacteriophage for Therapeutic Applications—A Quick Guide. Antibiotics [Online], 8.

FINN, R. D., MISTRY, J., TATE, J., COGGILL, P., HEGER, A., POLLINGTON, J. E., GAVIN, O. L., GUNASEKARAN, P., CERIC, G. & FORSLUND, K. 2010. The Pfam protein families database. Nucleic acids research, 38, D211-D222.

FITZGERALD, J. R., MEANEY, W. J., HARTIGAN, P. J., SMYTH, C. J. & KAPUR, V. 1997. Fine-structure molecular epidemiological analysis of Staphylococcus aureus recovered from cows. Epidemiology & Infection, 119, 261-269.

GARCÍA, P., MADERA, C., MARTÍNEZ, B., RODRÍGUEZ, A. & EVARISTO SUÁREZ, J. 2009. Prevalence of bacteriophages infecting Staphylococcus aureus in dairy samples and their potential as biocontrol agents. J Dairy Sci, 92, 3019-26.

GARNEAU, J. R., DEPARDIEU, F., FORTIER, L.-C., BIKARD, D. & MONOT, M. 2017. PhageTerm: a tool for fast and accurate determination of phage termini and packaging mechanism using next-generation sequencing data. Scientific reports, 7, 1-10.

GILCHRIST, C. L. M. & CHOOI, Y.-H. 2021. Clinker & clustermap. js: Automatic generation of gene cluster comparison figures. Bioinformatics, 37, 2473-2475.

GOFFART-ROSKAM, J. 1965. Quantitative study of sensitive and lysogenic bacteria surviving infection of a Staphylococcus by a temperate bacteriophage. Antonie van Leeuwenhoek, 31, 249-261.

GÖKER, M., GARCÍA-BLÁZQUEZ, G., VOGLMAYR, H., TELLERÍA, M. T. & MARTÍN, M. P. 2009. Molecular taxonomy of phytopathogenic fungi: a case study in Peronospora. PloS one, 4, e6319.

GÖLLER, P. C., ELSENER, T., LORGÉ, D., RADULOVIC, N., BERNARDI, V., NAUMANN, A., AMRI, N., KHATCHATOUROVA, E., COUTINHO, F. H. & LOESSNER, M. J. 2021. Multi-species host range of staphylococcal phages isolated from wastewater. Nature Communications, 12, 6965.

GONÇALVES, J. L., KAMPHUIS, C., VERNOOIJ, H., ARAÚJO JR, J. P., GRENFELL, R. C., JULIANO, L., ANDERSON, K. L., HOGEVEEN, H. & DOS SANTOS, M. V. 2020. Pathogen effects on milk yield and composition in chronic subclinical mastitis in dairy cows. The Veterinary Journal, 262, 105473.

GORDILLO ALTAMIRANO, F., FORSYTH, J. H., PATWA, R., KOSTOULIAS, X., TRIM, M., SUBEDI, D., ARCHER, S. K., MORRIS, F. C., OLIVEIRA, C. & KIELTY, L. 2021. Bacteriophage-resistant Acinetobacter baumannii are resensitised to antimicrobials. Nature microbiology, 6, 157-161.

GRANT, J. R., ENNS, E., MARINIER, E., MANDAL, A., HERMAN, E. K., CHEN, C.-Y., GRAHAM, M., VAN DOMSELAAR, G. & STOTHARD, P. 2023. Proksee: in-depth characterization and visualization of bacterial genomes. Nucleic Acids Research, gkad326.

GUMMALLA, V. S., ZHANG, Y., LIAO, Y.-T. & WU, V. C. H. 2023. The Role of Temperate Phages in Bacterial Pathogenicity. Microorganisms [Online], 11.

GUO, M., GAO, Y., XUE, Y., LIU, Y., ZENG, X., CHENG, Y., MA, J., WANG, H., SUN, J. & WANG, Z. 2021. Bacteriophage cocktails protect dairy cows against mastitis caused by drug resistant Escherichia coli infection. Frontiers in Cellular and Infection Microbiology, 11, 690377.

GUO, Y., SONG, G., SUN, M., WANG, J. & WANG, Y. 2020. Prevalence and therapies of antibiotic-resistance in Staphylococcus aureus. Frontiers in cellular and infection microbiology, 10, 107.

GUPTA, P., SINGH, H. S., SHUKLA, V. K., NATH, G. & BHARTIYA, S. K. 2019. Bacteriophage therapy of chronic nonhealing wound: clinical study. The international journal of lower extremity wounds, 18, 171-175.

GUTIÉRREZ, D., FERNÁNDEZ, L., RODRÍGUEZ, A. & GARCÍA, P. 2018. Practical method for isolation of phage deletion mutants. Methods and protocols, 1, 6.

HILL, C., MILLS, S. & ROSS, R. P. 2018. Phages & antibiotic resistance: are the most abundant entities on earth ready for a comeback? Future microbiology, 13, 711-726.

HITCHCOCK, N. M., DEVEQUI GOMES NUNES, D., SHIACH, J., VALERIA SARAIVA HODEL, K., DANTAS VIANA BARBOSA, J., ALENCAR PEREIRA RODRIGUES, L., COLER, B. S., BOTELHO PEREIRA SOARES, M. & BADARÓ, R. 2023. Current Clinical Landscape and Global Potential of Bacteriophage Therapy. Viruses, 15, 1020.

HOGEVEEN, H., STEENEVELD, W. & WOLF, C. A. 2019. Production diseases reduce the efficiency of dairy production: A review of the results, methods, and approaches regarding the economics of mastitis. Annual Review of Resource Economics, 11, 289-312.

HUSSAIN, W., YANG, X., ULLAH, M., WANG, H., AZIZ, A., XU, F., ASIF, M., ULLAH, M. W. & WANG, S. 2023. Genetic engineering of bacteriophages: Key concepts, strategies, and applications. Biotechnology Advances, 64, 108116.

INGMER, H., GERLACH, D. & WOLZ, C. 2019. Temperate phages of Staphylococcus aureus. Microbiology spectrum, 7, 7-5.

IWANO, H., INOUE, Y., TAKASAGO, T., KOBAYASHI, H., FURUSAWA, T., TANIGUCHI, K., FUJIKI, J., YOKOTA, H., USUI, M., TANJI, Y., HAGIWARA, K., HIGUCHI, H. & TAMURA, Y. 2018. Bacteriophage ΦSA012 Has a Broad Host Range against Staphylococcus aureus and Effective Lytic Capacity in a Mouse Mastitis Model. Biology (Basel), 7.

JENSEN, K. C., HAIR, B. B., WIENCLAW, T. M., MURDOCK, M. H., HATCH, J. B., TRENT, A. T., WHITE, T. D., HASKELL, K. J. & BERGES, B. K. 2015. Isolation and host range of bacteriophage with lytic activity against methicillin-resistant Staphylococcus aureus and potential use as a fomite decontaminant. PLoS One, 10, e0131714.

KEARY, R., MCAULIFFE, O., ROSS, R. P., HILL, C., O'MAHONY, J. & COFFEY, A. 2014. Genome analysis of the staphylococcal temperate phage DW2 and functional studies on the endolysin and tail hydrolase. Bacteriophage, 4, e28451.

KEBRIAEI, R., LEHMAN, S. M., SHAH, R. M., STAMPER, K. C., KUNZ COYNE, A. J., HOLGER, D., EL GHALI, A. & RYBAK, M. J. 2023. Optimization of Phage-Antibiotic Combinations against Staphylococcus aureus Biofilms. Microbiology Spectrum, e04918-22.

KHAMBHATI, K., BHATTACHARJEE, G., GOHIL, N., DHANOA, G. K., SAGONA, A. P., MANI, I., BUI, N. L., CHU, D. T., KARAPURKAR, J. K. & JANG, S. H. 2023. Phage engineering and phage-assisted CRISPR-Cas delivery to combat multidrug-resistant pathogens. Bioengineering & Translational Medicine, 8, e10381.

KILCHER, S. & LOESSNER, M. J. 2019. Engineering bacteriophages as versatile biologics. Trends in microbiology, 27, 355-367.

KING, A. M. Q., LEFKOWITZ, E., ADAMS, M. J. & CARSTENS, E. B. 2011. Virus taxonomy: ninth report of the International Committee on Taxonomy of Viruses, Elsevier.

KROPINSKI, A. M., PRANGISHVILI, D. & LAVIGNE, R. 2009. Position paper: the creation of a rational scheme for the nomenclature of viruses of Bacteria and Archaea. Environmental microbiology, 11, 2775-2777.

KRUEGER, F. 2015. Trim Galore!: A wrapper around Cutadapt and FastQC to consistently apply adapter and quality trimming to FastQ files, with extra functionality for RRBS data. Babraham Institute.

KUTTER, E. & SULAKVELIDZE, A. 2004. Bacteriophages: biology and applications, Crc press.

KWAK, H., KIM, J., RYU, S. & BAI, J. 2023. Characterization of KMSP1, a newly isolated virulent bacteriophage infecting Staphylococcus aureus, and its application to dairy products. International Journal of Food Microbiology, 390, 110119.

KWAN, T., LIU, J., DUBOW, M., GROS, P. & PELLETIER, J. 2005. The complete genomes and proteomes of 27 Staphylococcus aureus bacteriophages. Proceedings of the National Academy of Sciences, 102, 5174-5179.

KWIATEK, M., PARASION, S., MIZAK, L., GRYKO, R., BARTOSZCZE, M. & KOCIK, J. 2012a. Characterization of a bacteriophage, isolated from a cow with mastitis, that is lytic against Staphylococcus aureus strains. Arch Virol, 157, 225-34.

KWIATEK, M., PARASION, S., MIZAK, L., GRYKO, R., BARTOSZCZE, M. & KOCIK, J. 2012b. Characterization of a bacteriophage, isolated from a cow with mastitis, that is lytic against Staphylococcus aureus strains. Archives of virology, 157, 225-234.

LASLETT, D. & CANBACK, B. 2004. ARAGORN, a program to detect tRNA genes and tmRNA genes in nucleotide sequences. Nucleic acids research, 32, 11-16.

LE, S. Q. & GASCUEL, O. 2008. An improved general amino acid replacement matrix. Molecular biology and evolution, 25, 1307-1320.

LEE, C., KIM, H. & RYU, S. 2022. Bacteriophage and endolysin engineering for biocontrol of food pathogens/pathogens in the food: recent advances and future trends. Critical Reviews in Food Science and Nutrition, 1-20.

LEFORT, V., DESPER, R. & GASCUEL, O. 2015. FastME 2.0: a comprehensive, accurate, and fast distance-based phylogeny inference program. Molecular biology and evolution, 32, 2798-2800.

LEWIS, R., CLOONEY, A. G., STOCKDALE, S. R., BUTTIMER, C., DRAPER, L. A., ROSS, R. P. & HILL, C. 2020. Isolation of a novel jumbo bacteriophage effective against Klebsiella aerogenes. Frontiers in Medicine, 7, 67.

LI, H., HANDSAKER, B., WYSOKER, A., FENNELL, T., RUAN, J., HOMER, N., MARTH, G., ABECASIS, G., DURBIN, R. & GENOME PROJECT DATA PROCESSING, S. 2009. The sequence alignment/map format and SAMtools. bioinformatics, 25, 2078-2079.

LI, L. & ZHANG, Z. 2014. Isolation and characterization of a virulent bacteriophage SPW specific for Staphylococcus aureus isolated from bovine mastitis of lactating dairy cattle. Molecular biology reports, 41, 5829-5838.

LIANG, S., QI, Y., YU, H., SUN, W., RAZA, S. H., ALKHORAYEF, N., ALKHALIL, S. S., SALAMA, E. E. & ZHANG, L. 2023. Bacteriophage Therapy as an Application for Bacterial Infection in China. Antibiotics [Online], 12.

LINEHAN, K., ROSS, R. P. & STANTON, C. 2023. Bovine Colostrum for Veterinary and Human Health Applications: A Critical Review. Annual Review of Food Science and Technology, 14, 387-410.

LING, H., LOU, X., LUO, Q., HE, Z., SUN, M. & SUN, J. 2022. Recent advances in bacteriophage-based therapeutics: Insight into the post-antibiotic era. Acta Pharmaceutica Sinica B.

LIU, S., HON, K., BOURAS, G. S., PSALTIS, A. J., SHEARWIN, K., WORMALD, P. J. & VREUGDE, S. 2022. APTC-C-SA01: A Novel Bacteriophage Cocktail Targeting Staphylococcus aureus and MRSA Biofilms. Int J Mol Sci, 23.

LYONS, K. E., RYAN, C. A., DEMPSEY, E. M., ROSS, R. P. & STANTON, C. 2020. Breast Milk, a Source of Beneficial Microbes and Associated Benefits for Infant Health. Nutrients, 12.

MANGALEA, M. R. & DUERKOP, B. A. 2020. Fitness trade-offs resulting from bacteriophage resistance potentiate synergistic antibacterial strategies. Infection and immunity, 88, e00926-19.

MCARTHUR, A. G., WAGLECHNER, N., NIZAM, F., YAN, A., AZAD, M. A., BAYLAY, A. J., BHULLAR, K., CANOVA, M. J., DE PASCALE, G. & EJIM, L. 2013. The comprehensive antibiotic resistance database. Antimicrobial agents and chemotherapy, 57, 3348-3357.

MCNAIR, K., BAILEY, B. A. & EDWARDS, R. A. 2012. PHACTS, a computational approach to classifying the lifestyle of phages. Bioinformatics, 28, 614-618.

MEIER-KOLTHOFF, J. P., AUCH, A. F., KLENK, H.-P. & GÖKER, M. 2013. Genome sequence-based species delimitation with confidence intervals and improved distance functions. BMC bioinformatics, 14, 1-14.

MEIER-KOLTHOFF, J. P. & GÖKER, M. 2017. VICTOR: genome-based phylogeny and classification of prokaryotic viruses. Bioinformatics, 33, 3396-3404.

MEIER-KOLTHOFF, J. P., HAHNKE, R. L., PETERSEN, J., SCHEUNER, C., MICHAEL, V., FIEBIG, A., ROHDE, C., ROHDE, M., FARTMANN, B. & GOODWIN, L. A. 2014. Complete genome sequence of DSM 30083 T, the type strain (U5/41 T) of Escherichia coli, and a proposal for delineating subspecies in microbial taxonomy. Standards in genomic sciences, 9, 1-19.

MONTEIRO, R., PIRES, D. P., COSTA, A. R. & AZEREDO, J. 2019. Phage therapy: going temperate? Trends in microbiology, 27, 368-378.

MORARU, C., VARSANI, A. & KROPINSKI, A. M. 2020. VIRIDIC—A novel tool to calculate the intergenomic similarities of prokaryote-infecting viruses. Viruses, 12, 1268.

NAVILLE, M., GHUILLOT-GAUDEFFROY, A., MARCHAIS, A. & GAUTHERET, D. 2011. ARNold: a web tool for the prediction of Rho-independent transcription terminators. RNA biology, 8, 11-13.

NISHIMURA, Y., YOSHIDA, T., KURONISHI, M., UEHARA, H., OGATA, H. & GOTO, S. 2017. ViPTree: the viral proteomic tree server. Bioinformatics, 33, 2379-2380.

NURK, S., MELESHKO, D., KOROBEYNIKOV, A. & PEVZNER, P. A. 2017. metaSPAdes: a new versatile metagenomic assembler. Genome Research, 27, 824-834.

O'FLAHERTY, S., COFFEY, A., MEANEY, W. J., FITZGERALD, G. F. & ROSS, R. P. 2005a. Inhibition of bacteriophage K proliferation on Staphylococcus aureus in raw bovine milk. Lett Appl Microbiol, 41, 274-9.

O'FLAHERTY, S., ROSS, R. P., FLYNN, J., MEANEY, W. J., FITZGERALD, G. F. & COFFEY, A. 2005b. Isolation and characterization of two anti-staphylococcal bacteriophages specific for pathogenic Staphylococcus aureus associated with bovine infections. Letters in Applied Microbiology, 41, 482-486.

O'FLAHERTY, S., ROSS, R. P., MEANEY, W., FITZGERALD, G. F., ELBREKI, M. F. & COFFEY, A. 2005c. Potential of the polyvalent anti-Staphylococcus bacteriophage K for control of antibiotic-resistant staphylococci from hospitals. Appl Environ Microbiol, 71, 1836-42.

O'FLYNN, G., ROSS, R. P., FITZGERALD, G. F. & COFFEY, A. 2004. Evaluation of a cocktail of three bacteriophages for biocontrol of Escherichia coli O157: H7. Applied and environmental microbiology, 70, 3417-3424.

OOI, M. L., DRILLING, A. J., MORALES, S., FONG, S., MORAITIS, S., MACIAS-VALLE, L., VREUGDE, S., PSALTIS, A. J. & WORMALD, P.-J. 2019. Safety and tolerability of bacteriophage therapy for chronic rhinosinusitis due to Staphylococcus aureus. JAMA Otolaryngology–Head & Neck Surgery, 145, 723-729.

OROMÍ-BOSCH, A., ANTANI, J. D. & TURNER, P. E. 2023. Developing Phage Therapy That Overcomes the Evolution of Bacterial Resistance. Annual Review of Virology.

PANNARAJ, P. S., LY, M., CERINI, C., SAAVEDRA, M., ALDROVANDI, G. M., SABOORY, A. A., JOHNSON, K. M. & PRIDE, D. T. 2018. Shared and distinct features of human milk and infant stool viromes. Frontiers in microbiology, 9, 1162.

PARK, J.-M., KO, D.-S., KIM, H.-S., KIM, N.-H., KIM, E.-K., ROH, Y.-H., KIM, D., KIM, J.-H., CHOI, K.-S. & KWON, H.-J. 2023. Rapid Screening and Comparison of Chimeric Lysins for Antibacterial Activity against Staphylococcus aureus Strains. Antibiotics, 12, 667.

PARLET, C. P., BROWN, M. M. & HORSWILL, A. R. 2019. Commensal staphylococci influence Staphylococcus aureus skin colonization and disease. Trends in microbiology, 27, 497-507.

PAYASLIAN, F., GRADASCHI, V. & PIURI, M. 2021. Genetic manipulation of phages for therapy using BRED. Current Opinion in Biotechnology, 68, 8-14.

PETROVIC FABIJAN, A., LIN, R. C. Y., HO, J., MADDOCKS, S., BEN ZAKOUR, N. L., IREDELL, J. R. & WESTMEAD BACTERIOPHAGE THERAPY TEAM KHALID ALI 1 3 VENTURINI CAROLA 1 3 CHARD RICHARD 3 7 MORALES SANDRA 8 SANDARADURA INDY 2 3 GILBEY, T. 2020. Safety of bacteriophage therapy in severe Staphylococcus aureus infection. Nature microbiology, 5, 465-472.

PHILIPSON, C. W., VOEGTLY, L. J., LUEDER, M. R., LONG, K. A., RICE, G. K., FREY, K. G., BISWAS, B., CER, R. Z., HAMILTON, T. & BISHOP-LILLY, K. A. 2018. Characterizing phage genomes for therapeutic applications. Viruses, 10, 188.

PIRES, D. P., MONTEIRO, R., MIL-HOMENS, D., FIALHO, A., LU, T. K. & AZEREDO, J. 2021. Designing P. aeruginosa synthetic phages with reduced genomes. Scientific Reports, 11, 2164.

RAEISI, H., NOORI, M., AZIMIRAD, M., MOHEBBI, S. R., ASADZADEH AGHDAEI, H., YADEGAR, A. & ZALI, M. R. 2023. Emerging applications of phage therapy and fecal virome transplantation for treatment of Clostridioides difficile infection: challenges and perspectives. Gut Pathogens, 15, 1-20.

RANGEL-PINEROS, G., MILLARD, A., MICHNIEWSKI, S., SCANLAN, D., SIRÉN, K., REYES, A., PETERSEN, B., CLOKIE, M. R. J. & SICHERITZ-PONTÉN, T. 2021. From trees to clouds: PhageClouds for fast comparison of~ 640,000 phage genomic sequences and host-centric visualization using genomic network graphs. Phage, 2, 194-203.

RODRIGUEZ, R. A., BOUNTY, S., BECK, S., CHAN, C., MCGUIRE, C. & LINDEN, K. G. 2014. Photoreactivation of bacteriophages after UV disinfection: Role of genome structure and impacts of UV source. Water Research, 55, 143-149.

ROSS, A., WARD, S. & HYMAN, P. 2016. More is better: selecting for broad host range bacteriophages. Frontiers in microbiology, 7, 1352.

ROY, D., YE, A., MOUGHAN, P. J. & SINGH, H. 2020. Composition, structure, and digestive dynamics of milk from different species—A review. Frontiers in Nutrition, 7, 577759.

SABER, H., JASNI, A. S., JAMALUDDIN, T. & IBRAHIM, R. 2017. A Review of Staphylococcal Cassette Chromosome mec (SCCmec) Types in Coagulase-Negative Staphylococci (CoNS) Species. Malays J Med Sci, 24, 7-18.

SAMBROOK, J. & RUSSELL, D. W. 2006. Purification of bacteriophage λ particles by isopycnic centrifugation through CsCl gradients. Cold Spring Harbor Protocols, 2006, pdb-prot3968.

SAUNDERS, N. A. & HOLMES, A. 2007. Multilocus sequence typing (MLST) of Staphylococcus aureus. Methods Mol Biol, 391, 71-85.

SHAHIN, K., BOUZARI, M., WANG, R. & YAZDI, M. 2019. Prevalence and molecular characterization of multidrug-resistant Shigella species of food origins and their inactivation by specific lytic bacteriophages. Int J Food Microbiol, 305, 108252.

SHEN, A. & MILLARD, A. 2021. Phage genome annotation: where to begin and end. Phage, 2, 183-193.

SHEN, W., LE, S., LI, Y. & HU, F. 2016. SeqKit: a cross-platform and ultrafast toolkit for FASTA/Q file manipulation. PloS one, 11, e0163962.

SHORE, A. C., ROSSNEY, A. S., O'CONNELL, B., HERRA, C. M., SULLIVAN, D. J., HUMPHREYS, H. & COLEMAN, D. C. 2008. Detection of staphylococcal cassette chromosome mec-associated DNA segments in multiresistant methicillin-susceptible Staphylococcus aureus (MSSA) and identification of Staphylococcus epidermidis ccrAB4 in both methicillin-resistant S. aureus and MSSA. Antimicrob Agents Chemother, 52, 4407-19.

SHRIVASTAVA, S. R., SHRIVASTAVA, P. S. & RAMASAMY, J. 2018. World health organization releases global priority list of antibiotic-resistant bacteria to guide research, discovery, and development of new antibiotics. Journal of Medical Society, 32, 76.

SIMON, K., PIER, W., KRÜTTGEN, A. & HORZ, H.-P. 2021. Synergy between Phage Sb-1 and oxacillin against methicillin-resistant Staphylococcus aureus. Antibiotics, 10, 849.

SÖDING, J., BIEGERT, A. & LUPAS, A. N. 2005. The HHpred interactive server for protein homology detection and structure prediction. Nucleic acids research, 33, W244-W248.

STOTHARD, P. 2000. The sequence manipulation suite: JavaScript programs for analyzing and formatting protein and DNA sequences. Biotechniques, 28, 1102-1104.

STRATHDEE, S. A., HATFULL, G. F., MUTALIK, V. K. & SCHOOLEY, R. T. 2023. Phage therapy: From biological mechanisms to future directions. Cell, 186, 17-31.

SULLIVAN, M. J., PETTY, N. K. & BEATSON, S. A. 2011. Easyfig: a genome comparison visualizer. Bioinformatics, 27, 1009-1010.

TAMURA, K., STECHER, G. & KUMAR, S. 2021. MEGA11: molecular evolutionary genetics analysis version 11. Molecular biology and evolution, 38, 3022-3027.

TITZE, I., LEHNHERR, T., LEHNHERR, H. & KRÖMKER, V. 2020. Efficacy of Bacteriophages Against Staphylococcus aureus Isolates from Bovine Mastitis. Pharmaceuticals [Online], 13.

TOMANIĆ, D., SAMARDŽIJA, M. & KOVAČEVIĆ, Z. 2023. Alternatives to Antimicrobial Treatment in Bovine Mastitis Therapy: A Review. Antibiotics, 12, 683.

TONG, S. Y. C., DAVIS, J. S., EICHENBERGER, E., HOLLAND, T. L. & FOWLER JR, V. G. 2015. Staphylococcus aureus infections: epidemiology, pathophysiology, clinical manifestations, and management. Clinical microbiology reviews, 28, 603-661.

TURNER, D., KROPINSKI, A. M. & ADRIAENSSENS, E. M. 2021. A roadmap for genome-based phage taxonomy. Viruses, 13, 506.

TYNECKI, P., GUZIŃSKI, A., KAZIMIERCZAK, J., JADCZUK, M., DASTYCH, J. & ONISKO, A. 2020. PhageAI-bacteriophage life cycle recognition with machine learning and natural language processing. BioRxiv, 2020-07.

VAN BELLEGHEM, J. D., MERABISHVILI, M., VERGAUWEN, B., LAVIGNE, R. & VANEECHOUTTE, M. 2017. A comparative study of different strategies for removal of endotoxins from bacteriophage preparations. Journal of microbiological methods, 132, 153-159.

VENTURINI, C., PETROVIC FABIJAN, A., FAJARDO LUBIAN, A., BARBIRZ, S. & IREDELL, J. 2022. Biological foundations of successful bacteriophage therapy. EMBO Molecular Medicine, 14, e12435.

WALKER, B. J., ABEEL, T., SHEA, T., PRIEST, M., ABOUELLIEL, A., SAKTHIKUMAR, S., CUOMO, C. A., ZENG, Q., WORTMAN, J. & YOUNG, S. K. 2014. Pilon: an integrated tool for comprehensive microbial variant detection and genome assembly improvement. PloS one, 9, e112963.

WANG, S., HUANG, X., YANG, J., YANG, D., ZHANG, Y., HOU, Y., LIN, L., HUA, L., LIANG, W., WU, B. & PENG, Z. 2023. Biocontrol of methicillin-resistant Staphylococcus

aureus using a virulent bacteriophage derived from a temperate one. Microbiological Research, 267, 127258.

WANG, Z., ZHENG, P., JI, W., FU, Q., WANG, H., YAN, Y. & SUN, J. 2016. SLPW: A virulent bacteriophage targeting methicillin-resistant Staphylococcus aureus in vitro and in vivo. Frontiers in microbiology, 7, 934.

WEAVER, D. M., TYLER, J. W., VANMETRE, D. C., HOSTETLER, D. E. & BARRINGTON, G. M. 2000. Passive transfer of colostral immunoglobulins in calves. Journal of veterinary internal medicine, 14, 569-577.

WICK, R. R., SCHULTZ, M. B., ZOBEL, J. & HOLT, K. E. 2015. Bandage: interactive visualization of de novo genome assemblies. Bioinformatics, 31, 3350-3352.

XU, J., ZHANG, R., YU, X., ZHANG, X., LIU, G. & LIU, X. 2021. Molecular characteristics of novel phage vB_ShiP-A7 infecting multidrug-resistant Shigella flexneri and Escherichia coli, and its bactericidal effect in vitro and in vivo. Frontiers in Microbiology, 12, 698962.

YANG, D., WANG, S., SUN, E., CHEN, Y., HUA, L., WANG, X., ZHOU, R., CHEN, H., PENG, Z. & WU, B. 2022. A temperate Siphoviridae bacteriophage isolate from Siberian tiger enhances the virulence of methicillin-resistant Staphylococcus aureus through distinct mechanisms. Virulence, 13, 137-148.

YI, D. Y. & KIM, S. Y. 2021. Human breast milk composition and function in human health: from nutritional components to microbiome and microRNAs. Nutrients, 13, 3094.

YU, G. 2020. Using ggtree to visualize data on tree-like structures. Current protocols in bioinformatics, 69, e96.

YUKGEHNAISH, K., RAJANDAS, H., PARIMANNAN, S., MANICKAM, R., MARIMUTHU, K., PETERSEN, B., CLOKIE, M. R. J., MILLARD, A. & SICHERITZ-PONTÉN, T. 2022. PhageLeads: rapid assessment of phage therapeutic suitability using an ensemble machine learning approach. Viruses, 14, 342.

ZHANG, L., BAO, H., WEI, C., ZHANG, H., ZHOU, Y. & WANG, R. 2015. Characterization and partial genomic analysis of a lytic Myoviridae bacteriophage against Staphylococcus aureus isolated from dairy cows with mastitis in Mid-east of China. Virus Genes, 50, 111-117.

ZHANG, L., SHAHIN, K., SOLEIMANI-DELFAN, A., DING, H., WANG, H., SUN, L. & WANG, R. 2022. Phage JS02, a putative temperate phage, a novel biofilm-degrading agent for Staphylococcus aureus. Letters in Applied Microbiology, 75, 643-654.

ZHOU, S., LIU, Z., SONG, J. & CHEN, Y. 2023. Disarm The Bacteria: What Temperate Phages Can Do. Current Issues in Molecular Biology, 45, 1149-1167.

ZUKER, M. 2003. Mfold web server for nucleic acid folding and hybridization prediction. Nucleic acids research, 31, 3406-3415.

5.11 Supplementary material

Supplementary Tables:

Table S5.1 | Host ranges of phage cocktail containing phage HM1 and phage BC1 on S. aureus strains (n=33) determined by spot testing with serial dilutions of phage suspensions. Efficiency of plaquing (EOP) values determined for sensitive strains.

			Spot Test	Efficacy of Plaquing (EOP) (mean ± SD)
No.	**Strain**	**Source[a]**	**Cocktail**	**Cocktail**
1	0.0066(IIv)ST239	I	+	0.76 ± 0.1
2	0.1206(IV)ST250	I	+	0.25 ± 0.1
3	0.1239(III)ST239	I	-	no plaques
4	0.1345(II)ST5	I	-	no plaques
5	0073(III)ST239	I	+	0.23 ± 0.1
6	0104(III)ST239	I	+	0.33 ± 0.1
7	0220(II)ST5	I	+	0.32 ± 0.1
8	0242(IV)ST30	I	+	0.34 ± 0.2
9	0308(IA)ST247	I	+	0.14 ± 0.1
10	3045(IIv)ST8	I	+	0.37 ± 0.05
11	3144(IIv)ST8	I	+	0.45 ± 0.01
12	3488(vv)ST8	I	-	no plaques
13	3581(IA)ST247	I	-	no plaques
14	3594(II)ST36	I	+	0.62 ± 0.1
15	3596(IIv)ST8	I	+	0.36 ± 0.09
16	E1038(IIv)ST8	I	+	0.06 ± 0.03
17	E1139(IV)ST45	I	-	no plaques
18	E1174(IV)ST22	I	+	0.44 ± 0.1
19	E1185(IV)ST12	I	+	0.14 ± 0.02
20	E1202(II)ST496	I	+	0.34 ± 0.1
21	M03/0073(III)ST239	I	+	0.38 ± 0.12
22	DPC5646	II	+	0.81 ± 0.12
23	DPC5645	II	+	0.91 ± 0.14
24	DPC5647	II	-	no plaques
25	DPC5245*	II	+	1.0 ± 0
26	DPC5246	II	-	no plaques
27	DPC5247	II	+	0.36 ± 0.2
28	DPC5644	II	-	no plaques
29	DPC5970	II	+	0.23 ± 0.05
30	DPC5971	II	+	0.34 ± 0.01
31	DPC6868	II	+	0.54 ± 0.1
32	DPC6869	II	+	0.62 ± 0.12
33	DPC7016	II	+	0.33 ± 0.11

Results recorded as +, sensitive; −, no infection; * host strain of phage. [a]I, 21 MRSAs of differing sequence types obtained from the Irish National MRSA collection. [a]II, 12 *S. aureus* strains obtained from the DPC culture collection.

Table S5.2 | MRSAs strains of differing sequence types obtained from the Irish National MRSA collection.

			Efficacy of Plaquing (EOP) (mean ± SD)	
***S. aureus* Strain**	**SCCmec Type**	**MLST**	**vB_Sau_HM1**	**vB_Sau_BC1**
0.0066(IIv)ST239	II(2A) **	36	0.5 ± 0.1	no plaques
0.1206(IV)ST250	IVc(2B)	12	0.34 ± 0.12	0.44 ± 0.11
0.1239(III)ST239	III(3A)	239	no plaques	no plaques
0.1345(II)ST5	VIII(4A)	8	no plaques	no plaques
0073(III)ST239	III(3A)	239	0.55 ± 0.32	no plaques
0104(III)ST239	III(3A)	239	0.37 ± 0.04	no plaques
0220(II)ST5	IV(2B) **	8	0.46 ± 0.02	no plaques
0242(IV)ST30	II(2A)	496	0.16 ± 0.06	0.24 ± 0.01
0308(IA)ST247	I(1B)	247	0.05 ± 0.07	0.11 ± 0.04
3045(IIv)ST8	II(2A)	8	0.25 ± 0.01	0.31 ± 0.02
3144(IIv)ST8	II(2A)	8	0.12 ± 0.1	0.12 ± 0.04
3488(vv)ST8	IV(2B) **	8	no plaques	no plaques
3581(IA)ST247	VIII(4A) **	8	no plaques	no plaques
3594(II)ST36	III(3A)	239	0.62 ± 0.1	no plaques
3596(IIv)ST8	VIII(4A) **	8	0.36 ± 0.09	no plaques
E1038(IIv)ST8	II(2A)	8	0.06 ± 0.03	0.04 ± 0.01
E1139(IV)ST45	IVa(2B)	45	no plaques	no plaques
E1174(IV)ST22	IV(2B)	22	0.54 ± 0.01	0.46 ± 0.03
E1185(IV)ST12	IVc	12	0.14 ± 0.02	0.11 ± 0.04

E1202(II)ST496	VIII(4A) **	8	0.44 ± 0.07	0.51 ± 0.02
M03/0073(III)ST239	III(3A)	239	0.38 ± 0.12	no plaques

A mobile genetic element, staphylococcal cassette chromosome *mec* (SCC*mec*), carries *mecA* (methicillin-resistant gene) and plays an important role in staphylococci pathogenesis (Saber et al., 2017). Multilocus sequence typing (MLST) is a widely accepted method of DNA sequence-based typing that relies on analysis of relatively conserved genes that encode essential proteins. For *Staphylococcus aureus*, the level of discrimination provided by MLST is sufficient to provide a relatively detailed picture of the global dissemination of the organism (Saunders and Holmes, 2007). ** SCCmec type: two possible types suggested by SCCmecFinder with a hit of greatest coverage selected. Table adapted from (Arroyo-Moreno et al., 2022).

Table S5.3 | Strains obtained from the Dairy Products Research Centre (DPC) culture collection for phage host range screening.

			Spot Test	
DCP Code	Strain	Additional Info	HM	BC
DPC5646	*Staphylococcus aureus*	MRSA	+	+
DPC5645	*Staphylococcus aureus*	MRSA	+	+
DPC5647	*Staphylococcus aureus*	MRSA	-	-
DPC5245	*Staphylococcus aureus*	Bovine Mastitis strain Type I (RAPD type 5)	+	+
DPC5246	*Staphylococcus aureus*	Bovine Mastitis strain Type II (RAPD type 7)	-	-
DPC5247	*Staphylococcus aureus*	Bovine Mastitis strain Type III (RAPD type 4)	+	+
DPC5644	*Staphylococcus aureus*	Host for Ø TWORT	-	-
DPC5970	*Staphylococcus aureus*	Isolated from mastitic cow milk	+	+
DPC5971	*Staphylococcus aureus*	Isolated from mastitic cow milk	+	+
DPC6868	*Staphylococcus aureus*	Isolated from bovine milk for cheese production, enterotoxin C producer	+	+
DPC6869	*Staphylococcus aureus*	Isolated from bovine milk for cheese production, enterotoxin C producer	+	+

DPC7016	*Staphylococcus aureus*	Isolated from mastitic cow milk	+	+
DPC3572	*Listeria innocua*		-	-
DPC6868	*Streptococcus agalactiae*		-	-
DPC6010	*Staphylococcus epidermidis*	Coagulase-negative; bovine strain	-	-
DPC6012	*Staphylococcus chromogenes*	Coagulase-negative; bovine strain	-	-
DPC6013	*Staphylococcus capilis*	Coagulase-negative; bovine strain	-	-
DPC6014	*Staphylococcus hominis*	Coagulase-negative; bovine strain	-	-
DPC6015	*Staphylococcus haemolyticus*	Coagulase-negative; bovine strain	-	-
DPC6016	*Staphylococcus caprae*	Coagulase-negative; bovine strain	-	-
DPC6017	*Staphylococcus hyicus*	Coagulase-negative; bovine strain	-	-

Table S5.4 | Genomic annotation of Staphylococcus phage BC1.

ORF	Start (bp)	Stop (bp)	Length (aa)	Molecular Mass (kDa)	Function
BC_01c	3	1391	463	54.01	DNA invertase
BC_02c	1449	1952	167	18.66	hypothetical protein
BC_03c	1956	2447	163	18.96	hypothetical protein
BC_04c	2468	2926	152	18.14	ImmA/IrrE family metallo-endopeptidase protein
BC_05c	2938	3270	110	12.7	repressor
BC_06	3463	3702	79	9.16	transcriptional regulator, HTH cro/C1 type
BC_07	3717	4430	237	27.48	antirepressor protein
BC_08	4443	4535	30	3.65	hypothetical protein
BC_09	4532	4693	53	6.21	hypothetical protein
BC_10	4785	5045	86	10.15	hypothetical protein
BC_11	5053	5289	78	9.17	hypothetical protein
BC_12	5282	5761	159	18.51	host-nuclease inhibitor protein Gam

BC_13	5761	6399	212	23.71	essential recombination function protein
BC_14	6399	6824	141	15.85	single stranded DNA-binding protein
BC_15	6838	7533	231	26.81	putative HNHc nuclease
BC_16	7505	8326	273	32.47	replication initiation protein
BC_17	8339	9124	261	30.44	DNA replication helicase loader DnaC/DnaI
BC_18	9121	9279	52	6.19	hypothetical protein
BC_19	9292	9516	73	8.6	hypothetical protein
BC_20	9527	9931	156	18.70	hypothetical protein
BC_21	9936	10121	61	7.31	hypothetical protein
BC_22	10122	10739	205	24.00	hypothetical protein
BC_23	10739	10993	84	9.69	hypothetical protein
BC_24	10999	11241	80	9.58	hypothetical protein
BC_25	11256	11462	68	7.98	hypothetical protein
BC_26	11465	11893	142	16.30	hypothetical protein
BC_27	11970	12083	37	4.25	hypothetical protein
BC_28	12080	12364	94	11.32	putative acetyltransferase
BC_29	12357	12605	82	9.19	hypothetical protein
BC_30	12598	13131	160	17.50	dUTPase
BC_31	13198	13404	68	7.93	hypothetical protein
BC_32	13401	13589	62	7.1	hypothetical protein
BC_33	13591	13764	57	6.52	transcriptional activator rinB
BC_34	13765	14130	121	14.43	hypothetical protein
BC_35	14131	14277	48	5.72	hypothetical protein
BC_36	14301	14723	140	16.39	transcriptional activator RinA
BC_37	15054	15548	164	18.72	terminase small subunit
BC_38	15541	16764	407	47.16	terminase large subunit
BC_39	16761	18185	474	55.06	portal protein

BC_40	18154	19104	316	36.84	prohead
BC_41	19200	19784	193	22.41	scaffold protein
BC_42	19801	20715	304	33.62	major capsid protein
BC_43	20727	20870	47	5.36 k	head-tail adapter
BC_44	20876	21226	116	13.67	hypothetical protein
BC_45	21238	21573	111	12.94	hypothetical protein
BC_46	21560	21967	135	15.13	putative tail-component
BC_47	21980	22405	141	16.41	hypothetical protein
BC_48	22406	22963	185	20.47	major tail protein
BC_49	23030	23542	170	19.53	tail assembly chaperone protein
BC_50	23722	23871	49	5.88	hypothetical protein
BC_51	23875	27018	1047	113.63	tape measure protein
BC_52	27033	27974	313	36.18	distal tail protein
BC_53	27985	29871	628	70.53	tail protein
BC_54	29884	31782	632	72.59	putative major teichoic acid biosynthesis protein C
BC_55	31782	33605	607	66.89	baseplate upper protein
BC_56	33605	33991	128	14.49	hypothetical protein
BC_57	33984	34160	58	6.91	hypothetical protein
BC_58	34200	34505	101	12.06	hypothetical protein
BC_59	34642	34752	36	3.93	hypothetical protein
BC_60	35171	36865	564	63.92	mannosyl-glycoprotein endo-beta-N-acetylglucosaminidase
BC_61	36878	38890	670	75.79	tail fiber protein
BC_62	38941	39378	145	15.65	holin
BC_63	39359	40804	481	53.92	endolysin
BC_64	41209	41385	58	6.69	hypothetical protein
BC_65	41382	41996	204	23.7	acetyltransferase
BC_66c	42052	42159	35	3.89	hypothetical protein

Table S5.5 | Genomic annotation of Staphylococcus phage HM1.

ORF	Start (bp)	Stop (bp)	Length (aa)	Molecular Mass (kDa)	Function
HM_01c	2	1390	463	54.01	DNA invertase
HM_02c	1448	1951	167	18.66	hypothetical protein
HM_03c	1955	2446	163	18.96	hypothetical protein
HM_04c	2467	2925	152	18.14	ImmA/IrrE family metallo-endopeptidase protein
HM_05c	2937	3269	110	12.7	repressor
HM_06	3462	3701	79	9.16	transcriptional regulator, HTH cro/C1 type
HM_07	3716	4429	236	27.35	antirepressor protein
HM_08	4442	4534	30	3.65	hypothetical protein
HM_09	4531	4692	53	6.21	hypothetical protein
HM_10	4784	5044	86	10.15	hypothetical protein
HM_11	5038	5433	131	15.79	phage replisome organizer N-terminal domain-containing protein
HM_12	5446	6231	261	30.51	DNA replication helicase loader DnaC/DnaI
HM_13	6228	6386	52	6.15	hypothetical protein
HM_14	6399	6620	73	8.62	hypothetical protein
HM_15	6631	7035	134	16.13	hypothetical protein

HM_16	7040	7225	61	7.32	hypothetical protein
HM_17	7226	7735	169	19.85	hypothetical protein
HM_18	7735	7989	84	9.71	hypothetical protein
HM_19	7995	8237	80	9.59	hypothetical protein
HM_20	8251	8457	68	8.04	hypothetical protein
HM_21	8460	8864	133	15.58	hypothetical protein
HM_22	8861	9055	64	7.49	hypothetical protein
HM_23	9052	9504	150	17.38	hypothetical protein
HM_24	9501	10004	167	19.76	hypothetical protein
HM_25	10196	10447	83	9.45	hypothetical protein
HM_26	10437	10610	57	6.47	hypothetical protein
HM_27	10611	10892	93	11.39	hypothetical protein
HM_28	10893	10893	53	6.75	hypothetical protein
HM_29	11069	11602	117	20.56	dUTPase
HM_30	11639	11833	64	7.44	hypothetical protein
HM_31	11830	12033	67	7.83	hypothetical protein
HM_32	12026	12262	78	9.29	hypothetical protein
HM_33	12252	12641	129	15.15	hypothetical protein

HM_34	12638	12811	57	6.58	transcriptional activator RinB
HM_35	12812	13213	133	15.43	hypothetical protein
HM_36	13566	14060	164	18.72	terminase small subunit
HM_37	14053	15276	407	47.16	terminase large subunit
HM_38	15273	16697	474	55.06	portal protein
HM_39	16666	17616	316	36.84	prohead
HM_40	17712	18296	194	22.54	scaffold protein
HM_41	18313	19227	304	33.62	major capsid protein
HM_42	19239	19382	47	5.36	head-tail adapter
HM_43	19388	19738	116	13.67	hypothetical protein
HM_44	19750	20085	111	12.94	hypothetical protein
HM_45	20036	20479	147	16.63	putative tail-component
HM_46	20492	20917	141	16.41	hypothetical protein
HM_47	20918	21475	185	20.47	major tail protein
HM_48	20.47	22054	169	19.39	tail assembly chaperone protein
HM_49	22234	22383	49	5.88	hypothetical protein
HM_50	22387	25530	1047	113.63	tape measure protein
HM_51	25545	26486	313	36.18	distal tail protein

HM_52	26497	28383	628	70.53	tail protein
HM_53	28396	30294	632	72.59	putative major teichoic acid biosynthesis protein C
HM_54	30294	32117	607	66.89	baseplate upper protein
HM_55	32117	32503	128	14.49	hypothetical protein
HM_56	32496	32672	58	6.91	hypothetical protein
HM_57	32712	33017	101	12.06	hypothetical protein
HM_58	33154	33264	36	3.93	hypothetical protein
HM_59	33683	35377	564	63.92	mannosyl-glycoprotein endo-beta-N-acetylglucosaminidase
HM_60	35390	37402	670	75.79	tail fiber protein
HM_61	37453	37890	145	15.65	holin
HM_62	37871	39316	481	53.92	endolysin
HM_63	39721	39897	58	6.69	hypothetical protein
HM_64	39894	40508	203	23.57	acetyltransferase
HM_65_c	40564	40674	35	3.89	hypothetical protein

Table S5.6 | 56 conserved genes among phage BC1 and phage HM1 as determined by CoreGenes.

No.	**Product**	**BC1 locus tag**	**HM1 locus tag**
1	hypothetical_protein	BC_66	HM_65

2	acetyltransferase	BC_65	HM_64
3	hypothetical_protein	BC_64	HM_63
4	endolysin	BC_63	HM_62
5	holin	BC_62	HM_61
6	tail_fiber_protein	BC_61	HM_60
7	mannosyl-glycoprotein_endo-beta-N-acetylglucosaminidase	BC_60	HM_59
8	hypothetical_protein	BC_59	HM_58
9	hypothetical_protein	BC_58	HM_57
10	hypothetical_protein	BC_57	HM_56
11	hypothetical_protein	BC_56	HM_55
12	baseplate_upper_protein	BC_55	HM_54
13	putative_major_teichoic_acid_biosynthesis_protein_C	BC_54	HM_53
14	distal_tail_protein	BC_53	HM_52
15	distal_tail_protein	BC_52	HM_51
16	hypothetical_protein/ tape_measure_protein	BC_51	HM_50
17	hypothetical_protein	BC_50	HM_49
18	tail_assembly_chaperone_protein	BC_49	HM_48
19	major_tail_protein	BC_48	HM_47
20	hypothetical_protein	BC_47	HM_46
21	hypothetical_protein/ putative_tail-component	BC_46	HM_45
22	hypothetical_protein	BC_45	HM_44
23	hypothetical_protein	BC_44	HM_43
24	head-tail_adapter	BC_43	HM_42
25	major_capsid_protein	BC_42	HM_41
26	scaffold_protein	BC_41	HM_40
27	prohead	BC_40	HM_39
28	portal_protein	BC_39	HM_38

29	terminase_large_subunit	BC_38	HM_37
30	terminase_small_subunit	BC_37	HM_36
31	transcriptional_activator_RinB	BC_33	HM_34
32	hypothetical_protein	BC_31	HM_30
33	hypothetical_protein	BC_29	HM_25
34	hypothetical_protein	BC_28	HM_24
35	hypothetical_protein	BC_27	HM_22
36	hypothetical_protein	BC_26	HM_21
37	hypothetical_protein	BC_25	HM_20
38	hypothetical_protein	BC_24	HM_19
39	hypothetical_protein	BC_23	HM_18
40	hypothetical_protein	BC_22	HM_17
41	hypothetical_protein	BC_21	HM_16
42	hypothetical_protein	BC_20	HM_15
43	hypothetical_protein	BC_19	HM_14
44	hypothetical_protein	BC_18	HM_13
45	DNA_replication_helicase_loader_DnaC/DnaI	BC_17	HM_12
46	replication_initiation_protein/ hypothetical_protein	BC_16	HM_11
47	hypothetical_protein	BC_10	HM_10
48	hypothetical_protein	BC_9	HM_9
49	hypothetical_protein	BC_8	HM_8
50	antirepressor_protein	BC_7	HM_7
51	transcriptional_regulator_HTH_cro/C1_type	BC_6	HM_6
52	repressor	BC_5	HM_5
53	ImmA/IrrE_family_metallo-endopeptidase	BC_4	HM_4
54	hypothetical_protein	BC_3	HM_3
55	hypothetical_protein	BC_2	HM_2
56	invertase	BC_1	HM_1

Table S5.7 | BLASTn results of phage HM1 whole genome

Description	Max Score	Total Score	Query Cover	E value	Per. ident	Acc. Len	Accession
Staphylococcus phage DW2	34387	55846	85%	0	95.29	41941	NC_024391.1
Staphylococcus phage vB_SauS_I73	20811	37764	65%	0	92.14	43575	OM439672.1
Staphylococcus phage B166	15932	35694	63%	0	94.52	42881	NC_028859.1
Staphylococcus phage B122	15455	36393	63%	0	94.67	43108	NC_054979.1
Staphylococcus phage 3MRA	15383	39300	69%	0	93.57	41931	KJ452291.1
Staphylococcus phage WBG8381	15191	33754	63%	0	94.24	42493	CP071049.1
Staphylococcus phage DSP07	14790	37214	67%	0	95.02	42483	MZ041098.1
Staphylococcus phage vB_SauS_760	13572	36786	67%	0	96.11	42788	OM439669.1
Staphylococcus phage Sebago	12593	42593	71%	0	90.93	43878	NC_054982.1
Staphylococcus phage StauST398-3	12222	43288	73%	0	90.21	41392	NC_021332.1
Staphylococcus phage phiETA3	11958	33893	60%	0	89.22	43282	NC_008799.1
Staphylococcus phage phiJB	11793	36580	65%	0	88.92	43012	KT344895.1
Staphylococcus phage ROSA	11782	26665	50%	0	88.9	43155	NC_007058.1
Staphylococcus phage vB_SauS_Mh15	11666	37073	67%	0	96.09	43090	OM439674.1
Staphylococcus phage ECel-2020l	11596	34775	62%	0	90.71	43478	CP062422.1

Staphylococcus phage 96	11566	39274	69%	0	88.49	43576	NC_007057.1
Staphylococcus phage ASZ22RN	11561	40704	73%	0	88.48	43579	ON513432.1
Staphylococcus phage Hesat	11555	35877	66%	0	88.47	43129	OP947204.1
Staphylococcus phage phinm4	11529	36157	63%	0	90.57	43189	NC_028864.1
Staphylococcus phage vB_SauS_Mh1	10968	39553	72%	0	87.38	43800	OM439673.1
Staphylococcus phage IME1364_02	10802	34319	64%	0	87.07	42338	MW238767.1
Staphylococcus phage SA13	10338	23555	48%	0	88.12	42652	NC_021863.1
Staphylococcus phage ECel-2020q	10298	35806	68%	0	86.14	42844	CP062462.1
Staphylococcus phage vB_SauS_287	10189	34124	62%	0	87.82	43134	OM439663.1
Staphylococcus phage 55-3	9563	22515	49%	0	84.76	42309	KR709303.1

Table S5.8 | BLASTn results of phage BC1 whole genome

Description	**Max Score**	**Total Score**	**Query Cover**	**E value**	**Per. ident**	**Acc. Len**	**Accession**
Staphylococcus phage DW2	34387	67096	94%	0	95.29	41941	NC_024391.1
Staphylococcus phage vB_SauS_I73	20811	39461	66%	0	92.14	43575	OM439672.1
Staphylococcus phage B122	14347	35445	61%	0	94.5	43108	NC_054979.1

Staphylococcus phage B166	14316	31821	55%	0	94.45	42881	NC_028859.1
Staphylococcus phage WBG8381	14059	32094	59%	0	93.94	42493	CP071049.1
Staphylococcus phage DSP07	13681	35875	63%	0	94.81	42483	MZ041098.1
Staphylococcus phage 3MRA	13657	38502	66%	0	93.18	41931	KJ452291.1
Staphylococcus phage Sebago	12593	42618	68%	0	90.93	43878	NC_054982.1
Staphylococcus phage vB_SauS_760	12464	37702	66%	0	96.02	42788	OM439669.1
Staphylococcus phage StauST398-3	12222	46402	75%	0	90.21	41392	NC_021332.1
Staphylococcus phage phiETA3	11958	34740	59%	0	89.22	43282	NC_008799.1
Staphylococcus phage phiJB	11793	34024	59%	0	88.92	43012	KT344895.1
Staphylococcus phage ROSA	11782	28007	50%	0	88.9	43155	NC_007058.1
Staphylococcus phage ECel-2020l	11596	34301	59%	0	90.71	43478	CP062422.1
Staphylococcus phage 96, complete genome	11566	36088	63%	0	88.49	43576	NC_007057.1
Staphylococcus phage ASZ22RN	11561	39850	69%	0	88.48	43579	ON513432.1
Staphylococcus phage Hesat	11555	36228	64%	0	88.47	43129	OP947204.1
Staphylococcus phage phinm4	11529	32465	56%	0	90.57	43189	NC_028864.1
Staphylococcus phage vB_SauS_Mh1	10968	41395	72%	0	87.38	43800	OM439673.1

Staphylococcus phage IME1364_02	10802	33700	60%	0	87.07	42338	MW238767.1
Staphylococcus phage vB_SauS_Mh15	10619	36336	64%	0	96.09	43090	OM439674.1
Staphylococcus phage SA13	10338	27210	53%	0	88.12	42652	NC_021863.1
Staphylococcus phage ECel-2020q	10298	34622	64%	0	86.14	42844	CP062462.1
Staphylococcus phage vB_SauS_287	10189	33260	58%	0	87.82	43134	OM439663.1
Staphylococcus phage 55-2	9563	25338	51%	0	84.76	41898	KR709302.1

Table S5.9 |VIRIDIC Results of most closely related phages to phage HM1 and phage BC1.

Genome	**species_cluster**	**genus_cluster**
NC_054980.1_Staphylococcus_phage_Henu	10	6
NC_028669.1_Staphylococcus_phage_phiJ	6	3
NC_028864.1_Staphylococcus_phage_phinm4	7	3
NC_054979.1_Staphylococcus_phage_B122	9	5
OM439669.1_Staphylococcus_phage_vB_SauS_760	12	7
OM439674.1_Staphylococcus_phage_vB_SauS_Mh15	15	7
OM439673.1_Staphylococcus_phage_vB_SauS_Mh1	14	9
NC_028917.1_Staphylococcus_phage_3MRA	8	4
OM439672.1_Staphylococcus_phage_vB_SauS_I73	13	8
NC_007061.1_Staphylococcus_phage_vB_SauS_HM1	4	1

KJ140076.1_Staphylococcus_phage_DW2	1	1
NC_007061.1_Staphylococcus_phage_vB_SauS_BC1	3	1
NC_007057.1_Staphylococcus_phage_96	2	2
NC_021332.1_Staphylococcus_phage_StauST398-3	5	2
NC_054982.1_Staphylococcus_phage_Sebago	11	2

Table S5.10 | Phage clouds results for phage HM1

No.	Phage	Organism	Distance
1	KJ140076	Staphylococcus_phage_DW2	0.0383
2	JQ973847	Staphylococcus_phage_StauST398-3	0.0616
3	MK618716	Staphylococcus_phage_Sebago	0.065
4	NC_007057	Staphylococcus_virus_96	0.0751
5	AY954960	Staphylococcus_virus_96	0.0751
6	KJ452291	Staphylococcus_phage_3MRA	0.076
7	KP209285	Staphylococcus_phage_phiNM4-gamma4	0.0774
8	MK290764	Staphylococcus_virus_B122	0.0795
9	KT344895	Staphylococcus_phage_phiJB	0.0795
10	KP893289	Staphylococcus_phage_B166	0.0824
11	DQ530362	Staphylococcus_virus_phiNM4	0.0824
12	MW238767	Staphylococcus_phage_IME1364_02	0.0886
13	NC_008799	Staphylococcus_virus_phiETA3	0.0888
14	AP008954	Staphylococcus_virus_phiETA3	0.0888
15	CP071049	Staphylococcus_phage_WBG8381	0.0911

Table S5.11 | Phage clouds results for phage BC1

No.	Phage	Organism	Distance

1	KJ140076	Staphylococcus_phage_DW2	0.020179
2	JQ973847	Staphylococcus_phage_StauST398-3	0.058453
3	MK618716	Staphylococcus_phage_Sebago	0.067586
4	KJ452291	Staphylococcus_phage_3MRA	0.080535
5	NC_007057	Staphylococcus_virus_96	0.085513
6	AY954960	Staphylococcus_virus_96	0.085513
7	NC_008799	Staphylococcus_virus_phiETA3	0.087001
8	AP008954	Staphylococcus_virus_phiETA3	0.087001
9	MK290764	Staphylococcus_virus_B122	0.088581
10	KP209285	Staphylococcus_phage_phiNM4-gamma4	0.089547
11	KT344895	Staphylococcus_phage_phiJB	0.091234
12	MW238767	Staphylococcus_phage_IME1364_02	0.092853
13	DQ530362	Staphylococcus_virus_phiNM4	0.095222
14	KP893289	Staphylococcus_phage_B166	0.09586
15	CP071049	Staphylococcus_phage_WBG8381	0.098035

Supplementary Figure:

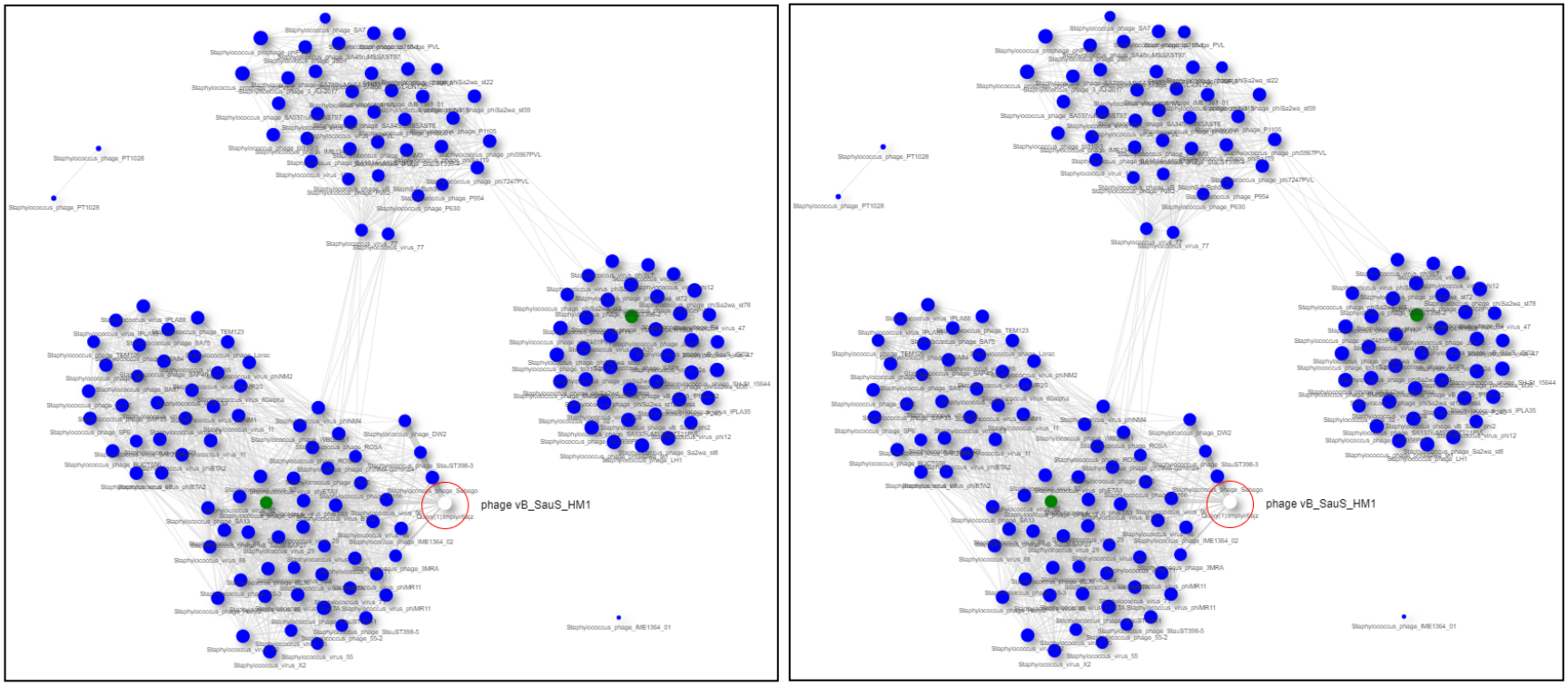

Figure S5.1 | (A) PhageCloud analysis of phage BC1 genomic relationship with the closest reference phage genomes on NCBI-GenBank. Intergenomic distances were calculated by dashing based on a threshold of 0.1. (B) PhageCloud analysis of phage vB_SauS_HM1 genomic relationship with the closest reference phage genomes on NCBI-GenBank. Intergenomic distances were calculated by dashing based on a threshold of

Chapter 6

6 Emulsion-Based Postbiotic Formulation is Comparable to Viable Cells in Eliciting a Localised Immune Response in Dairy Cows with Chronic Mastitis

Kevin Linehan is joint first author of this research paper which is published in:

Linehan, K., Mathur, H., Flynn, J., Byrne, N., Dillon, P., Conneely, M., Grimuad, G., Hill, C., Stanton, C. & Ross, R. P. 2022. Emulsion-Based Postbiotic Formulation Is Comparable to Viable Cells in Eliciting a Localised Immune Response in Dairy Cows With Chronic Mastitis. Frontiers in Microbiology, 13, 41.

6.1 Abstract

Bovine mastitis is a disease with a multi-etiological nature, defined as an infection and inflammation of the udder. Mastitis represents a significant ongoing concern in the dairy industry, leading to substantial losses in profits and revenue for farmers worldwide. The predominant causes of bovine mastitis include the pathogens Staphylococcus aureus, Streptococcus dysgalactiae, Streptococcus uberis, and Escherichia coli. Antibiotic administration is currently the main treatment option for mastitis. However, there is a pressing need for alternative therapies to treat and prevent the disease, especially with the emergence of antibiotic-resistant, mastitis-causing pathogens, resulting in antibiotic treatment failure. One such example is live bio-therapeutics (also known as probiotics), such as Lactococcus lactis DPC3147. The efficacy of this live bio-therapeutic has been demonstrated in several previous trials by our group. The most recent of these trials showed that an emulsion-based formulation of this strain was as effective as a commercial antibiotic formulation in treating sub-clinical and clinical cases of bovine mastitis. Here, we report the results of a follow-up field trial, in which we sought to gain insight into the mechanism of action of such live bio-therapeutics, focussing on chronic mastitis cases. We treated 28 cows with chronic mastitis with two separate emulsion-based formulations containing either viable L. lactis DPC3147 cells (15 cows) or heat-killed L. lactis DPC3147 cells (13 cows). We then evaluated the efficacies of the two formulations (two treatment groups) in terms of stimulating a localised immune response (quantified by measuring IL-8 concentrations in milk collected from udders affected by mastitis) and efficacies in terms of cure rates (quantified by reductions in somatic cell counts and absence of pathogens). We demonstrate that the presence of heat-inactivated bacteria (a postbiotic) was as effective as the live bio-therapeutic in eliciting a localised immune response in cows with chronic mastitis. The response to heat-killed cells (postbiotic) reported herein could have beneficial implications for farmers with regard to prolonging the shelf life of such emulsion-based formulations containing heat-killed cells of L. lactis DPC3147 for curing cows with mastitis.

6.2 Introduction

Milk is amongst the most versatile products in the food industry. World milk production was recorded at 823 million tons in 2017 and it is expected to increase by 22% by 2027 (Marcel et al., 2018). In addition to economic importance, milk and dairy products are important sources of macro and micronutrients in the human diet (Muehlhoff et al., 2013), including high-quality proteins, fatty acids, calcium, potassium, phosphorus, vitamin D, riboflavin, and vitamin B12 (Keast et al., 2013, O'Neil et al., 2018). Mastitis is the most prevalent and economically significant disease in dairy cattle worldwide (Castelani et al., 2019), primarily due to depleted milk production, discarded milk, premature culling, and treatment costs (Bar et al., 2008, Hertl et al., 2010, Halasa et al., 2007). In addition to negative impacts on milk production and quality (Detilleux et al., 2015), mastitis also influences the reproductive system of the animal (Kumar et al., 2017) and increases susceptibility to other diseases (Cha et al., 2013). Thus, decreasing the rates of mastitis and finding effective treatment options is crucial for ensuring a healthier herd, minimizing high somatic cell counts (SCCs) in cows, maximizing production yields and profits. The conventional treatment options for mastitis usually involve the use of antibiotics, such as pirlimycin, methicillin, cloxacillin, amoxicillin, novobiocin, penicillin G, dihydrostreptomycin, cephapirin, and erythromycin, which are all approved for bovine mastitis treatment and prevention (Nader-Macías et al., 2011).The principal etiological agents of bovine mastitis are *Staphylococcus aureus*, *Streptococcus dysgalactiae*, and *Streptococcus uberis* (Crispie et al., 2008, Zadoks et al., 2011b, Bi et al., 2016, Abebe et al., 2016). While antibiotics have proven to be effective in some cases against mastitis, a plethora of studies indicate that mastitis-causing pathogens are becoming resistant to antibiotics and the cure rates of conventional treatments are low (Freitas et al., 2018). Furthermore, mastitis caused by *S. aureus* can be recalcitrant to antibiotics due to its ability to evade the innate and adaptive immune response of the cow (Zaatout et al., 2020, Szweda et al., 2014, Zadoks et al., 2011a, Barkema et al., 2006), lending credence to the concern that antibiotics are no longer considered to be sufficient against *S. aureus*-induced bovine mastitis (Pietrocola et al., 2017).

The emergence of antimicrobial resistance (AMR) due to the overuse of antibiotics in food-producing animals has become a major concern (Xiong et al., 2018), especially

with respect to the risk of developing newly resistant bacteria that could be transmitted from animals to humans (Foutz et al., 2018). It is therefore imperative that preventative and alternative treatment plans are devised to reduce reliance on antibiotics in the dairy herd (McEwen and Collignon, 2018). To date, other forms of therapies (or combinations of antimicrobials) for mastitis have been reported with varying levels of efficacy (Angelopoulou et al., 2019, Cheng and Han, 2020). Bacteriocins such as nisin A have demonstrated antibacterial activity against mastitis pathogens (Malvisi et al., 2016). Immune stimulants such as ginseng (Beccaria et al., 2018) and the use of plant-derived compounds (Maia et al., 2018)and immune proteins such as lactoferrin (O'Halloran et al., 2016) have also been tested in this regard. Probiotic lactic acid bacteria (LAB) strains have been reported to eliminate mastitis-causing staphylococcal biofilms (Wallis et al., 2019). Furthermore, *Lactobacillus casei* BL23 has demonstrated anti-inflammatory properties on *S. aureus*-stimulated bovine mammary epithelial cells (Souza et al., 2018). However, there remains much mechanistic and trial work to elucidate the potential of probiotics as substitutes for antibiotics. Finally, phage therapy for treating bovine mastitis has been hampered on account of the inhibition of phages by compounds present in bovine milk (O'Flaherty et al., 2005). Phage endolysins, however, represent promising antimicrobial alternatives with proven potent activity against mastitis-causing pathogens (Zhou et al., 2017). However, endolysins require genetic engineering for both production and design, suggesting these are drugs of the future (Angelopoulou et al., 2019).

Our group has shown that the two-component bacteriocin produced by the LAB *L. lactis* DPC3147 inhibits a broad range of Gram-positive mastitis pathogens (Ryan et al., 1999, Ryan et al., 1998, Klostermann et al., 2008, Klostermann et al., 2010). *Lactococcus lactis* strains are routinely used as dairy starter organisms and numerous strains have been granted GRAS (generally regarded as safe) status in the dairy industry. Studies by Ryan et al. and Twomey et al., reported that lacticin 3147 combined with a bismuth-based teat seal prevented *Strep. dysgalactiae* infections in dry cows (Ryan et al., 1999) and *S. aureus* infections in lactating cows (Twomey et al., 2000). In a separate field trial, (Klostermann et al., 2008) evaluated the bactericidal activity of a freeze-dried preparation of the lacticin 3147-producing culture resuspended in sterile water and found that the treatment was as efficacious as conventional antibiotic treatment. Furthermore, that study noted that a Gram-negative,

lacticin 3147-insensitive *E. coli* strain was also one of the mastitis-causing pathogens that was eliminated by this freeze-dried preparation. Thus, it has been suggested that a mechanism other than bacteriocin production was contributing to the elimination of this Gram-negative pathogen (Klostermann et al., 2008). Additionally, (Crispie et al., 2008) reported that infusion with freeze-dried *L. lactis* DPC3147 rapidly stimulated the host intra-mammary immune system leading to the recruitment of lymphocytes and polymorphonuclear leukocytes (PMNs), to the mammary gland along with the localised production of acute-phase proteins (APP). A combination of these factors contributes to clear the mammary gland of the offending pathogen (Crispie et al., 2008). In a separate study (Klostermann et al., 2010), it was reported that a teat dip containing lacticin 3147 was efficacious at eliminating the mastitis pathogens *S. aureus*, *Strep. dysgalactiae* and *Strep. uberis* from cows' teats. However, producing sufficient quantities of pure antimicrobial peptides would be costly and is one of the main bottlenecks precluding the use of purified antimicrobial bacteriocins to treat bovine mastitis. More recently, our group developed a novel, live bio-therapeutic formulation, containing a liquid paraffin-based emulsion of *L. lactis* DPC3147. This live bio-therapeutic formulation displayed a 47% cure rate compared to a 50% cure rate for the routinely used commercial antibiotic formulation Terrexine™ for the treatment of cows with clinical and sub-clinical mastitis (Kitching et al., 2019).

The time-effective and inexpensive nature of producing this emulsion-based live bio-therapeutic formulation, compounded by its prolonged shelf life compared to previous aqueous-based formulations of the same, suggest that this product may represent a realistic alternative therapeutic option for bovine mastitis. In addition, the single-dose administration of this live bio-therapeutic formulation is a further advantage, as it can hasten the return of the milk to the milk pool and minimize or prevent withholding of milk from processing for several days, in comparison to some commercial antibiotics. The primary objective of this current trial was to investigate if such recently developed emulsion-based formulations derived from *L. lactis* DPC3147 need to contain viable cells or whether heat-inactivated cells thereof can elicit an equally potent localised immune response in cows with chronic mastitis. The outcome of this field trial reported herein demonstrates that a formulation containing heat-killed cells of *L. lactis* DPC3147 is equally efficacious at eliciting a localised interleukin 8 (IL-8) response upon infusion of udders affected by mastitis. The equally potent immuno-

stimulatory effects of emulsion-based formulations containing heat-killed cells of *L. lactis* DPC3147 could present farmers with additional alternative therapeutic options with a prolonged shelf life, for treating cows with mastitis.

6.3 Materials and Methods

6.3.1 Preparation of Liquid Paraffin-Based Emulsions Containing Viable and Heat-Killed *Lactococcus lactis* DPC3147 Cells

The emulsion-based formulations were prepared as described by (Kitching et al., 2019), with minor modifications. Briefly, liquid paraffin and polysorbate 80 were both purchased from Sigma-Aldrich (Vale Road, Arklow, Ireland). Polysorbate 80 (10%) was prepared in sterile autoclaved DNAase and RNAase-free water and sterilised by filtering twice through 0.2 μm syringe filters. Forty-five milliliters of liquid paraffin were poured into 250 ml glass beakers and sterilised under dry heat at 170°C for 2 h. This was subsequently allowed to cool to room temperature prior to use. Prior to preparation of the emulsion, the blade of an Ultra-Turrax® homogenizer was autoclaved and then steeped in 1% v/v Chlorus and UV-sterilised under laminar airflow for 1 h.

Ten milliliter overnight cultures of *L. lactis* DPC3147 were grown for 16 h at 30°C in LM17 (containing 0.5% lactose) broth (Merck). The overnight cultures were subsequently centrifuged at 8,000 x g for 15 min at 4°C using a Thermo Scientific Sorvall centrifuge to isolate the cell pellet. The cell pellets were washed twice with 10 ml of sterile autoclaved RNAase-free water between centrifugation steps. Finally, the cells were resuspended in 15 ml of 10% polysorbate 80. Forty-five milliliters of sterile liquid paraffin were homogenised with 15 ml of the 10% polysorbate 80 (mixed with cells) at 10,000 rpm in an Ultra-Turrax® homogenizer for 5 min under ice to yield a final cell concentration of approximately 1×10^9 cfu per 5 ml dose (equivalent to approximately 2×10^8 cfu/ml) in the emulsion. *Lactococcus lactis* DPC3147 cells resuspended in 10% polysorbate 80 were slowly poured into the liquid paraffin during homogenisation. Thus, the emulsion contained a final concentration of 2.5% polysorbate 80. To prepare heat-killed *L. lactis* DPC3147 cells, the above-mentioned steps were followed identically. However, just prior to resuspending the cells in 10% polysorbate 80, the cells were resuspended in 1 ml of sterile water and heat-treated in a boiling water bath at 100°C for 12 min. After boiling, the heat-killed cells were

cooled to room temperature before resuspending them in 14 ml of 10% polysorbate 80. Homogenisation steps were conducted with the Ultra-Turrax® as described above.

The number of viable cells was quantified in the emulsion formulations in terms of colony forming units/ml (cfu/ml) by conducting viable plate counts. Maximum recovery diluent (MRD, Oxoid, Basingstoke, Hampshire, United Kingdom) was utilised as a diluent in all cases. *Lactococcus lactis* DPC3147 (and heat-killed versions thereof) were plated onto LM17 agar. Plates were incubated for 24 h at 30°C and cfu/ml determined. Agar plates from heat-treated cells were incubated for up to 72 h at 30°C to ensure that all the cells were killed as confirmed by the absence of any colonies on agar plates after 72 h of incubation. While we did not check bacterial cell integrity after heat inactivation by microscopy, we concluded that the absence of any colonies whatsoever, even after a prolonged incubation of 72 h meant that our heat-killing procedure was 100% effective and no bacterial cells were able to recover and form colonies on agar plates.

6.3.2 Cows Selected for the Emulsion Formulation Trial, Intra-Mammary Infusion, and Sampling

This field trial was approved by the Teagasc Animal Ethics Committee (Approval number TAEC186-2018) and by the Health Products Regulatory Authority (HPRA; Project Authorisation number AE19132/P086). Holstein-Friesian dairy cows with mastitis were first identified in the herd using bulk cow somatic cell counts (SCCs) and only animals with a SCC >250,000 cells/ml were selected for the trial. Once cows were selected on the basis of these bulk cow SCCs, quarter sampling was conducted to identify the infected udder and quarter sample SCCs were quantified thereafter. Cows with clinical mastitis displayed obvious signs of udder inflammation and/or general malaise, clotted/abnormal milk production as well as the presence of pathogens in milk. G*Power calculations prior to conducting the trial revealed that $n = 13$ cows for each of the two treatment groups were sufficient for statistically valid results. However, this number was rounded off to $n = 15$ cows per treatment group to account for possible dropouts. To assess the response to each of the treatment groups, cows that were presenting with high SCC were identified in the herd and the affected quarter was infused at random with a one-time dose of emulsion preparation containing any one of the two formulations, which were made fresh (approximately 1×10^9 cfu of *L. lactis* DPC3147 or heat-killed versions thereof, per 5 ml dose;

equivalent to approximately 2×10^8 cfu/ml; *n* = maximum of 15 cows per treatment group). The selection of the treatment group was at random, to prevent bias and variability in the results. In specific cases where a cure was successful (defined by a reduction in SCC counts from initially high numbers to between 250,000 and 750,000 cells/ml and absence of pathogens upon plating within 5–7 days post-infusion), antibiotics were not required at all. However, in specific cases where there was treatment failure as a result of our formulations even after 7 days (and/or the cows were unable to mount a potent immune response naturally to result in a natural cure), conventional antibiotic intervention took place 7 days post-infusion to cure the cows, as per good veterinary and clinical practice. Any such cows were administered two doses of a commercial antibiotic. The commercial dual antibiotic formulation consists of cephalexin (200 mg) and kanamycin (100,000 I.U.) and is routinely utilised to treat lactating cows with clinical or sub-clinical mastitis in the Moorepark herd at the Teagasc Animal and Grassland Research and Innovation Centre, Moorepark, Ireland. The cows were considered still infected if the SCC was still high 7 days post-infusion, as the main criterion (and such cases of high SCCs were routinely validated by plating for pathogens as well, even after the conclusion of our investigative trial with our two treatment groups described here in this study).

All the treatments from each of the two treatment groups were directly administered into the teat sinus as previously described with minor modifications (Klostermann *et al.*, 2008, Crispie *et al.*, 2008). Briefly, the teat in question was swabbed with 70% v/v ethanol on cotton wool, prior to sampling. A milk sample from the affected quarter was collected just before infusion. After this, 5 ml of an emulsion-based formulation from one of the two treatment groups, containing approximately 1×10^9 cfu (or heat-killed versions thereof) per 5 ml dose (equivalent to approximately 2×10^8 cfu/ml) was infused into the mammary gland using sterile blunt-ended steel syringes (17 mm in length). Milk samples were taken at time 0 (just prior to infusion), 6 h post-infusion and subsequently at intervals up to 7 days post-infusion for analysis of SCC, interleukin (IL)-8 titres and the presence of mastitis-causing pathogens was detected by plating each of these milk samples on Blood agar (Oxoid Ltd., Basingstoke, Hampshire, United Kingdom). The respective pathogens were identified as follows: *S. aureus* produced creamy, greyish-white and occasionally golden-yellow colonies on blood agar, 3–5 mm in diameter with typical zones of haemolysis. Streptococci

produced small, smooth, translucent, cone shaped colonies on blood agar. *Strep. dysgalactiae* colonies produced characteristic narrow zones of pale green discoloration of the medium accompanied usually by a narrow zone of haemolysis. *Strep. uberis* colonies caused a diffuse browning of the aesculin blood agar. *Escherichia coli* produced large (3–4 mm) grey colonies. Such *E. coli* colonies can sometimes also show haemolysis and frequently produce mucoid colonies.

Overall, the cows with high bulk SCCs (and subsequently identified high quarter SCCs as briefly described above) as part of this trial were selected at random to prevent bias. The cows selected had a mixture of lactation ranks, ranging from ranks 1 to 7. Therefore, the cows were selected at random from early, mid and late lactation stages, as part of this trial to prevent bias. Upon retrospective assessments of the historical records of the cows, we concluded that the majority of cows had suffered from previous episodes of mastitis. Aside from the Moorepark herd (from where most of the cows were selected), there was one other nearby farm (Curtin's farm) from which cows were selected as well. The selection of cows took place in the time period between November 2018 and July 2019.

6.3.3 Somatic Cell Count Measurements

SCC/ml of milk samples were determined as previously described with a few minor modifications (Klostermann *et al.,* 2008, Klostermann *et al.,* 2010). Briefly, milk samples were collected from the relevant quarters at time 0 (just before treatment) and at designated time points post-treatment, as described above. SCC/ml in raw milk were measured using a Somacount 300® (Bentley Instruments Incorporated, United States).

6.3.4 Determination of IL-8 Titres in Milk Samples Using ELISA

Milk samples were collected as described above and centrifuged for 30 min at 44,000*g*, in order to remove the fat layer from the milk using a sterile pipette tip. After centrifugation, the supernatants from the milk samples were subjected to IL-8 analysis by ELISA or samples were frozen at −80°C for analysis at a later stage, as described previously (Kitching et al., 2019). The bovine IL-8 (CXCL8) ELISA development kit (Mabtech AB, Nacka Strand, Sweden) was utilised to quantify IL-8 titres in milk samples collected at different time points pre- and post-treatment, from cows treated with emulsion preparations containing one of the two treatment group formulations. Briefly, the following protocol was used: A 96-well Nunc-Immuno plate (Thermo

Scientific, Ballycoolen, Dublin, Ireland) was pre-coated with 100 µl of mAb MT8H6 at a concentration of 2 µg/ml (diluted in PBS pH 7.4) and the plate was stored at 4°C for 16 h. After 16 h, all wells were washed twice with 200 µl phosphate-buffered saline (PBS pH 7.4). The plate was subsequently blocked with 200 µl PBS (supplemented with 0.05% Tween 20 and 0.1% bovine serum albumin) and the plate was covered in tin foil and kept at room temperature for 1 h. After 1 h, the plate was washed five times using PBS supplemented with 0.05% Tween 20 (hereafter referred to as wash buffer). After this, 100 µl of IL-8 standards ranging from concentrations of 6.25 to 1,600 pg/ml were added to the wells in triplicate, as per the manufacturer's instructions. Milk samples collected at different time points were diluted 1:10, and 1:100 in PBS (pH7.4) and 100 µl of the undiluted samples, 1:10 dilutions and 1:100 dilutions were added to the wells in the microtiter plate in triplicate. The plate was covered in tin foil and incubated for 2 h at room temperature. After 2 h, each of the wells was washed with wash buffer five times. After these wash steps, 100 µl of mAb 26E5-biotin at a final concentration of 0.1 µg/ml was added to each well and the plate covered in tin foil and incubated for 1 h. As before, the wells were washed five times with wash buffer after the 1 h incubation step. One hundred microliters of Streptavidin-ALP diluted 1:1000 was added to each well and the plate covered in tin foil and incubated for 1 h at room temperature, followed by washing five times. Finally, phosphatase substrate (Sigma-Aldrich, Vale Road, Arklow, Ireland) at a final concentration of 1 mg/ml was prepared using sterile de-ionised water supplemented with 7.5 mg/ml glycine, 1 mM $ZnCl_2$ and 1 mM $MgCl_2$ and the pH was adjusted to pH 10.4 using 2 M NaOH. One hundred microliters of this substrate solution was added to each of the wells and the plate covered in tin foil and incubated for 1 h at 37°C. A plate reader (Synergy HT, BioTek) was used to take absorbance readings at 405 nm. Graph Pad Prism software (version v9.1.0) with five-parameter logistics was used to interpolate IL-8 values. However, in the rare event that five-parameter logistics failed to interpolate IL-8 values for certain quarters, the less stringent four-parameter logistics was utilised instead of five-parameter logistics in these specific cases.

6.3.5 Statistical Analyses

Statistical analyses described herein were performed in Graph Pad Prism v9.1.0. Comparison of the cure rate of the two treatment groups was performed using a Fisher's exact test. IL-8 and SCC data were first tested for normality using the

Shapiro–Wilk test. Non-parametric Wilcoxon tests were used to evaluate statistical differences between heat-killed *L. lactis* DPC3147 and viable *L. lactis* DPC3147 treatment groups in all cases. A spline-based statistical tool was also used to compare the whole time series (R package splinectomeR; Shields-Cutler et al., 2018). A difference was considered statistically significant if $p < 0.05$ in all cases.

To ordinate the sample, we first calculated dissimilarity matrices from the cows' time series using the "vegdist" function from the "vegan" R package (Bray–Curtis distances). Dissimilarity matrices were subjected to classical multidimensional scaling (PCoA) to obtain the first two principal coordinates, as well as the variance explained by each, using the "pcoa" function from the "ape" R package. The dissimilarity matrices used for PCoA were also used for permutational multivariate analysis of variance (PERMANOVA; "adonis2" function from "vegan"). Pairwise PERMANOVA were calculated using the "pairwiseAdonis" R package, and value of *p* were adjusted using the Bonferroni method. A difference was considered statistically significant if the adjusted $p < 0.05$. We finally calculated the Spearman correlation coefficients between SCC and IL-8 using the "cor.test" function from "stats" R package.

6.4 Results

6.4.1 *Lactococcus lactis* Cells Do Not Need to Be Viable to Elicit a Localised IL-8 Response

We opted to quantify the localised IL-8 response upon infusion of both treatment options as previous field trials of this nature in our group had indicated that IL-8 was the main cytokine involved in a localised inflammatory response and responsible for the recruitment of polymorphonuclear leucocytes and neutrophils to the site of infection (Beecher et al., 2009). While there was a large inter-animal variation of IL-8 concentrations in this trial as well, overall, it was apparent that heat-killed *L. lactis* DPC3147 cells elicited an equally potent IL-8 response as viable *L. lactis* DPC3147 cells (Figure 6.1). A Shapiro test of normality was initially used to show that the IL-8 values were not normally distributed ($p < 0.05$) and therefore, a non-parametric Wilcoxon test was used to compare the IL-8 titres elicited by viable *L. lactis* DPC3147 cells versus heat-killed DPC3147 cells. Figure 6.1 shows that there was no significant difference in IL-8 responses in cows treated with either viable

DPC3147 cells or heat-killed DPC3147 cells at any of the time points ($p > 0.05$). This indicates that formulations containing heat-killed cells were able to trigger an equally potent IL-8 response as formulations containing viable DPC3147 cells. In addition, a spline-based statistical tool was used to compare the value of *p* of IL-8 values in the whole time series (R package splinectomeR; Shields-Cutler et al., 2018; Figure 6.2). As shown in Figure 6.1, the differences in IL-8 values between the two treatment groups are not statistically significant for IL-8 ($p = 0.93$), further highlighting that heat-killed DPC3147 cells have the ability to cause an equally potent localised IL-8 response as viable DPC3147 cells (Figures 6.1, 6.2).

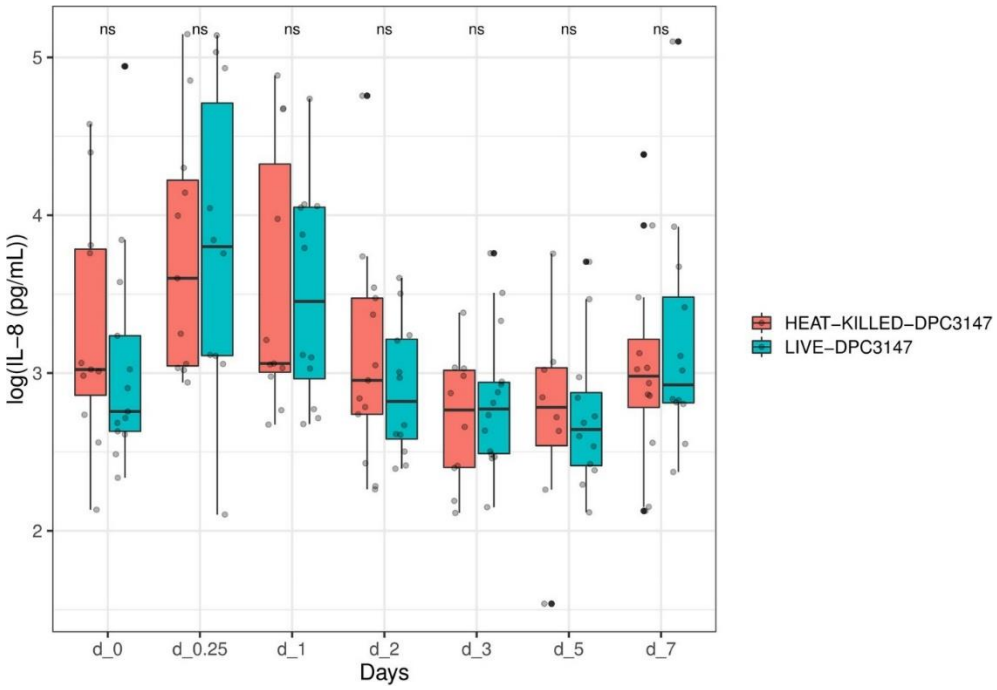

Figure 6.1 | A non-parametric Wilcoxon test was used to compare the IL-8 titres elicited by viable *Lactococcus lactis* DPC3147 cells versus heat-killed DPC3147 cells. The figure shows that there was no significant difference in IL-8 responses in cows treated with either viable DPC3147 cells or heat-killed DPC3147 cells at any of the time points ($p > 0.05$). This indicates that heat-killed cells can elicit an equally potent IL-8 response as viable DPC3147 cells.

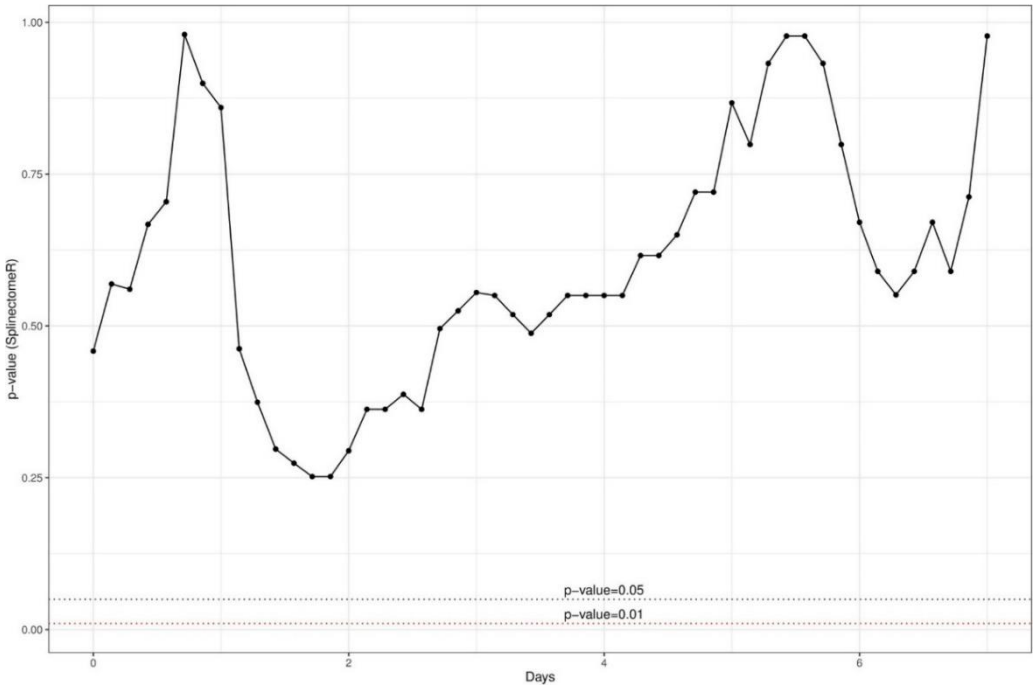

Figure 6.2 | A spline-based statistical tool was used to compare the value of *p* of IL-8 titres in the whole time series (R package splinectomeR; Shields-Cutler et al., 2018). The differences between the two treatment groups are not significant for IL-8 ($p = 0.93$), further highlighting that heat-killed cells have the ability to elicit an equally potent localised IL-8 response as do viable DPC3147 cells.

6.4.2 Cure Rates Based on SCC Are Statistically Similar for Treatment Groups Involving Either Viable or Heat-Killed *Lactococcus lactis* DPC3147 Cells

Quarters with a SCC of >250,000 cells/ml (log 5.4 cells/ml), were selected for this study as they were representative of mastitis. Somatic cell counts are an indicator of infection and inflammation in the udder, with a higher SCC generally indicative of inflammation. The criteria for defining chronic mastitis included cows that historically had suffered from recurrent cases of mastitis in the herd prior to the commencement of this current trial, and cows that were on occasion slow to recover from mastitis even with antibiotic therapy. These cows on occasion failed antibiotic therapy and recovered from mastitis naturally as a result of mounting a natural immune reaction to combat the infection. Such historical records were retrospectively checked upon completion of the trial, to prevent bias when initially selecting cows in the herd with high bulk (and high quarter) SCCs, as part of this current trial. The cure rates as part of this current trial were evaluated based on the initial SCC compared to counts after

7 days post-infusion. While a minimum SCC of >250,000 cells/ml (log 5.4 cells/ml) was chosen as a criterion for selecting cows with mastitis, the majority of animals selected had chronic mastitis and starting quarter SCCs which were significantly higher than this minimum criterion value of 250,000 cells/ml. Milk samples were taken from mastitic cows at the following time points: T0 (before treatment), T0.25 (6 h post-infusion), T1, T2, T3, T5, and T7 days. A clinical cure was considered as a reduction in SCC from initially high starting counts to a SCC of between 250,000 and 750,000 cells/ml within 5–7 days post-treatment, as well as the absence of pathogens upon plating (Tables 6.1 and 6.2). It was shown that the cure rate of both treatment groups was somewhat similar and there was no statistically significant difference between the groups in terms of cure rate (*L. lactis* DPC3147 viable cells = 46.67% cure rate, *L. lactis* DPC3147 heat-killed cells = 15.38% cure rate), ($p = 0.2616$ when cured numbers were compared to each other and $p = 0.5556$ when non-cured numbers were compared to each other, Fisher's exact test; Tables 6.1 and 6.2). Although there were no statistically significant differences ($p > 0.05$) in the cure rates between the two treatment groups, the percentage cure rates were higher for the live DPC3147 treatment group compared to the heat-killed treatment group. Such a difference in the percentage cure rates is likely to be due to inter-cow variation, which is an inherent part of field trials of this nature. It must also be noted that *S. aureus* was found to be the predominant etiological agent of mastitis in the cows investigated in this trial (Table 6.1).

Table 6.1| Total number of quarters infused with one of the four emulsion-based formulations, showing the etiological agents of mastitis.

Treatment	**Culture-positive cases**	**Identity of pathogens**	**Cure rate of culture-positive cases based on SCC results (%)**
L. lactis DPC3147 live (total N = 15 teats)	14/15	12/14 *S. aureus*, 2/14 *Strep. uberis*, 1/14 *Strep. dysgalactiae*	4/12 *S. aureus* (33.33%), 1/2 *Strep. uberis* (50%), 1/1 *Strep. dysgalactiae* (100%)
L. lactis DPC3147 heat-killed (total N = 13 teats)	9/13	7/9 *S. aureus*, 2/9 *Strep. uberis*	1/7 *S. aureus* (14.29%), 0/2 *Strep. uberis* (0%)

Cows with chronic mastitis were predominantly selected in this trial. N number denotes number of quarters infused per treatment group. A clinical cure was defined as a reduction in SCC to 250,000-750,000 cells/ml within 5-7 days of treatment and the absence of pathogens upon plating.

Table 6.2 | Overall cure rates for each of the treatment groups investigated in this trial.

Treatment group	**N (number of quarters)**	**Cure rate (%)**
L. lactis DPC3147 live	15	7/15 (46.67%)
L. lactis DPC3147 heat-killed	13	2/13 (15.38%)

Cows with chronic mastitis were mainly selected in this trial. A clinical cure was defined as a reduction in SCC to 250,000-750,000 cells/ml within 5-7 days of treatment and the absence of pathogens upon plating.

Overall, as was the case for IL-8 values, it was determined that the SCC data was not normally distributed, by performing a Shapiro test of normality ($p < 0.05$). Therefore, a non-parametric Wilcoxon test was used to compare the SCC values in cows treated with viable DPC3147 cells versus heat-killed DPC3147 cells (Figure 6.3). As was the case for the IL-8 values, there were no statistically significant differences in the SCC

values between the two treatment groups at the designated time points ($p > 0.05$ in all cases), except for time point Day 0.25 (6 h post-infusion), where there was a statistically significant difference in the SCC values between viable and heat-killed cells ($p < 0.05$), depicted by an asterisk at Day 0.25 (6 h). Due to the lack of statistically significant differences at all the other time points, the data indicate that heat-killed cells may be as efficacious as viable DPC3147 cells in terms of decreasing SCC counts in mastitic cows.

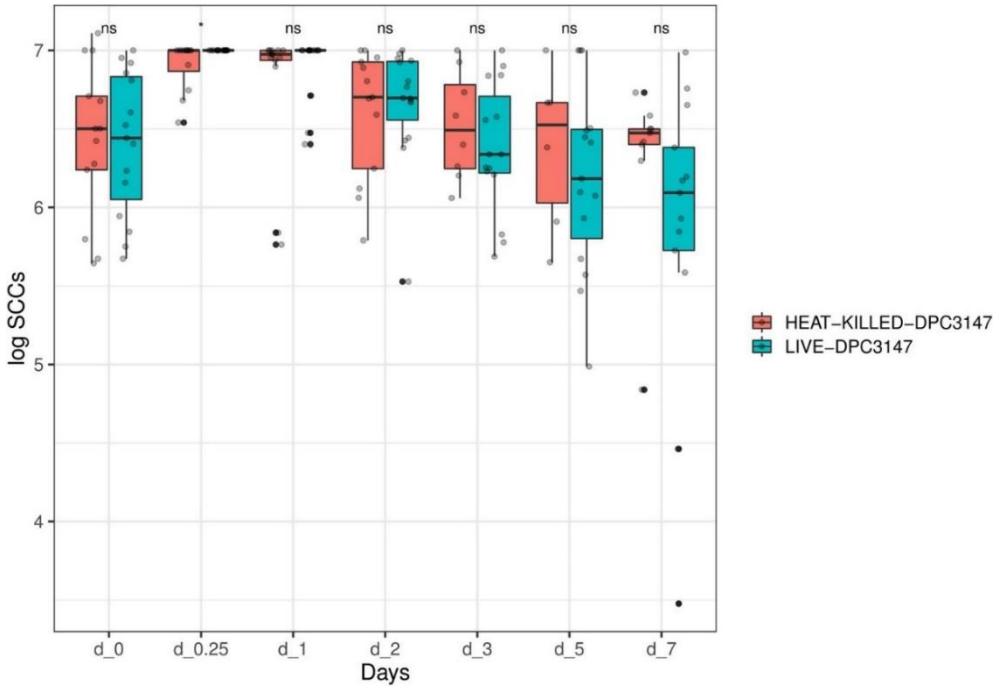

Figure 6.3 | A non-parametric Wilcoxon test was used to compare the SCC values in cows treated with viable DPC3147 cells versus heat-killed DPC3147 cells. There were no statistically significant differences in the SCC values between the two treatment groups at the designated time points ($p > 0.05$ in all cases), with the exception of time point Day 0.25 (6 h post-infusion), where there was a statistically significant difference in the SCC values between viable and heat-killed cells ($p < 0.05$), depicted by an asterisk at Day 0.25. Due to the lack of statistically significant differences at each of the time points except Day 0.25, the data indicates that heat-killed cells may be as efficacious as viable DPC3147 cells in terms of decreasing SCC count in mastitic cows.

In addition, a similar spline-based statistical tool as described in Figure 6.2 was used to compare the value of p of SCC values in the whole time series (R package splinectomeR; Shields-Cutler et al., 2018; Figure 6.4). As briefly mentioned above for Figure 6.3, overall, the differences in SCC values between the two treatment groups was not statistically significant ($p = 0.38$). However, this spline-based model could predict that the comparison was statistically significant between the two treatment groups at Day 0.25 (as shown previously in Figure 6.3) and also statistically significant on Day 5 and Day 7 ($p < 0.01$). Overall, this spline-based analysis also indicates that heat-killed DPC3147 cells can be as efficacious as viable DPC3147 cells in terms of decreasing SCC counts in mastitic cows (Figure 6.4). Furthermore, a Wilcoxon comparison between cured cows versus non-cured cows was conducted. The Wilcoxon test showed that there was a statistically significant difference in SCC values ($p < 0.05$) between cured cows versus non-cured cows at Day 5 post-infusion, indicating that it may take up to 5 days post-infusion to see clinical differences in the cows in terms of defining a clinical cure (Figure 6.5).

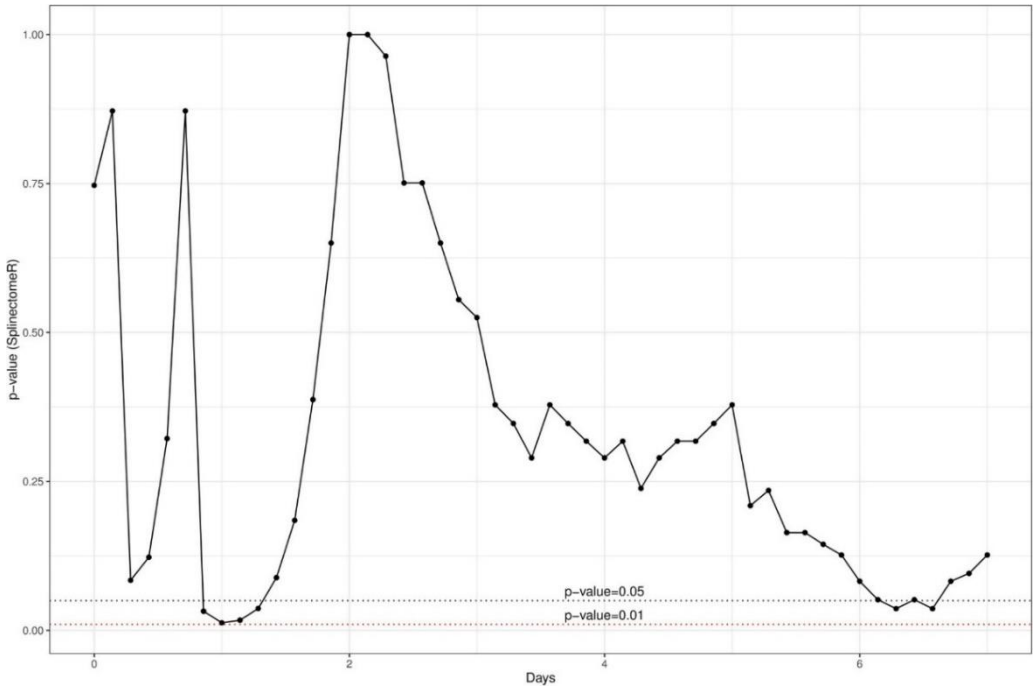

Figure 6.4 | A spline-based statistical tool was to compare the value of p of SCC values in the whole time series (R package splinectomeR; Shields-Cutler et al., 2018). Overall, the differences are not statistically significant for SCC between the two groups ($p = 0.38$). However, this spline-based model predicts that the comparison is statistically significant at Day 0.25 (as shown previously in Figure 6.2) and also

statistically significant between the two treatment groups on Day 5 and Day 7 ($p < 0.01$). Overall, this spline-based analysis also indicates that heat-killed DPC3147 cells can be as efficacious as viable DPC3147 cells in terms of decreasing SCC count in mastitic cows.

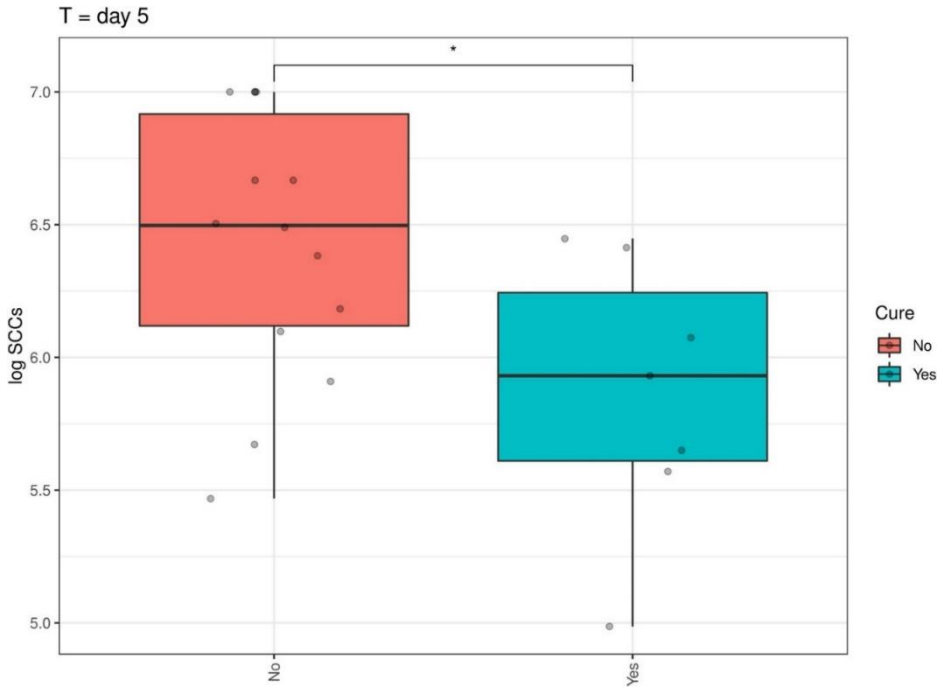

Figure 6.5 | A Wilcoxon comparison in SCC values between cured cows versus non-cured cows was conducted. The Wilcoxon test showed that there was a statistically significant difference in SCC values ($p < 0.05$) between cured cows versus non-cured cows at Day 5 post-infusion, indicating that it may take up to 5 days post-infusion to see clinical differences in the cows in terms of defining a clinical cure.

This trial established that the cure rates of both treatment groups were statistically non-significant (with the heat-killed *L. lactis* DPC3147 group showing somewhat lower cure rates, most likely due to inter-animal variation which is common in field trials of this nature). The focus of our previous trial was to compare the efficacies and cure rates of an emulsion-based formulation containing the live-biotherapeutic *L. lactis* DPC3147 versus commercial antibiotics to treat bovine mastitis. It is likely that any resolution and cure of the disease in trials of this nature is predominantly due to the cow's immune system mediated by IL-8 resulting from infusion with our treatment formulations, rather than the direct antimicrobial activity of lacticin 3147 against the pathogens. This was demonstrated here in this trial, as the cure rates of both treatment groups were statistically comparable to each other (Tables 6.1 and 6.2).

6.4.3 IL-8 Values Are Positively Correlated With SCC Values in Cured Cows but Not in Non-cured Cows

Spearman correlations were conducted between all the IL-8 values and SCC values as part of this trial. When compared overall, SCC and IL-8 were positively and significantly correlated ($R = 0.22$, $p < 0.01$; Figure 6.6). Such Spearman correlations were then conducted between IL-8 values and SCC values in cows which were cured (Figure 6.7). When compared overall, SCC and IL-8 are positively and significantly correlated in cured cows ($R = 0.44$, $p = 0.0012$). Although the concentrations of PMNs were not measured in this trial, the trends described above suggest that increased IL-8 values in response to infection (and therefore high SCC values) likely resulted in the recruitment of PMNs to the site of infection, which helped combat the offending pathogen, eventually resulting in a clinical cure (Figure 6.7).

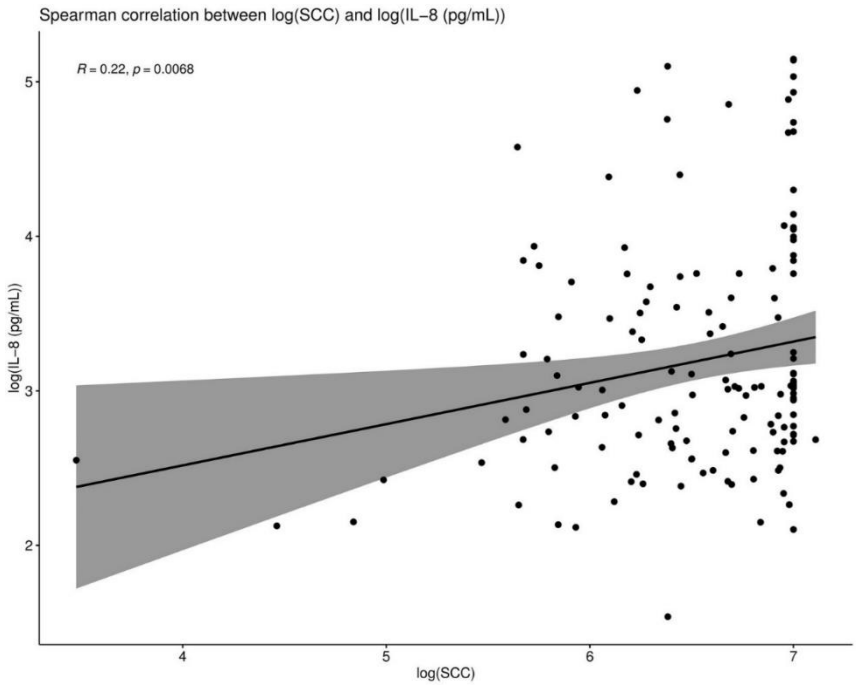

Figure 6.6 | Spearman correlations were conducted between IL-8 values and SCC values. When compared overall, SCC and IL-8 are positively and significantly correlated ($R = 0.22$, $p < 0.01$).

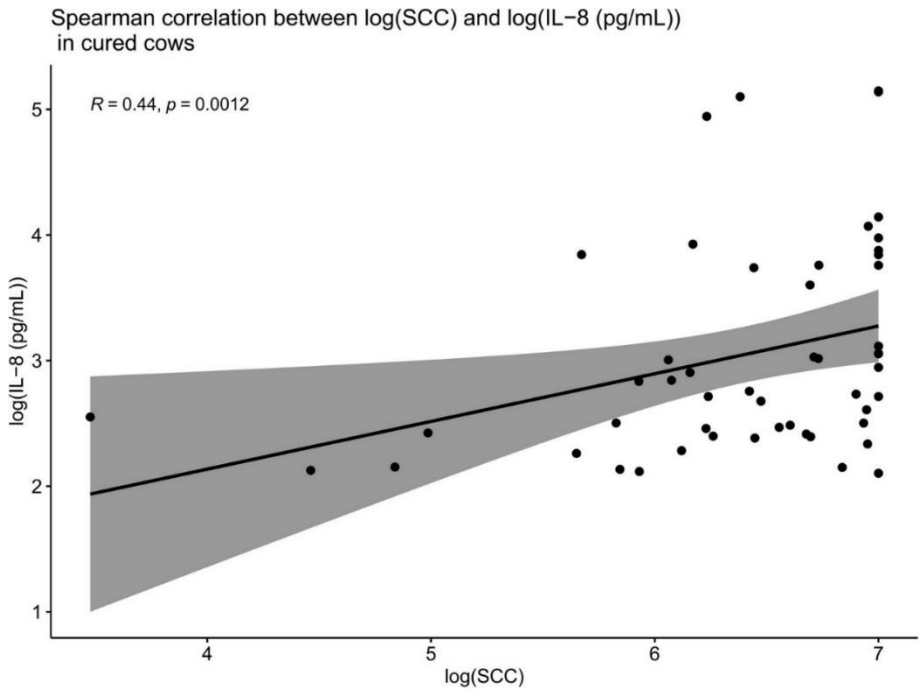

Figure 6.7 | Spearman correlations between IL-8 values and SCC values in cows which were cured showing that when compared overall, SCC and IL-8 are positively and significantly correlated in cured cows ($R = 0.44$, $p = 0.0012$). This suggests that increased IL-8 values in response to infection (and therefore high SCC values) result in the recruitment of PMNs to the site of infection, which likely combat the offending pathogen, eventually resulting in a clinical cure.

Such Spearman correlations were also conducted between IL-8 values and SCC values in cows which were not cured (Figure 6.8). When compared overall for cows which were not cured, SCC and IL-8 were no longer positively correlated ($R = 0.035$, $p = 0.73$). While we do not have data pertaining to PMN concentrations at the site of infection in this trial, the lack of positive correlations between SCC and IL-8 in non-cured cows described above suggests that these cows were likely unable to mount a sufficient localised IL-8 response, leading to inadequate recruitment of PMNs to the site of infection. This insufficient localised IL-8 response may help to explain why such cows may have been unable to combat the infection and thereby remained uncured.

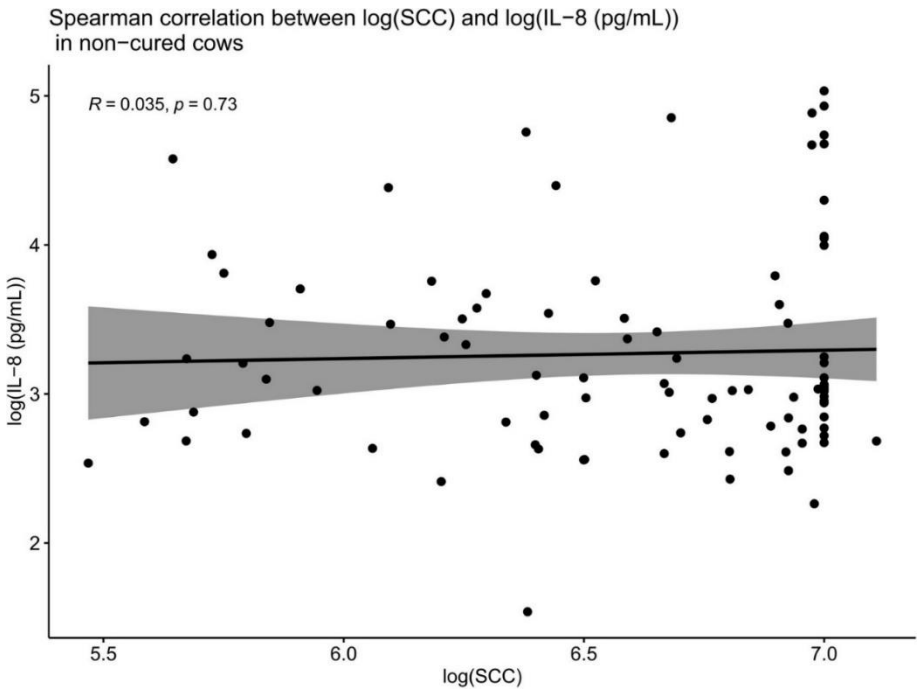

Figure 6.8 | Spearman correlations between IL-8 values and SCC values in cows which were not cured. When compared overall for cows which were not cured, SCC and IL-8 are no longer positively correlated ($R = 0.035$, $p = 0.73$). This suggests that these cows were likely unable to mount a sufficient localised IL-8 response, leading to inadequate recruitment of PMNs to the site of infection. This insufficient localised IL-8 response may explain why such cows were unable to combat the infection and thereby remained uncured.

6.4.4 Cows in This Trial Mounted an Equally Potent Localised IL-8 Immune Response, Irrespective of the Pathogenic Etiological Agent of Mastitis

A Wilcoxon comparison was conducted for IL-8 values in cows where the etiological agent of mastitis was identified to be (i) *Staphylococcus aureus*, (ii) *Streptococcus* species, (iii) *Staphylococcus aureus* and *Streptococcus* species together (co-infection), or (iv) pathogen negative (where there was no etiological agent detected but the cows still presented with mastitis). Overall, the statistical tests show that there were no significant differences in IL-8 values detected in milk samples from the cows infected by each of the above-mentioned pathogens ($p > 0.05$; Figure 6.9). However, there were statistical differences in IL-8 values detected in the milk samples in cows infected with *Streptococcus* species versus cows where there was no pathogen detected (but still suffered from mastitis). The average IL-8 values were higher in *Streptococcus*-infected cows compared to cows where there was no pathogen

detected. This may be due to the cows' natural immune response detecting the *Streptococcus* pathogen in the infected udder and mounting a natural localised IL-8 immune response as a result of detecting the pathogen.

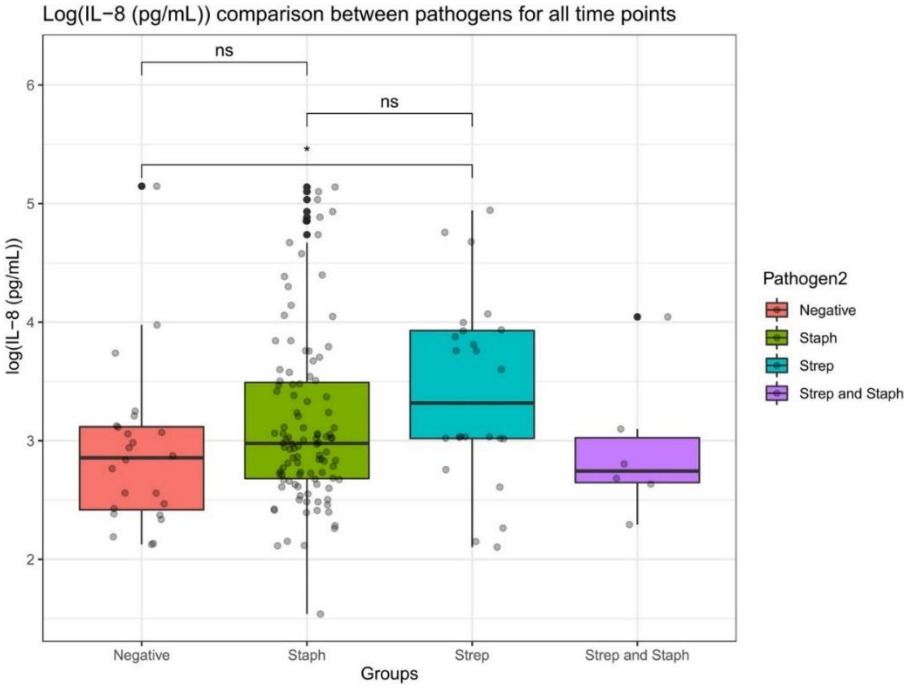

Figure 6.9 | A Wilcoxon comparison was conducted for IL-8 values in cows where the etiological agent of mastitis was identified to be *Staphylococcus*, *Streptococcus*, *Staphylococcus*, and *Streptococcus* together (co-infection) or pathogen negative (where there was no etiological agent detected but the cows still presented mastitis). Overall, the statistical tests show that there were no significant differences in IL-8 values detected in milk samples from the cows infected by each of the above-mentioned pathogens ($p > 0.05$). However, there were statistical differences in IL-8 values detected in the milk samples in cows infected with *Streptococcus* versus cows where there was no pathogen detected (but still suffered from mastitis; $p < 0.05$).

6.5 Discussion

Upon completion of this trial, we now have a more comprehensive hypothesis and a better understanding of the mechanism of action of emulsion-based formulations containing *L. lactis* cells. Prior to the commencement of the trial, we sought to answer one main key question: whether emulsion-based formulations need to contain viable *L. lactis* cells or not, in order to stimulate a localised immune response. Based on the

findings of this field trial, we have now established that infusion of emulsion-based formulations containing heat-killed *L. lactis* cells can evoke an equally potent localised IL-8 response in infected udders, as can viable cells. It may be the case that cell surface-associated structures are responsible for inducing a localised IL-8 immune response in cows with mastitis. In addition, differences in the composition of cell surface components between *S. aureus* and *Streptococcus* species may also account for the differences observed in IL-8 production in this trial, as shown in Figure 6.9. It is likely that any clinical cure is due to a stimulation of the cow's immune response, triggered by either viable *L. lactis* DPC3147 cells and/or partially degraded components of the cell walls of heat-killed DPC3147 cells. Indeed, there may be a combination of partially intact and partially degraded *L. lactis* cell wall components upon heat treatment. We aim to gain insights into the integrity of the *L. lactis* envelop by electron microscopy and ascertain the role of any such partially degraded or fully intact lactococcal cell wall components as part of future trials. Taken together however, the IL-8 data reported herein in this trial indicate that the immune response may be triggered by some other factor associated with the cell wall, perhaps fragments of peptidoglycan, or teichoic acid associated with *L. lactis* and/or Gram-positive cell walls, rather than being directly associated with viable cells. Indeed, it is highly likely that by heat-treating the *L. lactis* cells, such components of cell wall fragments such as peptidoglycan and teichoic acid are released into the emulsion. The presence of these foreign substances may in turn trigger an immune response in the udder, which likely explains the increase in IL-8 titres.

Previous trials of this nature investigating heat-killed and viable cells have shown that viable cells elicit a more pronounced influx of lymphocytes and neutrophils to the site of infection (Crispie et al., 2008a). Unlike some of these previous trials of this nature which focused on various aspects of the immune response, this current trial predominantly focused on a localised IL-8 response at the site of infection upon infusion with viable and heat-killed cells present in emulsion-based formulations, as a previous trial had indicated that this was the main cytokine involved in evoking an immune response and resolving the infection (Beecher et al., 2009). In the trial conducted by Crispie et al. (2008), heat-killed cells evoked a less potent influx of lymphocytes and neutrophils, relative to the viable cells. The mean neutrophil counts increased by 10-fold 1 day post-infusion, and the peak PMN counts occurred on day

3. Although there was a rise in PMN numbers, this was significantly lower than the numbers elicited by viable cells in the trial (Crispie et al., 2008). Infusion with live cultures resulted in the mean PMN values peaking on days 1 and 2 post-infusion. Similarly, the mean lymphocyte levels peaked on day 3 post-infusion. The viable cells evoked significant increases in milk amyloid A (MAA) and haptoglobin (Hp) levels. While heat-killed cells evoked an increase in APP levels, these levels were lower than those evoked by viable cells in that trial (Crispie et al., 2008). The stronger immune response elicited by viable cells in the trial conducted by Crispie et al. (2008), may have accounted for the differences between the clinical cure rates in that trial compared to our current trial. In contrast to the above-mentioned trial, our current trial here predominantly focussed on a localised IL-8 response in cows (the majority of which were affected with chronic cases of mastitis). We found that heat-killed cells present in emulsion-based formulations elicited a potent IL-8 response. However, it remains to be determined whether this increase in IL-8 triggered a substantial enough recruitment of PMNs to the site of infection. An insufficient recruitment of PMNs, below the threshold required to fight the infection, may account for the somewhat low cure rates found in this current study. It must also be emphasised that there was a large inter-animal variation in terms of immune responses in this trial.

While the cure rates in this study are somewhat lower than desired, it is important to note that most cows selected for this field trial suffered from recurrent chronic mastitis and thus were more likely to fail any type of antimicrobial therapy, including commercial antibiotics and/or our two treatment formulations. While we do not have data directly comparing the cure rates of antibiotics versus our two emulsion-based formulations in cows with chronic mastitis as part of this current trial here, we hope to ascertain the effects of antibiotics against such chronic cases of mastitis in these same cows as part of future field trials and compare the efficacy of antibiotics to our emulsion-based formulations containing heat-killed cells, pending ethical approval. In addition, as part of this current trial, *S. aureus* positive cultures were the most frequently seen cause of disease. *Staphylococcus aureus* has also been found to be the most common cause of mastitis in Irish dairy herds overall (Keane et al., 2013). Indeed, the phenotypic and genomic plasticity of *S. aureus* contributes to its persistence. *Staphylococcus aureus* persistence is most commonly linked to their ability to invade epithelial cells, form a biofilm and polysaccharide capsules (Bardiau

et al., 2014), all of which contribute to the ability of *S. aureus* to evade the innate and adaptive immune response of the cow, thus persisting in the mammary gland. For instance, the presence of small colony variants (SCVs) in dairy cows with a history of chronic intra-mammary *S. aureus* infection (Atalla et al., 2008) appear to have atypical morphological and biochemical properties, and it can survive in the intracellular environment that protects the bacteria from host defences and antibiotics (Atalla et al., 2011). Furthermore, the synthesis of polysaccharide capsules can stop the action of macrophages, mask the recognition of antibodies directed against the cell wall by PMNs and prevent complement activation (Zaatout et al., 2020). A combination of these evasive mechanisms of *S. aureus* in addition to selecting chronic mastitis cases may explain why the cure rates were relatively low in this study, in comparison to some previous trials. Interestingly, our current trial also showed that the cows mounted an equally potent IL-8 response, irrespective of the etiological pathogen involved (either *S. aureus* or *Streptococcus* species). However, the lower cure rates for *S. aureus*-associated mastitis cases in this trial are likely to be due to the above-mentioned phenomena, even though the IL-8 response mounted was statistically as potent as the response mounted in cows with *Streptococcus*-associated mastitis. Furthermore, with regard to cure rates, it was also interesting to note in this trial that SCC values and IL-8 titres were positively correlated in cured cows but there was no such positive correlation in non-cured cows. This may be due to a higher and more potent IL-8 response mounted in cured cows, and the insufficient IL-8 response mounted in non-cured cows may explain why such cows were unable to combat the infection.

Despite the variations seen in different animal trials of this nature, similar to our current trial, several *in vivo* trials have also demonstrated the efficacy of heat-killed cells in stimulating the immune response and potential probiotic effects of heat-killed cells. In one such study, Warda et al. (2019) (Warda et al., 2019) prepared a heat-killed preparation of ADR159 containing *Lactobacillus delbrueckii*. The study showed that heat-killed cells and components of the cell wall were able to elicit an immune effect. In a separate study, Wagner et al. (2000) tested the effects of administering heat-inactivated *Lactobacillus casei* and *Lactobacillus acidophilus* to *Candida albicans*-colonised immunosuppressed mice. The authors found that heat-killed probiotics conferred protection against *C. albicans*-induced systemic as well as mucosal

candidiasis infection. Piqué et al. (2019) summarised the health-promoting properties of tyndallised probiotics, mainly LAB and bifidobacteria, in a comprehensive review and described how heat-killed probiotic cells are still capable of eliciting immunomodulatory effects. Indeed, after inactivation of bacteria, dead cells can release bacterial components with key immunomodulating effects and with antagonizing properties against pathogens. Different bacterial components, such as lipoteichoic acids, peptidoglycans or exopolysaccharides (EPS), have been proposed to be mainly involved in these properties in preparations containing heat-killed bacteria (Taverniti and Guglielmetti, 2011; Sarkar and Mandal, 2016; Castro-Bravo et al., 2018). Another example includes a study by Jorjão et al. (2015) who reported that heat-killed *Lactobacillus rhamnosus* ATCC7469 cells were able to stimulate mouse macrophages to produce cytokines including IL-4, IL-6, IL-10, IL-12, among others. In other bovine mastitis-related studies, Blanchet et al. (2021) demonstrated the immunomodulatory efficacy of heat-killed *Lactobacillus gasseri* LA806 in the process of impairing *E. coli* and *S. aureus* colonisation of bovine mammary epithelial cells (bMEC) in *in vitro* models. A separate study by Fukuyama et al. (2020), also reported the immunomodulatory efficacy of LAB strains in stimulating Toll-like receptor-mediated inflammatory responses in *in vitro* bMEC models. Finally, Seridan Assis et al. (2015), demonstrated the efficacy of *L. lactis* V7 in stimulating the production of IL-8 in bMEC cell culture and by doing so, preventing the internalisation of *S. aureus* and *E. coli* pathogenic strains into bMEC cells.

While we have gained some further insights into the localised immune response that is elicited by our emulsion-based formulations containing *L. lactis* DPC3147 (and heat-killed cells thereof), this trial does have some limitations, and this is largely due to the limited number of animals (maximum $n = 15$ animals per treatment group) and limited treatment groups one can use in a trial, in keeping with the principles of the 3Rs. Although the inclusion of an antibiotic treatment group as a supplementary control treatment group may have been beneficial as part of this trial, the primary focus of this trial was to answer one main question: whether heat-killed *L. lactis* cells are as efficacious as viable *L. lactis* cells in evoking a localised IL-8 immune response in udders affected by mastitis. Indeed, upon completion of this trial, we now have greater insights into the immune response to heat-killed *L. lactis* cells.

It is anticipated that further trials of this nature with a few other treatment groups may have to be conducted to fully unravel the complex mechanisms involved in the resolution of this disease, pending approval by local animal ethics committees. Future trials of this nature may involve alternative *L. lactis* and/or other LAB strains which do not produce any bacteriocins/antimicrobials at all. A supplementary negative control treatment group may involve infusions with merely the emulsion-based formulation without any cells (live or heat-killed) whatsoever. This would provide insights as to whether the liquid paraffin-Tween 80 based emulsion-associated components trigger a minor immune response on their own and would enable us to quantify localised baseline IL-8 titres at the site of infection in the affected udder. In addition, as heat-killing cells is a very severe procedure, significantly degrading the bacterial cell wall and likely affecting heat-labile components which may have potential immunostimulatory activity, alternative methods such as UV irradiation could also be tested to determine what effect UV-inactivated cells with an intact cell wall have on the immune system. As UV irradiation damages the DNA inside bacterial cells and does not have a severe effect on the cell surface components, it may be the case that UV-inactivated cells are still capable of evoking a strong immune response. A separate negative control treatment group may include mastitic cows which have not been infused with any foreign substances at all after the initial detection of mastitis, in order to determine the strength of the natural immune response and baseline IL-8 titres evoked by the immune system of the cow itself in response to the pathogen. However, such a negative control treatment group would require us to treat the cows as soon as possible in the event of exacerbating mastitis, in accordance with good veterinary practice. Nonetheless, possible means to circumvent such issues may include a significantly reduced number of cows in such a negative treatment group and withholding treatment with antibiotics or other bio-therapeutic options for the shortest period of time possible. Finally, another possible study could involve assessing the impact of each of these treatment formulations on the microbiome of the teat canal and whether such alterations in the microbiome confer protection against mastitis-causing pathogens or not.

In addition, as part of future trials of a similar nature (pending ethical approval), we hope to quantify the concentrations of lacticin 3147 that are excreted in the milk samples at each of the time points post-infusion to use as an estimate of the amount of

lacticin 3147 produced in *in vivo* conditions. Our working hypothesis is that *L. lactis* DPC3147 cells may not be able to produce sufficient quantities of lacticin 3147 in these drastic *in vivo* conditions (and/or cells produce lacticin 3147 at sub-inhibitory concentrations, much lower than the minimum inhibitory concentrations actually required to have a killing effect on the offending pathogen). We aim to incorporate such lacticin 3147 concentration measurements as part of future trials of a similar nature, perhaps by including RP-HPLC and area under the curve analysis to quantify the concentrations of lacticin 3147 which are excreted in the milk samples post-infusion and use such concentrations as an estimate to gain insights into the concentrations produced *in vivo*. Also, further trials of this nature will help to determine whether other lactococci and/or other LAB strains in general, can mount an equally potent localised IL-8 response. Another interesting comparison would be to determine the difference in the potency of an immune response following infusions with other Gram-positive versus Gram-negative strains. However, for such a comparison to be conducted, the strain of choice would have to be carefully selected, ensuring that any such strains used have acquired GRAS and Qualified Presumption of Safety (QPS) status, and pass all the required regulatory safety assessments. Nonetheless, overall, the results of the trial reported here indicate that emulsion-based formulations containing heat-killed cells of *L. lactis* DPC3147 (a postbiotic) have the potential to sufficiently evoke a localised immune response in mastitic cows similar to that observed with the live strain. Furthermore, any such formulations containing heat-killed cells would significantly prolong the shelf life of such products compared to equivalent formulations requiring active viable cells, which would have a limited shelf life.

6.6 Data Availability Statement

The raw data supporting the conclusions of this article will be made available by the authors, without undue reservation.

6.7 Ethics Statement

The animal study was reviewed and approved by this field trial was approved by the Teagasc Animal Ethics Committee (Approval number TAEC186-2018) and by the Health Products Regulatory Authority (HPRA; Project Authorisation number AE19132/P086).

6.8 Author Contributions

HM and KL are researchers in Moorepark Food Research Centre, Teagasc and drafted the manuscript. HM prepared the various emulsion-based formulations for infusions, associated microbiological work, and ELISAs to quantify IL-8 titres. KL also conducted ELISAs to quantify IL-8 concentrations. JF conducted the SCC determinations and plating of pathogens. NB performed the infusions. GG performed the statistical analyses. JF, NB, PD, MC, CH, CS, and RR revised the manuscript. All authors contributed to the article and approved the submitted version.

6.9 Funding

HM is a researcher in Teagasc Food Research Centre, and this work was funded by the Science Foundation of Ireland (SFI)-funded Centre for Science, Engineering and Technology and the APC grant number SFI/12/RC/2273. Research in CH, CS, and RR laboratories is supported by the Science Foundation of Ireland (SFI)-funded Centre for Science, Engineering and Technology and APC Microbiome Ireland.

6.10 Conflict of Interest

The authors declare that the research was conducted in the absence of any commercial or financial relationships that could be construed as a potential conflict of interest.

6.11 Publisher's Note

All claims expressed in this article are solely those of the authors and do not necessarily represent those of their affiliated organisations, or those of the publisher, the editors and the reviewers. Any product that may be evaluated in this article, or claim that may be made by its manufacturer, is not guaranteed or endorsed by the publisher.

6.12 Abbreviations

AMR, Antimicrobial resistance; SCC, Somatic cell counts; PMN, Polymorphonuclear neutrophils/leucocytes; GRAS, Generally regarded as safe; QPS, Qualified presumption of safety; PBS, Phosphate-buffered saline; MRD, Maximum recovery diluent; IL-8, Interleukin 8; ELISA, Enzyme-linked immunosorbent assay.

6.13 References

ABEBE, R., HATIYA, H., ABERA, M., MEGERSA, B. & ASMARE, K. 2016. Bovine mastitis: prevalence, risk factors and isolation of Staphylococcus aureus in dairy herds at Hawassa milk shed, South Ethiopia. BMC Veterinary Research, 12, 270.

ANGELOPOULOU, A., WARDA, A. K., HILL, C. & ROSS, R. P. 2019. Non-antibiotic microbial solutions for bovine mastitis–live biotherapeutics, bacteriophage, and phage lysins. Critical reviews in microbiology, 45, 564-580.

ASSIS, B. S., GERMON, P., SILVA, A. M., EVEN, S., NICOLI, J. R. & LOIR, Y. L. 2015. Lactococcus lactis V7 inhibits the cell invasion of bovine mammary epithelial cells by Escherichia coli and Staphylococcus aureus. Beneficial Microbes, 6, 879-886.

ATALLA, H., GYLES, C., JACOB, C. L., MOISAN, H., MALOUIN, F. & MALLARD, B. 2008. Characterization of a Staphylococcus aureus small colony variant (SCV) associated with persistent bovine mastitis. Foodborne pathogens and disease, 5, 785-799.

ATALLA, H., GYLES, C. & MALLARD, B. 2011. Staphylococcus aureus small colony variants (SCVs) and their role in disease. Animal health research reviews, 12, 33-45.

BAR, D., TAUER, L. W., BENNETT, G., GONZALEZ, R. N., HERTL, J. A., SCHUKKEN, Y. H., SCHULTE, H. F., WELCOME, F. L. & GRÖHN, Y. T. 2008. The cost of generic clinical mastitis in dairy cows as estimated by using dynamic programming. Journal of dairy science, 91, 2205-2214.

BARDIAU, M., DETILLEUX, J., FARNIR, F., MAINIL, J. G. & OTE, I. 2014. Associations between properties linked with persistence in a collection of Staphylococcus aureus isolates from bovine mastitis. Veterinary microbiology, 169, 74-79.

BARKEMA, H. W., SCHUKKEN, Y. H. & ZADOKS, R. N. 2006. Invited review: The role of cow, pathogen, and treatment regimen in the therapeutic success of bovine Staphylococcus aureus mastitis. Journal of dairy science, 89, 1877-1895.

BECCARIA, C., SILVESTRINI, P., RENNA, M. S., ORTEGA, H. H., CALVINHO, L. F., DALLARD, B. E. & BARAVALLE, C. 2018. Panax ginseng extract reduces Staphylococcus aureus internalization into bovine mammary epithelial cells but does not affect macrophages phagocytic activity. Microbial pathogenesis, 122, 63-72.

BEECHER, C., DALY, M., BERRY, D. P., KLOSTERMANN, K., FLYNN, J., MEANEY, W., HILL, C., MCCARTHY, T. V., ROSS, R. P. & GIBLIN, L. 2009. Administration of a live culture of Lactococcus lactis DPC 3147 into the bovine mammary gland stimulates the local host immune response, particularly IL-1β and IL-8 gene expression. Journal of Dairy Research, 76, 340-348.

BI, Y., WANG, Y. J., QIN, Y., GUIX VALLVERDÚ, R., MALDONADO GARCÍA, J., SUN, W., LI, S. & CAO, Z. 2016. Prevalence of bovine mastitis pathogens in bulk tank milk in China. PLoS One, 11, e0155621.

BLANCHET, F., RAULT, L., PETON, V., LE LOIR, Y., BLONDEAU, C., LENOIR, L., DUBOURDEAUX, M. & EVEN, S. 2021. Heat inactivation partially preserved barrier and immunomodulatory effects of Lactobacillus gasseri LA806 in an in vitro model of bovine mastitis. Beneficial Microbes, 12, 95-106.

CASTELANI, L., ARCARO, J. R. P., BRAGA, J. E. P., BOSSO, A. S., MOURA, Q., ESPOSITO, F., SAUTER, I. P., CORTEZ, M. & LINCOPAN, N. 2019. Activity of nisin, lipid bilayer fragments and cationic nisin-lipid nanoparticles against multidrug-resistant Staphylococcus spp. isolated from bovine mastitis. Journal of dairy science, 102, 678-683.

CASTRO-BRAVO, N., WELLS, J. M., MARGOLLES, A. & RUAS-MADIEDO, P. 2018. Interactions of surface exopolysaccharides from Bifidobacterium and Lactobacillus within the intestinal environment. Frontiers in Microbiology, 9, 2426.

CHA, E., HERTL, J. A., SCHUKKEN, Y. H., TAUER, L. W., WELCOME, F. L. & GRÖHN, Y. T. 2013. The effect of repeated episodes of bacteria-specific clinical mastitis on mortality and culling in Holstein dairy cows. Journal of dairy science, 96, 4993-5007.

CHENG, W. N. & HAN, S. G. 2020. Bovine mastitis: risk factors, therapeutic strategies, and alternative treatments - A review. Asian-Australas J Anim Sci, 33, 1699-1713.

CRISPIE, F., ALONSO-GÓMEZ, M., O'LOUGHLIN, C., KLOSTERMANN, K., FLYNN, J., ARKINS, S., MEANEY, W., ROSS, R. P. & HILL, C. 2008a. Intramammary infusion of a live culture for treatment of bovine mastitis: effect of live lactococci on the mammary immune response. Journal of Dairy Research, 75, 374-384.

CRISPIE, F., ALONSO-GÓMEZ, M., O'LOUGHLIN, C., KLOSTERMANN, K., FLYNN, J., ARKINS, S., MEANEY, W., ROSS, R. P. & HILL, C. 2008b. Intramammary infusion of a live culture for treatment of bovine mastitis: effect of live lactococci on the mammary immune response. The Journal of dairy research, 75, 374.

DETILLEUX, J., KASTELIC, J. P. & BARKEMA, H. W. 2015. Mediation analysis to estimate direct and indirect milk losses due to clinical mastitis in dairy cattle. Preventive veterinary medicine, 118, 449-456.

FOUTZ, C. A., GODDEN, S. M., BENDER, J. B., DIEZ-GONZALEZ, F., AKHTAR, M. & VATULIN, A. 2018. Exposure to antimicrobials through the milk diet or systemic therapy is associated with a transient increase in antimicrobial resistance in fecal Escherichia coli of dairy calves. Journal of dairy science, 101, 10126-10141.

FREITAS, C. H., MENDES, J. F., VILLARREAL, P. V., SANTOS, P. R., GONÇALVES, C. L., GONZALES, H. L. & NASCENTE, P. S. 2018. Identification and antimicrobial suceptibility profile of bacteria causing bovine mastitis from dairy farms in Pelotas, Rio Grande do Sul. Brazilian Journal of Biology, 78, 661-666.

FUKUYAMA, K., ISLAM, M. A., TAKAGI, M., IKEDA-OHTSUBO, W., KURATA, S., ASO, H., VIGNOLO, G., VILLENA, J. & KITAZAWA, H. 2020. Evaluation of the immunomodulatory ability of lactic acid bacteria isolated from feedlot cattle against mastitis using a bovine mammary epithelial cells in vitro assay. Pathogens, 9, 410.

HALASA, T., HUIJPS, K., ØSTERÅS, O. & HOGEVEEN, H. 2007. Economic effects of bovine mastitis and mastitis management: A review. Veterinary quarterly, 29, 18-31.

HERTL, J. A., GRÖHN, Y. T., LEACH, J. D. G., BAR, D., BENNETT, G. J., GONZALEZ, R. N., RAUCH, B. J., WELCOME, F. L., TAUER, L. W. & SCHUKKEN, Y. H. 2010. Effects of clinical mastitis caused by gram-positive and gram-negative bacteria and other organisms on the probability of conception in New York State Holstein dairy cows. Journal of dairy science, 93, 1551-1560.

JORJÃO, A. L., OLIVEIRA, F. E. D., LEÃO, M. V. P., CARVALHO, C. A. T., JORGE, A. O. C. & OLIVEIRA, L. D. D. 2015. Live and heat-killed Lactobacillus rhamnosus ATCC 7469 may induce modulatory cytokines profiles on macrophages RAW 264.7. The Scientific World Journal, 2015.

KEANE, O. M., BUDD, K. E., FLYNN, J. & MCCOY, F. 2013. Pathogen profile of clinical mastitis in Irish milk-recording herds reveals a complex aetiology. Veterinary Record, 173, 17-17.

KEAST, D. R., FULGONI III, V. L., NICKLAS, T. A. & O'NEIL, C. E. 2013. Food sources of energy and nutrients among children in the United States: National Health and Nutrition Examination Survey 2003–2006. Nutrients, 5, 283-301.

KITCHING, M., MATHUR, H., FLYNN, J., BYRNE, N., DILLON, P., SAYERS, R., REA, M. C., HILL, C. & ROSS, R. P. 2019. A live bio-therapeutic for mastitis, containing Lactococcus lactis DPC3147 with comparable efficacy to antibiotic treatment. Frontiers in microbiology, 10, 2220.

KLOSTERMANN, K., CRISPIE, F., FLYNN, J., MEANEY, W., ROSS, R. P. & HILL, C. 2010. Efficacy of a teat dip containing the bacteriocin lacticin 3147 to eliminate Gram-positive pathogens associated with bovine mastitis. Journal of dairy research, 77, 231-238.

KLOSTERMANN, K., CRISPIE, F., FLYNN, J., ROSS, R. P., HILL, C. & MEANEY, W. 2008. Intramammary infusion of a live culture of Lactococcus lactis for treatment of bovine mastitis: comparison with antibiotic treatment in field trials. Journal of dairy research, 75, 365-373.

KUMAR, N., MANIMARAN, A., KUMARESAN, A., JEYAKUMAR, S., SREELA, L., MOOVENTHAN, P. & SIVARAM, M. 2017. Mastitis effects on reproductive performance in dairy cattle: a review. Tropical animal health and production, 49, 663-673.

MAIA, N. L., DE BARROS, M., DE OLIVEIRA, L. L., CARDOSO, S. A., DOS SANTOS, M. H., PIERI, F. A., RAMALHO, T. C., DA CUNHA, E. F. F. & MOREIRA, M. A. S. 2018. Synergism of Plant Compound With Traditional Antimicrobials Against Streptococcus spp. Isolated From Bovine Mastitis. Frontiers in Microbiology, 9, 1203.

MALVISI, M., STUKNYTĖ, M., MAGRO, G., MINOZZI, G., GIARDINI, A., DE NONI, I. & PICCININI, R. 2016. Antibacterial activity and immunomodulatory effects on a bovine mammary epithelial cell line exerted by nisin A-producing Lactococcus lactis strains. Journal of dairy science, 99, 2288-2296.

MARCEL, A., ENCISO, S. R. A., BOUBAKER, B.-B., JONATHAN, B., EMILY, C., CICERONE, G., KATIA, C., DE CAGNO, F., KOEN, D. & ANNELIES, D. 2018. OECD-FAO Agricultural Outlook 2018-2027. OECD-FAO Agricultural Outlook 2018-2027.

MCEWEN, S. A. & COLLIGNON, P. J. 2018. Antimicrobial resistance: a one health perspective. Antimicrobial resistance in bacteria from livestock and companion animals, 521-547.

MUEHLHOFF, E., BENNETT, A. & MCMAHON, D. 2013. Milk and dairy products in human nutrition, Food and Agriculture Organization of the United Nations (FAO).

NADER-MACÍAS, M. E. F., BOGNI, C., SESMA, F., ESPECHE, M. C., PELLEGRINO, M., SAAVEDRA, L. & FROLA, I. 2011. Alternative approaches for the prevention of bovine mastitis. Probiotics, bioactive compounds and vaccines: bioactives compounds. Nova Science Publishers Inc., New York, 1-34.

O'FLAHERTY, S., COFFEY, A., MEANEY, W. J., FITZGERALD, G. F. & ROSS, R. P. 2005. Inhibition of bacteriophage K proliferation on Staphylococcus aureus in raw bovine milk. Letters in applied microbiology, 41, 274-279.

O'HALLORAN, F., BEECHER, C., CHAURIN, V., SWEENEY, T. & GIBLIN, L. 2016. Lactoferrin affects the adherence and invasion of Streptococcus dysgalactiae ssp. dysgalactiae in mammary epithelial cells. Journal of Dairy Science, 99, 4619-4628.

O'NEIL, C. E., NICKLAS, T. A. & FULGONI III, V. L. 2018. Food sources of energy and nutrients of public health concern and nutrients to limit with a focus on milk and other dairy foods in children 2 to 18 years of age: National Health and Nutrition Examination Survey, 2011–2014. Nutrients, 10, 1050.

PIETROCOLA, G., NOBILE, G., RINDI, S. & SPEZIALE, P. 2017. Staphylococcus aureus manipulates innate immunity through own and host-expressed proteases. Frontiers in cellular and infection microbiology, 7, 166.

PIQUÉ, N., BERLANGA, M. & MIÑANA-GALBIS, D. 2019. Health benefits of heat-killed (Tyndallised) probiotics: an overview. International journal of molecular sciences, 20, 2534.

RYAN, M. P., FLYNN, J., HILL, C., ROSS, R. P. & MEANEY, W. J. 1999. The natural food grade inhibitor, lacticin 3147, reduced the incidence of mastitis after experimental challenge with Streptococcus dysgalactiae in nonlactating dairy cows. Journal of Dairy Science, 82, 2108-2114.

RYAN, M. P., MEANEY, W. J., ROSS, R. P. & HILL, C. 1998. Evaluation of lacticin 3147 and a teat seal containing this bacteriocin for inhibition of mastitis pathogens. Applied and environmental microbiology, 64, 2287-2290.

SARKAR, A. & MANDAL, S. 2016. Bifidobacteria—Insight into clinical outcomes and mechanisms of its probiotic action. Microbiological research, 192, 159-171.

SHIELDS-CUTLER, R. R., AL-GHALITH, G. A., YASSOUR, M. & KNIGHTS, D. 2018. SplinectomeR enables group comparisons in longitudinal microbiome studies. Frontiers in microbiology, 9, 785.

SOUZA, R. F. S., RAULT, L., SEYFFERT, N., AZEVEDO, V., LE LOIR, Y. & EVEN, S. 2018. Lactobacillus casei BL23 modulates the innate immune response in Staphylococcus aureus-stimulated bovine mammary epithelial cells. Beneficial microbes, 9, 985-995.

SZWEDA, P., SCHIELMANN, M., FRANKOWSKA, A., KOT, B. & ZALEWSKA, M. 2014. Antibiotic resistance in Staphylococcus aureus strains isolated from cows with mastitis in eastern Poland and analysis of susceptibility of resistant strains to alternative nonantibiotic agents: lysostaphin, nisin and polymyxin B. Journal of Veterinary Medical Science, 76, 355-362.

TAVERNITI, V. & GUGLIELMETTI, S. 2011. The immunomodulatory properties of probiotic microorganisms beyond their viability (ghost probiotics: proposal of paraprobiotic concept). Genes & nutrition, 6, 261-274.

WAGNER, R. D., PIERSON, C., WARNER, T., DOHNALEK, M., HILTY, M. & BALISH, E. 2000. Probiotic effects of feeding heat-killed Lactobacillus acidophilus and Lactobacillus casei to Candida albicans-colonised immunodeficient mice. Journal of food protection, 63, 638-644.

WALLIS, J. K., KRÖMKER, V. & PADUCH, J.-H. 2019. Biofilm challenge: lactic acid bacteria isolated from bovine udders versus Staphylococci. Foods, 8, 79.

WARDA, A. K., REA, K., FITZGERALD, P., HUESTON, C., GONZALEZ-TORTUERO, E., DINAN, T. G. & HILL, C. 2019. Heat-killed lactobacilli alter both microbiota composition and behaviour. Behavioural Brain Research, 362, 213-223.

XIONG, W., SUN, Y. & ZENG, Z. 2018. Antimicrobial use and antimicrobial resistance in food animals. Environmental Science and Pollution Research, 25, 18377-18384.

ZAATOUT, N., AYACHI, A. & KECHA, M. 2020. Staphylococcus aureus persistence properties associated with bovine mastitis and alternative therapeutic modalities. Journal of applied microbiology, 129, 1102-1119.

ZADOKS, R. N., MIDDLETON, J. R., MCDOUGALL, S., KATHOLM, J. & SCHUKKEN, Y. H. 2011a. Molecular epidemiology of mastitis pathogens of dairy cattle and comparative relevance to humans. Journal of mammary gland biology and neoplasia, 16, 357-372.

ZADOKS, R. N., MIDDLETON, J. R., MCDOUGALL, S., KATHOLM, J. & SCHUKKEN, Y. H. 2011b. Molecular epidemiology of mastitis pathogens of dairy cattle and comparative relevance to humans. Journal of mammary gland biology and neoplasia, 16, 357-372.

ZHOU, Y., ZHANG, H., BAO, H., WANG, X. & WANG, R. 2017. The lytic activity of recombinant phage lysin LysKΔamidase against staphylococcal strains associated with bovine and human infections in the Jiangsu province of China. Research in Veterinary Science, 111, 113-119.

Chapter 7

7 General Discussion

7.1 Discussion

Microbiome research, which focuses on the behaviour, interactions, and functions of microbial communities within a specified environment, has witnessed remarkable growth in recent years. These advances have largely been driven by the dramatic cost reduction of high-throughput sequencing and expansion of computational power. This progress has generated a wealth of data, which has provided profound insights into the nature of microbial communities, their interactions and effects within various hosts and ecological environments. Comprehensive understanding of the dynamic relationships between microbiota, hosts, and other microbes holds the potential to significantly enhance interventional strategies and diagnostic techniques across diverse domains, spanning from ecology and agriculture to medicine and forensics (Cullen et al., 2020). Deciphering the role of the microbiome in early-life is one of the most pivotal areas of microbiome research (Vemuri and Herath, 2023). Additionally, given the escalating antibiotic resistance crisis, exploring the potential of host-microbiome interactions as a means of developing microbiome-based therapeutics represents another compelling branch of microbiome research (Yadav and Chauhan, 2022). This thesis, therefore, endeavoured to provide novel insights into the early-life microbiomes of both bovines and humans and to explore innovative microbiome-based therapeutics applicable to both species.

Thorough understanding of the elements influencing initial microbiome transfer is of paramount importance to optimising neonatal health. Thus, in **Chapter 1**, we reviewed and discussed the decisive role of intrinsic and extrinsic factors, collectively named "perinatal factors", in the formation of the human infant gut microbiome. *Bifidobacterium, Bacteroides*, *Veillonella*, *Streptococcus, Collinsella*, *Lactobacillus* and *Akkermansia* species have repeatedly been shown to dominate the core infant gut microbiome. Perinatal factors, most ubiquitously birth mode, infant diet and mother-infant vertical transmission of microbes, significantly influence the manner in which these core members colonise the infant gut microbiome. Direct comparisons of studies of infant gut microbiota and perinatal factors are difficult due to the inherent limitations of currently available cultivation methodology, sequence techniques and reference databases. Therefore, our understanding of how such factors affect microbial colonisation and, in turn, influence infant health is mostly limited to correlation rather

than causation. Fortunately, the advent of metagenomics sequencing has begun to bridge this gap. For instance, reference catalogs such as the recently constructed Early-Life Gut Proteins (ELGP) and the Early-Life Gut Genomes catalog (ELGG), have provided new insights into the early-life human gut microbiome and will facilitate studies to better understand the development and mechanisms of disturbances of the human gut microbiome in early life (Zeng et al., 2022). Furthermore, studies adopting a multi-omics approach encompassing transcriptomics, metabolomics, lipidomics and proteomic investigations in combination with DNA and RNA sequencing will enable us to fully uncover the effects of perinatal factors on initial microbiome establishment and long-term functioning (Ferrocino et al., 2023).

In **Chapter 2**, we extensively reviewed the potential of bovine colostrum as a source of bioactive components with diverse applications in functional foods, nutraceuticals, and pharmaceuticals for both veterinary and human health. The cross-species bioactivity of bovine colostrum makes it an attractive option for research and development in both veterinary and human applications. A plethora of studies have demonstrated the therapeutic benefits of colostrum supplementation in promoting health and treating various diseases in humans and other animals. As the market for colostrum-based products expands, there is a need for stricter quality control and well-conducted clinical trials to assess dosage effectiveness and elucidate dose-response effects in clinical settings. Overcoming these obstacles and gaining a deeper understanding of the mechanisms behind colostrum's beneficial effects will pave the way for its broader adoption as a pharmaceutical product. Overall, bovine colostrum is an underutilised by-product of the dairy industry, and its potential as a valuable resource for human and veterinary health deserves further exploration.

The current consensus is that a disturbed microbiota during infancy can have a lasting impact on health in early life and beyond. As discussed in Chapter 1, perinatal factors can significantly impact the microbial bond between mother and infant and the establishment of the infant microbiome. Several intriguing questions persist concerning the infant microbiome during the early stages of life (Wang et al., 2020). In **Chapter 3** of this thesis, we delved into three of these questions. Firstly, we addressed the current debate on the sterility of the intrauterine environment and the timing at which microorganisms first colonise humans (Kennedy et al., 2023). Fetal

meconium has been shown to not have a detectable microbiota before birth (Kennedy et al., 2021), while the presence of a microbiome in neonatal (first-pass) meconium, which is formed before birth, has been debated (Kennedy et al., 2023). Similarly, the existence of a placental microbiome has been disputed (Briana et al., 2021, Blaser et al., 2021). As the existence of microorganisms is not established in these samples, they have been categorised as 'potential no (zero) biomass samples' (Kennedy et al., 2023). To elucidate the microbiome of placenta and meconium, we utilised methodological and bioinformatic approaches recommended for accurate microbial detection recommended for low biomass samples (de Goffau et al., 2018). *Staphylococcus*, *Bifidobacterium*, *Streptococcus*, *Enterococcus*, *Escherichia-shigella*, *Delftia*, *Afipia*, *Cutibacterium* and *Rothia* genera represented the core meconium microbiome in our samples, with *Staphylococcus epidermis* consistently present in all samples. In agreement with our findings, several studies have shown that neonatal meconium contains microbial profiles reflecting populations acquired during and after birth (Klopp et al., 2022, Kang et al., 2022, Rocha-Viggiano et al., 2022, Vemuri and Herath, 2023). Metabolic pathway analysis with PICRUST2 unveiled critical pathways essential for biosynthesis and energy production. There was no non-contaminant microbial profiles in placental samples. Therefore, these findings support the long-held view that microbial colonisation of the infant occurs at birth and the establishment of replicating microbial cells does not commonly occur in healthy pregnancies.

The existence of a fetal microbiome and its implications for medical practice are subjects of debate, posing a challenge to scientific progress. If confirmed, it could revolutionise our understanding of early immune system development and host-microbe interactions. Addressing this issue is crucial to prevent wasteful research and misguided attempts to manipulate a non-existent fetal microbiome. Furthermore, this challenge extends to studying microbiota in low-biomass samples, such as blood, brain, and cancer tissues. While we took extensive measures to minimise contamination and ensure accurate microbial identification, it is important to acknowledge that our study has limitations, which could be improved in further studies of this type. Prior to sequencing, an initial assessment of samples using quantitative methods (e.g., qPCR) and microscopic visualisation (e.g., Gram staining, fluorescence in situ hybridisation) is vital to confirm the presence of microorganisms, accuracy and

efficiency in the sequencing process. Repeating sample processing with different DNA extraction kits or methods (Lauder et al., 2016), with different operators and/or on different days is another informative method of control (Eisenhofer et al., 2019). Another useful addition to a future study would be the use of spike-in controls. These allow not only allow tracking of samples, but also aid absolute quantification and quantification of cross-contamination/index hopping (Hornung et al., 2019). We used PICRUSt2 to estimate metabolic functional differences between the groups rather than accurately measuring the relative abundance of functional genes using a shotgun metagenomic approach. A final critical and often overlooked aspect of low-biomass studies is the choice of primers targeting the 16S rRNA gene. We used the most commonly used primer pair in this study targeting the V3–V4 region of the gene. However, the use of V3-V4 primers has been associated with off-target effects and potential overestimation of bacterial abundance due to the amplification of human mitochondrial DNA (Walker et al., 2020). Therefore, alternative primers, such as those targeting the V1–V2 region have been recommended for studies of low biomass samples (Kennedy et al., 2023).

It has been well established that the gut, which harbours the most heavily populated microbiota in the human body, dominates the transmission of mother-to-infant microbiota (Wang et al., 2020). Therefore the second aim of this study was to analyse the contribution of the maternal oral cavity and vaginal microbiomes to the infant oral and gut microbiomes. Analysing the overall microbial composition of each sample type and deciphering vertical microbiota transfer in 18 mother-infant dyads, we found that the infant oral microbiome shared significant similarity with the maternal oral microbiome. Commensal bacteria such as *S. oralis*, *H. parainfluenzae*, *F. nucleatum* and *R. Mucilaginosa* exhibited high levels of sharing, similar to recent studies (Yu et al., 2023). Significantly lower levels of vertical transfer were observed between other maternal and infant body sites. *C. pyruvicproducens*, *F. nucleatum*, *R. mucilaginosa* and *B. longum* exhibited high levels of sharing between maternal and infant samples studied. By sampling multiple maternal and infant niches, we have identified various possible seeding routes, pointing toward auxiliary pathways in initial mother-to-infant seeding. Our study would have been further strengthened by including more maternal niches, specifically maternal feces and breastmilk.

Vertical mother-to-infant transmission of microbiota has been studied by several groups (Bogaert et al., 2023). These studies mainly focused on the infant gut microbiota and possible maternal source niches, including the vagina (Kait et al., 2023), breastmilk (Fehr et al., 2020) and maternal gut microbiota (Mitchell et al., 2020). Few studies however have explored vertical transmission events between a broader selection of maternal bacterial communities and infant niche, with a longitudinal design. A particularly interesting recent study examined the transmission pathways and early-life development of microbiota in infants born via C-section and vaginally. They characterised six maternal niches (vagina, nasopharynx, saliva, feces, skin, and breastmilk) and four infant niches (nasopharynx, saliva, feces, and skin) in 120 mother-infant pairs at five time points over the first month of life. The study revealed that 58.5% of the infant microbiota could be attributed to any of the maternal source communities (Bogaert et al., 2023). Incorporating placental samples and meconium into this type of study would also be particularly interesting. The majority of studies investigating vertical mother-to-infant transmission of microbiota have relied on 16S rRNA sequencing. Future research should consider employing shotgun sequencing, which provides accurate measurements of functional gene abundance and strain-level accuracy. While shotgun metagenomics sequencing offers several advantages, it has limitations, such as the inability to determine whether genes are functional and the uncertainty of organism viability. To address these issues, integrating culture-based techniques, meta-transcriptomics, and metabolomics analyses can be utilised. Additional metagenomics studies, similar to the one conducted by Wang et al. (2021), which analysed mother-infant gut microbiome transfer of 376 mother-infant dyads (468 mother and 1024 infant samples) of eight studies from six countries are warranted for other body sites (e.g., maternal-infant oral microbiome transfer) (Wang et al., 2021). By analysing a broader range of mother-infant dyads from different regions, generalised shared species and strains can be identified across different body sites. This knowledge can guide future research on infant microbiome development and identify primary targets for probiotics exploration. Finally, to harness the full benefit of investigating vertical mother-to-infant transmission, protocol standardisation from sample collection to microbiome profiling is essential (Szóstak et al., 2022). Every experimental procedure should be viewed as a detailed algorithm, requiring careful design and strict adherence. In metagenomic experiments, no step is negligible, from sample collection and DNA

isolation to sequencing, bioinformatics analyses, and statistical testing. Each part of the procedure plays a crucial role in obtaining reliable results and drawing meaningful conclusions. This is especially vital for vertical mother-to-infant transmission studies which use such a diverse array of sample types. In a recent study, Szóstak et al. (2022) provided a comprehensise analysis of DNA isolation, NGS library preparation, and bioinformatic analysis for identifying gut microbial taxa, offering a practical step-by-step guidance for metagenomic gut microbiome studies. Such valuable insights should also be extended to other types of microbiome research beyond the gut.

Finally, to add to the knowledge gathered in Chapter 1, we investigated the effect of perinatal factors on the microbial compositions of this cohort. Regarding maternal antibiotic usage, differences in beta diversity and differential abundance of specific bacterial genera were observed in meconium and maternal saliva samples. Notably, antibiotic exposure led to changes in bacterial pathways associated with pathogenicity and biofilm formation. Delivery mode also influenced the meconium and oral microbiomes, with C-section (CS) births showing increased species richness and differential abundance of certain bacteria associated with potential health implications. Breastfeeding was associated with a more diverse gut microbiome and health-promoting metabolic pathways. Gender had minimal effects, while preterm premature rupture of membranes (PROM) birth impacted alpha diversity and *Lactobacillus* spp. in vaginal samples. These findings have implications for understanding medical conditions in early life and informing preventive and therapeutic treatments. Studies investigating how multiple perinatal factors may interact with each other in the formation of the infant gut microbiome are also warranted. For instance, breastfeeding has been shown to beneficially alter the patterns of aberrant colonisation in CS born infants (Coker et al., 2021).

The virome, which encompasses the viral component of the microbiome, represents one of the least documented and poorly understood aspects of global biodiversity (Carlson Colin et al., 2022). Viral metagenomics have changed the perspective from which viruses are observed, from mere pathogens to recognising their role as architects in shaping the complex web of life. Numerous studies have explored the early life virome in humans (Shah et al., 2023). However, bovines have been relatively understudied in this area. Therefore, **Chapter 4** of this thesis explored the virome of

bovine colostrum. In this study, using a cohort of 72 cows, given dry cow therapy (n=48) or naturally dried off (n=24), we characterised the virome composition of first milking bovine colostrum. We developed a dedicated virome extraction protocol for colostrum samples. Through viral metagenomics analysis, we explored the virome's diversity, community structure, and potential ecological functions within colostrum. Notably, the study revealed a predominance of ssDNA viruses and dsDNA phages, with some phages carrying antibiotic resistance genes (ARGs).This finding raising important questions about their role in disseminating antibiotic resistance. Specific ARGs known to confer resistance to antibiotics used in the study were also identified. In terms of virome composition, *Circovius*, *Prunevirus*, and *Liefievirus* were the most abundant genera found in the samples. *Papillomaviruses*, known for their high pathogenicity to bovines, were also prevalent in the colostrum virome. Approximately 28% of the viral-like particles (VLPs) were identified as dsDNA phages, associated with specific host bacterial genera previously identified as core genera in bovine colostrum. The study also evaluated the influence of farm-level variables on the composition of the colostrum virome. Notably, antibiotic dry cow treatment significantly impacted virome composition. This study contributes to the growing field of virome research and emphasises the significance of characterising viral communities in livestock animals. These findings will enhance our understanding of the role of the virome in microbial ecosystems, animal health, and the broader implications for human health and the environment. These results could also have important implications for calf health, the spread of antimicrobial resistance in the environment and the transmission of diseases through colostrum-based products.

Given the fascinating and challenging nature of studying viruses, along with the growing evidence of the virome's impact on health and disease and the shifting paradigms surrounding certain viruses in various ecosystems, there is a strong need for continued advancement in viromics research. Virome research is currently primarily hindered by two factors: (i) the lack of standardised extraction and sequencing protocols and (ii) the absence of reference viral genomes. As with all microbiome studies, there is no “one size fits all” protocol for virome extractions and subsequent bioinformatics analysis (Thurber et al., 2009, Garmaeva et al., 2019). Fortunately, a growing body of diverse methodologies is becoming available for extracting viromes from different samples and handling the resulting sequencing data.

In our study, we attempted to optimise an extraction protocol based on polyethylene glycol (PEG) precipitation, widely used for studying the human gut virome (Wang et al., 2023). However, it would be worth revisiting our samples with other methods such as caesium chloride (CsCl gradients) for viral particle purification to see how the results could potentially improve. For instance, the majority of contigs recovered in our study were small in size, representing genome fragments. It has been reported that a CsCl step can improve the size of viral contigs recovered in virome studies (d'Humières et al., 2019).

Regarding sequencing methodology, we used short-read sequencing as it is commonly used in virome studies (Paez-Espino et al., 2016). However, this method is not without limitations. For instance, viruses which contain genomic islands and/or have high micro-diversity can cause genome fragmentation during assembly (Roux et al., 2017). Long-read sequencing technologies, such as Pacific Biosciences (PacBio) and Oxford Nanopore Technologies (ONT) offer solutions to such issues. The longer reads are potentially able to span the length of entire viral genomes, overcoming assembly issues resulting from repeat regions and low coverage (Olson et al., 2019). More recently, a Long-Read Linker-Amplified Shotgun Library (LASL) approach was developed that combines LASL library preparation with ONT MinION sequencing and has been found to recover more high-quality viral genomes than long or short-reads alone (Warwick-Dugdale et al., 2019, Cook et al., 2021). Such approaches could be applied to our extracted DNA to increase the number of VLPs for downstream analysis.

Owing to the lack of a universal marker gene across viral genomes, shotgun metagenomic sequencing is needed to fully address viral communities. Therefore, for metagenomic analysis of virome, reference viral genomes are important because they are used for taxonomic classification, estimation of viral taxa distribution, and identification of host-virus interactions and functional potential (Cook et al., 2023). Indeed, more than 50% of viral sequences generated by metagenomic sequencing remain unclassified (Cao et al., 2022). This hinders the accuracy of the generalisations and conclusions gleaned from the current studies. In recent years, work on building these essential reference data bases has been steadily increasing in a range of ecosystems. For instance, the IMG/VR database, the largest collection of publicly available viral genomes, primarily comprises genomes derived from the marine,

freshwater, and human gut (Camargo et al., 2023) and a bovine rumen viral catalog was recently constructed (Sato et al., 2023). To ensure the most accurate metagenomics analyses of viral diversity, it is essential to have sample-specific viral genome catalogs since viruses tend to exhibit habitat-specificity (Paez-Espino et al., 2016).

Once we overcome current virome research challenges, such as optimizing isolation protocols and expanding virus databases, future directions for virome study include: (i) identifying a core gut virome and viral genes through large longitudinal cohort studies, (ii) studying long-term bacteriome-virome interactions influenced by external factors, and (iii) establishing causality of host-related correlations using model systems, multi-omics approaches, and innovative bioinformatics, possibly adapted from environmental studies (Garmaeva et al., 2019).

In the final two chapters of this thesis, our focus shifted towards leveraging host-microbiome interactions to develop microbiome-based therapeutics, with a primary emphasis on tackling mastitis. The microbiome holds the potential to be one of the major game-changers in tackling the antibiotic resistance crisis (Sorbara and Pamer, 2022). Mastitis is a disease with a multi-etiological nature, characterised by inflammation of the mammary gland, affects lactating women and dairy cows, causing considerable discomfort and pain in both cases. The emergence of antibiotic-resistant, mastitis-causing pathogens, highlights the urgent necessity for alternative therapies to effectively treat and prevent the disease (Rizzo et al., 2023). In the case of mastitis, microbiome-based treatments present a number of advantages over antibiotic treatment, including reduced antibiotic resistance, selective targeting of mastitis-causing pathogens, and fewer side effects. Novel therapeutics for the prophylaxis and treatment of mastitis can include live-bio-therapeutics (also known as probiotics), bacteriocins and phages (Angelopoulou et al., 2019).

Following on from our investigation of the bovine colostrum virome in Chapter 4, we decided to culture phages with potential therapeutic applications. In addition, while the virome of human breast milk has recently been researched (Mohandas and Pannaraj, 2020), culturing of phages for therapeutic applications is scarcely reported. Therefore, in **Chapter 5**, we attempted to isolate and evaluate the therapeutic

applicability of *S. aureus* phages from bovine colostrum and human breast milk, which have remained largely unexplored for the isolation of phages. In this study, two novel temperate phages vB_SauS_HM1 (phage HM1) and vB_SauS_BC1 (phage BC1), belonging to subfamily *Azeredovirinae* and genus *Phietavirus*, were isolated. *In vitro* analysis revealed that these phages have a number of favourable therapeutic characteristics, including broad host ranges, species specificity and lytic activity in milk enabling their potential use for future therapeutic applications against *S. aureus* infections. Furthermore, either individually or applied as a cocktail, they displayed the ability to reduce the bacterial growth of *S. aureus* in pasteurised, raw and mastitic milk samples. *S. aureus* isolates are well-known for carrying multiple prophages within their genomes. Therefore, it is highly plausible that phage HM1 and phage BC1 originated as prophages already present in the screening strains used in the study. Although our assays were conducted on a small scale, the results support the consensus that phage cocktails may be effective at overcoming bacterial resistance to phage infections (Oromí-Bosch et al., 2023).

Temperate phages are not recommended for therapeutic applications due to their potential to facilitate the horizontal transfer of antibiotic resistance and virulence genes (Borodovich et al., 2022, Strathdee et al., 2023). Therefore, future studies involving these phages will utilise recently developed genetic engineering techniques, which have transformed seemingly innocuous temperate phages into viable candidates for therapeutic applications (Hussain et al., 2023, Zhou et al., 2023, Oromí-Bosch et al., 2023). Techniques including CRISPR-Cas genome editing (Balcha and Neja, 2023), bacteriophage recombineering of electroporated DNA (BRED) (Payaslian et al., 2021), yeast-based platforms (Pires et al., 2021) and homologous recombination (Kilcher and Loessner, 2019) could be utilised with these phages to make them more applicable for therapeutic usage. While phage therapy is considered safe for use in humans, it has not been explored for the treatment of human mastitis (Angelopoulou et al., 2019). In bovines, phage therapy for mastitis application has been hindered by the issues of phage activity in raw, mastitic bovine milk (O'Flaherty et al., 2005). The most important concept for the success of phages in reaching bacterial targets is ensuring that a minimum inhibitory concentration is surpassed. Recent attempts to enhance the *in vivo* application of phage for disease control, means that phage therapy will receive larger interest in the coming years. For instance, numerous methods have

been explored to enhance the stability and delivery of phage products to the site of infection including liposome encapsulation, polymer encapsulation, electrospun fibre-encapsulation and microneedling (Ling et al., 2022). Such methods would also be interesting to apply to phages which have previously failed during field trials of mastitis, such as Phage K (O'Flaherty et al., 2005).

Finally, in **Chapter 6**, we investigated the use of *Lactococcus lactis* (*L. lactis*) DPC3147, a live bio-therapeutic (also known as a probiotic), for the treatment of bovine mastitis. Building upon previous trials (Kitching et al., 2019), we sought to gain insight into the mechanism of action of this live bio-therapeutic, focussing on chronic mastitis cases, the most difficult to treat. We treated 28 cows with chronic mastitis with two separate emulsion-based formulations containing either viable L. lactis DPC3147 cells (15 cows) or heat-killed *L. lactis* DPC3147 cells (13 cows). We then evaluated the efficacies of the two formulations (two treatment groups) in terms of stimulating a localised immune response (quantified by measuring IL-8 concentrations in milk collected from udders affected by mastitis) and efficacies in terms of cure rates (quantified by reductions in somatic cell counts and absence of pathogens). We demonstrated that the presence of heat-inactivated bacteria (a postbiotic) was as effective as the live bio-therapeutic in eliciting a localised immune response in cows with chronic mastitis. The response to heat-killed cells (postbiotic) reported herein could have beneficial implications for farmers with regard to prolonging the shelf-life of such emulsion-based formulations containing heat-killed cells of *L. lactis* DPC3147 for curing cows with mastitis. Based on this study, a future trial has been granted ethical approval. The aim of this trial is to build upon our findings by including additional treatment groups. One group will include *L. lactis* strains which do not produce any bacteriocins/antimicrobials. A supplementary negative control treatment group will involve infusions with merely the emulsion-based formulation without any cells (live or heat-killed) whatsoever will also be applied. Finally, a supplementary negative control treatment group may involve infusions with merely the emulsion-based formulation without any cells (live or heat-killed) whatsoever will be included. This upcoming trial will help us fully unravel the complex mechanisms involved in the resolution of this disease when using live-biotherapeutic formulations.

Throughout this thesis, we have delved into the fascinating world of the early-life microbiome transfer and its therapeutic applications in bovines and humans. The collective findings underscore the importance of considering microbiome-host interactions in diverse contexts, from agriculture to human health. As we move forward, it is imperative to recognise the interconnectedness between human and bovine microbiomes, providing an opportunity for cross-species research collaborations and knowledge exchange. Understanding the parallels and differences between these two systems can lead to innovative approaches in therapeutic development and disease prevention for both species. In conclusion, the discoveries made herein provide a solid foundation for future research, guiding us towards further harnessing the power of the microbiome to improve the health and well-being of both bovines and humans. The implications of this work extend beyond the academic realm, promising tangible benefits for agriculture, medicine, and public health, making it a truly exciting and impactful field of study. Overall, studies of the micro environment will have impacts that reverberate at the macro scale.

7.2 References

ANGELOPOULOU, A., WARDA, A. K., HILL, C. & ROSS, R. P. 2019. Non-antibiotic microbial solutions for bovine mastitis–live biotherapeutics, bacteriophage, and phage lysins. Critical reviews in microbiology, 45, 564-580.

BÄCKHED, F., ROSWALL, J., PENG, Y., FENG, Q., JIA, H., KOVATCHEVA-DATCHARY, P., LI, Y., XIA, Y., XIE, H. & ZHONG, H. 2015. Dynamics and stabilization of the human gut microbiome during the first year of life. Cell host & microbe, 17, 690-703.

CARLSON COLIN, J., GIBB RORY, J., ALBERY GREGORY, F., BRIERLEY, L., CONNOR RYAN, P., DALLAS TAD, A., ESKEW EVAN, A., FAGRE ANNA, C., FARRELL MAXWELL, J., FRANK HANNAH, K., MUYLAERT RENATA, L., POISOT, T., RASMUSSEN ANGELA, L., RYAN SADIE, J. & SEIFERT STEPHANIE, N. 2022. The Global Virome in One Network (VIRION): an Atlas of Vertebrate-Virus Associations. mBio, 13, e02985-21.

COKER, M. O., LAUE, H. E., HOEN, A. G., HILLIARD, M., DADE, E., LI, Z., PALYS, T., MORRISON, H. G., BAKER, E. & KARAGAS, M. R. 2021. Infant feeding alters the longitudinal impact of birth mode on the development of the gut microbiota in the first year of life. Frontiers in microbiology, 524.

CULLEN, C. M., ANEJA, K. K., BEYHAN, S., CHO, C. E., WOLOSZYNEK, S., CONVERTINO, M., MCCOY, S. J., ZHANG, Y., ANDERSON, M. Z. & ALVAREZ-PONCE, D. 2020. Emerging priorities for microbiome research. Frontiers in microbiology, 11, 136.

DE GOFFAU, M. C., LAGER, S., SALTER, S. J., WAGNER, J., KRONBICHLER, A., CHARNOCK-JONES, D. S., PEACOCK, S. J., SMITH, G. C. S. & PARKHILL, J. 2018. Recognizing the reagent microbiome. Nat Microbiol, 3, 851-853.

FERROCINO, I., RANTSIOU, K., MCCLURE, R., KOSTIC, T., DE SOUZA, R. S. C., LANGE, L., FITZGERALD, J., KRIAA, A., COTTER, P. & MAGUIN, E. 2023. The need for an integrated multi-OMICs approach in microbiome science in the food system. Comprehensive reviews in food science and food safety, 22, 1082-1103.

KENNEDY, K. M., DE GOFFAU, M. C., PEREZ-MUÑOZ, M. E., ARRIETA, M.-C., BÄCKHED, F., BORK, P., BRAUN, T., BUSHMAN, F. D., DORE, J., DE VOS, W. M., EARL, A. M., EISEN, J. A., ELOVITZ, M. A., GANAL-VONARBURG, S. C., GÄNZLE, M. G., GARRETT, W. S., HALL, L. J., HORNEF, M. W., HUTTENHOWER, C., KONNIKOVA, L., LEBEER, S., MACPHERSON, A. J., MASSEY, R. C., MCHARDY, A. C., KOREN, O., LAWLEY, T. D., LEY, R. E., O'MAHONY, L., O'TOOLE, P. W., PAMER, E. G., PARKHILL, J., RAES, J., RATTEI, T., SALONEN, A., SEGAL, E., SEGATA, N., SHANAHAN, F., SLOBODA, D. M., SMITH, G. C. S., SOKOL, H., SPECTOR, T. D., SURETTE, M. G., TANNOCK, G. W., WALKER, A. W., YASSOUR, M. & WALTER, J. 2023. Questioning the fetal microbiome illustrates pitfalls of low-biomass microbial studies. Nature, 613, 639-649.

KITCHING, M., MATHUR, H., FLYNN, J., BYRNE, N., DILLON, P., SAYERS, R., REA, M. C., HILL, C. & ROSS, R. P. 2019. A live bio-therapeutic for mastitis, containing

Lactococcus lactis DPC3147 with comparable efficacy to antibiotic treatment. Frontiers in microbiology, 10, 2220.

OROMÍ-BOSCH, A., ANTANI, J. D. & TURNER, P. E. 2023. Developing Phage Therapy That Overcomes the Evolution of Bacterial Resistance. Annual Review of Virology.

SHAH, S. A., DENG, L., THORSEN, J., PEDERSEN, A. G., DION, M. B., CASTRO-MEJÍA, J. L., SILINS, R., ROMME, F. O., SAUSSET, R. & JESSEN, L. E. 2023. Expanding known viral diversity in the healthy infant gut. Nature Microbiology, 1-13.

SORBARA, M. T. & PAMER, E. G. 2022. Microbiome-based therapeutics. Nature Reviews Microbiology, 20, 365-380.

VEMURI, R. & HERATH, M. P. 2023. Beyond the Gut, Emerging Microbiome Areas of Research: A Focus on Early-Life Microbial Colonization. Microorganisms [Online], 11.

WANG, S., RYAN, C. A., BOYAVAL, P., DEMPSEY, E. M., ROSS, R. P. & STANTON, C. 2020. Maternal vertical transmission affecting early-life microbiota development. Trends in microbiology, 28, 28-45.

YADAV, M. & CHAUHAN, N. S. 2022. Microbiome therapeutics: exploring the present scenario and challenges. Gastroenterology report, 10.

YU, J. C., KHODADADI, H., SALLES, É. L., NAEINI, S. E., THRELKELD, E., BHANDARI, B., MEGHIL, M., WANG, P. L. & BABAN, B. 2023. Oral Microbiome and Innate Immunity in Health and Disease: Building a Predictive, Preventive and Personalised Therapeutic Approach. Microbiome in 3P Medicine Strategies: The First Exploitation Guide, 391-409.

ZENG, S., PATANGIA, D., ALMEIDA, A., ZHOU, Z., MU, D., PAUL ROSS, R., STANTON, C. & WANG, S. 2022. A compendium of 32,277 metagenome-assembled genomes and over 80 million genes from the early-life human gut microbiome. Nature Communications, 13, 5139.